ACTA CHIMICA

ACADEMIAE SCIENTIARUM HUNGARICAE

ADIUVANTIBUS

V. BRUCKNER, GY. DEÁK, K. POLINSZKY,
E. PUNGOR, G. SCHAY, Z. G. SZABÓ

REDIGIT

B. LENGYEL

TOMUS 72 FASCICULUS 1

AKADÉMIAI KIADÓ, BUDAPEST

1972

ACTA CHIM. (BUDAPEST) ACASA 2 72 (1) 1–109 (1972)

ACTA CHIMICA

A MAGYAR TUDOMÁNYOS AKADÉMIA KÉMIAI TUDOMÁNYOK OSZTÁLYÁNAK IDEGEN NYELVŰ KÖZLEMÉNYEI

SZERKESZTI

LENGYEL BÉLA

TECHNIKAI SZERKESZTŐK

DEÁK GYULA és HARASZTHY-PAPP MELINDA

Az Acta Chimica német, angol, francia és orosz nyelven közöl értekezéseket a kémiai tudományok köréből.

Az Acta Chimica változó terjedelmű füzetekben jelenik meg, egy-egy kötet négy füzetből áll. Évente átlag négy kötet jelenik meg.

A közlésre szánt kéziratok a szerkesztőség címére (Budapest 112/91 Műegyetem) küldendők.

Ugyanerre a címre küldendő minden szerkesztőségi levelezés. A szerkesztőség kéziratokat nem ad vissza.

Megrendelhető a belföld számára az „Akadémiai Kiadó"-nál (Budapest V., Alkotmány utca 21. Bankszámla 05-915-111-46), a külföld számára pedig a „Kultúra" Könyv- és Hírlap Külkereskedelmi Vállalatnál (Budapest I., Fő utca 32. Bankszámla: 43-790-057-181) vagy annak külföldi képviseleteinél és bizományosainál.

Die Acta Chimica veröffentlichen Abhandlungen aus dem Bereiche der chemischen Wissenschaften in deutscher, englischer, französischer und russischer Sprache.

Die Acta Chimica erscheinen in Heften wechselnden Umfanges. Vier Hefte bilden einen Band. Jährlich erscheinen 4 Bände.

Die zur Veröffentlichung bestimmten Manuskripte sind an folgende Adresse zu senden:

Acta Chimica
Budapest 112/91 Műegyetem

An die gleiche Anschrift ist auch jede für die Redaktion bestimmte Korrespondenz zu richten. Abonnementspreis pro Band: $ 16.00.

Bestellbar bei dem Buch- und Zeitungs-Außenhandels-Unternehmen »*Kultúra*« (Budapest I., Fő utca 32. Bankkonto No. 43-790-057-181) oder bei seinen Auslandsvertretungen und Kommissionären.

ACTA CHIMICA

ACADEMIAE SCIENTIARUM HUNGARICAE

ADIUVANTIBUS

V. BRUCKNER, GY. DEÁK, K. POLINSZKY,
E. PUNGOR, G. SCHAY, Z. G. SZABÓ

REDIGIT

B. LENGYEL

TOMUS 72

AKADÉMIAI KIADÓ, BUDAPEST

1972

ACTA CHIM. ACAD. SCI. HUNG.

ACTA CHIMICA

TOMUS 72

Fasciculus 1 : 1972
Fasciculus 2 : 1972
Fasciculus 3 : 1972
Fasciculus 4 : 1972

INDEX

AHMED, Z. F. s. KARAWYA, M. S.

APJÓK, J. and BARTÓK, M.: Химия 1,3-бифункциональных соединений, XIII. Изучение превращений циклических ацеталей на катализаторе Pt/T с помощью микрореакторной техники. 1,3-Диоксоланы и 1,3-диоксепаны. (The Chemistry of 1,3-Bifunctional Systems, XIII. Conversions of Cyclic Acetals on Pt/T Catalysts, Studied by Micro-reactor Technique. 1,3-Dioxalans and 1,3-Dioxepans) 281

ÁRVAY, GY. s. ZSADON, B.

BARTHOS, É. s. SZABÓ, J.

BARTÓK, M. s. APJÓK, J.

BARTÓK, M., BOZÓKI-BARTÓK, G. and KOVÁCS, K.: The Chemistry of 1,3-Bifunctional Systems, XIV. Kinetic Study of the Alkaline Hydrolysis of the 2,2-Disubstituted Homologues of Trimethylene Chlorohydrin 297

BARTÓK, M. and BOZÓKI-BARTÓK, G.: The Chemistry of 1,3-Bifunctional Systems, XV. Kinetic Study of the Alkaline Hydrolysis of the 1-Monosubstituted Homologues of 3-Chloropropanol 423

BARTÓK, M. and BOZÓKI-BARTÓK, G.: The Chemistry of 1,3-Bifunctional Systems, XVI. Reaction Kinetical Study of the Alkaline Hydrolysis of 1,1-Disubstituted Derivatives of 3-Chloro-1-propanol 433

BITTER, I. s. CSŰRÖS, Z.

BODOR, E., JÓNÁS, K. and WELTHER, M.: Thermal Decomposition of Pyridine-Borane 111

BOGNÁR, R. s. LIPTÁK, A.

BOZÓKI-BARTÓK, G. s. BARTÓK, M.

BUREWICZ, A. s. WOLSKI, W.

CASTIŇEIRA M. s. SZEJTLI, J.

CLAUDER, O. and HORVÁTH-DÓRA, K.: Alkaloids Containing the Indolo [2,3-c] Quinazolino [3,2-a] Pyridine Skeleton, I. New Syntheses and Reduction of Rutecarpine.... 221

CSŰRÖS, Z., SOÓS, R., BITTER, I. and PÁLINKÁS, J.: Use of Amide Chlorides in Ring Closure Reactions, IV. A New Synthesis of 4-Aminoquinazoline Derivatives 59

DETREKŐY, E. s. KALLÓ, D.

DIAB, A. M. s. KARAWYA, M. S.

DINYA, Z.: Calculation of the Infrared Carbonyl Stretching Frequencies and Ionization Potentials of 4-Substituted Acetophenones 323

DINYA, Z. and SZABÓ, S.: Infrared Spectroscopic Studies on Flavonoids and Model Compounds, I. Investigations on some Infrared Frequencies of 4-Substituted Acetophenones by means of HMO Calculations 65

DOBIS, O. s. GIBER, J.

DOSS, S. H.: Infrared Absorption Bands Associated with the Sultam Ring..... 341

DUDAR, E. s. SZŐKE, S.

DWIVEDI, A. N. s. SINGH, D.

EGYED, J., VINKLER, P. and GÁL, S.: Thermolytic Disproportionation of Cyanoacetate Salts 451

FAUVELOT, G. s. LADÁNYI, L.

GADÓ, P. s. KISS, A. B.

GÁL, S. s. EGYED, J.

GIBER, J. and VAJASDY-PERCZEL, I.: Study of the Rest and Polarization Potentials of Chemically Treated Germanium Single Crystal Surfaces, I. Effect of the pH and Anion Adsorption 33

GIBER, J., WÉGNER, M. and DOBIS, O.: Adsorption of Water Vapour on the Chemically Treated Surface of a Germanium Single Crystal 393
HAMMOUDA, F. M. s. KARAWYA, M. S.
HASKÓ, I. s. KORACH, M.
HAUFFE, K. und HEGEDŰS, A. J.: Zum Mechanismus der Desorption und aktivierten Adsorption von Sauerstoff an unbelichtetem und UV-belichtetem Zinkoxid. (On the Mechanism of the Desorption and Activated Adsorption of Oxygen for Non-irradiated and UV-irradiated Zinc Oxide) 1
HEGEDŰS, A. J. s. HAUFFE, K.
HEGEDŰS, A. J. s. KISS, A. B.
HENRIQUES, R. D. s. SZEJTLI, J.
HILD, E. s. KISS, A. B.
HOLLY, S. s. KISS, A. B.
HORÁNYI, G., KŐNIG, P. and TELCS, I.: Oxidation of Secondary Alcohols on a Platinum Electrode, I. The Oxidation Products 165
HORÁNYI, G., VÉRTES, GY. and KŐNIG, P.: Oxidation of Secondary Alcohols on a Platinum Electrode, II. Study of the Connection Between Oxygen Adsorption and the Reaction 179
HORÁNYI, G. and NAGY, F.: Investigation of Adsorption Phenomena on Platinized Pt Electrodes by Tracer Methods, X. Studies with ^{14}C-labelled Acetone 261
HORÁNYI, G., KŐNIG, P. and NAGY, F.: Investigation of Adsorption Phenomena on Platinized Pt Electrodes by Tracer Methods, XI. Study of the Adsorption of Isopropanol 269
HORVÁTH-DÓRA, K. s. CLAUDER, O.
ILLÉS, V.: The Pyrolysis of Gaseous Hydrocarbons, V. The Kinetics of the Thermal Decomposition of an Isobutane-*n*-Butane Mixture 117
ILLÉS, V.: The Pyrolysis of Gaseous Hydrocarbons, VI. Product Distribution as the Function of the Degree of Decomposition in the Pyrolysis of an Isobutane-*n*-Butane Mixture 133
JALSOVSZKY, G. s. SZŐKE, S.
JÓNÁS, K. s. BODOR, E.
KALLÓ, D., DETREKŐY, E. and SCHAY, G.: Mechanistic Study of the Isomerization of *n*-Butene on Acid Catalysts, I. Kinetics of Monomolecular Catalytic Interconversion of Three Components 189
KARAWYA, M. S., RIZK, A. M., HAMMOUDA, F. M., DIAB, A. M. and AHMED, Z. F.: Phytochemical Investigation of Certain Cestrum Species Growing in Egypt. Alkaloids and Saponins 317
KÁLMÁN, E.: Untersuchungen zum Verhalten der Uranylsalze in wäßrigen binären und ternären Systemen. (Investigation of the Behaviour of Uranyl Salts in Aqueous Binary and Ternary Systems) 407
KISFALUDY, L. and NYÉKI, O.: Racemization During Peptide Azide Coupling (Short Communication) 75
KISS, A. B., GADÓ, P. and HEGEDŰS, A. J.: Investigations on the Thermocondensation of Ammonium Paratungstate Pentahydrate by a Combined Thermoanalytical and IR Spectrophotometric Method, and Additional Methods 371
KISS, A. B., HOLLY, S. and HILD, E.: Characteristic Vibrational Frequencies of Crystalline Ammonium Polymolybdates Consisting of Octahedral MoO_6 Units, in the 400—4000 cm^{-1} Range 147
KORACH, M. and HASKÓ, L.: Development of Petroleum Refining Technologies in Graph Theoretical Representation, I. Distillation 77
KOVÁCS, K. s. BARTÓK, M.
KŐNIG, P. s. HORÁNYI, G.
LADÁNYI, L. s. PHAM HAI TUNG
LADÁNYI, L., PHAM HAI TUNG, FAUVELOT, G. and SZÓKÁN, G.: Hydrazo-9-Acridine, a New Acid–Base Indicator for Titrations in Glacial Acetic Acid, I 359
LEMPERT, K. s. LEMPERT-SRÉTER, M.
LEMPERT-SRÉTER, M. and LEMPERT, K.: Alkaline Cleavage of Some (1-Phenylsulfonyl-2-Pyrazolin-5-Ylmethyl) Ketones (Short Communication) 349
LIPTÁK, A. and BOGNÁR, R.: N-Glycosides, XV. The Validity of Hudson's Isorotational Rule for Aromatic O- and N-Glucoside Derivatives of Analogous Structures 309
LITOMISKY, J.: Über die Anwendung zweiatomiger Moleküle als Vergleichselemente bei der spektrochemischen Analyse nichtleitender Stoffe. (On the Use of Diatomic Molecules as Comparing Elements in the Spectrometric Analysis of Non-Conducting Substances) 231

MENCZEL, GY., SAMAY, G. and SIMON, K.: Crystal and Molecular Structure of Acetone 4-Nitrophenylhydrazone 441
NAGY, F. s. HORÁNYI, GY.
NYÉKI, O. s. KISFALUDY, L.
PÁLINKÁS, J. s. CSŰRÖS, Z.
PAÁL, Z. and TÉTÉNYI, P.: C_5-Cyclization of Unsaturated Hydrocarbons on Platinum Black (Short Communication) 277
PHAM HAI TUNG and LADÁNYI, L.: Hydrazo-9-Acridine, a New Acid–Base Indicator for Titrations in Glacial Acetic Acid, II. Determination of the Indicator Dissociation Constant 363
PHAM HAI TUNG s. LADÁNYI, L.
Г. В. ПУТЫРСКАЯ и Ю. СИЛАДИ: Синтез моно- и дисульфопроизводных дифенилпикрилгидразила (ДФПГ). — (PUTIRSKAJA, G. V. and SZILÁGYI, J.: Synthesis of Mono- and Disulfonated Derivatives of 1,1-Diphenyl-2-picrylhydrazyl (DPPH) .. 329
Recensiones 93, 357
RIZK, A. M. s. KARAWYA, M. S.
SAMAY, G. s. MENCZEL, GY.
SCHAY, G. s. KALLÓ, D.
SIMON, K. s. MENCZEL, GY.
SINGH, D. and DWIVEDI, A. N.: Influence of Hydrogen Ion Concentration on the Anodic Polarization of p-Germanium Electrodes 255
SOÓS, R. s. CSŰRÖS, Z.
SZABÓ, J., VARGA, I., VINKLER, E. and BARTHOS, É.: Preparation of 2,3-Dihydro-4*H*-1,3-Benzothiazine Derivatives 213
SZABÓ, S. s. DINYA, Z.
SZEJTLI, J., HENRIQUES, R. D. and CASTIÑEIRA, M.: Methanolysis of Inulin and Hydrolysis of Methyl-β-D-Fructofuranoside 459
SZILÁGYI, J. s. PUTIRSKAJA, G. V.
SZÓKÁN, G. s. LADÁNYI, L.
SZŐKE, S., JALSOVSZKY, G. and DUDAR, E.: Electronic Structure of Isoelectronic Molecules 241
TELCS, I.: A Method for the Determination of Hydrogen Adsorption on Palladium Electrodes (Short Communication) 209
TELCS, I. s. HORÁNYI, G.
TÉTÉNYI, P. s. PAÁL, Z.
TÉTÉNYI, P. s. ZSADON, B.
VAJASDY-PERCZEL, I. s. GIBER, J.
VARGA, I. s. SZABÓ, J.
VÉRTES, GY. s. HORÁNYI, G.
VINKLER, E. s. SZABÓ, J.
VINKLER, P. s. EGYED, J.
WELTHER, M. s. BODOR, E.
WÉGNER, M. s. GIBER, J.
WOLSKI, W. and BUREWICZ, A.: Ferromagnetic Products of the Explosion Reaction Between $Co(NO_3)_2$ and $(NH_4)_4[Fe(CN)_6]$ 25
ZSADON, B., ÁRVAY, GY. and TÉTÉNYI, P.: Alkaloids from Vinca Major L. (Apocynaceae) (‡)-Vincadifformine (Preliminary Communication) 355

Acta Chimica Academiae Scientiarum Hungaricae, Tomus 72 (1), pp. 1—24 (1972)

ZUM MECHANISMUS DER DESORPTION UND AKTIVIERTEN ADSORPTION VON SAUERSTOFF AN UNBELICHTETEM UND UV-BELICHTETEM ZINKOXID

K. HAUFFE und A. J. HEGEDŰS

(Institut für physikalische Chemie der Universität Göttingen, BRD und Tungsram, Forschungsinstitut, Budapest-Újpest)

Eingegangen am 23. Juli 1970

Es wurde die durch Evakuierung und Belüftung verursachte Desorption und Adsorption bei verschiedenen konstanten Temperaturen sowie die durch Temperaturänderungen hervorgerufene Desorption und Adsorption, bzw. Thermolyse und Chemisorption bei $1—2 \cdot 10^{-5}$ Torr und 1 atm, an Zinkoxid gemessen. Bei $1{,}2 \cdot 10^{-5}$ Torr wurde auch die Photosorption von $O_2 + H_2O$ untersucht und stets nur eine Photolyse, nie eine Photoadsorption festgestellt. Aufgrund der Ergebnisse ist der Versuch unternommen worden, die möglichen Reaktionsschritte im einzelnen zu behandeln.

1. Problemstellung

Da Ausmaß und Art der Fehlordnung in der Oberflächenschicht der ZnO-Kristallite für die elektrischen und elektrophotographischen Eigenschaften von ausschlaggebender Bedeutung sind, ist es das Ziel dieser Arbeit, weitere Informationen über die Erzeugung definierter Oberflächenzustände zu erhalten. An verschiedenen ZnO-Sorten wird die Änderung der Fehlordnungskonzentration in oberflächennahen Bereichen sowohl durch thermolytische als auch durch photolytische Prozesse studiert. Neben elektrischen Leitfähigkeitsmessungen ist die Ermittlung der zeitlichen Änderung der Masse eine bequeme Methode, um die Änderung der Fehlordnungskonzentration in den Oberflächenbereichen, den sogenannten Randschichten, zu studieren. Während eine Vakuum-Behandlung zur Desorption von Gasen und bei höheren Temperaturen zur Thermolyse von Zinkoxid führt, findet darauffolgend im Bereich niedriger Temperaturen in Anwesenheit von Sauerstoff eine Aufoxydation des aktivierten Zinkoxids statt, die bei höheren Sauerstoffdrucken rascher verläuft.

Wenn auch Einstrahlung von UV-Licht auf Zinkoxid stets zu einer Photolyse, d. h. zu Desorptionsprozessen führen sollte, sofern Temperatur, Druck und Zusammensetzung der umgebenden Gasphase konstant bleiben, wird in der Literatur immer wieder auch auf Photoadsorption von Sauerstoff an Zinkoxid hingewiesen. Durch die Ergebnisse der nachfolgend beschriebenen Untersuchungen angeregt, haben wir uns an anderer Stelle auch mit den theoretischen Zusammenhängen dieser Erscheinung ausführlich befaßt und konnten zeigen, daß an reinem Zinkoxid kaum mit einer Photoadsorption von Sauerstoff gerechnet werden kann [1].

Ein anderes Problem — ebenfalls sehr wichtig für den Oberflächenzustand — ist die Neigung von Zinkoxid, H_2O und CO_2 ebenfalls bevorzugt zu chemisorbieren. Auf Grund dieses Verhaltens ist es auch nicht verwunderlich, wenn Zinkoxid-Pulver, das lange an H_2O-haltiger Luft gelagert hat, eine beachtliche Menge an H_2O in der Randschicht aufweist. Eine ähnliche Situation gilt für CO_2. Demzufolge erscheint es wünschenswert, durch thermogravimetrische Untersuchungen weitere Informationen über die Fehlordnung im Oberflächenbereich der ZnO-Kristallite zu erhalten.

2. Experimentelles

Zur Bestimmung des zeitlichen Verlaufs der Massenänderung während thermolytischer und photolytischer Vorgänge wurde eine thermogravimetrische Versuchsanordnung mit einer elektronischen Mikrowaage von Sartorius aufgebaut. Über die Arbeitsweise dieser Versuchsanlage wurde bereits an anderer Stelle berichtet [2—4]. Zur Untersuchung wurden vier ZnO-Präparate verwandt, u. zw. ein a-ZnO (p. a., REANAL, Budapest), dann b-ZnO (Fotosiegel A von der Zinkweiß-Forschungsgesellschaft Oberhausen), c-ZnO (das REANAL-Präparat mit 0,27 Atom-% Li, 2 Stunden bei 1000 °C in Luft getempert) und ein d-ZnO (das 2 Stunden bei 1000 °C in Luft getemperte REANAL-Präparat). Über ausführlichere Kenndaten dieser Proben muß gleichfalls auf frühere Stellen verwiesen werden [2, 4].

3. Versuchsergebnisse ohne Belichtung und Diskussion

Vermindert man den Gasdruck über ein ZnO-Pulver, das an der Luft gelagert hat, dann beobachtet man eine Masseabnahme wegen Verflüchtigung und Desorption von kondensiertem Wasser und adsorbierten Gasen. Eine darauffolgende Belüftung mit Luft verursacht die Herstellung des Ausgangszustandes. Die mehrmalige Wiederholung dieser Reaktionsschritte bewies nicht nur die Reversibilität der Adsorption, sondern auch die lineare Abhängigkeit der Gewichtsabnahme bzw. Gewichtszunahme von der ZnO-Einwaage. Eine Abweichung von dieser Linearität nach kleineren Werten machte sich nur dann bemerkbar, wenn mit größerer Einwaage die Schichtdicke des Pulverhaufens in der Wägeschale zu stark anwuchs. Nahm man zu einer größeren Einwaage einen Tiegel von größerem Durchmesser, so blieb die Linearität auch bei größeren Einwaagen erhalten. Im Falle einer Querschnittsfläche von 1,58 cm^2 verschwand die bei 100 und 200 mg Einwaage gemessene Abweichung von der Linearität bereits bei ZnO-Mengen von 50 und 100 mg.

Der lineare Zusammenhang mit der Einwaage bedeutet aber nur bei derselben Probe die gleichzeitige lineare Abhängigkeit von der BET-Oberfläche. Der Befund einer größeren Adsorption und Desorption von ± 695 $\mu g/g$ ZnO beim b-ZnO (statt 565 μg beim a-ZnO) mit einer annähernd gleichen BET-Oberfläche von 3,8—3,9 m^2/g, kann als ein Beweis dafür angesehen werden, daß bei der Adsorption nicht nur die Oberfläche, sondern auch die Oberflächenaktivität eine wichtige Rolle spielt.

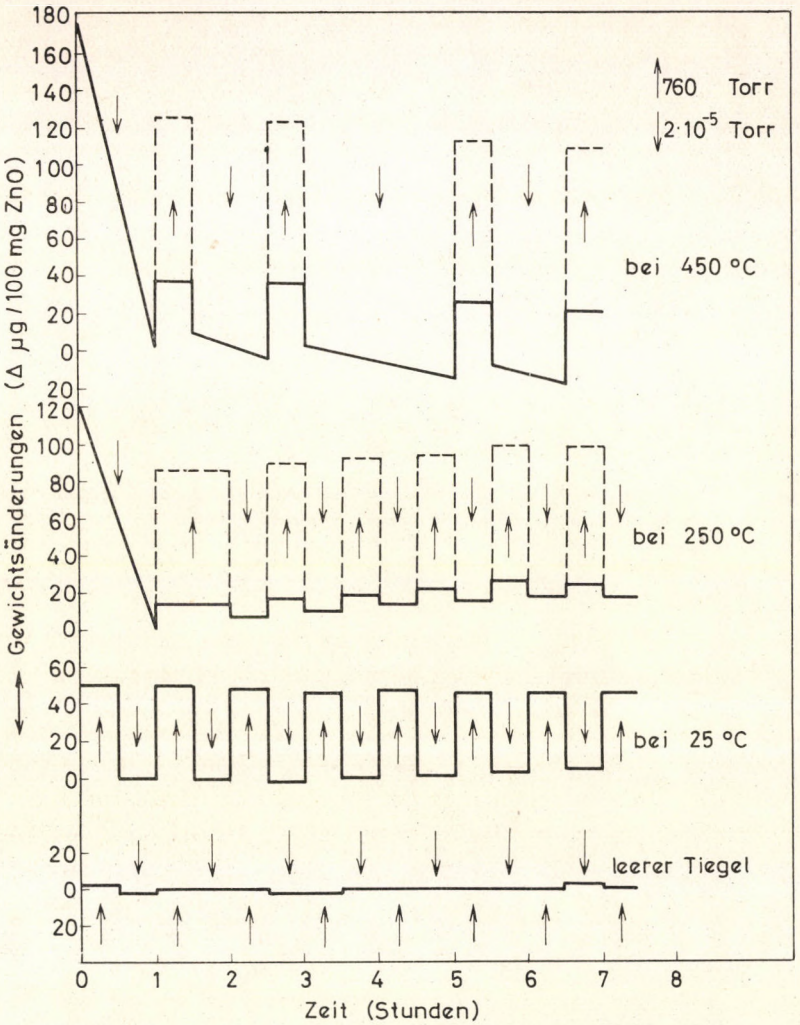

Abb. 1. Einfluß der öfters wiederholten Druckänderung der umgebenden Zimmerluftatmosphäre auf das Gewicht von 100 mg a-ZnO-Pulver. Die Bewegung des ZnO allein ist durch normal ausgezogene Linien, die des mit ZnO beladenen Tiegels durch gestrichelt verlängerte angedeutet

Registriert man die durch periodisch wiederholte Evakuierung und Belüftung erhaltenen Gewichtsänderungen, wie z. B. in Abb. 1, so bemerkt man, daß die Gewichtsänderungen langsam, wahrscheinlich einem Grenzwert zustrebend, abnehmen. Auf Grund dieses Sachverhalts darf man annehmen, daß es sich bei diesem Vorgang nicht nur um eine Adsorption handeln kann, da ja z.B. mit dem Austritt von H_2O auch chemische Oberflächen-Reaktionen ablaufen, wie z. B.:

$$Zn(OH)_2 = ZnO + H_2O \qquad (1)$$

und

$$Zn(CO_3)_{1-x} \cdot (OH)_{2x} \cdot yH_2O = ZnO_x(CO_3)_{1-x} + (x+y)H_2O \qquad (2)$$

Vermutlich tragen diese chemischen Vorgänge zur Änderung der Oberflächenaktivität und der Fehlstellenkonzentration in der Randschicht bei. Demnach besteht zwischen Randschicht und umgebender Atmosphäre eine ständige Wechselwirkung, derzufolge Struktur und chemische Zusammensetzung der Randschicht geändert wird, wenn sich

a) das Komponentenverhältnis des mehrkomponentigen Sorbats (z. B. Änderung des H_2O- und CO_2-Gehalts der Luft), oder

b) auch die Zahl der in der Gasphase auftretenden Komponenten (z. B. von Säuredämpfen, Halogenen, Ammoniak, Kohlenwasserstoffe, usw.) während der Lagerung verändern.

Wenn die zur Belüftung verwendete Luft der Reihe nach mit konzentriertem H_2SO_4, granuliertem KOH, Silikagel und einer Falle mit flüssiger Luft vorgetrocknet wurde, dann gelangten wir zu den in Tabelle I — gemein-

Tabelle I

Einfluß des Druckes auf die Masseänderung des a-ZnO mit einer BET-Oberfläche = 3,9 m^2/g und einer freien geometrischen Oberfläche in der Wägeschale von 1,58 cm^2

Evakuierung und Belüftung mit nicht getrockneter Luft $760 \rightarrow 2 \cdot 10^{-5} \rightarrow 760$ Torr			
	Mittelwerte		
bei 25 °C	−55	+ 58 µg/ 98,86 mg ZnO	±565 µg/g ZnO
	−97	+107 µg/193,46	527
			546
bei 250 °C	−17	+ 17 µg/100,25	170
bei 450 °C	−35	+ 37	360
Evakuierung und Belüftung mit getrockneter Luft			
	Mittelwerte		
bei 25 °C	− 9,8	+ 9,2 µg/100,25 mg ZnO	±95 µg/g ZnO
	−25	+ 27 µg/193,46	134
			115
bei 250 °C	−10	+ 12 µg/100,25	110
	−23	+ 23 µg/193,46	119
			115
bei 450 °C	−16	+ 16 µg/100,25	160
	−31	+ 33 µg/193,46	165
			163

sam mit den vorangehend geschilderten Versuchsergebnissen — angegebenen Werten, aus denen hervorgeht, daß die bei 25 °C adsorbierten Stoffe aus etwa 80% H_2O+CO_2 bestehen müssen. Dabei kann der Anteil an CO_2 höchstens 4% betragen, weil das Ausschalten einer Falle mit flüssiger Luft keine größere Abweichung als ± 1 μg pro Einwaage verursachte. Es steht noch die Frage offen, ob die Differenz von ~20% überwiegend der Adsorption anderer Gase (O_2, N_2, CO, Kohlenwasserstoffe) oder dem Meßfehler zugeschrieben werden

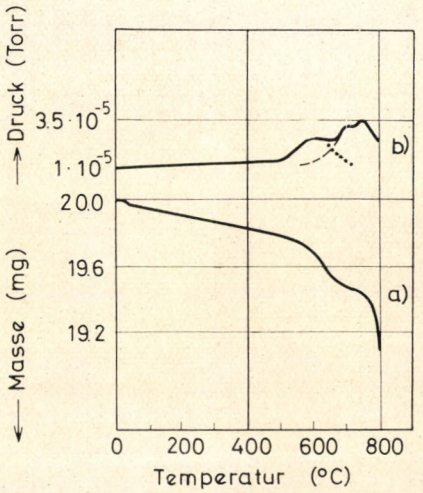

Abb. 2. Thermolyse des a-ZnO-Pulvers. Zeitliche Gewichtsabnahme, *a)* TG-Kurve; zeitliche Änderung des Druckes, *b)* Druckkurve (punktiert: abnehmender p_{CO_2}, gestrichelt: ansteigender p_{O_2}). Einwaage = 20 mg im Pt-Tiegel, Temperaturanstieg = 6 °C/Minute, Grundvakuum $p = 1 \cdot 10^{-5}$ Torr

muß. Wenn man die starke H_2O-Adsorption unterdrücken will, um die Adsorption der anderen Stoffe studieren zu können, dann muß man beim Einsetzen einer neuen Probe solange einige Male evakuieren und mit hochgetrockneter Luft vorbelüften, bis gleiche Desorptions- und Adsorptionswerte erhalten werden. Ungenügende Trocknung führt sofort zu höheren Gewichtsänderungen infolge zusätzlicher Adsorption von H_2O.

Eine simultane thermogravimetrische und massenspektrometrische Aufnahme mit dem Mettler Vakuum-Thermoanalyser und Balzers QMG 101 Massenspektrometer [5] ergab bei einer Aufheizgeschwindigkeit von 6 °C/min und einem Ausgangsvakuum von $1 \cdot 10^{-5}$ Torr die in Abb. 2 wiedergegebenen Druck- und Gewichtsänderungen. Das Massenspektrometer zeigte innerhalb m = 0—50 eine Restgaszusammensetzung von 2 H_2^+ : 3 O^+ : 22 H_2O^+ : 10 CO^+ und N_2^+ : 3,5 O_2^+ an. Der Ionenstrom von H_2O^+ wies bei ~240°C ein Maximum und bei ~595 °C ein Minimum auf, während der von CO_2^+ schon ab 120 °C

anzusteigen begann und bei ~595 °C ein Maximum durchlief. Der Anwuchs von O_2^+ fing bei ~450 °C an und nahm über etwa 750 °C exponentiell zu. Die Schwankungen der CO^+-Menge verliefen annähernd parallel mit den Änderungen des CO_2^+-Ionenstromes. Zum Vergleich sollten ähnliche massenspektrometrische Messungen von KODERA, KUSUNOKI und SHIMIZU [6] herangezogen werden. Leider haben die Autoren keine Analysen über das untersuchte ZnO mitgeteilt. Aus unseren und ihren Ergebnissen kann man aber ohnedem sofort entnehmen, daß eine solche Methode, die die simultane Aufnahme der Gewichts- und Enthalpieänderungen (beim ZnO zeigt natürlich die DTA-Kurve keine solchen Änderungen an) der festen Phase sowie der genauen mengenmäßigen Verteilung der desorbierten und exhalierten Gase in Abhängigkeit von Temperatur und Zeit ermöglicht, wohl die gegenwärtig zuverlässigste Information über Vorgeschichte und thermische Eigenschaften eines Feststoffes liefert. Aus dem Unterschied, daß die Hauptmenge des CO_2 im Falle unseres Präparats bei einer um etwa 200 °C höher liegenden Temperatur entweicht als bei KODERA, KUSUNOKI und SHIMIZU, kann man auf verschiedene Herstellungs- und Lagerungsbedingungen des Oxids schließen. Ihre Aufnahmen stammen von einer ZnO-Probe, die längere Zeit gelagert wurde. Bereits bei einer unmittelbar nachher ausgeführten zweiten Aufnahme schrumpften die massenspektrometrischen Intensitäten auf ganz niedrige Werte zusammen. Außerdem wechselten auch die Intensitätsverhältnisse der desorbierten Stoffe beträchtlich. Nur die O^+- und O_2^+-Linien erschienen bei derselben Temperatur und mit unveränderter Intensität. Als weiterer Beitrag zu diesen Erwägungen seien noch die Befunde von MORIMOTO, NAGAO und TOKUDA [7] herangezogen. Sie haben mit im Vakuum bei verschiedenen Temperaturen vorbehandelten ZnO-Proben Desorptions- und Adsorptionsversuche mit H_2O ausgeführt und gefunden, daß die Vorbehandlung für das Auftreten von schwächer und stärker gebundenem Wasser verantwortlich ist, das bei niedrigeren oder höheren Temperaturen abgespalten und chemisorbiert wird.

Es ist eine an Oxiden oft beobachtete Tatsache, daß sie beim Erhitzen im Vakuum zwischen 200—800 °C CO abgeben, manchmal in überraschend großer Menge [6]. Dabei hat es sich gezeigt, daß sowohl entweichendes CO als auch CO_2 am oder im ZnO nicht unbedingt als CO oder CO_2, d.h. nicht als Adsorbat oder Einschlußverbindung vorhanden sein müssen. Kohlendioxid kann sich auch aus Zinkkarbonatresten, CO aus Zinkkarboxylat bilden. Im letzteren Fall wird wohl CO_2 chemisorbiert, aber CO desorbiert. Eine auf den ersten Blick unverständliche CO-Desorption wird jedoch verständlich, wenn man berücksichtigt, daß beim Erhitzen im Vakuum sich thermolytisch Zink an der Oberfläche bildet. Dieses chemisorbiert beim Abkühlen CO_2 als Karboxylat, das beim Wiedererhitzen unter CO-Abgabe zersetzt wird. Unlängst haben wir auch darüber berichtet [4], daß die thermische Dissoziation des ZnO im Vakuum bei 400—500 °C bereits eine gut meßbare Geschwindigkeit erreicht.

Das hierbei entstehende O^-(ads) oder O(ads) kann nun mit adsorbierten Kohlenwasserstoffen und ihren Zersetzungsprodukten, mit Kohle oder CO(ads) abreagieren und CO_2 bilden. Als Brutto-Reaktion wird das Entweichen von CO_2 und bei monoton steigender Temperatur auch eine vorübergehende Anhäufung von Zn an der Oberfläche beobachtet. Durch diese Zink-Anreicherung könnte die Abnahme des Masseverlustes in der Umgebung von 700 °C an der Kurve *a)* in Abb. 2, bzw. das Minimum bei etwa 650 °C an der Kurve *b)* verursacht sein. Bei weitersteigender Temperatur nimmt dann die Desorptionsgeschwindigkeit des Zinks zu; Kurve *a)* zeigt eine beginnende steile zeitliche

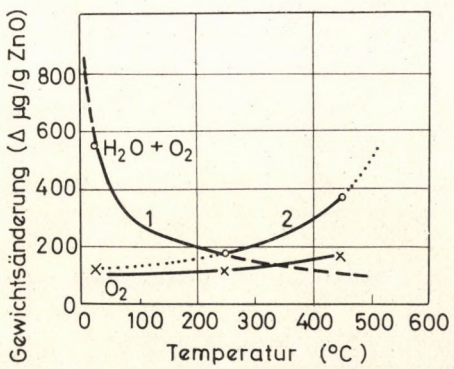

Abb. 3. Masseänderung (Normalatmosphäre → $2 \cdot 10^{-5}$ Torr Restgas) verursacht durch reversible $H_2O + O_2$- (obere ausgezogene Kurve) und O_2-Adsorption (untere ausgezogene Kurve), $\Delta\mu g/g$ ZnO, bei konstanten Temperaturen (Tabelle I). Gestrichelt verlängerter Kurventeil, Kondensation und Physisorption; punktiert verlängerter, Chemisorption. Erklärung im Text

Gewichtsabnahme, und Sauerstoff bzw. Zink sollten im Massenspektrum mit zunehmender Intensität erscheinen. Können aber bei gleichzeitiger Druckabnahme weder Zinkdämpfe noch Sauerstoff nachgewiesen werden, dann dürfte hierfür ein unzweckmäßiger Versuchsaufbau verantwortlich sein [verfälschte Druckwerte bei arbeitender Diffusionspumpe; Ermöglichung von Zn(gas) und O_2(gas) Rekombination oder Zn-Kondensation und Zn-Getterwirkung in zu langen, kühleren und engen Rezipientgängen zwischen Massenspektrometeranalysator und Probe, usw.].

Die durch jähe Druckänderung hervorgerufene Desorption und Adsorption haben wir auch bei 250 und 450 °C gemessen. Die Endwerte dieser Messungen sind ebenfalls in Tabelle I angegeben. Sie zeigen, daß die so aufgetretene reversible Adsorption auch bei höheren Temperaturen abhängig von der Einwaage und damit bei derselben Probe auch abhängig von der BET-Oberfläche ist. Die graphische Wiedergabe der Ergebnisse ist aus Abb. 3 zu entnehmen. Hieraus erkennt man die Tendenz der Temperaturabhängigkeit der reversiblen H_2O+O_2- bzw. O_2-Adsorption. Die H_2O+O_2-Kurve zeigt ein Minimum etwa zwischen 200—250 °C. Auch andere Autoren [7, 8] haben auf einen solchen Wendepunkt im erwähnten Temperaturbereich hingewiesen. Der in Abb. 3

wiedergegebene Verlauf der H_2O+O_2-Kurve kann aus zwei Kurventeilen zusammengesetzt angenommen werden, von denen der Kurventeil 1 einschließlich der gestrichelten verlängerten Teile die Physisorption bzw. -desorption des H_2O aus dem Gasgemisch darstellt, die mit steigender Temperatur kleiner wird. Aus dem Kurventeil 2 kann man dagegen annehmen, daß die merkliche Gewichtszunahme mit steigender Temperatur auf einer chemischen Oberflächenreaktion des H_2O mit dem fehlgeordneten ZnO-Gitter beruht:

$$H_2O(gas) + Zn^{\cdot} = 2OH|O|^{\cdot} + e' + ZnO \qquad (3)$$

wobei $OH|O|^{\cdot}$ ein OH-Ion auf einem Sauerstoffionen-Gitterplatz, $Zn^{\cdot}$ ein Zinkion auf Zwischengitterplatz und e' ein freies Elektron repräsentieren. Wie in Gl. (3) schematisch angedeutet, kann es bei etwas höheren Temperaturen zu einer merklichen Hydroxid-Bildung kommen, die bei weiter ansteigenden Temperaturen dann wieder abnimmt und schließlich durch Ablauf des Teilschrittes von rechts nach links in Gl. (3) wieder rückgängig gemacht wird.

Wie man aus Abb. 3 weiterhin erkennt, ist der Anteil der Sauerstoff-Adsorption erheblich kleiner als der von H_2O. Dieses ist offenbar auch der Grund, daß ein im Vakuum thermisch behandeltes ZnO am stärksten für H_2O wie ein »Getter« wirkt.

Aus der schematischen Darstellung der Meßreihen, die bei 250 bzw. 450 °C durchgeführt wurden, ergibt sich bei 250 °C bzw. bei 450 °C eine wesentlich höhere Ausheilung von Kristallfehlern als bei 25°C. Die allmähliche Gewichtszunahme der Probe nach mehrfacher Adsorption und Desorption weist darauf hin, daß ein Teil des Sauerstoffs zur Ausheilung der Kristallfehler verbraucht und damit irreversibel eingebaut wird. Bei 450 °C verläuft die Ausheilung so schnell, daß sich bereits nach der ersten De- und Adsorptionsperiode eine konstante Oberflächenaktivität einstellt.

In Abb. 4 ist die durch jähe Temperaturänderung verursachte Desorption und Adsorption — einschließlich Oberflächenreaktion — von O_2 bzw. H_2O bei 1 atm (Kurve *a* und *b*), sowie bei $1{,}2 \cdot 10^{-5}$ Torr (Kurve *c*) gegen die Temperatur aufgetragen. Dabei bedeutet die schnelle Temperaturänderung auf 250 °C oder zurück auch im weiteren stets $\sim$13 Minuten, auf 450 °C oder zurück stets $\sim$7 Minuten. Nach maximal 2 Stunden war im allgemeinen ein stationärer Zustand erreicht. Während Kurve *a* mit H_2O-haltiger Luft erhalten wurde, stellt Kurve *b* eine analoge Meßreihe mit H_2O-freier Luft dar. Wie man aus dem Verlauf der Kurven *a* und *b* erkennt, ist bei wasserdampfhaltiger Luft von 1 atm die Chemisorption von H_2O um etwa eine Größenordnung höher als die von Sauerstoff. Wenn auch die bei 1 atm Luft erhaltenen Versuchsergebnisse infolge der thermisch asymmetrisch aufgebauten Waage und der hierdurch verursachten Störungen [2, 3, 4] nicht so zuverlässig wie die in Vakuum gemessenen sind, so scheint doch der bei 250° C erhaltene Wert von

50 μg O_2/1 g ZnO nicht unvernünftig zu sein, weil 50 μg O_2 nur $\sim$0,16 m^2/g von der 3,9 m^2/g verfügbaren BET-Oberfläche des untersuchten ZnO bedecken. Die Aktivität der ZnO-Oberfläche steigt durch die geschilderten thermischen Behandlungen etwa bis zu jener Temperatur an, bei welcher eine merkliche Sinterung zu einer Abnahme der Oberflächengröße führt. Bei unserer Probe lag diese Temperatur in der Umgebung von 500 °C, so daß das Maximum der Adsorptionskapazität in der Nähe dieser Temperatur zu erwarten wäre, was mit Untersuchungen anderer Autoren [7] im Einklang zu sein scheint.

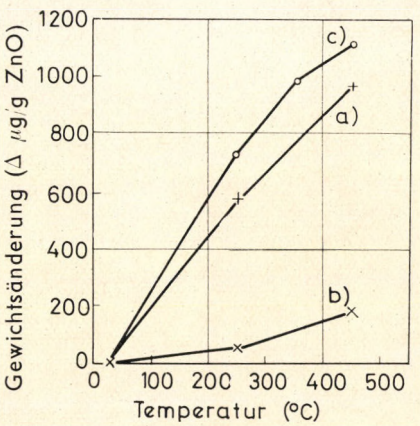

Abb. 4. Durch Temperaturänderung verursachte reversible Adsorption von $H_2O + O_2$ (Kurve *a*) und O_2 allein (Kurve *b*), $\Delta\mu$g/g ZnO, bei Normalatmosphärendruck bzw. bei $1{,}2 \cdot 10^{-5}$ Torr Restgas (Kurve *c*)

Bei genügend niedrigen Drucken von $<10^{-4}$ Torr ist auch bei einer geometrisch-thermisch asymmetrisch aufgebauten Apparatur völlige Störungsfreiheit der Wägung zu erlangen. Dies ermöglicht die Durchführung von exakten Desorptions- und Adsorptionsmessungen bei einem konstanten Restgasdruck von $1{,}2 \cdot 10^{-5}$ Torr bzw. bei einem konstanten Sauerstoffdruck von $1 \cdot 10^{-5}$ Torr [9], wobei von einer konstanten Desorptionstemperatur rasch auf die konstante Adsorptionstemperatur von 25 °C abgekühlt wird. Zwecks Erreichen eines stationären Wertes ließen wir die Desorption bei der gewünschten Versuchstemperatur etwa 2 Stunden lang laufen, kühlten dann rasch ab und verfolgten die nun einsetzende Adsorption etwa 6 Stunden lang. Danach ließen wir die Probe in der Waage bei $3—5 \cdot 10^{-4}$ Torr während einer Nacht stehen, belüfteten anschließend für kurze Zeit ($\sim$30 min) und wiederholten eine solche De- und Adsorptionsperiode mehrmals mit derselben Einwaage. Die erhaltenen Meßwerte haben wir in den Tabellen II—IV zusammengefaßt und die aufgenommenen Kurven in den Abbildungen 5—7 wiedergegeben.

Die Kurven bestätigen erneut die in Tabelle I und Abb. 1 bereits angegebene durch Druckverminderung verursachte Gewichtsabnahme (Abb. 5—7,

senkrechte — — — Linien), die wir als Vakuumdesorption benennen können. Bei dieser Desorption stellt sich das Gleichgewicht erfahrungsgemäß ziemlich schnell ein (Abb. 5—7, obere dünn ausgezogene Linien, Gleichgewichts-

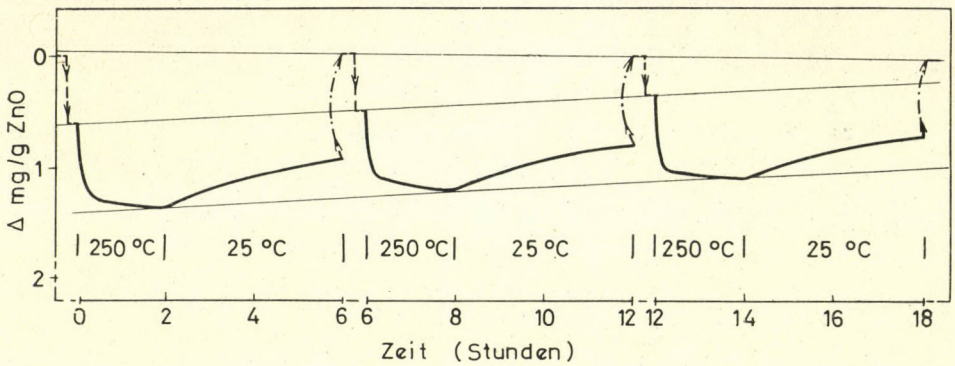

Abb. 5. Zeitlicher Verlauf der Desorption und Thermolyse bei 250 °C und der darauffolgenden Sauerstoffadsorption mit Oberflächenreaktion bei 25 °C, in einem konstanten Vakuum von $1{,}2 \cdot 10^{-5}$ Torr Restgas (ausgezogene Kurven). Mit 182,7 mg a-ZnO gemessen und auf 1 g ZnO umgerechnet. Erklärung in Tabelle II und im Text

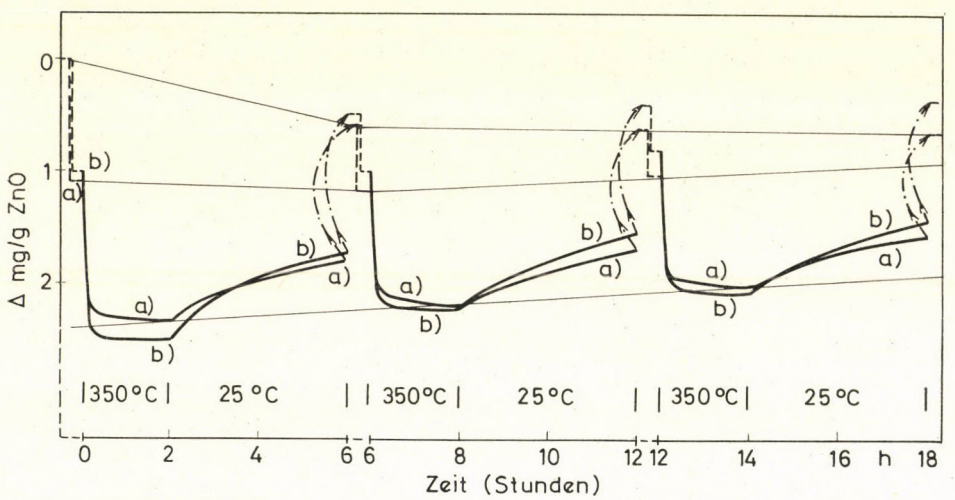

Abb. 6. Zeitlicher Verlauf der Desorption und Thermolyse bei 350 °C und der darauffolgenden Sauerstoffadsorption mit Oberflächenreaktion bei 25 °C, in einem konstanten Vakuum von $1{,}2 \cdot 10^{-5}$ Torr Restgas (ausgezogene Kurven). Mit 185,89 (Kurve *a*) bzw. 86,33 mg a-ZnO gemessen (Kurve *b*) und auf 1 g ZnO umgerechnet. Erklärung in Tabelle III und im Text

zustand bei Normalatmosphäre; mittlere dünn ausgezogene Linien, Gleichgewichtszustand bei $1{,}2 \cdot 10^{-5}$ Torr Restgasdruck). Die bei $1{,}2 \cdot 10^{-5}$ Torr und 250, 350 bzw. 450 °C erhaltenen Werte geben die Kinetik der Thermodesorption (Tabelle II—IV, obere Zahlensäulen; Abb. 5—7, konkav ausgezogene Kurven) wieder, während die ohne Unterbrechung bei gleichem Druck

aber bei 25 °C aufgenommenen Kurven die Kinetik der Adsorption anzeigen (Tabelle II—IV, untere Zahlensäulen; Abb. 5—7, konvex ausgezogene Kurven). Schließlich wird die Meßperiode durch eine Lagerung während einer Nacht in einem Vakuum von $3—5 \cdot 10^{-4}$ Torr und infolge einer kurzen Belüftung durch Adsorption beendet (Abb. 5—7, —·—·— Kurven).

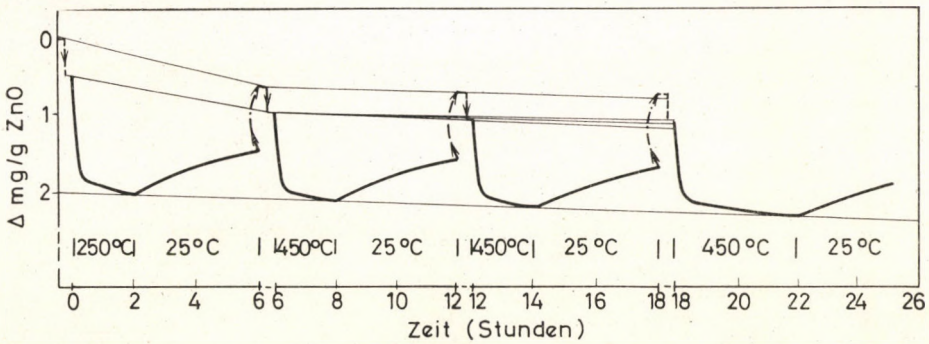

Abb. 7. Zeitlicher Verlauf der Desorption und Thermolyse bei 450 °C und der darauffolgenden Sauerstoffadsorption mit Oberflächenreaktion bei 25 °C, in einem konstanten Vakuum von $1{,}2 \cdot 10^{-5}$ Torr Restgas (ausgezogene Kurven). Mit 185,33 mg a-ZnO gemessen und auf 1 g ZnO umgerechnet. Erklärung in Tabelle IV und im Text

Quantitativ können die Ergebnisse in den Tabellen II—IV z. B. mit der ROGINSKY—ZELDOVITSCH Gleichung [8] erfaßt werden:

$$\frac{\mathrm{d}n}{\mathrm{d}t} = a \cdot e^{-bn} \tag{4}$$

wo n die desorbierte bzw. adsorbierte Gasmenge, die Konstanten a und b die Anfangsgeschwindigkeit und die Änderung der Aktivierungsenergie bedeuten.

Wir haben bereits erwähnt, daß infolge Evakuierung bei 25 °C vom b-ZnO um 36,6% mehr Gase desorbiert werden als vom a-ZnO trotz gleicher BET-Oberflächen. Die thermischen Desorptionsversuche bewiesen aber, daß beim b-ZnO auch die durch Erhitzung abgegebene Gasmenge um 30—40% größer ist als beim a-ZnO. Der Umstand, daß diese Differenz mit der Aktivität in Zusammenhang steht, die Aktivität jedoch eine Funktion der Fehlstellenkonzentration der Oberfläche ist, erlaubt die Folgerung, daß bei bestimmten Feststoffen, so auch beim ZnO, die thermodesorbierte Gasmenge zur Berechnung der Fehlstellenkonzentration geeignet sein müßte. Solange die desorbierte Gasmenge in jedem Zeitpunkt proportional der Einwaage und BET-Oberfläche ist, gilt der Zusammenhang:

$$n = a \cdot m \cdot v = a \cdot m \cdot k \cdot c \tag{5}$$

Tabelle II

Desorption und Thermolyse von a-ZnO (182,7 mg) bei konstantem Druck von 1,2 · 10^{-5} Torr beim Erhitzen von 25 auf 250 °C und Adsorption mit Oberflächenreaktion beim Abkühlen von 250 auf 25 °C

Mit derselben Einwaage wurde jeweils nacheinander gemessen und zwischen den einzelnen Messungen 14 Stunden lang in einem Vakuum von 3—5 · 10^{-4} Torr gelagert. Vor der erneuten Evakuierung wurde 10 Minuten gelüftet

25 → 250 °C	Desorption und Thermolyse µg/g ZnO		
nach 6 min	355	443	509
9	520	558	613
15	645	618	667
21	684	640	679
30	706	657	690
45	717	679	701
60	722	706	712
90	750	712	722
120	777	722	728

Mittelwert an Massenverlust nach 2 Stunden

742 µg/g ZnO

250 → 25 °C	Adsorption und Oberflächenreaktion		
nach 30 min	93	77	60
50	159	148	120
90	213	203	181
120	257	252	224
150	301	301	263
180	345	334	296
210	383	367	328
240	416	400	361

Mittelwert an Massengewinn nach 4 Stunden

392 µg/g ZnO

wo n die desorbierte Gasmenge, a eine Konstante (spezifische Oberfläche), m die Masse des ZnO, v die Geschwindigkeit der Adsorption, k die Geschwindigkeitskonstante der Adsorption und c die Fehlstellenkonzentration (Aktivität) sind.

Diese Formel ist identisch mit der Ausgangsformel von PANASSJUK, DANTSCHEWSKAJA und KOBOSLEW [10], die für die massenspektrometrische

Tabelle III

Desorption und Thermolyse von a-ZnO (185,89 und 86,33 mg) bei konstantem Druck von 1,2 · 10^{-5} Torr beim Erhitzen von 25 auf 350 °C und Adsorption mit Oberflächenreaktion beim Abkühlen von 350 auf 25 °C

Mit derselben Einwaage wurde jeweils dreimal nacheinander gemessen, zwischen den einzelnen Messungen 14 Stunden lang in einem Vakuum von 3—5 · 10^{-4} Torr gelagert und vor der erneuten Evakuierung 10 Minuten belüftet

25→ 350 °C	Desorption und Thermolyse µg/g ZnO					
	mit 185,89 mg ZnO			mit 86,33 mg ZnO		
nach 6 min	802	608	672	1100	950	1008
9	1114	828	818	1402	1066	1124
15	1173	909	888	1460	1124	1193
21	1194	936	904	1494	1147	1216
30	1205	963	920	1506	1158	1239
45	1221	979	936	1517	1170	1263
60	1232	990	947	1529	1182	1274
90	1243	995	958	1529	1182	1274
120	1253	1006	973	1529	1182	1274

Mittelwert an Massenverlust nach 2 Stunden

990 µg/g ZnO *1228* µg/g ZnO

350→ 25 °C	Adsorption und Oberflächenreaktion					
nach 30 min	129	91	81	220	151	151
60	221	183	156	359	255	255
90	307	247	221	475	348	336
120	366	312	285	556	417	405
150	420	360	339	625	498	487
180	468	414	393	683	556	544
210	511	457	430	741	614	602
240	554	495	473	811	672	649

Mittelwert an Massengewinn nach 4 Stunden

507 µg/g ZnO *711* µg/g ZnO

Intensität des aus ZnO verdampfenden Zn-Überschusses diese Formel ableiteten, um daraus die Fehlstellenkonzentration des ZnO zu errechnen. Dabei wurde allerdings vorausgesetzt, daß die Thermolyse des ZnO erst über 800 °C beginnt, während bei niedrigeren Temperaturen nur das überschüssige, d. h. nur das auf Zwischengitterplatz befindliche Zn verdampft und mit dem

Tabelle IV

Desorption und Thermolyse von a-ZnO (185,33 mg) bei konstantem Druck von 1,2 · 10^{-5} Torr beim Erhitzen von 25 auf 450 °C und Adsorption mit Oberflächenreaktion beim Abkühlen von 450 auf 25 °C

Mit derselben Einwaage wurde jeweils viermal nacheinander gemessen und zwischen den einzelnen Messungen 14 Stunden lang in einem Vakuum von 3—5 · 10^{-4} Torr gelagert und vor der erneuten Evakuierung 10 Minuten belüftet

25 → 450 °C	Desorption und Thermolyse µg/g ZnO			
nach 6 min	442	362	399	405
9	1012	761	777	820
15	1279	928	912	950
21	1327	971	960	993
30	1370	1009	993	1025
45	1419	1047	1025	1052
60	1446	1068	1047	1068
90	1500	1101	1079	1101
120	1533	1127	1106	1127
150				1160
180				1187
210				1203
240				1230

Mittelwert an Massenverlust nach 2 Stunden

1120 µg/g ZnO

450 → 25 °C	Adsorption und Oberflächenreaktion			
nach 30 min	119	92	70	65
60	221	189	149	140
90	302	270	232	210
120	372	340	291	281
150	426	399	356	335
180	480	448	410	394
210	529	502	464	442
240	577	545	512	491

Mittelwert an Massengewinn nach 4 Stunden

531 µg/g ZnO

Massenspektrometer nachgewiesen wird. Diese Annahme können wir aber auf Grund unserer Versuchsergebnisse nicht bestätigen, weil in einem Vakuum von $2 \cdot 10^{-5}$ Torr die Thermolyse bereits ab etwa 200 °C anfängt einen merklichen Zn-Überschuß an der Oberfläche zu erzeugen, der bei der gegebenen Empfindlichkeit unserer Meßeinrichtung ab 450 °C so groß wurde, daß eine zeitlich konstante Verdampfung gemessen werden konnte [4], die in der Nähe von 500 °C zur vollständigen Verflüchtigung der Probe führte. Demzufolge müssen wir die von PANASSJUK, DANTSCHEWSKAJA und KOBOSLEW erhaltenen Werte für die Fehlstellenkonzentration mit gewissem Vorbehalt aufnehmen.

Die Druckabhängigkeit der thermischen Dissoziation und damit die Druckabhängigkeit der Verdampfungsgeschwindigkeit des ZnO ist allgemein bekannt [11, 12, 13, 14]. Druckabhängig ist natürlich auch die desorbierte Gasmenge. Dieser Sachverhalt wurde auch immer wieder aus unseren Messungen gefunden, so z. B. aus Abb. 4 und Tabelle II und IV, wo für die Druckänderung von $p_{O_2} = 160$ auf $p_{O_2} = 1 \cdot 10^{-5}$ Torr bei 250 °C 580 (Abb. 4, Kurve *a*) und 580 + 742 μg/g ZnO (Abb. 4, Kurve *a* + *c*); bei 450 °C dagegen 970 (Abb. 4, Kurve *a*) und 970 + 1120 μg/g ZnO (Abb. 4, Kurve *a* + *c*) angegeben sind. Weniger bekannt ist aber jene in Abb. 1 auffallende Tatsache, daß sich die Menge des desorbierten Gases mit der unmittelbar aufeinander folgenden Wiederholung von De- und Adsorptionsperioden vermindert. Bei 250 °C beschränkt sich diese Erscheinung überwiegend auf die der Thermodesorption vorangehenden H_2O-Vakuumdesorption bei 25 °C (Abb. 5, senkrechte — — — Linien). Bei 350 °C jedoch macht sich der Effekt auch bei der Thermodesorption bemerkbar (Abb. 6, konkav ausgezogene Kurve). Diese Erscheinung führen wir nicht nur bei der Vakuumdesorption des H_2O, sondern auch hier bei der Thermodesorption auf Ausheilungsvorgänge von Kristallfehlern zurück. Bei 450 °C spielt sich dieses Ereignis bereits während der ersten Desorption ab und es bildet sich infolge der Zn-Verdampfung am Ende jeder einzelnen Periode eine praktisch gleiche Oberflächenstruktur aus, weil bereits nach der ersten Periode annähernd eine Gleichgewichtsmenge an Zn und Zn^+ an der Oberfläche zustandekommt.

Die beiden mit verschiedenen Einwaagen gewonnenen Kurven in Abb. 6 beweisen die Einwaageabhängigkeit der Thermodesorption und der Adsorption bei Zimmertemperatur. Gleichzeitig machen sie aber auch darauf aufmerksam, daß bereits bei ganz kleinen Pulverschichtdicken Abweichungen von diesem linearen Zusammenhang auftreten, indem mit wachsender Schichtdicke kleinere Gasmengen desorbiert und nach Abkühlen wieder adsorbiert werden. Die Tendenz der ungenügenden Bedeckung, der Richtung der Abweichung bei den beiden ausgezogenen Kurven beweist fernerhin, daß bei kleineren Einwaagen, also bei kleineren Schichtdicken, der stationäre Zustand sich viel schneller erreichen läßt. Schon bei so dünnen Schichten kommen

Unterschiede in der Schichtdicke durch eine wesentlich bessere Entgasbarkeit der dünneren Schicht zum Vorschein. Sowohl dieser Befund, als auch der Graustich des in Vakuum erhitzten ZnO muß selbstverständlich mit der Änderung der Steilheit der p_{O_2}-Gradienten an der geometrischen Oberfläche des Pulverhaufens im Zusammenhang stehen insofern, als der Sauerstoffdruck

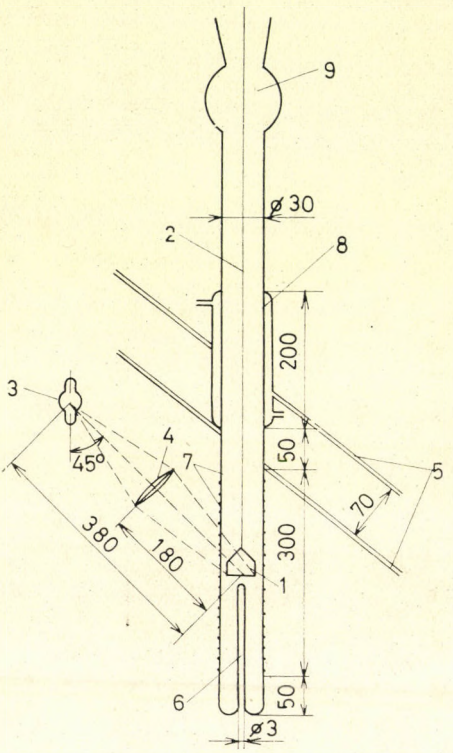

Abb. 8. Schematische Darstellung des Reaktionsrohres mit Belichtungseinrichtung (alle Maße sind in mm angegeben). 1: Wägeschälchen mit ZnO-Pulver, 2: Pt-Draht als Waageaufhängung, 3: Hg-Hochdrucklampe 500 W, 4: Quarzglaslinse, 5: Asbestplatten, 6: Thermoelement-Zuführung, 7: Heizwicklung, 8: Mantel zur Wasserkühlung, 9: Einhängehaken zum Arm der elektronischen Mikrowaage

nach innen schreitend einem Grenzwert zustrebend allmählich zunimmt, d. h. das Gefälle von p_{O_2} an der Oberfläche am steilsten ist.

4. Versuchsergebnisse bei Belichtung und abschließende Diskussion

Die Belichtung erfolgte nach Abb. 8 seitlich durch das Quarzrohr auf die Oberfläche des im Wägeschälchen befindlichen ZnO-Pulvers. Wegen Einzelheiten muß auf frühere Arbeiten [2—4] verwiesen werden. Bei der Auswertung wurde der Wärmeeffekt gemäß Abb. 9 berücksichtigt. Belichtet man 53,53 mg a-ZnO unter Luft von 1 atm und bei Zimmertemperatur, so wird

eine Gewichtsabnahme von ~ 71 μg beobachtet, die bei Entfernung des Lichts (Beschattung) verschwand. Die Reproduzierbarkeit dieses Photoeffekts war jedoch merklich schlechter als die Reproduzierbarkeit der mit Druck- oder Temperaturänderung hervorgerufenen Gewichtsänderung. Mit steigender Einwaage stieg auch diese reversible Gewichtsänderung an, jedoch nicht linear, sondern einem Grenzwert zustrebend. Anwendung von Wärmefiltern hatte eine vermindernde Wirkung im Sinne der Abb. 9, so daß sich bei der Verwen-

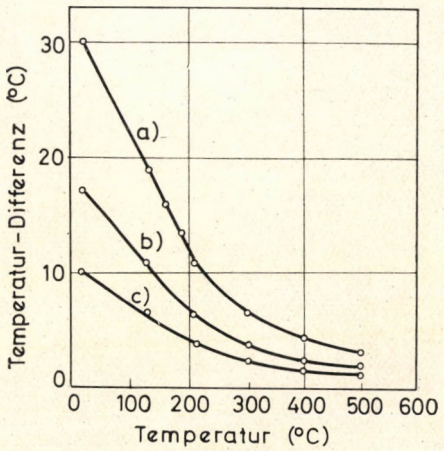

Abb. 9. Temperaturabhängigkeit der Überhitzung der Probe (ΔT °C) bei UV-Bestrahlung ohne Wärmefilter *a)*, durch Wärmefilter NG 11 oder 15 mm H_2O-Schicht *b)* und durch 15 mm Schicht einer wäßrigen $CuSO_4$-Lösung *c)*

dung des NG 11 Filters statt 71 μg eine Gewichtsabnahme von 40 μg ergab. Bemerkenswert ist der Befund, daß der leere Tiegel auf Belichtung und Beschattung sein Gewicht um ± 11 μg änderte, während der mit einer Zn-Scheibe von 180 mg beladene eine Gewichtsänderung von ± 25 μg zeigte. In diesen beiden letzten Fällen war die Reproduzierbarkeit der Messungen gegenüber den mit ZnO durchgeführten Messungen unerwartet gut. Der hier gefundene Zusammenhang zwischen den erhaltenen Zahlen, leerer Tiegel 11, mit 54 mg ZnO-Pulver beladener 71 und mit 180 mg Zn-Blech beladener 25 μg, war nicht vorausschaubar, weil wir allein die Auftriebskraft errechnen können, den Anteil der Konvektionskraft, der thermomolekularen und der elektrostatischen Kraft jedoch nicht. Will man den Anteil dieser Kräfte bei einer geometrisch-thermisch asymmetrischen Apparatur für eine Korrektionsrechnung einzeln erforschen, dann muß man unbedingt den Umstand in Betracht ziehen, daß das ZnO-Pulver durch Belichtung und Beschattung elektrostatisch (manchmal, je nach Oberflächenbehandlung des Oxids, mit überraschender Auswirkung) umgeladen wird. Das Einstrahlen von UV-Licht während des Erwärmungs-

oder Abkühlungsvorganges verursachte manchmal über 400 μg große, stundenlang und bis zu einem undefinierten Quasigleichgewicht abklingende Gewichtsänderungen. Es erschien daher empfehlenswert, für eine elektrische Ableitung ales Tiegels und von den exponiertesten Stutzenwandteilen zur Erde zu sorgen und die Versuche bei einem Vakuum von $< 1 \cdot 10^{-4}$ Torr durchzuführen, wo thermomolekulare Störungen und Konvektionseffekte *ab ovo* ausbleiben. Damit konnte erreicht werden, daß in einem Vakuum von $5 \cdot 10^{-5}$—$5 \cdot 10^{-6}$ Torr sich weder der leere Tiegel zwischen 25—550 °C, noch der mit

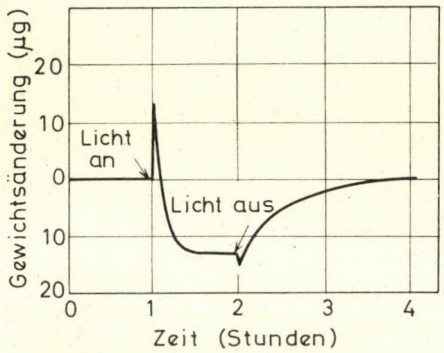

Abb. 10. Wirkung von kurzwelligem Licht auf das Gewicht von 53,53 mg ZnO von 1,58 cm² geometrischer Pulveroberfläche, in einem Vakuum von $2 \cdot 10^{-5}$ Torr, bei 25 °C. Belichtung, Desorption; Beschattung, Adsorption

Zn-Blech beladene zwischen 25—150 °C [4] durch Erwärmung, Abkühlung, Belichtung oder Beschattung, in welcher Variation auch immer, bewegte.

In Abb. 10 ist der zeitliche Verlauf der Gewichtsänderung einer a-ZnO-Probe bei 25 °C bei Belichtung mit UV-Licht und anschließender Dunkelperiode wiedergegeben. Der bei laufender Pumpe eingestellte Restgasdruck betrug etwa $2 \cdot 10^{-5}$ Torr. Im ersten Augenblick der Lichteinwirkung kam es sowohl zu einer vorübergehenden Druckerhöhung als auch zu einer Gewichtszunahme. Durch die explosionsartige Druckerhöhung im Tiegel wird dieser vorübergehend nach unten gestoßen, aber aus dem weiteren Verlauf der Gewichtsänderung in Abb. 10 ergibt sich diejenige Gewichtsabnahme, die durch die Photolyse bei aufrechterhaltenem Vakuum verursacht wird gemäß:

$$\mathrm{ZnO} + h\nu \rightarrow 1/2\ \mathrm{O_2(gas)} + \mathrm{Zn^{\cdot}} + e' \tag{6a}$$

oder auch

$$\mathrm{Null} + h\nu \rightarrow 1/2\ \mathrm{O_2(gas)} + |\mathrm{O}|^{\cdot} + e' \tag{6b}$$

wobei $|\mathrm{O}|^{\cdot}$ eine Sauerstoffionen-Leerstelle kennzeichnet, die neben Zn-Ionen $\mathrm{Zn^{\cdot}}$ auf Zwischengitterplatz auftreten kann. Das Symbol »Null« soll den hypothetisch fehlordnungsfreien Zustand darstellen. Wie man ferner aus Abb. 10

erkennt, ist nach etwa 30 Minuten unter unseren Versuchsbedingungen der stationäre Zustand erreicht, wo keine Masseänderung der ZnO-Probe während der Belichtung erfolgt. Sie betrug bei 53,5 mg ZnO-Einwaage bei 1,58 cm^2 geometrischer Oberfläche des ZnO-Pulvers im Wägeschälchen 13 ± 3 μg. Nach Abschalten des Lichtes konnte die Gewichtsabnahme bei gleichbleibendem Druck ($2 \cdot 10^{-5}$ Torr) quantitativ rückgängig gemacht werden. Man muß allerdings darauf achten, daß eine frische ZnO-Einwaage, die mit der Normalatmosphäre in Berührung war, mehrmalige Belichtungs- und Dunkelperioden mitmachen muß, bevor sich die reversible gleichmäßige Gewichtsänderung einstellt. Die vorübergehende kleine Gewichtsabnahme bei der Beschattung entsteht infolge des Sogs, der wegen der plötzlichen adsorptionsverursachten Druckerniedrigung im Tiegel zustandekommt.

Mit abnehmendem Druck steigt die photodesorbierte Gasmenge und die Desorptionszeit wird kürzer, die Adsorptionszeit länger. Mit wachsender geometrischer Pulveroberfläche wächst die photolytisch abgespaltete Sauerstoffmenge praktisch linear an. Dagegen ist die Einwaageabhängigkeit im allgemeinen nicht linear. Sie strebt mit wachsender Schichtdicke einem Grenzwert zu, so daß bei dickeren Schichten eine Unabhängigkeit von der Einwaage zur Geltung kommt. Thermo- und Photolyse waren stets additiv und ließen sich in unserer Versuchseinrichtung mit Hilfe der Abb. 9 ziemlich genau trennen.

Um mit Thermodesorption die gleiche Gasmenge abzuspalten wie mit der Photodesorption, mußten wir statt der durch das UV-Licht verursachten Erwärmung von 25 auf 30° (Abb. 9) auf etwa 95 °C erwärmen. Die Thermolyse verlief deutlich langsamer als die zum gleichen Masseverlust führende Photolyse. Auf Grund unserer Versuchsergebnisse ist die photolytische Wirkung von UV-Licht auf Zinkoxid außer Zweifel.

Im folgenden wurde nun der Verlauf der Adsorption von Sauerstoff an reinem a-ZnO, an mit 0,27 Mol% Li_2O dotiertem c-ZnO und an d-ZnO bei 25 °C und einem Druck von $1 \cdot 10^{-5}$ Torr Sauerstoff sowohl im Dunkeln als auch unter UV-Lichteinstrahlung untersucht. In Abb. 11 sind einige Ergebnisse dieser Versuchsreihen wiedergegeben. Zur Zeit $t = 0$ wurde die Temperatur von 400 °C auf 25 °C erniedrigt und dann 3 Stunden lang die zeitliche Aufnahme des Sauerstoffs im Dunkeln (obere Kurven in Abb. 11) und auch unter Lichteinwirkung (untere Kurven in Abb. 11) registriert, wobei im letzteren Fall mit der Belichtung vor der Abkühlung der Probe, noch in der Desorptionsperiode begonnen wurde. Bemerkenswert ist der Befund, daß die aufgenommene Sauerstoffmenge beim Li_2O-dotierten c-ZnO weniger war als beim undotierten reinen a-Oxid; mit dem unter den gleichen Bedingungen – jedoch ohne Li-Zusatz – hergestellten reinen d-Oxid von gleicher <1 m^2/g BET-Oberfläche konnte aber praktisch kein unterschiedliches Verhalten festgestellt werden. In Übereinstimmung mit sämtlichen Experimenten ergab ein Einstrahlen von UV-Licht stets eine Abbremsung der zeitlichen Aufnahme von Sauerstoff, wenn vor-

her im Dunkeln gemessen wurde (siehe die oberen Kurvenverläufe in Abb. 11) oder es wurde eine Zunahme der Geschwindigkeit der Sauerstoffaufnahme beobachtet, wenn das Licht abgeschaltet wurde (siehe die unteren Kurvenverläufe in Abb. 11).

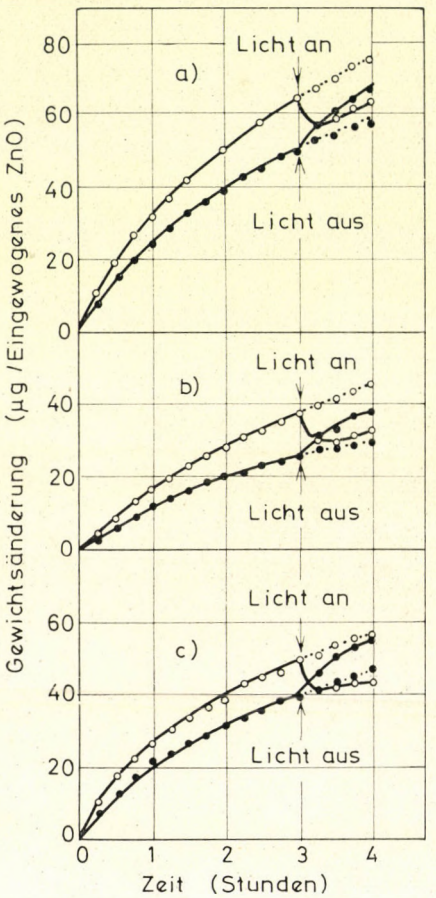

Abb. 11. Einwirkung von kurzwelligem Licht auf die Kinetik der Sauerstoffaufnahme an 145 mg (Kurven *a*) bzw. 58 mg a-ZnO (Kurven *c*) von gemeinsamer 1,58 cm^2 freier geometrischer Oberfläche und 3,9 m^2/g BET-Oberfläche, bei 25 °C und $p_{O_2} = 1 \cdot 10^{-5}$ Torr. Die Kurven *b* wurden mit 223 mg c-ZnO von ebenfalls 1,58 cm^2 freier geometrischer aber <1 m^2/g BET-Oberfläche erhalten. Obere Kurven im Dunkeln, untere Kurven in UV-Licht aufgenommen

Wie man aus den Versuchsergebnissen der Abbildungen 1, 5, 6 und 7 sowie aus den Tabellen II bis IV entnehmen kann, verläuft die Aufnahme und Abgabe von Sauerstoff unter gleichen Versuchsbedingungen reproduzierbar. Bemerkenswert ist hierbei der experimentelle Befund, daß die Gewichtsabnahme sowohl bei 250° als auch bei 350° und 450 °C wesentlich rascher ab-

läuft als die Massenzunahme bei Absenken der Temperatur auf 25 °C unter Konstanthaltung des Sauerstoffdruckes von etwa $1 \cdot 10^{-5}$ Torr. Ein ähnliches Ergebnis wird bei Belichtungsversuchen erhalten. Hier wurde bei Lichteinwirkung mit UV-Licht eine wesentlich raschere Gewichtsabnahme beobachtet als die im Dunkeln eintretende Gewichtszunahme (siehe Abb. 10 und 11). Die Änderung des Halbleitercharakters des Sorbenten von n-Typ auf p-Typ durch Li_2O-Dotierung erbrachte auch in dieser Hinsicht keinen mit der verwendeten Methode erfaßbaren Unterschied zwischen dotiertem und undotiertem ZnO.

Es ist kaum anzunehmen, daß die über Stunden ablaufenden Gewichtsänderungen auf reine Adsorptions- und Desorptionsvorgänge zurückgeführt werden können. Vielmehr handelt es sich, wie bereits oben hingewiesen, um thermo- und photolytische Vorgänge auf der einen Seite und um Oberflächenreaktionen mit fehlgeordneten Ionen und Elektronen der Randschicht im ZnO auf der anderen Seite. Im folgenden soll der Versuch unternommen werden, diese möglichen Reaktionsschritte im Einzelnen zu behandeln. Wir betrachten zunächst einmal die bei höheren Temperaturen (250—450 °C) im Vakuum ($\leq 1 \cdot 10^{-5}$ Torr) thermolytischen Vorgänge im Zinkoxid. Unter der Annahme eines, insbesondere bei höheren Temperaturen, eingestellten Oberflächen-Gleichgewichts:

$$ZnO \rightleftarrows Zn^+(ads) + O^-(ads) \tag{7}$$

bzw.

$$Null \rightleftarrows |O|^{\cdot} + O^-(ads) \tag{8}$$

mit den sich anschließenden Folgeschritten:

$$2\,O^-(ads) \rightarrow O_2^-(ads) + e' \tag{9}$$

und

$$O_2^-(ads) \rightarrow O_2(gas) + e' \tag{10}$$

wird es in der Nähe der Oberfläche der ZnO-Körner zu einer Bildung von überschüssigen Zn-Ionen und Sauerstoffionen-Leerstellen $|O|^{\cdot}$ kommen, neben freien Elektronen. Auf Grund der Anreicherung von Elektronen e' und Zinkionen können leicht verdampfbare Zinkatome gebildet werden, gemäß:

$$Zn^+(ads) + e' \rightarrow Zn(gas) \tag{11}$$

Die nun wesentlich langsamer ablaufende Aufnahme von Sauerstoff bei Zimmertemperatur wird verständlich, wenn man die exponentiell mit der Temperatur abnehmende Ionenbeweglichkeit in der Raumladungs-Randschicht

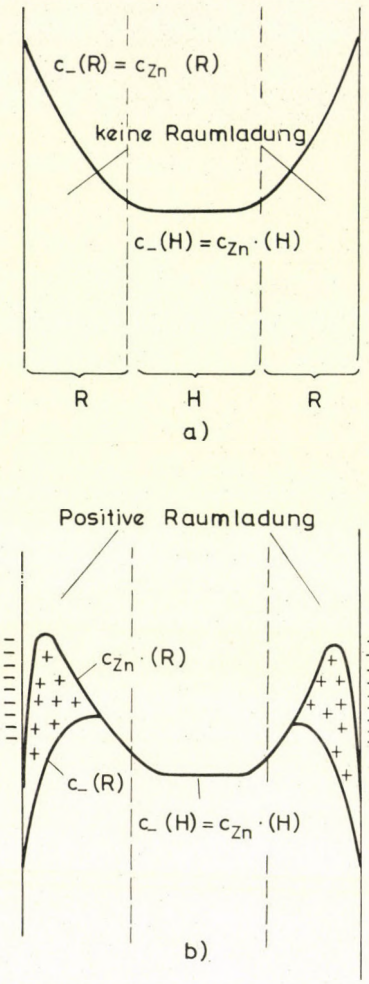

Abb. 12. Schematische Darstellung des örtlichen Konzentrationsverlaufs c_- und c_{Zn}. der freien Elektronen und der Zinkionen auf Zwischengitterplatz in einem ZnO-Korn, *a)* während der Thermolyse, *b)* während der Wiederauf nahmevon Sauerstoff. (R) und (H) kennzeichnen die Raumladungszone und das Halbleiterinnere

der ZnO-Körner berücksichtigt. Zur Erläuterung dieses Sachverhalts ist der in den ZnO-Körnern auftretende örtliche Verlauf der Fehlordnungskonzentration c_- und c_{Zn}. während der Thermolyse und während der Oberflächenreaktion (Wieder-Aufoxidation) schematisch in Abb. 12 wiedergegeben. Wie man erkennt, bildet sich während der Thermolyse eine Anreicherungs-Randschicht sowohl an Elektronen als auch an Zn-Ionen auf Zwischengitterplatz aus, gekennzeichnet durch

$$c_-(\mathrm{R}) = c_{Zn}.(\mathrm{R}) \gg c_-(\mathrm{H}) = c_{Zn}.(\mathrm{H}) \qquad (12)$$

Bei konstant gehaltenem Sauerstoffdruck wird bei Absenken der Temperatur von 250 oder 450 °C auf 25 °C nunmehr eine Sauerstoff-Chemisorption einsetzen gemäß:

$$O_2(gas) + e' \rightleftarrows O_2^-(ads) \tag{13}$$

die relativ rasch abläuft. Hierdurch wird eine Verarmung an Elektronen hervorgerufen, so daß sich nunmehr eine positive Raumladungs-Randschicht ausbildet, wie dies in Abb. 12 *b)* angedeutet ist. Die nun einsetzenden Folgeschritte

$$e' + O_2^-(ads) + Zn^{\cdot} \rightarrow ZnO + O^-(ads) \tag{14}$$

und

$$O^-(ads) + Zn^{\cdot} \rightarrow ZnO \tag{15}$$

werden nur langsam ablaufen und in vernünftigen Reaktionszeiten (z. B. 4 Stunden) auch nicht die durch die Thermolyse verursachte Fehlordnung bzw. den Masseverlust wieder aufheben, was auch beobachtet wird.

Diesen Vorgängen überlagert laufen die durch UV-Lichteinstrahlung einsetzenden Teilschritte (6a) und (6b) ab, die zur Photolyse der ZnO-Kristallite führen, was mit einer Ausscheidung von metallischem Zink verbunden sein kann gemäß:

$$Zn^{\cdot} + e' \rightarrow Zn^{\times}(\text{Zn-Keim}), \tag{16}$$

wobei sich die in übersättigter Konzentration vorhandenen $Zn^{\cdot}$ und e' als Zn-Atome an bereits vorhandene Zinkkeime anlagern. Teilschritt (16) spielt auch besonders im Falle der Thermolyse eine Rolle. Hier kann man das Auftreten von metallischem Zink an der Oberfläche der ZnO-Körner durch die Dunkelfärbung nachweisen.

Nach Abb. 3 und 9 scheint der Anteil des reversibel physisorbierten Wassers und die Einwirkung von UV-Licht mit steigender Temperatur sehr ähnlich abzunehmen. Demgemäß könnte man annehmen, daß die Photolyse nur in Gegenwart von H_2O stattfindet, also ebenso wie beim ZnS [11, 15]. Da wir aber auch zwischen 160—225 °C eine starke Lichtempfindlichkeit der Oxidanlaufschicht an Zinkblech messen konnten [4], neigen wir zu der Anschauung, daß die Hydrolyse bei der Photolyse des ZnS eine bedeutende Rolle spielt und daher die Anwesenheit von H_2O bei der Photolyse des ZnS vielleicht als Bedingung angesehen werden kann, auf die Photolyse des ZnO jedoch nur eine fördernde Wirkung ausübt.

*

Der Mettler Instrumente AG möchten wir für die simultane thermoanalytische und massenspektrometrische Aufnahme und der Deutschen Forschungsgemeinschaft für die Sachmittel und für die Finanzierung des Aufenthaltes in Göttingen des einen von uns (A. J. H.) verbindlichst danken.

LITERATUR

1. HAUFFE, K., STECHEMESSER, R.: Zur Randschicht-Theorie der Adsorption und Katalyse an Halbleiter-Katalysatoren; in: Electronic Phenomena in Chemisorption and Catalysis on Semiconductors, herausg. von HAUFFE, K. und WOLKENSTEIN, TH., Walter de Gruyter, Berlin, 1969
2. HEGEDŰS, A. J.: Bericht über meine Forschungsarbeit vom 7. 9. 67—2. 9. 68 in der Abteilung für augewandte physikalische Chemie des Instituts für Physikalische Chemie der Universität Göttingen. Tungsram, Forschungsinstitut, Arbeitsbericht, Budapest, 1969
3. HEGEDŰS, A. J., MARTIN, K.: Vakuumthermomikrowaagetechnik — Einrichtungen und Wägeerfahrungen. VI. Internationales Symposium für Mikrochemie, 7—11. 9. 1970, Vol. C, D, Seite 165. Verlag der Medizinischen Akademie, Wien, 1970
4. HAUFFE, K., HEGEDŰS, A. J.: Über die Beeinflussung der Verdampfungsgeschwindigkeit von ZnO durch kurzwelliges Licht. Acta Chim. Acad. Sci. Hung. **69,** 123 (1971) und: Über die vakuumthermomikrogravimetrische Messung der UV-Lichteinwirkung auf die Verdampfungsgeschwindigkeit von ZnO bzw. Zn, und auf die Desorption und aktivierte Adsorption von Sauerstoff an ZnO. Vortrag gehalten von A. J. HEGEDŰS an der IX. Konferenz über Mikrowägung im Vakuum, Berlin-West, 11. Juni 1970
5. Mettler Instrumente AG, Greifensee—Zürich, Techn. Bull. T—107; GIOVANOLI, R., WIEDEMANN, H. G.: Helv. Chim. Acta **51,** 1134 (1968) und HEGEDŰS, A. J.: Mikrochim. Acta **1971,** 40
6. KODERA, K., KUSUNOKI, I., SHIMIZU, SH.: Bull. Chem. Soc. Japan **41,** 1039 (1968)
7. MORIMOTO, T., NAGAO, M., TOKUDA, F.: Bull. Chem. Soc. Japan **41,** 1533 (1968)
8. BARRY, T. I., STONE, F. S.: Proc. Roy. Soc. **A255,** 124 (1960)
9. KUBALA, H., MÜLLER, K.: Vakuum-Techn. **17,** 87 (1968)
10. PANASSJUK, G. P., DANTSCHEWSKAJA, M. N., KOBOSLEW, N. I.: Zh. fiz. Chim. **41,** 691 (1967)
11. Gmelins Handbuch der anorganischen Chemie, Zink, System-Nr. 32, Verlag Chemie, Weinheim/Bergstr.–Berlin, 1924 und 1956
12. HIRSCHWALD, W., STOLZE, F., STRANSKI, I. N.: Z. phys. Chem. Neue Folge **42,** 96 (1964) und STOLZE, F.: Kinetik der thermischen Dissoziation von Zinkoxid. Diss., T. U. Berlin, 1969
13. SOMORJAI, G. A., LESTER, J. E.: Progr. Solid State Chem. **4,** 1 (1967)
14. HEGEDŰS, A. J., KISS, A. B.: Mikrochim. Acta **1966,** 813
15. SVISZT, P.: Fiz. Szemle **17/7,** 217 (1967)

Karl HAUFFE; Göttingen, Bürgerstrasse 50. BRD
András J. HEGEDŰS; Budapest IV., Váci út 77.

Acta Chimica Academiae Scientiarum Hungaricae, Tomus 72 (1), pp. 25—32 (1972)

FERROMAGNETIC PRODUCTS OF THE EXPLOSION REACTION BETWEEN $Co(NO_3)_2$ AND $(NH_4)_4[Fe(CN)_6]$

W. WOLSKI and A. BUREWICZ

(Department of Magnetochemistry, Adam Mickiewicz University, Poznan, Poland)

Received October 14, 1970

Ammonium ferrocyanide reacts with cobalt nitrate explosively when heated to 220 °C. The reaction takes place at the $Co(NO_3)_2$ to $(NH_4)_4$ $[Fe(CN)_6]$ mole ratio range of 1 : 5 to 5 : 1. The nature of products depends basically on the composition but also on the atmosphere in which the explosion is carried out.

X-ray studies, magnetic measurements and chemical analysis indicate that the ferromagnetic properties of the products are due to the presence in the residue of metallic iron, metallic cobalt, magnetite and sometimes cobalt ferrite. If the process occurs with free access of air, more non-ferromagnetic α-iron oxide is formed. The highest values of saturation magnetization have been found among the salt mixtures with the ratio $Co(NO_3)_2 : (NH_4)_4$ $[Fe(CN)_6] = 2 : 1$. The richest in crystalline phases are the residues after the explosion of mixtures with a 1 : 1 ratio.

Explosion reactions involving ferrocyanides are of short history. The literature available so far is very scarce and almost completely patented.

The first works concerning explosion reactions of ferro- and ferricyanides, mixed with nitrates of metals (mainly divalent), were published in 1959—1960 [1, 2]. It is stated there that ammonium or potassium ferro- and ferricyanides not only react explosively with nitrates of metals but these reactions yield ferromagnetic products. From these works it follows that the composition of products is complex and contains also ferritic phases. From this time on a number of very interesting patents have been claimed, chiefly in the USA, formulating the compositions of explosive mixtures based on ferro- and ferricyanides designed for specific applications as blasting explosives or catalysts of solid fuels in jet engines [3—8].

Further results on the explosion reactions of mixtures of cobalt nitrate with ammonium ferrocyanide, taken in mole ratios from 5 : 1 to 1 : 5 and heated to 220 °C, are reported in the present paper. The explosion reaction of ammonium ferrocyanide alone has also been examined. Owing to sometimes very strong explosions, resulting in destruction of the experimental equipment, the sample weight had to be reduced to 5 g. The experiments were carried out in air. Some explosions were effected by supplying a given volume of air to the bottom of the vessel containing the mixture or by passing air above the mixture. Other experiments were conducted in open vessels under free access of air and still another group of experiments concerned the reactions taking

place in a closed vessel without the access of air. Reactions took place usually in 5 to 20 min after the mixture had reached the temperature of 220 °C. As a rule the mixtures rich in ammonium ferrocyanide reacted in times close to 5 min, whereas those containing much cobalt nitrate required nearly 20 min. It is believed that here the crystallization water is the chief cause of retardation.

Beginning at a 1 : 1 cobalt nitrate to ammonium ferrocyanide ratio and increasing the ammonium ferrocyanide content, the products of explosions were powders of brown or deep brown colour. The explosion products arising from mixtures rich in cobalt nitrate, with $Co(NO_3)_2$ to $(NH_4)_4[Fe(CN)_6]$ ratios of 4 : 1, 3 : 1 and 2 : 1, had the form of hard lumps with a metallic lustre. Their colour was black after grinding in a mortar. The preparations with still higher cobalt content were again powders or slags, always black but without a metallic lustre.

The magnetization values of the explosion products (Table I) show that, depending on the method of air supply, ammonium ferrocyanide alone gives products of strongly varying magnetic properties. The highest magnetization value of the product occurs at a 2 : 1 ratio of cobalt nitrate to ammonium ferrocyanide, regardless of whether the reaction takes place in an open or a closed vessel, and of the method of air supply. Relatively high values are obtained at a 3 : 1 ratio and considerably lower ones at a 4 : 1 ratio. At the 5 : 1 composition a drastic drop of the σ value is observed. The increase of the ammonium ferrocyanide content in the mixture also sharply decreases the magnetization value. For instance in the case of a 2 : 1 ratio of the two salts, $\sigma_{20°C}$ is reduced almost fourfold. A further increase in the $(NH_4)_4[Fe(CN)_6]$ content from 1 : 1, through 1 : 2, 1 : 3, 1 : 4, to 1 : 5 gives products of much the same values of saturation magnetization. They are even very close, as may be seen from the table, to the magnetization reached by preparations obtained on heating ammonium ferrocyanide alone.

Thus the magnetic measurements indicate a distinct effect of the mole ratio of the starting salts on the reaction products. These data also help in the identification of ferromagnetic phases present in the products of explosion reactions. The very high magnetization values, observed for the explosion residue of a 2 : 1 cobalt nitrate and ammonium ferrocyanide mixture, indicate that at least one metallic phase must be present or else the products must contain iron nitride Fe_4N, because only metallic iron, metallic cobalt or iron nitride can reach the magnetization values, $\sigma_{20°C}$, in excess 150 $G_s \cdot cm^3 \cdot g^{-1}$. In addition these results were of valuable help in X-ray pattern identification and interpretation.

X-ray pattern identification has disclosed that metallic iron and cubic β-Co are responsible for the ferromagnetism in the explosion products of a 2 : 1 mixture of cobalt nitrate with ammonium ferrocyanide. The reactions were carried out in air fed above the mixture at the rate of 5, 20 and 40 l/hr

Table I

Saturation magnetization values $G_S \cdot cm^3 \cdot g^{-1}$ of the products of explosion reactions

	$Co(NO_3)_2$: $(NH_4)_4[Fe(CN)_6]$									Ammonium ferro-cyanide
	5 : 1	4 : 1	3 : 1	2 : 1	1 : 1	1 : 2	1 : 3	1 : 4	1 : 5	
Limited access of air										
prep.→sample	1	2	3	4	5	6	7	8	9	10
20 °C	57.7	108.8	124.0	125.6	43.5	41.6	42.4	37.2	42.9	31.5
Free access of air										
prep.→sample	11	12	13	14	15	16	17	18	19	20
20 °C	46.9	90.2	103.5	107.9	38.9	36.2	38.1	39.8	40.4	26.5
Maximum rate of air flow*										
prep.→sample	21	22	23	24	25	26	27	28	29	30
20 °C	23.6	93.0	111.7	109.0	53.5	62.6	56.4	43.1	41.7	36.7
5 l/hr of air passed over the sample										
prep.→sample	31	32	33	34	35	36	37	38	39	40
20 °C	21.8	33.5	85.2	153.6	45.8	46.0	35.9	44.2	2.75	2.57
20 l/hr of air passed over the sample										
prep.→sample	41	42	43	44	45	46	47	48	49	50
20 °C	25.3	36.43	76.0	143.6	37.5	49.8	46.0	46.9	6.9	24.5
40 l/hr of air passed over the sample										
prep.→sample	51	52	53	54	55	56	57	58	59	60
20 °C	24.3	35.6	88.5	144.5	37.6	41.6	39.9	39.7	38.4	48.7
5 l/hr of air led into the bulk of the sample										
prep.→sample	61	62	63	64	65	66	67	68	69	70
20 °C	26.4	24.9	87.8	147.2	44.0	40.9	27.5	51.1	37.0	14.4
20 l/hr of air led into the bulk of the sample										
prep.→sample	71	72	73	74	75	76	77	78	79	80
20 °C	19.9	25.4	76.8	159.4	40.6	41.0	44.0	36.6	37.6	2.4
40 l/hr of air led into the bulk of the sample										
prep.→sample	81	82	83	84	85	86	87	88	89	90
20 °C	19.9	23.3	108.7	151.1	35.4	37.4	35.4	31.9	31.0	35.6

* max ~50 l/hr

(Fig. 1, patterns 1, 2, 3). Metallic iron is the predominant carrier of ferromagnetism when air penetrates into the mixture at a rate of 5 l/hr (pattern 4). To a lesser extent cobalt, accompanied by magnetite, also contributes to this ferromagnetism but these components are hardly visible on the X-ray diagram. At an air flow of 20 l/hr, conducted into the mixture, the identifiable ferromagnetic phases are metallic iron and magnetite, distinctly visible this time (pattern 5). The same phases are also responsible for the ferromagnetism when air is led into the bulk of the sample at a rate of 40 l/hr (pattern 6). Small amounts of Co_3O_4 and CoO are observed in samples obtained at all flow rates in the case of a 2 : 1 mole ratio of cobalt nitrate and ammonium ferrocyanide. β-Co and α-Fe occur on the X-ray patterns in agreement with the high values of magnetization. At the extreme ratio of 5 : 1, metallic cobalt, Co_3O_4 and CoO are found in the reaction products (patterns 7 and 8). The distribution of cobalt between these three crystalline phases as a function of the air supply method is rather difficult to establish. In the case of the second extreme composition (ammonium ferrocyanide alone), the observed low ferromagnetism is also confirmed by the X-ray picture. For example, preparation 40 (pattern 9) of very low ferromagnetism is Prussian blue, $Fe_4[Fe(CN)_6]_3$, while sample 50, obtained at an air flow of 20 l/hr shows considerable magnetization when compared with the preceding one, obtained at 5 l/hr. Here the pattern contains magnetite besides Prussian blue. The amount of magnetite rises as the air flow increases during the heating of ammonium ferrocyanide. The products of heating have lower magnetization values when conducting air in depth of the sample. This is due to the appearance of a non-ferromagnetic α-Fe_2O_3 phase. The same phase has also been observed in the products obtained under conditions of passing air above the sample at the maximum flow rate. The phases are similar regardless of the way air is introduced (outside the sample or into the bulk). A somewhat higher α-Fe_2O_3 content is observed only in the case of products with the in-bulk method.

The diffraction method has been very useful in the interpretation of crystalline phases. With its aid, an attempt was made to identify the magnetite $d_{220} = 2.95$ line.

In Fig. 2 are shown two sectors of the X-ray diagrams. The first represents the preparation No. 40, where the characteristic line of magnetite (2.95) appears as a very weak reflection. Magnetic data confirm the low magnetization value of this sample, 2.6 $G_s \cdot cm^2 \cdot g^{-1}$. The lower curve in Fig. 2 illustrates the build-up of the ferromagnetic phase in the samples with excess ammonium ferrocyanide. This is demonstrated on the second sector by the increase of the 2.95 magnetite line, which is accompanied by enhanced magnetic properties.

Thermomagnetic analysis disclosed magnetic (and chemical) changes taking place after exposure to elevated temperatures and permitted a closer

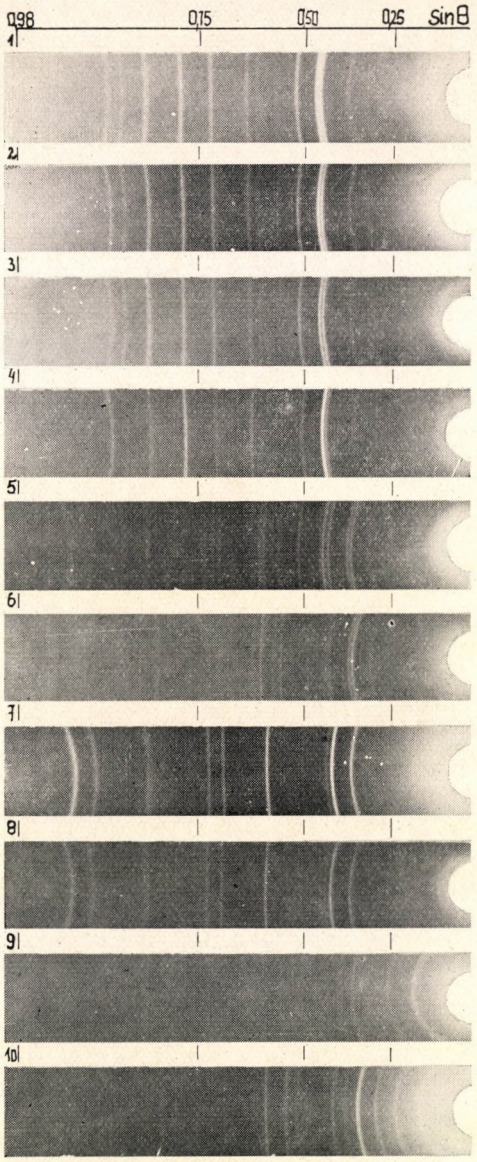

Fig. 1. X-ray patterns of the explosion products of cobalt nitrate–ammonium ferrocyanide mixtures in air

1 — prep. → sample 34 — $Co(NO_3)_2 : (NH_4)_4 [Fe(CN)_6] = 2 : 1$ air over the sample, 5 l/hr
2 — prep. → sample 44 — $Co(NO_3)_2 : (NH_4)_4 [Fe(CN)_6] = 2 : 1$ air over the sample, 20 l/hr
3 — prep. → sample 54 — $Co(NO_3)_2 : (NH_4)_4 [Fe(CN)_6] = 2 : 1$ air over the sample, 40 l/hr
4 — prep. → sample 64 — $Co(NO_3)_2 : (NH_4)_4 [Fe(CN)_6] = 2 : 1$ air into the bulk of the sample, 5 l/hr
5 — prep. → sample 74 — $Co(NO_3)_2 : (NH_4)_4 [Fe(CN)_6] = 2 : 1$ air into the bulk of the sample, 20 l/hr
6 — prep. → sample 84 — $Co(NO_3)_2 : (NH_4)_4 [Fe(CN)_6] = 2 : 1$ air into the bulk of the sample, 40 l/hr
7 — prep. → sample 31 — $Co(NO_3)_2 : (NH_4)_4 [Fe(CN)_6] = 5 : 1$ air over the sample, 5 l/hr
8 — prep. → sample 51 — $Co(NO_3)_2 : (NH_4)_4 [Fe(CN)_6] = 5 : 1$ air over the sample, 40 l/hr
9 — prep. → sample 40 — $(NH_4)_4 [Fe(CN)_6]$ air over the sample, 5 l/hr
10 — prep. → sample 50 — $(NH_4)_4 [Fe(CN)_6]$ air over the sample, 20 l/hr

The patterns were obtained in a chamber, 57.3 mm in diameter, with CoK_α radiation (exposure time = 3 hr; 35 kV; 18 mA)

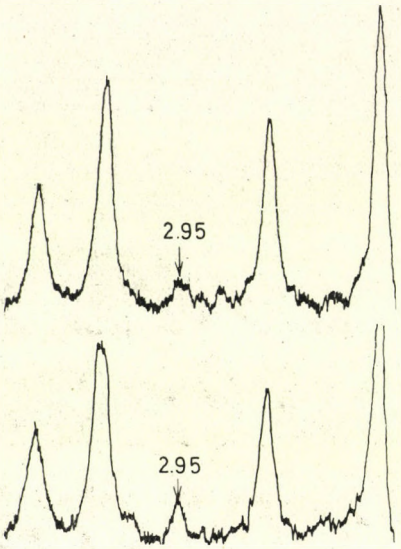

Fig. 2. Diffraction curves representing the rise of the $d = 2.95$ line

upper curve — sample 40 — $(NH_4)_4[Fe(CN)_6]$ air over the sample, 5 l/hr, lower curve — sample 49 — $Co(NO_3)_2 : (NH_4)_4[Fe(CN)_6] = 1 : 5$ air over the sample, 20 l/hr (CoK_α radiation)

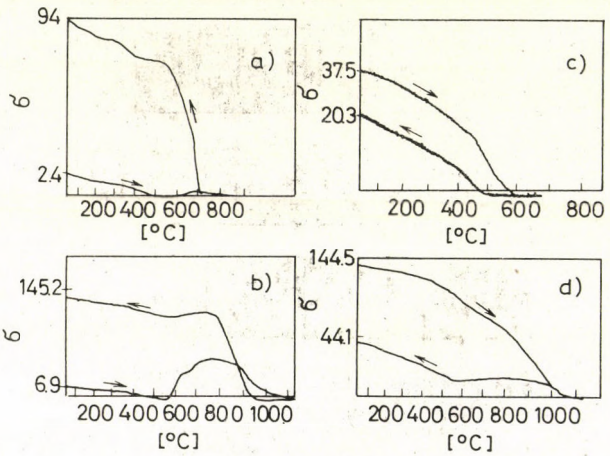

Fig. 3. Thermomagnetic curves

a — sample 80 $(NH_4)_4[Fe(CN)_6]$; air led into the bulk 20 l/hr
b — sample 49 $Co(NO_3)_2 : (NH_4)_4[Fe(CN)_6] = 1 : 5$ air passed over the sample, 20 l/hr
c — sample 45 $Co(NO_3)_2 : (NH_4)_4[Fe(CN)_6] = 1 : 1$ air passed over the sample, 20 l/hr
d — sample 54 $Co(NO_3)_2 : (NH_4)_4[Fe(CN)_6] = 2 : 1$ air passed over the sample, 40 l/hr

investigation of the mixture composition after explosions. Fig. 3 represents the thermomagnetic curves obtained on heating ammonium ferrocyanide at an air flow of 20 l/hr, conducted into the bulk. The magnetization value of this

sample is low: 2.4 $G_s \cdot cm^3 \cdot g^{-1}$. The constituent ferromagnetism is lost below 550 °C. The magnetic properties are improved on further heating, reaching their maximum at 710 °C. Up to 580 °C transformations of iron ferrocyanide take place resulting in the formation of iron cyanide. The decrease of original magnetization is caused by the disappearance of Fe_3O_4, the only magnetic phase detected. Owing to the decomposition of iron cyanide from about 580 °C, a rise of the magnetization value is observed. On cooling, the magnetization curve rises beginning from about 750 °C, a fact pointing to the formation of metallic iron. Further inflexions observed while cooling indicate the occurrence of iron nitride, iron carbide and magnetite. Such curves are typical for all samples of initially low magnetization.

The next curve (Fig. 3b) demonstrates the magnetization *vs.* temperature relationship for the explosion product of a mixture low in cobalt content. The first portion of this diagram is similar to the curve presented in Fig. 3a but from the temperature of about 570 °C the improvement of magnetic properties is different due to the formation of metallic iron and cobalt. Hence the deterioration of magnetic properties after reaching a certain maximum is caused by approaching the Curie point for iron and then for cobalt. On cooling, the magnetization sharply rises beginning from 960 °C, then falls slightly and rises again at about 570 °C. The first rise in magnetization is due to the formation of a cobalt–iron alloy, the second to iron–cobalt ferrite.

The chemical analyses of this sample as well as of all those belonging to the low-magnetization group yield high contents of nitrogen (25—30%) and carbon (15—24%).

Samples of higher magnetization values have thermomagnetic curves of quite different shapes (Fig. 3c). Their carbon and nitrogen contents are 3–7% and 1—1.5%, respectively. These are products obtained with a 1 : 1 initial ratio of cobalt nitrate and ammonium ferrocyanide. In these cases ferromagnetism is mainly due to magnetite, with some contribution from iron and cobalt which are barely discernible on the X-ray patterns. The returning line on the thermomagnetic diagram runs much below the initial one and the beginning of its ascent becomes observable at a temperature of about 500 °C. This is probably associated with the formation of a solid solution of magnetite and cobalt–iron ferrite.

The fourth and last type of thermomagnetic curves (Fig. 3d) is yielded by samples with very good magnetic properties, and a 2 : 1 initial ratio of the components. β-Co and α-Fe have been detected by X-ray analysis. The magnetic properties of these products are lost gradually on heating. Some tendency toward reaching the Curie point is observed for magnetite, iron and cobalt (for the latter, at about 1120 °C). The return of the curve beyond this temperature is a sufficient demonstration of metal oxidation and oxide formation together with the appearance of a ferritic phase.

In general, the pure metals, magnetite and sometimes a ferritic phase are the main carriers of magnetic properties among the 90 samples prepared in the course of the present work. The ratio of the starting salts is the deciding factor in the phase composition of explosion products. The method of air supply has a strong quantitative but no qualitative effect. Larger amounts of α-Fe_2O_3 are formed when air is conducted into the bulk of the sample. The preparations with a 2 : 1 ratio of cobalt nitrate and ammonium ferrocyanide show the highest magnetization values. The greatest differentiation of crystalline phases (including the ferromagnetic ones) occurs in the case of a 1 : 1 proportion of $Co(NO_3)_2$ and $(NH_4)_4[Fe(CN)_6]$, irrespective of the method of air supply.

REFERENCES

1. WOLSKI, W.: Rocz. Chem. **33,** 231 (1959)
2. WOLSKI, W.: Rocz. Chem. **33,** 1237 (1959)
3. PROELL, W., STANLEY, W.: US Patent 3 137 598 (1964)
4. SAGERS, D.: US Patent 3 011 883 (1961)
5. PARTI, P.: US Patent 2 946 672 (1960)
6. EISZNER, J., STANLEY, W.: US Patent 2 942 961 (1960)
7. HERRING, L. G.: US Patent 3 157 025 (1959)
8. MORELLO, E., BROELL, W., BOWMAN, N.: US Patent 2 942 962 (1960)

Wlodzimierz WOLSKI
Andrzej BUREWICZ
} Poznan, ul. Grundwaldzka nr. 6. Poland.

Acta Chimica Academiae Scientiarum Hungaricae, Tomus 72 (1), pp. 33—57 (1972)

STUDY OF THE REST AND POLARIZATION POTENTIALS OF CHEMICALLY TREATED GERMANIUM SINGLE CRYSTAL SURFACES, I

EFFECT OF THE pH AND ANION ADSORPTION

J. GIBER and I. VAJASDY-PERCZEL

(Semiconductor Development Department, United Incandescent Lamp and Electric Company Tungsram, Budapest)

Received August 23, 1970

1. The conditions were elaborated for the measurement of the electrode potential on germanium single crystal surfaces with a reproducibility of ±10 mV.

2. The rest potential of germanium was measured in 0.1*N* K_2SO_4, KCl, KBr and KI solutions in the pH interval 2—12. With the increase of pH the potential is shifted linearly in the negative direction. The effect of anions causes a potential shift in the negative direction, increasing in the above series; this is greater in acidic than in neutral solution.

3. The polarization potential of germanium was measured in acidic, neutral and alkaline 0.1*N* solutions of the above salts in the cathodic and then the anodic region in the current density interval 10^{-7}—10^{-3} A/cm². The anodic and the cathodic polarization curves are composed of one and two sections, respectively, all of which can be described by Tafel equations.

4. The formation of the surface layers was studied with an ellipsometer on an electrode at rest and during the polarization process. In the rest state and with anodic polarization, for a certain time a clear thickening of the layer can be demonstrated; the cathode process, however, is not accompanied by a clear decrease of the thickness of the surface layer.

5. On the basis of the experimental results, it can be stated with high probability that the rest potential is of a corrosion nature. It is likely that the cathode and anode reactions are identical with the low current density polarization reactions. If this is accepted, the anion effect in the case of the rest potential can be simply explained as the effects of the adsorbed anions in decreasing the overvoltage of the anode reaction.

From an analysis of all the available data, it is likely that the determining anode reaction of the corrosion rest potential is the oxidation process of germanium. According to our assumptions about the cathode reactions in question, it can be said that the rate of the oxide reduction process can be neglected. The determining reaction is the evolution of hydrogen, with the intermediate step of germanium hydride formation.

As regards the anode reactions, it is likely that we are concerned with different oxidation steps of germanium, depending on the current density. The cathode reactions agree at low current densities with those of the rest state, but at higher current densities the rate of hydrogen formation is already significant.

A number of authors [1—13] have made experimental studies of the *rest potential* (φ_r) of germanium, but with regard to the dependence on the composition of solution and the pH these provide only few and contradictory data.

The problem has been dealt with systematically only by LOVREČEK and BOCKRIS [1], HARVEY and GATOS [2] and BODDY and BRATTAIN [4]. These authors studied the pH-dependence of the potential in a wide interval, and found that the rest potential of the germanium electrode has a similar

pH-dependence to that of the hydrogen electrode. The experimental results reported by them, however, differ significantly from each other (Fig. 1).

The different authors made different assumptions as to the nature of the electrode potential and the mechanism of the processes determining the potential. Without making any concrete investigations, and assuming that the reactions determining the potential are reversible, POURBAIX [14] gives many possible reactions based on thermodynamic data for germanium electrolyte solution systems, and calculates the equilibrium electrode potentials of these

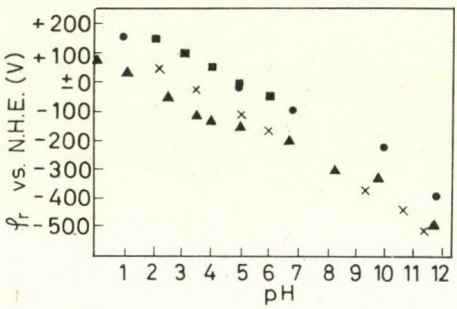

Fig. 1. Rest potential data from the literature
▲ K_2SO_4; KOH—H_2SO_4, pH adjustment [1]. ■ N Na_2SO_4; sulfate-bisulfate buffer; O_2 atmosphere [2]. ● 0.1N K_2SO_4; KOH—H_2SO_4, pH adjustment [4]. × 0.1N K_2SO_4; KOH—H_2SO_4, pH adjustment (this work)

reversible reactions. From a comparison of their experimental data with thermodynamic calculations, LOVREČEK and BOCKRIS [1] consider that their results can be explained by the reversible reactions

$$Ge + H_2O \rightleftharpoons GeO_{brown} + 2H^+ + 2e^- \quad (1a)$$

$$Ge + H_2O \rightleftharpoons GeO_{yellow} + 2H^+ + 2e^- \quad (1b)$$

Since their measured potential values depend on the stirring, it is not excluded that the potential-determining processes, which in their opinion can be characterized by anode reaction (1) and the cathodic evolution of hydrogen, give a mixed potential. (The calculated mixed potential data differ slightly from the reversible potential data.) HARVEY and GATOS [2] assume a mixed potential which, in agreement with the fact that their solution was saturated with oxygen, can be explained by the reactions

in acidic medium:

$$Ge + H_2O \rightarrow GeOH + H^+ + e^- \quad (2)$$

$$O_2 + H^+ + e^- \rightarrow HO_2 \quad (3)$$

in alkaline medium:

$$Ge + OH^- \rightarrow GeOH + e^- \quad (4)$$

$$O_2 + H_2O + e^- \rightarrow HO_2 + OH^- \quad (5)$$

According to LOVREČEK and BOCKRIS [1], the pH-dependence of the rest potential is in good agreement with the interpretation that the potential is determined mainly by reactions (1a) and (1b): reaction (1a) is predominant in the pH range 0—4, and reaction (1b) in the pH range 6—12. HARVEY and GATOS [2] explain the pH-dependence by a mixed potential derived from Eqs (2)—(5).

The effect of anions on the rest potential of germanium has not been studied, but data are available [2] on the relation between the dissolution of germanium and the adsorption of anions (Cl^-, Br^-, I^-). It can be found from this paper that, by means of specific adsorption, anions accelerate the dissolution of germanium.

Of the measurements giving an indication of the nature of the potential, the study of the dependence on the GeO_2 concentration must be mentioned: LOVREČEK and BOCKRIS [1] found the rest potential to be independent of the GeO_2 concentration, whereas according to HARVEY and GATOS [8], φ_r becomes more positive with increasing GeO_2 concentration.

It can be established that the nature of the rest potential and the mechanism of the processes have still not been cleared up. The effect of anions on the rest potential has not been studied. The reported experimental results on the value of the rest potential, on its pH-dependence, and on its dependence on the GeO_2 concentration, contain significant differences and contradictions.

Numerous papers deal with the study of the *polarization potential* (φ) of germanium, but these primarily cover either the anodic polarization region of higher current density (10^{-4}—10^{-1} A/cm^2) [10, 15 –23], or the cathodic polarization region of higher current density [24, 25]. Only a few authors (HARVEY, LAFLEUR and GATOS [3], BOROVKOV [10], GERISCHER and BECK [18]) measure the cathodic and anodic polarization regions together, but two of these [10, 18] treat merely the region of higher current density.

On the other hand, from the viewpoint of the general study of the classification, the nature and mechanism of polarization phenomena, it is of fundamental importance to carry out a joint, parallel investigation of the anode and cathode processes with current densities smaller than the 10^{-4} A/cm^2 region. In this low current density interval, BODDY [26] studied the same *anodic* polarization region as our own polarization measurements, BOHNENKAMP and ENGEL [27] and HARVEY and GATOS [3] studied an interval smaller by one order of magnitude, while the data of YEFIMOV and YERUSALIMCHIK [23] and GERISCHER, HOFFMANN-PEREZ and MINDT [28] provide sporadic experimental points; in the *cathodic* region, however, our own studies can be compared only with the data of HARVEY, LAFLEUR and GATOS [3] (Fig. 2).

The mechanism of the polarization processes was studied by TURNER [21], BARDELEBEN [29], GERISCHER, HOFFMANN-PEREZ and MINDT [28], GE-

RISCHER, MAURER and MINDT [30] and HOFFMANN-PEREZ and GERISCHER [31] with anodic-cathodic cyclic measurements.

In the *mechanism of the anodic dissolution* of germanium (in the region of high current densities) BOROVKOV [10], JIRSA [15] and HARVEY, SHEFF

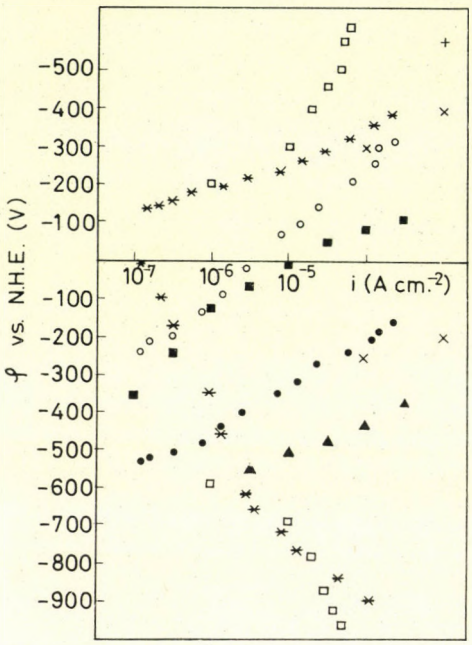

Fig. 2. Comparison of the present polarization potential data with those in the literature ✳ 0.1*N* K_2SO_4; pH = 2.1 (this work). ○ 0.1*N* K_2SO_4; pH = 6.3 (this work). ■ 0.1*N* K_2SO_4; pH = 7.4 [26]. ▲ *N* KOH [27]. □ 0.1*N* Na_2SO_4 + 10^{-4} *N* KI [3]. × 0.1*N* H_2SO_4 [21]. ● 0.1*N* KOH (this work)

and GATOS [32] assume GeO_2 as oxidation product while GeO is formed as a secondary product in the reaction

$$Ge + GeO_2 \rightarrow 2GeO \tag{6}$$

PLESKOV [17] and TURNER [21] propose a mechanism for the anodic dissolution according to which the covalent bond of a surface Ge atom is broken by the capture of two holes.

BOROVKOV [10] and JIRSA [15] have observed saturation phenomena for N-type semiconductors at high current densities (above 10^{-3} A/cm^2) in agreement with GERISCHER and BECK [18] and YEFIMOV and YERUSALIMCHIK [23]; they explain this as confirmation that the rate-determining step in the anodic dissolution is the transport of a hole within the germanium to the boundary

surface of the semiconductor. BODDY [26] accepts the detailed mechanism elaborated by BECK and GERISCHER [33, 34] for the anodic dissolution of germanium.

As the *cathode process of the polarization*, BOROVKOV [10], YEFIMOV and YERUSALIMCHIK [24] and GREEN [25] consider it probably to be hydrogen evolution; according to BOROVKOV [10] and YEFIMOV and YERUSALIMCHIK [24], the rate-determining step is neutralization and it can be described by the Tafel equation in the formulation of VOLMER and FRUMKIN. GREEN [25] proposes the following mechanism

$$Ge + H_3O^+ + e^- \xrightarrow{\text{fast}} GeH + H_2O \tag{7}$$

$$H_3O^+ + GeH + e^- \xrightarrow{\text{slow}} Ge + H_2 + H_2O \tag{8}$$

From a study of the hydrogen evolution process GREEN [35] finds that the neutralization of the proton is not the rate-determining step in the case when the process is controlled by the diffusion of minority charge-carriers in the semiconductor.

On the basis of their cyclic polarization measurements, GERISCHER, MAURER and MINDT [30] propose the following mechanism for the anodic–cathodic polarization transition:

$$\gtrdot Ge - OH + e^- + H^+ \rightleftharpoons \gtrdot Ge^{\cdot} + H_2O \tag{9}$$

$$\gtrdot Ge^{\cdot} + H^+ \rightleftharpoons \gtrdot Ge - H + e^+ \qquad \text{in acidic medium}$$

$$\gtrdot Ge - OH + e^- \rightleftharpoons \gtrdot Ge^{\cdot} + OH^- \tag{10}$$

$$\gtrdot Ge^{\cdot} + H_2O \rightleftharpoons \gtrdot Ge - H + OH^- + e^+ \qquad \text{in alkaline medium}$$

From capacity measurements, HOFFMANN-PEREZ and GERISCHER [28, 31] assume a surface covered with hydroxide in the anodic polarization region, and a surface covered with hydride in the cathodic polarization region, and the joint presence of hydroxide and hydride in the transitional region of small current density.

From capacity and charging curve measurements, BODDY and BRATTAIN [4], BODDY [26], HOFFMANN-PEREZ and GERISCHER [31] and MYAMLIN and PLESKOV [36] propose the following mechanism for *the explanation of the pH-dependence of the polarization potential*: on both the surface covered with hydroxide and that covered with hydride, a dissociation double layer develops in accordance with the following dissociation equations:

$$Ge - OH + H_2O \rightleftharpoons GeO^- + H_3O^+ \tag{11}$$

$$Ge - H + H_2O \rightleftharpoons Ge^- + H_3O^+ \tag{12}$$

and the slope of the pH-dependence of the potential can be expressed from a consideration of these.

The effect of anions on the polarization potential at higher anodic current densities has been studied by HOLMES [16], YEFIMOV and YERUSALIMCHIK [19, 20] and TOSHIMA and UCHIDA [37]. From their measurements, the conclusion was drawn that reducing ions are oxidized by electron injection. As a result of electron injection, the electron concentration on the surface increases, this gives rise to the presence of a greater number of holes on the surface, and this in turn increases the rate of anodic dissolution. HARVEY, LAFLEUR and GATOS [3] studied the effect of iodide ion adsorption on the polarization potential in the lower current density region on both the cathode and the anode. The mechanism of the process was not clarified. YEFIMOV and YERUSALIMCHIK [24] studied the mechanism of cathodic hydrogen evolution in the higher current density region by anion and cation adsorption measurements. They found that hydrogen evolution proceeds by a slow neutralization mechanism on germanium. From the results of their polarization potential and capacity measurements, BRATTAIN and BODDY [38] have concluded that the iodide ion exerts a specific effect. In the anodic polarization region the effect is characterized by the reaction

$$\mathrm{Ge-OH} + \mathrm{I^-} \rightarrow \mathrm{Ge-I} + \mathrm{OH^-} \tag{13}$$

The following assumptions as to the mechanism of the process are considered compatible with the results: (a) Iodide ion displaces the OH ion from the surface, and the resulting change in dipole moment contributes to the internal potential difference. (b) The iodide bonded to the surface exerts an inductive effect and brings about changes in $\mu^{\circ}_{\mathrm{GeO}}$ — and $\mu^{\circ}_{\mathrm{GeOH}}$.

From a survey of the literature on polarization potential measurements it can be established that so far there have been no comprehensive systematic polarization measurements, a joint study of the cathodic and anodic processes has not been made, and, at present, opinions are divided as to the kinetic nature of polarization reactions and even more as to the presumable polarization mechanism.

In summary, it can be established that the germanium rest potential data of individual authors do not agree, the study of the effects of the parameters is incomplete, and the nature of the potential has not been elucidated. It is therefore our object to carry out reproducible additional measurements on the dependence of the rest potential on pH, anion effect and GeO_2 concentration, and also to clarify the effect of surface treatment of the electrode.

In order to support our conclusions on the nature of the rest potential, and also because of the incompleteness of the germanium polarization potential studies, it seemed reasonable to produce anodic–cathodic polarization curves in a wide polarization current density interval (10^{-7}—10^{-3} A/cm^2).

Experimental method

Measuring cell. Rest and polarization potentials were measured in the pyrex-glass apparatus to be seen in Fig. 3. The measuring cell consists of 3 parts (*A*, *B*, *C*), separable from each other by taps.

A is the measuring vessel proper, into which extends
B, a vessel containing an auxiliary electrode (platinum), and
C, a vessel containing a comparative (normal calomel) electrode.

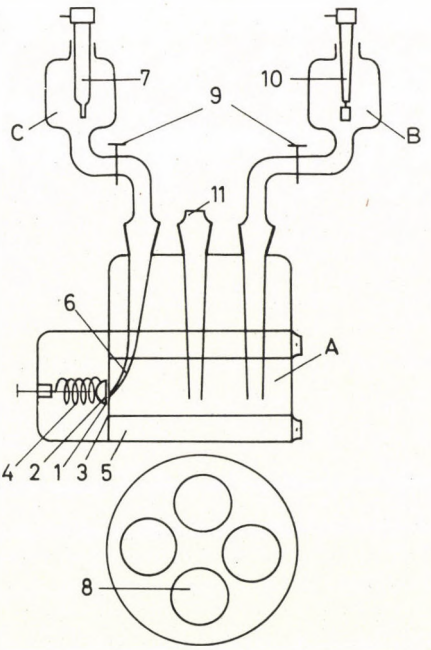

Fig. 3. Measuring cell. *A:* measuring compartment, *B:* auxiliary electrode, *C:* normal calomel electrode. 1: circular opening, 2: sealing ring, 3: germanium electrode, 4: clamping spring, 5: clamping device, 6: Luggin capillary (⌀ 1 mm), 7: calomel electrode, 8: gas scrubber, 9: taps, 10: platinum electrode, 11: N_2 gas inlet

The end of the latter, which finishes as a bent capillary of 1 mm internal diameter, extends to the surface of the Ge sample. The Ge disc used as measuring electrode (3) is pressed from outside to a circular, polished-rimmed hole in the side of vessel A by a clamping device (5). A plastic ring (2) was used for sealing.

This measuring electrode arrangement, which was also used by SHEFF, GATOS and ZWERDLING [39], is more advantageous than the usual electrode arrangement: here only the germanium surface comes into contact with the solution, and hence the possibility of contamination is markedly reduced.

The measuring cell was placed in a dark thermostat, and the measurements made at 25 °C. The accuracy of the thermostating was ± 0.1 °C.

Electrodes. N-type germanium of 6—10 ohm · cm specific resistance, and (111) orientation, was prepared from a single crystal. After cutting to size ($11 \times 11 \times 0.4$ mm), grinding and polishing, the samples were classified by the following control measurements:

measurement of specific resistance,
measurement of dislocation density,
orientation measurement,
microscopic surface study,
interference microscopic study.

After classification the samples were degreased by boiling for 5 min in CCl_4, rinsed in distilled water, etched at 70 °C for 30 sec in CP-4A etching solution (25 ml acetic acid, 25 ml nitric acid, 15 ml hydrofluoric acid), washed in deionized water, and then rinsed in distilled water. An ohmic contact was prepared by alloying. (The contact material was tin foil; the alloying was made in a hydrogen furnace at 420 °C with rapid heating-up, and lasted 20 min.)

The ohmic nature of the contact was checked by recording the characteristics, and the side of the contact was then covered with epokit resin.

The final electrode surface was formed with a further etching at 70 °C for 2 min with CP-4A etching solution, followed by thorough washing with doubly distilled water. The ready samples were kept for four days in doubly distilled water: ellipsometric studies showed that

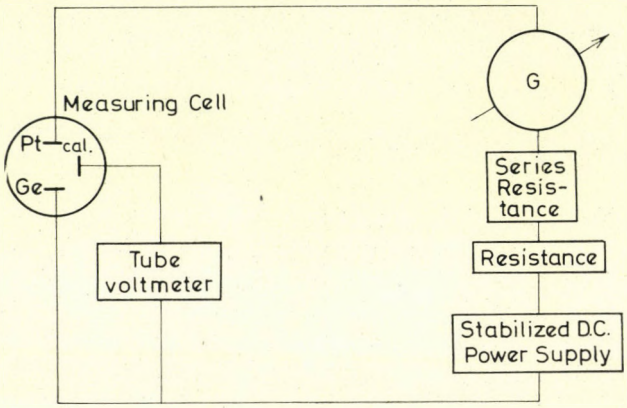

Fig. 4. Measuring circuit

during this soaking the thickness of the oxide layer increases (see Table IV). The reproduction of the measurements on the oxide surface formed *in this way* was good (the scatter decreased by a factor of three).

Preparation and purification of the solutions. The measuring solutions were prepared from analytical grade reagents and water which had been deionized and doubly distilled in a quartz vessel; they were then purified by a standard shaking procedure with a given amount of germanium powder.

The nominal GeO_2 content of the measuring solutions thus prepared was adjusted to 0.003 g/l. For the study of the effect of GeO_2, the 'GeO_2' contents of K_2SO_4 solutions with nominal GeO_2 contents of 4.0 g/l and 0.4 g/l were adjusted with a solution of GeO_2 dissolved in 2*N* KOH, before the adjustment of the pH. The GeO_2 content in the prepared solutions was checked analytically by a spectrophotometric method [40]. The pH of the solutions was adjusted with H_2SO_4 or KOH in nitrogen atmosphere. Stable and *measurable* pH values were obtained after 10 min in acidic solution, after 25 min in neutral or weakly basic solutions, and after 100 min in strongly alkaline solution.

Measuring equipment. A high input-resistance tube voltmeter (Radelkis type OP 401/1) was used for potential and pH measurements, while a transistor-stabilized rectifier served as a direct current source for the galvanostatic polarization measurements. The experimental set-up is shown in Fig. 4.

Procedure. The measuring cell was cleaned in a mixed solution of hydrogen peroxide and sulfuric acid, and then washed with deionized, doubly distilled water. After the apparatus had been set up, it was filled with distilled water, left to stand for 24 hours, and then washed thoroughly with the measuring solution and filled with this.

The rest potential was measured against a normal calomel reference electrode as a function of time up to the attainment of a stationary state; during this, nitrogen gas (purified by passage through a deoxygenator, a portion of the measuring solution, and a G-4 glass filter) was bubbled through to ensure the absence of oxygen and carbon dioxide.

In the polarization potential measurements the measuring system was first cathodically polarized (with the use of a platinum auxiliary electrode). The current density was varied

between 10^{-7} and 10^{-3} A/cm^2, proceeding from lower to higher current densities. The individual polarization potentials were read off after attainment of the stationary state (generally 5 min). After the cathodic polarization was stopped, the re-establishment of the rest potential value was awaited, and then an anodic polarization curve was recorded, similarly to the cathodic one. The measured potentials were converted to those relative to the normal hydrogen electrode. Before the polarization measurements the rest potential was always measured as described above.

Conditions of reproducibility of potential measurements. Deciding roles are played in the reproducibility of the results by the internal (type, specific resistance) and surface (mechanical and chemical surface treatment, orientation) parameters of the electrode, the temperature and

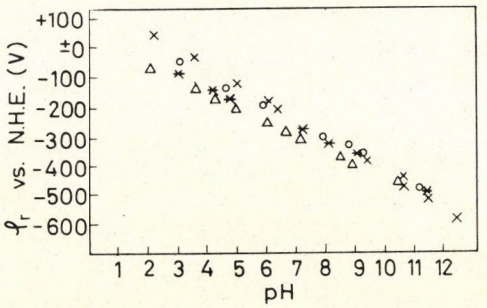

Fig. 5. Dependence of φ_r on pH

× 0.1*N* K_2SO_4; ○ 0.1*N* KCl; ⋇ 0.1*N* KBr; △ 0.1*N* KI; adjustment of pH with H_2SO_4 and KOH at 25 °C in N_2 atmosphere

lighting conditions, the composition of the solutions, its purity, pH, and freedom from oxygen and carbon dioxide. This latter can be achieved by the continuous passage of an inert gas (*e.g.* nitrogen).

The change of the pH of the solution during the measurements was never more than 0.2—0.3 pH unit.

The pH of KI measuring solution changes in time on the effect of light, as a result of the well-known photocatalytic reaction. In order for the pH to be stabilized, it was necessary to keep the solution in the dark.

In the case of using an inert gas atmosphere and keeping the solutions in the dark, the reproducibility of the rest potentials is ±10 mV with 80% of the samples used; however, with the other 20% it was only 40—50 mV. A pre-polarization for 10 min at an anodic current density of 1×10^{-6} A/cm^2 brought about a further improvement in the reproducibility. The reproducibility was similar in the measurement of the polarization potentials.

Experimental results

Study of the rest potential

According to our experimental data, the rest potential depends on the *pH of the solution* and in the pH interval 2—12 in all the solutions studied can be described within experimental error by a linear relation (Fig. 5, Table I).

If the results of our measurements in potassium sulfate solution are compared (see Fig. 1) with the potential measurements of HARVEY and GATOS [2] (taken only in acidic solutions) and the potential values calculated from

Table I

Rest potential data at different pH values (referred to the normal hydrogen electrode)

Electrolyte solution	pH				
	2.5	4	6	9	11
0.1*N* K_2SO_4	+45	− 55	−182	−370	−500
0.1*N* KCl	−20	−100	−210	−360	−470
0.1*N* KBr	−55	−135	−233	−370	−470
0.1*N* KI	−92	−170	−265	−450	−500

capacity measurements by BODDY and BRATTAIN [4], it is seen that these authors report values which are significantly more positive than our own data. The results of LOVREČEK and BOCKRIS [1], however, agree well with our measurements. The pH region studied comprises three straight sections of different slopes; these correspond to the equilibrium reactions $Ge \rightarrow GeO_{brown}$, $Ge \rightarrow GeO_{yellow}$, and $Ge \rightarrow GeO_3^{2-}$. BODDY and BRATTAIN obtained a linear relation in the pH interval 4.5—11.

It can be seen from Fig. 5 that with the increase of pH the potential is displaced in the negative direction.

In the alkaline region φ_r can be said to be independent of *the anion in the solution*, while proceeding towards the acidic region the φ_r values at a given pH are shifted more in the negative direction, the better adsorbed is the ion in question (Fig. 5). The greatest anion effect can be observed in the case of the iodide solution in the acidic region.

The described relation between the rest potential and the pH holds also in many *buffer solutions* (Fig. 6). According to our observations, and in contrast to the previous opinion (BODDY [5]), the potassium hydrogen phthalate buffer solution shows an anomaly in the acidic region, and, to extents depending on the pH, shifts φ_r in the positive direction compared with the other buffer solutions.

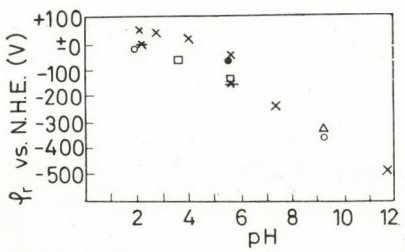

Fig. 6. Dependence of φ_r on the pH in buffer solutions

○ Clark-Lubs; △ Sörensen; ✳ McIlvaine; □ Walpole; × potassium hydrogen phthalate; 25 °C, N_2 atm.

The gradient of the pH-dependence of the rest potential ($\Delta\varphi_r/\Delta$pH) likewise depends on the anion in the solution: it decreases in the order of the adsorption series as shown in Table II.

Table II

Slope ($\Delta\varphi_r/\Delta pH$) of the rest potential vs. pH curves

	0.1*N* K_2SO_4	0.1*N* KCl	0.1*N* KBr	0.1*N* KI	potassium hydrogen phthalate 0.2*M*
$\frac{\Delta\varphi_r}{\Delta pH}$	0.063	0.053	0.049	0.047	0.055

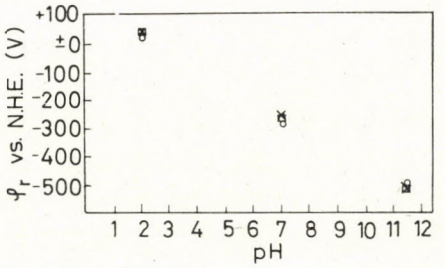

Fig. 7. Dependence of φ_r on GeO_2 concentration in 0.1*N* K_2SO_4 solution at 25 °C; N_2 atmosphere × 0.003 g/l; □ 0.4 g/l; ○ 4.0 g/l GeO_2

For the further clarification of the nature of the potential, a study was made of the effect of the GeO_2 content of the solution at three concentrations (4.0, 0.4 and 0.003 g/l GeO_2).

The results (Fig. 7) show that in a wide concentration range the rest potential is independent of the GeO_2 content: this agrees with the observation of LOVREČEK and BOCKRIS [1], according to which the further addition of GeO_2 to a solution containing 0.036 *M* GeO_2 does not cause any perceptible change in the potential. Attention must be drawn to the opposite experimental observations of HARVEY and GATOS [8], according to which the rest potential shifts in the positive direction with increasing GeO_2 concentration (these measurements were made in an atmosphere of oxygen!).

A study was also made of the effect of *various chemical treatments* on the rest potential of germanium electrodes, and on the change of the potential with time (Fig. 8). It can be seen from the measurements that the forms of the potential *vs.* time curves are different for the variously treated electrodes, but there is no significant difference between the rest potentials obtained. The nature of the curves depicting the change in time depends on the quality of the oxide layer formed during the treatment.

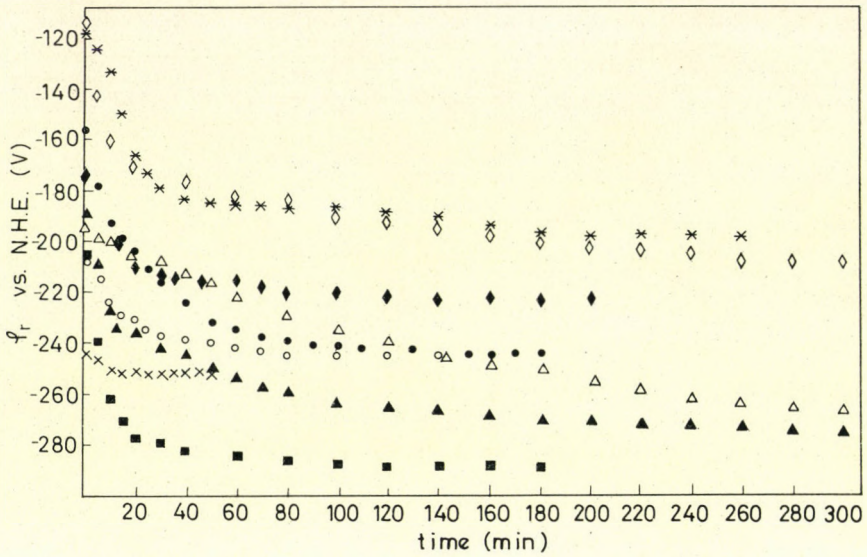

Fig. 8. Dependence of φ_r on time on differently treated electrode surfaces, in 0.1*N* K_2SO_4 at 25 °C, in N_2 atmosphere
× CP-4A; ○ CP-4A + standing in distilled water; ● CP-4A + H_2 reduction; ⚹ HNO_3; △ H_2O_2 + Li_2CO_3; ■ H_2O_2 + Li_2CO_3 + standing in distilled water; ♦ hot H_2O_2; ◇ hot H_2O_2 + standing in distilled water; ▲ etchant 8 (period of standing in distilled water: 24 hrs)

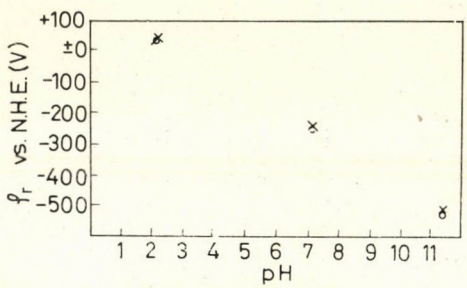

Fig. 9. Dependence of φ_r on the rotation. 0.1*N* K_2SO_4 solution, 25 °C, N_2 atmosphere

As Fig. 9 shows, the rest potential in a solution which is strongly stirred with a stream of nitrogen depends very slightly on the *rotation of the electrode.*

From a study of the *temperature-dependence* of the rest potential, it was observed that if the temperature is increased from 25 °C to 60 °C, the potential is shifted in the negative direction by about 100 mV (Fig. 10).

Study of the polarization potentials

It can be seen from Figs 11—16, 20 and 21 that for all the solutions examined, *the anodic polarization curves* consist of one section in the current density range 5×10^{-7}—10^{-4} A/cm², and follow the Tafel relation. At current

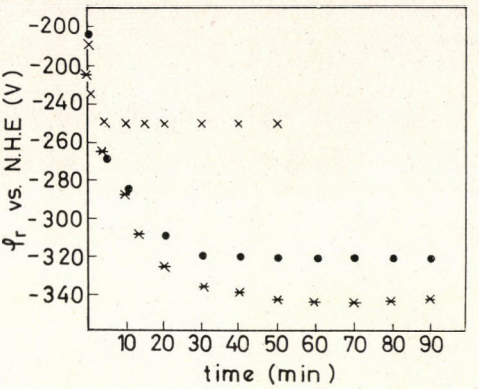

Fig. 10. Dependence of φ_r on temperature. 0.1*N* K_2SO_4 solution, N_2 atmosphere
× 25 °C; ● 40 °C; ⚹ 60 °C

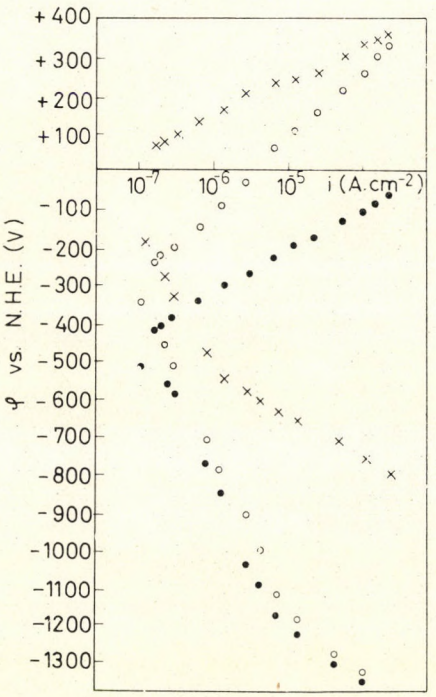

Fig. 11. Polarization curve in 0.1*N* K_2SO_4 solution at 25 °C, N_2 atmosphere
× pH 2.21; ○ pH 6.5; ● pH 11.4

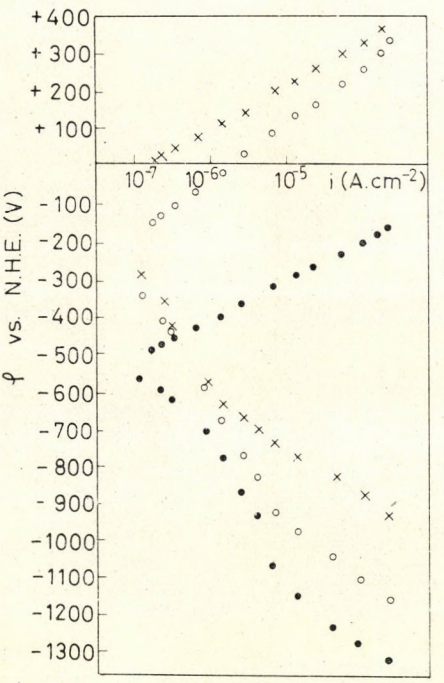

Fig. 12. Polarization curve in 0.1*N* KCl solution at 25 °C, N_2 atmosphere
× pH 2.53; ○ pH 6.0; ● pH 11.6

densities greater than 10^{-4} A/cm^2, a new polarization stage begins, for which the Tafel equation is not valid. Our data in the low current density region agree with the measurements of BODDY [26] made under almost the same conditions, but in our case a wider current density interval can be described with the same constant *b*.

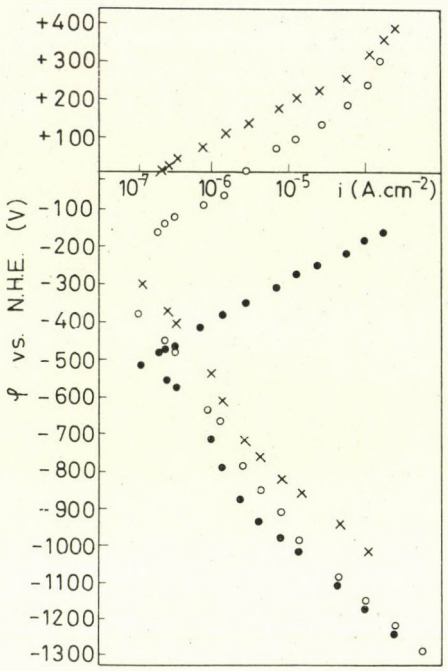

Fig. 13. Polarization curve in 0.1*N* KBr solution at 25 °C, in N_2 atmosphere
× pH 2.71; ○ pH 6.5; ● pH 11.3

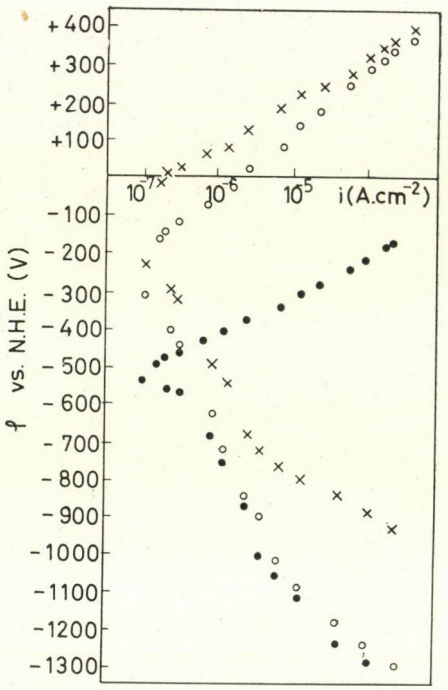

Fig. 14. Polarization curve in 0.1*N* KI solution at 25 °C, in N_2 atmosphere
× pH 2.22; ○ pH 6.59; ● pH 11.5

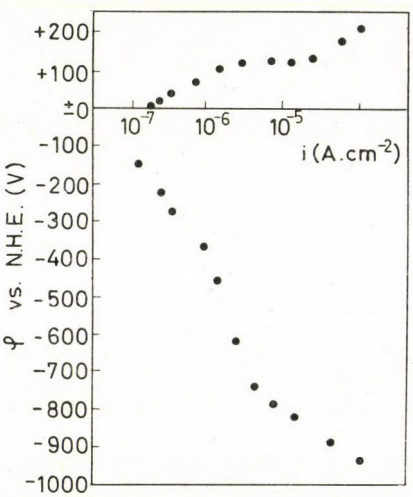

Fig. 15. Polarization curve in potassium hydrogen phthalate solution at pH 5.6

The cathodic polarization curves after the attainment of the necessary overvoltage can be considered as consisting of two sections, I_c and II_c, proceeding towards higher current densities, with different slopes, but both following the Tafel relation. The point of break between the two sections shifts towards higher current densities in solutions of higher pH.

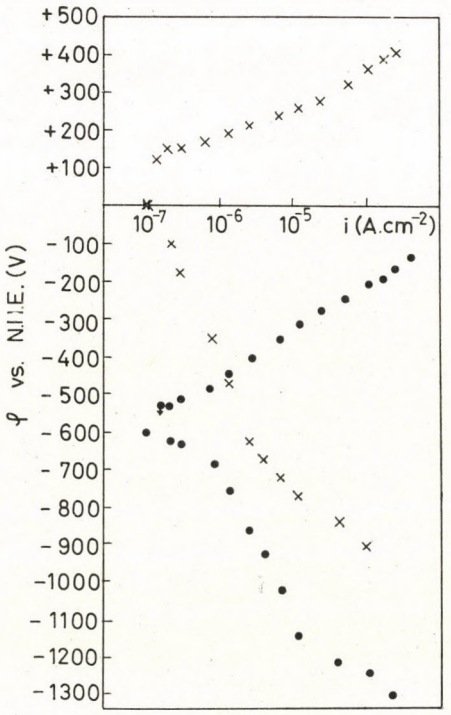

Fig. 16. Polarization curves in H_2SO_4 and in KOH
× pH 2.4; ● pH 11.6

The *b* values of the Tafel equations for the individual sections were calculated (Table III); it should be noted that while the *b* values for the anodic curve and the cathodic II sections for the various solutions are 0.100—0.120 (a little higher in neutral solution: 0.130—0.160) and agree well with the literature data (0.12—0.16 [10, 18, 23, 24, 25]), the first sections of the cathodic curves are very steep with *b* values of about 0.4. Similar observations were made by YEFIMOV and YERUSALIMCHIK [24]; on the cathodic curves taken in 0.1*N* HCl at higher current densities they distinguish 3 sections, for which the *b* values are 0.12, 0.47 and 0.12.

The polarization curves follow the tendency of the *pH-dependence* of φ_r; with the increase of pH, at a given current density the polarization potentials shift in a more negative direction. However, the gradient of the pH-

Table III

The coefficient b of the Tafel relation

Solution composition	pH	Anodic polarization	Cathodic polarization	
		b	b_I	b_{II}
0.1*N* K_2SO_4	acidic	0.098	0.370	0.122
	neutral	0.188	0.440	0.120
	alkaline	0.095	0.418	0.120
0.1*N* KCl	acidic	0.120	0.360	0.140
	neutral	0.155	0.420	0.110
	alkaline	0.100	0.400	0.130
0.1*N* KBr	acidic	0.100	0.330	0.130
	neutral	0.147	0.380	0.170
	alkaline	0.115	0.360	0.160
0.1*N* KI	acidic	0.110	0.320	0.140
	neutral	0.150	0.380	0.150
	alkaline	0.100	0.395	0.130
potassium hydrogen phthalate	neutral	0.020	0.520	0.125

dependence of the polarization potential does not agree with the gradient of the pH-dependence of the rest potential. Although the potential difference between the anodic curves recorded in acidic and alkaline solutions corresponds approximately to the difference of the rest potentials, the polarization curve measured in neutral solution is no longer parallel to these two. In the section I_c of the cathodic polarization curves the pH-dependence of the polarization potentials is generally less than that of the rest potentials, and indeed there is scarcely any difference between the polarization potentials measured in neutral and alkaline media. The pH-dependence of the II_c section is about the same as the usual pH-dependence of hydrogen electrodes.

In the case of the solutions of different pH, the potential values (Figs 11—14), beginning at which our anodic curves are well reproducible (5×10^{-7} A/cm^2), and where the II_c sections of our cathodic curves begin, agree with these potential values reported by GERISCHER *et al.* [28] (for solutions containing less readily adsorbing ions, such as H_2SO_4, nitrate buffer, phosphate buffer, glycol buffer, KOH), relative to which, at more positive and negative potentials, the authors presume a pure hydroxide (anodic curve) and a pure hydride (cathodic curve) surface.

The polarization curves in the current density range measured by us are essentially determined, within experimental error, by the pH. The effects of other ionic species are substantially smaller, but in the anodic current density

range studied, an overvoltage-decreasing effect of the iodide was readily observable. The experimental results of HOLMES [16] and YEFIMOV and YERUSALIMCHIK [19] are similar in the high current density region.

The polarization curves are temperature-dependent in every section (Fig. 17). From our experimental results a temperature difference of 20 °C

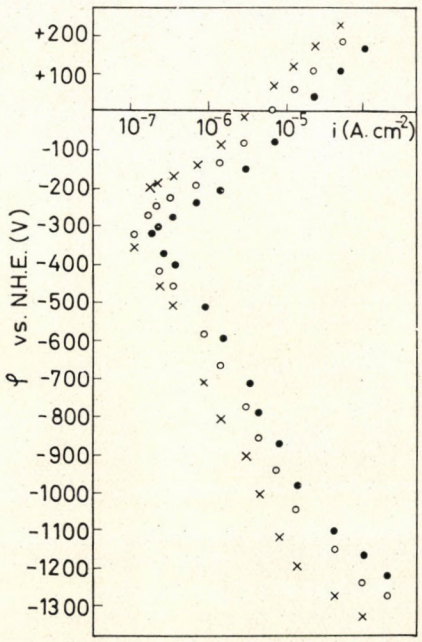

Fig. 17. Dependence of the polarization curve on temperature. 0.1*N* K_2SO_4 solution, N_2 atmosphere. × 25 °C; ○ 40 °C; ● 60 °C

corresponds to a potential difference of 80—100 mV. With the decrease of temperature the anodic curves shift in the direction of more positive potentials. The temperature coefficient of current densities referring to the same potentials is 1.4/10 °C, and the calculated activation energy is 7.1 kcal/mol. According to HARVEY and GATOS [2, 41], the dissolution of germanium at low oxygen concentrations is determined by diffusion (the calculated activation energy is 4.6 kcal/mol), while at high oxygen concentration the activation energy is 16.2 kcal/mol [41], which points to the presence of an activation overvoltage.

In both the anodic and cathodic sections the polarization potentials rapidly *attain the stationary value* (Fig. 18).

If the polarization current is discontinued, in the low current density ($i_a = 10^{-5}$ A/cm²) section of the anodic curve and the I_c section of the cathodic curve, the potential is restored in a short time to the potential φ_r before the

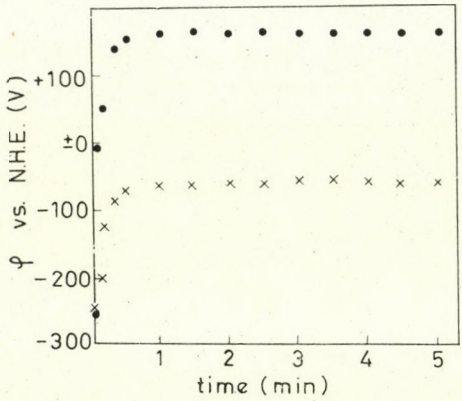

Fig. 18. Dependence of polarization potential on time. 0.1*N* K_2SO_4 × $1 \cdot 10^{-6}$ A/cm²; ● $1 \cdot 10^{-5}$ A/cm²

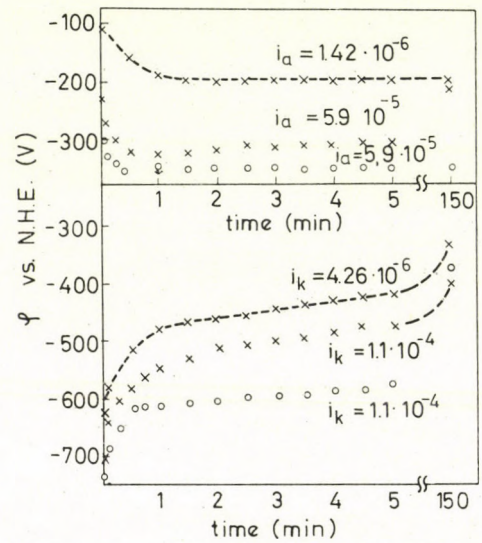

Fig. 19. Anodic–cathodic drop-out curves. 0.1*N* K_2SO_4, N_2 atmosphere × 25 °C; ○ 60 °C

polarization. In the higher current density sections of the anodic curves the restoration takes a longer time. The time necessary for the restoration of φ_r in II_c is very long, as can be seen in Fig. 19. The conclusion can be drawn from the curves that at small anodic and cathodic currents the surface formed does not differ substantially from the equilibrium surface, while at high cathodic polarization a surface of significantly different character must be present. Our observations have led to conclusions which agree with those drawn by GERISCHER *et al.* [28, 31] from measurements of a different nature (see introductory section).

From a study in a wide concentration interval of the effect on the polarization curves of the concentration of germanium oxide in the solution (this was expressed as GeO_2, but in part other germanium compounds may be present) (Fig. 20), it was found that the course of the curves is identical, the current and potential values of the break-points agree, and thus the polarization curves are independent of the GeO_2 content.

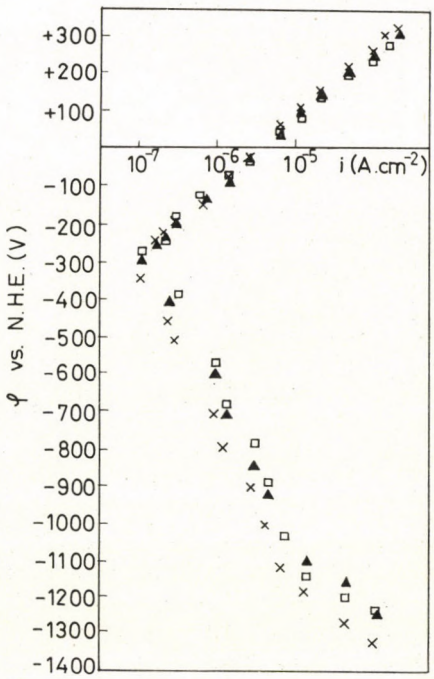

Fig. 20. Dependence of the polarization curve on GeO_2 concentration. 0.1N K_2SO_4 solution. × 0.003 g/l GeO_2; □ 0.4 g/l; ▲ 4.0 g/l

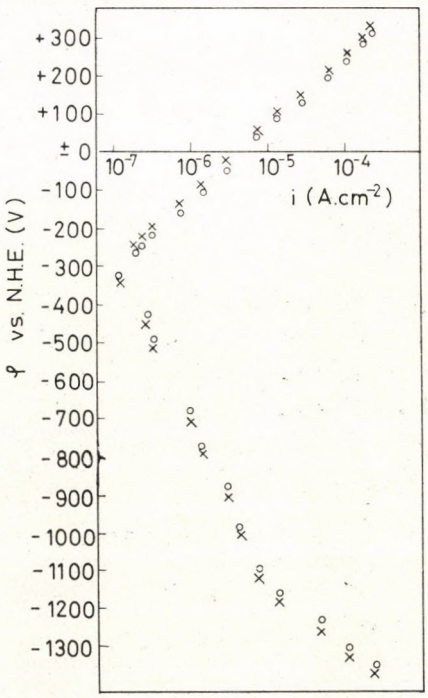

Fig. 21. Dependence of the polarization curve on electrode rotation. × non-rotating electrode; ○ rotating electrode

The study of the effect of electrode rotation (Fig. 21) shows that within experimental error the anodic and the I_c polarization sections are independent of the rotation, while the potential values of the II_c section are shifted slightly (by 10—30 mV) in the direction of less negative potentials. This practical lack of dependence on the rotation indicates that in the polarization regions studied no significant diffusion polarization need be considered.

To supplement and to support the conclusions drawn from the previous experimental results, the *thickness of the oxide layer* was measured by an *ellipsometric method.*

Germanium samples which had been freshly etched under standard conditions were placed in doubly distilled water immediately after being washed. The thickness of the surface oxide layer formed during the etching varies with the soaking period according to the data given in Table IV. These measurements explain the effect of the soaking in distilled water.

Table IV

Increase of oxide thickness during soaking in deionized, doubly distilled water

	After etching	Soaking for		
		1 day	3 days	6 days
Oxide layer thickness, Å	23.0	49.5	64.5	62.0

A study was also made with this method of the effect of electrochemical treatment (anodic or cathodic polarization) on similarly freshly etched electrodes. From the measurement the increase of the layer thickness can be established during both anodic and cathodic polarizations (Table V).

Table V

Effect of electrochemical treatment on the change of oxide layer thickness on a chemically treated germanium single crystal electrode

Sample number	φ_r	Polarization characteristics A/cm²			Increase of oxide layer thickness Å
		$i_{=a}$	$i_{=c}$	time min.	
1	−280	1.05×10^{-4}		60	27.1
2	−284	5×10^{-5}		60	10.8
3	−286	2.8×10^{-6}		60	9.9
4	−263		1.1×10^{-4}	60	51.4
5	−285		5.0×10^{-5}	60	49.6
6	−282		2.8×10^{-6}	60	18.1

The measurements were made in a 0.1*N* K_2SO_4 solution of pH 6.7.

Considering the oxidation conditions, the layer formed in the anodic process can only be some germanium oxide. The nature of the surface compound formed in the cathodic process is not so clearly defined. In accordance with the reduction conditions during the cathodic electrochemical treatment, the probable process is the decomposition of the surface oxide layer or the formation and increase of some germanium-hydrogen compound. Although the

data are difficult to evaluate in this section because of the lack of refractive indices, it seems likely that this section is not characterized by simple reduction of the oxide in the direction opposite to the anodic reaction.

Discussion of the experimental results

As regards the nature of the reactions determining the rest potential, it can be established from the experimental results that the rest potential is not a reversible ion-exchange, nor a reversible redox potential, but a corrosion potential. The corrosion potential is determined by the simultaneous progress of two (or more) anode and cathode processes with identical rates but opposite directions. The stationary state in the two or more reactions is obtained at a rate leading to charge equilibrium, but at the same time a material equilibrium does not develop. The reversible ion-exchange reactions can be excluded because of the anion effect and the pH-dependence, and the reversible redox reaction from the germanium dioxide content. The corrosion character is indicated by the fact that (as shown by our ellipsometric measurements) the thickness of the surface oxide layer of the germanium electrode increases for a certain time in a current-free state. In other words, the facts show that besides the oxidation anode reactions the reduction of the oxide does occur at a low rate, but this is not the determining process.

The analysis of the experimental results leads to the conclusion that the reactions determining the rest potential and the polarization potential are closely connected with one another. The reactions forming the corrosion rest potential are presumably identical with the polarization processes of low current density. This is supported by the fact that the exchange current potential extrapolated from the I_a and I_c polarization curve sections (Figs 11—14) is almost the same as the rest potential, and also by the fact that the polarization potential in the I_a and I_c sections rapidly returns to the original rest potential level after the current is discontinued. It can be concluded from this that the nature of the surface formed under these polarization conditions is completely or partially the same as that existing under the conditions of the rest potential.

To prove the corrosion nature of the *rest potential*, it is necessary to select and confirm those anode and cathode processes the joint progress of which determines this potential at the $\Sigma i_a = \Sigma i_c$ charge equilibrium.

In the third part of this series [42] we study the possible reversible reactions. The scheme for the overall process leading to the corrosion potential is shown in Fig. 22 for the case of pH 2.2.

The most probable of the germanium oxidation reactions producing the corrosion potential are:

$$Ge + H_2O \rightleftharpoons GeO_{brown} + 2H^+ + 2e^- \text{ in acidic and neutral medium,}$$
$$Ge + OH^- \rightleftharpoons GeO_{brown} + H^+ + 2e^- \text{ in alkaline medium}$$

since that anodic reaction is the most probable the thermodynamic potential of which is the most positive from among the reactions with reversible potentials more negative than the corrosion. Of the several possible oxidation steps, for the sake of simplicity, only this one has been given in the figure.

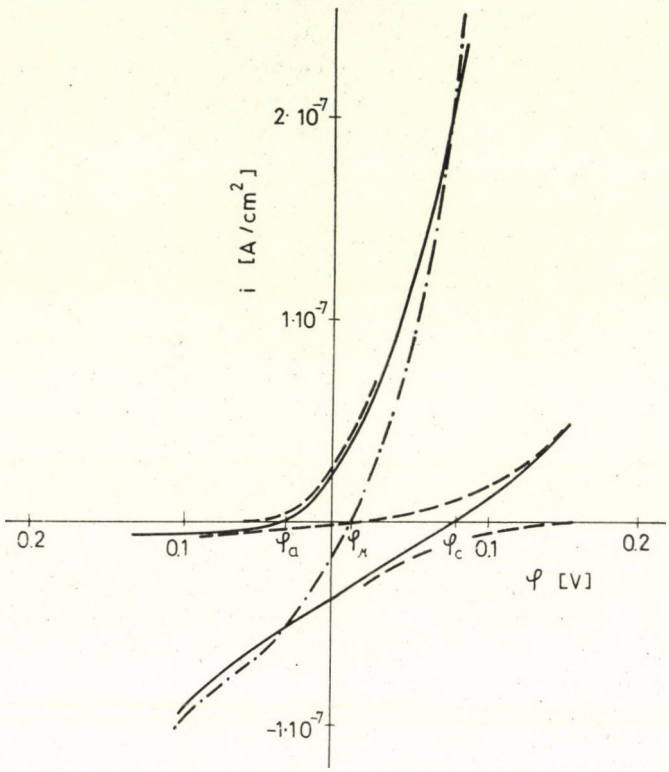

Fig. 22. Potential–current relationships in the region of the rest potential. ·—·—·—· experimental polarization curve; ——— oxide formation and decomposition, and hydride and hydrogen formation and decomposition curves; - - - - - partial current curves of the reactions; φ_a, φ_c: reversible potentials of the corresponding processes; φ_r: rest (mixed) potential

The reaction determining the cathodic potential cannot be only the above-mentioned reduction of the oxide. Of the possible reactions, the evolution of hydrogen can occur with a very low rate, as is indicated by the very small exchange current of the reaction [24, 45]. Under our experimental conditions it can be assumed with high probability that one of the steps of the hydrogen evolution process, hydride formation, occurs with a considerable rate:

$$Ge + H^+ + e^- \rightleftharpoons Ge - H \qquad \text{in acidic and neutral medium}$$
$$Ge + H_2O + e^- \rightleftharpoons Ge - H + OH^- \qquad \text{in alkaline medium}$$

There are no data in the literature on the reversible potential of this reaction, and the thermodynamic data necessary for the calculation are also lacking. We shall return to the confirmation of the reaction in parts II and III [42].

The points $i = 0$ of the reactions described were assigned at the calculated reversible potential values; in the construction of the polarization curves we made use of the assumptions for the measured overall reaction, the most decisive of which was that because of the nature determining the corrosion (irreversible) potential, the oxidation and reduction directions of the oxide reaction are strongly asymmetric; it could thus be explained that although our experimental conditions were close to the equilibrium, the rate of the oxide reduction appears negligible beside the other cathode reactions assumed.

The pH-dependence of the corrosion potential is determined by the pH-dependence of the individual reactions.

The anion effect too can easily be explained on the basis of our model. In accordance with the literature already mentioned and our own measurements [43], the specific chemisorption of the iodide ion can be accepted as a fact on the current-free electrode. GIBER *et al.* [43] have also shown experimentally that this adsorption decreases with the increase of the current density. According to our assumption, as a result of this adsorption, the i *vs.* φ curve of the germanium oxidation reaction will be more steep. This can lead to the shift of the corrosion potential towards more negative values. Other authors [44] have also dealt with such an explanation of the anion effect in other systems.

Discussion of some characteristics of the polarization curves

The *anodic* polarization process is some oxidation reaction. This is supported by the fact that the growth of the oxide layer can be demonstrated ellipsometrically during the anodic polarization, and by the fact that in the high current density part of the measured current density range, prolonged anodic polarization causes a pH shift in the solution in the acidic direction.

If it is assumed that the polarization reaction in the current density interval of the anodic section measured by us is the same as the anode reaction of the rest potential, then the following anodic polarization reaction can be presumed:

$$Ge + H_2O \rightleftharpoons GeO + 2H^+ + 2e^-$$

It is assumed in this reaction that the free germanium surface is oxidized. This assumption neglects the fact that at low current densities the surface is not exclusively covered with oxide, but also with germanium hydride, and during the anodic polarization the oxidation of the hydride also takes place, with a low rate and as a non-typical process.

In anodic polarization in the above oxidation reaction, an activation mechanism is assumed in acidic and alkaline media. The current densities studied by us are too small for their effects to be felt by the low state of the hole concentration in the N-type germanium. The hole diffusion limiting current calculated from the known relations for room temperature in the case of a specific resistance of 6—10 ohm·cm turned out to be greater than 1×10^{-4} A/cm^2, and during anodic polarization this limiting current region was not reached. The b value of these polarization regions also points to an activation mechanism. In neutral medium the b value differs slightly. In our view this can be explained by the fact that some process connected with the state of the oxide layer forming (in neutral medium the solubility of the oxide is different, and the density of the oxide may be different) also plays a part in the determination of the rate of the overall process.

From similar considerations for the *cathodic* polarization, and from the fact that there is no thinning of the surface layer in either the I_c or the II_c sections, it can be concluded that the rate of reduction of the oxide is not appreciable in the potential region studied; the characteristic processes are rather hydride formation and hydrogen evolution according to the following reactions;

$$\begin{aligned} &Ge + H_3O^+ + e^- \rightleftharpoons Ge - H + H_2O \quad \text{in acidic solution} \\ &Ge + H_2O + e^- \rightleftharpoons Ge - H + OH^- \text{ in neutral and alkaline solution} \end{aligned} \tag{1}$$

$$Ge - H + H^+ + e^- \rightleftharpoons Ge + H_2 \tag{2}$$

The slopes of the polarization sections I_c and II_c differ; the slope of the I_c section ($b = 0.4$) is much higher than that of the II_c section ($b = 0.12$—0.14). From this the conclusion can be drawn that at a given polarization potential during cathodic polarization a change of mechanism occurs, *i.e.* the rate-determining step of the above reaction is different in the I_c section from that in the II_c section. The position of the appearance of this change of mechanism depends on the pH of the solution. In acidic solution it occurs at a lower overvoltage than in alkaline and neutral solutions.

As regards the kinetic nature of the process, the following can be said for the I_c section. The formation of a diffusion overvoltage is not likely since there is no need in the electrode process for a reagent the slow diffusion of which to the electrode surface would impede the electrode process.

The best explanation for the experimental data is the assumption that at low current densities the rate of reaction (2) can still be neglected compared with that of reaction (1), and thus in the I_c section reaction (1) can be taken as potential-determining.

In the II_c section, however, the rate of reaction (2) is also significant.

The rates of the above reactions are affected in a decisive way by the nature of the surface in the given polarization section.

REFERENCES

1. LOVREČEK, B., BOCKRIS, J. O'M.: J. Phys. Chem. **63,** 1368 (1959)
2. HARVEY, W. W., GATOS, H. C.: J. Electrochem. Soc. **107,** 65 (1960)
3. HARVEY, W. W., LAFLEUR, W. J., GATOS, H. C.: J. Electrochem. Soc. **109,** 155 (1962)
4. BODDY, P. J., BRATTAIN, W. H.: J. Electrochem. Soc. **110,** 570 (1963)
5. BODDY, P. J.: J. Electroanal. Chem. **10,** 199 (1965)
6. VASENIN, R. M.: Zhur. Fiz. Khim. **27,** 878 (1953)
7. UKSHE, E. A., LEVICH, A. I.: Zhur. Fiz. Khim. **29,** 219 (1955)
8. HARVEY, W. W., GATOS, H. C.: J. Appl. Phys. **29,** 1267 (1958)
9. YEFIMOV, E. A., YERUSALIMCHIK, I. G.: Zhur. Fiz. Khim. **33,** 441 (1959)
10. BOROVKOV, I. V.: Zhur. Fiz. Khim. **34,** 2682 (1960)
11. DYERYAGINA, O. G.: Elektrokhimiya **1,** 267 (1965)
12. PLESKOV, YU. V.: Elektrokhimiya **3,** 4 (1967)
13. ROMANOV, O. V., KONOROV, R.: Fiz. Tverd. Tiela **8,** 13 (1966)
14. POURBAIX, M.: Atlas d'Equilibres Electrochimiques. Gauthier-Villars, 1963
15. JIRSA, F.: Z. anorg. allg. Chem. **268,** 84 (1952)
16. HOLMES, P. J.: The Electrochemistry of Semiconductors. Academic Press, London and New York, 1962
17. PLESKOV, YU. V.: Khim. Nauka i Prom. **3,** 443 (1958)
18. GERISCHER, H., BECK, F.: Z. Phys. Chem. **13,** 389 (1957)
19. YEFIMOV, E. A., YERUSALIMCHIK, I. G.: Dokl. Akad. Nauk. SSSR **128,** 124 (1959)
20. YEFIMOV, E. A., YERUSALIMCHIK, I. G.: Zhur. Fiz. Khim. **35,** 543 (1961)
21. TURNER, D. R.: J. Electrochem. Soc. **103,** 252 (1956)
22. YEFIMOV, E. A., YERUSALIMCHIK, I. G.: Zhur. Fiz. Khim. **32,** 1103 (1958)
23. YEFIMOV, E. A., YERUSALIMCHIK, I. G.: Zhur. Fiz. Khim. **32,** 413 (1958)
24. YEFIMOV, E. A., YERUSALIMCHIK, I. G.: Zhur. Fiz. Khim. **9,** 1967 (1959)
25. GREEN, M.: Nature **182,** 1592 (1958)
26. BODDY, P. J.: J. Electrochem. Soc. **111,** 1136 (1964)
27. BOHNENKAMP, K., ENGEL, H. J.: Z. Elektrochemie **61,** 1184 (1957)
28. GERISCHER, H., HOFFMANN-PEREZ, M., MINDT, W.: Berichte Bunsenges. **69,** 130 (1965)
29. BARDELEBEN, J.: Z. Phys. Chem. **17,** 39 (1958)
30. GERISCHER, H., MAURER, A., MINDT, W.: Surface Sci. **4,** 431 (1966)
31. HOFFMANN-PEREZ, M., GERISCHER, H.: Ber. Bunsenges. **65,** 771 (1961)
32. HARVEY, W. W., SHEFF, S., GATOS, H. C.: J. Electrochem. Soc. **107,** 560 (1960)
33. BECK, F., GERISCHER, H.: Z. Elektrochem. **63,** 500 (1959)
34. GERISCHER, H., BECK, F.: Z. Phys. Chem. Neue Folge **23,** 113 (1960)
35. GREEN, M.: J. Phys. Chem. Solids **14,** 77 (1960)
36. MYAMLIN, V. A., PLESKOV, YU. V.: Elektrokhimiya poluprovodnyikov. 1965.
37. TOSHIMA, S., UCHIDA, I.: Private communication, 1966
38. BRATTAIN, W. H., BODDY, P. J.: Surface Sci. **4,** 18 (1966)
39. SHEFF, S., GATOS, H. C., ZWERDLING, S.: Rev. Sci. Inst. **29,** 531 (1958)
40. Veszprém University of Chemical Industry, Dept. of Analytical Chemistry: Germanium determinations. Veszprém, 1966
41. HARVEY, W. W., GATOS, H. C.: J. Electrochem. Soc. **105,** 654 (1958)
42. GIBER, J., VAJASDY-PERCZEL, I., MARTON, D.: Acta chim. Acad. Sci. hung. (In press)
43. GIBER, J., FÜLÖP, M., KÁMORY, L., SZEKRÉNYESY, T.: Magy. Kém. Foly. (In press.)
44. FRUMKIN, A. N.: Acta Phys. et Chim. Debr. **XII,** 37 (1966)
45. GREEN, M.: Modern Aspects of Electrochemistry, No. 2. Ed. J. O'M. BOCKRIS, Chap. 5. Butterworth, London, 1959

János GIBER
Irma VAJASDY-PERCZEL } Budapest IV., Váci út 77.

Acta Chimica Academiae Scientiarum Hungaricae, Tomus 72 (1), pp. 59—64 (1972)

USE OF AMIDE CHLORIDES IN RING CLOSURE REACTIONS, IV

A NEW SYNTHESIS OF 4-AMINOQUINAZOLINE DERIVATIVES

Z. CSŰRÖS, R. SOÓS, I. BITTER and J. PÁLINKÁS

(Institute of Organic Chemical Technology, Technical University, Budapest)

Received August 26, 1970

N,N-Dimethyl-N′-(2-cyanophenyl)-formamidine hydrochloride was prepared from anthranilic amide and dimethylformamide chloride. N-substituted 4-aminoquinazoline derivatives were obtained from the resulting trisubstituted amidine in cyclization and simultaneous isomerization reactions with ammonia, primary aliphatic and aromatic amines, and hydrazine.

The group of aminoquinazolines includes several analgesics, antimalarial and antiviral agents [1, 2, 3]. The literature lists numerous procedures for their preparation. In almost all of them, the quinazoline skeleton is built up first, and the required product is then obtained by ammonolysis or aminolysis of a suitable group (chloro, alkoxy, mercapto, etc.). There are only a few methods known in which the amino group is introduced simultaneously with the cyclization reaction.

TAYLOR *et al.* [4] prepared 4-aminoquinazolines from anthranilic nitrile derivatives and nitriles. The above authors also described another procedure [5] in which the self-condensation of 5-nitroanthranilic nitrile gave a 4-aminoquinazoline derivative.

STEVENS and KREUTZBERGER [6] also used anthranilic nitrile derivatives as starting materials. Cyclization was accomplished with *s*-triazine. Just like in the methods described previously, the intermediate of cyclization was supposed to be N-(2-cyano-4-alkylphenyl)-formamidine.

The above syntheses require long reaction times and high temperatures and give only medium yields. These procedures are unsuitable for the preparation of N-substituted derivatives.

In our procedure, anthranilic amide (I) is used as the starting material. This compound is allowed to react with an equimolar quantity of dimethylformamide chloride(II) in chloroform solution.

This reaction resulting in N,N-dimethyl-N′-(2-carboxamidophenyl)-formamidine hydrochloride(III) was described in a previous paper [7].

On further addition of dimethylformamide chloride the acid amide group of the amidine is dehydrated and N,N-dimethyl-N′(2-cyanophenyl)-formamidine hydrochloride(IV) is obtained.

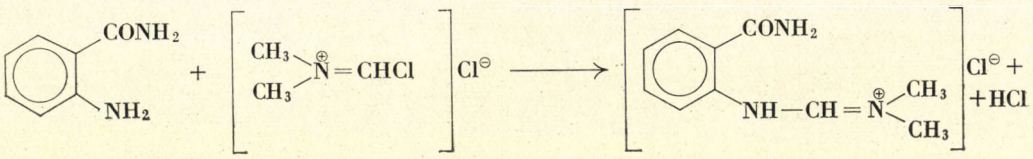

I II III

Of course, this product can also be prepared in one step by the reaction of anthranilic amide with 2 moles of amide chloride.

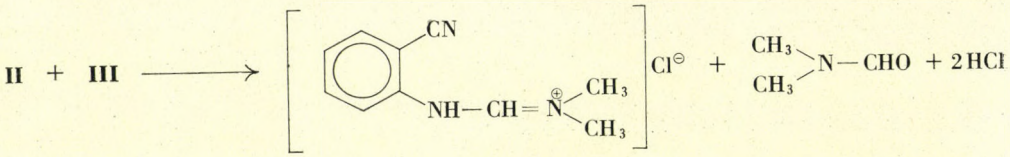

IV

N,N-dimethyl-N′-(2-cyanophenyl)-formamidine hydrochloride is not a new compound. SEEFELDER prepared it and its derivatives from substituted isatin-β-oxime and amide chloride; some of the products are important intermediates in the pharmaceutical, dye and insecticide industry [8].

Since the melting points of the substances prepared according to the two methods were different, the structure of the product obtained in our procedure was studied. The chloride content determined by titration with silver nitrate, as well as the result of the C, H, N analyses were in good agreement with the calculated data. The infrared spectrum of the substance is shown below, together with the spectrum of N,N-dimethyl-N′-phenylformamidine hydrochloride, in order to make the identification easier. (This latter compound was prepared from aniline and dimethylformamide chloride and identified on the basis of the melting point and the chloride content.)

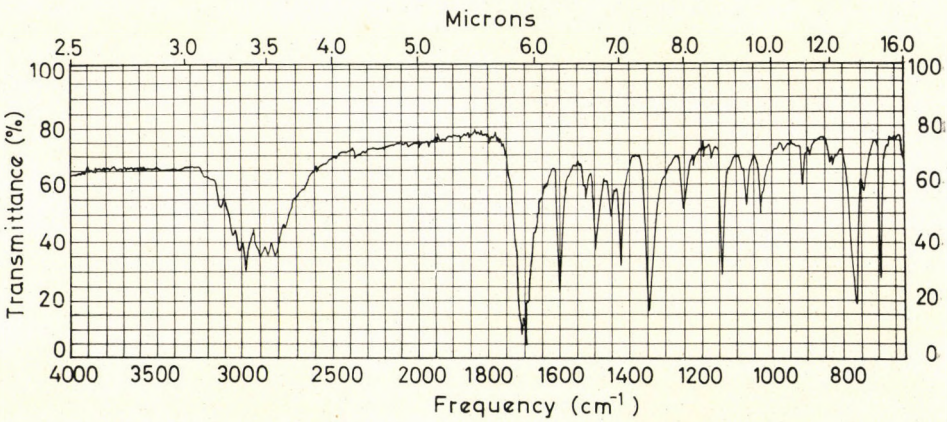

Fig. 1. N,N-dimethyl-N′-phenylformamidine hydrochloride

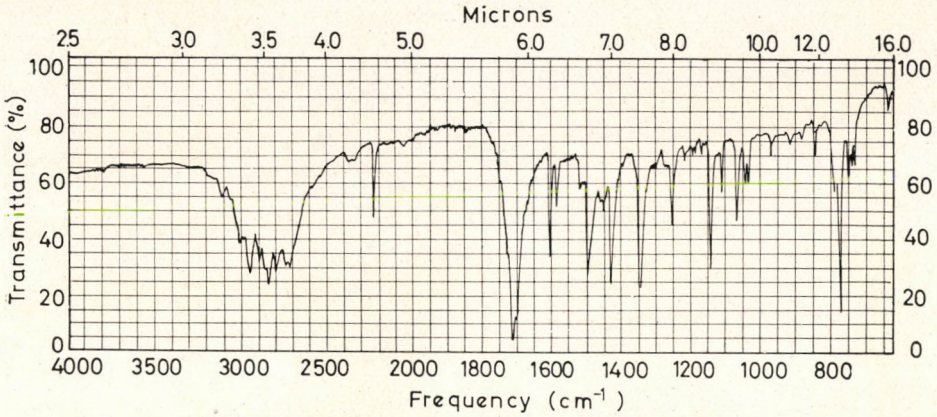

Fig. 2. N,N-dimethyl-N′-(2-cyanophenyl)-formamidine hydrochloride

As can be seen, the two spectra are very similar to each other. The bands corresponding to the $>C=\overset{\oplus}{N}<$ bond appear at 1709 cm^{-1} and 1700 cm^{-1}. The deviations are due to the presence of the nitrile group. The band of the nitrile group is found at 2230 cm^{-1}; the out-of-plane deformational skeletal vibration at 690 cm^{-1}, which is characteristic of monosubstitution, disappears in Spectrum 2, owing to aromatic *o*-disubstitution.

N,N-dimethyl-N′-(2-cyanophenyl)-formamidine hydrochloride was cyclized to 4-aminoquinazolines (**V**) in reactions with ammonia, aliphatic and aromatic primary amines and with hydrazine.

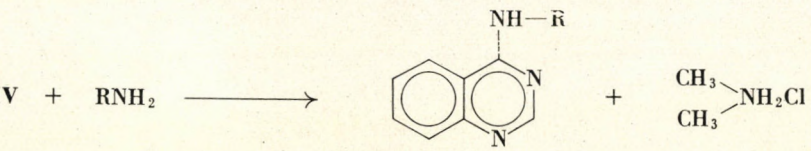

(R = H, butyl, hydroxyethyl, phenyl, *p*-tolyl, *p*-aminophenyl, $-NH_2$)

In contrast with the above discussed procedures, this method is suitable for the preparation of N-substituted derivatives, too. Its further advantage is that the 4-aminoquinazolines are obtained in a short reaction period at relatively low temperature, in satisfactory yield.

In order to identify the products, the required derivatives were also synthetized from 4-chloroquinazoline. The infrared spectra of the substances obtained in the two different procedures were found to be perfectly identical.

As an example, the spectrum of one of the derivatives is shown in Fig. 3.

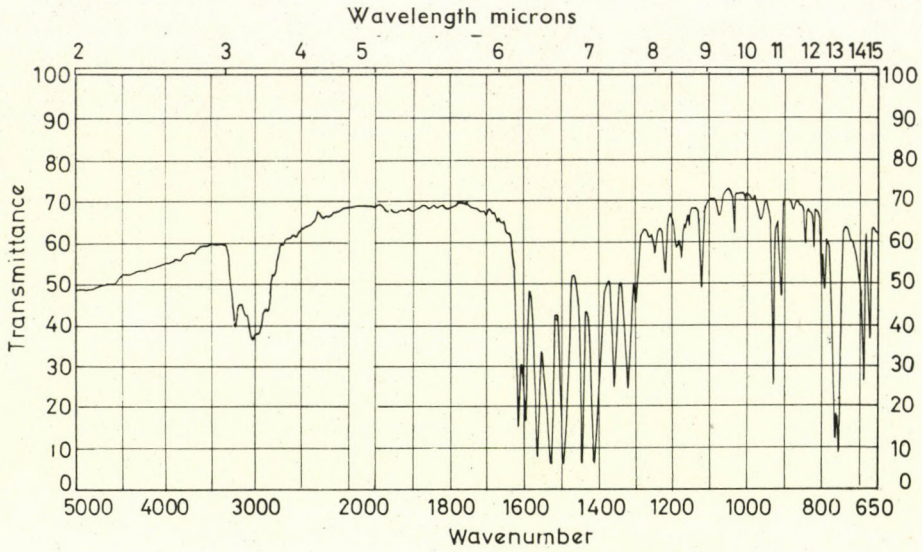

Fig. 3. Infrared spectrum of 4-(N-phenylamino)-quinazoline

Similarly to the case of the other compounds, the infrared spectrum of 4-(N-phenylamino)-quinazoline contains a high number of bands. The three skeleton valence vibrational bands characteristic of quinazolines, called quinazoline I, II and III bands, appear at 1614 cm^{-1}, 1565 cm^{-1} and 1497 cm^{-1}, respectively.

On the analogy of other reactions and on the basis of our earlier results [7, 9, 10], the following reactions are supposed to be involved in the cyclization mechanism.

The first step is an aminolytic splitting. This results in the mono- or disubstituted amidine base which is transformed to 4-aminoquinazoline probably through the 4-iminoquinazoline derivative, under the conditions of the reaction.

Our further studies on cyclization, as well as the utilization of this procedure for the preparation of other heterocyclic compounds will be reported in another paper.

Experimental

Dimethylformamide chloride [7]

N,N-Dimethyl-N′-(2-cyanophenyl)-formamidine hydrochloride

27 g (0.21 mole) of dimethylformamide chloride was dissolved in 300 ml of absolute chloroform. Under vigorous stirring, 13.6 g (0.1 mole) of finely ground anthranilic amide was added at a rate allowing to maintain the temperature of the mixture below 40 °C. After completing the addition, the mixture was stirred at room temperature for 30 min and the white precipitate was filtered off and dried. The filtrate was concentrated on a water bath, the residue

was filtered off, washed with some chloroform and dried. The total quantity of the product obtained was 20.1 g (95.8%); m. p. 245—247 °C.

Formula: $C_{10}H_{12}ClN_3$ M. W. 209.5

Calcd. C 57.28; H 5.73; N 20.05; Cl 16.94. Found C 57.08; H 5.80; N 19.89; Cl 16.97%.

4-Aminoquinazoline

20.95 (0.1 mole) of N,N-dimethyl-N′-(2-cyanophenyl)-formamidine hydrochloride was dissolved in 150 ml of methanol. Ammonia was introduced into the solution until saturation. After standing for 2 hrs, the solution was evaporated on a water bath. The residue was washed with some water and dried. The total quantity of the product obtained was 13.5 g (93.5%); m. p. 264—267 °C.

Formula: $C_8H_7N_3$ M. W. 145

Calcd. C 66.21; H 4.83; N 28.96. Found C 66.50; H 4.91; N 29.14%.

4-(N-Butylamino)-quinazoline

20.95 g (0.1 mole) of N,N-dimethyl-N′-(2-cyanophenyl)-formamidine hydrochloride was dissolved in 150 ml of methanol. 7.31 g (0.1 mole) of butylamine was added. The solution was stirred at room temperature for 1 hr and evaporated. The light yellow oil obtained was rubbed with a mixture of water–acetone (1 : 1). The precipitated crystals were filtered off and dried. The yield was 18.6 g (92.6%); m. p. 114—117 °C.

Formula: $C_{12}H_{15}N_3$ M. W. 201

Calcd. C 71.64; H 7.64; N 20.90. Found C 71.55; H 7.36; N 20.91%.

4-[N-(2-Hydroxyethyl)-amino]-quinazoline

20.95 g (0.1 mole) of N,N-dimethyl-N′-(2-cyanophenyl)-formamidine hydrochloride was dissolved in 150 ml of methanol. 6.11 g (0.1 mole) of ethanolamine was added, and the solution was stirred at room temperature for 1 hr. The solvent was evaporated, the residue diluted with water, filtered off, washed with some cold alcohol and dried to obtain 16.8 g (88.6%) of the of product; m. p. 172—176 °C.

Formula: $C_{10}H_{11}N_3O$ M. W. 189

Calcd. C 63.57; H 5.70; N 22.06. Found C 63.49; H 5.82; N 22.22%.

4-(N-Phenylamino)-quinazoline

20.95 g (0.1 mole) of N,N-dimethyl-N′-(2-cyanophenyl)-formamidine hydrochloride was dissolved in 150 ml of methanol. 9.8 g (0.105 mole) of aniline was added. The solution was boiled for 1 hr, and evaporated. A light yellow oil was obtained, which crystallized on rubbing with water–acetone. The precipitate was filtered off, washed with some dioxan and dried to obtain 20.4 g (91.9%) of the product; m. p. 216—219 °C.

Formula $C_{14}H_{11}N_3$ M. W 221

Calcd. C 70.02; H 4.90; N 19.00. Found C 76.30; H 4.91; N 19.15%.

4-(N-p-Tolylamino)-quinazoline

20.95 g (0.1 mole) of N,N-dimethyl-N′-(2-cyanophenyl)-formamidine hydrochloride was dissolved in 150 ml of methanol. 11.3 g (0.105 mole) of p-toluidine was added. The solution was boiled for 1 hr, then evaporated. The residual crystalline mass was diluted with water, filtered off and dried to give 21.9 g (93.5%) of the product; m. p. 177—180 °C.

Formula: $C_{15}H_{13}N_3$ M. W. 235

Calcd. C 76.60; H 5.53; N 17.87. Found C 76.79; H 5.36; N 17.69%.

4-[N-(4-Aminophenyl)-amino]-quinazoline

20.95 g (0.1 mole) of N,N-dimethyl-N′-(2-cyanophenyl)-formamidine hydrochloride was dissolved in 150 ml of methanol. 11.35 g (0.105 mole) of *p*-phenylenediamine was added. The

solution was boiled for 1 hr, then evaporated. The residue was diluted with water, filtered off and dried. 21.8 g (92.3%) of the product was obtained; m. p. 215—217 °C.

Formula: $C_{14}H_{12}N_4$ M. W. 236

Calcd. C 71.19; H 5.08; N 23.73. Found C 71.20; H 5.25; N 23.81%.

4-Hydrazinoquinazoline

20.95 g (0.1 mole) of N,N-dimethyl-N′-(2-cyanophenyl)-formamidine hydrochloride was dissolved in 150 ml of methanol. 5.0 g (0.1 mole) of hydrazine hydrate was added. The solution was stirred for 1 hr, then evaporated. The residue was filtered off, washed with water and dried to obtain 14.2 g (88.9%) of the product; m. p. 184—185 °C.

Formula: $C_8H_8N_4$ M. W. 160

Calcd. C 60.00; H 5.00; N 35.00. Found C 60.16; H 5.03; N 35.12%.

REFERENCES

1. HOEFFE, M. L.: U.S. Pat. 3,305,553 (1967)
2. CURD, F. H. S.: J. Chem. Soc. **1947,** 775
3. DAVOLL, J.: Brit. Pat. 1,045,180 (1966)
4. TAYLOR, E. C., BORROR, A. L.: J. Org. Chem. **26,** 4967 (1961)
5. TAYLOR, E. C., KNOPF, R. J., BORROR, A. L.: J. Am. Chem. Soc. **82,** 3152 (1960)
6. STEVENS, M. F. G., KREUTZBERGER, A.: Angew. Chem. **81,** 84 (1969)
7. CSŰRÖS, Z., SOÓS, R., PÁLINKÁS, J., BITTER, I.: Acta chim. Acad. Sci. hung. **63,** 215 (1970)
8. SEEFELDER, M.: German Pat. 1,204,663 (1965)
9. CSŰRÖS, Z., SOÓS, R., PÁLINKÁS, J., BITTER, I.: Acta chim. Acad. Sci. hung. (In press)
10. TAYLOR, E. C., LOEFFLER, P. K.: J. Am. Chem. Soc. **82,** 3147 (1960)

Zoltán CSŰRÖS
Rudolf SOÓS
István BITTER
János PÁLINKÁS

Budapest XI., Műegyetem rkp. 3.

Acta Chimica Academiae Scientiarum Hungaricae, Tomus 72 (1), pp. 65—74 (1972)

INFRARED SPECTROSCOPIC STUDIES ON FLAVONOIDS AND MODEL COMPOUNDS, I

INVESTIGATIONS ON SOME INFRARED FREQUENCIES OF 4-SUBSTITUTED ACETOPHENONES BY MEANS OF HMO CALCULATIONS

Z. DINYA and S. SZABÓ

(Organic Chemical Institute of the L. Kossuth University, Debrecen)

Received August 29, 1970

The π bond order of the carbonyl group was calculated for 4-substituted acetophenones using the simple HMO method with suitably chosen parameters. The results are in good agreement with the literature data calculated in other ways.

In the case of band '*e*' appearing in the 1200—1300 cm^{-1} region in the infrared spectra of the compounds examined, linear relationships were found between the wavenumbers of these bands and the Hammett-σ values of the substituents in para position, the π-bond order of the carbonyl group, and the π-bond order of the bond linking the carbon atom of the aromatic ring to the C=O carbon atom. These relationships are in agreement with the usual interpretation of the character of band '*e*' given in the literature.

The characteristics of the out-of-plane deformation vibrational band of the hydrogen atoms attached to the aromatic ring of 4-substituted acetophenones were also studied. In accordance with the literature data and according to our measured and calculated results, the decisive factor in the wavenumber of this band is the $-M$ effect of the substituents.

Investigations on the relations between the infrared spectroscopical properties and the structure of 3- and 4-substituted acetophenones [1a—h] have revealed a linear relationship between the wavenumber of the stretching vibration of the carbonyl group and the Hammett σ values of the substituents.

TANAKA *et al.* [1e] were the first to study the electron structure of 4-substituted acetophenones by means of the quantum chemical method. In connection with the ESR spectra of carbonyl anions, RIEGER and FRAENKEL [2] carried out HMO (Hückel Molecular Orbital) calculations for acetophenone, 4-CN- and 4-NO_2-acetophenone; however, they reported only the bond orders between the aromatic and carbonyl carbon atoms.

It is well known that all aromatic carbonyl compounds have a strong band in the 1150—1300 cm^{-1} region. In the literature this band is denoted with "*e*" [4a—c], as suggested by KOHLRAUSCH [3]. This band is assigned to a complex vibration which is due — in addition to the vibration of the aromatic ring — to the substituents attached to the ring [4d—f].

As a part of our studies on the structure of flavonoids, an investigation of the relationship between the infrared spectral properties and the charge distribution of 4-substituted acetophenones seemed desirable. For similar purposes, several authors [5a—h] have applied successfully the simple HMO

method in the case of aromatic carbonyl compounds. Such investigations on substituted acetophenones have not been reported in the literature.

Calculations

Our calculations were carried out by means of the simple HMO method [6a—e]. The Coulomb (α_i) and resonance (β_{ij}) integrals of the substituents were used in the usual form:

$$\alpha_i = \alpha_0 + h_i \beta_0$$

$$\beta_{ij} = k_{ij} \beta_0$$

Of the several parameter pairs (α_i, β_{ij}) applied in similar calculations for the C=O group the $h_0 = 2.0$ and $k_{C=O} = \sqrt{2} \simeq 1.41$ values used by FUENO *et al.* [7] proved to be the best.

The following parameters were applied for the substituents:

Table I

Substituent in position 4	$-NH_2$	$-OH$	$-OCH_3$	$\rangle C-C\equiv H_3$	$-Cl$	$-Br$	$-I$	$\rangle C-\overset{\oplus}{N}\overset{O^{\ominus}}{\underset{O^{\ominus}}{O}}$
Lit. data	[9a, b]	[9c]	[9d]	[9e]	[6b]	[6b]	*	[9e]
h_i	1.0	1.3	1.0	$h_{\rangle C} = -0.15$ $h_C(\equiv H_3) = -0.10$ $h_{\equiv H_3} = -0.50$	2.0	1.5	1.4	$h_{\rangle C} = 0.25$ $h_N = 1.8$ $h_O = 1.5$
k_{ij}	0.9	0.8	1.2	$k_{\rangle C-C(\equiv H_3)} = 0.7$ $k_{C-H_3} = 2.5$	0.4	0.3	0.25	$k_{\rangle C-\overset{\oplus}{N}} = 0.9$ $k_{\overset{\oplus}{N}-\overset{\ominus}{O}} = 1.7$

* Extrapolated on the basis of the electronegativities [8] from the parameters of the halogens.

On the basis of literature data [5a, b, d], the frequencies of the carbonyl stretching vibrations were calculated by means of the following equations:

$$k_{C=O} = \xi P_{C=O} + \sigma(1 - P_{C=O})$$

$$\nu = 2\pi \sqrt{\frac{k_{C=O}}{M}} \ (\mathrm{cm}^{-1})$$

where

$$\xi = 13 \cdot 95 \cdot 10^5 \ \mathrm{dyn/cm}$$

$$\sigma = 5 \cdot 10^5 \ \mathrm{dyn/cm}$$

$k_{C=O}$ = force constant of the C=O bond
$P_{C=O}$ = mobile: π-bond order of the C=O bond
ν = vibrational frequency (cm^{-1})
M = reduced mass of the C=O group.

Our calculations indicate that the methyl group attached to the carbonyl group should most properly be considered on the basis of the so-called 'hetero-atom model' [6b] using the $h_{CH_3} = 2.0$ and $k_{C-CH_3} = 0.7$ parameter pair.

The calculations were made on the Type ODRA-1013 instrument of the University Computing Centre, Debrecen.

Experimental

The infrared spectra were obtained with Zeiss UR-10 W and Unicam Sp-200 G spectrophotometers. The instruments were calibrated with a polystyrene foil: the accuracy of the measurement was ± 2 cm^{-1}. The spectra were recorded in liquid films, KBr pellets and in carbon tetrachloride solutions of 0.1—0.2 mole/l concentration and with 0.1—0.3 mm layer thickness.

The purity of the substances examined is characterized by the m.p. and b.p. data listed below:

1. 4-Aminoacetophenone m. p. 120 °C
2. 4-Hydroxyacetophenone m. p. 109 °C
3. 4-Methoxyacetophenone m. p. 39 °C; b. p. 160 °C/30 mmHg
4. 4-Methylacetophenone b. p. 113 °C/15 mmHg
5. Acetophenone b. p. 97 °C/16 mmHg
6. 4-Chloroacetophenone b. p. 126 °C/25 mmHg
7. 4-Bromoacetophenone m. p. 50 °C; b. p. 120 °C/20 mmHg
8. 4-Iodoacetophenone m. p. 85—86 °C
9. 4-Nitroacetophenone m. p. 80—81 °C

Results

The measured and computed results are summarized in Table II. The following explanation will help in understanding the data in the Table. For calculation purposes, the atoms of the compounds examined are numbered in the following way:

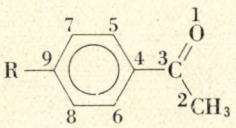

The numbers given in the column 'Serial Numbers' in Table II also indicate the individual points in the graphs representing relationships to be discussed later. In column 'R—' the substituents in position 4 are shown.

In the first column of 'Experimental values' the measured wavenumbers of the bands of the carbonyl stretching vibrations are given, the second column

Table II

Serial numbers	R—	Experimental values			Calculated values			
		ν(C=O) cm^{-1} *	'e' band cm^{-1} *	$\gamma(\diagup\!\!\diagdown C—H)$ cm^{-1} **	ν(C=O) cm^{-1}	$P_{C=O}$	$P_{Ar-C\neq O}$	$\sum_{i=5}^{8} qi$
1.	$-NH_2$	1675	1281	818	1668	0.637	0.420	3.380
2.	$-OH$	1680	1288***	820	1672	0.642	0.419	3.350
3.	$-OCH_3$	1684	1274	835	1677	0.650	0.414	2.512
4.	$-CH_3$	1688	1270	819	1694	0.674	0.408	3.356
5.	$-H$	1692	1266	—	1699	0.678	0.397	3.200
6.	$-Cl$	1692	1262	830	1696	0.677	0.402	1.908
7.	$-Br$	1693	1261	829	1969	0.677	0.401	1.902
8.	$-I$	1693	1262	825	1697	0.678	0.400	1.818
9.	$-NO_2$	1700	1248***	855	1701	0.687	0.379	1.560

* solutions in CCl_4
** liquid films and KBr pellets
*** spectra obtained in KBr pellets

contains the wavenumbers of the bands '*e*', while in the third column, designated with $\gamma(\diagup\!\!\diagdown C—H)$, the wavenumbers of the bands due to the out-of-plane C—H deformational vibration of the 1,4-disubstituted aromatic nucleus can be found.

The first column of the calculated values gives the calculated wavenumber of the band of the carbonyl stretching vibration. Columns $P_{C=O}$ and $P_{Ar-C\neq O}$ contain the mobile bond orders of the bond of the carbonyl group and that existing between the carbonyl group and the aromatic nucleus, respectively, introduced by COULSON [10]. Finally in column $\sum_{i=5}^{8} qi$ the sum of the π charges on the C-5, C-6, C-7 and C-8 carbon atoms, *i.e.* the carbon atoms in *o*,*o'* and *m*,*m'* positions of the aromatic ring, can be found.

Discussion

The data in Table II show a good agreement between the calculated and found wavenumber values of the bands assigned to the carbonyl valence vibration.

Further on, it can be stated that the bond order values calculated by us are in excellent agreement with those obtained by TANAKA *et al.* [1e], using another method. Also the π-bond order of the bond between the aromatic ring and the carbonyl carbon atom is in good agreement with the results given by RIEGER and FRAENKEL [2].

In using the results of the HMO calculations, our purpose was to obtain further information on the characteristics of the intense band '*e*' appearing in the 1200—1300 cm^{-1} region of the infrared spectrum, as well as on the properties of the band attributed to the out-of-plane deformation vibration of the aromatic $\gg C-H$ found in the 800—900 cm^{-1} region.

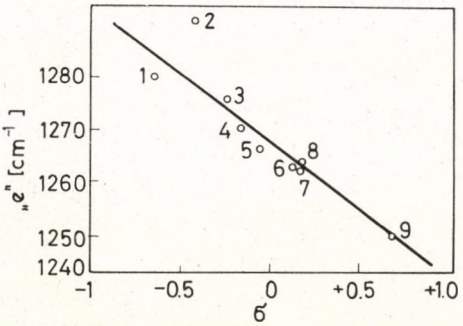

Fig. 1. Wavenumber values of the '*e*' bands as a function of the Hammett σ values of the substituents in position 4

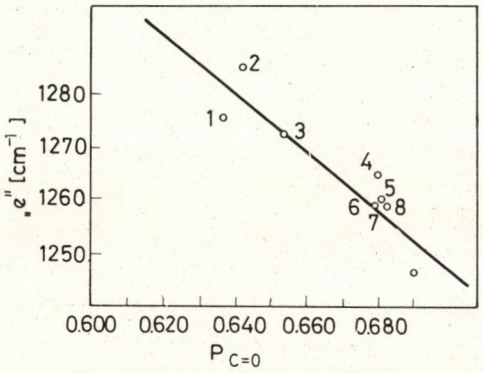

Fig. 2. Wavenumber values of the '*e*' bands as a function of the calculated π-bond order of the carbonyl group

Plotting the wavenumber value of band '*e*' as a function of the Hammet σ [11] values of the substituents in position 4, Fig. 1 is obtained.

It can be seen that increasing electronegativities of the substituents result in a linearly decreasing function whose character is opposite to that of the carbonyl stretching vibrational band studied from a similar point of view [1a—h].

Fig. 2 shows the wavenumber of band '*e*' as a function of the bond order ($P_{C=O}$) of the carbonyl group calculated by us.

As can be seen, a function of roughly similar course though somewhat different in character as the previous one was obtained, with some scattering.

Fig. 3 gives the wavenumber value of band '*e*' as a function of the bond order of the bond connecting the carbonyl carbon atom to the aromatic ring.

It is seen that a definite linear relationship — with small scattering — can be detected between the wavenumber value of band '*e*' and the mobile band order of the bond connecting the carbon atom of the C=O group and the aromatic ring.

Of the relationships regarding the wavenumber of band '*e*', the most definitely linear relationship is that involving the mobile bond order of the bond between the aromatic and carbonyl carbon atoms (Fig. 3). This indicates

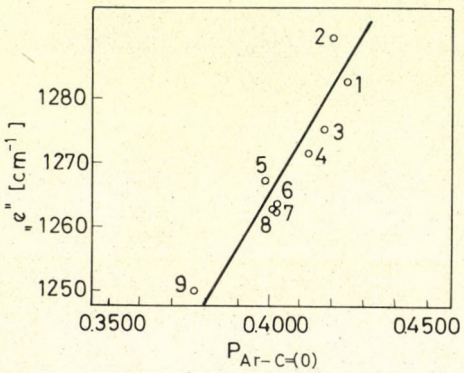

Fig. 3. Wavenumber values of the '*e*' bands as a function of the π-bond order existing between the aromatic ring and the carbonyl-C atom

the significant role of the vibration of this bond in the development of band '*e*', as also reported in the literature [3, 4a—c]. The charge density along this bond decreases with increasing electronegativities of the substituents in position 4, involving a decrease in the wavenumber of the vibration, in the direction $(-\sigma) < 0 < (+\sigma)$, as also confirmed by the experimental data. Our results regarding the alteration of the bond order and the electron distribution of the bond existing between the aromatic ring and the carbonyl-C atom are well supported by mass spectrometric measurements carried out on 4-substituted acetophenones [12, 13]. According to these, the relative percentage occurrence of the (CH_3CO) ion decreases in the direction 4-NO_2 (4.5%) → 4-NH_2 (0.26%), indicating the change in the strength of this bond.

Brigodiot and Lebas [4c] have shown that the frequency of the corresponding band is primarily decided by the valence vibration of the Ar—C=O bond, and aromatic skeletal vibration is of secondary importance.

The significant contribution of the Ar—C bond to the appearance of this band is also supported by our quantum chemical calculations described above.

The charge displacements caused in the 4-substituted acetophenone molecules by the substituents are verified by the characteristics of the bands appearing in the 800—900 cm^{-1} region, which are due to the out-of-plane deformation vibrations, $\gamma(\diagdown\!\!\diagup C—H)$, of the hydrogen atoms of the aromatic ring. KROSS *et al.* [14] have shown that the frequency of this vibration increases with the increasing *M* effect of the substituents. In the case of aromatic carbonyl compounds, BELLAMY [1d] observed a parallel relationship between

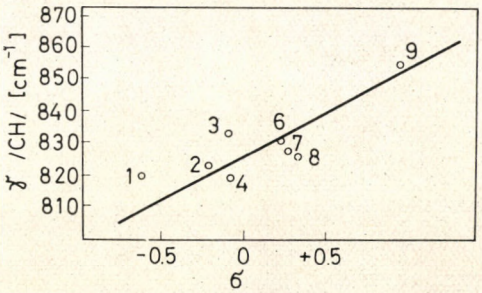

Fig. 4. The $\gamma(CH)_{Ar}$ wavenumber values of 4-substituted acetophenones as a function of the Hammett σ values

the frequency alterations of the out-of-plane deformation vibrations of the hydrogen atoms of the aromatic ring and the stretching vibration of the carbonyl group. In *meta*- and *para*-substituted compounds a linear relationship was detected between the Hammett σ values of the substituents and the frequency of the $\gamma(\diagdown\!\!\diagup C—H)$ band. On the other hand, VARSÁNYI [15] questioned the existence of an unambiguously linear relationship between the Hammett σ values and the frequencies of the $\gamma(\diagdown\!\!\diagup C—H)$ band, however, a linear relationship was observed by him between the spectroscopic moments, introduced by PLATT [16], and the frequency values of the $\gamma(\diagdown\!\!\diagup C—H)$ band.

In our case, the graphical representation of the wavenumbers of the $\gamma(\diagdown\!\!\diagup C—H)$ vibrations of 4-substituted acetophenones, as a function of the Hammett σ values of the substituents, gives the relationship shown in Fig. 4.

Obviously, the measured wavenumber values fall within a zone of linearly increasing character; there is medium scattering.

The relationship between the wavenumbers of the $\gamma(\diagdown\!\!\diagup C—H)$ bands and the PLATT spectroscopic moments is given in Fig. 5.

If the wavenumbers of the $\gamma(\diagdown\!\!\diagup C—H)$ bands are plotted as a function of the PLATT moments, the measured values fall within a zone of decreasing tendency; the scattering is about the same as in the former case.

Finally, Fig. 6 shows the wavenumber values of the $\gamma(\diagdown\!\!\diagup C—H)$ bands as a function of the overall π charge density at the C-5, C-6, C-7 and C-8 carbon atoms (*i.e.* those in *o,o'*- and *m,m'*-positions).

According to KROSS *et al.* [14], the relationships observed can be explained as follows. The bonds between the carbon and hydrogen atoms of the

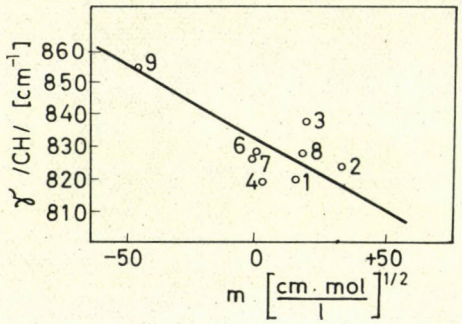

Fig. 5. The $\gamma(CH)_{Ar}$ wavenumber values as a function of the PLATT moments

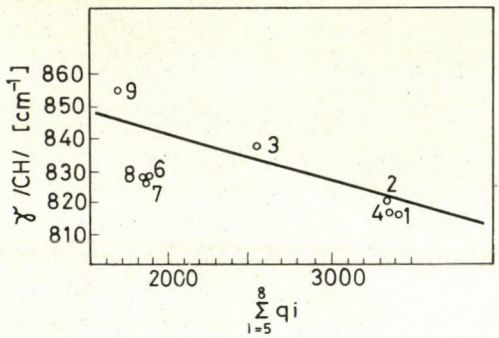

Fig. 6. Wavenumber values of the $\gamma(CH)_{Ar}$ band as a function of the sum of the π charges calculated for the *o,o'*- and *m,m'*-positions of the aromatic ring

aromatic ring are established by sp^2 hybride orbitals. In the course of the out-of-plane deformation vibrations, when the hydrogen atom leaves the plane of the benzene ring, the C—H bond undergoes a rehybridization towards the sp^3 state, owing to interaction with the π-electron cloud of the ring. This results in a decrease of the force constant and the frequency of the out-of-plane vibration. However, a decrease in the π-electron density at the carbon atom carrying the hydrogen atom will be accompanied by a similar decrease in the energy of the interaction. This can conveniently be pictured by considering the activation energy of the transition into the sp^3 state to be increasing. Owing to this, the C—H bond becomes more rigid against the out-of-plane

deformation vibration, and the force constant, as well as the frequency of the vibration will increase. Thus the crucial factor is the change of the π-electron density at the carbon atoms of the ring, depending on the $-M$ effect of the substituents. These considerations are completely supported by the relationship shown in Fig. 6 representing the wavenumber values of the $\gamma(\diagdown\!\!\diagup C-H)$ bands of 4-substituted acetophenones as a function of the sum of the π-charges at the carbon atoms in positions 5, 6, 7 and 8 (*i.e.* the *o*,*o'* and *m*,*m'* positions), calculated by means of the HMO method. As can be seen, a descending function has been obtained, verifying the earlier empirical explanation.

*

The authors' thanks are due to Prof. R. BOGNÁR for his interest in this work, to Prof. R. GÁSPÁR for valuable discussions, and to the workers of the University Computing Centre for their help in the calculations.

REFERENCES

1. a. CROSS, R. P., FUGASI, P.: J. Am. Chem. Soc. **71,** 223 (1949)
   b. FRIESS, S. L., SOLOWAY, A. H.: J. Am. Chem. Soc. **73,** 3968 and 5000 (1951)
   c. FUSON, N., JOSIEN, M. L., SHELTON, E. M.: J. Am. Chem. Soc. **76,** 2526 (1954)
   d. BELLAMY, L. J.: J. Chem. Soc. **1955,** 4221
   e. TANAKA, J., NAGAKURA, S., KOBAYASHI, M.: J. Chem. Phys. **24,** 311 (1956)
   f. JONES, R. N., FORBES, W. F., MUELLER, W. A.: Can. J. Chem. **35,** 505 (1967)
   g. JONES, R. N., SPINNER, E.: Can. J. Chem. **36,** 1020 (1958)
   h. ROSSETTI, G. P., SUSZ, B. P.: Helv. Chim. Acta **47,** 299 (1964)
2. RIEGER, P. H., FRAENKEL, G. K.: J. Chem. Phys. **37,** 2811 (1962)
3. KOHLRAUSCH, K. W. F.: Phys. Z. **37,** 59 (1936)
4. a. GARRIGOU-LAGRANGE, C., CLAVERIE, N., LEBAS, J. M., JOSIEN, M. L.: J. Chim. Phys. **58,** 559 (1961)
   b. LEBAS, J. M.: J. Chim. Phys. **59,** 1072 (1962)
   c. BRIGODIOT, M., LEBAS, J. M.: J. Chim. Phys. **62,** 347 (1965)
   d. GARRIGOU-LAGRANGE, C., LE CALVE, N.: Compt. rend. **262,** 947 (1966)
   e. SCHERRER, J. R.: Spectr. Acta **20,** 345 (1964)
   f. CALVE, N., LABARBE, P.: Spectr. Acta **26A,** 77 (1970)
5. a. BONINO, G. B., SCROCCO, E.: Rend. Accad. Naz. Linc. **6,** 421; **8,** 183 (1950)
   b. SCROCCO, E., CHIORBOLI, P.: Rend. Accad. Naz. Linc. **8,** 248 (1950)
   c. BERTHIER, G., PULLMAN, B., PONTIS, J.: J. Chim. Phys. **40,** 367 (1952)
   d. JOSIEN, M. L., DESCHAMPS, J.: J. Chim. Phys. **52,** 213 (1955)
   e. BAUDET, J., BERTHIER, G., PULLMAN, B.: J. Chim. Phys. **54,** 282 (1957)
   f. DESCHAMPS, J.: Compt. rend. **246,** 3061 (1958)
   g. PÁRKÁNYI, C., HORAK, V., PECKA, J., ZAHRADNIK, R.: Coll. Czechoslov. Chem. Comm. **31,** 835 (1966)
   h. PASPALEEV, E., KOJUCHAROVA, A.: Monatsh. f. Chem. **100,** 1213 (1969)
6. a. HÜCKEL, E.: Z. Elektrochem. **43,** 752 and 827 (1937)
   b. STREITWIESER, A.: Molecular Orbital Theory for Organic Chemists. John Wiley and Sons, New York, 1961.
   c. PULLMAN, B., PULLMAN, A.: Quantum Biochemistry. Intersci. Publ., John Wiley and Sons, New York, 1963
   d. HEILBRONNER, E., BOCK, H.: Das HMO-Modell und seine Anwendung. Verlag Chemie GmbH., Weinheim, 1968
   e. SINANOGLU, O.: Modern Quantum Chemistry. Acad. Press, New York, 1965. (Part I: J. KOUTECKY: pp. 171, R. DAUDEL, pp. 195)
7. FUENO, T., MORUKUMA, K., FURUKAWA, J.: Bull. Inst. Chem. Res. Kyoto Univ. **36,** 96 (1958)

8. SKINNER, H. A., PRITCHARD, H. O.: Trans. Faraday Soc. **49**, 1254 (1953)
9. a. TERRAGO, G., PULLMAN, B.: J. Chim. Phys. **55**, 793 (1958)
b. BOCHVAR, D. A., STANKEVICH, V., KORSAK, V. V., RUSANOV, A. L.: Dokl. Akad. Nauk. USSR, **154**, 95 (1969)
c. ROCHE, E. B., KIER, L. B.: Tetrahedron **24**, 1673 (1968)
d. NEMCOVA, I., MALATA, M., ZAHRADNIK, M.: Coll. Czechoslov. Chem. Comm. **34**, 2880 (1969)
e. SCHUSTER, P., POLANSKY, O. E.: Monatsh. f. Chem. **96**, 396 (1965)
10. COULSON, C. A.: Proc. Roy. Soc. (London) **A169**, 413 (1939)
11. SWAIN, C. G., LUPTON, E. C.: J. Am. Chem. Soc. **90**, 4329 (1958)
12. FREEMAN, S. K.: Interpretive Spectroscopy, p. 95, Reinhold Publ., New York, 1965
13. CHIN, M. S., HARRISON, A. C.: Org. Mass Spectr. **2**, 1073 (1970)
14. KROSS, R. D., FASSEL, V. A., MARGOSHES, M.: J. Am. Chem. Soc. **78**, 1332 (1956)
15. VARSÁNYI, G.: Acta chim. Acad. Sci. hung. **57**, 51 (1968)
16. PLATT, J. R.: Chem. Phys. **19**, 263 (1951)

Zoltán DINYA
Sándor SZABÓ
} KLTE Szerves Kémia Int., Debrecen 10, Hungary.

Acta Chimica Academiae Scientiarum Hungaricae, Tomus 72 (1), pp. 75—76 (1972)

RACEMIZATION DURING PEPTIDE AZIDE COUPLING

(SHORT COMMUNICATION)

L. KISFALUDY and O. NYÉKI

(Research Laboratory of the Chemical Works of Gedeon Richter, Budapest)

Received March 13, 1971

Recently, it has been reported [1—3] that under certain conditions racemization may occur during acylation with peptide azides. Therefore, it was of interest to investigate the extent of racemization depending upon the quantity and quality of the base applied, under various conditions of the azide coupling. The reaction Z-Gly-Ala-N_3 + H-Leu-OBzl has been chosen since, according to IZUMIYA and MURAOKA [4], after removal of the protecting groups in the usual way, the quantity of the D-Ala isomer in the free H-Gly-Ala-Leu-OH can be determined simply and with 0.1% accuracy, by means of an amino acid analyzer.

Table I

Racemization during the coupling of Z-Gly-Ala-N_3 with Leu-OBzl

No.	Moles per mole of hydrazide		Amine[a]	Solvent[b]	Z-Gly-Ala-Leu-OBzl		Racemization,[d] %
	Leu-OBzl	Amine			M.p.,[c] °C	Yield %	
1	1.1	1.1	Et_3N	Et_2O	95—96	49[e]	0
2	1	1	Et_3N	Et_2O[f]	96—97	43	0
3	1.18	1.18	Et_3N	Et_2O	95—97	47	4.5
4	1.3	2.6	Et_3N	$CHCl_3$—Et_2O	96—97	35	9.5
5	1.3	6.5	Et_3N	$CHCl_3$—Et_2O[g]	95—97	42	15.0
6	1.3	1.3	NMM	$CHCl_3$—Et_2O	95—97	39.5	5.5
7	1.3	2.6	NMM	$CHCl_3$—Et_2O	95—96	30	9.7
8	1.3	1.3	$EtNPr^i_2$	$CHCl_3$—Et_2O	96—97	37	11.4
9	1.3	2.6	$EtNPr^i_2$	$CHCl_3$—Et_2O	96—97	21	12.4
10	1.2	1.2	DEAiP	$CHCl_3$—Et_2O	96—97	42	0
11	1.1	2.4	DEAiP	$CHCl_3$—Et_2O	96—97	31	0

[a] NMM = N-methylmorpholine; DEAiP = 1-diethylamino-2-propanol. [b] Unless otherwise noted, the reactions were run at −5 °C for 30 min. and at room temperature for 20 hrs. [c] The crude products were homogeneous by tlc., R_f 0.58 in $CHCl_3$—MeOH (95 : 5). [d] Determined by the method of Ref. [4]. [e] Once recrystallized. [f] 2 hrs at −5 °C. [g] 3 hrs at −5 °C and 20 hrs at room temperature.

The above peptide azide was prepared as described in the literature [5] and since the pH of the ethereal solution of the azide was between 6—6.5, it was extracted with cold water only. This solution was then reacted with freshly prepared H-Leu-OBzl (see Table, Reactions 1—3) or with H-Leu-OBzl *p*-toluenesulfonate (see Table, Reactions 4—11) in chloroform solution containing the required quantity of the appropriate amine. The reaction mixture was worked up in the usual way; the protected tripeptide was hydrogenated without further purificaton, and the crude tripeptide was submitted to analysis. The results are summarized in Table I.

From the results it can be seen that in this reaction under definite conditions, racemization increases with the amount of the amine applied, and with some bases it may be significant even if only one equivalent of the base is used. No racemization takes place when 1-diethylamino-2-propanol is applied even in amounts as high as one equivalent. This observation is in agreement with experiments carried out on highly activated peptide esters [6].

*

The authors wish to express their sincere gratitude to Dr. T. DÉVÉNYI for the analyses.

REFERENCES

1. ANDERSON, G. W., ZIMMERMAN, J. E., CALLAHAN, F. M.: J. Am. Chem. Soc. **88,** 1338 (1966)
2. SIEBER, P., RINIKER, B., BRUGGER, M., KAMBER, RITTEL, W.: Helv. Chim. Acta **53,** 2135 (1970)
3. KEMP, D. S., BERNSTEIN, Z., REBEK, J.: J. Am. Chem. Soc. **92,** 4756 (1970)
4. IZUMIYA, N., MURAOKA, M.: J. Am. Chem. Soc. **91,** 2391 (1969)
5. BERGMANN, M., ZERVAS, L.: J. Biol. Chem. **113,** 341 (1936)
6. KISFALUDY, L., NYÉKI, O., SZIRTES, T.: Proc. 11th Europ. Peptide Symp. **1971** (in press)

Lajos KISFALUDY
Olga NYÉKI
Budapest X., Gyömrői út 19—21.

Acta Chimica Academiae Scientiarum Hungaricae, Tomus 72 (1), pp. 77—91 (1972)

DEVELOPMENT OF PETROLEUM REFINING TECHNOLOGIES IN GRAPH THEORETICAL REPRESENTATION, I

DISTILLATION

M. KORACH* and L. HASKÓ**

* *Research Institute of Technical Chemistry, Hungarian Academy of Sciences and*
** *Construction Bureau of Petroleum and Natural Gas Industry, Budapest*

Received June 2, 1970

Graph theoretical representation made possible the quantitative study of the course of development of industrial refinery technologies. The representation of the types of distillation equipments as a function of their year of introduction permitted to establish that the corresponding graphs lead from the open and uniflow type gradually to cyclic graphs of increasing complexity and, on the other hand, that the number of graph elements of the single systems shows an increasing trend with time, and the curve seems to approach a limiting value.

1. Objectives and means of the study

Our studies on the general laws and structure of the systems of chemical technology were begun about ten years ago. Several communications [1—5] and the review article "Graph theoretical representation of chemical technological processes" [6] report on this work.

The object of the present research is *to investigate the technological development of the most important chemical industries* on the basis of graph theoretical representation, with the expectation that *this might uncover further correlations between chemical technological systems.*

Up to now we have studied two chemical industries of the greatest importance, looking back on a long past. One is the petroleum refining industry, the other the production of sulfuric acid. Petroleum industry has been selected for investigation because, in addition to furnishing the most important raw material of modern chemical industry and energy supply, the petroleum refining determined the first development of the "process engineering".

One of the preconditions of this research was the critical study of publications treating the technology and the history of industry, using not only the dialectic approach but also that of historical materialism. Indeed, the course of development (*e.g.* the transition from the open process or open graph type to the cyclic process or cyclic graph type, or the trend of increasing number of graph elements) had also to be proved historically besides representation, because essential "new features" are of necessity reflected not by the bare statement of facts, but possibly only by the conclusions drawn from them.

However, historical works [15—18] list and describe only the new technologies or their modifications appearing in successive periods, giving often different and even contradictory data, so that it was rather difficult to piece together the correct chronological data.* However, in accordance with our object, the development of basic technologies had to be studied as a function of time. As will be seen, certain trends, and periods within these, could be established in this development. Period means here the space of time between the appearance of two technologies new in their principle, because only the time of appearance can be established with adequate reliability, while the time of utilization and life of a technology may be completely different in each country depending on local conditions, and even within the industry of the same country, as will be shown on hand of some examples.

The petroleum industry had to meet the steadily increasing quantitative and qualitative requirements of society. However, it was not our aim to investigate each of the several hundred processes realized for the purpose of manufacturing a multitude of petroleum products. Our petroleum technological investigations concern only the two principal directions of development:

1. distillation and
2. characteristic processes used in refineries, involving chemical conversion.

Practical production is realized by numerous combinations of the two directions. The object of this first study is *to investigate the development of the ancient petroleum technology, distillation*, still in versatile use in each refinery. Several other processes of the industry, characteristic of its development, in-

* In his book "A History of Industrial Chemistry" [26], Sherwood F. TAYLOR considers the successful drilling performed by DRAKE in 1859 in Titusville (Pennsylvania, USA) the beginning of modern petroleum industry. However, in another part of the book we can read that 90 years earlier, "at about 1770, systematic petroleum production existed in the neighbourhood of Baku". In contrast to this, on p. 270 the author states that in Baku the utilization of petroleum began in 1873. Finally, according to the text on p. 106, the use of petroleum for lighting was known already in ancient times in Babylon and in Girgenti (Sicily).

Naturally the "beginning" of petroleum industry should be marked by that time from which the manufacture of petroleum products can be referred to as "industry", and this depends on the conceptional content of the word "industry", which is far from being unequivocal. Possibly, it is in this sense that TAYLOR considers the drilling by DRAKE as the actual beginning of petroleum industry. However, according to SCHÖNWALDER [15], the first period of the petroleum industry can be traced back much farther. This author writes in his work "Erdöl in der Geschichte" that in Russia there are earlier data, from 1650, on petroleum production, and adds that "the concept according to which we can speak of a petroleum industry only since the drilling by DRAKE, is actually valid only in general". "In Northern Italy, in the environs of Amiano, petroleum was produced at about 1800 in a quantity sufficient for lighting the towns Genua, Parma and Borgo san Donnino". Peter the Great issued orders as early as 1723 on the transportation of petroleum from Baku, and already in 1735 petroleum for lighting was manufactured in Baku by distillation. Well, was this not "industry"?

According to Harold F. WILLIAMSON [17], "The American was not the first but the second petroleum industry ever realized" [Not rather fourth? (Remark of the authors)]. A period of 5000 years separated the first petroleum industry (Mesopotamia) from the second. In summary, according to TAYLOR the year of birth of petroleum industry was 1895, according to SCHÖNWALDER, this is the year of birth only in general; and finally, WILLIAMSON traces it back to about 3000 B.C. Indeed, this cannot be called a serious historical registration!

volving mainly the chemical conversion of the components of petroleum, will be examined in a second communication on the example of the *manufacture of Otto engine fuel and lubricating oil.*

The means of our investigation is graph theoretical representation by the method developed by us for the chemical industry [6]. In this study, semi-technological graphs, *similar to the theoretical type of graph*, will be constructed, comprising besides the reactor the essential allactors, cooling and heating allactors and conduits. For each graph its graph-theoretical type will be established, and for the characterization of its technological complexity the number of elements constituting the graph will be given.

It should be mentioned finally that the graphs constructed were not developed by direct representation of flowsheets of the most various degrees of abstraction found in the literature, but these were converted as far as possible to a similar level of abstraction, because otherwise the degrees of technical development shown in the figures would not have been comparable. Sometimes, due to the lack of flowsheets, figures were reconstructed on the basis of descriptions alone.

2. Development of distillation

As is well known, in the history of petroleum distillation two working principles have been realized:

1. fractional distillation and
2. fractional condensation.

2.1 *Equipment in fractional distillation*

In fractional distillation, petroleum is heated to increasing temperatures, and first the light, then the heavier distillates are obtained. For this purpose, two kinds of technical implementation have been developed:

2.1.1 *Simple distillation*

Petroleum was distilled already by the Copts in 100 B. C. in stills, the neck of which was cooled [17, p. 7]. The condensation of vapours in coiled tubes was already used in the 18th century. An industrial scale distillation plant was constructed in 1832 in Russia by the BUDININ brothers for black oil production. The plant was closed after a few years [15], but later a series of similar plants was built in the environment af Baku [25].

In the United States from 1862 on several coal oil plants were converted after the successful drilling by DRAKE into petroleum distillation plants, but new plants were also erected in the vicinity of New York, Boston and Pitts-

burgh [17, p. 202]. First, these plants used without changes the directly heated, cast iron stills of coal distillation plants, to the highest point of which a water-cooled coil was connected. Distillates were collected according to temperature ranges. Operation was of the batch type and slow, particularly owing to the long cooling time. The first stills were replaced later by vertical or horizontal cylindrical types made of wrought iron and later of steel plates, and built

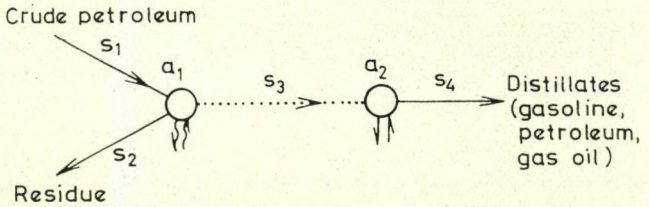

Fig. 1. Petroleum refinery distillation. Simple distillation (according to THORPE's Dict. Vol. 9, p. 325, Fig. 3). (Vertical still, 1860) Theoretical graph
Allactors: a_1 = distillation still; a_2 = condenser. Conduits: s_1 = crude petroleum; s_2 = distillation residue; s_3 = distillate vapours; s_4 = distillates (according to increasing boiling point). Type of graph: uniflow, open. Number of graph elements: 6

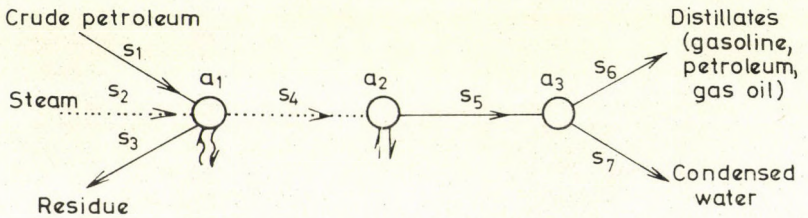

Fig. 2. Petroleum refinery distillation. Simple distillation (with steam) (1863, according to the description of WILLIAMSON, I. p. 216). Theoretical graph
Allactors: a_1 = distillation still; a_2 = condenser; a_3 = settler. Conduits: s_1 = crude petroleum; s_2 = steam; s_3 = distillation residue; s_4 = distillate + steam; s_5 = condensate; s_6 = distillates; s_7 = condensed water. Type of graph: uniflow, open. Number of graph elements: 10

into masonry furnace chambers. The capacity of the stills was increased with the increase of product demand to 600—800 barrels and more. Several other innovations were introduced in the design of stills, distillation being carried out with steam and under vacuum.

In spite of the innovations this method of distillation did not change from the viewpoint of the process; it is characterized only by two operations: *evaporation and the condensation of vapours.* Distillation is of the batch type, distillates are collected between increasing boiling point limits. The literature contains the scheme of several apparatuses of this kind. Starting from any of these, the graph shown in Fig. 1 is obtained. The graph is *uniflow and open.* If distillation is carried out with steam, a separator must be used after the condenser for the separation of water and oil. The graph of such a plant is shown in Fig. 2. This graph is also *uniflow and open.*

To obtain a sharper separation, European refineries used already in the 1870's fractionating columns built on top of the still, as has been customary in distilleries. The plant operates periodically, as a simple distillation apparatus. The graph of such apparatus is shown in Fig. 3. This graph too is *uniflow and open.* The angle point A_1 in the graph is an allactor series consisting of two units (still, column), between which there is a countercurrent process, as can be seen from subgraph II.

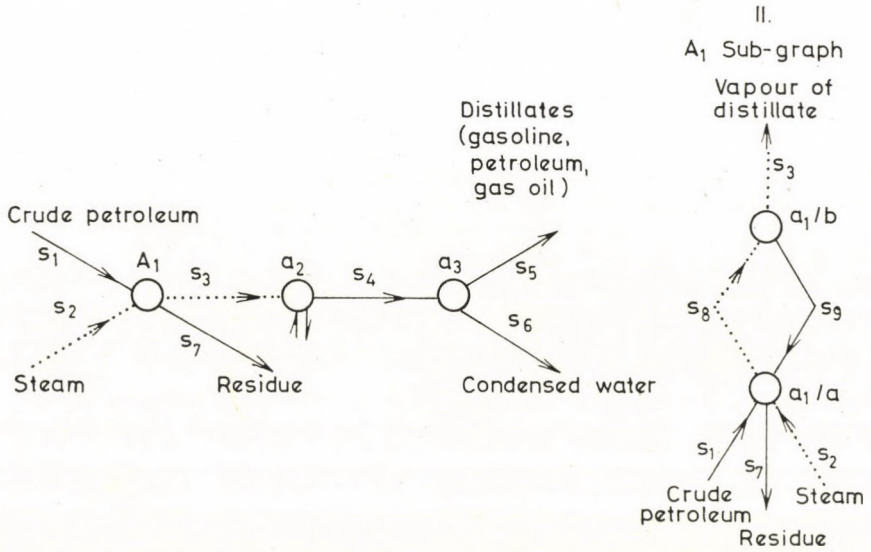

Fig. 3. Petroleum refinery distillation. Distillation still with fractionating column (Europe, in the 1870's). (According to THORPE's Dict. Vol. 9. p. 326, Fig. 5). Theoretical graph
Number of graph elements (I and II): 12
Allactors: A_1 = still with column; a_2 = condenser; a_3 = separator. Allactors of A_1: a_1/a = heated still; a_1/b = column

Conduits: s_1 = crude petroleum; s_2 = steam; s_3 = vapour of distillate; s_4 = distillates; s_5 = distillates; s_6 = condensed water; s_7 = still residue. Conduits: s_8 = ascending steam; s_9 = reflux. Type of graph: uniflow, open. II. Type of graph: uniflow, open (with countercurrent)

2.1.2 *Continuous battery distillation*

In view of the rapidly growing quantitative demands and qualitative requirements of the market, the disadvantages of "simple" still distillation (low performance, poor heat utilization, uncertain separation, high manpower) were felt increasingly in high capacity plants. The rise in social demand required a new technology. Recommendations with this goal in view were not missing in countries with refining industries, thus in the U.S.A., as witnessed by numerous patent applications in the 1860's and 1870's. Some of the recommendations were used transitorily; however, the U.S. monopolies peculiarly refused to consider the innovations (battery distillation, fractionating column) during the whole nineteenth century.

The new distillation of continuous operation was solved in Russia, by using batteries consisting of a series of stepwise arranged horizontal cylindrical oil-heated distillation stills. Each had separate heating and was equipped with a dephlegmator of special design. According to one source, inventors were the NOBEL brothers [17, p. 26], while TUREVITCH gives the credit to the Russian engineer A. F. INTCHIK [25, p. 347]. At the beginning of the 1880's the process was already in use in Baku. In his report [21] on a study tour in 1885, ENGLER attributes only the transport in pipelines to the NOBEL brothers.

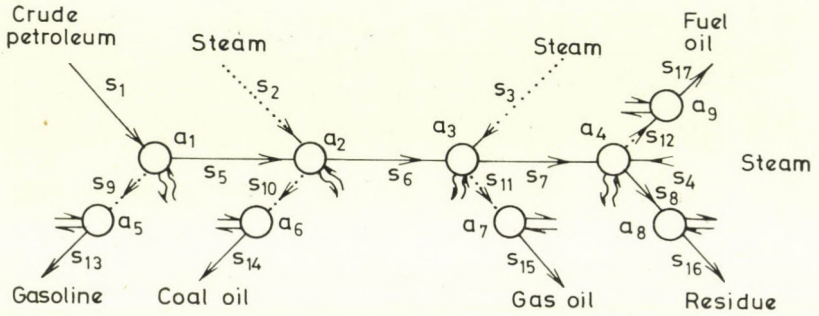

Fig. 4. Petroleum refinery distillation. Battery type continuous distillation without recuperation (1880). (Reconstructed according to THORPE's Dict. Vol. 9, p. 326, Fig. 6). Theoretical graph. Allactors: $a_1 - a_4$ = distillation stills; $a_5 - a_9$ = coolers. Conduits: s_1 = crude petroleum; $s_2 - s_4$ = steam; $s_5 - s_7$ = bottom product of still; s_8 = distillation residue; $s_9 - s_{12}$ = vapour of distillate; $s_{13} - s_{17}$ = products. Type of graph: uniflow, open. Number of graph elements: 26.

As compared to simple distillation, the new process represents a considerably more advanced stage of development, its specific performance is higher, the thermal energy and labor requirement lower. The desired products are obtained simultaneously, with a sharper separation, and the repeated distillation of distillates is avoided.

The process was quickly adopted by the larger European refineries, and with modifications it was still in use in the first decades of the twentieth century. A great number of modifying patents were filed, concerning mainly details of the apparatus. The number of the stills is determined by the quality of the raw material and by the number of the target products, which often is 4, 5, 6 or more. On his tour mentioned, ENGLER saw in Baku batteries composed of as many as 17—18 stills [21].

A substantial innovation in the process was also the improvement of thermal economy: crude petroleum was preheated by the distillates in heat exchangers. Of the many possible variants, 3 stages of development will be shown. Fig. 4 represents the graph of a plant built at the early stages (about 1880) of the battery process, with no heat recovery. *The graph is open and uniflow.*

Fig. 5 shows the graph of a plant similar to that seen by ENGLER in 1885 in Baku (but with only 4 stills represented), where crude oil is preheated with hot mazout in heat exchangers. Material moves in *uniflow and open* also here, but the *cyclic process* represented by the *circulation of part of the heat* transferred to the oil already appears in it, as can be seen from the figure. The battery plant shown in Fig. 6, with *complete heat recuperation*, is similar.

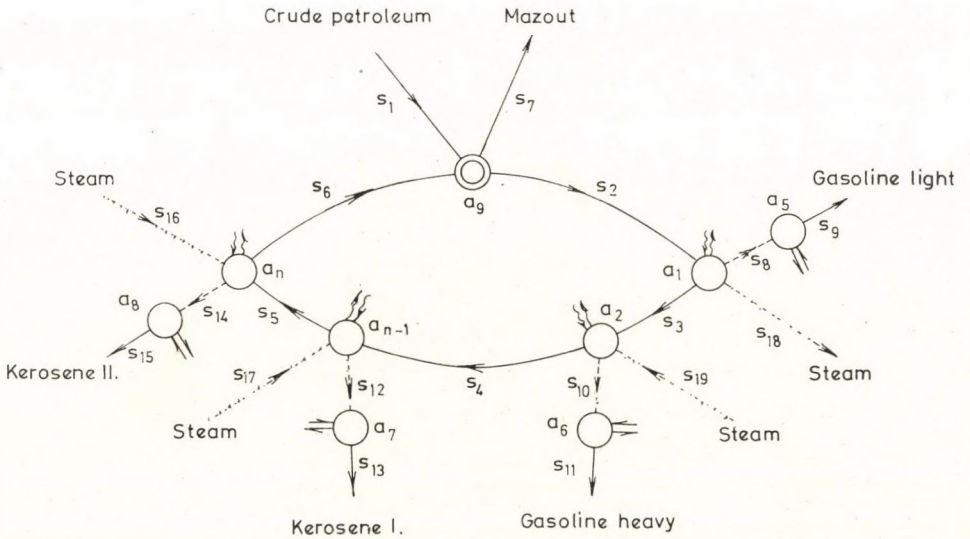

Fig. 5. Petroleum refinery distillation (battery type continuous distillation). System Baku 1885. (On the basis of the report on the study tour of C. ENGLER in 1885). Theoretical graph Allactors: a_1, a_2 = distillation still; a_n, a_{n-1} = distillation still; a_5—a_8 = condenser; a_9 = heat exchanger (mazout — crude petroleum). Conduits: s_1, s_2 = crude petroleum; s_3—s_5 = bottom product of still; s_6—s_7 = mazout; s_8 = light gasoline vapours; s_9 = light gasoline liquid; s_{10} = heavy gasoline vapour; s_{11} = heavy gasoline liquid; s_{12} = kerosene I vapour; s_{13} = kerosene I liquid; s_{14} = kerosene II vapour; s_{15} = kerosene II liquid; s_{16}—s_{19} = steam. Type of graph: uniflow, open (material); cyclic (heat); countercurrent dephlegmation. Number of graph elements: 28

In our graphs, the distillation stills of the battery plants are marked by a single angle point, but actually these units called stills consist of several allactors (still and dephlegmator), between which there is *countercurrent flow*, resulting in a sharper separation. In Fig. 6 this is shown by the sub-graph.

2.2 *Apparatus with fractional condensation*

The rapid development of distillation in the petroleum refining industry is due to *the use of pipe stills*. The pipe still was employed for the first time at the beginning of the 20th century by California refineries for the dehydration of crude oils forming tenacious emulsions [9, p. 136]. The pipe still design was

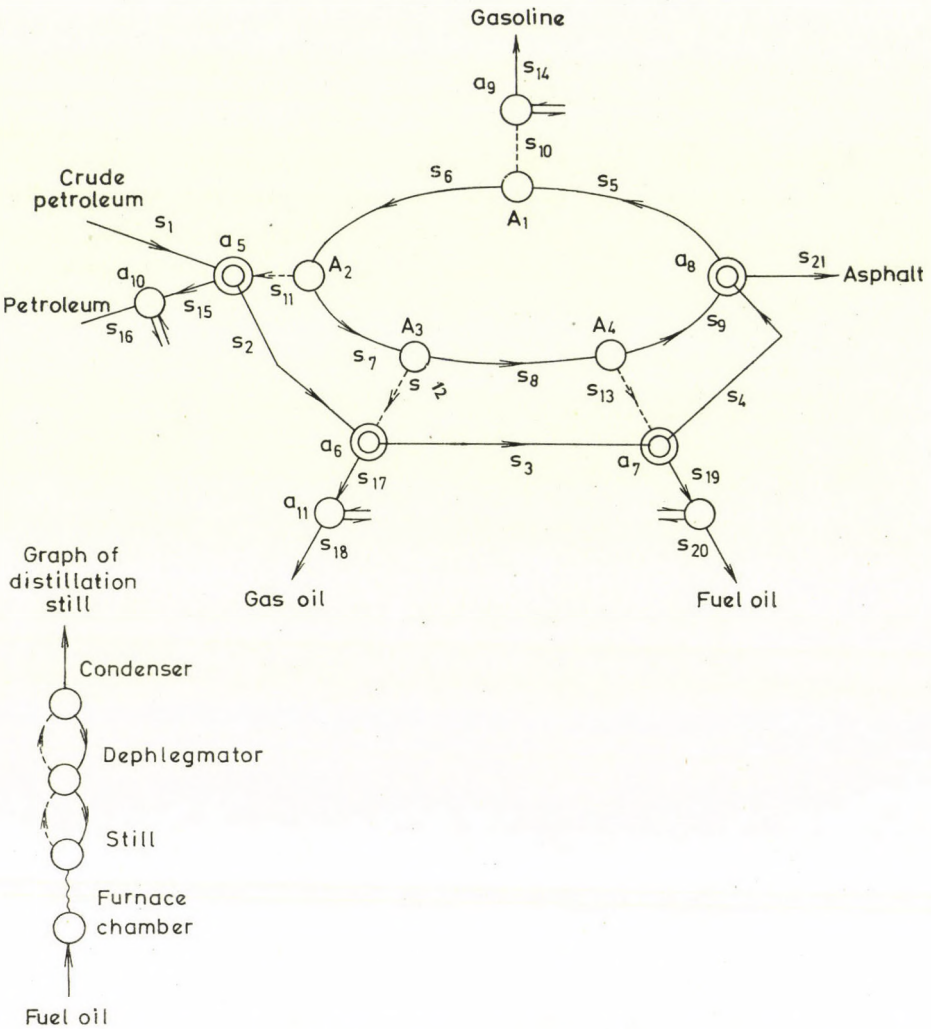

Fig. 6. Petroleum refinery distillation. Battery type continuous distillation with complete recuperation, Europe (1890). (According to WINNACKER—KÜCHLER I., Fig. III-26). Theoretical graph. Allactors: A_1-A_4 = distillation still; a_5-a_8 = heat exchanger; a_9-a_{11} = condenser. Conduits: s_1-s_5 = crude petroleum; s_6-s_9 = bottom product of still; $s_{10}-s_{13}$ = vapour of distillate; $s_{14}-s_{20}$ = distillate; s_{21} = asphalt. Type of graph: uniflow, open (material) with cyclic process (heat); countercurrent dephlegmation. Number of graph elements: 33

further developed by the California refineries, and experiments were carried out on its application in the distillation of crude petroleum. The problem of industrial realization was solved by J. TRUMBLE in 1912, in the Martinez plant of Shell Co. [18, p. 129].

TRUMBLE's process changed the working principle of distillation. In distillation carried out in stills, *fractional distillation* takes place. In TRUMBLE's

process, raw petroleum is heated in the pipe still to the boiling point of the highest-boiling product, when under the pressure prevailing in the pipe still the components remain partly liquid, and so called "*equilibrium*" *evaporation* occurs. From the pipe still the liquid–vapour mixture passes into an evaporator, where, as a result of the pressure drop, the components to be obtained are evaporated. The vapours leaving the evaporator pass through a series of dephlegmators where they are gradually cooled, and first the heavier then the lighter hydrocarbons are condensated. Thus, *fractional condensation* takes place. The graph of the system is shown in Fig. 7. The temperature of the dephlegmators is regulated by changing the amount of reflux. *The process is continuous, and here already three material cycles are present.*

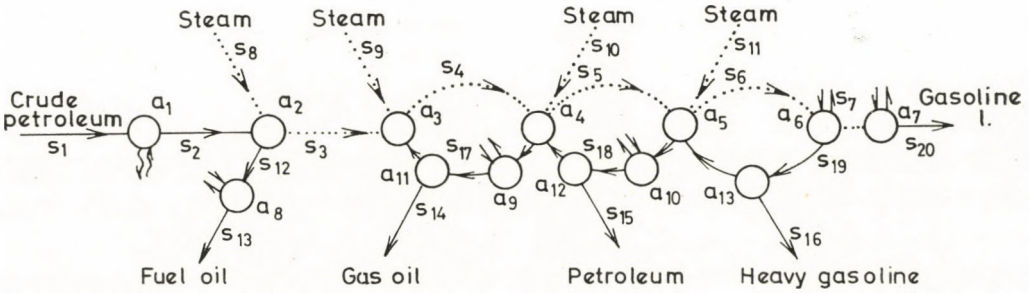

Fig. 7. Petroleum refinery distillation. System Trumble. Pipe still — dephlegmator distillation (Shell 1912). (According to ULLMANN, 3rd Ed. Vol 6, p. 614, Fig. 30). Theoretical graph. Allactors: a_1 = pipe still; a_2 = evaporator; a_3—a_5 = dephlegmators; a_6—a_7 = condensers; a_8—a_{10} = coolers; a_{11}—a_{13} = pumps. Conduits: s_1 = crude petroleum, s_2 = crude petroleum hot; s_3—s_7 = crude vapour passage; s_8—s_{11} = steam; s_{12}—s_{13} = fuel oil; s_{14}—s_{16} = distillates; s_{17}—s_{19} = bottom product; s_{20} = light gasoline. Type of graph: uniflow, open, with cyclic processes (material). Number of graph elements: 38

The development of distillation in the petroleum industry during the 1920's is based on the principle of fractional condensation, and has begun by *coupling the pipe still and the fractionating column* for the distillation of crude petroleum. Modern petroleum distillation, which gradually displaced battery and Trumble distillation from the industry, has been developed by improving the design of pipe stills and fractionating columns (bubble-cap tray) and by distillating the heavy components in vacuum. There are no data either on the development of the new distillation system, or on the time required for introducing important innovations. These data can only be estimated, as development took place independently in several countries having their own refining industry. Development occurred in two directions: sharper separation of the fractions and improvement of the heat economy. One way to attain sharp separation is multi-column distillation, which was introduced at about 1920. The system consists of four columns with bubble-cap trays. The columns may be connected in different ways. Fig. 8 shows the graph of a distillation, in

which the products are obtained partly as heads, partly as side draws, and partly as bottoms. Here, *two material cycles are involved.*

The other mode of sharp separation, most frequently used, is to strip with steam from the side streams of the principal column the lighter products in a *stripper column.* The graph of this type of distillation is shown in Fig. 9, which comprises two side streams. In this apparatus, crude petroleum passes through two heat exchangers before it enters the pipe still, utilizing thus the

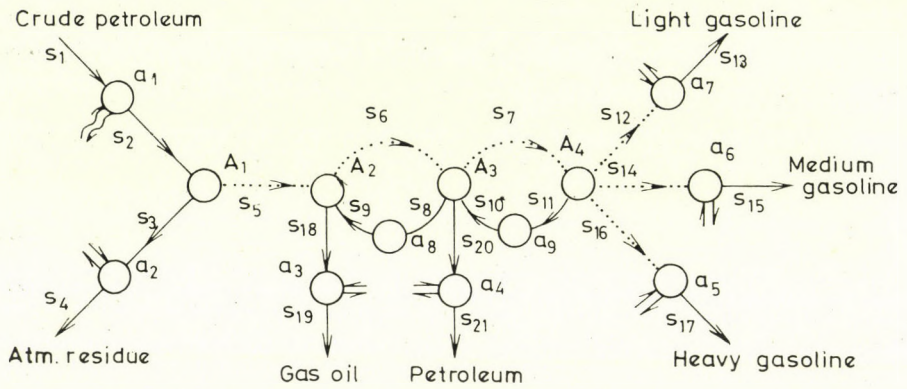

Fig. 8. Petroleum refinery distillation. Multicolumn atmospheric crude distillation (Europe—USA, about 1920). (According to WINNACKER—KÜCHLER I, p. 258, Fig. III-326b). Theoretical graph.
Allactors: A_1-A_4 = rectification columns; a_1 = pipe still; a_2-a_7 = coolers; a_8-a_9 = pumps. Conduits: s_1-s_2 = crude petroleum; s_3-s_4 = atm. residue; $s_5 = A_1$ head product vapours; $s_6 = A_2$ head product vapours; $s_7 = A_3$ head product vapours; $s_8-s_9 = A_3$ bottom product reflux; $s_{10}-s_{11} = A_4$ bottom product reflux; $s_{12}-s_{13}$ = light gasoline vapours; $s_{14}-s_{15}$ = medium gasoline vapours; $s_{16}-s_{17}$ = heavy gasoline vapours; $s_{18}-s_{19}$ = gas oil; $s_{20}-s_{21}$ = petroleum. Type of graph: uniflow, open, interrupted by material cycles, in A_1-A_4 by countercurrents. Number of graph elements: 34

heat content of the head and bottom products. According to data in the literature, the first distillation plants of this kind were built in the USA starting from 1924 [18, p. 104]. The graph shows *multiple cycles.*

The complete fractionation of crude petroleum in a single plant was solved around 1925 by the *combination of atmospheric and vacuum columns.* The bottom product of the atmospheric column is heated in the pipe still and passes on to the vacuum column, the products of which are: heavy gas oil, lubricating oil fractions, etc. The graph of such a plant is shown in Fig. 10. The equipment, comprising a *double cycle*, contains also a pre-distillation column for the separation of gasoline.

3. Conclusions

Graphs representing the principal types of petroleum distillation since 1860 have been shown. The initial period of the refining industry was associated

with simple batch discontinuous distillation. The graphs of distillations are *uniflow, open graphs* (Figs 1, 2, 3). This is the first period of development. In the second period, at about 1880, battery systems of continuous operation were introduced. These systems were formed by the division and repetition of

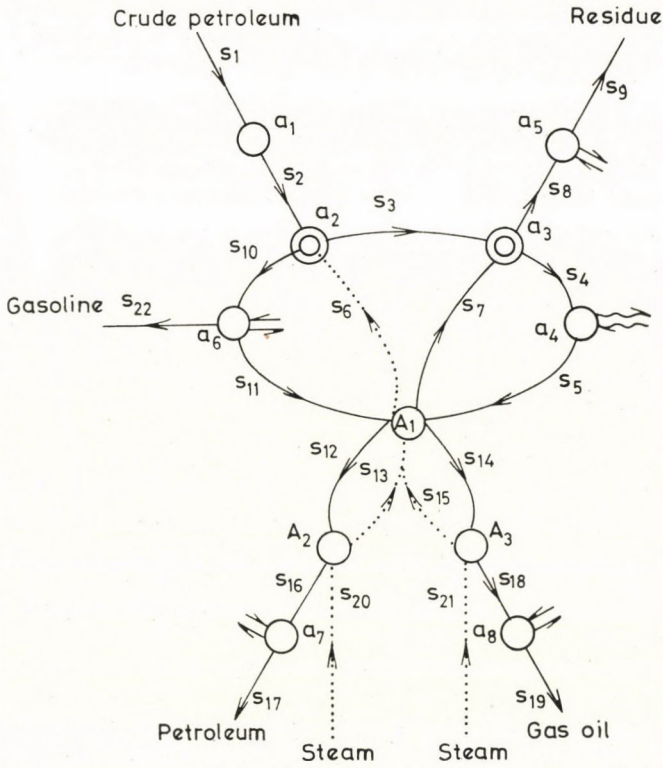

Fig. 9. Petroleum refinery distillation. Single stage crude petroleum distillation (with two lateral streams and heat exchanger, from 1924 on). (According to WINNACKER—KÜCHLER I, p. 257, Fig. III-29). Theoretical graph.
Allactors: A_1 = rectification column; A_2 = petroleum stripper; A_3 = gas oil stripper; a_1 = pump of crude petroleum; a_2—a_3 = heat exchanger; a_4 = pipe still; a_5—a_8 = coolers. Conduits: s_1—s_4 = crude petroleum; s_5 = hot crude petroleum; s_6 = gasoline vapour; s_7—s_9 = residue; s_{16}—s_{22} = gasoline; s_{11} = gasoline reflux; s_{12} = petroleum side draw; s_{13} = petroleum stripping; s_{14} = gas oil side draw; s_{15} = gas oil stripping; s_{16}—s_{17} = petroleum; s_{18}—s_{19} = gas oil; s_{20}—s_{21} = steam. Type of graph: cyclic (heat and material); (columns are countercurrent). Number of graph elements: 33

simple distillation. The principal material flow is uniflow, open, but *due to heat economy, a specific circulation appeared*, which is manifested also in the graphs.

An essential element of the system is *countercurrent dephlegmation* (Figs 4, 5, 6).

The development of continuous operation combined with the economy of heat and manpower and with safe control was attained by the use of the

pipe still and of *fractionated condensation* methods, the forerunner of which was Trumble distillation. The graph of this system (Fig. 7) is *still uniflow, open*, but this too is *combined with cyclic processes.*

The dominant type of the graphs of the pipe still—fractionating column systems is the *cyclic process* (Figs 8, 9, 10).

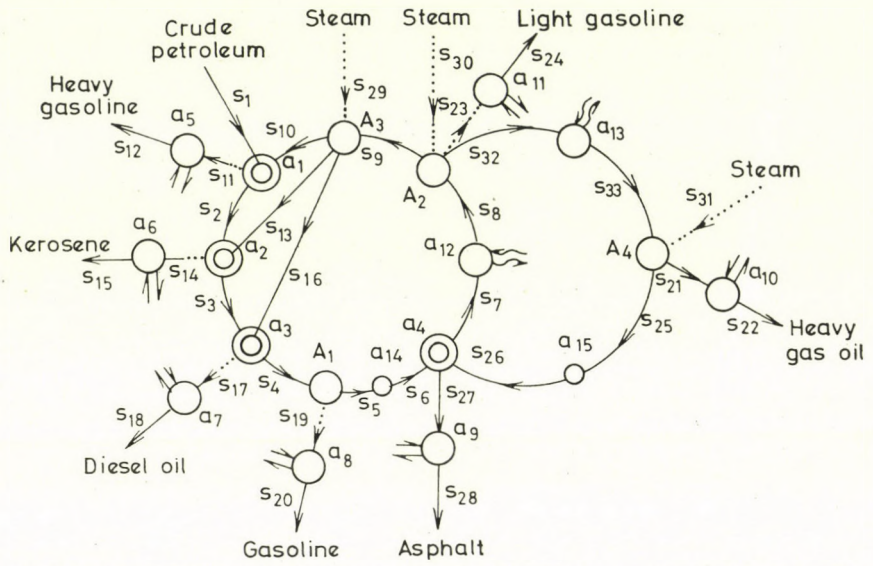

Fig. 10. Petroleum refinery distillation. Atmospheric and vacuum distillation plant (Shell Oil 1925). (According to H. S. BELL: American Petroleum Refining, p. 198, Fig. XII-8).
Theoretical graph.
Allactors: A_1 = pre-distillation column; A_2 = atmospheric distillation column; A_3 = stripper column; A_4 = vacuum column; a_1—a_4 = heat exchangers; a_5—a_{11} = coolers; a_{12}—a_{13} = pipe stills a_{14}—a_{15} = pumps. Conduits: s_1—s_8 = crude petroleum; s_9 = side stream; s_{10}—s_{12} = heavy gasoline; s_{13}—s_{15} = kerosene; s_{16}—s_{18} = Diesel oil; s_{19}—s_{20} = gasoline; s_{21}—s_{22} = heavy gas oil; s_{23}—s_{24} = light gasoline; s_{25}—s_{28} = asphalt; s_{29}—s_{31} = steam; s_{32}—s_{33} = bottom product of atmospheric column. Type of graph: countercurrent, open cyclic.
Number of graph elements: 48

Thus, in the case of distillations in the petroleum industry the trend of development is the same as in other technologies of the chemical industry: technology starts with simple apparatus, the graph is uniflow and open; the increasing quality demand and the improvement of economy are met by the introduction of countercurrent and cyclic processes, which is reflected also in our graphs.

Even on simple inspection, the graphs shown are indicative of the fact that the distillation equipment becomes increasingly complicated. The growing complexity is illustrated by the diagram given in Fig. 11. Years are plotted on the abscissa, while the number of graph elements as shown in the graphs (group A) and the number of graph elements per product (group B), respective-

ly, are represented on the ordinate. Both groups show an *increasing trend.* This trend which appears simultaneously with the introduction of countercurrent and cyclic methods, results from the law of reducing the cost of production [see 1, p. 23]. However, the reduction of cost parameters has also factors which are not directly reflected by the graphs, as *e.g.* the increasing performance of processes within the operational units. The distillation of petroleum illustrates this well. The largest still used in simple distillation in USA plants had a capacity of 800 barrel = 128 t/day, whereas atmospheric

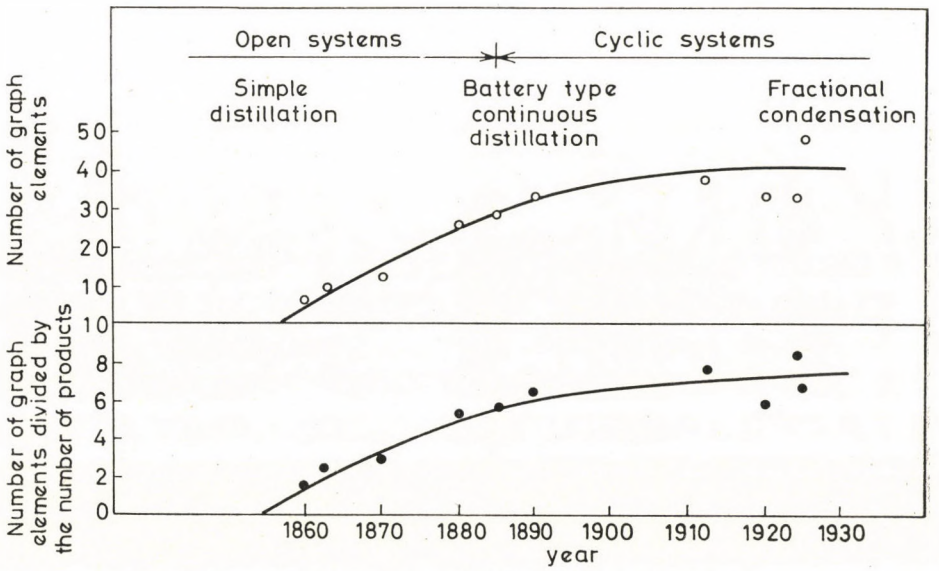

Fig. 11. Number of graph elements in Figures 1—10

crude petroleum columns are built today already often for a yearly capacity of 3 million tons (about 10,000 t/day). This is almost 80 times larger than its predecessor of the past century. The advantages are evident. Notwithstanding this fact, in our graphs both units are presented by *one* angle point. The higher performance indirectly affects the structure of the graphs to a certain degree, because larger equipment usually requires more auxiliary equipment, which is manifested in the number of the graph elements. Other cost factors can be similarly reduced by additional equipment; thus *e.g.* the utilization of heat requires heat exchangers. This *trend towards complexity* and the *periods* are evident in the mentioned diagram plotted from data of the graphs representing actual distillations (Table I and Fig. 11). A trend of this kind cannot give a precise curve. However, Fig. 11 seems to have approximately an asymptotic course in displaying the regularities of the development of chemical technology (see [29]).

Table I

The complexity of distillation

(see Fig. 11)

Graph No.	Year	Number (n) of graph elements	Number (t) of products	$m = n/t$
1	1860	6	4	1.5
2	1863	10	4	2.5
3	1870	12	4	3
4	1880	26	5	5.2
5	1885	28	5	5.6
6	1890	33	5	6.6
7	1912	38	5	7.6
8	1920	34	6	5.7
9	1924	33	4	8.2
10	1925	48	7	6.8

REFERENCES

1. KORACH, M.: General Chemical Technology, I—II (In Hungarian). Tankönyvkiadó. Budapest, 1962—64
2. KORACH, M.: XXXIV. Congrès International de Chimie Industrielle. Beograd, 1964
3. KORACH, M.: Conference on Intensified Chemical Technological Processes. Kecskemét, 1964
4. KORACH, M.: Acta chim. Acad. Sci. hung. Budapest, **50**, 457—470 (1966)
5. KORACH, M.: Scientific World, London, No. 4, 1967, pp. 16—20
6. KORACH, M., HASKÓ, L.: Magyar Tudományos Akadémia Kémiai Közl., Budapest, **29**, 263—290 (1968)
7. WINNACKER, K., KÜCHLER, L.: Chemical Technology (in Hungarian). Műszaki Kiadó. Budapest, 1962
8. NELSON, W. L.: Petroleum Refinery Engineering. McGraw-Hill, New York, 1960
9. BELL, H. S.: American Petroleum Refining. Van Nostrand Co., New Jersey, 1969
10. RUF, H.: Kleine Technologie des Erdöls. Birkhäuser Vlg., Basel, 1963
11. KISSLING, R.: Chemische Technologie des Erdöls. Vieweg und Sohn, Braunschweig, 1915
12. VAJTA-KRÁLIK, Zs., VÁMOS, E.: Petroleum Processing Industry (in Hungarian). Népszava. Budapest, 1951
13. ULLMANN, S.: Enzyklopädie, 3. Aufl. Bd. 6. Urban u. Schwarzenberg, München, 1955
14. KIRK, R. E., OTHMER, D. F.: Encyclopedia of Chemical Technology, Vol. 10. Interscience, New York, 1953
15. SCHÖNWALDER, G.: Erdöl in der Geschichte. Vlg. Hüthig und Dreyer, Mainz, 1958
16. CLARK, J. A.: The Chronological History of the Petroleum and Natural Gas Industries. Clark Book Co., Houston, 1963
17. WILLIAMSON, H. F., DAUN, A. R.: The American Petroleum Industry. The Age of Illumination. Northwestern University Press, 1859—1899
18. WILLIAMSON, H. F., DAUN, A. R.: The American Petroleum Industry. The Age of Energy. Northwestern University Press, 1899—1959
19. PHILLIPOVICH, A.: Die Betriebsstoffe für Verbrennungskraftmaschinen. Springer Vlg., Wien, 1949
20. Petroleum World Conference: Petroleum Processing. NIM Műszaki Dokumentációs és Fordítóiroda, Budapest, 1967
21. ENGLER, C.: Das Erdöl von Baku. Ein Reisebericht. Vlg. I. G. Cotta, Stuttgart, 1886

22. ENGLER, C., HÖFER, H.: Das Erdöl. Band III. Die Technologie des Erdöls und seiner Produkte. Vlg. S. Hirzel, Leipzig, 1911
23. THORPE, S.: Dictionary of Applied Chemistry. Vol. 9. Longmans, Green and Co., London, 1949
24. FREUND, M.: Petroleum Industry (in Hungarian). Nehézipari Kiadó, Budapest, 1951
25. TUREVITCH: Teknologia Nefti. p. 347. Moscow, 1952
26. TAYLOR, S. F.: A History of Industrial Chemistry. Heinemann, London, 1956
27. LEHMANN, G. H.: Das Erdöl und seine Verarbeitung. Vlg. Hüthig und Dreyer, Mainz, 1963
28. KORACH, M.: Chemistry Conference, Veszprém, 1962

Mór KORACH
Lajos HASKÓ
Budapest XI., Budafoki út 47.

RECENSIONES

G. HESSE: *Chromatographisches Praktikum. (Eine Anleitung zur kritischen Durchführung chromatographischer Arbeiten)*

Band 6 der Reihe »Methoden der Analyse in der Chemie«. Akademische Verlagsgesellschaft, Frankfurt am Main, 1968

Die äußerst rasche Entwicklung der chromatographischen Methoden in allen Gebieten der analytischen Chemie gab den Anlaß zum Schreiben von mehreren umfangreichen, je eine chromatographische Methode ausführlich behandelnden und die gesamte einschlägige Literatur bearbeitenden Monographien. Diese sind für Fachleute, die die Methode kennen und in der Praxis anwenden, äußerst wertvoll und nützlich, jedoch zu mühsam für Anfänger und für jene, die sich über verschiedene chromatographische Methoden informieren wollen. Diese Tatsache veranlaßte den Verfasser das vorliegende Buch zu schreiben, das im wesentlichen das Material des durch den Verfasser früher an der Universität von Erlangen geleiteten chromatographischen Praktikums enthält.

Das Buch ist in vier Abschnitte gegliedert; der erste Abschnitt, der mehr als die Hälfte des Gesamtumfanges ausmacht, behandelt die Methoden der chromatographischen Trennung aus Lösungen. Im säulenchromatographischen Teil werden — nach den grundlegenden Experimenten und theoretischen Fragen der chromatographischen Trennung — spezielle Arbeitsmethoden der Säulenchromatographie, Adsorptions-, Ionenaustauscher-, Verteilungs-, Molekularsieb- und Gelfiltrationschromatographie behandelt. Anschließend folgt die Darstellung der Dünnschichtchromatographie und der Papierchromatographie sowie deren spezielle Ausführungsart, die Circularchromatographie. Zu jedem Verfahren wird die Durchführung mehrerer einfacher Übungsaufgaben ausführlich beschrieben; durch ihre Ausführung kann sich jeder Anfänger die nötigen praktischen Kenntnisse leicht aneignen.

Der zweite Abschnitt befaßt sich mit der Gaschromatographie. Nach der Einleitung folgt die Beschreibung der grundlegenden Demonstrationsversuche. Die Begriffe der Elutionsgaschromatographie, deren Zusammenhänge und Benützung bei der Auswertung der Chromatogramme werden ausführlich erklärt. Es folgt der Aufbau der für analytische Zwecke verwendeten Gaschromatographen, Vorrichtungen zum Messen der Gasgeschwindigkeit und zum Dosieren, das Einführen des Prüfstoffes in das Instrument, die Art der Vorbereitung der Säulen und schließlich die wichtigsten Trägermaterialien und Trennflüssigkeiten. Auch die Fragen der Thermostatierung der Säulen, die verschiedenartigen Detektoren und Schreibvorrichtungen werden behandelt.

Nach der Diskussion der wichtigsten Gesichtspunkte der qualitativen und quantitativen Analyse werden praktische Ratschläge zur Auswahl des für die gegebene Aufgabe am besten geeigneten Instruments gegeben. Anschließend folgt die Beschreibung einiger sorgfältig ausgewählter Übungsaufgaben.

Nach einer kurzen Behandlung der Pyrolysechromatographie und der präparativen Gaschromatographie macht der Verfasser den Leser auf die reversiblen und irreversiblen Änderungen aufmerksam, die der zu untersuchende Stoff in der Kolonne gegebenenfalls erleiden kann.

Im letzten, kurzen Abschnitt werden Anhaltspunkte gegeben, mit deren Hilfe selbst der in der chromatographischen Praxis wenig bewanderte Chemiker die geeigneteste chromatographische Methode zum Trennen eines Stoffgemisches mit gegebenen Eigenschaften auswählen kann.

Das Buch ist eine wertvolle Hilfe für Chemiker, die die Hochleistungsmethoden der Chromatographie kennen lernen wollen.

L. MÁZOR

D. JENTZSCH und E. OTTE: *Detektoren in der Gaschromatographie*

Band 14 der Reihe »Methoden der Analyse in der Chemie«. Akademische Verlagsgesellschaft, Frankfurt am Main, 1970

Einen äußerst wichtigen Bestandteil des Gaschromatographen bildet der Detektor; seine richtige Wahl und einwandfreie Funktion übt einen entscheidenden Einfluß auf die Empfindlichkeit des Nachweises oder der Bestimmung und auf die Verläßlichkeit der Ergebnisse aus. Dieser Umstand begründet die Notwendigkeit der Ausgabe einer Monographie, die sich ausschließlich mit gaschromatographischen Detektoren befaßt.

Im Vorwort weisen die Verfasser darauf hin, daß im Laufe der vergangenen 20 Jahre viele neue Detektorentypen entwickelt und mehrere, auf andersartigen physikalischen Prinzipien beruhende Vorrichtungen für Detektierungszwecke in der Gaschromatographie verwendet wurden; dennoch werden bei den im Handel vertriebenen Instrumenten fast ausschließlich Wärmeleitfähigkeits- oder Flammenionisationsdetektoren angewendet, obwohl diese weder hinsichtlich der Spezifität, noch hinsichtlich der Eichbarkeit den heutigen gesteigerten Anforderungen entsprechen. Mikrocoulometer, Reaktionscoulometer, Massenspektrometer bzw. die verschiedenen spektrophotometrischen Detektoren werden kaum angewendet, obwohl z.B die Spezifität und Eichbarkeit sowie die einfache Betätigungsweise der letzteren die entsprechenden Kenngrößen der Wärmeleitfähigkeits- und Flammenionisationsdetektoren übertrifft. Ein wichtiges Ziel des Buches ist die Beschreibung dieser Detektorentypen und ihrer Vorteile.

Im ersten Abschnitt des Buches werden — nach der Behandlung der gaschromatographischen Meßtechnik und dem Überblick der meßtechnischen Definitionen — die allgemeinen Gesichtspunkte behandelt, die zur Charakterisierung der gaschromatographischen Detektoren dienen. Der zweite Abschnitt — in einem Umfang von fast 400 Seiten — behandelt den Aufbau, die Funktionsweise und die Leistungsfähigkeit der Detektoren. Der erste Teil dieses Abschnitts befaßt sich mit den theoretischen und praktischen Problemen des am häufigsten angewendeten Detektorentyps, des Wärmeleitfähigkeitsdetektors. Anschließend folgen die mechanischen und thermischen Detektoren, sowie die auf optische und elektrische Eigenschaften ansprechenden Detektorentypen. Jeder Teil beginnt mit einer theoretischen Einleitung, wonach die Geschichte der Entwicklung des betreffenden Detektorentyps, sein Aufbau und seine Meßanordnung, seine Arbeitsweise und Leistungsfähigkeit sowie die gesamte bezügliche Literatur folgen.

Im nächsten Abschnitt werden die theoretischen und praktischen Probleme jener Detektoren behandelt, die auf dem Prinzip des Ladungstransportes im elektrischen Feld beruhen. Nach den Vorrichtungen mit radioaktiven Quellen folgt die Diskussion der einfachen Flammenionisationsdetektoren, dann der Thermoionen-Flammendetektoren, der Thermoionen-Spektrophotometerdetektoren, der Entladungsdetektoren, der Photoionisations-, Feldemissions- und selbständigen Entladungsdetektoren. Ein besonderer Teilabschnitt behandelt die Kontrolle der Radioaktivität und des Ledung/maß-Quotienten. Es folgen die Detektierung auf der Grundlage von physikalisch-chemischen Reaktionen (im wesentlichen Coulometrie- und sonstige elektrochemische Methoden) und die Verwendung der Dünnschichtchromatographie als Detektiermethode.

Der dritte Abschnitt des Buches befaßt sich mit praktischen Fragen. Hier werden die Detektoren als Teil der gesamten gaschromatographischen Apparatur vor den Leser hingestellt. Der Teil »Prüfung der Detektoren« befaßt sich mit dem Prüfen auf Linearität mit einem Gasverdünner. Der letzte Abschnitt befaßt sich schließlich mit den Zusammenhängen zwischen Detektor und Analyse und gibt praktische Ratschläge zum Abstimmen der Parameter der Säule, der Füllung und des Detektors.

Die wertvolle, theoretisch auf hohem Niveau geschriebene und zugleich auch die praktischen Fragen nicht vernachlässigende Monographie leistet gute Dienste allen Analytikern und Physikochemikern, die sich in theoretischer oder praktischer Beziehung mit gaschromatographischen Detektoren befassen.

L. MÁZOR

Z. G. SZABÓ: *Anorganische Chemie. Eine grundlegende Betrachtung*

Heidelberger Taschenbücher, Springer-Verlag, Berlin—Heidelberg—New York, 1969. 159 Seiten, 16 Abbildungen und 20 Tabellen

Das Kenntnismaterial, das Chemiestudenten im Laufe ihres Studiums zu bewältigen haben, wird immer größer, weshalb es äußerst wichtig ist, die unbedingt notwendigen Angaben zweickmäßig auszuwählen. Es ist unmöglich, aber auch unnötig, alle physikalischen und chemischen Eigenschaften sämtlicher Verbindungen zu beschreiben; es sollen vielmehr jene grundlegende Gesetzmäßigkeiten erläutert werden, aus denen entsprechende Schlußfolgerungen gezogen werden können.

Das Buch von Professor Z. G. SZABÓ ist in 8 Hauptabschnitte gegliedert. Der Behandlung der allgemeinen, teilweise physikalisch-chemischen Grundlagen (I) folgt die Beschreibung der Eigenschaften der einzelnen Elementgruppen (II) und Verbindungen (III). Die weiteren Abschnitte sind den anorganischen Redoxvorgängen (IV), der biologischen Bedeutung der Elemente und deren Verbindungen (V), dem geochemischen Vorkommen der Elemente und ihrer Häufigkeit (VI), den Darstellungsverfahren der Elemente sowie anorganischen Verbindungen (VII) und abschließend ihrer praktischen Anwendung (VIII) gewidmet.

Neben dem bündigen aber dennoch klaren und leicht verständlichen Stil des Buches ist die Art der Behandlung des Materials ein besonders wertvoller Zug. Es wurde hier die deskriptive, eine Unzahl von Angaben enthaltende Schreibweise der früheren Lehrbücher der anorganischen Chemie aufgegeben; an ihre Stelle tritt eine auf moderne Kenntnisse der Atom- und Molekülstruktur aufgebaute Diskussion der angeführten Themenkreise. Das Ziel liegt nicht darin, massenhaft physikalische und chemische Kenngrößen und Zahlenwerte anzuführen, sondern darin, Zusammenhänge, Gesetze, periodische Funktionen gründlich darzustellen, woraus dann hinsichtlich der verschiedenartigen wichtigen Eigenschaften mehr oder minder sichere Schlüsse gezogen werden können. Aus diesem Gesichtspunkt ergibt sich eine einheitliche Behandlung all dessen, was die Grundlagen der modernen anorganischen Chemie bildet, fundiert auf das Verständnis der Gesetzmäßigkeiten des Elektronenschalenaufbaus, der im periodischen System zusammengefaßten Änderung der Eigenschaften der Elemente, der Atom- und Ionengröße, der Ionenbildung, der Bindungstypen, dem Übergang zwischen den Bindungstypen, der Elektronegativität, der durch die Bindungstypen bestimmten Eigenschaften.

Der Rezensent ist davon überzeugt, daß dieses Buch nicht allein für Chemiestudenten sondern auch für die in verschiedensten Gebieten arbeitenden Fachleute von hohem Wert und Nutzen sein wird.

J. CSÁSZÁR

U. GRIGULL: *Technische Thermodynamik*

Zweite erweiterte Auflage, S. 173. Sammlung Göschen Band 1084/1084a, Walter de Gruyter und Co. Berlin, 1970

Dieser Band der über außerordentlich edle Traditionen verfügenden Göschen Serie ist wieder ein Beweis dafür, daß die Möglichkeit gegeben ist, ein weites Anwendungsgebiet der Physik, die durch die Technische Thermodynamik repräsentiert ist, in einem minimalen Umfang und auf anspruchsvollen theoretischen Grundlagen in Betracht zu ziehen. Im Büchlein können wir außer den Grundbegriffen, Größen, Einheiten und Hauptsätzen der Thermodynamik und der logischen didaktischen und exakten Bekanntgabe deren mathematischer Formulierung auch die physikalische Beschreibung der Arbeitsstoffe von Kraft und Arbeitsmaschinen vorfinden sowie die Beschreibung von Kreisprozessen charakteristisch für die technische Thermodynamik.

Im Werk sind 9 Kapitel enthalten, von welchen das I., II. und IV. Kapitel den Grundbegriffen der Thermodynamik bzw. der Bekanntgabe des ersten und zweiten Hauptsatzes gewidmet ist. In diesen Kapiteln ist die exakte und konzise Entwicklung der Grundlagen der Theorie vorzufinden, auf welche die weiteren Anwendungen wie auf feste Grundlagen gebaut sind. Kapitel III ist mit Hinsicht auf die Theorie und deren Anwendungen von übergänglichem Charakter. In diesen Abschnitten werden die physikalischen Eigenschaften von idealen Gasen

und Mehrphasen-Systemen in einer sehr anspruchsvollen Art behandelt. Kapitel VI—IX befassen sich hauptsächlich mit Anwendungen. In diesem Teil des Werkes sind außer der Bekanntgabe der Kreislaufprozesse von idealen Gasen und Dämpfen die Elemente der Gasdynamik, die Beschreibung der Zustandsänderungen und Eigenschaften von Gas–Dampf-Gemischen beschrieben.

Wir empfehlen das Werk herzlichst nicht nur den sich für die technische Thermodynamik eingehend interessierenden Fachleuten, sondern auch Universitätshörern und auch sämtlichen Personen, die rasch eingehende Kenntnisse in diesem Gebiet der Ingenieurwissenschaft erringen möchten. Es scheint, daß in der internationalen Literatur im Themenkreis der technischen Thermodynamik kein anderes Werk existiert, in welchem die Bekanntgabe des Themas in einem so limitierten Umfang mit ähnlicher Logik und Genauigkeit geboten wäre.

I. GYARMATI

D. KILSHAW: *Steroids; Principles and Techniques*

Butterworth, London 1970

This book, consisting of 64 pages, is divided into 10 chapters and contains 50 references. As shown by the sub-title (Principles and Techniques) the work is intended primarily for laboratory practice. For this purpose as a concise and clearly written guide, it will apparently find good use, primarily in clinical practice. The Appendix at the end of the book is very helpful, as it indicates, in addition to the rational names, the trivial names used in clinical practice.

A special merit of the book is that it comprises steroid determinations which are in the foreground of research and interest today, such as those used in endocrinological and gynecological tests.

The part on the structure of steroids in Chapter 1 is insufficient and unsatisfactory. It does not contain any new information for the expert, and cannot be used by the non-specialist. The first formula is incorrect, because it gives the pregnane skeleton as a cyclopentenoperhydrophenanthrene ring system. It is not advantageous that the scope of the book is rather limited (colour reactions, mainly the Zimmermann reaction), and it does not deal with other methods, *e.g.* the use of radioisotopes, etc. Some parts of the book are too short, and are written almost in telegram style. The references are cited in an unusual way. They are not numbered, but listed in alphabetical order.

The book has been published as a member of the "Laboratory Aids Series".

Notwithstanding its considerable shortcomings, the book can be recommended for practical use.

K. KOVÁCS

E. JUCKER, Ed.: *Progress in Drug Research*

Vol. 14, 586 pp. Birkhäuser Verlag, Basel, 1970

In the first chapter (E. J. ARIËNS: Reduction of drug action by drug combination) of the new, 14th volume of the known series, the author deals very concisely (47 pages), still with reference to a large number of works, with the reduction of drug action occurring in the use of drug combinations, and systematizes these cases. In the first part of the survey (Reduction in the action of a drug due to a decrease in its biological availability) the following possibilities of the reduction of drug action are discussed: a compound may change the gastrointestinal function (*e.g.*, $MgSO_4$, cholinolyticum), the pH in the body fluids, one compound may bind the other in the stomach or after absorption, the compounds may influence the transport of another drug, they can enhance its biochemical conversion, its metabolism, or may reduce its bioactivation. The second part of the work (Reduction of the response to drugs due to interactions which take place on the pharmacodynamic level) is a concise summary of the possibilities partly discussed earlier in more detail: competitive, non-competitive, combined, irreversible, functional antagonism. Several examples are given (combinations of antibiotics and chemotherapeutic compounds, drugs acting on the central nervous system and hormones,

which reduce the action of each other), and finally a short survey deals with the problems of cross resistance, tolerance, and tachyphylaxis. Though concise, the work treats many problems. Owing to its lucid style, well arranged tables and clear schematic diagrams, this summary is interesting and easy to understand also for readers less acquainted with the particular field discussed.

The second chapter (S. EHRENPREIS: Drug-macromolecular interactions: implications for pharmacological activity) deals with the relationship between the linking to macromolecules of a drug and its action. The summary gives a clear picture of many new aspects on the problem of the dependence of drug action on the linkage to receptors or acceptors. This latter binding, which may be called aspecific, might be the cause of untoward side-effects. In addition to a theoretical and methodological summary, the author discusses extensively the binding of anti-inflammatory agents, anticoagulants, chemotherapeutic agents, anesthetics and psychopharmacological agents to macromolecules. Special mention should be made of the part the compilation of which discusses the binding of monoamines to their antagonists and the resulting effect.

The third comprehensive study of the book (O. LINET: Interactions between androgenic anabolic steroids and glucocorticoids) describes primarily those investigations (observations in laboratory animals and in clinical tests), which attempt the elimination of the untoward side-effects of glucocorticosteroids by means of anabolic steroids (according to the nomenclature of the author: androgenic-anabolic steroids). In the paper, summarizing an immense experimental material and literature, the conclusion is reached that the various toxic side-effects of glucocorticoids can be prevented by the use of anabolic steroids without a decrease in therapeutic effect. Indeed, the therapeutic effect is even increased in certain cases in combined administration.

In the next chapter, G. B. WEST and M. S. STAR (A new approach to the medical interpretation of shock) elucidate the development of allergic reactions and anaphylactic shock from a new aspect. They start with the fact that one part of Wistar strain rats is not sensitive to ovalbumin and dextran, and this property can be inherited. The authors establish that the amount of bradykinin formation and liberation and the measure of the outflow of catecholamine are very important factors in the sensitivity behaviour. The histamine and bradykinin sensitivity of sensitive and non-sensitive animals is also different. The experiments described help to solve the problem why some people are sensitive to ovalbumin while others are resistant.

The chapter "Biological activity in the quinazolone series" (A. H. AMIN, D. R. MEHTA and S. S. SAMARTH) true to the traditions of the series demonstrates the structure and biological activity relationship for a group of compounds with important biological activity, in the present case on the example of quinazolone derivatives. It is remarkable that although several derivatives of the basic compound, 4(3H)-quinazolone, have been known for almost half a century, only "the isolation of an antimalarial alkaloid from the Chinese plant Ch'ang Shan in 1946 and an identical alkaloid from hydrangea in 1952, gave the great impetus to the . . . investigations of biological activity of quinazolone derivatives . . .". Extensive research being in progress since that time which the authors give a representative picture in 43 pages, has led finally to two derivatives of therapeutic importance: 2-methyl-3-(o-tolyl)-4(3H)-quinazolone (methaqualone), a hypnotic and anticonvulsant, and 7-chloro-2-ethyl-1,2,3,4-tetrahydro-4-oxo-6-quinazoline sulfonamide (quinethazone), a diuretic. The summary discusses the subject in the following grouping: quinazolones as antimalarials; quinazolones acting on the central nervous system; methaqualone; quinazolones as diuretics; quinethazone; quinazolones as antihypertensives, as antituberculotic agents, as bronchodilators, as anti-inflammatory agents; antiamoebic action of quinazolones, and finally, miscellaneous biological activities.

The sixth chapter of the volume is the work of K. MÜNZEL: Galenische Formgebung und Arzneimittelwirkung — Neue Erkenntnisse und Feststellungen, Teil 1 (Galenic formulation and drug action — New knowledge and findings). It is a long-needed summary on a very important problem. Its importance lies in the fact well-known to every medicinal chemist and pharmacologist that it is not sufficient to prepare compounds with favourable activity, but they must be introduced into the organism in a form which ensures optimum action. In this first part of the work, the "drug forms" of pesticides, official problems ("Biopharmazie als Politikum" [Policy in Biopharmacy]), the possible reasons of unsatisfactory drug action and the possibilities of the reduction of the side-effects of drugs are briefly dealt with.

The mode in which the chemical, physico-chemical and physical properties (salt and ester form, crystal form, solubility, particle size, etc.) affect the absorption of drugs is discussed in detail. The last chapter of the first part deals with the role played by auxiliary (carrier) substances in the absorption of drugs: stabilizers, various complexing agents, tensides (surface-active substances, detergents), etc. The important work of 117 pages gains further value by the more than 300 references, given with full title.

In the last review of the volume (K. E. SCHULTE und G. RÜCKER: Synthetische und natürliche Acetylen-Verbindungen als Arzneistoffe [Synthetic and natural acetylene compounds as drugs]) the authors clearly systematize about 1500 compounds containing acetylene groups, both from the point of view of chemical structure and biological activity. Considering the material treated, the extent of the work is not large: 176 pages, out of which the text is about 55 pages, tables occupy 88 pages, while 1092 references are listed on 33 pages.

The grouping of the compounds is twofold, being based on the pharmacological action and on the chemical structure. The seven groups of pharmacological action are: (1) narcotics, hypnotics, sedatives and anticonvulsants; (2) compounds acting on the sympathetic nervous system; (3) amine oxidase inhibitors; (4) analgesics, antitussives, local anesthetics and smooth muscle spasmolytics; (5) hypotensive agents; (6) cytostatics; (7) bactericides and fungicides. An interesting feature of the work is that the about 80 natural acetylene derivatives occurring in plants of higher and lower order are discussed in separate chapters.

Within the groups of pharmacological action, the compounds are grouped in 56 tables according to their chemical structures. These tables are well arranged, easy to survey, and contain, wherever possible, in addition to the chemical structure also the pharmacological data. This allows in several cases a quick and good orientation on the relationship between chemical structure and biological activity.

The work describes the preparation of the most important compounds, gives references to the chemical literature and the pertinent patents. It gives a detailed description of the biological, pharmacological, toxicological, biochemical effects and side-effects of the most important and characteristic compounds, discusses their metabolic fate and transformation within the organism, and indicates their possible uses in clinical practice. The structure of the work permits a quick orientation in the immense subject both for the pharmacologist and the chemist.

GY. DEÁK, L. GYÖRGY, K. PFEIFER

NMR Basic Principles and Progress. Vol. 4. *Natural and Synthetic High Polymers*

Editors: P. DIEHL, E. FLUCK, R. KOSFELD
Springer Verlag, Berlin—Heidelberg—New York, 1971

This volume contains the main lectures presented at the Seventh Colloquium on NMR Spectroscopy held in Aachen, Germany, April 13—17, 1970; of 17 lectures presented, 12 dealing with NMR spectroscopy, the remaining 5 are devoted to such related topics as copolymerization theory, electron spin resonance, dielectric relaxation and infrared spectroscopy. The volume (309 pp.) contains 202 figures; 13 papers are written in English, 4 in German.

In the field of high resolution NMR, F. A. BOVEY (New Jersey) reviews recent results obtained in his laboratory, using a 220 MHz superconducting spectrometer.

Analysis of the spectra of polypropylene, polyvinylchloride are discussed in detail with special reference to stereochemical analysis. The 13 C method is also reviewed briefly. The paper is not introductory and does not intend to cover the whole field. The examples chosen are very important and the results are illustrative.

The second main field dealt with is the analysis of copolymers by high resolution NMR (4 papers). α-methylstyrene-butadiene copolymers are treated by H. J. CANTOW, K. F. ELGERT, E. SEILER and H. FRIEBOLIN (Freiburg, Germany). In this paper the stereochemical analysis of pure poly-α-methylstyrene is discussed on the basis of 220 MHz NMR spectra, and the sequence lengths of its copolymers with butadiene are determined. Methyl methacrylate-methacrylic acid copolymers are discussed in the paper of E. KLESPER, W. GRONSLEI and A. JOHNSEN (Freiburg).

Copolymers containing aromatic rings such as styrene-methyl methacrylate, styrene-butadiene, styrene-methacrylonitrile are discussed in detail by H. J. HARWOOD (Akron, Ohio). The problem of cotacticity in acrylonitrile-methyl methacrylate copolymers is studied by Q. T. PHAM (France), using the 60 MHz technique.

In 2 papers theoretical problems of copolymerization are dealt with: the kinetic study of the penultimate effects in radical copolymerization by J. GUILLOT (France) and new concepts in copolymer statistics by C. TOSI (Italy). In these papers the NMR method is not used.

The third main field discussed in the book is the application of the NMR method for studying polymeric solids. This field is excellently reviewed by E. P. SLICHTER (New Jersey).

In his paper the physical basis of the method is described very briefly and the possible applications to various polymeric systems are illustrated by well chosen examples. In this volume SLICHTER's paper is the only one which fulfills the aim expressed in the editorial preface, namely that the papers should "take the reader from the introductory stage to the latest development of the field".

From this review it appears clearly how the problem of multiple relaxation phenomena and molecular motion in polymers can be studied by measuring nuclear magnetic relaxation times. The results of NMR experiments are compared with those obtained by dielectric and mechanical relaxation methods. The problem of molecular mobilities in polymeric solids is also discussed in K. BERGMANN's (Ludwigshafen) paper. This paper is centered on a phenomenological analysis of the wide-line NMR line shapes in amorphous and crystalline systems.

A special paper of T. M. CONNOR is devoted to the rotating frame spin-echo method for measuring magnetic relaxation in polymers. This powerful new method for studying molecular mobilities in polymers is extensively reviewed in the paper.

Three fields related to the NMR technique are discussed in the last three papers of the book: dielectric relaxation of amorphous polymers by G. WILLIAMS and D. C. WATTS (Wales), conformation of chains as revealed by infrared spectroscopy by SHIMANOUCHI (Tokyo) and ESR by FISCHER (Zürich). In these papers special problems of the corresponding fields are discussed with no intention to review the recent results. In a book dealing with NMR spectroscopy it would have been more useful to include such review articles which would inform the reader about the possible connections between NMR and the related fields. The papers presented in this book certainly do not fulfill this requirement, they are written for specialists of the particular field rather than for those of NMR.

P. HEDVIG

Fortschritte der chemischen Forschung

New Results in Boron Chemistry
Volume 15, Number 2, July 1970. Springer Verlag, Berlin. 280 pp., illustrations and tables.

This part of the excellent series provides information on the following topics: the new chemistry of smaller boron hydrides (H. D. JOHNSON and S. G. SHORE), the preparative aspects of cyclic boron nitrogen compounds (A. MELLER), the 1,3,2-diazoboracycloalkanes (K. NIEDENZU and C D. MILLER) and finally, the representation and systematization of borates and polyborates (G. HELLER). It does not seem likely that, according to the editors, the topics listed have special significance in today's boron chemistry: on the contrary, some papers deal with not quite "fashionable" subjects. Thus, for example the hydride chemistry of boron seems lately to predominate over the chemistry of borates in our opinion, without convincing reasons. The intention of the editors to draw attention to such topics is, therefore, to be appreciated. Of course, there are also "top-hits" in the book, such as the B—N ring and the similarly exciting cyclic diazo-boron-alkanes.

The first paper deals with "conventional" boron hydrides containing a maximum of eight boron atoms. The author reviews and systematizes the papers published since 1964. The main virtue of the paper is its uniform aspect, based on molecular structure and reactivity. From this point of view a very interesting classification principle has been applied: the boranes can be divided into two large groups depending on whether or not they contain a BH_2 group. The paper discusses recent structural and energy data regarding the B—H—B bridge and the 3-center bond. The summary given in tabulated form is of great value; it represents the first detailed review on the adducts of borane, describing 61 compounds. It gives their structures, the physicochemical information reported up to now, as well as their source. After the tabulated summary, preparative details are also reported for selected groups of compounds, and the reactions and properties interesting from the viewpoint of general inorganic chemistry are emphasized. The presentation of the experiments and results based on the analogy of BH_3 and oxygen suggested by MULLIKEN is very interesting. The adducts of BH_3 and phosphine provide a picture about the electronic structure of the latter compounds. Also the relative basicities of transition metal carbonylates could be evaluated on the basis of the stabilities of the BH_3 adducts. The paper gives an excellent summary of the chemistry of the different boronium ions formed from B_2H_6. Here, as in other parts, the author shows a preference for collecting analogies and, indisputably, this is of the greatest value for the reader.

In accordance with their nature, the higher boranes provide a more limited subject. The following topics should be mentioned from this field. In complexes of the octahydrotriborate(1-) ion, a double hydrogen bridge is formed, the third kind of the B—H bond known up to now. The tautomerism of the $B_5H_8^-$ ion draws attention to the fact that the field most closely related to organic chemistry is the boron-hydrogen chemistry (and not silicon chemistry!). In the discussion of the chemistry of higher boranes one has to realize the great contribution of the NMR method and radiochemistry to the investigation of the structure of the often very complicated cage-molecules and isomers.

The survey by A. MELLER, the second in the book, discusses the subject in three parts: symmetric borazines which are essentially rings consisting of B—N units; boron nitrogen rings containing also B—B bonds and, finally, those involving N—N bonds. The two latter chapters are short, but the first gives a complete survey. We have to point out the value of reviews on the derivatives, *e.g.*, of the first tabulated summary of organofluor borazines. The preparative methods are critically evaluated in each case and, whenever possible, the relative reactivities and stabilities of the products are also given. In the B—N chemistry the hydrolytic stability and polymerizability are particular topics. These aspects are continuously present in the paper. The author emphasizes the new, advancing and most exciting trends, such as the substitution reactions (at both the boron and nitrogen atoms) and their products, the π-complexes formed of chromium and molybdenum with borazines and CO, as well as the group of s-diazoborines which seems to be very attractive from several points of view, though no satisfactory preparative path has been developed for them.

K. NIEDENZU and C. D. MILLER review an interesting group of σ-bonded heterocycloalkanes, 1,3,2-diazoboracycloalkanes. Practical expectations and bond-theoretical interests are attached to these compounds, since some of them and their derivatives may act as carcinostatic and sedative drugs, insecticides, and fungicides. With suitable substituents at the boron atom they can perhaps be condensed to larger molecules, possibly polymers of considerable thermal stability. The authors make no attempt to predict whether or not these expectations will come true, but they give an excellent summary of the development of preparative methods applied for these compounds, their characteristic reactions and of the results dealing with their molecular structure. We have to emphasize the fact, for which there is now ample evidence that the rings, in spite of their apparent σ-character, involve π-type bonding and their coplanarity extends even to the alkane component.

The data regarding these compounds are summarized in three tables; the physicochemical aspects are based on molecular spectroscopic and mass-spectrometric investigations.

The last, very detailed paper of the book written by G. HELLER, can be regarded as an original work, rather than just a review of the literature. The author sets out from the correct inorganic chemical idea that the chemistry of borates has undergone too much distortion because of an attitude overemphasizing the similarity between borates and other polyacid derivatives, such as silicates and phosphates. The author is right in speaking against this and suggesting original approach and systematization in borate chemistry. For this purpose, he goes back to the fundamentals, presenting the subject as a whole, in addition to reviewing the most recent results in this field. His bond-theoretical systematization is based on the three rules of Edwards and Ross to which he attaches his own, very detailed investigations. These involve a very ingenious preparative technique, *viz.*, the hydrolysis of boric esters with a stoichiometric amount of water in an organic solvent, followed by the ^{11}B—NMR and ^1H—PMR determination of the borate insoluble in the organic solvent, thus forming a precipitate. The method suggested by the author provides information on several new structures, since this procedure gives substances free of hydrate-water, thus eliminating the interference from water; species sensitive to hydrolysis can also be detected. The paper provides detailed information on the data with respect to the cations and suggests a systematization principle for borates and polyborates. Its essence is very simple: the classification should be based on the isolated or polymeric character of the complex and on the number of boron atoms in the structural unit. Doubtless, a simple nomenclature can be constructed in accordance with this system, the only question being whether or not the compounds included in the individual classes are really related to each other. The main virtue of the paper seems to be not the presentation of this system but the excellent review of the new result and the literature.

T. SZÉKELY

B. Lőcsei: *Molten Silicates and their Properties*

Akadémiai Kiadó, Budapest, and Chemical Publishing Co. Inc., New York, co-publishers, 1970. 135 pp., 13 tables, 129 figures, 199 references. English translation by F. Sós

The book is the extended English translation of the work of B. Lőcsei: "Molten silicates and their properties", published as the 8th volume of the series "Monographs on Silicate Chemistry (Akadémiai Kiadó, Budapest 1967).

Today molten silicates form one of the targets of scientific research and practical interest. In Hungary, Béla Lőcsei is one of the pioneers of this research work. His book summarizes scientific results, obtained in Hungary and abroad, relevant to molten silicates. A considerable part of the former constitutes his own research work.

Petrurgical (molten rock) and vitroceramic products can be prepared by crystallization from melts. Characteristic of the products of both groups is the fact that they can be prepared from the melts by casting, cooling and heat treatment according to exact prescriptions.

After a short introduction and historical survey, the author discusses the basic principles of the preparation of molten silicates. The conditions of primary nucleation of molten rocks and of secondary nucleation of vitroceramic products (produced by mineralizers) are given.

The next chapter on the oriented crystallization of glasses is a high-level scientific description of the nucleation process. The influence of the activation energy on the nucleation rate is discussed. In connection with this, the author discusses his own theoretical considerations under the name "microeutectic principle", and compares his own results with those reported in the literature. He elucidates the effect of nucleators, the effect of cooling rate, *liquidus* temperature, and viscous energy on nucleation. Unfortunately, this chapter is not sufficiently long and detailed.

The definition of "mineralizer" and "nucleator" used in this chapter (IV/B) may be disputed. In the English literature these two concepts are clearly distinguished, whereas the author uses them alternatively at the expense of clarity.

Chapter V discusses in general the operations of the preparation of molten silicates such as preparation of the raw material, melting, processing of the melt, casting and crystallization. This short chapter, giving a good summary of the technology, does not call for the amplification on crystallization, added in the American edition. This very valuable material could have been arranged more suitably as part C in Chapter IV.

The chapter discussing vitroceramics on feldspar – diopside basis contains the results of the author, according to which the vitroceramic products can be prepared on blast furnace slag basis by some corrections in the chemical composition and by the use of mineralizators. Thereby, the principle of the preparation of vitroceramics is actually extended to "molten artificial stones". The properties and the texture of the product obtained are described in detail.

The last chapter of the book deals in general with the properties and possible applications of vitroceramics.

A bibliography of 199 references completes the monograph.

In the Hungarian literature, the book is a pioneering work. The research work undertaken by Béla Lőcsei in the field of molten silicates has brought recognition from various parts of the world. Unfortunately, he has not used the American edition for a more extensive discussion of his own results and hypotheses made in this field. It is regrettable that sometimes the borderline between the individual findings of the author and the review of the pertinent literature becomes indistinct. The book has no author or subject indexes, which substantially hinders its easy handling.

The figures and microscopic photos are much better in the American than in the Hungarian edition.

This book will be of great interest also in other countries for theoretical and practical experts in silicate chemistry.

It can be recommended also as a university textbook.

M. Déry

W. Demtröder: *Laser Spectroscopy*

Springer Verlag, Berlin, 1971. III + 95 pp., 16 figures

The rapid development of laser techniques in recent years widened substantially the possible applications of lasers in the most various fields of physics and chemistry. Several thousand kinds of laser beams, with wavelengths from the microwave to the ultraviolet region,

can be produced today, which permit the spectroscopic utilization of lasers. Lasers enable the solution of problems which are unsolvable with conventional light sources, and experiments unfeasible with other light sources can be easily carried out. The advantages of lasers can be summarized as follows:

1. A single spectroscopic transition produces radiation of very high energy.
2. The coherence of the induced emission permits almost perfect focussing.
3. The natural spectral line-width is by several orders of magnitude smaller than in the case of common monochromatic light sources.
4. Within a narrow frequency range, the frequency of laser beams can be tuned, which makes lasers particularly suitable for special investigations.
5. The peak power of pulsating lasers may attain 10 GW, and at the same time the pulse-width may be reduced to 0.1 μs, which permits the study of very rapid processes (decay of excited states, lifetime measurements, flash-photolysis, etc.).

The text of about 80 pages is divided into four parts. In the first part the characteristic properties of lasers are discussed and compared with those of other light sources from the viewpoint of spectroscopical application.

The second, and longest, part deals with spectroscopic experiments which use "external" light sources, *i.e.* the system studied is outside the laser resonator. The examples given concern the following spectroscopic fields: absorption, fluorescence, lifetime measurements of excited states, investigation of collision processes, photochemical processes, Raman spectroscopy, measurement of light scattering, plasma spectroscopy, microanalysis and spectrophotometry, spectroscopy of solids.

In the third part the author discusses those new methods of high-resolution spectroscopy which are based on various saturation phenomena. Some of the experiments are carried out within the laser resonator; this results in the coupling between the absorption of radiation and the mechanism by which radiation is produced. The feed-back effects arising from this permit high precision frequency stabilization and the measurement of frequency shifts and line shapes, with an accuracy far beyond the reach of earlier methods. By studying the interaction of light radiation and matter, the results of theoretical calculations can be checked.

The fourth part is concerned with the spectroscopic study of various laser processes. These investigations are aimed at clarifying the nature of excitation, the precise assignment of transitions and the fundamental collision processes. For chemists, the study of chemical lasers (quantum generators) is of particular interest. In these, the heat of reaction is directly converted into light energy.

W. DEMTRÖDER, Head of the Physics Department of the University of Trier—Kaiserslautern, treats a very wide field, but in view of the restricted extent of the book, obviously, the discussion can be neither complete nor detailed. From objectivity towards the topics discussed, the author did not even unify the units used by the different authors. The aim of the author was to give a survey on those methods of modern spectroscopy, the introduction of which was made possible by the discovery of the laser. Reviews of this kind do excellent service to those researchers who work in related fields, and wish to keep abreast of the rapid technical development.

Gy. VARSÁNYI

Reactive Intermediates. Topics in Current Chemistry

R. A. ABRAMOVITCH, R. G. SUTHERLAND: Chemistry of Sulphonyl Nitrenes, — H. HEANEY: Chemistry of Highly Halogenated Arynes, — E. WINTERFELDT: Hetero-Cope-Reaktionen. Fortschritte der Chemischen Forschung, Band 16, Heft 1, Nov. 1970. Springer-Verlag, Berlin, Heidelberg, New York, pp. 102

As indicated by the title page of the book, "Reactive Intermediates" contains 3 reviews. *Chemistry of Sulphonyl Nitrenes.* Sulphonyl nitrenes, like other nitrenes and the isoelectronic carbenes can exist in either the singlet ($RSO_2\ddot{N}$) or triplet state ($RSO_2\dot{\ddot{N}}\cdot$) and their chemical and physical properties will vary accordingly. Though the intermediate is usually generated as the singlet, since the ground state is the triplet, inter-system crossing can occur if the intermediate survives several collisions or if the substrate is relatively inert. It is important to bear in mind that the reaction observed may not be due only to a nitrene intermediate but to a precursor such as the sulphonyl azide, *e.g.* triazoline formation followed by loss of nitrogen

to give the same product as would be derived from the free nitrene. The chemical reactions through the sulphonyl nitrenes are sometimes complicated and diversified.

The review gives a survey on the formation of sulphonyl nitrenes and on their various reactions. The following titles of chapters illustrate the scope of the material which is completed by a list of nearly 80 up-to-date references: Generation of sulphonyl nitrenes from sulphonyl azides (by thermolysis, photolysis and metal catalysis) and other compounds. Reactions occurring through nitrenes: 1. Hydrogen abstraction, 2. Insertion into aliphatic C—H bonds, 3. Aromatic substitution, 4. Addition to olefines, 5. Trapping by nucleophiles, 6. Molecular rearrangement, 7. Applications (including the synthesis of cyclic sulphonamides).

Chemistry of Highly Halogenated Arynes. Recently, attention was directed towards arynes (dehydrobenzenes), regarded as strongly electrophilic intermediates reacting with nucleophiles and entering into cycloadditions with various compounds. The author gives a survey on studies which are concerned with the preparation and reactions of arynes of enhanced electrophilic character due to the presence of 4 electron-withdrawing substituents. Of special interests are the studies aimed at the preparation and reactions of tetrafluorobenzyne and other halogenobenzynes. Thus, by reacting *e.g.* butyl lithium with bromopentafluorobenzene, products are formed which indicate the presence of a tetrafluorobenzyne intermediate. Benzyne formation was observed in the pyrolytic decomposition of numerous compounds. A convenient synthetic route is aryne formation through diazotization of tetrasubstituted anthranilic acids, in which benzyne gives a 1,4-cycloadduct with benzene present as the solvent. The reactions of benzynes with other aromatic hydrocarbons, styrenes, alkoxyaromatic compounds, thioethers, dimethylaniline, steroid dienes and carbonyl compounds are also treated in the review.

Together with the author's own publications, the review is completed with a list of 172 references.

Hetero Cope Reactions. The term Hetero Cope Reaction refers to a special class of sigmatropic rearrangements in which two allyl radicals are simultaneously formed and recombined. According to modern terminology, this may involve only a transition state allowed by the principle of orbital symmetry conservation. The author's objective is to give a summary on the so-called 3,3-sigmatropic rearrangements (Cope reactions) of substrates containing heteroatoms. The energy of the transition state is decreased by the presence of the heteroatom, thus the rearrangement can be carried out even at relatively low temperatures.

The review begins with the description of Claisen-analogous hetero rearrangements, then new details are given concerning the thio Claisen and aza Claisen reactions. A separate chapter is devoted to Fischer-analogous hetero Cope reactions, and finally, the reactions involving ionic transition states are discussed. The monograph contains 97 references.

The reviewer wishes to express his greatest appreciation of the high standard of monographs published in the series "Fortschritte der Chemischen Forschung", but considers it necessary to call attention to an ambiguity in the title of this volume. Of the three reviews in the present volume, the first is concerned with nitrenes, and the second with arynes, which are indeed reactive intermediates. The subject of the third review (Hetero Cope Reactions). however, is a reaction occurring in a single step, apparently without any intermediate. In the reviewer's opinion, this excellent monograph either should have been published in another volume or, if included in the present one, its title should have been modified. An introductory note calling the reader's attention to these essential differences in the mechanism would have served the same purpose.

A. MESSMER

E. PARHAM: *Syntheses and Reactions in Organic Chemistry*

John Wiley and Sons, Inc., New York, 1970. 553 pp.

This book provides a program for some studies by undergraduates and young graduates on organic chemical reactions. In the reviewer's opinion, the author has reached his aim.

The book consists of ten main chapters: aromatic substitutions, electrophilic reactions in aliphatic systems, molecular rearrangements, nucleophilic reactions in aliphatic systems, elimination reactions, nucleophilic substitutions, nucleophilic additions (including organometallic compounds), condensation reactions of carbonyl compounds, reduction processes, preparation and reactions of free radicals, molecular reactions, photochemistry. The sequence of

the chapters corresponds to that applied in the textbook written by R. C. FUSON ("Reactions of organic compounds", Wiley, New York, 1962), so the latter is recommended by the author as a supplementary text.

The purpose of the book is not to present a great number of reactions, processes and encyclopedic information in the field of organic chemistry, but to group various organic processes which may seem very different at first sight, and to analyze them in such detail as to obtain a reasonable formulation of the mechanisms involved. This aspect must be given strong emphasis from the viewpoint of up-to-date teaching since in this way the treatment of the subject, by focusing attention on the reaction mechanism, reveals the essential features, applying a dialectic method and stimulating the students to concentrate on the most important parts of the great amount of organic chemical information. This approach based on the mechanisms of the different processes permits to show the interrelation of several apparently independent reactions, thus they can be remembered more easily. In fact, some of the reaction mechanisms are oversimplified, thus not perfectly accurate, but this does not reduce the value of the book. The simplifications serve to reach the purpose of the book more easily and the omission of complications hindering the understanding promotes learning the subject.

It can be considered very useful that the author, being a university professor, utilized in the book the results of his own research and his educational experience. The definitions regarding the reactions are concise, accurate and clear. The use of advanced, easily available monographs and well-known journals in collecting the subject material greatly assists the reader who wishes to find an auxiliary textbook or searches for additional information. The list of references also increase the usefulness of the book. Its special virtue is its shortness. Instead of lengthy and verbose explanatory texts, an exact, easily understandable discussion method offered by organic chemical formulas is applied, which is to be greatly appreciated. With respect to its textbook character, however, certain formal additions would have made the handling of the book easier. The omission of titles to the chapters and the absence of a clear separation of the sub-chapters is a shortcoming. So, at the first sight the structure of the individual chapters and, in some cases, also the selected material seems to be questionable, and the logical construction is not always clear.

From the viewpoint of didactics, the following suggestions of the author on the treatment of the subject are approvable; in each exercise period the students should study the text first, supplement their knowledge from the Fuson book or other sources, and then answer the questions given at the end of each chapter.

Beside didactic aspects, the author took special care to treat only those organic processes having mechanisms properly confirmed on the basis of our present knowledge. The construction of the book is such that no superfluous encyclopedic information is given and no descriptive sections are included.

Finally, emphasis must be placed on the merits of the book in pointing out the characteristics of its subject and in stimulating the modern approach to organic chemistry. The entire structure of the book reflects this purpose of discussing and clearing up the most important relations by means of selected practical examples and by presenting the mechanism — and the stereochemistry, when necessary — of the reactions. In the process of learning, this aspect is of great importance.

In accordance with its character discussed above, W. E. PARHAM's book is a very useful source for the modernization of organic chemical teaching of university students and in increasing its level.

M. BARTÓK

F. W. EASTWOOD, J. M. SWAN, JEAN B. YOUATT: *Organic Chemistry*

Cambridge University Press 1970, 2nd edition, 245 pages + index

The authors working at the Monash University (Australia) designed this volume as a handbook for the first university course of the programmed teaching of organic chemistry. The book is not intended for replacing the conventional organic chemistry textbooks but only for enabling the students to learn the subject included in the program.

The reader with less experience in programmed education and unfamiliar with the topics of the subsequent organic chemical courses at this particular university, has a rather difficult task in forming an objective opinion. One must resist the temptation of detailed criticism, using the pretext of reviewing the book, therefore, it is more advisable to remain restricted to a general characterization. The book must be very useful for students attending the actual course, but a more general result seems to be also achieved by the authors: they arouse interest

in their method and suggest several very useful ideas to teachers of organic chemistry. Beyond this, all teachers who have read this book will recommend it to students, even if the topics of the lectures are different in volume and in details, together with the methods of teaching. The positive result is unquestionable for the students in spite of these differences: in fact, students not participating in programmed teaching but having a certain knowledge of the subject will perhaps be more stimulated to study the book, since it is not obligatory for them and helps them to check their knowledge by means of a new and interesting method.

The question arises how effective the connection can be between organic chemistry as a subject and the programmed teaching method. In view of the strongly descriptive character of the subject, requiring the communication of information in great amounts, the advantages of programmed teaching cannot always be as definite as in the case of other subjects. This method seems to be the most successful in those fields of organic chemistry where the primary aim is to teach the fundamentals effectively and rapidly. With respect to our teaching methods, this book could be used in training biologists or a certain group of chemical engineers.

The first two programs ("Naming organic compounds" and "Formulae, structures, equations and reaction mechanisms") suppose a certain knowledge of chemistry by the reader and discuss step by step and in a strict logical sequence all the concepts and information essential for learning the fundamentals of organic chemistry, as well as those facilitating the use of subsequent programs. The "frame" system used in constructing the programs permits the use of simple examples (formulated as questions) after a systematic description of definitions and simple information. These questions are simple, easy to understand, being designed with the purpose of at least making the reader to study the text thoroughly and re-read it sometimes. The purpose of the "test frames" is evidently different, they presume the knowledge and understanding of the subject. However, the first two programs cannot be regarded as "evening studies" for one evening each, as recommended by the authors. On the contrary, it is advisable to re-read them attentively before starting with the following programs. The sequence and content of the other programs essentially correspond to the conventional, generally applied treatment of organic chemistry.

On the basis of our experience with domestic teaching methods and traditions, a few critical comments may be made. Although the authors allow an optional sequence in the use of the programs — except for Program 12 ("Synthesis of organic compounds") — it seems to be advisable to study Program 11 ("Isomerism") before Program 6 ("Alcohols"). Here we may point out an unusual feature of the book, namely that in the sections dealing with different groups of compounds no mention is made of geometrical and optical isomerism, playing a very important role in organic chemistry; this strongly narrows the horizon of the student. On the other hand, the relatively low number of examples given in Program 11 does not satisfactorily promote the understanding of these important concepts. The construction and size of Program 9 ("Benzene derivatives") are also unusual. Although isolated and condensed polycyclic aromatic hydrocarbons are evidently discussed in subsequent organic chemical courses, the usefulness of the book as a whole would have been enhanced by supplementing Program 9 with this fundamental information and thus the program could have carried the title "Aromatic hydrocarbons". Owing to similar reasons, it is regrettable that no programs are devoted to the fundamentals of the chemistry of heterocyclic compounds. As compared with other capters, Program 10 ("Arylamines and diazonium salts") seems to be somewhat oversized, although the theoretical and practical importance of this group of compounds is evident.

The presentation and structure of the book are attractive. The "flip card" system serving for the repetition and deepening of the material treated in the programs is very useful. The special arrangement of the Programs 1—6 and 7—12 is worth of attention.

Á. KUCSMAN

Peptides: Chemistry and Biochemistry

Boris Weinstein and Saul Lande (editors), Marcel Dekker, Inc., New York, 1970. XV + 538 pp.

The first symposium of European peptide chemists was held in Prague in 1958. Its main scope included synthetic methodology and the synthesis of natural peptides. This first meeting was followed by ten such symposia on extended and varying topics, with the participation of peptide chemists from other continents as well. Since the interest in these useful conferences was increasing rapidly but the number of guests remained limited, independent meetings were soon organized in Japan and the United States. The complete texts of the lectures held at the European Peptide Symposia were regularly published. The book reviewed

here represents such a trend, being the publication of lectures presented at the first American Peptide Symposium held at Yale University in 1968. Since the book contains only the lectures, this review deals actually with the scientific session itself.

Similarly to the European Peptide Symposia, the first American Symposium was also concerned with the most urgent and then up-to-date problems of peptide chemistry. Since the synthetic methodology, the selective application of sensitive protecting groups, the accomplishment of coupling without racemization, as well as the purification of the products are always returning and actual problems, it is not surprising that 60% of the papers were devoted to these topics.

The other extensive subject of the symposium was the relationship between the structure (chemical composition and conformation) and the biological effect of peptides. A few lectures involved structural studies and some special subjects, but these were of lesser significance.

The only thing the reader feels the absence of is the material of the discussions following the individual lectures. This is always the most valuable at symposia, since the lecturers rarely emphasize the difficulties and perhaps never the contradictions; the tables mostly include favourable data only and certainly everybody reproduces his most beautiful chromatogram for public demonstration. The curious, sometimes slightly suspicious questions asked in the discussions provide an opportunity to obtain a more realistic picture of the subject discussed in the lecture; so this material is strongly lacking. The editors may have been deterred from its publication by the difficulties of getting the discussions on record.

The first lecture of the symposium — and thus the first paper in the book — is a summary by BODÁNSZKY on the strategy of peptide synthesis and its perspectives. This lecture represents a new battle in the seven-year war between the classical synthetic paths (stepwise and fragment condensation) and the Merrifield solid phase synthesis. After reading this paper one feels that neither will win: a compromise may be reached, or the two principles will merge to produce a better approach to the ideal solution. It is noteworthy that in this paper BODÁNSZKY has introduced the concept of "efficiency yield" into the calculation of the yields of individual synthetic steps, taking into account also the large excess of the acylating agent present during the coupling steps.

Among the topics of the other lectures both synthetic methods are abundantly represented. BAYER has studied the performance of solid state synthesis as a function of the molecular weight of the polypeptide to be prepared. MERRIFIELD illustrates the applicability of his method also for the preparation of cyclic depsipeptides on the synthesis of valinomycin. ANFINSEN has prepared a fragment, consisting of 43 amino acids, of a nuclease isolated from a culture of *Staphylococcus aureus*, on a polymer carrier and points out the inadequacy of the methods available for determining the identity and homogeneity of the product.

Six papers deal with the phenomenon of racemization which accompanies the formation of the peptide bond. These cover the detection of racemization, as well as the determination of its degree (ANDERSON, IZUMIYA, WESTLEY, WEINSTEIN) and studies on the mechanism of racemization (GOODMAN, KOVÁCS).

The papers on the relationship between biological activity and structure cover a rather extended field; the effects of angiotensin, thyrocalcitonin, the polypeptide hormones of the stomach and intestines, and the fat-mobilizing peptides were discussed in different lectures. MAZUR and coworkers investigated the relationship between the structure and taste of peptides of low molecular weight. Almost all papers clearly indicate that the structural changes (altered functional groups) affect so many characteristics of the molecule (polarity, dipole moment, lipid solubility, disappearance or development of essential functions, conformation) that the change in the effect cannot be attributed to a single factor. MARSHALL emphasizes the importance of physico-chemical methods (NMR spectroscopy combined with the computation of the most stable conformation of the molecule in solution).

Of the special subjects that could not be included in the chapters discussed above, the structural studies on the antibiotic nisine (GROSS), the synthesis of actinomycin-D (MEIENHOFER) and the synthesis of amino acids and peptides containing selenium instead of sulfur (WALTER) should be noted. The latter compounds can be conveniently used in studying the biological importance of the sulfur atom and permit radioactive indication, as well as X-ray crystallographic investigations.

Almost all of the papers in the book are illustrated with drawings, diagrams, photographs and formula tables. The material, complete with extensive lists of references, is indispensable for those wishing to keep up with modern peptide chemistry, and is very useful for chemists and biologists engaged in related fields, as well as for endocrinologists and pharmacologists dealing with peptide hormones.

K. MEDZIHRADSZKY

Organic Peroxides

Vol. 1. Daniel SWERN, Ed. Wiley — Interscience. New York, London, Sidney, Toronto, 1970.

The first organic peroxides were prepared about 100 years ago. However, owing to their unpleasant properties, they are dealt with extensively only since the beginning of the 1930's. The per-compounds were introduced into the industrial practice at the beginning of the 1930's in connection with the preparation of various polymers. Though the majority of peroxides is hazardous, their industrial importance and field of application increased at a high rate in the last thirty years.

The technical literature dealing with peroxides suffers from the same faults which are mentioned more and more frequently also in connection with the literature of other fields. Volumes of comprehensive character summarize either only theoretical problems, or the fundamentals of practice. Among the books published so far on peroxides, the better known discuss either the preparation of peroxides (MESROBIAN—TOBOLSKY: Organic Peroxides) or only theoretical problems (HAWKINS: Organic Peroxides). Therefore, chemists concerned with both theoretical and practical problems of peroxides must look forward with high expectations to the work edited by D. SWERN, to be published in three volumes. As mentioned by the Editor in the introduction to Volume 1, reviewed below, this work attempts to give a comprehensive picture on the chemistry, properties, reactivity and field of application of organic per-compounds, in such a manner that it could serve as a useful handbook for both theoretical experts and the users of peroxides.

Volume 1 is divided into 11 chapters. Authors of the single chapters are specialists well known to those studying the literature, thus *e.g.* L. A. SINGER, the renowned specialist of peroxy esters, S. W. BENSON, the eminent physico-chemist, K. F. O'DISCOLL, expert on radical polymerization, to mention only a few of the contributors.

The first chapter gives a survey on the classification of per-compounds and the general characteristics of their syntheses, summarizes briefly the problems associated with the application of peroxides and the most important safety regulations. Chapter 2 discusses practical problems relevant to the thermochemistry of per-compounds. This chapter, though dealing with several important practical problems, is nevertheless the weakest part of the book. To understand this chapter, a knowledge of the subject published in periodicals in connection with the theme is indispensable. Without this, the methods described cannot be understood. Chapter 3 describes the most important types and chemical reactions of radicals formed from organic per-compounds. Chapter 4 summarizes the mechanisms of polar peroxide reactions. The introductory part of the chapter gives useful advice concerning the investigation of the reactions. Chapters 5, 6 and 7 discuss the preparation of organic peroxy acids and peresters, to a depth giving concrete prescriptions, their properties and the analytical problems connected with these compounds. Chapters 8, 9 and 10 give a good summary of the peroxide reactions catalyzed by bases. Chapter 11 treats the role of organic peroxides in vinyl polymerization. It is regrettable that this last chapter summarizes practical problems but briefly, while it discusses the theoretical aspects more extensively.

The literature dealing with the topics of the single chapters is practically complete. The more important references for the period 1930—1967 are all listed. The literature on the preparation of peroxides duly emphasizes the possible sources of hazard during the operations, and gives useful recommendations in connection with the storage and use of per-compounds. The same holds true for the summaries in connection with the analytical procedures. Some problems are treated for the first time in this book in an encyclopedic manner, as *e.g.* the summary on the peroxy ester reactions catalyzed by metal ions, used today in an increasingly wide field for the oxidation of saturated and unsaturated hydrocarbons.

If the two volumes to follow will give a similarly modern treatment of the other problems concerning per-compounds, then a useful handbook which was lacking very much in the last ten years has finally been published.

B. LOSONCZI

R. F. Heck, F. W. Frey, H. Shapiro, A. Gumboldt, H. Weber, A. Bokranz, H. Plum: *Organometallic Compounds io Industry*

A new volume in the series "Fortschritte der Chemischen Forschung. Topics in Current Chemistry", Vol. 16, Nos 3/4, February 1971. Springer Verlag, Berlin, Heidelberg, New York. 182 pp., 27 tables, 5 flowsheets and 5 figures

The volume "Organometallic Compounds in Industry" is composed of monographs by renowned authors in this field. The book deals with several problems, furnishing important information not only to theoretical specialists but also to engineers and researchers working in the industry. Particularly in recent years, organometallic chemistry developed very rapidly. The synthetic organic and plastics industries apply and use organometallic compounds in increasing amounts.

Therefore, this volume fills a gap by discussing the properties of individual organometallic compounds and their possible application in combination with theoretical problems. Among others, it describes the mechanism of some chemical processes interesting also from the viewpoint of theoretical organic chemistry.

The monograph contains the following chapters:

1. R. H. Heck: The addition–elimination reactions of palladium compounds with olefins (pp. 221—242)

In this chapter the author gives a general description of the complexes of palladium with olefins and of their addition–elimination reactions from the viewpoint of organic chemistry. The addition–elimination reactions of palladium compounds with olefins provided new ways for the preparation of vinyl and allyl derivatives, even in those cases where other conventional methods were unsuccessful. A detailed description is given of the addition reaction of palladium chloride with olefins in aqueous and alcoholic media and of various elimination reactions in the presence of palladium chloride, palladium acetate and copper(I) chloride. In this way, several vinyl halide and pseudohalide (cyanide) monomers, as well as vinyl acetate can be prepared, and by means of carboxylation reactions oxo-olefin derivatives can also be obtained.

2. F. W. Frey, H. Shapiro: Commercial organolead compounds (pp. 243—298)

After a historical review, the types of organic lead compounds, their bond structures and methods of preparation are discussed together with their physical and chemical properties. In this chapter, the mechanism of antiknock action in the internal combustion chamber of engines and its economic aspects are discussed in detail by the authors.

Other possible applications of organic lead compounds are also given: they may serve as additive to paints protecting sea-going ships against corrosion, and as additives to lubricants. The poisoning effect of organic lead compounds and their toxicological mode of action are discussed.

3. A. Gumboldt: Metallorganische Verbindungen als Katalysatoren der Olefin-Polymerisation [Organometallic compounds as olefin polymerization catalysts] (pp. 299—328)

After an introduction, the author deals with the catalysis of polyreactions, mainly from the viewpoint of Ziegler type catalysts. The subjects of discussion are the polymerization mechanism of olefins in the presence of Ziegler catalysts, mixed organometallic catalysts, industrial manufacture of the catalysts and the steric conformations and modifications of the polymers formed. The relationship between catalyst structure and catalyst efficiency is also dealt with. In this part, the author reviews very thoroughly but at the same time with moderation the industrial catalysts of polyaddition reactions, and their theoretical problems.

4. H. Weber: Metallorganische Verbindungen als Katalysatoren zur Herstellung von Stereokautschuken [Organometallic catalysts used in the preparation of stereo-caoutchouc] (pp. 329—364)

An introduction is followed by the discussion of the polymerization and co-polymerization of conjugated diolefins in the presence of organic alkali, alkaline earth and earth metals. The polymerization of olefins and diolefins in the presence of Ziegler catalysts is described. Various properties and fields of application of the polymers prepared on butadiene, isoprene and propylene basis are dealt with in detail.

5. A. Bokranz, H. Plum: Technische Herstellung und Verwendung von Organozinnverbindungen [Technical preparation and use of organic tin compounds] (pp. 365—400)

The authors discuss extensively the possible industrial preparation of organic tin compounds, technological and economic aspects included. They describe the individual tin compounds according to the number of functional groups and their field of application, as *e.g* biocides, PVC stabilizers, silicone rubber vulcanizing agents, lubricant additives, etc. The poisonous effects of organic tin compounds are also discussed in detail.

The monograph "Organometallic Compounds in Industry" is an excellent technological and theoretical book comprising well selected topics which will be useful to chemical engineers, chemists, and particularly to industrial specialists active in the synthetic and plastics industries. Each chapter is complete with ample bibliography, helping the reader to obtain more detailed information.

J. NAGY

ERRATUM

In the issue *71* (1), p. 97.: *Direct preparation of phtiocol*, the sentence beginning at the end of the 4th row had unfortunately been misprinted, its correct spelling is: The solution is heated on a water-bath at 100 °C for about 15 min, while the solution turns progressively red. After cooling the solution is acidified with 40 ml of 2 N acetic acid.

INDEX

INORGANIC AND ANALYTICAL CHEMISTRY – ANORGANISCHE UND ANALYTISCHE CHEMIE – НЕОРГАНИЧЕСКАЯ И АНАЛИТИЧЕСКАЯ ХИМИЯ

HAUFFE, K. und HEGEDŰS, A. J.: Zum Mechanismus der Desorption und aktivierten Adsorption von Sauerstoff an unbelichtetem und UV-belichtetem Zinkoxid (On the Mechanism of the Desorption and Activated Adsorption of Oxygen for Non-irradiated and UV-irradiated Zinc Oxide) 1

WOLSKI, W. and BUREWICZ, A.: Ferromagnetic Products of the Explosion Reaction between $Co(NO_3)_2$ and $(NH_4)_4[Fe(CN)_6]$ 25

PHYSICAL CHEMISTRY – PHYSIKALISCHE CHEMIE – ФИЗИЧЕСКАЯ ХИМИЯ

GIBER, J. and VAJASDY-PERCZEL, I.: Study of the Rest and Polarization Potentials of Chemically Treated Germanium Single Crystal Surfaces, I. Effect of the pH and Anion Adsorption 33

ORGANIC CHEMISTRY – ORGANISCHE CHEMIE – ОРГАНИЧЕСКАЯ ХИМИЯ

CSŰRÖS, Z., SOÓS, R., BITTER, I. and PÁLINKÁS, J.: Use of Amide Chlorides in Ring Closure Reactions, IV. A New Synthesis of 4-Aminoquinazoline Derivatives ... 59

DINYA, Z. and SZABÓ, S.: Infrared Spectroscopic Studies on Flavonoids and Model Compounds, I. Investigations on some Infrared Frequencies of 4-Substituted Acetophenones by means of HMO Calculations 65

KISFALUDY, L. and NYÉKI, O.: Racemization during Peptide Azide Coupling (Short Communication) 75

CHEMICAL TECHNOLOGY – CHEMISCHE TECHNOLOGIE – ХИМИЧЕСКАЯ ТЕХНОЛОГИЯ

KORACH, M. and HASKÓ, L.: Development of Petroleum Refining Technologies in Graph Theoretical Representation, I. Distillation 77

RECENSIONES 93

Printed in Hungary

A kiadásért felel az Akadémiai Kiadó igazgatója — Műszaki szerkesztő: Várhelyi Tamás
A kézirat nyomdába érkezett: 1971. X. 18. — Terjedelem: 10 (A/5) ív, 61 ábra

72.72558 Akadémiai Nyomda, Budapest — Felelős vezető: Bernát György

ACTA CHIMICA

ТОМ 72—ВЫП. 1

РЕЗЮМЕ

Механизм десорбции и активированной адсорбции кислорода на окиси цинка, облученной УФ светом и в отсутствии облучения

К. ХАУФФЕ и А. Й. ХЕГЕДЮШ

Были исследованы десорбция и адсорбция на окиси цинка, вызванные эвакуированием и введением воздуха при постоянной температуре, а также были измерены вызванные изменением температуры десорбция и адсорбция, термолиз и хемисорбция при остаточных давлениях $1—2 \cdot 10^{-5}$ торр и 1 атмосфере. При остаточном давлении $1{,}2 \cdot 10^{-5}$ торр была исследована также фотосорбция $O_2 + H_2O$, где был найден только фотолиз, а фотоадсорбцию обнаружить не удалось. На основе результатов измерений проводятся попытки обсуждения отдельных возможных ступеней реакции.

Ферромагнитные продукты реакции взрыва между $Co(NO_3)_2$ и $(NH_4)_4[Fe(CN)_6]$

В. ВОЛЬСКИ и А. БУРЕВИЧ

Нагрев аммониевого ферроцианида с нитратом кобальта при температуре 220°C приводит к взрывообразной реакции. Реакция носит такой характер при молекулярном отношении $Co(NO_3)_2 : (NH_4)_4[Fe(CN)_6]$ от 1 : 5 до 5 : 1. Состав продуктов зависит в основном от и сходного состава, а также от атмосферы, в которой проводится взрыв.

На основе рентгеновских исследований, магнитных измерений и химического анализа было установлено, что ферромагнитные свойства продуктов обусловлены присутствием в осадке металлических железа и кобальта, а также магнетита и, иногда, феррита кобальта. Если процесс проводится при большом избытке воздуха, то образуется большее количество неферромагнитной α-окиси железа. Наибольшие величины магнитного насыщения были найдены в смеси солей с отношением $Co(NO_3) : (NH_4)_4[Fe(CN)_6] = 2 : 1$. Осадки, наиболее богатые кристаллической фазой, были получены при составе исходных солей 1 : 1.

Изучение потенциала в состоянии покоя и поляризационного потенциала на поверхности химически обработанного монокристалла германия, I

Эффект pH и анионной адсорбции

Я. ГИБЕР и И. ВАЯШДИ—ПЕРЦЕЛ

Были разработаны условия измерения электродного потенциала на поверхности монокристалла германия в пределах воспроизводимости ± 10 мв. Были измерены потенциалы в состоянии покоя для германия в 0,1 N растворах K_2SO_4, KCl, KBr и KJ в интервале pH = 2 — 12. С возрастанием pH потенциал линейно сдвигается в отрицательном направлении; анионы вызывают возрастающий сдвиг потенциала в отрицательном направлении в вышеупомянутом ряду. Был измерен поляризационный потенциал германия в

растворах этих солей при различных pH в катодной, а затем в анодной областях в интервале плотности тока 10^{-7} — 10^{-3} А/см². Анодные и катодные поляризационные кривые состоят из одного и двух участков, описываемых уравнением Тафеля, соответственно. Образование поверхностных слоев в состоянии покоя и в процессе поляризации исследовалось с помощью эллипсометра.

На основе результатов измерений кажется вероятным, что потенциал в состоянии покоя представляет собой коррозионный потенциал, что катодные и анодные реакции являются идентичными с поляризационными реакциями, протекающими при небольших плотностях тока; анодная реакция является окислением германия, а катодная реакция является выделением водорода с образованием гидрида германия на промежуточной стадии.

Использование амидохлоридов в реакциях циклизации. IV

Новый синтез производных 4-аминохиназолина

З. ЧЮРЁШ, Р. ШООШ, И. БИТТЕР и Й. ПАЛИНКАШ

Из амида антраниловой кислоты и хлористого диметилформамида приготовлялся гидрохлористый N,N-диметил-N'-(2-цианофенил)-формамидин. Из полученного таким образом трехзамещенного амидина под действием аммиака, первичных алифатических и ароматических аминов, а также гидразина за счет циклизации с одновременной изомериацией были синтезированы N-замещенные производные 4-аминохиназолина.

Изучение флавоноидов и их модельных соединений с помощью ИК спектроскопии, I

Исследование некоторых частот ИК спектра 4-замещенных ацетофенонов с помощью метода МО Хюккеля

З. ДЫНЯ и Ш. САБО

С помощью упрощенного метода МО Хюккеля при подходящим выборе параметров были рассчитаны π-характер карбонильной группы в 4-замещенных ацет фенонах. Расчетные данные хорошо согласуются с литературными данными, полученными другими путями.

В случае появления полосы «е» в области 1200—1300 $см^{-1}$ ИК спектра изученных соединений, были получены линейные зависимости между волновыми числами полос и значениями δ Гамметта для n-замещенных, а также между π-характером карбонильной группы и π-характером связи карбонильного углерода с ароматическим кольцом. Наблюдаемые зависимости также подтверждают обычное в литературе объяснение характера полосы «е».

Были исследованы свойства полос деформационных колебаний водородных атомов ароматического кольца 4-замещенных ацетофенонов, перпендикулярных к плоскости кольца. На основе результатов измерений и расчетов, в согласии с литературными данными, было найдено, что фактором, определяющим волновое число этой полосы, является (—)М-эффект заместителя.

Графтеоретическое изображение развития промышленной технологии нефтепереработки, I

Дистилляция

М. КОРАХ и Л. ХАШКО

Применение графтеоретических изображений позволяло количественное изучение хода развития промышленных технологий нефтепереработки. Изображение типов дистилляционных установок в зависимости от года появления отдельных типов приводит к заключению, что, с одной стороны, соответствующий граф приводит от открытого прямоточного типа к все усложняющемуся типу графов с несколькими циклическими процессами; с другой стороны, число элементов графов отдельных систем в зависимости от времени обладает возрастающим характером и, вероятно, стремится к предельному значению.

The Acta Chimica publish papers on chemistry in English, German, French and Russian.

The Acta Chimica appear in volumes consisting of four parts of varying size, 4 volumes being published a year.

Manuscripts should be addressed to

Acta Chimica
Budapest 112/91 Műegyetem

Correspondence with the editors should be sent to the same address.

The rate of subscription is $ 16.00 a volume.

Orders may be placed with "*Kultúra*" Foreign Trade Company for Books and Newspapers (Budapest I., Fő utca 32. Account No. 43-790-057-181) or with representatives abroad.

Les Acta Chimica paraissent en français, allemand, anglais et russe et publient des mémoires du domaine des sciences chimiques.

Les Acta Chimica sont publiés sous forme de fascicules. Quatre fascicules seront réunis en un volume (4 volumes par an).

On est prié d'envoyer les manuscrits destinés à la rédaction à l'adresse suivante:

Acta Chimica
Budapest 112/91 Műegyetem

Toute correspondance doit être envoyée à cette même adresse.

Le prix de l'abonnement est de $ 16.00 par volume.

On peut s'abonner à l'Entreprise pour le Commerce Extérieur de Livres et Journaux «*Kultúra*» (Budapest I., Fő utca 32. Compte-courant No. 43-790-057-181) ou à l'étranger chez tous les représentants ou dépositaires.

«*Acta Chimica*» издают трактаты из области химической науки на русском, французском, английском и немецком языках.

«*Acta Chimica*» выходят отдельными выпусками разного объема. 4 выпуска составляют один том. 4 тома публикуются в год.

Предназначенные для публикации рукописи следует направлять по адресу:

Acta Chimica
Budapest 112/91 Műegyetem

По этому же адресу направлять всякую корреспонденцию для редакции.

Подписная цена — $ 16.00 за том.

Заказы принимает предприятие по внешней торговле книг и газет «*Kultúra*» (Budapest I., Fő utca 32. Текущий счет № 43-790-057-181) или его заграничные представительства и уполномоченные.

Reviews of the Hungarian Academy of Sciences are obtainable at the following addresses:

ALBANIA

Drejtorija Qändrone e Pärhapjes
dhe Propagandimit tä Librit
Kruga Konferenca e Päzes
Tirana

AUSTRALIA

A. Keesing
Box 4886, GPO
Sydney

AUSTRIA

GLOBUS
Höchstädtplatz 3
A-1200 Wien XX

BELGIUM

Office International de Librairie
30, Avenue Marnix
Bruxelles 5
Du Monde Entier
5, Place St. Jean
Bruxelles

BULGARIA

HEMUS
11 pl Slaveikov
Sofia

CANADA

Pannonia Books
2, Spadina Road
Toronto 4, Ont.

CHINA

Waiwen Shudian
Peking
P. O. B. 88

CZECHOSLOVAKIA

Artia
Ve Smečkách 30
Praha 2
Poštovní Novinová Služba
Dovoz tisku
Vinohradská 46
Praha 2
Mad'arská Kultura
Václavské nám. 2
Praha 1
SLOVART A. G.
Gorkého
Bratislava

DENMARK

Ejnar Munksgaard
Nörregade 6
Copenhagen

FINLAND

Akateeminen Kirjakauppa
Keskuskatu 2
Helsinki

FRANCE

Office Internationa' de Documentation
et Librairie
48, rue Gay-Lussac
Paris 5

GERMAN DEMOCRATIC REPUBLIC

Deutscher Buch-Export und Import
Leninstraße 16
Leipzig 701
Zeitungsvertriebsamt
Fruchtstraße 3—4
1004 Berlin

GERMAN FEDERAL REPUBLIC

Kunst und Wissen
Erich Bieber
Postfach 46
7 Stuttgart S.

GREAT BRITAIN

Blackwell's Periodicals
Oxenford House
Magdalen Street
Oxford
Collet's Subscription Import
Department
Dennington Estate
Wellingsborough. Northants.
Robert Maxwell and Co. Ltd.
4—5 Fitzroy Square
London W. 1

HOLLAND

Swetz and Zeitlinger
Keizersgracht 471—487
Amsterdam C.
Martinus Nijhof
Lange Voorhout 9
The Hague

INDIA

Hind Book House
66 Babar Road
New Delhi 1

ITALY

Santo Vanasia
Via M. Macchi 71
Milano
Libreria Commissionaria Sansoni
Via La Marmora 45
Firenze
Techna
Via Cesi 16
40135 Bologna

JAPAN

Kinokuniya Book-Store Co. Ltd.
826 Tsunohazu 1-chome
Shinjuku-ku
Tokyo
Maruzen and Co. Ltd.
P. O. Box 605
Tokyo-Central

KOREA

Chulpanmul
Phenjan

NORWAY

Tanum-Cammermeyer
Karl Johansgt 41—43
Oslo 1

POLAND

RUCH
ul. Wronia 23
Warszawa

ROUMANIA

Cartimex
Str. Aristide Briand 14—18
Bucureşti

SOVIET UNION

Mezhdunarodnaya Kniga
Moscow G—200

SWEDEN

Almquist and Wiksell
Gamla Brogatan 26
S—101 20 Stockholm

USA

F. W. Faxon Co. Inc.
15 Southwest Park
Westwood Mass. 02090
Stechert Hafner Inc.
31. East 10th Street
New York, N. Y. 10003

VIETNAM

Xunhasaba
19, Tran Quoc Toan
Hanoi

YUGOSLAVIA

Forum
Vojvode Mišića broj 1
Novi Sad
Jugoslovenska Knjiga
Terazije 27
Beograd

ACTA CHIMICA

ACADEMIAE SCIENTIARUM HUNGARICAE

ADIUVANTIBUS

V. BRUCKNER, GY. DEÁK, K. POLINSZKY,
E. PUNGOR, G. SCHAY, Z. G. SZABÓ

REDIGIT

B. LENGYEL

TOMUS 72 FASCICULUS 2

AKADÉMIAI KIADÓ, BUDAPEST

1972

ACTA CHIM. (BUDAPEST) ACASA 2 72 (2) 111—230 (1972)

ACTA CHIMICA

A MAGYAR TUDOMÁNYOS AKADÉMIA KÉMIAI TUDOMÁNYOK OSZTÁLYÁNAK IDEGEN NYELVŰ KÖZLEMÉNYEI

SZERKESZTI

LENGYEL BÉLA

TECHNIKAI SZERKESZTŐK

DEÁK GYULA és HARASZTHY-PAPP MELINDA

Az Acta Chimica német, angol, francia és orosz nyelven közöl értekezéseket a kémiai tudományok köréből.

Az Acta Chimica változó terjedelmű füzetekben jelenik meg, egy-egy kötet négy füzetből áll. Évente átlag négy kötet jelenik meg.

A közlésre szánt kéziratok a szerkesztőség címére (Budapest 112/91 Műegyetem) küldendők.

Ugyanerre a címre küldendő minden szerkesztőségi levelezés. A szerkesztőség kéziratokat nem ad vissza.

Megrendelhető a belföld számára az „Akadémiai Kiadó"-nál (Budapest V., Alkotmány utca 21. Bankszámla 05-915-111-46), a külföld számára pedig a „Kultúra" Könyv- és Hírlap Külkereskedelmi Vállalatnál (Budapest I., Fő utca 32. Bankszámla: 43-790-057-181) vagy annak külföldi képviseleteinél és bizományosainál.

Die Acta Chimica veröffentlichen Abhandlungen aus dem Bereiche der chemischen Wissenschaften in deutscher, englischer, französischer und russischer Sprache.

Die Acta Chimica erscheinen in Heften wechselnden Umfanges. Vier Hefte bilden einen Band. Jährlich erscheinen 4 Bände.

Die zur Veröffentlichung bestimmten Manuskripte sind an folgende Adresse zu senden:

Acta Chimica
Budapest 112/91 Műegyetem

An die gleiche Anschrift ist auch jede für die Redaktion bestimmte Korrespondenz zu richten. Abonnementspreis pro Band: $ 16.00.

Bestellbar bei dem Buch- und Zeitungs-Außenhandels-Unternehmen »*Kultúra*« (Budapest I., Fő utca 32. Bankkonto No. 43-790-057-181) oder bei seinen Auslandsvertretungen und Kommissionären.

Acta Chimica Academiae Scientiarum Hungaricae, Tomus 72 (2), pp. 111–116 (1972)

THERMAL DECOMPOSITION OF PYRIDINE-BORANE

E. BODOR, K. JÓNÁS and M. WELTHER

(Institute of General and Inorganic Chemistry, University of Chemical Industries, Veszprém, Hungary)

Received September 10, 1970

It was proved by derivatographic, infrared and chemical analysis that pyridine-borane undergoes rearrangement at about 120°C. In this reaction the hydrogens bonded to the boron migrate to the pyridine ring and the ring becomes partially saturated. The product is a chain polymer involving boron–boron bonds. Competitive reactions are: the thermal dissociation of pyridine-borane and the decomposition of the chain polymer at higher temperatures. Studies with boranes of similar type (*e.g.* quinoline-borane, etc.) indicate that a rearrangement of this kind always occurs to some extent during the heating of borane adducts in which the nitrogen donor is in an aromatic ring.

The thermal decomposition of organoboron compounds is generally a complex process. The final products are not pure, well-defined compounds owing to the many side reactions taking place during heating [1]. The thermal reactions of the relatively simple $R_xH_{3-x}N \cdot BH_3$ amine-boranes, however, are rather well understood. The type of thermal decomposition depends on the substituents attached to the nitrogen. If there is no hydrogen on the nitrogen, thermal dissociation takes place, producing the corresponding free amine and diborane. However, borazene and borazol type compounds are formed, in combination with hydrogen evolution, in the case of di- and mono-substituted amine ligands, respectively. Some other reaction types are also known from the literature. An interesting example is the behaviour of the adducts of volatile cyanides with diborane ($R \cdot CN \cdot BH_3$; where R: CH_3 or C_2H_5). These dissociate at room temperature or between —10° C and 0° C, but at the same time a rearrangement reaction also takes place. In this process hydrogens bonded to the boron atom migrate to the carbon adjacent to the nitrogen, and borazene and borazol are produced without hydrogen evolution [2, 3, 4]:

$$CH_3 \cdot CN \cdot BH_3 \rightarrow CH_3 \cdot CH = N = BH_2 \rightarrow (CH_3 \cdot CH_2 - N = BH)_3$$

Similar hydrogen migration was observed by MIKHEEVA and FEDNEVA [5] in the case of pyridine-borane. These authors supposed, without any experimental proof, that the following rearrangement takes place if pyridine-borane is heated, or allowed to stay at room temperature:

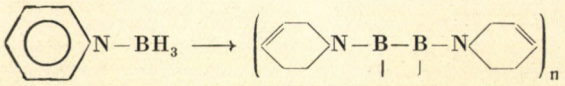

The aim of the present work was to study this reaction and the structure of its product.

Experimental

Pyridine- and piperidine-borane were prepared by the direct reaction of diborane with the ice-cold ether solution of the corresponding free amine. Piperidino-borane has been obtained by the thermal decomposition of piperidine-borane at about 130° C. The progress of the reaction was followed by measuring the volume of the hydrogen evolved.

A PAULIK—PAULIK—ERDEY type MOM derivatograph (N_2 gas atmosphere, heating rate 6°C/min) was used for the study of the thermal reactions of pyridine-borane. Thermal decompositions were also carried out with greater sample weights in an oil bath of given constant temperature. In these experiments the volume of the non-condensable gases evolved was also measured.

Starting materials and decomposition products were identified by chemical analysis and infrared spectra. Boron has been titrated in the presence of mannitol after acid hydrolysis and distillation with methanol; nitrogen was analysed by the Kjeldahl method. The number of B–H bonds was determined by measuring the amount of hydrogen evolved upon acid hydrolysis of the products.

Infrared spectra were recorded with a UR-10 (Zeiss) spectrophotometer.

Results and discussion

A very violent exothermic reaction takes place at about 150—160° C if pyridine-borane is heated in the derivatograph. In the presence of an inert material (Al_2O_3) the exothermic peak is resolved into several steps (curves *a* and *b*, Fig. 1). An orange-yellow residue was found in the crucible in each case if the reaction was stopped at 300° C and the mixture cooled. Products obtained in experiments stopped at higher temperatures were darker, due to some tarry constituents.

As the reaction is very violent at 150—160° C, a lower temperature was applied in the decompositions carried out in the oil bath. If pyridine-borane was kept at 120° C in a thermostat, the viscosity of the originally colourless liquid increased gradually, its colour changed to yellow, and after about 4—6 hours the same orange-yellow solid was obtained as in the derivatograph. We recorded the DTA curves of the decomposition products formed at 120° C after various times of treatment. The exothermic peak at about 150—160° C was observed to decrease gradually with increasing time of thermal pretreatment. After a sufficiently long treatment at 120° C the transformation is complete. This is evident also from the DTA curve, which does not show the exothermic peak any more (curves *c* and *d* Fig. 1).

According to the TG curves, the exothermic reactions at about 150—160° C are accompanied by weight loss. The magnitude of the weight loss is badly reproducible, amounting to about 20 w.%.

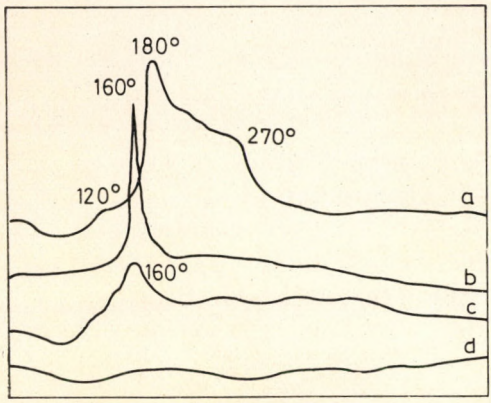

Fig. 1. DTA curves of pyridine-borane and of its decomposition products. a) Pyridine-borane (68.0 mg; sensitivity 1/10), inert material: Al_2O_3. b) Pyridine-borane without inert material (66.2 mg; sensitivity 1/20). c) Pyridine-borane treated previously at 120°C for 5 hrs (176.2 mg; sensitivity 1/10). d) Pyridine-borane treated previously at 120°C for 10 hrs (158.5 mg; sensitivity 1/20)

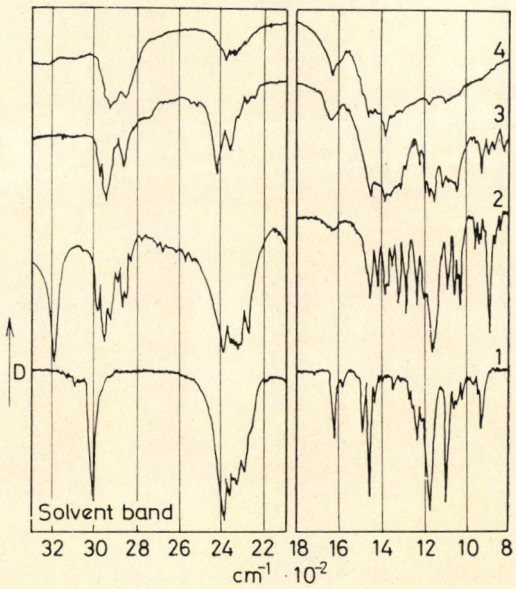

Fig. 2. Infrared spectrum of (1) pyridine-borane, (2) piperidine-borane, (3) piperidino-borane, (4) decomposition product of pyridine-borane. (Spectrum (1) in $CHCl_3$, spectra (2)—(4) in KBr)

The decomposition products obtained in the derivatograph or in the thermostat were found to have nearly identical physical and chemical properties. They are insoluble in both polar and non-polar solvents; the mole ratio of boron and nitrogen is about 1 : 1; one mole of hydrogen is evolved per boron atom upon hydrolysis in acid. The results of boron, nitrogen and active hydro-

gen determinations scatter around the above values, depending on the degree of unavoidable tarrification taking place during the thermal treatment.

Attempts at purification of the products with selective solvents were unsuccessful.

The characteristic infrared bands of the pyridine ring do not appear in the spectrum of the decomposition product, but there are new bands in the 2800—3000 cm^{-1} range, which correspond to the C—H stretching vibration of saturated hydrocarbons. At the same time the B—H stretching vibrations (2300—2500 cm^{-1}) are gradually suppressed; they are absent in the spectra of products treated for sufficient time at 120°C. In Fig. 2 (curves *1* and *4*) the spectrum of pyridine-borane is compared with that of an incompletely transformed product; in the latter weak B—H bands are still observed. Thus the partial saturation of the pyridine ring on heating, by the hydrogens bonded originally to the boron, is proved by the infrared spectra.

The following structures may be supposed for the intermediates and final products of the rearrangement reaction:

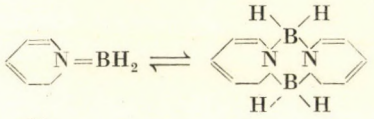

I/a I/b

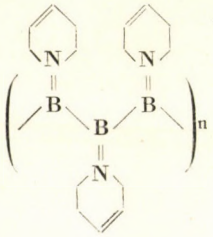

II

These structures seem to be supported by the presence of B—N double bonds as shown by the infrared spectra and by the amount of hydrogen evolved in the hydrolysis of completely transformed samples which do not contain B—H bonds at all.

The assignment of the B—N vibrations is a much disputed problem in the literature. In the case of boron–nitrogen dative bonds (single bond), spectroscopic studies suggest a value in the range between 980 and 1250 cm^{-1}. Later it has been concluded on the basis of the spectra of deuterated derivatives that the B—N band appears in the 650—750 cm^{-1} region [6, 7]. In practice, however, the formation of a dative B—N bond is accompanied always by the appearance of a strong band near 1100—1250 cm^{-1}, the exact position of which can be correlated with the relative donor strength of the ligand. Thus to the B—N coordinate bond we have assigned the strong band of

1095 cm^{-1} of pyridine-borane, in accordance with KATRITZKY's value [8], and the 1235 cm^{-1} medium intensity band of piperidine-borane, corresponding to the B—N frequency reported in the literature [9] for piperidine-boron trichloride (1245 cm^{-1}).

The B–N bands are at 1300—1550 cm^{-1} in the case of borazenes and borazols, where partial double-bonding may occur as a results of back-donation by the non-bonding electrons of nitrogen. There are, however, many assignment problems in the spectra of these compounds too. NIEDENZU *et al.* [10] have investigated the spectra of compounds containing $R-B\begin{smallmatrix}N\\N\end{smallmatrix}-$ units (R: alkyl or aryl). They found not only one, but generally two, new strong bands in the 1300—1600 cm^{-1} region; one at 1340—1400 cm^{-1}, and one around 1500 cm^{-1}. It was concluded that the second band is rather a manifestation of a B—N vibration than of an aromatic C–H bond. The bands belonging to the four-membered B—N—B—N rings, composed of B–N single bonds in the dimeric amino-boranes, are at frequencies higher by about 250—400 cm^{-1} than that of the coordinate B—N bond in the corresponding amine-borane [11]. If we also consider that the most significant aliphatic and aromatic C—H vibrations are also in the frequency range discussed above, and that these might suffer considerable wave-number and intensity changes in the borane adducts, it is clear that the spectra of the boron-nitrogen compounds must be analyzed with great precaution.

Due to the difficulties mentioned, we compare the spectrum of the decomposition product with that of a model compound, the structure of which is similar to the compounds assumed to be present in the decomposition product. For this purpose, piperidino-borane was chosen. It is known that there is a monomer-dimer equilibrium in the piperidino-borane [12]:

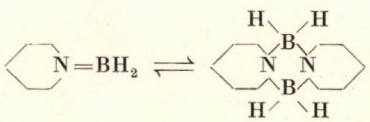

It can be seen from Fig. 2 that there is a prominent resemblance between the spectra of piperidino-borane and the orange-yellow decomposition product, especially in the frequency region characteristic of the B—N double bond (1300—1500 cm^{-1}). On the basis of the spectra one may assume the presence of intermediates I/a and I/b in the decomposition product, but it is certain that the B—N bond order has increased correlative to that in the starting pyridine-borane.

The presence of B—B bonds in structure II may be supported by the hydrolysis data for this compound. As mentioned, about one mole of hydrogen is evolved per boron atom during the hydrolysis of a completely transformed

product. Bearing in mind that, according to the spectrum, this material does not contain B—H bonds any more, we must suppose that the hydrogen originates from the B—B bonds *via* the following reaction scheme:

$$— B — B — + H — O — H \text{ (acid)} \rightarrow — B — H + H — O — B —$$
$$— B — H + H — O — H \rightarrow B — O — H + H_2$$

The hydrolysis of one B—B bond gives one mole of hydrogen, that is 0.5 mole of hydrogen per boron atom. Thus our data correspond to *two* boron–boron bonds for one boron atom.

The presence of B_4 or B_6 rings is not likely, among others, because the molecular weight of these rings would still allow dissolution of the product in some solvents. Owing to the insolubility of the product, we could not determine the molecular weight. The X-ray spectrum of the decomposition product also supports the supposition of a chain structure.

We may thus conclude from the results of the infrared studies that the thermal rearrangement of pyridine-borane, supposed by MIKHEEVA and FEDNEVA, actually takes place. In this reaction a chain polymer is formed. It is evident from the DTA and TG curves and from the qualitative analysis of the products released by the system upon heating that competitive reactions also occur. One of these is the thermal dissociation of the non-reacted pyridine-borane. The product of rearrangement, the chain polymer, is not thermally stable: it decomposes slowly between 150 and 450°C with the formation of tarry products containing mainly aliphatic amines.

Further studies on the thermal behaviour of boranes of similar type (*e.g.* quinoline-borane, etc.) indicate that the above rearrangement always takes place to some extent during the heating of borane adducts in which the nitrogen donor is in the aromatic ring.

REFERENCES

1. FINCH, A., GARDNER, P. J.: Thermochemistry of Boron Compounds, in: Progress in Boron Chemistry. Vol. 3, p. 177. Pergamon Press, 1970
2. SCHLESINGER, H. J., BURG, A. B.: Chem. Rev. **31,** 1 (1942)
3. BURG, A. B.: Record of Chemical Progress (Kresge-Hooker Science Library) **15,** 159 (1954)
4. EMELEUS, H. J., WADE, K.: J. Chem. Soc. **1960,** 2614
5. MIKHEEVA, V. I., FEDNEVA, E. M.: Zh. Neorg. Khim. **1,** 894 (1956)
6. TAYLOR, R. C., CLUFF, C. L.: Nature **182,** 390 (1958)
7. TAYLOR, R. C.: in "Advances in Chemistry Series", Vol. 42, p. 59. Am. Chem. Soc., 1964
8. KATRITZKY, A. R.: J. Chem. Soc. **1959,** 2049
9. GREENWOOD, N. N., WADE, K.: J. Chem. Soc. **1960,** 1130
10. NIEDENZU, K., BEYER, H., DAWSON, J. W.: Inorg. Chem. **1,** 738 (1962)
11. NÖTH, H., DOROCHOV, W. A., FRITZ, P., PFAB, F.: Z. anorg. allg. Chem. **318,** 293 (1962)
12. NÖTH, H., VAHRENKAMP, H.: Chem. Ber. **100,** 3353 (1967)

Endre BODOR
Klára JÓNÁS
Mária WELTHER
Veszprém, Schönherz Z. u. 10. Hungary.

Acta Chimica Academiae Scientiarum Hungaricae, Tomus 72 (2), pp. 117—131 (1972)

THE PYROLYSIS OF GASEOUS HYDROCARBONS, V

THE KINETICS OF THE THERMAL DECOMPOSITION OF AN ISOBUTANE–*n*-BUTANE MIXTURE

V. ILLÉS

(Hungarian Oil and Gas Research Institute, Veszprém)

Received March 23, 1970,
In revised form May 18, 1971

The thermal cracking of a 50—50 mole% i-butane–*n*-butane mixture was studied, at 1 atm total pressure, in a temperature range of 640—790° C, using a flow reactor. Kinetic equations, describing the overall decomposition rate in function of the fictive and actual reaction time, were given. The constants of the equations expressing the decomposition rate of the components, *n*-butane and i-butane, were determined.

The degree of decomposition of hydrocarbon mixtures was characterized by the sum of the conversions of the components, weighted by the mole fractions of the original components of the mixture. For multicomponent mixtures relative expansion was defined. In kinetic equations elaborated for flow reactors conversion was replaced by the degree of decomposition and equations were obtained describing the overall decomposition rate of hydrocarbon mixtures. The constants of the equations were determined. By using these equations the degree of decomposition could be evaluated for given temperature and reaction time.

The preparation of unsaturated C_2—C_4 hydrocarbons, which are the starting compounds in a large number of industrial scale chemical syntheses, is performed either by the thermal cracking (pyrolysis) of individual hydrocarbons (ethane, propane) or hydrocarbon mixtures (gas mixtures, petrol distillates). Detailed investigations have been carried out on the thermal decomposition of several pure hydrocarbons; the pyrolysis of mixtures, however, has been less extensively studied, and very few reliable data are known. As far as data on the decomposition rates of hydrocarbon mixtures are concerned the situation is even worse.

In studies on the pyrolysis of petrol distillates the severity function, introduced by LINDEN *et al.* [1, 2], is most widely used for the description of the cracking process. This function gives the change of the yield of ethylene product in terms of a variable consisting of the outlet temperature of the furnace multiplied by the 0.06th power of the average sojourn time. Recently, ZDONIK *et al.* [3] introduced the so-called kinetic severity function, which characterizes the degree of the cracking of petrol distillates by the decomposition rate constant calculated from the conversion of *n*-pentane under the given conditions, or, more precisely, from the first order kinetic equation based on the above.

No method has been found so far for expressing product yields or the composition of reaction mixture as a function of the conditions of the pyrolysis of mixtures. Calculations of such type, however, would be of vital importance in the analysis of up to date pyrolysing tube furnaces and in the setting of their optimal operating conditions.

For characterizing the degree of decomposition of hydrocarbon mixtures we have introduced the sum of the conversions of the components of the feed mixture, weighted by their mole fractions. For multicomponent mixtures relative expansion has been introduced. By using these terms a method has been developed for the determination of overall decomposition rate and product yield curves. We report the application of this method on the pyrolysis of a 50—50 mole% i-butane–*n*-butane mixture.

Experiments were carried out in a flow reactor [4], in a temperature range of 640—790°C, under isotherm and isobar conditions.

Definition of the decomposition grade in terms of the expansion

In the cracking of multicomponent hydrocarbon mixtures the decomposition of the components can be described by the following system of equations:

$$\begin{aligned} A_1 &\rightarrow v_{11}R_1 + v_{12}R_2 + v_{13}R_3 + \ldots + v_{1i}R_i + \ldots \\ A_2 &\rightarrow v_{21}R_1 + v_{22}R_2 + v_{23}R_3 + \ldots + v_{2i}R_i + \ldots \\ &\cdot \\ &\cdot \\ &\cdot \\ A_j &\rightarrow v_{j1}R_1 + v_{j2}R_2 + v_{j3}R_3 + \ldots + v_{ji}R_i + \ldots \end{aligned} \qquad (1)$$

where $A_1, A_2 \ldots A_j$ are molar amounts of the components of the feed mixture,
$R_1, R_2 \ldots R_j$ are molar amounts of the products,
$v_{1i}, v_{2i} \ldots v_{ji}$ are the mole numbers of the ith reaction product formed by the complete decomposition of one mole of $A_1, A_2 \ldots A_j$, respectively (*i.e.* overall stoichiometrical coefficients),
$j = 1,2 \ldots k$ is the number of components in the feed mixture,
$i = 1,2 \ldots k'$ is the number of components formed in the cracking reaction.

In the above reaction scheme it has been assumed that the stoichiometry of the decomposition of a given component in the mixture is not influenced by the presence of the other components.

The number of moles fed into the reactor during unit time (not taking inert diluents into account) can be given by the following expression:

$$n^0 = \sum_j^k n_j^0 = \sum_j^k y_j n^0 \qquad \text{(mole/sec)} \qquad (2)$$

where y_j is the mole fraction of component j of the feed mixture.

The number of moles leaving the reactor during unit time can be given by the following expression:

$$\sum n = \sum_j^k n_j + \sum_j^{k'} m_i = n^0 \left[\sum_j^k y_j (1 - x_j) + \sum_i^{k'} \sum_j^k y_j v_{ji} x_j \right] \qquad \text{(mole/sec)} \qquad (3)$$

where $x_j = \dfrac{n_j^0 - n_j}{n_j^0}$ is the conversion of component j of the feed mixture, and

$m_i = n^0 \sum_j^k y_j v_{ji} x_j$ is the amount of product i formed during unit time.

The first term of the right-hand side of Eq. (3) refers to the amount of the still unchanged feed hydrocarbons, whereas the second term represents the amount of reaction products.

Expansion is defined by the ratio of the mole numbers of the mixture leaving and fed into the reactor during unit time [4] and can be expressed by the following relation:

$$E = \frac{\Sigma n}{n^0} = \sum_j^k y_j + \sum_j^k \sum_i^k v_{ji} y_j x_j - \sum_j^k y_j x_j =$$

$$= 1 + \sum_j^k y_j x_j \left(\sum_i^{k'} v_{ji} - 1 \right) = y_1 \left[1 + \left(\sum_i^{k'} v_{1i} - 1 \right) x_1 \right] +$$

$$+ y_2 \left[1 + \left(\sum_i^{k'} v_{2i} - 1 \right) x_2 \right] + \ldots + y_j \left[1 + \left(\sum_i^{k'} v_{ji} - 1 \right) x_j \right] + \ldots + = \sum_j^k y_j E_j \qquad (4)$$

where $E_j = 1 + \left(\sum_i^{k'} v_{ji} - 1 \right) x_j$ is the expansion due to the decomposition up to a conversion value of x_j of component j of the feed mixture.

According to Eq. (4), in the pyrolysis of hydrocarbon mixtures, expansion can be given as the sum of the expansions arising from the decomposition of the components of the feed mixture. Consequently, if the composition of the feed mixture and the $E(x)$ function, or the stoichiometrical coefficients of the reaction products in the decomposition reaction of individual components, as well as the conversions of components in the mixture are known, the expansion of the mixture can be evaluated.

The expansion of the mixture can also be obtained by an other method. Expansion for the pyrolysis of pure hydrocarbons is defined by the following expression [4]:

$$E = 1 + \left(\sum_{i}^{k'} v_i - 1\right) x = 1 + (E_v - 1)\, x \tag{5}$$

By replacing conversion and overall stoichiometric coefficients with the corresponding sums of conversions and stoichiometric coefficients, weighted by the mole fractions of the components, the following equation is obtained:

$$E = 1 + \left(\sum_{j}^{k} \sum_{i}^{k'} y_j v_{ji} - 1\right) \sum_{j}^{k} y_j x_j = 1 + (E_v - 1)\, X \tag{6}$$

where

$X = \sum_{j}^{k} y_j x_j$ is the degree of decomposition and

$E_v = \sum_{j}^{k} \sum_{i}^{k'} y_j v_{ji}$.

The expansion values calculated from Eqs (4) and (6) using pyrolysis data of pure iso-butane [5] and *n*-butane [4], as well as the corresponding values measured by the pyrolysis of the mixture of the above hydrocarbons are listed in Table I. The data refer to several temperatures and degrees of

Table I

A comparison of the calculated and experimental expansion values

Temperature °C	Conversion		Degree of decomposition	Expansion		
	x_{i-B}	x_{n-B}	X	Calculated from Eq. (4)	Calculated from Eq. (6)	Exp.
644	0.6846	0.8344	0.7557	1.8582	1.8520	1.851
644	0.2866	0.3287	0.3060	1.3317	1.3330	1.328
644	0.1642	0.1971	0.1797	1.1863	1.1880	1.203
675	0.7926	0.8885	0.8539	2.0024	1.9967	2.026
675	0.4750	0.5724	0.5210	1.5755	1.5724	1.593
675	0.3053	0.3677	0.3263	1.3486	1.3492	1.376
712	0.9349	0.9456	0.9346	2.1992	2.1923	2.226
712	0.7737	0.7431	0.7536	1.9072	1.9035	1.881
712	0.4623	0.4408	0.4487	1.4971	1.5206	1.521
752	0.9627	0.9586	0.9548	2.3267	2.3186	2.331
752	0.7565	0.7623	0.7548	1.9179	1.9134	1.900
792	0.9895	0.9942	0.9859	2.4035	2.3948	2.473
792	0.6934	0.6847	0.6848	1.8192	1.8163	1.834

decomposition. The good agreement of the calculated and experimental data proves the validity of the assumption made at the construction of Eq. (1).

The diagram in Fig. 1 shows a plot of the expansion values obtained at the pyrolysis of the mixture against the degree of decomposition. In this type of plot expansion can be given by a "single-curve", independent of temperature. In the case of decomposition reactions of simple stoichiometry expansion is a linear function of conversion, or, in the case of mixtures, that of the degree of decomposition over the whole range [4]. If the degree of decomposition is higher than 50%, the actual expansion curve deviates gradually upwards from the tangent drawn to the initial section of the curve. This

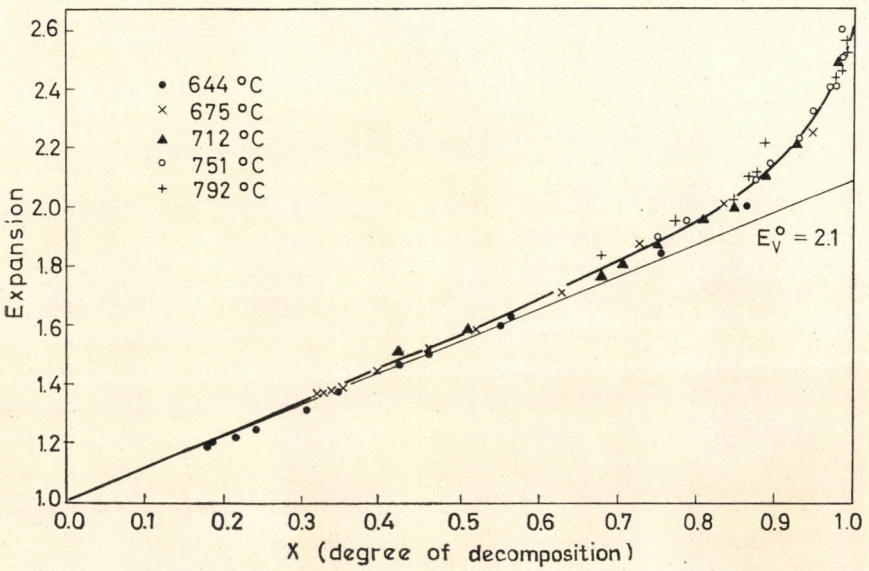

Fig. 1. The variation of expansion as a function of the degree of decomposition in the mixture

behaviour is due to the growth of mole numbers caused by secondary reactions. Similarly to the value of expansion, the value of E_v also changes with the degree of decomposition. In the case of simple mixtures (containing but a few components) the value of E_v belonging to a given degree of decomposition can be calculated from Eq. (6) or determined graphically from Fig. 1.

The application of Eqs (4) or (6) for multicomponent mixtures (*e.g.* petrol distillates) is not straightforward, since the conversion values of the components of the feed mixture cannot be determined with the required accuracy; and for the above calculations pyrolysis data of a great number of pure hydrocarbons would be needed.

In order to overcome these difficulties, the degree of decomposition in multicomponent mixtures has been characterized, on the basis of Eqs (5)

and (6), by the relative expansion [6]. By rearranging equations (5) and (6) conversion, or the degree of decomposition can be expressed by the following relation:

$$X = \frac{E - 1}{E_v - 1} \tag{7}$$

where X is the degree of decomposition of the mixture,
E is the instant value of the expansion,
E_v is the value of the expansion corresponding to the complete decomposition of one mole of the feed mixture (necessarily $E \leq E_v$).

The numerical value of the degree of decomposition defined above, similarly to the value of the conversion, should lie between zero and one. The use of Eq. (7) is theoretically supported by the fact that for pure substances the degree of decomposition defined there becomes identical to the conversion.

When applying Eq. (7) difficulties arise at the determination of the value of E_v. Namely, for multicomponent mixtures the summation of the overall stoichiometric coefficients, required in Eq. (6), cannot be carried out due to the lack of sufficient data, and, at the same time, the conversion values of the components are unknown. In this case the value of E_v should be determined graphically, on the basis of expansion curves, where expansion is plotted against the reaction time or against the conversion of a slowly decomposing component (*e.g. n*-pentane). It should be stressed that if equations containing E_v are used for designing industrial reactors, the value of E_v must be determined from experimental data that belong to pressure, temperature and reaction time ranges used in industrial reactors. This is important because under conditions that differ substantially from the above parameters the value of E_v may be quite different due to secondary reactions.

Overall decomposition rate of the isobutane–n-butane mixture

If in the overall decomposition rate equations of pure hydrocarbons conversion is replaced by the degree of decomposition defined by Eqs (6) and (7), a relatively simple expression is obtained for the evaluation of the overall decomposition rate of mixtures.

Equations constructed by us for expressing the overall decomposition rate of hydrocarbons (conversion curves) are based on first order kinetic equations. For isotherm, isobar flow reactors these equations are the following [4]:

$$\omega = \frac{1}{k}\left[E_v \ln \frac{1}{1 - x} - (E_v - 1)\, x\right] \tag{8}$$

$$\tau = \frac{1}{k} \ln \frac{1}{1 - x} \tag{9}$$

where $\omega = \dfrac{V_R}{B_0}$ is a fictive reaction time (sec), and

$\tau = \displaystyle\int_0^{\omega} \frac{d\omega}{E}$ is the actual reaction time (sec), which can be evaluated from the fictive reaction time and the expansion, and

k is the rate constant of the decomposition (sec^{-1}).

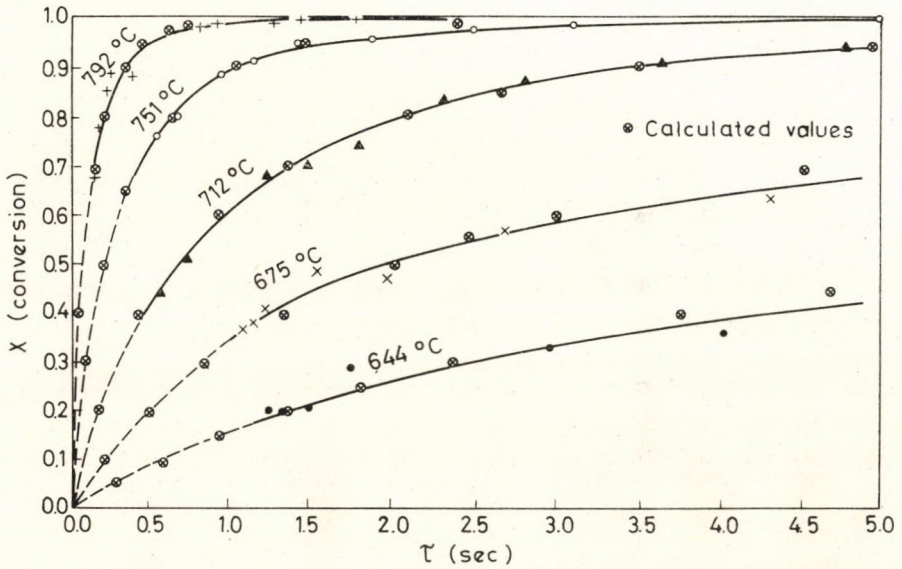

Fig. 2. The variation of *n*-butane conversion as a function of the actual reaction time in the mixture

It has been investigated whether on the basis of Eqs (8) and (9) the individual conversion curves of *n*-butane and iso-butane measured in the mixture, as well as the variation of the degree of decomposition defined by Eq. (6), and characteristic of the mixture, can be given as a function of the actual and fictive reaction times. This investigation may be based on any of the equations, because the *k*-values calculated for the same experimental points from both equations are equal to each other.

Conversions measured in the mixture have been plotted against actual reaction time at different temperature values. The conversion curves obtained are given for *n*-butane in Fig. 2 and for iso-butane in Fig. 3. The decomposition rate of both components significantly increases with increasing tempera-

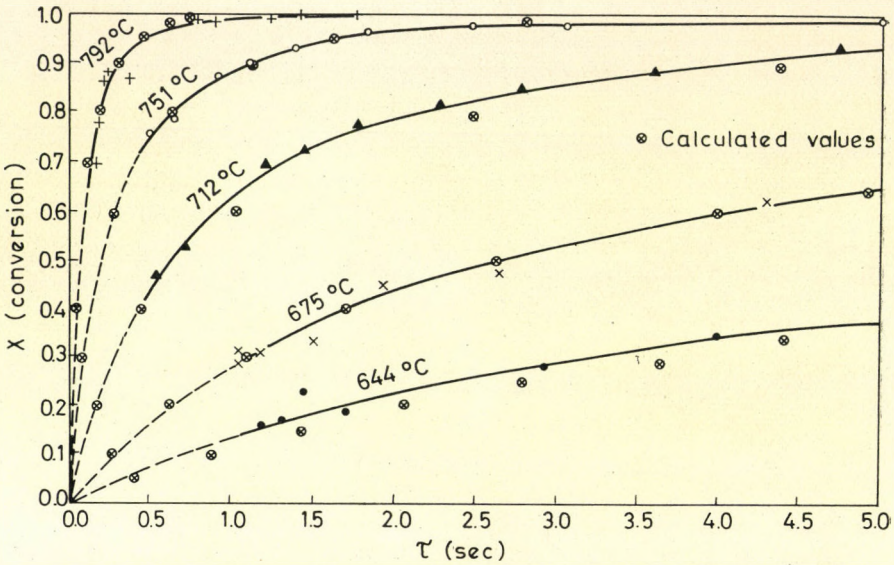

Fig. 3. The variation of i-butane conversion as a function of the actual reaction time in the mixture

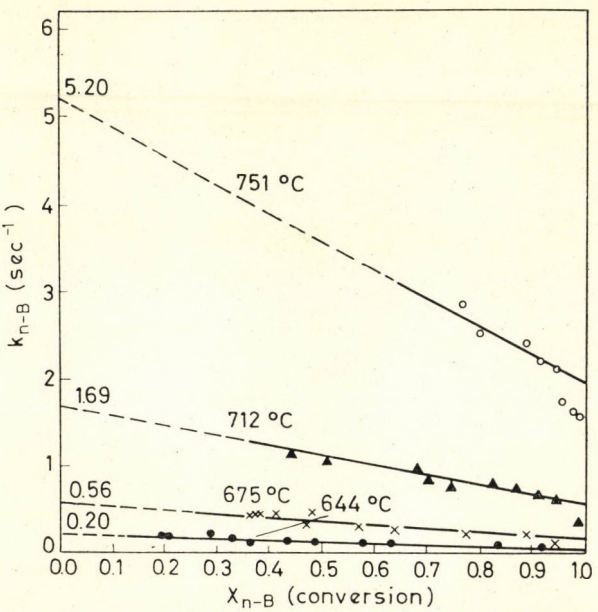

Fig. 4. The variation of the decomposition rate 'constant' of *n*-butane as a function of the conversion in the mixture

ture (*i.e.* conversion curves become more and more steep). It turns out from the more detailed investigation of the curves that below 700° C the decomposition rate of *n*-butane is higher, whereas at higher temperatures the decomposition rates of the above two substances are approximately the same. At the pyrolysis of pure *n*-butane and iso-butane just the opposite behaviour was found; below 700° C the decomposition of iso-butane, above that temperature the decomposition of *n*-butane was faster [4, 5]. These facts indicate that the decomposition rate of the components differs in the mixture from that of the pure substances. This may be due to the different conditions (partial pressure, concentration of chain-carrier radicals) existing in the mixture.

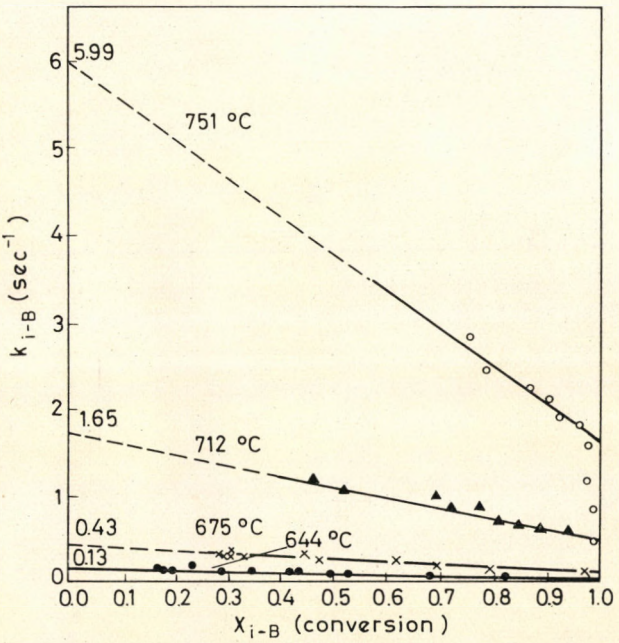

Fig. 5. The variation of the decomposition rate 'constant' of i-butane as a function of the conversion in the mixture

Decomposition rate constants were determined on the basis of Eq. (9) from the data shown in Figs 2 and 3. The values obtained were plotted against conversion. These plots are given in Fig. 4 for *n*-butane and in Fig. 5 for iso-butane. It can be established on the bases of these diagrams that, at a given temperature, the value of the decomposition rate 'constants' calculated from first order kinetic equations decreases with the conversion. The variation can be given by the following linear function:

$$k = k^0 - \beta x \tag{10}$$

where k^0 is the rate constant of decomposition extrapolated to zero conversion, and

β is a 'restraining coefficient' representing the inhibition effect of the reaction products exerted on the feed hydrocarbon.

On substituting Eq. (10) into the integrated Eqs (8) and (9) the conversion curves of normal- and iso-butane can be expressed in function of the actual and fictive reaction times. The functions can be given by the following expressions (using decimal logarithms):

$$\omega = \frac{1}{k^0 - \beta x}\left[E_v\, 2.303 \log \frac{1}{1-x} - (E_v - 1)\, x\right] \tag{11}$$

$$\tau = \frac{2.303}{k^0 - \beta x} \log \frac{1}{1-x} \tag{12}$$

The values of k^0 and β constants in Eqs (10), (11) and (12) are determined from experimental data on the basis of Figs 4 and 5. The temperature dependence of k^0 and β is given in Fig. 6 for *n*-butane and in Fig. 7 for isobutane. These diagrams are Arrhenius-type plots, where the logarithms of the

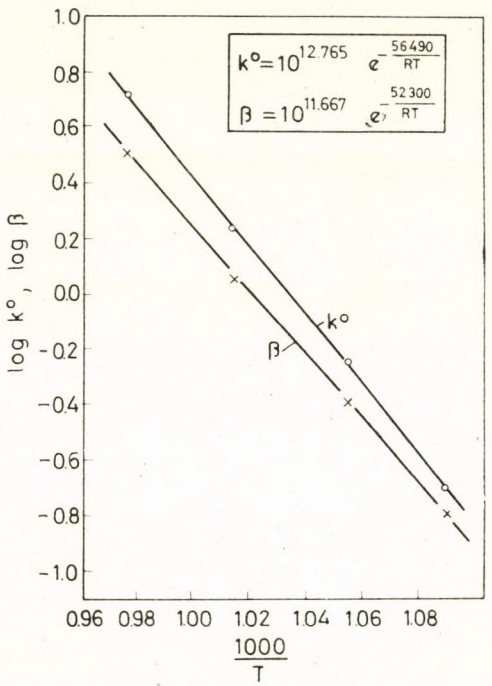

Fig. 6. Temperature dependence of the decomposition rate 'constant' and restraining coefficient of *n*-butane in the mixture

constants are plotted against the reciprocal temperature measured in Kelvin degrees. It has been found that the temperature dependence of both constants can be described by Arrhenius-type expressions. The expressions have the following numerical forms:

For *n*-butane:

$$\log k^0 = 12.765 - \frac{56490}{4.576\ T}$$

$$\log \beta = 11.667 - \frac{52300}{4.576\ T}$$

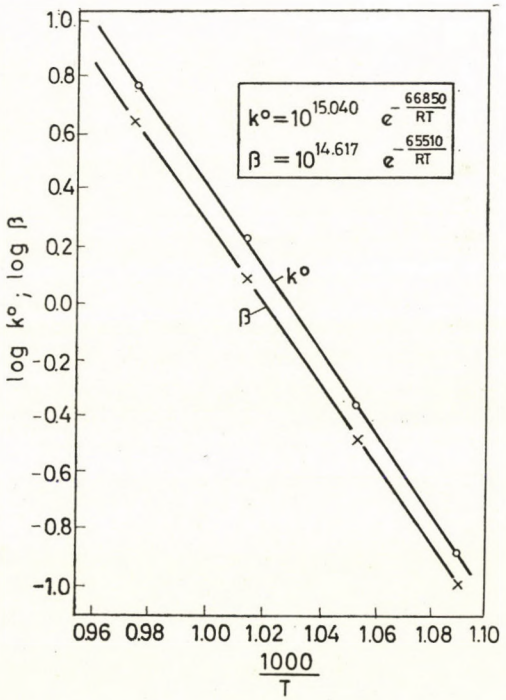

Fig. 7. Temperature dependence of the decomposition rate 'constant' and restraining coefficient of i-butane in the mixture

For *i*-butane:

$$\log k^0 = 15.040 - \frac{66850}{4.576\ T}$$

$$\log \beta - 14.617 - \frac{65510}{4.576\ T} \qquad (14)$$

In order to check relations (10)—(14) the conversion curves, belonging to the temperature used in the experiments, were calculated. For this purpose first k^0 and β values were evaluated for the given temperature using Eqs (13) and (14). These constants were substituted into Eq. (12), and actual reaction times, belonging to different conversion values, were calculated. The calculated points, given in Figs 2 and 3, are in a good agreement with the curves fitted to the experimentally determined points.

In the following paragraphs the overall decomposition rate of mixtures will be discussed. In the discussion the degree of decomposition defined by

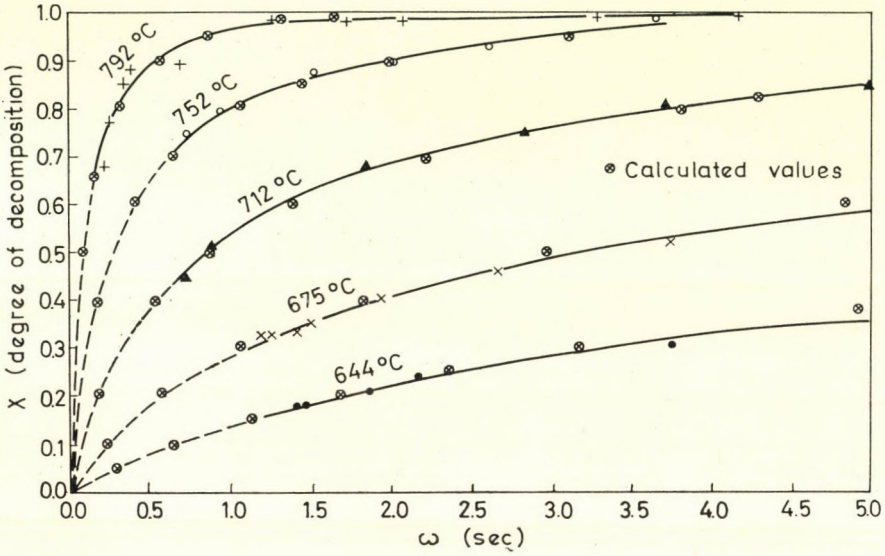

Fig. 8. The variation of the degree of decomposition in the mixture as a function of the fictive reaction time

Eq. (6) will be used. The variation of the degree of decomposition as the function of the fictive and actual reaction time is given in Figs 8 and 9. According to the diagrams, the degree of decomposition of mixtures can be expressed by curves quite similar to the conversion curves of the individual components. The slope of the curves (which is proportional to the decomposition rate) rapidly increases with increasing temperature.

The study of the overall decomposition rate (curves in Figs 8 and 9) is based on the method given earlier in this paper. From Eqs (8) and (9), by replacing conversion with the degree of decomposition the values of k were calculated for different experimental points. The values obtained were plotted against the degree of decomposition (Fig. 10). It can be seen that the decomposition rate constants calculated for the mixture decrease with the increasing extent of decomposition and at a fixed temperature, Eq. (10) also holds.

Hence, at a given temperature, the variation of the degree of decomposition for mixtures can be expressed in function of the actual and fictive reaction time by equations similar to Eqs (11) and (12). The constants k^0 and β were evaluated from Fig. 10. Their temperature dependence is given in Fig. 11, and by the following functions:

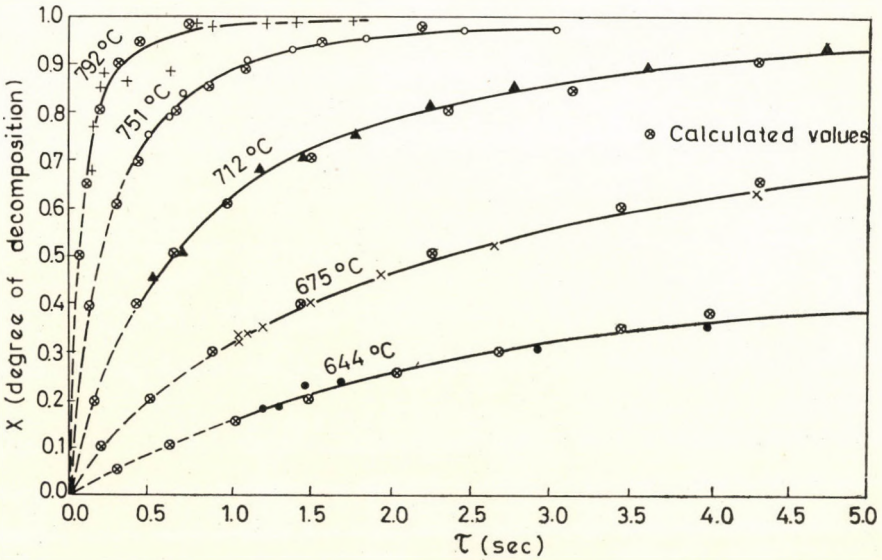

Fig. 9. The variation of the degree of decomposition in the mixture as a function of the actu a reaction time

$$\log k^0 = 13.113 - \frac{58134}{4.576\ T}$$

$$\log \beta = 11.811 - \frac{52878}{4.576\ T} \qquad (15)$$

Using the method described above, and on the basis of Eqs (15), (11) and (12) the variation of the degree of decomposition was calculated as a function of the fictive and actual reaction time. Calculations were carried out for the temperature used in the experiments. The calculated points are shown in Figs 8 and 9. Calculated values are in a good agreement with the curves fitted to the experimental values. Consequently, the method and the relations discussed in the paper provide an adequate description of the overall decomposition rate of mixtures.

Finally, it has been examined whether the constants of the kinetic equations for the description of the decomposition rate of i-butane and *n*-butane

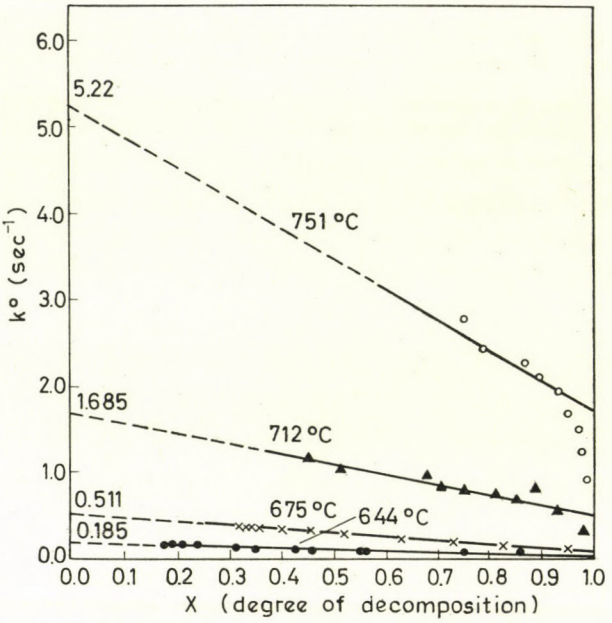

Fig. 10. The variation of decomposition rate 'constants' of the mixture as a function of the degree of decomposition in the mixture

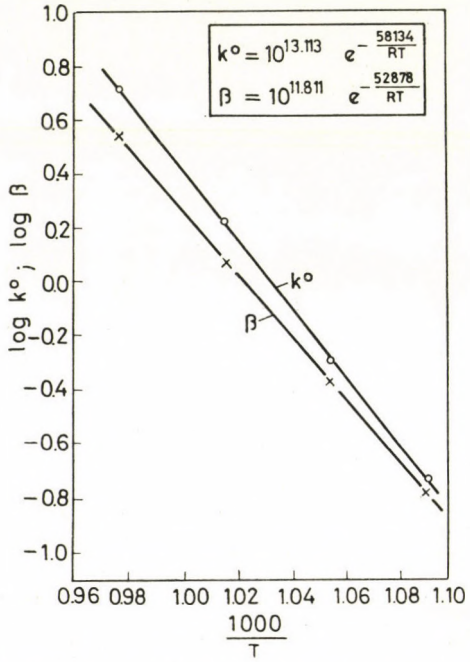

Fig. 11. Temperature dependence of the restraining coefficient and decomposition rate constant of the mixture

(both in pure state and in mixtures) can be correlated to the constants of the kinetic equations that describe the decomposition rate of mixtures in function of the degree of decomposition. For the time being, no quantitative relationship has been found between the constants of the above equations. The existence of such a relationship would mean that the pyrolysis of mixtures could be completely interpreted by the pyrolysis data of pure hydrocarbons alone. No such attempt has been published in the literature so far, hence, according to our present knowledge, the experimental study of the pyrolysis of mixtures is indispensable.

REFERENCES

1. LINDEN, H. R., *et al.:* Ind. Eng. Chem. **47,** 2467 (1955)
2. LINDEN, H. R., REID, J. M.: Chem. Eng. Progr. **55,** 71 (1959)
3. ZDONIK, S. B., GREEN, E. J. and HALLE, L. P.: The Oil and Gas J., July 10, 192 (1967)
4. ILLÉS, V.: Acta Chim. Acad. Sci. Hung. **59,** 35 (1969); *ibid.* **59,** 229 (1969)
5. ILLÉS, V.: Acta Chim. Acad. Sci. Hung. **67,** 339 (1971)
6. ILLÉS, V.: Magy. Kém. Foly. **76,** 664 (1970)

Vendel ILLÉS; Magyar Ásványolaj és Földgáz Kísérleti Intézet, Veszprém, Hungary.

Acta Chimica Academiae Scientiarum Hungaricae, Tomus 72 (2), pp. 133—146 (1972)

THE PYROLYSIS OF GASEOUS HYDROCARBONS, VI

PRODUCT DISTRIBUTION AS THE FUNCTION OF THE DEGREE OF DECOMPOSITION IN THE PYROLYSIS OF AN ISOBUTANE–*n*-BUTANE MIXTURE

V. ILLÉS

(Hungarian Oil and Gas Research Institute, Veszprém)

Received March 23, 1970
In revised form May 18, 1971

The distribution of the reaction products as a function of the degree of decomposition was studied at different temperatures. The qualitative and quantitative distribution of the reaction products as well as their variation were interpreted on the basis of free radical chain theory.

It was pointed out that the yields of the main reaction products, in the temperature and reaction time range used in industrial pyrolysis, can be given in function of the degree of decomposition by temperature independent 'single-curves'.

A relation was given by which the product yields of the pyrolysis of mixtures could be calculated using the pyrolysis data of pure components.

It was also pointed out that the variation of the molecular weight of the product mixture can also be given in function of the degree of decomposition by a temperature independent 'single curve'.

In the thermal cracking process of *n*-butane and isobutane, according to the free radical chain mechanism, the chain carrying radicals split off hydrogen atoms from the butane molecules. This reaction leads to the formation of primary and secondary *n*-butyl radicals in the case of *n*-butane and to primary and tertiary i-butyl radicals in the case of iso-butane, as well as to saturated products according to the following equations:

$$C_4H_{10} + \cdot H \rightarrow H_2 + C_4H_9\cdot$$

$$C_4H_{10} + \cdot CH_3 \rightarrow CH_4 + C_4H_9\cdot$$

$$C_4H_{10} + \cdot C_2H_5 \rightarrow C_2H_6 + C_4H_9\cdot$$

The decomposition of butyl radicals of different types produces olefin hydrocarbons of low molecular weight, and the chain carrying radicals are regenerated in the reaction. The decomposition of butyl radicals proceeds according to the following equations.

n-butyl radicals:

$$CH_3—CH_2—CH_2—CH_2\cdot \longrightarrow C_2H_4 + C_2H_5\cdot$$

$$CH_3—CH_2—\underset{\cdot}{CH}—CH_3 \longrightarrow C_3H_6 + CH_3\cdot$$

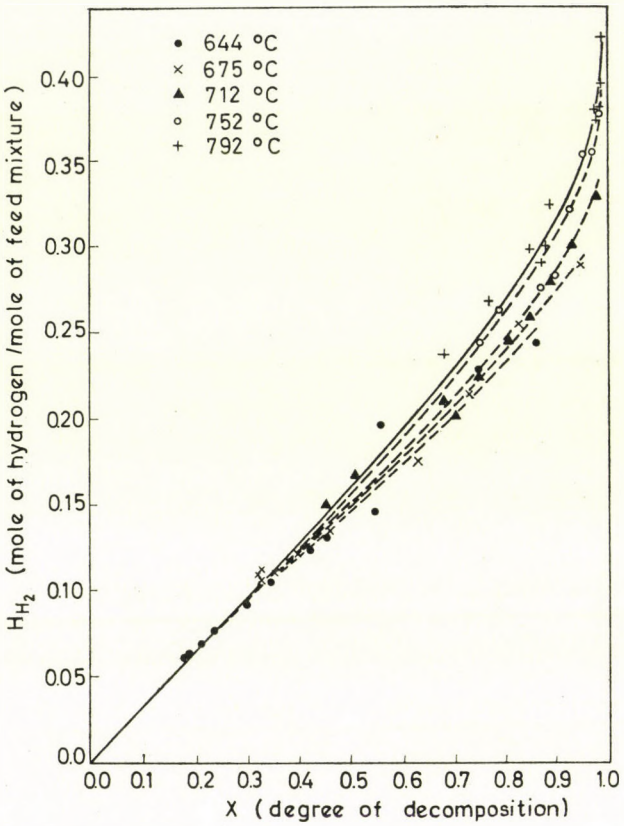

Fig. 1. The variation of hydrogen yield at the pyrolysis of the mixture, in function of the degree of decomposition

Iso-butyl radicals:

$$CH_3-\underset{\displaystyle CH_3}{\overset{\displaystyle |}{CH}}-CH_2\cdot \longrightarrow CH_3-CH=CH_2 + CH_3\cdot$$

$$CH_3-\underset{\displaystyle CH_3}{\overset{\displaystyle |}{\dot{C}}}-CH_3 \longrightarrow CH_3-\underset{\displaystyle CH_3}{\overset{\displaystyle |}{C}}=CH_2 + H\cdot$$

A part of the ethyl radicals formed in the decomposition reaction of *n*-butyl radicals yields ethylene and hydrogen in the following reaction:

$$C_2H_5^{\cdot} \longrightarrow C_2H_4 + H\cdot$$

Accordingly, the primary decomposition reaction of *n*-butane yields ethylene, propylene, hydrogen, ethane and methane, whereas that of i-butane yields propylene, iso-butylene, hydrogen and methane.

According to experiments on the thermal decomposition of *n*-butane and i-butane, the primary distribution of products was in qualitative and quantitative agreement with the distribution calculated on the basis of the free radical chain mechanism [1, 2]. It can be expected that the thermal decomposition of the mixture of these hydrocarbons proceeds *via* the same reactions, yielding the following main reaction products: hydrogen, methane, ethane, ethylene, propylene and iso-butylene.

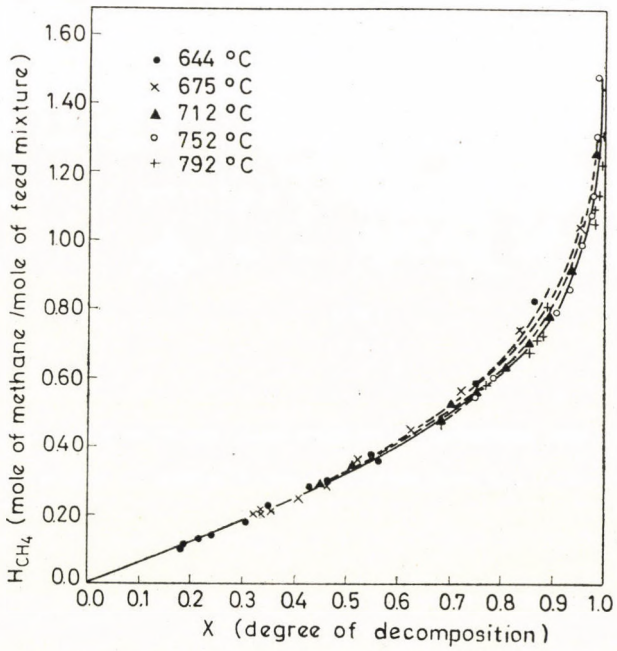

Fig. 2. The variation of methane yield at the pyrolysis of the mixture in function of the degree of decomposition

Figs 1—6 show the yields of the main reaction products (mole of product/mole of feed mixture) plotted against the degree of decomposition defined by Eq. (6) of the preceding paper [3]. (In the diagrams yield data belonging to different temperatures are marked with different symbols.) It can be seen from the diagrams that it is the above listed products that are formed in reasonably high amount (*i.e.* exceeding 10 mole%). The yield values of the reaction products show different variation with the degree of decomposition and temperature.

Hydrogen and methane yields increase with the degree of decomposition over the whole range studied. These products are stable under the conditions of the pyrolysis. The ethylene yield also increases until $X = 0.95$, and the yield curves corresponding to higher temperatures have maxima. The

yield curves of propylene and iso-butylene are also maximum curves. The maxima of propylene yield curves appear in the range of $X = 0.77 - 0.8$, and those of iso-butylene yield curves can be found in the range of $X = 0.7 - - 0.76$.

Among the above reaction products the yields of hydrogen and ethylene at a fixed degree of decomposition increase, whereas those of ethane and iso-

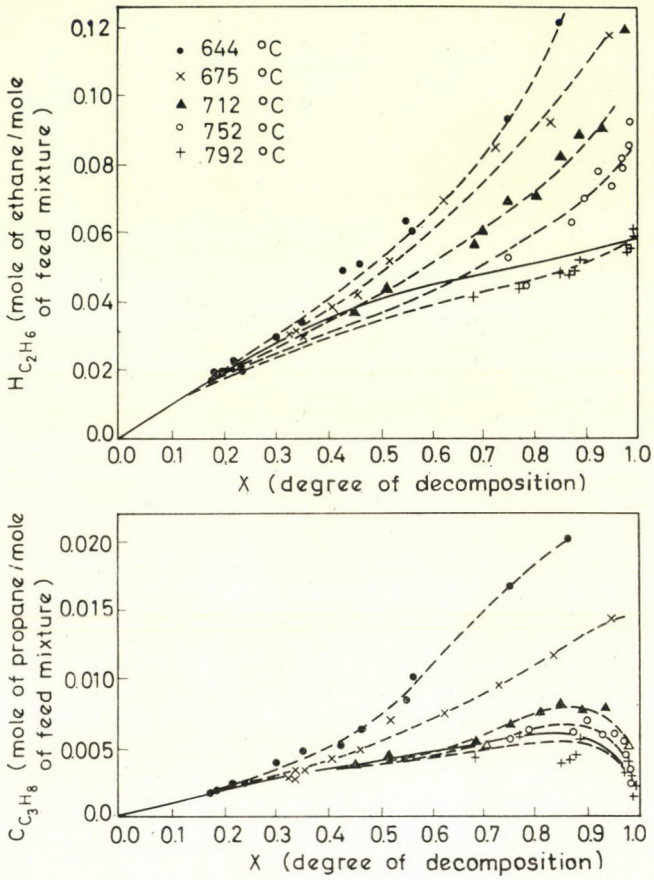

Fig. 3. The variation of ethane and propane yields at the pyrolysis of the mixture, in function of the degree of decomposition

butylene decrease with the temperature. The methane yield slightly decreases, and the yield of the coupled product, propylene, slightly increases with the temperature. The very low yield of propane further decreases with increasing temperature.

The above changes with the temperature are due to the following facts. The activation energies of the abstraction reactions of hydrogen atoms bound

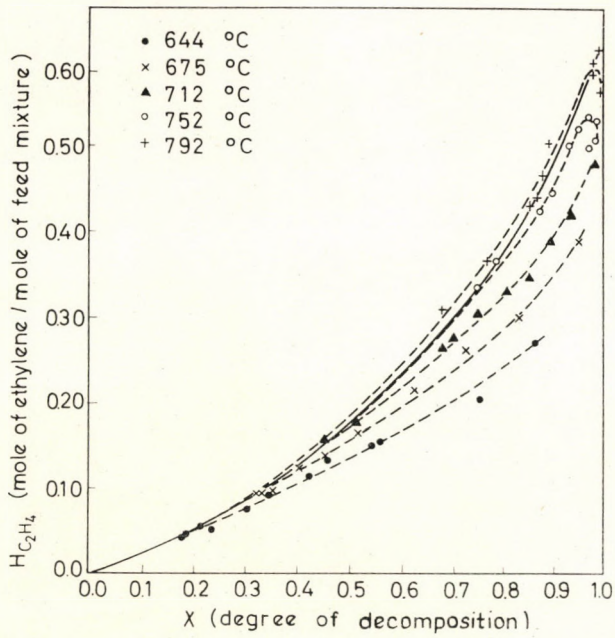

Fig. 4. The variation of the ethylene yield at the pyrolysis of the mixture, in function of the degree of decomposition

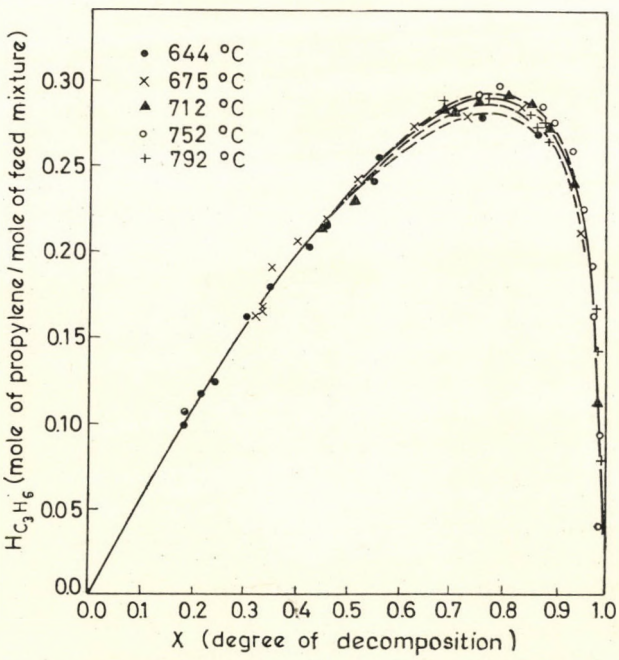

Fig. 5. The variation of propylene yield at the pyrolysis of the mixture, in function of the degree of decomposition

to primary, secondary and tertiary carbons of butane molecules as well as those of the two-way reactions of ethyl and propyl radicals are different; moreover the radicals of different types formed in the hydrogen abstraction reaction may isomerize before the decomposition reaction.

According to KOSIAKOV and RICE [4] the difference between the activation energies required for hydrogen abstraction from carbon atoms of different type is cca. 2 kcal/mole. (The highest activation energy is required for the splitting of hydrogens bound to primary carbon atoms.) Consequently,

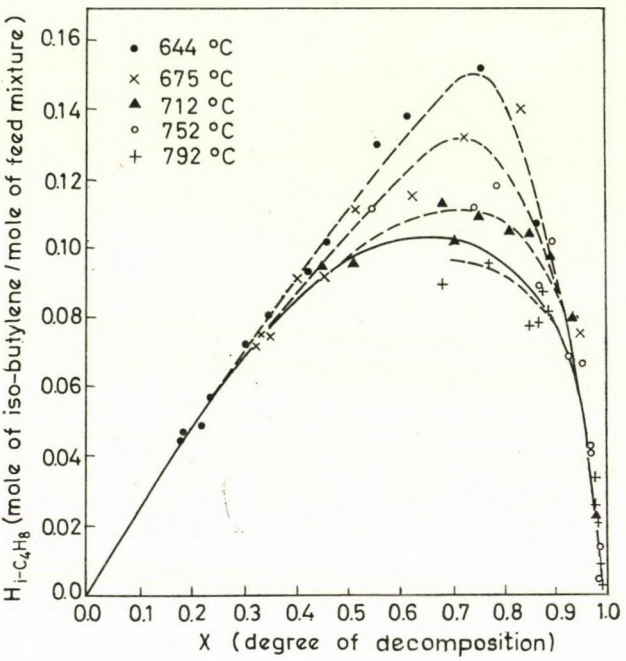

Fig. 6. The variation of iso-butylene yield at the pyrolysis of the mixture, in function of the degree of decomposition

with increasing temperature, the amount of primary butyl radicals slightly increases in comparison with the amount of secondary and tertiary radicals. It follows from this fact that in the decomposition of iso-butyl radicals the amount of propylene and methyl radicals increases, whereas that of iso-butylene and hydrogen atoms decreases with increasing temperature. On the other hand, in the decomposition of *n*-butyl radicals the amount of ethylene and ethyl radicals increases, while that of propylene and methyl radicals decreases. Methyl radicals, apart from the very low fraction that take part in recombination reactions, give rise to methane.

Methane yield curves shown in Fig. 2 and iso-butylene yield curves shown in Fig. 6 indicate the above discussed effect; the amount of both

products decreases with the temperature, at constant degree of decomposition.

Since methane and propylene are coupled products (methyl radicals and propylene molecules are formed in the same reaction), it can be expected that the yield of propylene also decreases with the temperature. As it can be seen in Fig. 5, however, the yield of propylene, at constant degree of decomposition slightly increases with the temperature. This experience may be attributed to the fact that besides the decomposition of secondary butyl radicals and primary iso-butyl radicals there is another reaction that takes part, to a small extent, in the propylene formation. This reaction is the decomposition of secondary propyl radicals formed *via* the thermal dissociation of iso-butane molecules. The products of this decomposition are hydrogen atoms and propylene. (Secondary propyl radicals may also be formed in the addition reactions of chain carrying hydrogen atoms on the produced propylene molecules.) A fraction of secondary propyl radicals takes part in hydrogen abstraction reactions yielding propane. With increasing temperature the decomposition reaction becomes dominant due to its higher temperature coefficient. Consequently, at constant degree of decomposition the yield of propane decreases (Fig. 3), whereas that of propylene increases (Fig. 5).

The subsequent reactions of ethyl radicals formed in the decomposition of primary *n*-butyl radicals have much greater influence on the hydrogen, ethane and ethylene yields than the reactions discussed above [1]. A fraction of the ethyl radicals takes part in hydrogen abstraction reactions yielding ethane; the other fraction decomposes into ethylene and hydrogen. With increasing temperature the decomposition reaction becomes dominant, since the temperature coefficient of this reation is substantially higher. Consequently, in accordance with the experimental results, hydrogen and ethylene yields increase, whereas ethane yield decreases with increasing temperature (Figs 1, 4 and 3).

The maxima of propylene and iso-butylene yield curves are due to secondary decomposition reactions of propylene and iso-butylene, and to the isomerization reactions of propyl and butyl radicals of different types prior to the decomposition. The first step of decomposition reactions is the addition of chain carrying radicals (hydrogen atoms) on propylene and iso-butylene molecules. In this step different types of propyl and isobutyl radicals are formed, which partly isomerize to yield primary propyl and butyl radicals. The decomposition of primary propyl radicals yields ethylene and methyl radicals, that of primary isobutyl radicals propylene and methyl radicals. The substantial increase of methane and ethylene yields in the $X > 0.7$ range may be attributed to the above reactions.

Butadiene and aromatic hydrocarbons also appear among the decomposition products and their amount increases with increasing degree of decom-

position (Figs 7 and 8). This fact indicates that olefin hydrocarbons also take part in subsequent secondary reactions. Butadiene and aromatic hydrocarbons are formed from ethylene, propylene and butylene, presumably by radical mechanisms. For example, if a hydrogen atom is split off from ethylene or propylene molecules by chain carrying radicals, vinyl or allyl radicals are

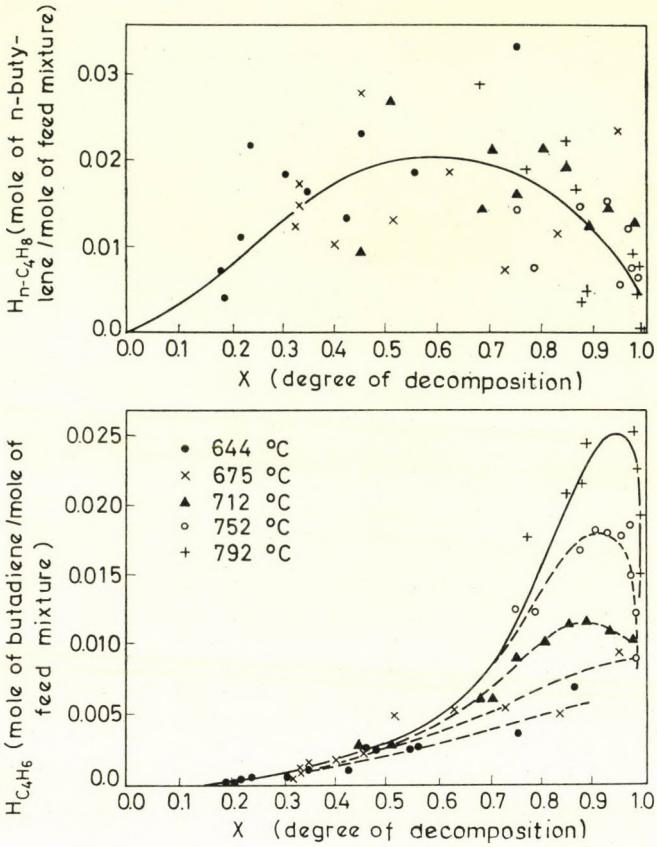

Fig. 7. The variation of *n*-butylene and butadiene yields at the pyrolysis of the mixture, in function of the degree of decomposition

formed, capable of reacting with each or with olefins. These reactions yield dienes or aromatic hydrocarbons.

The role of secondary reactions increases with the degree of decomposition of the feed mixture, at constant temperature, because parallel to the cracking process the concentration of the components that may take part in secondary reactions increases, and at the same time the concentration of the feed hydrocarbons, which consume the free radicals, decreases. At the maxima

of the yield curves the rates of the primary reactions yielding these intermediates are equal to the rates of secondary reactions of the intermediates.

Figs 1—8 contain all the experimental data. A substantial part of the data belong to reaction times longer than 1.5 sec, the maximal sojourn time applied in industrial pyrolysing furnaces. Regarding only the yield data belonging to reaction times of $0 \leq 1.5$ sec, the corresponding points fit to a 'single-curve', independent of the temperature. As an example, Fig. 9 shows the

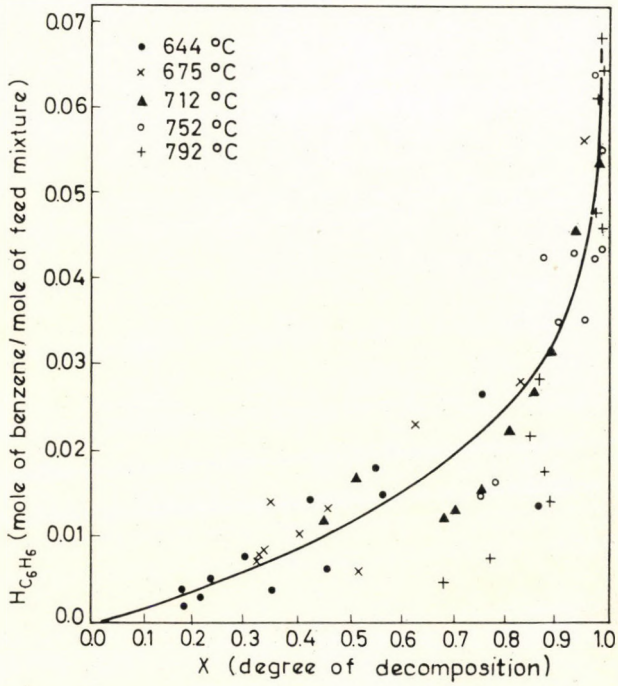

Fig. 8. The variation of benzene yield at the pyrolysis of the mixture, in function of the degree of decomposition

yield data of ethylene measured in the above time interval. A 'single-curve', as drawn in the diagram, can well be fitted to these points. Also in the remaining diagrams solid lines represent yield curves belonging to conditions characteristic of industrial pyrolysing furnaces. Some points of these yield curves are given in Table I. These yield curves can be sufficiently well approximated by mathematical functions (*e.g.* third order polynomials).

It has been investigated whether the product yields in the pyrolysis of mixtures may be calculated from the yield curves determined from the pyrolysis data of pure butanes. The calculation was based on the following relation:

$$H_i = \frac{m_i}{n^0} = \sum_j^k y_j \, v_{ji} \, x_j = \sum_j^k y_j \, H_{ji}$$

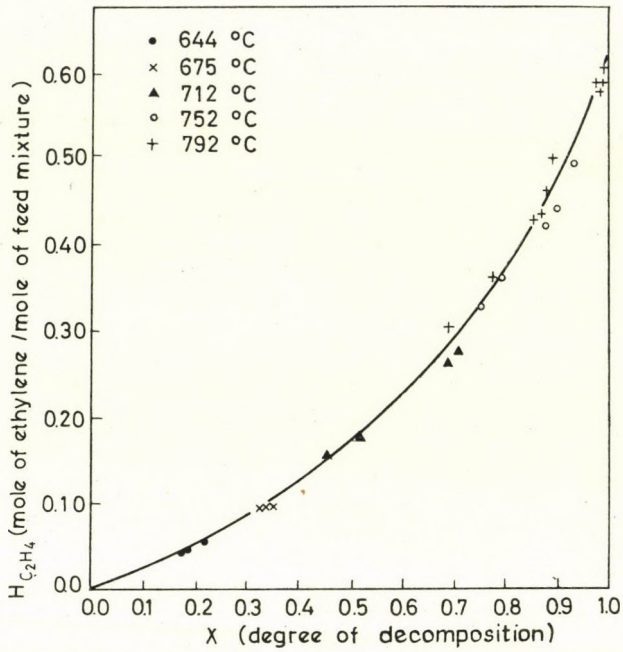

Fig. 9. The variation of ethylene yield at the pyrolysis of the mixture, in function of the degree of decomposition ($0 < \tau < 1.5$ sec)

where H_i is the yield of the ith product in the pyrolysis of the mixture,
m_i is the amount of the ith product formed during unit time (mole/sec),
n^0 is the amount of feed mixture per unit time (mole/sec),
y_j is the mole fraction of the jth component in the feed mixture,
x_j is the conversion of the jth component in the pyrolysis of the mixture,
v_{ji} is the overall stoichiometric coefficient of the ith product in the decomposition reaction of the jth component, belonging to x_j conversion,
H_{ji} is the yield of the ith product in the pyrolysis of the jth component, belonging to x_j conversion.

The calculation was carried out in the following way. Yield data corresponding to the conversion x_j in the mixture were taken from the yield curves determined by pyrolysis of pure substances in experiments carried out practically at the temperature of the pyrolysis of the mixture. These yield data were multiplied by the mole fraction y_j of the hydrocarbon in question, measured in the feed mixture, and the products were summed.

Yield values determined by the pyrolysis of the mixture and those calculated by the above method using the pyrolysis data of pure *n*-butane and

Table I

Product yields at the pyrolysis of isobutane–n-butane mixture, as a function of the degree of decomposition (mole of product/mole of feed mixture)

Degree of decomposition / Products	0.10	0.20	0.30	0.40	0.50	0.60	0.70	0.80	0 90	0.95
H_2	0.033	0.065	0.096	0.127	0.160	0.194	0.231	0.271	0.318	0.350
CH_4	0.060	0.120	0.183	0.251	0.328	0.408	0.500	0.612	0.785	0.950
C_2H_6	0.0095	0.0185	0.0270	0.0350	0.0405	0.0450	0.0475	0.0505	0.0538	0.0555
C_2H_4	0.024	0.052	0.086	0.126	0.177	0.230	0.295	0.375	0.480	0.548
C_3H_8	0.0010	0.0022	0.0028	0.0034	0.0045	0.0046	0.0053	0.0058	0.0055	0.0045
C_3H_6	0.056	0.108	0.155	0.196	0.233	0.264	0.283	0.290	0.268	0.225
i-C_4H_8	0.0245	0.0470	0.0675	0.0840	0.0965	0.1025	0.1003	0.0960	0.0800	0.0590
n-C_4H_8	0.0024	0.0080	0.0132	0.0175	0.0200	0.0208	0.0196	0.0170	0.0124	0.0088
C_4H_6	0.0000	0.0001	0.0005	0.0015	0.0027	0.0047	0.0080	0.0155	0.0248	0.0250
C_6H_6	0.0012	0.0032	0.0056	0.0084	0.0116	0.0152	0.0194	0.0250	0.0332	0.0420

Table II

A comparison of the calculated and experimental yields of the main products

Temperature °C	Conversion		Degree of decomposition	Calculated yield of products (mole of product/ mole of feed mixture)					Experimental yield of products (mole of product/ mole of feed mixture)				
	x_{i-B}	x_{-n-B}	X	H_2	CH_4	C_2H_4	C_3H_6	C_4H_8	H_2	CH_4	C_2H_4	C_3H_6	C_4H_8
644	0.6846	0.8344	0.7557	0.208	0.579	0.287	0.314	0.119	0.226	0.580	0.205	0.278	0.152
644	0.2866	0.3287	0.3060	0.093	0.186	0.097	0.162	0.066	0.091	0.175	0.075	0.161	0.072
644	0.1642	0.1971	0.1797	0.053	0.106	0.055	0.096	0.040	0.060	0.108	0.044	0.098	0.044
675	0.7926	0.8885	0.8539	0.246	0.689	0.361	0.309	0.111	0.257	0.740	0.298	0.285	0.140
675	0.4750	0.5724	0.5210	0.154	0.335	0.193	0.252	0.098	0.154	0.359	0.164	0.241	0.111
675	0.3053	0.3677	0.3263	0.103	0.200	0.107	0.168	0.069	0.106	0.211	0.096	0.164	0.075
712	0.9349	0.9456	0.9346	0.310	0.894	0.495	0.230	0.077	0.303	0.914	0.421	0.240	0.079
712	0.7737	0.7431	0.7536	0.239	0.559	0.341	0.319	0.113	0.226	0.560	0.305	0.289	0.109
712	0.4623	0.4408	0.4487	0.144	0.280	0.166	0.219	0.094	0.150	0.292	0.157	0.213	0.095
752	0.9627	0.9586	0.9548	0.336	0.958	0.561	0.232	0.071	0.323	0.988	0.522	0.224	0.066
752	0.7565	0.7623	0.7548	0.247	0.545	0.374	0.310	0.114	0.244	0.547	0.334	0.291	0.111
792	0.9895	0.9942	0.9859	0.372	1.067	0.653	0.157	0.027	0.383	1.136	0.600	0.142	0.021
792	0.6934	0.6847	0.6848	0.231	0.467	0.333	0.291	0.115	0.238	0.477	0.308	0.288	0.090

isobutane are compared in Table II. Comparison has been made for a number of different temperature and degree of decomposition values.

For hydrogen, methane, propylene and butylene the agreement of calculated and measured data is sufficient; for ethylene the deviation exceeds 15% at some points, so the discussed method is suitable for approximative calculations.

The variation of the molecular weight of the mixture, as the function of the degree of decomposition, is given in Fig. 10. According to the diagram, the molecular weight of the reaction mixture, when plotted against the degree of decomposition, is on a single curve, independent of the temperature. Hence, the decomposition grade of the feed mixture can also be characterized by the molecular weight of the product gas. The value extrapolated from the curve to zero degree of decomposition is equal to the molecular weight of the feed mixture. The molecular weight of the reaction mixture decreases with increasing degree of decomposition because the majority of the products formed in the cracking process has lower molecular weight than the components of the feed mixture.

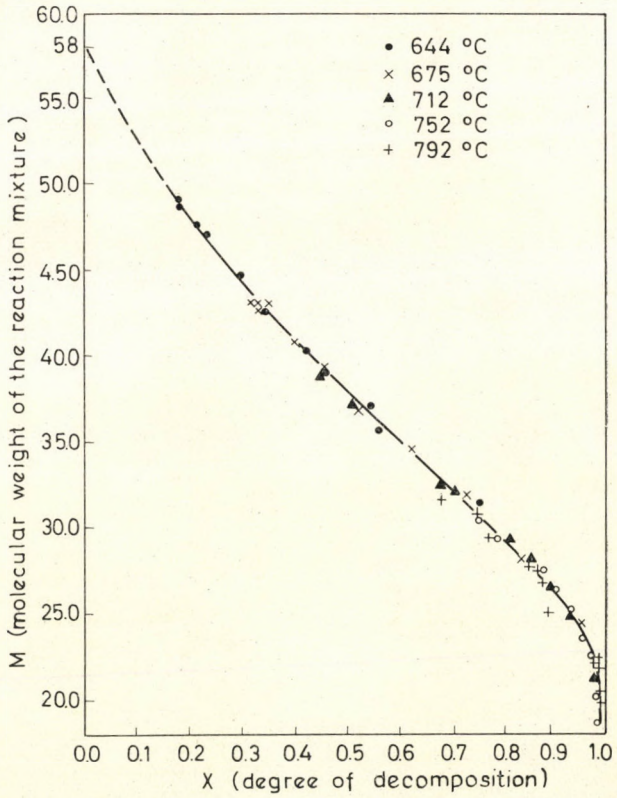

Fig. 10. The variation of the molecular weight of the reaction mixture at the pyrolysis of the mixture, in function of the degree of decomposition

REFERENCES

1. ILLÉS, V.: Acta Chim. Acad. Sci. Hung. **59,** 229 (1969)
2. ILLÉS, V.: Acta Chim. Acad. Sci. Hung. **67,** 339 (1971)
3. ILLÉS, V.: Acta Chim. Acad. Sci. Hung. **72,** 117 (1972)
4. KOSIAKOV, A., RICE, F. O.: J. Am. Chem. Soc. **65,** 590 (1943)

Vendel ILLÉS; Magyar Ásványolaj és Földgáz Kísérleti Intézet, Veszprém Hungary.

Acta Chimica Academiae Scientiarum Hungaricae, Tomus 72 (2), pp. 147—164 (1972)

CHARACTERISTIC VIBRATIONAL FREQUENCIES OF CRYSTALLINE AMMONIUM POLYMOLYBDATES CONSISTING OF OCTAHEDRAL MoO_6 UNITS, IN THE 400—4000 cm^{-1} RANGE

A. B. KISS, S. HOLLY* and E. HILD

(Tungsram Research Institute, Central Research Institute for Chemistry, Hungarian Academy of Sciences, Budapest)*

Received August 29, 1970

The vibrational frequencies of microcrystalline ammonium polymolybdates were studied in the range of 400—4000 cm^{-1}. The IR spectra reflect very sensitively the structural variations in polyanions built up of MoO_6 units. The frequencies of stretching vibrations of the Mo—O and the Mo—O—Mo bridges containing oxygen in various coordinations have been approximately assigned. The character of the stretching vibrations has been established for the hepta- and octamolybdates with the aid of the $O_h \rightarrow C_{2v} \rightarrow C_{2h} \rightarrow$ and the $O_h \rightarrow C_{2h} \rightarrow C_i$ correlations, respectively.

The shift of the Mo—O(I) bond frequencies in the infrared and Raman range was correlated with the variation of the extent of polycondensation, the average coordination numbers of the central Mo nuclei and the variation of the ratio $[NH_4^+] : [Mo—O(I)] = K$. The frequency shift of the $\nu_3(F_2)$ vibrational mode of the NH_4^+ ion was interpreted similarly. The relationships allow for the estimation of the number of Mo—O(I) bonds in the polyanions of unknown structure and, in simple cases, the position of the NH_4^+ ions as well. It is likely that the NH_4^+ ions of octamolybdate are symmetrically located with respect to the i-th center of the C_i^1 triclinic cell.

Several authors dealt with the infrared and Raman spectra of various molybdates [1—9]. However, only a limited number of references can be found which pertain to the infrared spectrometric study of crystalline polymolybdates composed of octahedral MoO_6 units. A most characteristic representative of the latter group is the ammonium heptamolybdate tetrahydrate. The infrared spectrum of this compound was published by MILLER *et al.* [1, 2], while its Raman spectrum together with that of the octamolybdate can be found in AVESTON's paper [10], in which a study of the polycondensation processes of aqueous molybdate solutions is reported.

It is known that during the stepwise acidification of basic molybdate solutions, polymolybdates of growing condensation degree are initially formed, depending on the pH and the $(H^+) : (MoO_4^{2-})$ concentration ratio. At $pH \leq 1$ monomeric MoO_2^{2+} cations appear. A similar polycondensation reaction takes place in the solid phase during the thermal treatment of ammonium heptamolybdate tetrahydrate in the air. In this process the formation of at least four intermediate polymolybdates with independent structures prior to the formation of MoO_3 was proved by recent investigation [11]. The most important characteristics of the solid and liquid phase polycondensation reactions and their correlations were discussed in an earlier paper [11].

In this communication we report the characteristic vibrational frequencies (in the 400—4000 cm^{-1} range) of a few polymolybdates precipitated from solution, as well as of the one formed in the solid phase reaction.

Experimental

The spectra of polymolybdates were recorded on a Type UR 10 spectrophotometer, in KBr pellets, nujol mull or a hexachlorobutadiene suspension. The samples were prepared using AnalaR reagent grade and Tungsram ammonium heptamolybdate tetrahydrates. Both of these chemicals showed an X-ray diffraction pattern characteristic of the heptamolybdates and their composition was in agreement with the formula $(NH_4)_6[Mo_7O_{24}] \cdot 4H_2O$. The structures of some polymolybdates studied are known whereas only the composition is given for the others [11]. For the latter compounds the formula of composition referred uniformly to 1 $(NH_4)_2O$ is given (Table I).

Table I

Data on the structure and composition of ammonium polymolybdates

Structure	Substance	Space group	Z	Reference
Known	$(NH_4)_2[Mo_2O_7]$	$C_i^1 - P_1$	2	[12]
	$(NH_4)_6[Mo_7O_{24}] \cdot 4H_2O$	$C_{2h}^5 - P2_{1/c}$	4	[13—15]
	$(NH_4)_4[Mo_8O_{26}]$	$C_i^1 - P_1$	1	[16]
	MoO_3	$D_{2h}^{16} - Pbnm$	4	[17—20]
Unknown	$(NH_4)_2O \cdot 2.5MoO_3$	—	—	[11]
	$(NH_4)_2O \cdot 4MoO_3 \cdot 1.3H_2O$	—	—	
	$(NH_4)_2O \cdot 14MoO_3$	—	—	
	$(NH_4)_2O \cdot 14MoO_3 \cdot 3H_2O$	—	—	
	$(NH_4)_2O \cdot 22MoO_3$	—	—	

The octa-, 2,5-, 14-, 22-molybdates and molybdenum trioxide were prepared by the method described in the study of the thermal decomposition of heptamolybdate [11]. The 14-molybdate · $3H_2O$, whose X-ray and infrared spectrometric characteristics were identical with the 14-molybdate formed in a thermal reaction, was precipitated from solution [11]. The 4-molybdate exhibiting an $(NH_4)_2O : MoO_3$ ratio identical with that of the octamolybdate was obtained by NEUGEBAUER from solution [11]. Its structure as studied by X-ray diffraction was found to be significantly different from that of octamolybdate [11]. Investigating a Merck product labelled 'ammonium heptamolybdate', we found that its infrared spectrum differed significantly from the published pattern [1, 2].

The structure of this substance, identified by X-ray diffraction using the dÅ and the I/I_1 intensity values given by MA [21], was identical with that of the dimolybdate. Its chemical composition was found to be $(NH_4)_2O \cdot 2.1\ MoO_3$. It is worth mentioning that the dimolybdate $(NH_4)_2Mo_2O_7$ used in the X-ray diffraction study by LINDQVIST [12] was also a commercial product labelled 'heptamolybdate'.

There is only a slight deviation between the spectra recorded in KBr pellets and in nujol mull, indicating the lack of any significant interaction between the polymolybdates and KBr. The most important parts of the spectra are shown in Figs 1 and 2, whereas the wavenumbers observed in different media are listed in Table II.

The complete molybdate series would require inclusion of the monomeric $(NH_4)_2MoO_4$ as well; however, we were not able to prepare the ammonium salt of the 1-molybdate using the methods reported in the literature [22]. Although the chemical composition of our products closely approximated the mole ratio $(NH_4)_2O : MoO_3 = 1$ in several cases, ammonia losses and polymerization occurred during pellet formation in air; therefore the spectra exhibited mostly the characteristics of the di- and heptamolybdates.

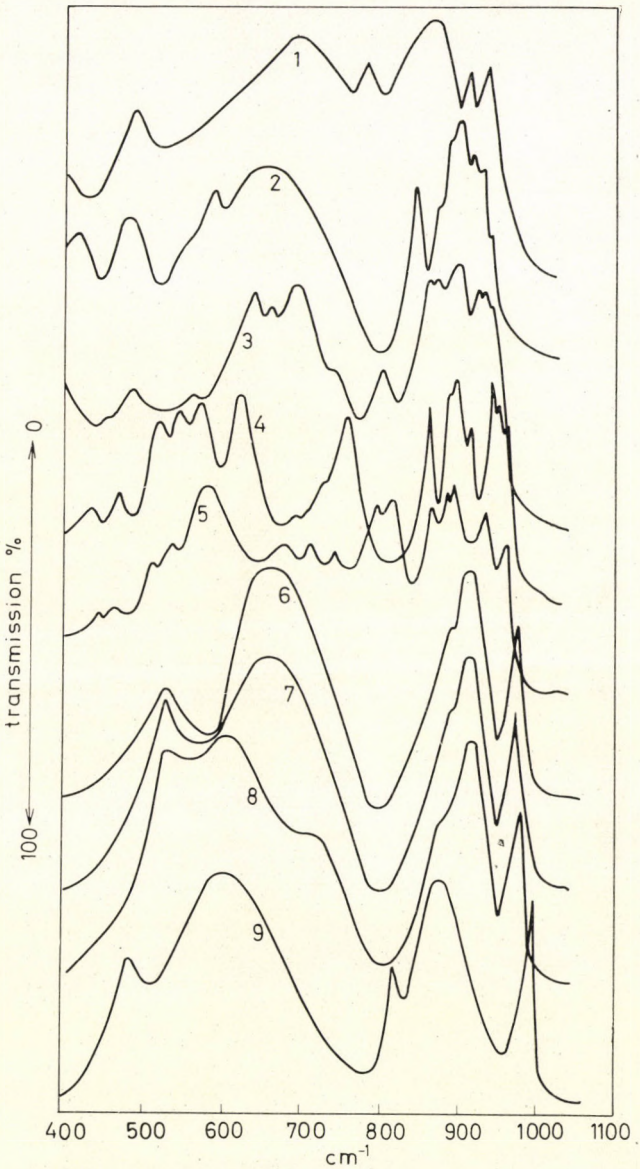

Fig. 1. Infrared spectra (in KBr pellets) of 1: dimolybdate; 2: heptamolybdate; 3: 2,5-molybdate; 4: octamolybdate; 5: 4-molybdate · 1.3 H_2O; 6: 14-molybdate · 3 H_2O; 7: 14-molybdate; 8: 22-molybdate; 9: MoO_3

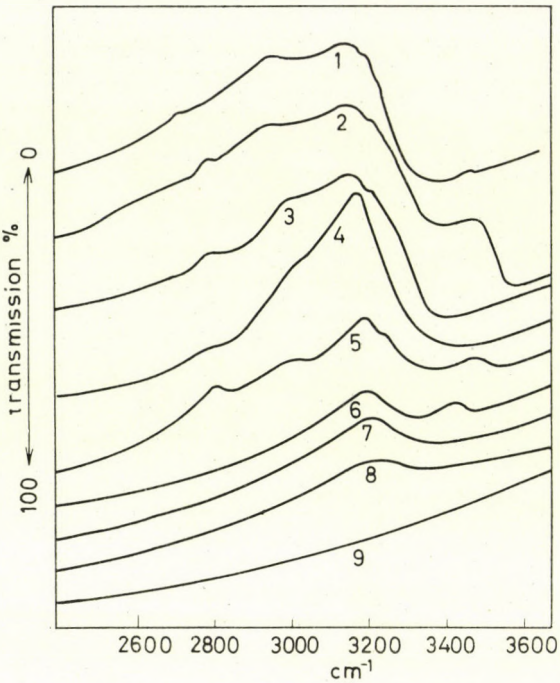

Fig. 2. Infrared spectra (in KBr pellets) of the same samples as in Fig. 1

Problems of the IR spectrometric study of polymolybdates

The analysis of the vibrational spectra of crystalline inorganic compounds with molecules consisting of too many atoms is rather complicated. If the unit cell best reflecting the symmetry properties of the substance is chosen as basis, one finds that the number of vibrations may be very large and difficulties may be encountered when attempting the reliable assignment of the vibrational modes. This holds particularly true for the case of macromolecular inorganic polymers, since the polyanions often contain 30—50 atoms and the unit cell is occupied by several molecules.

A characteristics feature of the crystalline forms of the various molybdates is that the coordination number for the molybdenum atom is 4 or 6. The problem is somewhat simpler with molybdates of the schelit [4, 7, 9] or the spinel [3, 4] structure containing four-coordinate molybdenum, where the unit cell is occupied by independent MoO_4 tetrahedra. With the aid of the site symmetries arising from the structure found by X-ray diffraction *(e.g.* S_4, T_d*)* and the corresponding selection rules the absorption bands can be interpreted.

The situation is much more complex in the case of six-coordinate polymolybdates. There are 7 and 8 MoO_6 octahedra sharing edges in heptamolybdate [13—15] and octamolybdate [16], respectively, which results in the formation of a 3-dimensional, compact anion with a net structure (Fig. 3). The last member of the condensation series, the MoO_3, is also built up of MoO_6 units [17—20].

With regard to the structure and the coordination number the dimolybdates are intermediate between these two extreme cases. Their unit cells are built up by MoO_6 octahedra and MoO_4 tetrahedra sharing corners; owing to chain formation, the dimolybdates do not form as compact a structure as the polymolybdates containing MoO_6 units only (Fig. 4).

In general even the structures of those polymolybdates studied by X-ray diffraction are not elucidated in full detail. The positions of the NH_4^+ ions in the di- [12], hepta- [12—15] and octamolybdates [16] are not known and, with the exception of the heptamolybdate, even the positions of the oxygen atoms were not determined experimentally but only derived from the positions of the molybdenum atoms by means of geometrical considerations. In these molybdates the molybdenum and oxygen atoms occupy a rather general position with no special characteristics [12—16], which therefore renders impossible even an approximate treatment on the basis of site symmetries relating to crystal systems.

It is an empirical fact that the spectra of polymolybdates built up of MoO_6 units are much more complex than those of molybdates containing tetrahedra. In the region of the Mo—O stretching frequencies, several intense, overlapping absorption bands appear with a number of inflexions, which can be more or less reliably evaluated. However, the number of theoretically possible infrared-active internal vibrations is so large compared with the number of the absorption bands, that extensive experimental work and theoretical considerations are necessary for their reliable assignment. It is not the aim of this paper to give a complete analysis of the spectra but only to interpret the approximate and general relationships.

1. It is assumed that the interaction between vibrations of the coordinated groups $(NH_4)_2O$ and MoO_3 is negligible [23—25].

2. The considerations will be applied which relate to the coordination number of a cation contained in an MoO_n group and the frequency range of the absorption bands [25] as well as to the stretching frequencies of metal–oxygen bonds containing the oxygen atoms in isolated or condensed positions [23—30].

The validity of the first assumption is strongly supported by crystallographic considerations and by the spectra. The general composition of the polymolybdates is usually given by the formula $x(R_2O) \cdot yMoO_3$. If $R = NH_4^+$ the coordinated groups would be $(NH_4)_2O$ and MoO_3. However, contrary to

Table II

The wave-numbers of the absorption

1		2		3		4		5	
a	*b*	*a*	*b*	*a*	*b*	*a*	*b*	*a*	*b*
		412		457		434		445	
483		475		485		471		469	
						520		510	
		550		560		548		535	
		580				575		577	
		650		642		625			
				662					
685				690				683	
				738	736	728		712	
						754	753	742	740
778	776			798	790			790	788
850	850	841	838					817	815
		868	865	855	850	861	859	863	860
		880	877	873	875	887	884	883	880
		895	892	895	890	895	890	895	892
						913	912		
913	912	918	918	922	923	940	937	938	935
933	932	923		933	936	948			
		935	930	940		958	955	959	957
1403		1405		1406		1412		1405	
1540				1460					
		1628						1630	
		1645						1645	
		1740				1740		1745	
2040				2030					
2780		2810	2780	2800	2780	2820	2800	2820	2800
3020	2950	3022	2960	3015	2980	2960	2950	3035	3020
3180	3160	3155	3155	3165	3160	3200	3200	3185	3180
3230		3215		3217				3260	
		3410	3420					3480	3470

1 : dimolybdate, 2 : heptamolybdate, 3 : 2,5-molybdate, 4 : octamolybdate, 5 : 4-molybdate · pellet, *b* : in Nujol or hexachlorobutadiene.

alkali, alkaline-earth and other positive metals, the oxide of the NH_4^+ ion does not exist in free state, therefore, the $(NH_4)_2^{2+} \cdot O^{2-}$ group can be regarded as a real coordinated group only with certain restrictions. The oxygen

bands of ammonium polymolybdate

6		7		8		9		Assignment
a	*b*	*a*	*b*	*a*	*b*	*a*	*b*	
						485		δ Mo—O—Mo
528		526		533				
600		650		610		600		ν Mo—O(V)
				710				ν Mo—O(IV)
								ν Mo—O(III)
						820	820	
880	880	876	875	876	875			ν Mo—O—Mo
						880	880	
918	918	918	918	918	918			
								ν Mo—O(I)
973	974	973	974	975	976	995	995	
1405		1405		1405				$\nu_4(F_2)$
1445		1445						
1625								δ H_2O
								$\nu_2 + \nu_6$
								$\nu_4 + \nu_6$
								$2\nu_4$
								$\nu_2 + \nu_4$
3220	3200	3225	3220	3225	3220			$\nu_3(F_2)$
								$\nu_1 + \nu_5$
3490	3490							ν H_2O

· $1,3H_2O$, 6 : 14-molybdate · $3H_2O$, 7 : 14-molybdate, 8 : 22-molybdate, 9 : MoO_3. *a* : in KBr

ion of this group belongs to the $(Mo_xO_y)^{z-}$ complex ion, to which the NH_4^+ ion is attached by typical electrostatic bonding. Consequently, in the spectra there will be Mo—O stretching frequencies characteristic of the lattice struc-

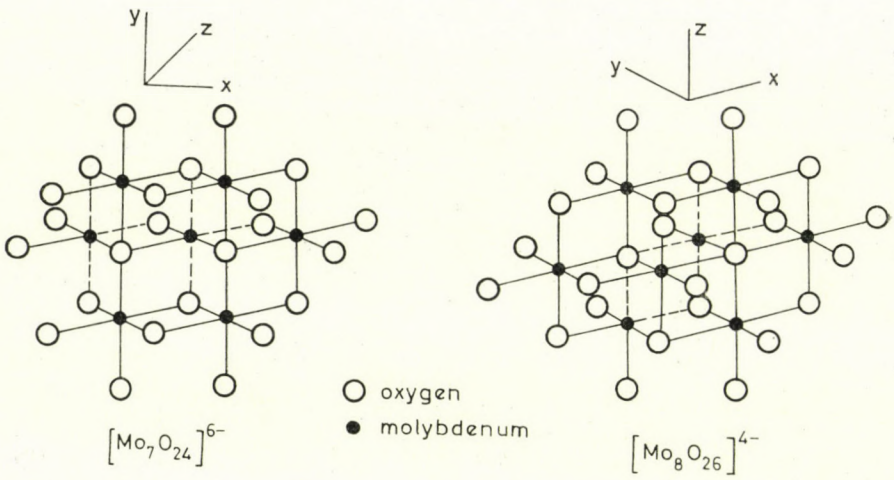

Fig. 3. Structure of the hepta- and octamolybdate ions

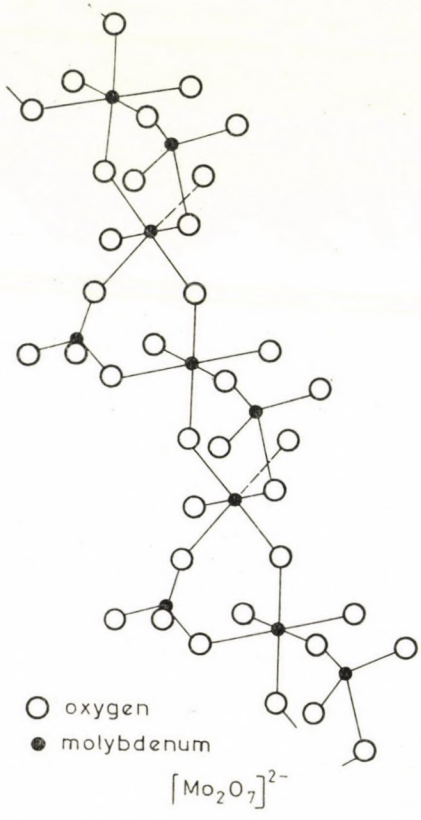

Fig. 4. Structure of the dimolybdate ion

ture of complex ions which are independent of the coordinated '$(NH_4)_2O$' group. To these frequencies the bands of the NH_4^+ ion are added, whose frequencies are, according to the spectra, approximately independent of the $(NH_4)_2O : MoO_3$ ratio.

In molybdates consisting of octahedral groups, the structure of the ions is determined by the metal–oxygen bonds involving variously coordinated oxygen atoms. The study of several compounds led to the conclusion that the stretching frequencies of the terminal M=O and M—O bonds are always higher than those of the M—O—M bonds containing a common oxygen atom in different layers of the lattice [27—30]. Therefore, of the three MoO_3 bands observed in the 800—1000 cm^{-1} region, the one at 985 cm^{-1} was assigned to the terminal Mo—O bond, whereas the bands at 870 and 813 cm^{-1} were assigned to the Mo—O—Mo and Mo—O=Mo_2 stretching vibrations, respectively, which contain 2- and 3-coordinate oxygen atoms in the layer [27, 28]. The Raman and infrared study of a MoO_3 single crystal gave strong support to the above assignment of the Mo—O and Mo—O—Mo frequencies, however, a lower frequency was assigned to the vibrations of the Mo—O=Mo_2 groups (545 cm^{-1}) [30].

Approximate interpretation of the spectra of polymolybdates

a) Mo—O vibrations

There are 7 octahedra in the heptamolybdate and eight in the octamolybdate ion, connected to each other in an arrangement shown in Fig. 3 [14—16]. According to LINDQVIST [12], the MoO_6 and MoO_4 units form a chain structure; the idealized structure corresponding to this assumption is shown in Fig. 4. For other molybdates only the dimensions and the symmetry of the unit cells are known and no reliable structural formula exists [11]. Thus it has not yet been proved that these molybdates are actually composed of MoO_6 octahedra. This however seems likely from Fig. 5 constructed from data for molybdates of known structure. The average coordination number is shown as a function of the $(NH_4)_2O : MoO_3$ mole ratio (characteristic of the given polymolybdate) and O : Mo ratio in the ions.

The coordination number of the molybdenum in the monomeric molybdate is 4 [3, 4, 7, 12, 31], whereas its value is 6 in the hepta- and octamolybdates and in MoO_3 [13—20]. At the same time, due to the equal number of MoO_6 and MoO_4 units in the infinite $Mo_2O_7^{2-}$ chain, this value will be $\bar{n} = 5$ (Fig. 4). The conclusion can be drawn that all the polymolybdates for which $\alpha \leq 0.43$ or O : Mo ≤ 3.43, are characterized by coordination number $\bar{n} = 6$, *i.e.* the ions in molybdates whose structure has not yet been elucidated are composed exclusively of MoO_6 units as well. For the compositions of various

degree of condensation ranging from monomeric molybdate to heptamolybdate, the expected coordination number is $6 > \bar{n} > 4$. Of the condensates of this type only the dimolybdate is known thus far.

It is seen from Fig. 1 and Table II that with increasing degree of condensation the spectra first become more complex but then assume a simpler structure and become similar to that of MoO_3. Generally it could be concluded that the spectra of polymolybdates — apart from the splitting of the bands — exhibit certain similarity to the spectrum of MoO_3. There is a wide intense band in the 880—900 cm^{-1} region and a sharp maximum with an increasing frequency in the range of 900—1000 cm^{-1} which initially shows multiple

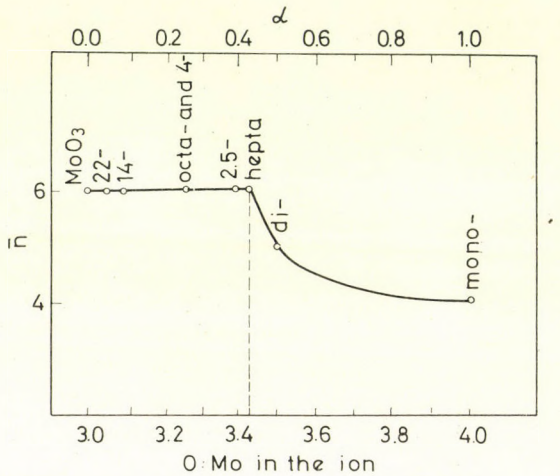

Fig. 5. Variation of the coordination number of the central Mo atoms

splitting. A separate maximum and an inflection can be observed in the 800—850 cm^{-1} region. In the interval of 550—680 cm^{-1}, a very wide and intense band appears whose complexity increases with increasing degree of condensation and with increasing size of the polyanion. From the 14-molybdate, the band becomes simple and similar to that of MoO_3.

In order to explain the properties of the spectra common with those of MoO_3, it should be borne in mind that the polyanions of the heptamolybdate → MoO_3 condensation series are composed of an increasing number of MoO_6 octahedra, whereas in MoO_3, the MoO_6 units form an infinite three-dimensional polymer. Consequently, in the general formula $n \cdot (MoO_6)$, $n \to \infty$ with increasing degree of condensation. If the value of n is small, *i.e.* the size of the polyanion is not too large, the individual spectral properties (*e.g.* splittings) characteristic of the symmetry of complex anions will appear beside those of the MoO_6 octahedra. If, however, the value of n is large or $n \to \infty$,

breaks in the three-dimensional polymer chain will occur rarely and the spectrum as well as the structure of such condensates will be very similar to those of the MoO_3. This similarity with the structure of MoO_3 can already be observed for the 14-molybdate.

It is first of all the spectrum of the octamolybdate which exhibits discrete, separate bands in accordance with the fact that this ion is composed of symmetric MoO_6 octahedra yielding a relatively regular stucture [16]. Consequently the extent of broadening and overlapping of bands due to lattice distortions is less compared with other molybdates. Upon inspection of Fig. 3 the following four different types of bonding can be postulated with respect to the coordination number of oxygen: Mo—O(I), Mo—O(II), Mo—O(III), Mo—O(V). (I, II, etc. denote the coordination number of oxygen.)

Similarly, depending on the coordination number of oxygen there are four different types of bonding in the $(Mo_7O_{24})^{6-}$ ion, which are as follows: Mo—O(I), Mo—O(II), Mo—O(III) and Mo—O(IV). Since the heptamolybdate is built up of more strongly distorted octahedra [14, 15], certain bands — especially in the 850—950 cm^{-1} region — collapse.

The assignments of the stretching vibrations of MoO_3 [27, 28, 30, 32] suggest the assignments shown in Table II for the 400—1000 cm^{-1} region of the polymolybdate spectra. Considering the character of bonds it can be established that the vibrations of the types νMo—O, ν_s O—Mo—O and ν_{as} O—Mo—O may be all active in the infrared region.

The normal frequencies of polymolybdates composed of MoO_6 octahedra can be derived from those of the XY_6 molecules taking into account the point symmetry of the ion and the degradation of symmetry determined by the space group.

The splitting of the O_h species in the point groups C_{2v} and C_{2h} and in the factor groups C_{2h} and C_i are shown in Table III.

The frequency ranges studied and the spectra recorded with microcrystalline powder samples do not allow for a more precise assignment of the frequencies. However, the data in Table III show that in the general case both the symmetric and asymmetric O—Mo—O stretching vibrations may be infrared active.

For example in the case of $(Mo_7O_{24})^{6-}$ the A_1, B_1, B_2 species, which refer to the C_{2v} point group derived from the ν(XY) mode of F_{1u}, and the B_u species referring to the C_{2h} group are infrared active. The character of these modes is: ν_{as} O—Mo—O. However, the character of the A_1 and the A_1, B_1 species derived, respectively, from A_{1g} and E_g is: ν_s O—Mo—O. These statements can be verified for the octamolybdate too with the aid of Table III.

Below 550 cm^{-1}, bands due to deformation modes also appear, which can be derived from the F_{1u}, F_{2g} or F_{2u} normal vibrations of the O_h point group, if the ion symmetry and the corresponding factor group are known.

Table III

Splitting of the O_h point group into the species of the $C_{2v} \rightarrow C_{2h}$ and $C_{2h} \rightarrow C_i$ point groups

$[Mo_7O_{24}]^{6-}$		„MoO_6"	$[Mo_8O_{26}]^{4-}$	
Factor group C_{2h}	Ion symmetry C_{2v}	O_h XY_6	Ion symmetry C_{2h}	Factor group C_i
A_g	A_1	A_{1g}	A_g	A_g
		A_{1u}		
		A_{2g}		
A_u	A_2	A_{2u}	A_u	
		E_g		
		E_u		
B_g	B_1	F_{1g}	B_g	A_u
		F_{1u}		
B_u	B_2	F_{2g}	B_u	
		F_{2u}		

$C_2 = C_2(z)$
$\delta_h = \delta_v(xz)$
$\delta_d = \delta_v(yz)$

$C_4^2 = C_2(z)$
$\delta_h = \delta_h(xy)$

b) The NH_4^+ and H_2O absorption bands

The NH_4^+ ion of T_d symmetry has two infrared active normal vibrations namely the $\nu_3(F_2)$ and the $\nu_4(F_2)$. According to Fig. 2 and Table II, other bands of lower intensity, assigned to the vibration of the ammonium ion appear as well [33]. With the exception of the octamolybdate, the $\nu_4(F_2)$ frequency of the polymolybdates remains practically unchanged, only the $\nu_3(F_2)$ mode exhibits a slight shift with increasing degree of polycondensation. Of the combination bands identified by WAGNER [34], PLUMB and HORNIG [35, 36] and VEDDER [37], several can be observed especially for molybdates with higher content of ammonia. These bands are, however, weak compared with those arising from NH_4Cl, therefore, the wave numbers cannot be determined reliably. It can be concluded from the presence of the $\nu_4(F_2) + \nu_6$ (torsional lattice vibration) combination bands in the spectra of hepta-, octa- and 14-molybdate, that in these crystals the free rotation of the NH_4^+ ion is hindered [34, 37]. It should be mentioned that the very weak bands in the

region between 1650—1660 cm^{-1} and the more intense ones in the vicinity of 3020 cm^{-1} do not arise necessarily from combined modes. Since these frequencies may correspond to the ν_1 and ν_2 Raman-active vibrations in T_d, it can be assumed as well that these modes become infrared active due to lattice distortions or the symmetry of the crystal lattice.

The shape and frequency of the νH_2O and δH_2O bands are identical with those characteristic of the water of crystallization. According to our observations, the anhydro-molybdates are non-hygroscopic. No spectral changes indicating water absorption were found.

General relationships

The frequencies of polymolybdates are characteristic and reflect sensitively the structural changes of polycondensates. Consequently, the infrared spectra can be of great use in the identification of molybdates.

It can be seen from Fig. 1 and Table II that of the characteristic frequencies of polymolybdates those assigned to the terminal Mo—O(I) bonds exhibit a continuous shift in a definite direction. The magnitude of this shift is the largest for the MoO_3.

If the frequency shift is plotted against the value of $(NH_4)_2O : MoO_3 = \alpha$, or log α, these changes can be correlated with the degree of polycondensation (Fig. 6).

It is apparent from this figure that there is no break in the $\nu_{Mo-O(I)} = f(\log \alpha)$ relationship as far as the average coordination number of molybdenum is 6 in the ions, *i.e.* the crystal lattice is formed of MoO_6 octahedra only. However, a sharp change in the frequency is observed if the value of $\bar{n}$ changes. This phenomenon is observed in the case of dimolybdate, for which $\bar{n} = 5$, since there are MoO_4 tetrahedra beside MoO_6 in the lattice. Consequently, the appearance of the break indicates a significantly different structure.

To interpret the relationship expressed in Fig. 6 (restricting the considerations to the molybdates characterized by $\bar{n} = 6$) it should be remembered that the locations of the lower frequency bands (*e.g.* the most intense peak at 900 cm^{-1}) assigned to the stretching modes of the Mo—O—Mo or O—Mo—O bridges, are identical or vary within narrow limits. A definite shift of frequency can be observed for the stretching vibrations of the Mo—O(I) bonds only. Thus it is obviously the differences in the outer coordination sphere of the ions as opposed to internal structural changes, that are responsible for the frequency shifts. The dependence of this shift upon the degree of condensation already indicates a connection of this kind (Fig. 6), since the variation of α involves the change of the electric charge referred to one MoO_3 ($(NH_4)_2^{2+}O^{2-} : MoO_3$). Thus the frequency shift seems to be correlated with the electrostatic interactions within the molecule.

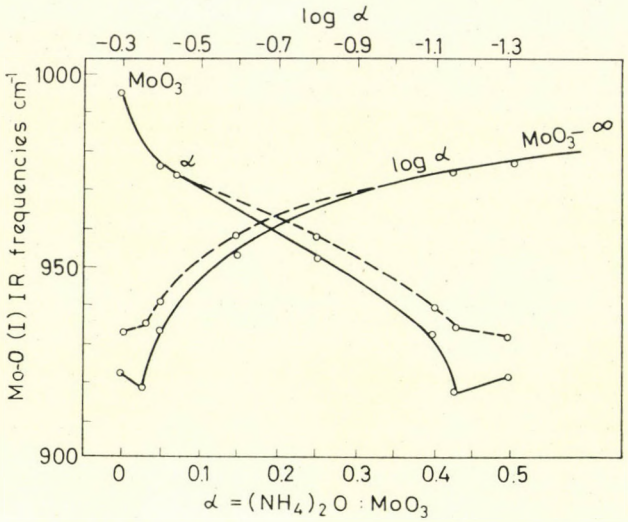

Fig. 6. Frequency shift of the Mo—O(I) stretching vibrations. – – – – – – : on the basis of the highest frequency bands; ———— : from the wave number of the envelope constructed graphically for all of the Mo—O(I) bands

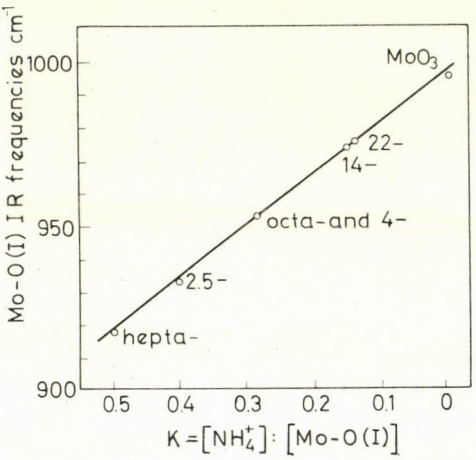

Fig. 7. Frequency shift of the Mo—O(I) stretching vibrations

Since the ions are composed electrostatically the Mo—O(I) bonds should be regarded Mo—O^- . . .NH_4^+ groups. According to the spectra, the change of the charge expressed by α shifts only the frequencies of the Mo—O(I) stretching vibrations but the vibrations of Mo—O—Mo on O—Mo—O bridges are not affected. From this fact the conclusion can be drawn that the electrostatic interaction between the NH_4^+ ion and the polyanions shown in Fig. 3 (and also others) involves mainly positions at least as concerns spectroscopic observ-

ability. This assumption seems to be supported by Fig. 7 where the frequencies of the Mo—O(I) bonds are shown as a function of the amount of positive charge referred to one Mo—O(I) bond in the molecule.

The $[NH_4^+]$: [Mo—O(I)] ratio is easily obtained for the hepta- and octamolybdates of known structure from the composition of the molecules using Fig. 3. $K_{hepta} = [6\ NH_4^+] : [12\ Mo—O(I)] = 0.5\ K_{octa} = [4\ NH_4^+] : [14\ Mo—O(I)] = 0.286$; for the MoO_3 naturally $K = 0$. According to Fig. 7, these values give a linear relationship.

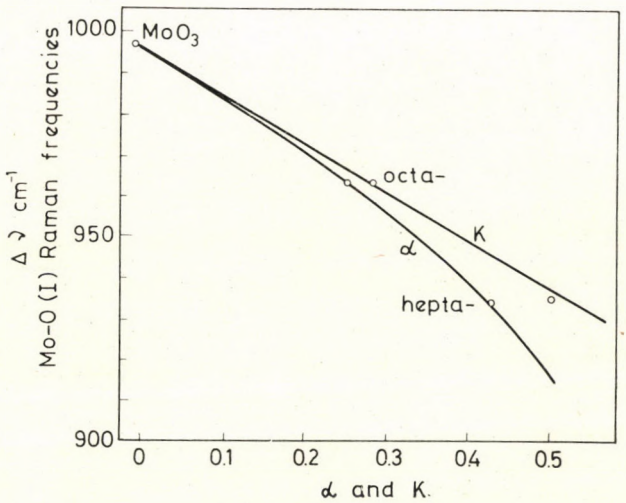

Fig. 8. Variation of the Raman frequencies of the Mo—O(I) bond

The gradual shift of the bands of highest intensity and frequency can be observed in the Raman spectra of hepta- and octamolybdate [10] and of MoO_3 [30, 38]. For the MoO_3 this band (996 cm^{-1}) was assigned to the Mo—O(I) stretching vibration. No attempt was made to interpret the Raman spectra of the hepta- and octamolybdate [10] but it follows almost certainly from Table III, that the frequencies 934 cm^{-1} and 963 cm^{-1} can be assigned to the A_1, A_g or A_g, A_g species of total symmetry, derived from A_{1g}. According to Fig. 8, the dependence of the mentioned Raman frequencies on the α values is similar to that shown in Fig. 6, whereas they give a linear relationship as a function of K.

In the case of molybdates of unknown structure only the wave numbers of the Mo—O(I) bonds are known. However, assuming that the anions of these molybdates involve the most compact association of MoO_6 units, the K values and the number of Mo—O(I) bonds can be estimated with a certain probability using the linear relationship in Fig. 7. The α, K and the derived characteristic values are shown in Table IV.

Table IV

Spectral and structural data related to the α and K values for ammonium polymolybdates

Molybdate	α	Wave-number of the envelope of Mo—O(I) bonds	$[NH_4^+]$: [Mo—O(I)] K	Number of Mo—O(I) bonds : ion
hepta-	0.43	918	0.5	12
2.5-	0.40	933	0.395	*nx* 5.05
octa-	0.25	952	0.286	14
4-	0.25	952	0.286	*nx* 7
14-	0.0715	973	0.15	*nx* 13.4
22-	0.0455	975	0.14	*nx* 14.3
MoO_3	0.0	995	0.0	—

For molybdates of unknown structure the true structural formula may be the integer multiple of the formula shown in Table I; this should be taken into account when considering the number of Mo—O(I) bonds. If, *e.g.* the structural formulas $(NH_4)_8$ $[Mo_{10}O_{34}]$, $(NH_4)_2$ $[Mo_{14}O_{43}]$ or $(NH_4)_2$ $[Mo_{22}O_{67}]$ are assumed for the 2,5-, 14- and the 22-molybdates [11], respectively, it can be shown that several realistic variants can be conceived by linking together 10, 14 or 22 MoO_6 units, that satisfy the calculated and rounded values [20 and 14] obtained for the number of Mo—O(I) bonds.

The K values can also be interpreted as the ratio of the number of negative charges carried by the polyanion and the number of Mo—O(I) bonds in it. Since $K < 1$ in each case, it follows that no oxygen atom can be assumed in a preferred terminal position which would bear one or more units of negative charge, but the total charge of the ions or at least that part falling on the Mo—O(I) bonds is uniformly distributed over all the oxygen atoms in terminal positions.

The above interpretation of the frequency shift serves as a spectroscopic proof to support the general statements relating to the ionic crystals, according to which the effect of the electrostatic attraction is uniform in all directions, *i.e.* there are no preferred bond directions. Consequently, in this aspect the NH_4^+ ions cannot be assigned to preferred Mo—O(I) bonds. A correct picture is obtained only if the ammonium ions are placed into the crystal lattice in accordance with the uniform distribution of charges. As mentioned above, the position of the NH_4^+ ions was not determined either in the hepta- or in the octamolybdate. However, the following scheme would closely correspond to the above picture: assume that around the octamolybdate ion in Fig. 3 the four NH_4^+ ions are placed symmetrically with respect to the symmetry centre of the C_{2h} point group, or to the C_i triclinic unit cell.

The frequency of the $\nu_3(F_2)$ mode of ammonium ions also depends on the degree of polycondensation, although to a lesser extent (Fig. 9). The dependence on α and K of this frequency is similar to those shown previously. This fact supports the above assumptions as well.

As a next step, if we succeed in preparing suitable molybdate single-crystals, the detailed analysis of these highly complicated systems and the theoretical confirmation of the frequencies will be attempted with the aid of Raman and polarized spectra.

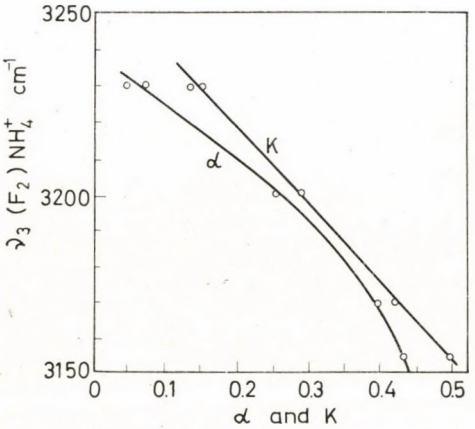

Fig. 9. Frequency change of the $\nu_3(F_2)$ mode of the NH_4^+ ion

REFERENCES

1. MILLER, F. A., CARLSON, F. L., BENTLEY, F. F., JONES, W. H.: Spectrochimica Acta **16,** 135 (1960)
2. MILLER, F. A., WILKINS, C. H.: Anal. Chem. **24,** 1253 (1952)
3. BUSEY, R. J., KELLER, O. L. Jr.: J. Chem. Phys. **41,** 215 (1964)
4. CLARK, G. M., DOYLE, W. P.: Spectrochimica Acta **22,** 1441 (1966)
5. DUPUIS, Th., VILTANGE, M.: Microchimica Acta **2,** 232 (1963)
6. DUPUIS, Th., VILTANGE, M.: Compt. rend. **255,** 2582 (1962)
7. KHANNA, R. K., LIPPINCOTT, E. R.: Spectrochim. Acta **24A,** 905 (1968)
8. CAILLET, P., SAUMAGUE, P.: J. Anal. Struct. **4,** 191 (1969)
9. BROWN, R. G., DENNING, J., HALLETT, A., ROSS, S. D.: Spectrochim. Acta **26A,** 963 (1970)
10. AVESTON, J., ANACKER, E. W., JOHNSON, J. S.: Inorg. Chem. **3,** 735 (1964)
11. KISS, B. A., GADÓ, P., ASZTALOS, I., HEGEDÜS, J. A.: Acta Chim. Acad. Sci. Hung. **66,** 235 (1970)
12. LINDQVIST, I.: Nova Acta Regiae Soc. Sci. Upsaliensis Ser. IV. **15,** No. 1. 1 (1950)
13. STURDIVANT, J. H.: J. Am. Chem. Soc. **59,** 630 (1937)
14. LINDQVIST, I.: Arkiv. Kemi. **2,** 325 (1950)
15. SIMAO, E.: Bull. Chem. Soc. Jap. **40,** 1609 (1967)
16. LINDQVIST, I.: Arkiv. Kemi **2,** 349 (1950)
17. BRAEKKEN, H.: Z. Krist. **78,** 484 (1931)
18. WOOSTER, N.: Z. Krist. **80,** 504 (1931)
19. ANDERSON, G., MAGNÉLI, A.: Acta Chem. Scand. **7,** 739 (1950)
20. KIHLBORG, L.: Arkiv. Kemi **21,** 357 (1963)
21. MA, E.: Bull. Chem. Soc. Jap. **37,** 171 (1964)
22. GMELINS, Handbuch No. 53. Molibden **253,** (1935)
23. TARTE, P.: Spectrochim. Acta **18,** 467 (1962)

24. TARTE, P.: Mém. Acad. Roy. Belg. **35,** 4(a), 4(b), (1965)
25. TARTE, P.: Spectrochim. Acta **23A,** 2127 (1967)
26. MATOSSI, F.: J. Chem. Phys. **17,** 679 (1949)
27. BARRACLOUGH, C. G., LEWIS, J., NYHOLM, R. S.: J. Chem. Soc. 3552 (1959)
28. BARRACLOUGH, C. G., STALS, J.: Aust. J. Chem. **19,** 741 (1966)
29. FODOR, M., POKÓ, Z., MINK, J.: Microchimica Acta **4—5,** 865 (1966). MTA Közp. Fiz. Kut. Int. Közl. **15,** 133 (1967)
30. BEATTIE, I. R., GILSON, T. R.: J. Chem. Soc. (A) 2332 (1969)
31. LINDQVIST, I.: Acta Chem. Scand. **4,** 1066 (1950)
32. MATTES, R., SCHRÖDER, F.: Z. Naturforsch. **24,** 1095 (1969)
33. NAKAMOTO, K.: Infrared Spectra of Inorganic and Coordination Compounds, p. 104—105. John Wiley, 1963, New York, London.
34. WAGNER, E. L., HORNIG, D. F.: J. Chem. Phys. **18,** 296, 305 (1950)
35. PLUMB, R. C., HORNIG, D. F.: J. Chem. Phys. **21,** 366 (1953)
36. PLUMB, R. C., HORNIG, D. F.: J. Chem. Phys. **23,** 947 (1955)
37. VEDDER, W., HORNIG, D. F.: J. Chem. Phys. **35,** 1560 (1961)
38. KRASSER, W.: Naturwissenschaften, **56,** 213 (1969)

András B. KISS: Budapest IV., Váci út 77.
Sándor HOLLY: Budapest II., Pusztaszeri út 57—69.
Erzsébet HILD: Budapest IV., Váci út 77.

Acta Chimica Academiae Scientiarum Hungaricae, Tomus 72 (2), pp. 165—178 (1972)

OXIDATION OF SECONDARY ALCOHOLS ON A PLATINUM ELECTRODE, I

THE OXIDATION PRODUCTS

G. HORÁNYI, P. KŐNIG and I. TELCS

(Central Research Institute for Chemistry, Hungarian Academy of Sciences, Budapest)

Received October 8, 1970

The electrooxidation of secondary alcohols (i-propanol, *sec*-butanol and cyclohexanol) was studied in acidic medium. The information obtained from studies with stationary and potentiodynamic methods was classified in groups.

It was found that the chemical events in the oxidation of alcohols can be separated into two groups.

1. The interaction of the metal and the alcohol is irreversible adsorption occurring with charge transfer; this is not a step of stationary oxidation.
2. There is a well-defined reaction path leading from the dissolved starting substance to the dissolved product.

It was found that the products of oxidation are the corresponding ketones

It is clear from a number of monographs [1—4] that in recent years studies of the electrooxidation of alcohols have occupied an increasingly important place in the electrochemical literature. The bulk of the work concerns the oxidation of primary alcohols, and relatively few papers are found which deal with the oxidation of secondary alcohols [5, 6].

This may be due to inherent differences in the practical importance of the two types of compounds, but from the point of view of the better understanding of questions concerning the mechanism of oxidation of alcohols it is our opinion that the study of the oxidation of secondary alcohols should not be neglected.

Several different possibilities arise with primary and secondary alcohols for the study of individual steps in the multi-stage oxidation processes. In the case of secondary alcohols, the ketone formed in the first steps of the oxidation reaction is relatively stable and the rate of its oxidation is small. If this assumption is true, then hydroxy–oxo transition in the oxidation of secondary alcohols can be studied without interfering factors.

In this paper it is primarily intended to give an answer to the question of whether or not the reaction given by the overall equation

$$\mathrm{R{-}\underset{\displaystyle OH}{\underset{|}{CH}}{-}R' \longrightarrow R{-}\overset{\displaystyle O}{\overset{\|}{C}}{-}R' + 2\,H^+ + 2\,e}$$

can be studied without interfering side-reactions (R and R′ are alkyl or aryl groups). It is obvious that only after this question has been decided can it be attempted to form some idea of the mechanism of oxidation by analysis of the polarization curves.

Method of investigation

The apparatus was essentially the same as in earlier studies of electrohydrogenation [7]. Two types of electrolytic cells were used; the outline of one of these is given in Fig. 1.

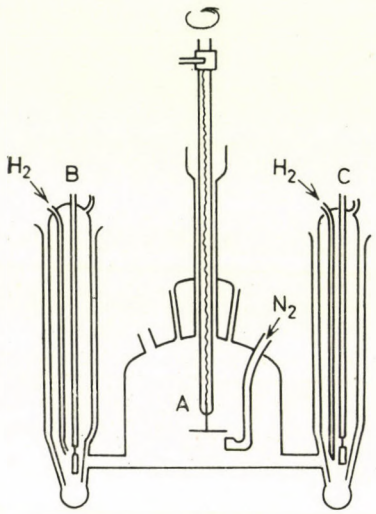

Fig. 1. Electrolytic cell. *A* main electrode, *B* reference electrode, *C* auxiliary electrode

The geometrical area of the main electrode, a disk-shaped platinum electrode, was 10 cm^2. By platinization a roughness factor of 500—1000 was attained. The magnitude of the roughness factor was determined from charging curves. 1 *N* $HClO_4$ was used as background solution, and the electrode potential was measured against a 1 atm. hydrogen electrode immersed in this solution. In order to eliminate the rate-determining role of transport processes, either the solution was stirred or the electrode was rotated.

This cell was used in the main to study the potential dependence of the rate by the determination of the polarization curves. With the further aim of product analysis, a cell was constructed in which a considerable yield could be achieved without giving up the simultaneous study of the potential dependence of the rate.

An outline of the cell used for preparative purposes is shown in Fig. 2. The main electrode, which had a geometrical surface of 160 cm^2, was platinized platinum in the form of a hollow cylinder. The auxiliary electrode, which

was placed at the centre of the cylinder formed by the main electrode and which was separated from it by a glass filter, had a geometrical surface about 2 orders of magnitude smaller than that of the main electrode. By means of the glass filter the oxidation products can easily approach the auxiliary electrode and there be reduced. If the geometrical surface of the auxiliary electrode (cathode) is small, then the reduction of a product formed during the oxidation can be neglected.

Today potentiodynamic methods are generally used to study the oxidation of alcohols and so the different stationary methods are being forced increasingly into the background [8, 9].

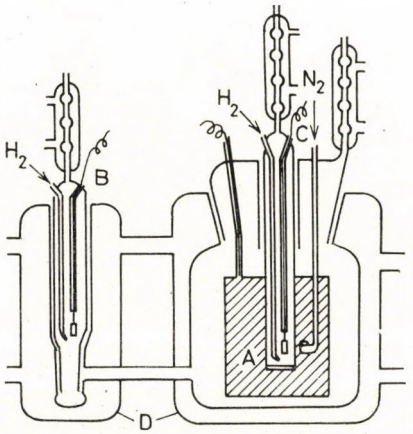

Fig. 2. Cell for preparative purposes. *A* main electrode, *B* reference electrode, *C* auxiliary electrode

In parallel with this the nature of the electrodes used has changed, the potentiodynamic methods usually employing bright, and the stationary methods platinized platinum electrodes. We wished to use both methods to study the oxidation of secondary alcohols, but even at the outset of the investigation we were forced to conclude that the two methods give information on two different at times only loosely related areas of the phenomena.

An attempt is made below to classify the information obtained by the two methods according to whether phenomena are considered to be directly related to the oxidation reaction studied, or whether they result from interfering factors. For this the types of information yielded by the individual methods must first be examined.

A. Stationary methods

As regards the pairs potential–current values in measurements with stationary methods, the polarization curves produced from these are by no means the only type of information. In the application of the stationary

method it must first be made clear whether the stationary measurements are practicable, that is, whether the stationary or quasi-stationary state is attainable.

Many workers use only the potentiodynamic method in the oxidation of alcohols because they do not consider that the stationary or quasi-stationary state can be achieved.

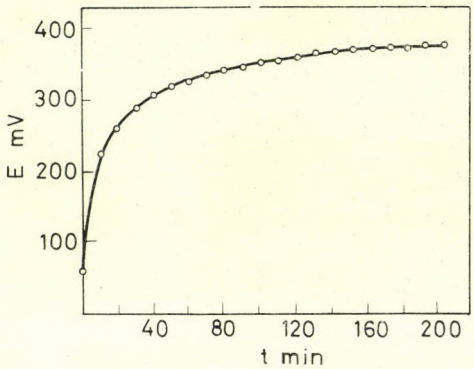

Fig. 3. Change of potential with time in a galvanostatic measurement (5×10^{-2} *M* i-propanol)

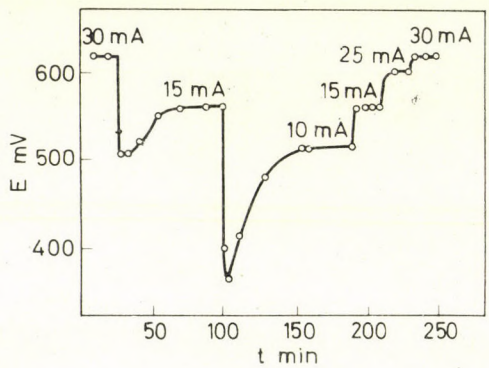

Fig. 4. Phenomena during change-over (i-propanol)

This misgiving is to a certain extent justified for the attainment of, or the approach to, the stationary state is often an extremely lengthy process.

Accordingly, how the setting in of the stationary state depends on time and on other parameters of the system studied may also be important information.

In Fig. 3 is shown the potentical change at given current value in a galvanostatic measurement as a function of time. As can be seen from the figure, the establishment of the stationary state requires an extremely long time. Further valuable information is obtained when a change is made from one stationary state to another.

The phenomena observed during the change-over in the case of a galvanostatic method are shown in Fig. 4.

It can be seen in Fig. 4 that significant changes occur in the case of certain change-over modes (from high currents to low currents), but in spite of this the measurements are reproducible.

Fluctuation or periodic phenomena form a further group. Periodic potential oscillations can be observed at certain currents in the galvanostatic measurement method; this is shown in Fig. 5 for the case of the oxidation of cyclohexanol.

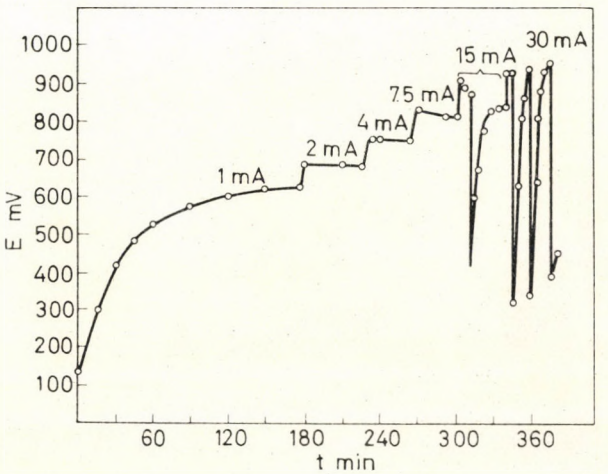

Fig. 5. Galvanostatic measurement in the case of 4 ml cyclohexanol (~0.5 *M*)

It can be seen from the figure that the stationary state is established at low currents, but on the increase of the current a periodic potential oscillation can be observed. This phenomenon has already been observed by numerous authors in the oxidation of alcohols and organic substances [3], and thus in the case of the oxidation of secondary alcohols all those factors must be reckoned with which were considered in the explanation of potential fluctuations.

To summarize the above, the information obtained with the stationary methods can be classified into the following groups.

1. The stationary potential–current relation.
2. The transient processes during change-overs.
3. The periodic phenomena during the galvanostatic processes.

B. Potentiodynamic methods

Two types of potentiodynamic method are in use for the purpose of kinetic investigations; the difference between them is the mode of changing the potential.

a) In the cyclic potentiodynamic measurement mode (cyclic voltammetry), the controlled potential varies cyclically at a constant rate between two constant potential values; its time-course can be seen in Fig. 6a.

b) In the single potentiodynamic measurement mode (single sweep), the controlled potential proceeds at constant rate in a previously determined potential interval; its time-course is shown in Fig. 6b.

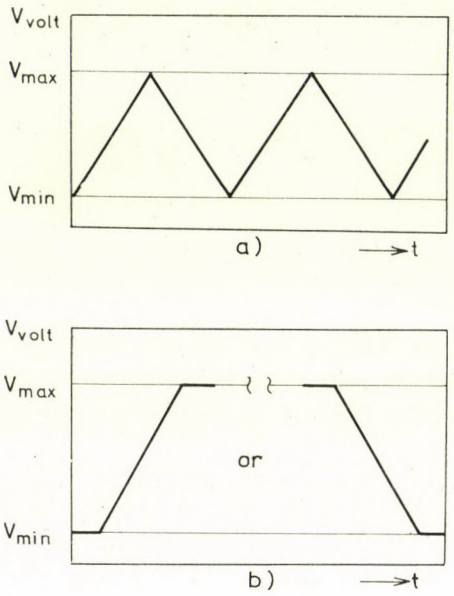

Fig. 6. Potential–time diagram

In our studies both modifications of the method were used. The experimental set-up was essentially the same as already mentioned, but a bright platinum disk of geometrical surface 1.68 cm^2 or a weakly platinized roughness factor ca. 100 platinum needles of geometrical surface $\sim$ 0.1 cm^2 were used as measuring electrodes.

The desired rate of change of the potential was ensured with a controlled-sweep potentiostat. The change of potential between 0 and +2 V was linear with time between wide rate limits.

The current passing between the measuring and auxiliary electrodes in the cell was recorded as a function of the potential by an XY plotter. In certain cases, beginning at a suitably selected point of time the charge passed through the cell was recorded simultaneously with the current; this was achieved by electronic integration of the current.

The preparation of the electrode depended on the desired mode of measurement. In the cyclic mode, a measurement was accepted after a single

anodic regeneration ($\sim$ 2 V, 1 minute) if it did not show a change during several cycles. There is no such control possibility in the case of polarization curves determined with a single potential change, and therefore a strictly standardized preparation procedure was adopted in this case; in general the diagram of this was the following.

After the regeneration in stage "*a*", the oxygen formed during regeneration was displaced from the solution by a stream of nitrogen in stage "*b*"; meanwhile the electrode, which was covered with an oxide layer, was at a

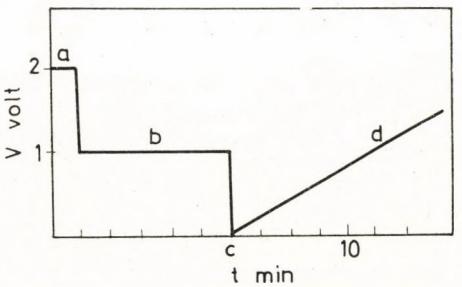

Fig. 7. Potential–time diagram

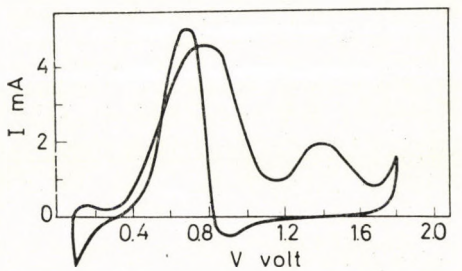

Fig. 8. Potentiodynamic curve. 1 *N* $HClO_4$ background solution, 0.1 *M* i-propanol

potential where there is no appreciable reaction (1.0—1.1 V). Stage "*c*" (generally $\sim$ 1 sec) was the total reduction of the surface oxide and stage "*d*" the measurements (Fig. 7).

These two methods are used alternately at random in the literature to obtain the potentiodynamic polarization curve, and are considered equivalent from the point of view of the result. With 1 *N* $HClO_4$ or 1 *N* H_2SO_4 containing primary alcohols, these curves have characteristic shapes with 2 definite maxima. In our experiments with secondary alcohols the shapes of the potentiodynamic polarization curves were found to be similar (Fig. 8). No difference can be found either in the shape of the polarization curve or in the positions of the maxima compared with the polarization curves reported in the literature to illustrate the electrooxidation of methanol or ethanol.

The shape of the potentiodynamic polarization curve depends on the experimental conditions, *viz.* on

a. the mode of changing the potential,
b. the rate of changing the potential,
c. the extreme values of the potential interval,
c. the sweep frequency of the potential interval.

The effect of these parameters is the same as in the case of secondary alcohols. Omitting the detailed discussion of our results we refer to [10, 11].

C. Comparison of stationary and potentiodynamic methods

If the differences in current density are disregarded, there is a large difference between the shapes of the potential–current curves obtained by the potentiodynamic and stationary methods.

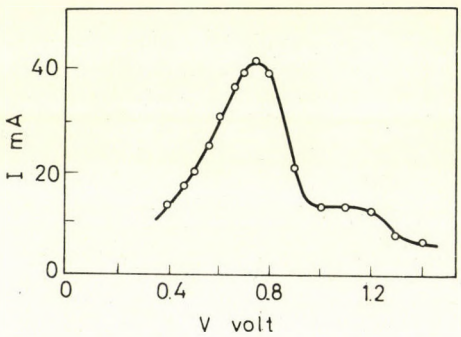

Fig. 9. Potentiostatic stationary polarization curve

Fig. 9 shows a quasi-stationary current–potential curve obtained with a potentiostatic method on a Pt black electrode. If this curve is compared with the curve produced with a potentiodynamic method, which can be seen in Fig. 8, it is found that there are two maxima on the potentiodynamic curve and only one on the stationary curve.

In the opinion of several authors the second maximum observed during the oxidation of alcohols can be attributed to an oxidation reaction on platinum oxide. The question rightly arises: if the oxidation reaction indeed occurs on the oxide, then why is it not observed in the stationary case too? The second maximum also appears if the electrode is immersed in i-propanol, washed, and the potential changed in the positive direction from some medium potential value in an alcohol-free background solution. As can be seen in Fig. 10 under such conditions only the stage corresponding to the second maximum can be observed, signifying that this current is used for the oxidation of the substance adsorbed earlier.

There are also similar difficulties in the explanation of the first stages of the curves obtained with the potentiodynamic method and the polarization curves taken under stationary conditions. In the case of i-propanol, similarly to the other alcohols, the adsorption is connected with a considerable change in charge, that is, the adsorption is essentially a surface redox reaction, the products of which remain predominantly or completely adsorbed (chemisorption, which may be accompanied by a certain amount of decomposition of

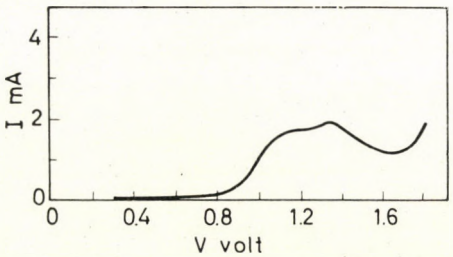

Fig. 10. Potentiodynamic oxidation curve of i-propanol adsorbed in open circuit

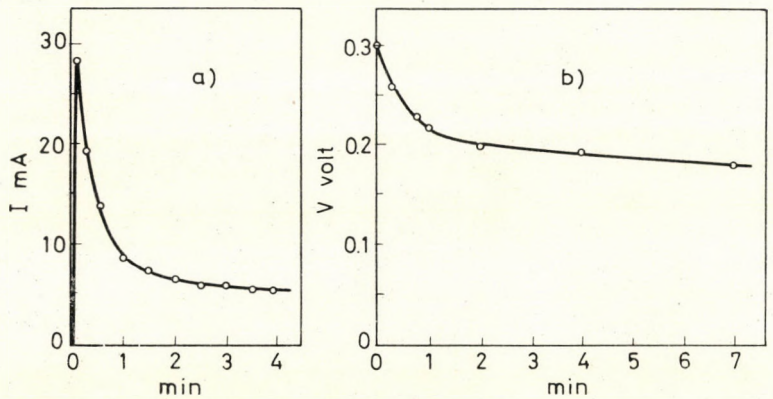

Fig. 11. a) Change of the current after addition of i-propanol at constant potential (300 mV). b) Change of the potential after the addition of i-propanol in open circuit

the initial molecule). The change in charge accompanying the adsorption is well shown by Fig. 11. In case a) the i-propanol was added to a 1*N* $HClO_4$ background solution, the potential being maintained constant with a potentiostat; in the case of the open circuit in case b) the electrode at a given potential came into contact with i-propanol.

All these observations prove that in the potentiodynamic method the changes in charge accompanying the adsorption process and the amount of charge corresponding to the oxidation process can barely be distinguished from each other. Further results, which will be reported in another paper,

were obtained from measurements using a tracer technique. At this time we wish to report only a few fundamental findings. Fig. 12 shows the potential dependence of the adsorption of i-propanol labelled with ^{14}C. It can be seen that the adsorption hardly changes with the potential over a fairly wide potential interval. In this potential interval the adsorbed labelled i-propanol cannot be exchanged with unlabelled i-propanol. At these potentials the adsorbed molecules are not removed from the surface during the oxidation reaction; this means that the adsorption and the reaction cannot be directly related to each other, that is, a significant part of the adsorbed molecules do not take part in the reaction.

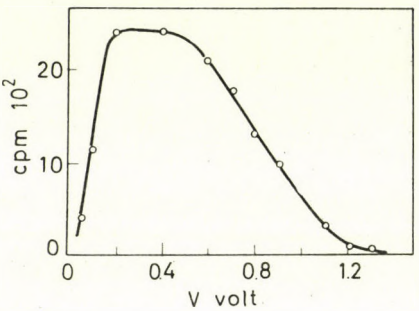

Fig. 12. Potential dependence of the adsorption

To summarize the above it can be stated that the chemical events in the oxidation of alcohols can ebsepar ated into two groups.

1) The interaction of the metal and the alcohol is irreversible adsorption occurring with charge transfer; this is not a step of stationary oxidation.

2) There is a well-defined reaction path leading from the dissolved starting substance to the dissolved product.

The processes mentioned in the first point show up in the transient sections of the stationary processes and in the potentiodynamic measurements.

Thus, these are the phenomena which disturb the processes in the second group. A knowledge of them is indispensable for a correct interpretation of electrode processes. At the same time it must be seen that the two types of processes in the potentiodynamic methods do not differ from each other.

In the stationary methods, however, the processes in the first group can be assigned as the single cause of the slow transient processes.

Thus, we have arrived at a very vital conclusion. The stationary methods appear much more suitable for the study of the oxidation processes than do the potentiodynamic methods which have recently become widespread.

This is the reason why we shall primarily use the stationary methods in our following investigations.

Detection and study of the oxidation product by electrochemical methods

The detection, and possible determination, of the reaction product can be made in the same system as the oxidation without disturbing the system.

From earlier investigations of the electrohydrogenation of oxo compounds, it is well known [8] that the ketone presumably formed during the oxidation of secondary alcohols can be reduced in acidic medium according to the reaction

$$\mathrm{R{-}\underset{\underset{\mathrm{O}}{\|}}{C}{-}R' + 4\,H^{+} + 4\,e \longrightarrow R{-}CH_2{-}R' + H_2O}$$

even at potentials where the evolution of hydrogen need not be considered. From this it follows that if a secondary alcohol is oxidized for a suitable time a section corresponding to the reduction of the ketone must appear on the polarization curve.

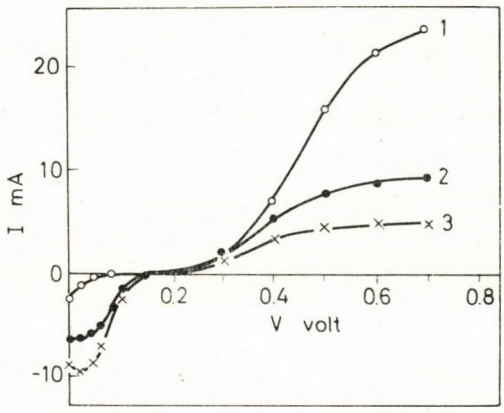

Fig. 13. Change of shape of the polarization curve as the oxidation proceeds

This is shown in Fig. 13. Curve 1 was determined from potentiostatic measurements at an i-propanol concentration of 10^{-2} *M*. Curves 2 and 3 were obtained after oxidation with a given current for different times.

Only the sections corresponding to the oxidation of i-propanol, and the formation of hydrogen at about 0 mV, appear on the first polarization curve. On the other two curves the section corresponding to the hydrogenation of the oxidation product begins at potentials more negative than 200 mV. In the section corresponding to the oxidation, the current and the rate of oxidation decrease with decreasing i-propanol concentration. Parallel to this, the rate of reduction increases with increasing amount and concentration of the product.

On the oxidation of i-propanol any other product which may be hydrogenated, apart from acetone, is difficult to conceive. Hence, this observation supports the view that a significant amount of acetone is formed during the oxidation of i-propanol. Similar phenomena can be observed in the oxidations of *sec*-butanol and cyclohexanol.

If one accepts that the oxo compound is one of the oxidation products, then we can study its proportion to the other products by electrochemical means. A necessary condition of this is that if other products are formed in the oxidation, then these must be derived from the oxidation of the oxo compound. In this way the question may be answered by comparing the

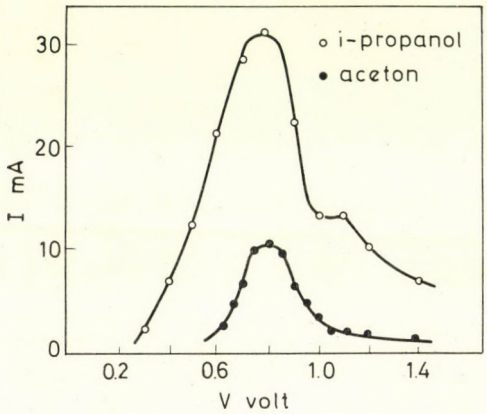

Fig. 14. Comparison of the oxidations of acetone and i-propanol at concentrations of 5×10^{-2} *M*

polarization curves with the oxo compound and the corresponding alcohol present.

In Fig. 14 the comparison is made for the case of i-propanol and acetone.

It can be seen from the figure that the disturbing effect of ketone oxidation in the case of i-propanol need only be considered at potentials more positive than 600 mV. With *sec*-butanol and cyclohexanol, the behaviour of which is exactly similar, the oxidation of the ketone is not involved.

The ratio of the rates of oxidation of i-propanol and acetone is not sufficiently clear from the polarization curves, considering that the charge equivalents necessary for the oxidation also appear in the current ratios, quite apart from the rate ratios.

The most simple and the most probable [12] equation for the oxidation of acetone is

$$CH_3{-}\underset{\underset{O}{\|}}{C}{-}CH_3 + H_2O \longrightarrow CO_2 + CH_3COOH + 8\,H^+ + 8\,e$$

Thus, the relations between the oxidation rate of acetone (w_0) and the current, and the rate of formation (w_f) and the current are

$$8\ F\ w_0 = i_0$$

and

$$2\ F\ w_f = i_f$$

Hence

$$\frac{w_f}{w_0} = 4\,\frac{i_f}{i_0}$$

When both reactions occur the current will be the sum of i_0 and i_f. From what has been said it is clear that the acetone will be in excess among the products while the current corresponding to the oxidation of acetone is not larger than that necessary for the oxidation of i-propanol. However, this can only follow in the case of high acetone and low i-propanol concentrations, both reaction rates being concentration dependent.

Study of the products by analytical methods

With the electrochemical methods it was only indirectly proved that the product of oxidation is the corresponding ketone. Therefore, two analytical procedures were applied for the detection and determination of the oxo compounds formed. One of the methods was the gravimetric determination of the 2,4-dinitrophenylhydrazone of the oxo compound.

A 0.2—0.5 *M* solution of the secondary alcohol was prepared. Electrolysis was carried out by a galvanostatic method in order to form several mmoles of the product. The solution was then transferred from the electrolytic cell to an Erlenmeyer flask, and the 2,4-dinitrophenylhydrazone precipitated according to Ref. [13]. The determination did not give satisfactory results, particularly in the case of acetone, because of the relatively high solubility of the 2,4-dinitrophenylhydrazone, but from the point of view of qualitative analysis it was important. From the m.p. and crystalline form of the 2,4-dinitrophenylhydrazones it was found that in each case only one oxo compound, corresponding to the alcohols concerned, is formed during the oxidation.

Good results were obtained in the semi-micro acidimetric determination of the oximes. Following a similar preparation to the above, the determination was carried out according to Ref. [13].

It was found that in the case of *sec*-butanol and cyclohexanol the electric charge introduced was used 100% to the formation of the oxo compound. In the case of i-propanol too, practically only acetone is formed, particularly at the beginning of the reaction at not too positive potentials.

REFERENCES

1. PIERSMA, B. I., GILEADI, E.: The Mechanism of Electrochemical Oxidation of Organic Fuels, Modern Aspects of Electrochemistry, 4. Ed. J. O' M. Bockris, Plenum Press, London (1966)
2. CONWAY, B. E.: Rev. Pure and Appl. Chem. **18,** 105 (1968)
3. WEINBERG, N. L., WEINBERG, H. R.: Chem. Reviews **68,** 449 (1968)
4. VIJH, A. K., CONWAY, B. E.: Chem. Reviews **67,** 623 (1967)
5. KURENNIEMI, T., TOMMILA, E.: Suomen Kemistilenti **9B** 25 (1936); Chem. Abstr. **31,** 1299 (1937)
6. NIKOLOV, Y., YNCHUK, B., BESKOROVAINAYA, S. S., VASILIEV, Yu. B., BAGOTSKII, V. S.: Elektrokhimia **6,** 597 (1970)
7. HORÁNYI, GY., SOLT, J., SZABÓ, S., NAGY, F.: Acta Chim. Acad. Sci. Hung. (In press)
8. WILL, F. G., KNORR, C. A.: Z. Electrochem. **64,** 258 (1960)
   BREITER, M. W.: Electrochim. Acta **8,** 447, 457 (1963)
   VIELSTICH, W.: Z. Instrumentekunde **71,** 29 (1963)
   BUCH, R. P., GRIFFITH, L. R.: J. Electrochem. Soc. **109,** 1005 (1962)
   SRINIVASAN, S., GILEADI, E.: Electrochim. Acta **11,** 32 (1966)
9. BAGOTSKII, V. S., VASILIEV, Yu. B.: Electrochim. Acta **12,** 1323 (1967); **11,** 1439 (1966)
10. GILMAN, J., BREITER, M. W.: J. Electrochem. Soc. **109,** 1099 (1962)
11. JULIARD, A. L., SHALIT, H.: J. Electrochem. Soc. **110,** 1002 (1963)
12. KHOMIAKOV, V. G., BAKHCHISARAITSAN, N. G., TOMILOV, A. P.: Trudi chetvortovo soveshchanyiya po elektrokhimii, Izd. Akad. Nauk. S.S.S.R., Moscow (1959)
13. HOUBEN—WEYL: Methoden der Organischen Chemie, Georg Thieme Verlag Stuttgart **2,** 457 (1959)

György HORÁNYI
Péter KŐNIG
Iván TELCS
Budapest II., Pusztaszeri út 59—67.

Acta Chimica Academiae Scientiarum Hungaricae, Tomus 72 (2), pp. 179—187 (1972)

OXIDATION OF SECONDARY ALCOHOLS ON A PLATINUM ELECTRODE, II

STUDY OF THE CONNECTION BETWEEN OXYGEN ADSORPTION AND THE REACTION

G. HORÁNYI, G. VÉRTES and P. KŐNIG

(Central Research Institute for Chemistry of the Hungarian Academy of Sciences, Budapest)

Received November 5, 1970

1. The oxidation of secondary alcohols was studied on platinum surfaces partially or completely covered with oxygen.

2. It was found that the oxidation takes place with a considerable rate only on the free metal surface.

3. With the study of the oxidation reaction, the possibility arises for the investigation of the adsorption and desorption properties of the adsorbed oxygen.

From an examination of the literature concerning the electrooxidation of alcohols on noble metal electrodes it can be established that, according to the views of different authors, the reactions may be classified into the following types [1, 2].

1. The reaction occurs by electron transfer or dehydrogenation with the molecule adsorbed on the metal.

2. Reaction takes place on the oxygen-covered surface in a similar way to the above.

3. Reaction occurs with the adsorbed oxygen or the oxide.

Considering all these reactions, it is hardly possible to find a unified treatment for the oxidation processes on the platinum electrode. The analysis of polarization curves therefore runs into difficulties, because the ratio of the metal surface and the surface covered with oxide or adsorbed oxygen varies as a function of the electrode potential, and this complicates the situation considerably. It appears practical to limit the study first to those conditions in which we are concerned either only with a metal surface or only with oxygen-covered surfaces. In the present paper we study the role in the reaction of oxide or oxygen-covered surfaces with regard to the oxidation of secondary alcohols.

Experimental method

The method and equipment were as already reported [3]. In the study of the platinum electrode – alcohol interaction, either the preparatory operations necessary with the electrode were carried out in a separate vessel and the electrode was then placed in the cell containing the alcohol solution, used in the study, or the preparatory operations were carried out in the cell and the alcohol added at the appropriate moment. This preparatory work was mainly anodic polarization lasting for a definite time. Similarly to our earlier studies, a 1 *N* $HClO_4$ background solution was used.

Reaction of the previously oxidized metal surface and the alcohol

It has already been mentioned in the introduction that a number of authors consider that a direct chemical reaction occurs between oxygen chemisorbed on the platinum and the alcohols or other organic compounds; as a result a clean platinum surface is formed. In the absence of an external polarizing effect, the reaction is accompanied by a change of the electrode potential, and the exhaustion of the adsorbed oxygen is indicated by a jump in the potential [4, 7].

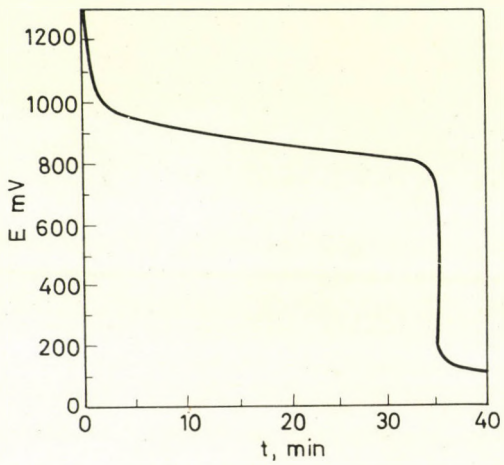

Fig. 1. Discharge curve of a previously oxidized, platinized Pt electrode in 1 *N* $HClO_4$ + 0.1 *M* i-propanol

As is shown in Fig. 1, this phenomenon can also be observed in the case of secondary alcohols. The reduction of chemisorbed oxygen takes place in stage *a*. The length of this stage depends on the concentration of alcohol too. In contrast with literature findings [4], the experiments are not well reproducible even when an identical preparation is always applied. At given alcohol concentrations the length of stage *a* depends significantly on the prior anodic polarizing potential and period. A long pre-treatment causes the lengthening of stage *a* to be seen in Fig. 1.

Disregarding these uncertainties, it must be stated that from the length of stage *a* or from the reaction time only an average reaction rate can be given; it is not known how the reaction rate varies with the amount of chemisorbed oxygen (which changes during the reaction). Therefore the literature finding [4] that the reaction rate is proportional to the amount of oxygen on the surface appears arbitrary. Further data are required to decide what function describes the reaction between the oxide and the alcohol.

We were faced with essentially these questions in our studies of oxidation processes on the nickel hydroxide electrode [5]. The method applied there was used here too. The essence of the study was that the electrode in contact with the alcohol was cathodically polarized with various currents at the same time as the reaction. The shape of the potential–time curve in this case is similar to that in Fig. 1. From the relation between the current and the lengths of the corresponding *a* stages, conclusions can be drawn on the kinetics of the reaction between the oxide and the alcohol.

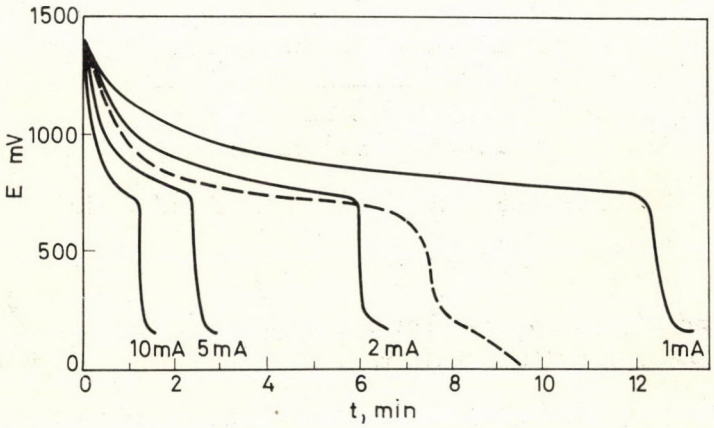

Fig. 2. Discharge curves of a platinized Pt electrode in 0.1 *M* i-propanol, determined with cathodic polarization. The discharge curve determined with a current of 5 mA in the pure background solution is given by a broken line

Figure 2 shows the potential–time curves obtained with the different polarizing currents. From the curves it was found that (disregarding the very small currents) the product of the time corresponding to stages *a* and the currents concerned (*i.e.* the amount of charge introduced) gives almost identical values. This constant charge value is a considerable fraction (ca. one third) of the charge equivalent to the oxygen chemisorbed on the electrode in the given way. This observation permits the conclusion that until a considerable part of the adsorbed oxygen has been removed from the surface the reaction is extremely slow, and its rate can be neglected compared with the currents applied.

Another experimental observation also points to the very slow reaction between the previously strongly oxidized metal surface and the alcohol. If a charged electrode is left to stand for 10 min in a 1 *M* i-propanol solution, and then after rinsing is discharged in pure background solution, a discharge curve agreeing with the curve shown by a broken line in Fig. 2 is obtained. At the same time this is experimental proof that indeed only average rates can be

calculated from curves such as that shown in Fig. 1, since in the first ten minutes the reaction rate can practically be neglected.

From the fact that only about one third of the oxygen chemisorbed on the electrode is removed by the current in the joint discharge with alcohol and cathodic polarization, and also from the observation that the chemisorbed oxygen is practically not removed by the alcohol in the first ten minutes but the reaction still proceeds (Fig. 1), the conclusion must be drawn that after a certain time (the removal of a given amount of oxygen or the attainment of a certain electrode potential) the rate of reaction increases to a significant extent.

From studies with methanol, formaldehyde and formic acid, it is assumed [6] that initially a slow chemical reaction takes place between the adsorbed oxygen and the organic substance.

In the present case this would be formulated by the equation

$$PtO + R{-}\underset{\displaystyle OH}{\underset{|}{CH}}{-}R' \longrightarrow R{-}\underset{\displaystyle O}{\overset{\|}{C}}{-}R' + H_2O + Pt \qquad (1)$$

where R and R′ are alkyl or aryl groups. However, the rapid change of potential is caused by the setting up of a local cell, at one pole of which the reaction

$$Pt + R{-}\underset{\displaystyle OH}{\underset{|}{CH}}{-}R' \longrightarrow Pt + R{-}\underset{\displaystyle O}{\overset{\|}{C}}{-}R' + 2\,H^+ + 2\,e \qquad (2)$$

takes place, and at the other the process

$$PtO + 2\,H^+ + 2\,e \longrightarrow Pt + H_2O \qquad (3)$$

The view is well known [7] that reaction (1) never takes place directly, and only the reactions (2) and (3) need be considered. In this case it is assumed that the anodic pre-treatment of the electrode leaves free sites on the surface on which reaction (2) occurs. The number of free sites varies depending on the manner and period of the pre-treatment, and so it could be explained to a certain extent why the average rate of reduction of the oxide is smaller in the case of a longer anodic polarization. Leaving aside the disputed questions, the above experimental observations permit the conclusion that when part of the metal surface is covered with oxygen in the case of the oxidation of secondary alcohols too, only the oxidation reaction taking place on the free metal surface need be taken into consideration.

In the following an answer is sought to the question of what possibilities there are of following changes in the state of the surface and the ratio of free and oxygen-covered surface.

Potentiostatic study of the oxidation reaction on an electrode prepared by anodic polarization

The electrode is immersed in a solution containing the secondary alcohol after prolonged anodic polarization with a high current, the potential is adjusted to an initial 1500 mV with the help of a potentiostat, then this is changed in the negative direction; even after a long waiting period (10—20 min) no considerable current flows in a fairly wide potential interval. Thus, in agreement with what was said earlier, the rate of the oxidation reaction cannot be significant.

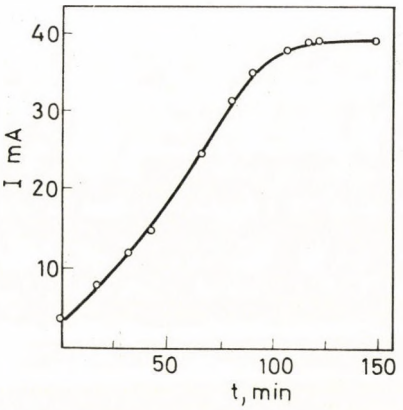

Fig. 3. Change of the current at a platinized Pt electrode at 800 mV in 1 *N* $HClO_4$ + 0.1 *M* i-propanol

Beginning from certain potentials (more negative than 900 mV) an extremely slow increase of current can be observed. This is shown in Fig. 3. As can be seen from the figure, it remains at the studied potential value for almost two hours until the stationary state is attained. (This observation again supports the earlier finding [3] that in the case of the use of potentiodynamic methods many important, slowly occurring phenomena can escape attention.) In a potential interval of about 100 mV the phenomena shown in Fig. 3 are repeated with the change of potential; this can be seen in Fig. 4. In the case of different initial potentials on electrodes prepared by anodic polarization, the rates of attainment of the stationary state will also be different, as is to be seen in Fig. 5.

The above experimental observations bear witness to the fact that in the case of oxidized surfaces the rate of the oxidation reaction is controlled by a slow process which depends to a considerable extent on the electrode potential. Since the rate of this process depends on the potential, it must play the part of a charge transfer process in the reaction, and so the reaction

concerned cannot be the direct chemical reaction between the alcohol and the adsorbed oxygen.

From what has been said in the previous part we must come to the conclusion that the process controlling the rate of oxidation of the alcohol is probably the electrochemical reduction of oxygen (process [3]), or the rate of formation of the free surface.

On repeating the previous experiments with solutions not containing alcohol, as Fig. 6 shows, it was observed that at potentials where the rate of oxidation attains the stationary value only very slowly, the reduction of the adsorbed oxygen is likewise a very slow process. From a comparison of Figs 4, 5 and 6, therefore, we come to the interesting conclusion that the phenomena connected with the reduction of adsorbed oxygen during the oxidation of alcohol appear with strongly opposite signs.

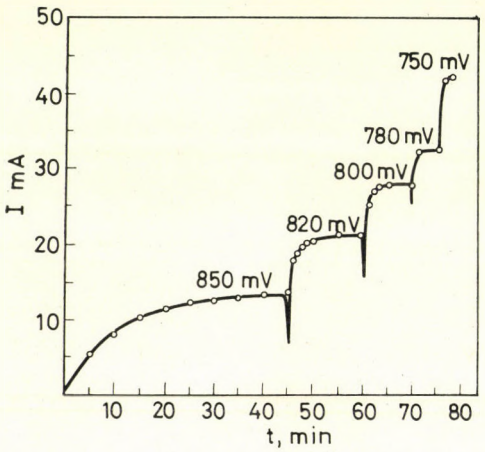

Fig. 4. Potentiostatic 'determination' of the polarization curve in 1 *N* $HClO_4$ + 0.1 *M* i-propanol

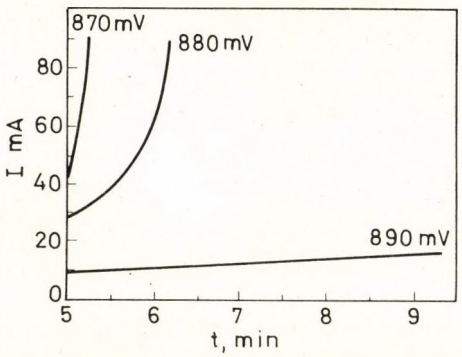

Fig. 5. The electrode was previously oxidized (5 min at 1500 mV), and then the oxide formed was reduced for 5 min at a given potential. Next, i-propanol was added to the cell (to 0.1 *M*) and the oxidation current was measured at this same potential

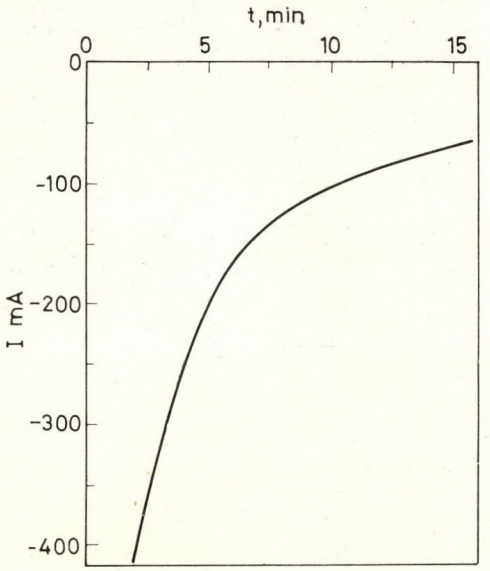

Fig. 6. Change with time at 900 mV of the reduction current of the chemisorbed oxygen on a previously oxidized electrode

In the experiments shown in Figs 3 and 4 the stationary state was attain ed after a certain time. The establishment of the stationary state can be explained by the fact that the ratio of the 'free metal surface' to the oxide-covered surface no longer changes, that is the rates of formation and removal of the oxide are the same. If, in agreement with [6], the formation of the oxide is described by the equation

$$\mathrm{Pt} + \mathrm{H_2O} \rightleftharpoons \mathrm{PtOH} + \mathrm{H^+} + e \tag{4}$$

then in the stationary state or at equilibrium in the case studied by us a relation

$$k_1(1 - \theta_0 - \theta_s)10^{bE} = k_{-1}\,\theta_0\,10^{-bE} \tag{5}$$

can be given, where k_1 is the adsorption rate constant, k_{-1} the desorption rate constant, θ_0 the coverage with regard to oxygen, θ_s that with regard to the substrate, b a constant ($b = \alpha\, zF/RT$, $\alpha = 0.5$) and E the potential. At the same time, the rate (i) of the oxidation reaction can be given by the relation

$$i = k_3 c(1 - \theta_s - \theta_0) = k_4\,\theta_s\,10^{b'E} \tag{6}$$

The first part of Eq. (6) refers to the rate of adsorption of the substrate, and the second part to the oxidation reaction (c is the concentration of alcohol

in the solution; k_3, k_4 and b' are constants). By combining relations (5) and (6), one obtains for the oxygen coverage

$$\frac{k_1}{k_{-1} k_3 c} i \cdot 10^{2bE} = \theta_0 \tag{7}$$

It may be seen from Eqs (6) and (7), corresponding to observations illustrated in Figs 3 and 4, that the change of θ_0 in time must be connected with the simultaneous change of i.

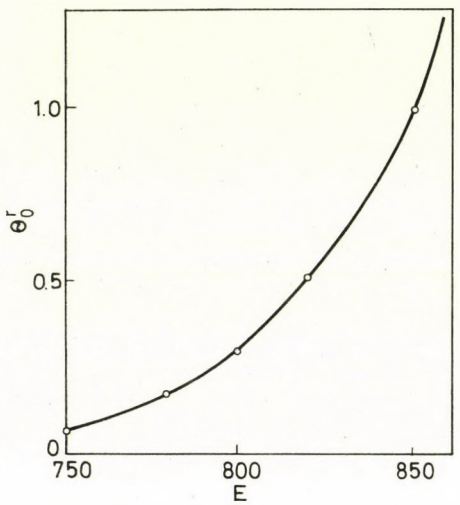

Fig. 7. Change with the potential of the relative oxygen coverage referred to the 850 mV data, according to Eq. (8), from the data of Fig. 4

For the determination of the absolute value of θ_0, the values of k_1, k_{-1}, k_3 and b are needed, apart from the experimentally measured i and E. However, these data are not available. It seems practical to calculate relative coverage values starting from some definite θ_0^1 and E_1 pair. The relative coverage, θ_0^r, is given by the relation

$$\frac{i}{i_1} 10^{2b(E-E_1)} = \frac{\theta_0}{\theta_0^1} = \theta_0^r \tag{8}$$

θ_0^r can be determined using Eq. (8) if the value of b is known. For this the literature value of 1/120 mV^{-1} was used.

If θ_0^1 does not differ greatly from unity, then there is not a large difference in the values of θ_0^r and θ_0. At any rate, conclusion can readily be made from the values of θ_0^r as to the potential dependence of the reversible oxygen adsorption.

In our view, the study principle introduced in this paper (and, in the case of further development of the precision, the measurement method) can be a valuable aid in the investigation of oxygen adsorption. The possibility for this is provided by the fact that it could be unambiguously confirmed that the oxidation reaction in the studied cases occurs only on the free metal surface.

REFERENCES

1. CONWAY, B. E.: Rev. Pure and Appl. Chem. **18,** 105 (1968)
2. GILMAN, S.: J. Electroanal. Chem. **12,** 111 (1967)
3. HORÁNYI, G., KŐNIG, P., TELCS, I.: Acta Chim. Acad. Sci. Hung. **72,** 165 (1972)
4. DRAZIC, D. M., DRAZIC, V. J.: Electrochim. Acta **11,** 1235 (1966)
5. VÉRTES, G., HORÁNYI, G., NAGY, F.: Acta Chim. Acad. Sci. Hung. **68,** 217 (1971)
   VÉRTES, G., HORÁNYI, G., NAGY, F.: Magy. Kém. Foly. **74,** 172 (1968)
6. CONWAY, B. E., MARINCIC, N., GILROY, D., RUDD, E.: Electrochem. Soc. **113,** 1144 (1966)
7. HOFFMAN, A., KUHN, A. T.: Electrochim. Acta **9,** 835 (1964)
8. HOLLNAGEL, M., LOHSE, U.: Z. phys. Chem. **232,** 237 (1966)

György HORÁNYI
György VÉRTES
Péter KŐNIG
Budapest II., Pusztaszeri út 59–67.

Acta Chimica Academiae Scientiarum Hungaricae, Tomus 72 (2), pp. 189—207 (1972)

MECHANISTIC STUDY OF THE ISOMERIZATION OF *n*-BUTENE ON ACID CATALYSTS, I

KINETICS OF MONOMOLECULAR CATALYTIC INTERCONVERSION OF THREE COMPONENTS

D. KALLÓ, E. DETREKŐY and G. SCHAY

(Central Research Institute for Chemistry, Hungarian Academy of Sciences, Budapest)

Received November 11, 1970

The rate equations for the transformation of a component i were derived for the following mechanisms: (1) transformation to both j and k proceeds by adsorption, surface reaction and desorption; (2) without a surface reaction one of the adsorbed forms if i is desorbed into j, the other into k; (3) adsorbed i transforms to adsorbed forms of j and k, which are desorbed into j and k; (4) the common adsorbed form of two components transforms to the adsorbed form of the third component; (5) the components transform into each other *via* a common surface intermediate. In the derivation of the rate equations for the individual mechanisms, either the surface reaction or the sorption were considered as rate-determining steps. The relations obtained for r^0_{ij}, the initial rate of some transformation $i \rightarrow j$ are easier to evaluate; these can be given always by an equation of the form $1/r^0_{ij} = m_{ij}/p^0_i + b_{ij}$ as a function of the initial pressure p^0_i (at low coverages $m_{ij}/p^0_i \gg b_{ij}$, and at high coverages $m_{ij}/p^0_i \ll b_{ij}$). If $b_{ij} \neq b_{kj}$, in principle it can be observed only that the elementary steps of the monomolecular interconversion of the three components follow each other according to a triangular scheme [mechanisms (1) and (2) and (3) if the surface reaction is rate-determining]; if $b_{ij} = b_{kj}$, it can be observed only that the transformation proceeds according to an Y scheme *via* a common surface intermediate or an equilibrium mixture of products [mechanisms (3), (4) and (5), when the sorption steps are rate-determining]; if equilibrium is very rapidly established between any two components, the reaction proceeds by a slow surface reaction according to mechanism (4). As well as this elucidation of the mechanism, the kinetic method at times also provides a possibility for the determination of the constants of the elementary steps.

In the present series of papers we wish to report the results of a study of the isomerization of *n*-butene as model reaction, in respect of the so-called acid catalysts, their active groups. To start with, we endeavour to elucidate the mechanism of the reaction, the first and most obvious possibility for this being offered by the reaction kinetic methods. The evaluation of the kinetically elucidated elementary steps and the constants determined for these can serve as the basis of further investigations. However, there are restrictions of principle to the kinetic study of the mechanism. For the clarification and the sizing up of all this it is necessary *(a)* to know the kinetic relations concerned, and *(b)* to establish with their help the limitation of calculations and evaluations from the experimental data.

The kinetics of the catalytic transformation of the three *n*-butene isomers have been cleared up in so far as the process can be phenomenologically described by the triangular scheme

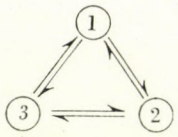

in which the individual steps are reversible and, within the limits of experimental error, first order with respect to the composition expressed in *mole fractions* at a given, constant pressure [*e.g.* 1—3]; that is, the rate of transformation of the i-th component ($i = 1, 2, 3$) is

$$r_i = (k_{ij} + k_{ik})\, y_i - k_{ji}\, y_j - k_{ki}\, y_k \qquad (1)$$

where y is the mole fraction; k_{ij} is the empirical rate constant of the overall transformation $i \rightarrow j$; $i, j, k = 1, 2, 3$; and $i \neq j \neq k$.

Nevertheless, it may be observed that at times the rate of transformation increases not with the first, but a smaller power of the total *pressure* of the reacting gas mixture. Under such conditions the experimental data can be described on the basis of a reaction scheme in which surface reactions take place between the adsorbed isomers [4] (see scheme **III** in Fig. 1); in addition to this they can also be described on the basis of a scheme in which the individual isomers are transformed into each other via a common intermediate [5, 6] (see scheme **V** in Fig. 1). From other measurements, however, it could be concluded that the two 2-butene isomers give a common surface intermediate which transforms into the adsorbed form of the third isomer [7] (see scheme **IV** in Fig. 1). All these observations prompted us to extend our studies related to this system, *i.e.* to take into account all the kinetic cases for the possible schemes of catalytic transformation, including the conditions prevailing under extremely large and extremely small coverages.

1. Reaction schemes for the catalytic transformation

Fig. 1 shows those monomolecular transformation schemes for which kinetic equations have been derived. Only the non-activated surface intermediates are given in the schemes, and not the activated complexes.

The schemes shown in Fig. 1 do not comprise the total variety of formal possibilities, the reaction paths appearing fairly reasonable were regarded only on the basis of the following considerations.

I represents the conception (today already considered as classic) according to which three processes were considered for every reaction direction: adsorption, surface reaction and desorption. Accordingly, each individual isomer would be adsorbed in two forms of surface intermediate, which thus transform in the surface reactions; this means then that the 3 isomers would occur in a total of six types of adsorbed state. With this the most complicated transformation scheme was taken into consideration.

II is simpler than **I** in so far as the surface reaction step does not occur. Here too each isomer is adsorbed in two ways, but in such a manner that their intermediates are common in pairs, and hence these can be desorbed in two ways.

In the case of **III** the transformation takes place between the isomeric forms adsorbed on the surface.

IV represents the case when the process occurs by the surface reaction between the common intermediate of two isomers and the adsorbed form of the third. This picture appears reasonable if on adsorption a π-complex is formed which in the 2-butenes has an identical structure, and in 1-butene a structure different from this.

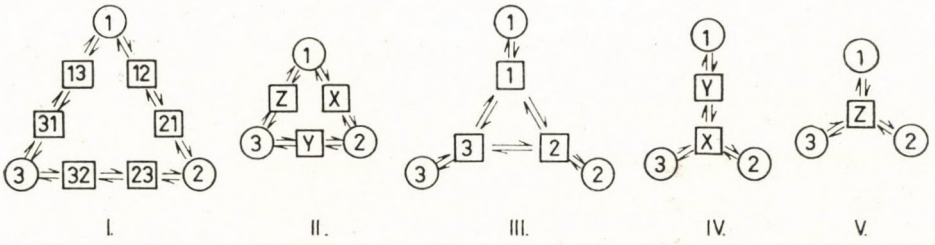

Fig. 1. Transformation schemes considered in the kinetic calculations; ○ = gas phase component; □ = adsorbed state

In **V** all three isomers form a common surface complex. This seems likely because upon the addition of a proton from the acid catalyst an identical σ-complex and the same *sec*-butyl carbonium ion may be formed from all three isomers.

2. Kinetic relations

The kinetic cases which are studied for the transformation schemes shown in Fig. 1 are as follows:

r: the rate-determining step is the *surface reaction* with surface coverages corresponding to an adsorption equilibrium; extreme sub-cases are

r_0: there are very small surface coverages, *i.e.* the adsorption equilibrium constants are very small: $K_a p_i \ll 1$ (K_a is the adsorption equilibrium constant; p_i — the partial pressure of the i-th component);

r_1: the coverage of the surface is complete, *i.e.* the adsorption equilibrium constants are very large: $K_a p_i \gg 1$.

s: the *sorption* steps are rate-determining, while the surface reaction (if there is one) can be considered as being in equilibrium; extreme sub-cases are

ads : the rate-determining step is the adsorption, *i.e.* $k_a p_i \ll k_d$ (k_a, k_d are the adsorption and desorption rate constants, resp.), resulting in very small coverages;

des : the rate-determining step is the desorption, *i.e.* $k_a p_i \gg k_d$, resulting in very high surface coverages.

Our investigations do not extend to those cases when (*a*) neither the sorption nor the surface reaction (if there is one) is the rate-determining step, as the practical probability of such general cases is very small, (*b*) the adsorption is strong or weak for only one or two components, and further when one surface reaction is fast and the other slow, as large differences in such a sense cannot be expected for closely related compounds.

In the following are given the kinetic equations for r_i, the rate in steady state, related to unit catalyst surface, of the transformation of some component ($i = 1, 2, 3$) expressed in partial pressures, as directly measurable independent variables. The equations were derived by assuming a catalyst surface of homogeneous activity; the steady state was taken into consideration in such a way that $\Sigma r_i = 0$, or equivalently $\dfrac{d\theta}{d\tau} = 0$, *i.e.* the various coverages and the fraction of vacant surface θ_0 do not change in time. The basic equations from which we set out can be given in the following general forms:
for the sorption process $\textcircled{i} \rightleftarrows \boxed{\alpha}$:

$$r_{i,a} = k_{i,a}\, p_i\, \theta_0 - k_{i,d}\, \theta_\alpha$$

for the surface reactions $\boxed{\alpha} \rightleftarrows \boxed{\beta}$:

$$r_{\alpha\beta} = k_{\alpha\beta}\, \theta_\alpha - k_{\beta\alpha}\, \theta_\beta .$$

The fraction of vacant surface is stressed in our equations since this is clearly of identical significance in any conception of the mechanism, while the coverages refer to different systems and different intermediates. The indices denote the transitions according to Fig. 1 in an unambiguous way and as simply as possible.

———

In case *I-r*, conditions of which are $k_{ij} \ll k_{ij,i}$, $k_{ik} \ll k_{ik,i}$, $k_{ji} \ll k_{ji,j}$ and $k_{ki} \ll k_{ki,k}$:

$$r_i = \theta_0 \left[(k_{ij} K_{i,ij} + k_{ik} K_{i,ik})\, p_i - k_{ji} K_{j,ij}\, p_j - k_{ki} K_{k,ki}\, p_k \right] \qquad (2)$$

$$\theta_0 = \frac{1}{1 + \Sigma K_i\, p_i}$$

(k_{ij} is the rate constant of transformation of the adsorbed intermediate $\boxed{ij}$ to $\boxed{ji}$, in accordance with the designation to be seen in scheme **I** in Fig. 1; also in this sense
$k_{ij,i}$ is the rate constant of desorption $\boxed{ij} \rightarrow (j)$;
$K_{i,ij}$ is the equilibrium constant of adsorption of the gas phase component (i) into $\boxed{ij}$;
$K_i = K_{i,ij} + K_{i,ik}$ = adsorption equilibrium constant of i;
p is the partial pressure; while in the indices
$i = 1, 2, 3$; $j = 1, 2, 3$; $k = 1, 2, 3$; $i \neq j$; $j \neq k$; and $k \neq i$).

In case *I-r*$_0$:

$$r_i = \left[(k_{ij} K_{i,ij} + k_{ik} K_{i,ik})\, p_i - k_{ji} K_{j,ji}\, p_j - k_{ki} K_{l,ki}\, p_k\right] \tag{4}$$

In case *I-r*$_1$:

$$r_i = \frac{\left[(k_{ij} K_{i,ij} + k_{ik} K_{i,ik})\, y_i - k_{ji} K_{j,ji}\, y_j - k_{ki} K_{k,ki}\, y_k\right]}{\Sigma K_i\, y_i} \tag{5}$$

(y is the mole fraction in the gas phase, since $p = yP$ and the total pressure P can be eliminated).

In case *I-s*:

$$r_i = \theta_0 \left[\left(k_{i,ij} \frac{k_{ji,j} K_{ij}}{k_{ij,i} + k_{ji,j} K_{ij}} + k_{i,ik} \frac{k_{ki,k} K_{ik}}{k_{ik,i} + k_{ki,k} K_{ik}} \right) p_i - \right.$$
$$\left. - k_{j,ji} \frac{k_{ij,i}}{k_{ij,i} + k_{ji,j} K_{ij}} p_j - k_{k,ki} \frac{k_{ik,i}}{k_{ik,i} + k_{ki,k} K_{ik}} p_k \right] \tag{6}$$

$$\theta_0 = \left[1 + (1 + K_{12}) \frac{k_{1,12} p_1 + k_{2,21} p_2}{k_{12,1} + k_{21,2} K_{12}} + \right.$$
$$\left. + (1 + K_{23}) \frac{k_{2,23} p_2 + k_{3,32} p_3}{k_{23,2} + k_{32,3} k_{23}} + (1 + K_{31}) \frac{k_{3,31} p_3 + k_{1,13} p_1}{k_{31,1} + k_{13,1} K_{31}} \right]^{-1} \tag{7}$$

($k_{i,ij}$ is the rate constant of the adsorption $(i) \rightarrow \boxed{ij}$;
$k_{ji,j}$ is the rate constant of the desorption $\boxed{ji} \rightarrow (j)$;
K_{ij} is the equilibrium constant of the surface reaction $\boxed{i} \rightleftharpoons (j)$).

In case *I-ads:*

$$r_i = \left[\left(k_{i,ij} \frac{k_{ji,j} K_{ij}}{k_{ij,i} + k_{ji,j} K_{ij}} + k_{i,ik} \frac{k_{ki,k} K_{ik}}{k_{ik,i} + k_{ki,k} K_{ik}} \right) p_i - \right.$$
$$\left. - k_{j,ji} \frac{k_{ij,i}}{k_{ij,i} + k_{ji,j} K_{ij}} p_j - k_{k,ki} \frac{k_{ik,i}}{k_{ik,i} + k_{ki,k} K_{ik}} p_k \right] \tag{8}$$

In case *I-des:*

$$r_i = \left[\left(k_{i,ij}\frac{k_{ji,j}K_{ij}}{k_{ij,i}+k_{ji,j}K_{ij}} + k_{i,ik}\frac{k_{ki,k}K_{ik}}{k_{ik,i}+k_{ki,k}K_{ik}}\right)y_i - k_{j,ji}\frac{k_{ij,i}}{k_{ij,i}+k_{ji,j}K_{ij}}y_i - k_{k,ki}\frac{k_{ik,i}}{k_{ik,i}+k_{ki,k}K_{ik}}y_k\right] \times \left[(1+K_{12})\frac{k_{1,12}y_1+k_{2,21}y_2}{k_{12,1}+k_{21,2}K_{12}} + (1+K_{23})\frac{k_{2,23}y_2+k_{3,32}y_3}{k_{23,2}+k_{32,3}K_{23}} + (1+K_{31})\frac{k_{3,31}y_3+k_{1,13}y_1}{k_{31,3}+k_{13,1}K_{31}}\right]^{-1} \tag{9}$$

As in (5) it was possible to eliminate the pressure.

In case *II-s:*

$$r_1 = \theta_0\left[\left(k_{1X}\frac{k_{X2}}{k_{X1}+k_{X2}} + k_{1Z}\frac{k_{Z3}}{k_{Z3}+k_{Z1}}\right)p_1 - k_{2X}\frac{k_{X1}}{k_{X1}+k_{X2}}p_2 - k_{3Z}\frac{k_{Z1}}{k_{Z3}+k_{Z1}}p_3\right] \tag{10}$$

$$\theta_0 = \left[1 + \frac{k_{1X}p_1+k_{2X}p_2}{k_{X1}+k_{X2}} + \frac{k_{2Y}p_2+k_{3Y}p_3}{k_{Y2}+k_{Y3}} + \frac{k_{3Z}p_3+k_{1Z}p_1}{k_{Z3}+k_{Z1}}\right]^{-1} \tag{11}$$

(*k* is the adsorption or desorption rate constant, depending on the indices; the indices refer to the transformations according to scheme II in Fig. 1; thus for example the rate constant of the adsorption ① → [X] is k_{1X}).

In case *II-ads:*

$$r_1 = \left[\left(k_{1X}\frac{k_{X2}}{k_{X1}+k_{X2}} + k_{1Z}\frac{k_{Z3}}{k_{3Z}+k_{Z1}}\right)p_1 - k_{2X}\frac{k_{X1}}{k_{X1}+k_{X2}}p_2 - k_{3Z}\frac{k_{Z1}}{k_{Z3}+k_{Z1}}p_3\right] \tag{12}$$

In case *II-des:*

$$r_1 = \left[\left(k_{1X}\frac{k_{X2}}{k_{X1}+k_{X2}} + k_{1Z}\frac{k_{Z3}}{k_{Z3}+k_{Z1}}\right)y_1 - k_{2X}\frac{k_{X1}}{k_{X1}+k_{X2}}y_2 - k_{3Z}\frac{k_{Z1}}{k_{Z3}+k_{Z1}}y_3\right] \times \left[\frac{k_{1X}y_1+k_{2X}y_2}{k_{X1}+k_{X2}} + \frac{k_{2Y}y_2+k_{3Y}y_3}{k_{Y2}+k_{Y3}} + \frac{k_{3Z}y_3+k_{1Z}y_1}{k_{Z3}+k_{Z1}}\right]^{-1} \tag{13}$$

r_2 and r_3 are obtained from Eqs (10), (12) and (13) by the simultaneous substitution of the index numbers and index symbols according to the cycles

$$\begin{matrix} & 1 & & \\ \nearrow & & \searrow & \\ 3 & \leftarrow & 2 & \end{matrix} \quad \text{and} \quad \begin{matrix} Z & \rightarrow & X \\ & \nwarrow \swarrow & \\ & Y & \end{matrix} .$$

In case *III-r:*

$$r_i = \theta_0 \left[(k_{ij} + k_{ik}) K_i p_i - k_{ji} K_j p_j - k_{ki} K_k p_k \right] \tag{14}$$

$$\theta_0 = \frac{1}{1 + \Sigma K_i p_i} \tag{15}$$

(k_{ij} is the rate constant of the surface reaction [i] → [j], indexed according to scheme **III** in Fig. 1; *e.g.* k_{12} for [1] → [2];
K_i is the adsorption equilibrium constant of component i).
In case *III-r*$_0$*:*

$$r_i = \left[(k_{ij} + k_{ik}) K_i p_i - k_{ji} K_j p_j - k_{ki} K_k p_k \right] \tag{16}$$

In case *III-r*$_1$*:*

$$r_i = \frac{(k_{ij} + k_{ik}) K_i y_i - k_{ji} K_j y_j - k_{ki} K_k y_k}{\Sigma K_i y_i} \tag{17}$$

In case *III-s* (general indexing is not possible here):

$$r_1 = \theta_0 \left[(k_1 k_{-2}^{***} + k_1 k_{-3}^{***}) p_1 - k_2 k_{-1}^{***} p_2 - k_3 k_{-1}^{***} p_3 \right] \tag{18}$$

$$\theta_0 = \frac{k_{-1} + k_{-2} K_{12} + k_{-3} K_{13}}{(1 + K_{12} + K_{13}) \Sigma k_i p_i + k_{-1} + k_{-2} K_{12} + k_{-3} K_{13}} \tag{19}$$

and

$$k_{-1}^{***} \equiv k_{-1} (k_{-1} + k_{-2} K_{12} + k_{-3} K_{13})^{-1} \tag{20}$$

$$k_{-2}^{***} \equiv k_{-2} K_{12} (k_{-1} + k_{-2} K_{12} + k_{-3} K_{13})^{-1} \tag{21}$$

$$k_{-3}^{***} \equiv k_{-3} K_{13} (k_{-1} + k_{-2} K_{12} + k_{-3} K_{13})^{-1} \tag{22}$$

considering that $K_{ij} = 1/K_{ji}$ and $K_{ik}/K_{jk} = K_{ij}$, if the numerators and denominators of (19)—(22) are divided by any optional K_{ij}, equivalent expressions are obtained.

(k_i is the adsorption rate constant of i;
k_{-i} is the desorption rate constant of i;
K_{ij} is the equilibrium constant of the surface reaction [i] → [j]).

In case *III-ads:*

$$r_1 = [(k_1 k_{-2}^{***} + k_1 k_{-3}^{***})\, p_1 - k_2 k_{-1}^{***} p_2 - k_3 k_{-1}^{***} p_3] \tag{23}$$

In case *III-des:*

$$r_1 = \frac{[(k_1 k_{-2} K_{12} + k_1 k_{-3} K_{13})\, y_1 - k_2 k_{-1} y_2 - k_3 k_{-1} y_3]}{(1 + K_{12} + K_{13}) \Sigma k_i y_i} \tag{24}$$

which naturally can be transcribed in the sense of what was said after (22). r_2 and r_3 can be obtained from Eqs. (18), (23) and (24) by altering the indices according to the cycle $\begin{matrix} & 1 & \\ \nearrow & & \searrow \\ 3 & \leftarrow & 2 \end{matrix}$.

In case *IV-r* (general indexing is not possible here):

$$r_1 = \theta_0 \left(k_{YX} K_1 p_1 - k_{XY} \frac{k_2}{k_{-2} + k_{-3}} p_2 - k_{XY} \frac{k_3}{k_{-2} + k_{-3}} p_3 \right) \tag{25}$$

since the adsorption equilibrium has set in, components 2 and 3 are also permanently equilibrated through X:

$$r_2 = K'_{32}\, r_3 = \frac{1}{1 + K'_{23}}\, \theta_0 \,(k_{XY} K_j p_j - k_{YX} K_1 p_1) \tag{26}$$

that is

$$\frac{k_2 p_2 + k_3 p_3}{k_{-2} + k_{-3}} = K_j p_j \tag{27}$$

$$\theta_0 = \frac{1}{1 + K_1 p_1 + K_j p_j} \tag{28}$$

(k_{XY}, k_{YX} are the rate constants of the surface reaction according to scheme IV in Fig. 1;
K_1, K_j are adsorption equilibrium constants; $j = 2, 3$;
K'_{32}, K'_{23} are equilibrium constants of the overall transformations ③ → ② and ② → ③).

In case *IV-r*$_0$*:*

$$r_1 = (k_{XY} K_1 p - k_{XY} K_j p_j) \tag{29}$$

$$r_2 = K'_{32}\, r_3 = \frac{1}{1 + K'_{23}} (k_{XY} K_j p_j - k_{YX} K_1 p_1) \tag{30}$$

In case *IV-r*$_1$:

$$r_1 = \frac{(k_{YX} K_1 y_1 - k_{XY} K_j y_j)}{K_1 y_1 + K_j y_j} \tag{31}$$

$$r_2 = K'_{32} r_3 = \frac{1}{1 + K'_{23}} \frac{(k_{XY} K_j y_j - k_{YX} K_1 y_1)}{K_1 y_1 + K_j y_j} \tag{32}$$

In case *IV-s* (general indexing is not possible here):

$$r_1 = \theta_0 [(k_1 k^{**}_{-2} + k_1 k^{**}_{-3}) p_1 - k_2 k^{**}_{-1} p_2 - k_3 k^{**}_{-1} p_3] \tag{33}$$

$$\theta_0 = \frac{k_{-1} + k_{-2} K_{YX} + k_{-3} K_{YX}}{(1 + K_{XY}) \Sigma k_i p_i + k_{-1} + k_{-2} K_{YX} + k_{-3} K_{YX}} \tag{34}$$

and $k^{**}_{-1} \equiv k_{-1}(k_{-1} + k_{-2} K_{YX} + k_{-3} K_{YX})^{-1}$ (35)

$$k^{**}_{-2} \equiv k_{-2} K_{YX}(k_{-1} + k_{-2} K_{YX} + k_{-3} K_{YX})^{-1} \tag{36}$$

$$k^{**}_{-3} \equiv k_{-3} K_{YX}(k_{-1} + k_{-2} K_{YX} + k_{-3} K_{YX})^{-1} \tag{37}$$

since $K_{XY} = 1/K_{YX}$, on dividing by K_{YX} the equivalent expressions of (34)—(37) are obtained

(k_i is the adsorption rate constant of i;
k_{-i} is the desorption rate constant of i;
K_{XY} is the equilibrium constant of the surface reaction $|X| \rightarrow |Y|$).

In case *IV-ads:*

$$r_1 = [(k_1 k^{**}_{-2} + k_1 k^{**}_{-3}) p_1 - k_2 k^{**}_{-1} p_2 - k_3 k^{**}_{-1} p_3)] \tag{38}$$

In case *IV-des:*

$$r_2 = \frac{[(k_1 k_{-2} K_{YX} + k_1 k_{-3} K_{YX}) y_1 - k_2 k_{-1} y_2 - k_3 k_{-1} y_3]}{(1 + K_{YX}) \Sigma k_i y_i} \tag{39}$$

r_2 and r_3 can be obtained from Eqs (33), (38) and (39) by changing the index-numbers according to the cycle $\begin{matrix} & 1 & \\ \nearrow & & \searrow \\ 3 & \leftarrow & 2 \end{matrix}$.

In case *V-s* (the general indices have been disregarded in order to simplify comparison with cases *III-s* and *IV-s*):

$$r_1 = \theta_0[(k_1k^*_{-2} + k_1k^*_{-3})p_1 - k_2k^*_{-1}p_2 - k_3k^*_{-1}p_3] \tag{40}$$

$$\theta_0 = \frac{\Sigma k_{-i}}{\Sigma k_i p_i + \Sigma k_{-i}} \tag{41}$$

and the probability of desorption of the common intermediate to i is

$$k^*_{-i} \equiv \frac{k_{-i}}{\Sigma k_{-i}} \tag{42}$$

(k_i is the adsorption rate constant of i;
k_{-i} is the desorption rate constant of i).

In case *V-ads:*

$$r_1 = [(k_1k^*_{-2} + k_1k^*_{-3})p_1 - k_2k^*_{-1}p_2 - k_3k^*_{-1}p_3)] \tag{43}$$

In case *V-des:*

$$r_1 = \frac{[(k_1 k_{-2} + k_1 k_{-3})y_1 - k_2 k_{-1} y_2 - k_3 k_{-1} y_3]}{\Sigma k_i y_i} \tag{44}$$

r_2 and r_3 can be obtained from Eqs (40), (43) and (44) by changing the index-numbers according to the cycle $\begin{matrix} & 1 & \\ \nearrow & & \searrow \\ 3 & \leftarrow & 2 \end{matrix}$.

It should be noted that the equations established for the simpler cases can be derived from those valid for the more involved cases by using appropriate simplifications. This compatibility confirms the correctness of the equations set up. Thus, *IV-r* can be derived from *III-r*, *IV-s* from *III-s* and *V-s* from *IV-s* (and all these from the rate equations deduced for scheme **III** if no rate determining step is involved).

3. Initial rate equations

Although the rate of the reaction may be obtained for any partial pressures with the use of the kinetic expressions given above (in so far as one or other of these reflect the correct mechanism), as a result of their complexity they are scarcely suitable for the calculation of the unknown constants from known partial pressures and reaction rates (at least in as much as this is possible at all in principle; see later at the end of this section).

Simpler expressions easier to evaluate, are obtained, if instead of the rate of disappearance of (*i*) in steady state, the initial rate of the overall transformation (*e*) → (*j*), r_{ij}^0 is regarded in steady state when the partial pressure of reactant is p_i^0 ($p_j = p_k = 0$). All the kinetic equations derived for the different cases can then be rearranged in linear form (see the symbols in the equations cited):

In case *I-r*, the rate of transformation of *i* is deduced from (2) as

$$\frac{1}{r_{ij}^0} = \frac{1}{k_{ij} K_{i,ij}} \left[\frac{1}{p_i^0} + (K_{i,ij} + K_{i,ik}) \right] \tag{45}$$

In case $I\text{-}r_0$ the second term can be neglected in comparison with the first:

$$r_{ij}^0 = k_{ij} K_{i,ij} p_i^0 \tag{46}$$

In case $I\text{-}r_1$ the first term can be neglected:

$$r_{ij}^0 = \frac{k_{ij} K_{i,ij}}{K_{i,ij} + K_{i,ik}} \tag{47}$$

In case *I-s*, from (6)

$$\frac{1}{r_{ij}^0} = \frac{k_{ji,j} K_{ij} + k_{ij,i}}{k_{i,ij} k_{ji,j} K_{ij}} \left[\frac{1}{p_i^0} + \frac{k_{i,ij}(1 + K_{ij})}{k_{ij,i} + k_{ji,j} K_{ij}} + \frac{k_{i,ik}(1 + K_{ik})}{k_{ik,i} + k_{ki,k} K_{ik}} \right] \tag{48}$$

In case *I-ads*, from (8)

$$r_{ij}^0 = k_{i,ij} \frac{k_{ji,j} K_{ij}}{k_{ji,j} K_{ij} + k_{ij,\,i}} p_i^0 \tag{49}$$

In case *I-des*, from (9)

$$r_{ij}^0 = [k_{i,ij} k_{ji,j} K_{ij} (k_{ki,k} K_{ik} + k_{ik,i})] \times [k_{i,ij}(k_{ki,k} K_{ik} + k_{ik,i})(1 + K_{ij}) + \\ + k_{i,ik}(k_{ji,j} K_{ij} + k_{ij,i})(1 + K_{ik})]^{-1} \tag{50}$$

In case *II-s*, from (10)

$$\frac{1}{r_{12}^0} = \left(\frac{1}{k_{1X}} \frac{k_{X1} + k_{X2}}{k_{X2}} \right) \left[\frac{1}{p_1^0} + \frac{k_{1X}}{k_{X1} + k_{X2}} + \frac{k_{1Z}}{k_{Z1} + k_{Z3}} \right] \tag{51}$$

In case *II-ads*, from (12)

$$r_{12}^0 = k_{1X} \frac{k_{X2}}{k_{X1} + k_{X2}} p_1^0 \tag{52}$$

In case *II-des*, from (13)

$$r_{12}^0 = \frac{k_{1X}\, k_{X2}\, (k_{Z3} + k_{Z1})}{k_{1X}\, (k_{Z3} + k_{Z1}) + k_{1Z}\, (k_{X1} + k_{X2})} \tag{53}$$

In case *III-r*, from (14)

$$\frac{1}{r_{ij}^0} = \frac{1}{k_{ij}\, K_i}\, \frac{1}{p_i^0} + \frac{1}{k_{ij}} = \frac{1}{k_{ij}\, K_i} \left[\frac{1}{p_i^0} + K_i \right] \tag{54}$$

In case *III-r*$_0$, from (16)

$$r_{ij}^0 = k_{ij}\, K_i\, p_i^0 \tag{55}$$

In case *III-r*$_1$, from (17)

$$r_{ij}^0 = k_{ij} \tag{56}$$

In case *III-s*, from (18)

$$\frac{1}{r_{12}^0} = \frac{k_{-1} + k_{-2}\, K_{12} + k_{-3}\, K_{13}}{k_1\, k_{-2}\, K_{12}} \left[\frac{1}{p_1^0} + \frac{k_1 (1 + K_{12} + K_{13})}{k_{-1} + k_{-2}\, K_{12} + k_{-3}\, K_{13}} \right] \tag{57}$$

In case *III-ads*, from (23)

$$r_{12}^0 = k_1\, k_{-2}^{***}\, p_1^0 \tag{58}$$

In case *III-des*, from (24)

$$r_{12}^0 = \frac{k_{-2}\, K_{12}}{1 + K_{12} + K_{13}} \tag{59}$$

In case *IV-r*, from (25) because of the established equilibrium ② ⇄ ③

$$\frac{1}{r_{12}^0} = \frac{1 + K'_{23}}{k_{YX}\, K_1} \left[\frac{1}{p_1^0} + K_1 \right] \tag{60}$$

while

$$-\frac{1}{r_1^0} = \frac{1}{k_{XY}\, K_j} \left[\frac{1}{p_j} + K_j \right] \text{ if } p_1 = 0$$

$$(j = 2,\ 3 \text{ and } p_2 = K'_{32} p_3 \text{ and } K_2 = K'_{23} K_3)$$

In case *IV-r*$_0$, from (29)

$$r_{12}^0 = \frac{k_{YX}\, K_1}{1 + K'_{23}}\, p_1^0, \quad -r_1^0 = k_{XY}\, K_j\, p_j \text{ if } p_1 = 0 \tag{61}$$

In case *IV-r*$_1$, from (31)

$$r_{12}^0 = \frac{k_{YX}}{1 + K'_{23}}, \quad -r_1^0 = k_{XY} \text{ if } p_1 = 0 \tag{62}$$

In case *IV-s*, from (33)

$$\frac{1}{r_{12}^0} = \frac{k_{-1} + k_{-2} K_{YX} + k_{-3} K_{YX}}{k_1 k_{-2} K_{YX}} \left[\frac{1}{p_1^0} + \frac{k_1(1 + K_{YX})}{k_{-1} + k_{-2} K_{YX} + k_{-3} K_{YX}} \right] \tag{63}$$

In case *IV-ads*, from (38)

$$r_{12}^0 = k_1 k_{-2}^{**} p_1^0 \tag{64}$$

In case *IV-des*, from (39)

$$r_{12}^0 = \frac{k_{-2} K_{YX}}{1 + K_{YX}} \tag{65}$$

In case *V-s*, from (40)

$$\frac{1}{r_{ij}^0} = \frac{\Sigma k_{-i}}{k_i k_{-j}} \left[\frac{1}{p_i^0} + \frac{k_i}{\Sigma k_{-i}} \right] \tag{66}$$

In case *V-ads*, from (43)

$$r_{ij}^0 = k_i k_{-j}^* p_i^0 \tag{67}$$

In case *V-des*, from (44)

$$r_{ij}^0 = k_{-j} \tag{68}$$

From a consideration of Eqs (45)—(68) it is evident that they agree in form; that is, in the monomolecular, catalytic interconversion of 3 components the initial rate of transformation of pure component i into j can be given in the following general form:

$$\frac{1}{r_{ij}^0} = m_{ij} \left[\frac{1}{p_i^0} + b_i \right] \tag{69}$$

or in the more usual form of rate equations of catalytic transformations

$$r_{ij}^0 = \frac{\frac{1}{m_{ij}} p_i^0}{1 + b_i p_i^0} \tag{69/a}$$

where m_{ij} and b_i are the quantities characteristic of the transformation concerned. Their values can be determined from the experimentally measured r_{ij}^0 and p_i^0 pairs with the help of the linear relation

$$\frac{1}{r_{ij}^0} = m_{ij} \frac{1}{p_i^0} + b_{ij} \tag{69/b}$$

where

$$b_{ij} \equiv m_{ij} b_i \tag{70}$$

and so, of necessity,

$$\frac{m_{ij}}{m_{ik}} = \frac{b_{ij}}{b_{ik}} \tag{71}$$

Only in the range of medium coverages is there a possibility of the simultaneous calculation of the two constants in (69/b). In the case of small coverages (in cases r_0 and *ads*) $p_i^0 \to 0$ and so $m_{ij}/p_i^0 \gg b_{ij}$, and in the case of large coverages (in cases r_1 and *des*) $p_i^0 \to \infty$, when $m_{ij}/p_i^0 \ll b_{ij}$; in the former case it is only possible to determine m_{ij}, and in the latter case only b_{ij}.

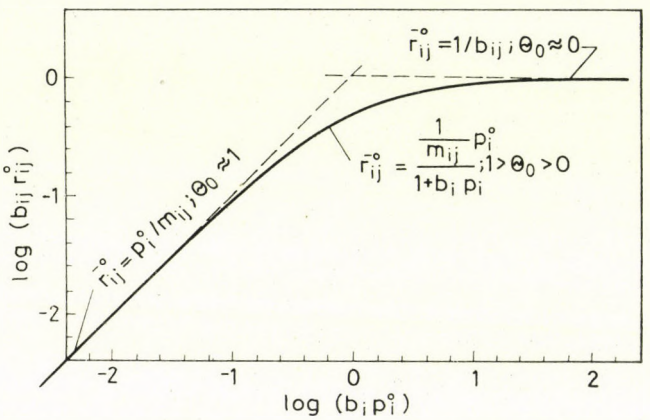

Fig. 2. General form of the pressure function of the initial overall conversion rate $r_{ij}^0 = \frac{1}{m_{ij}} p_i^{\nu}(1 + b_i\, p_i^0)^{-1}$, normalized for the maximum rate ($p_i^0 \to \infty$, $r_{ij}^0 \to 1/m_{ij}\, b_i = 1/b_{ij}$)

By rearranging (69/a) and substituting for m_{ij} according to (70), the function of the general form

$$b_{ij}\, r_{ij}^0 = \frac{b_i\, p_i^0}{1 + b_i\, p_i^0} \tag{72}$$

is obtained, with dimensionless variables; its plot is shown in Fig. 2. In the logarithmic scale it can be well perceived that for a given system (substrate, catalyst, temperature) there exists an interval of about two orders of magnitude, within which the pressure may vary so that both m_{ij} and b_{ij} could be determined, while in the range $\theta_0 \approx 1$ and in the range $\theta_0 \approx 0$ only m_{ij} or b_{ij}, respectively, can be calculated.

For the constants m of the forward and reverse transformations, it holds that

$$\frac{m_{ij}}{m_{ji}} = K'_{ji} \tag{73}$$

(K'_{ji} is the equilibrium constant of the overall transformation $(-) \to (i)$), which must be taken into account in their determination according to (69/b) for

greater accuracy [we pass over the proof of (73)]. However, the initial selectivity is given by the ratio of the constants m of the parallel transformations:

$$\frac{m_{ij}}{m_{ik}} = \frac{r^0_{ik}}{r^0_{ij}} \tag{74}$$

as can easily be seen from (69).

Nevertheless, a problem arises from the fact that, even if the determination of the quantities m_{ij} and b_{ij} is successful, in some of the kinetic cases presented we do not obtain a sufficient number of independent equations for the calculation of every unknown constant. [It should be noted that the determination of six b_{ij} values using substitution (70) in fact means a knowledge of only three b_i values.]

In *I-r*, 6 adsorption equilibrium constants and 6 surface reaction rate constants, *i.e.* 12 unknowns, should be determined from 6 m_{ij} and 3 b_i values, *i.e.* from 9 independent equations;

In *I-s*, 6 adsorption and 6 desorption rate constants and 3 surface reaction equilibrium constants, *i.e.* 15 unknowns, should be determined from 6 m_{ij} and 3 b_i values, *i.e.* from 9 independent equations;

In *II-s*, 6 adsorption and 6 desorption rate constants, *i.e.* 12 unknowns, must be determined from 6 m_{ij} and 3 b_i values, bearing in mind that the sum of the desorption probabilities $\left(e.g.\ \dot{k}_{X1} \equiv \frac{k_{X1}}{k_{X1} + k_{X2}}\right)$ is equal to unity ($e.g.\ \dot{k}_{X1} + \dot{k}_{X2} = 1$) and that this results in further 3 independent equations (for the desorptions of X, Y and Z), *i.e.* from 12 independent equations;

In *III-r*, 3 adsorption equilibrium constants and 5 independent rate constants of the triangular surface reaction ($K_{12}K_{23}K_{31} = 1 = k_{12}/k_{21}\ k_{23}/k_{32}\ k_{31}/k_{13}$ and hence five k_{ij} values determine the sixth), *i.e.* 8 unknowns, must be determined from 6 m_{ij} and 3 b_i values, *i.e.* from 9 independent equations;

In *III-s*, 3 adsorption and 3 desorption rate constants and 2 surface reaction equilibrium constants (as in *III-r* this determines the third), *i.e.* 8 unknowns, should be determined from 6 m_{ij} and 3 b_i values, *i.e.* from 9 independent equations; the unknown equilibrium constants K_{ij}, however, cannot be separated;

In *IV-r*, 2 adsorption equilibrium constants and 2 rate constants of the surface reaction, *i.e.* 4 unknowns, must be determined from 2 m_{ij} and 2 b_i values, *i.e.* from 4 independent equations;

In *IV-s*, 3 adsorption and 3 desorption rate constants and 1 surface reaction equilibrium constant, *i.e.* 7 unknowns, should be determined from 6 m_{ij} and 3 b_i values, *i.e.* from 9 independent equations; the unknown equilibrium constant K_{YX}, however, is not separable;

In *V-s*, 3 adsorption and 3 desorption rate constants, *i.e.* 6 unknowns, must be determined from 6 m_{ij} and 3 b_i values, *i.e.* from 9 independent equations.

4. Possibilities of determining the reaction mechanism by kinetic methods

The elucidation of the mechanism by kinetic methods is restricted by the agreement between the kinetic equations which are valid for individual mechanisms. The consequences of this are as follows.

(a) The similarity between the initial rate equations deduced for the various transformation schemes above is striking [see general equations (69) and (69/a), and the criteria for their constants in (73) and (74)].

(b) No difference can be revealed from the relative change of the composition of the reacting mixture, with the exception of the special requirements in cases *IV-r* to which we shall return later. The differential equation of this composition change

$$\frac{dy_i}{dy_j} = f(y_i, y_j) \tag{75}$$

can be given as the quotient of two kinetic equations r_i/r_j [5]. These differential equations can thus be obtained from the derived kinetic equations [(1), (2), (4), (5), (6), (8), (9), (10), (12), (13), (14), (16), (17), (18), (23), (24), (33), (38), (39), (40), (43), (44)]. On the formation of the quotient, θ_0 and the common denominators (if there are any) of the kinetic equations are eliminated, and the partial pressures can be simply substituted by the corresponding mole fractions y [5] (for $\theta_0 = 0$ these appear already). The obtained relations are formally and thus experimentally indistinguishably identical for each of the reaction schemes studied, whatever the rate-determining process, *viz.*

$$\frac{dy_i}{dy_j} = \frac{\frac{1}{m_{ij}}(y_i - K'_{ji}y_i) + \frac{1}{m_{ki}}\left[y_i(K'_{ik}+1) + y_j - 1\right]}{\frac{1}{m_{ij}}(K'_{ji}y_j - y_i) + \frac{1}{m_{jk}}\left[y_j(K'_{kj}+1) + K'_{kj}y_i - K'_{kj}\right]} \tag{76}$$

if (73) and the relation $\sum_1^3 y_i = 1$ are taken into account; with the substitution $1/m_{ij} = k_{ij}$, however, (76) agrees with that relation which can be obtained from (1) for the phenomenological triangular scheme. Including cases *IV-r-r*$_1$-*r*$_0$ the pressure independence of the relative change of composition, which was observed experimentally (see an example in Fig. 3), follows from these differential equations.

As a check on the determination of the parameter m_{ij} reported in section 3, its relative values related to some m_{jk} can be approximately calculated with relatively high accuracy from the experimentally measured $y_i = f(y_j)$ curves [6] by numerical integration of (76). In the case of large coverages, however, when m_{ij} cannot be determined and therefore it is possible to cal-

culate fewer kinetic constants only, valuable data may thus be obtained (*e.g.* in *III*-r_1 the relative equilibrium constants may be determined, and in *V-des* the relative values of the adsorption rate constants).

(c) In addition, a common feature of each of the transformation schemes studied is that at small total pressure, when the coverages are low, the transformations are of first order in the entire conversion range [see (4) and (8) for *I*; (12) for *II*; (16) and (23) for *III*; (29) and (30) for *IV*; and (43) for *V*]; in the region of higher pressures, where the coverage is no longer negligibly small, because of the pressure dependence of θ_0 this does not hold any more:

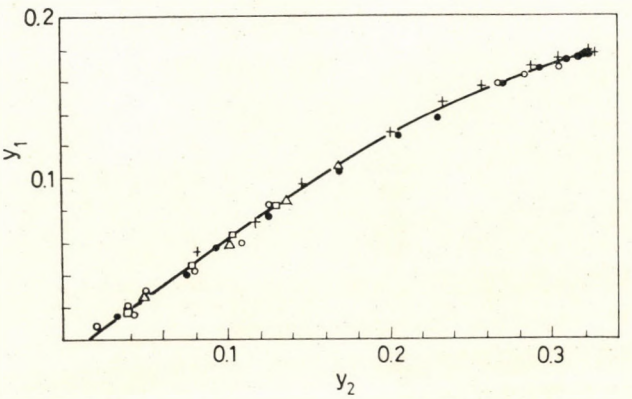

Fig. 3. Relative change of composition during the isomerization of *trans*-2-butene at 250°C on H form of clinoptilolite; y_1 : 1-butene; y_2 : *cis*-2-butene; + 70 torr, ○ 120 torr, △ 130 torr, □ 215 torr, ● 560 torr

the transformation rates are apparently proportional to the total pressure to a power less than unity. When total coverage is attained, the transformation rates depend only on the composition and not on the pressure [see (5) and (9) for *I*; (13) for *II*; (17) and (24) for *III*; (31), (32) and (39) for *IV*; and (44) for *V*]. Thus, rate equation (1) given in the introduction can strictly never be correct (except in the range $\theta_0 \approx 1$), since the composition dependence of the rate is more complicated than it is expressed by Eq. (1).

Despite such comprehensive similarity of the kinetics fundamental differences can be revealed.

Although the transformation always seems formally to be a triangular reaction, the kinetic cases can be classified into two main groups *on the basis of the mechanisms* describing the catalytic transformation: in the one it is observable in principle that the elementary steps of the transformation follow each other according to the triangular scheme, while in the other in principle it can only be observed that the transformation occurs *via* some common intermediate, that is, according to an Y scheme.

It can easily be seen that the *catalytic* transformation follows the triangular scheme in all cases of schemes *I* and *II*, and in cases *III-r*, *III-r*$_0$, and *III-r*$_1$; cases *III-s*, *III-ads*, *III-des*, *IV-s*, *IV-ads*, *IV-des*, *V-s*, *V-ads* and *V-des* are characterized by an Y scheme mechanism, while *IV-r*, *IV-r*$_0$ and *IV-r*$_1$ are the special cases of the Y scheme when the transformation occurs *via* the rate-determining reaction of two surface intermediates. As a result of the established sorption equilibria, two gas phase components are always in equilibrium with each other *via* their intermediate, *i.e.* $p_k/p_j = K'_{jk}$

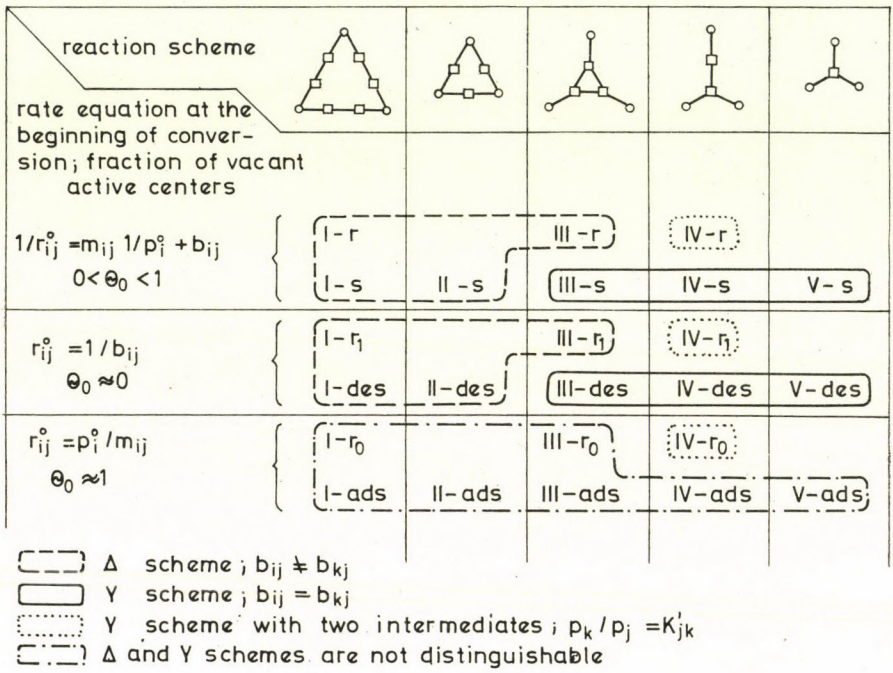

Fig. 4. Reaction mechanisms distinguishable by kinetic methods; the cases within the same borders are kinetically identical, and the groups are unambiguously separable from each other (for the designations of the kinetic cases in the grouping according to Fig. 1, see at the beginning of section 2)

(this is a special requirement of the *IV-r* cases, which was mentioned earlier, and therefore the transformation can be regarded as a particular case of the formal triangular reaction).

It is possible to draw conclusions on the mechanism according to the triangular scheme in the range of medium coverages, *i.e.* in cases *I-r*, *I-s*, *II-s* and *III-r*, and also for large coverages, *i.e.* in cases *I-r*$_1$, *II-des* and *III-r*$_1$, when $b_{ij} \neq b_{kj}$ in Eqs (69/b) [see the term(*s*) not containing $1/p_i^0$ on the right side of Eq. (45) for *I-r*, and *I-r*$_1$, of (48) for *I-s* and *I-des*, of (51) for *II-s* and *II-des*, and of (54) for *III-r*, and *III-r*$_1$].

The mechanism according to the Y scheme can be demonstrated for medium coverages, *i.e.* in cases *III-s*, *IV-s* and *V-s*, and for large coverages in cases *III-des*, *IV-des* and *V-des*; then in (69/b) $b_{ij} = b_{kj}$, which can be ascertained from the equations reported in section 3. At the same time, however, it is not possible to decide on kinetic grounds alone whether the process proceeds *via* a single common intermediate or *via* a mixture of two or three surface intermediates in equilibrium, since the equilibrium constants of the surface reactions in these equations cannot be separated [see the term not containing $1/p_i^0$ on the right hand side of Eq. (57) for *III-s* and *III-des*, of (63) for *IV-s* and *IV-des*, and of (66) for *V-s* and *V-des*].

In the range of low coverages the triangular and Y schemes become indistinguishable. Under such circumstances it is helpful if a medium coverage can be attained by decreasing the temperature or by increasing the pressure, when the question can be decided; the results can then be evaluated accordingly.

All the above groupings are given in Fig. 4, together with the direct possibilities and theoretical limits of the kinetic elucidation of the mechanism. Within the individual groups (except for the cases relating to the Y scheme) further differences may be made from an examination of the reality of the determinable kinetic constants (*e.g.* the investigation of temperature dependence).

These findings will be used in the evaluation of the experimental results in our further work.

REFERENCES

1. HAAG, W. O., PINES, H.: J. Am. Chem. Soc. **82,** 387, 2488 (1960)
2. KALLÓ, D., SCHAY, G.: Acta Chim. Acad. Sci. Hung. **39,** 183 (1963)
3. HIGHTOWER, J. W., HALL, W. K.: J. Phys. Chem. **71,** 1014 (1967)
4. AMENOMYA, Q., CVETANOVIC, R. J.: Can. J. Chem. **40,** 2130 (1962)
5. KALLÓ, D.: Acta Chim. Acad. Sci. Hung. **57,** 313 (1968)
6. KALLÓ, D., PRESZLER, I., SCHAY, G.: Acta Chim. Acad. Sci. Hung. **64,** 211 (1970)
7. FORNI, L., ZANDERIGHI, L., CARRA, S.: J. Catalysis **12,** 298 (1968)

Dénes KALLÓ
Emil DETREKŐY
Géza SCHAY
Budapest II., Pusztaszeri út 57—69.

Acta Chimica Academiae Scientiarum Hungaricae, Tomus 72 (2), pp. 209—212 (1972)

A METHOD FOR THE DETERMINATION OF HYDROGEN ADSORPTION ON PALLADIUM ELECTRODES

(SHORT COMMUNICATION)

I. TELCS

(Central Research Institute for Chemistry of the Hungarian Academy of Sciences)

Received April 15, 1971

In contrast to the platinum electrode on which hydrogen adsorption has been investigated in detail, on the palladium electrode hydrogen adsorption has, to our knowledge, only been determined indirectly [1] by taking charging curves in an indifferent electrolyte and in the presence of halogenide ions. The difference between the two charging curves was regarded as the charging curve of hydrogen adsorption on the assumption that in the presence of an adequate halogenide ion concentration hydrogen adsorption is practically suppressed. This indirect method was chosen because of the important amount of hydrogen dissolved in palladium in the range between 60 to 400 mV, masking adsorption. Determination of hydrogen adsorption by a less indirect method seemed desirable.

The idea is as follows. At a given potential the amount of hydrogen adsorbed is proportional to the surface area, the amount dissolved to the volume of palladium. The ratio of surface area/volume of the palladium specimen is a function of the particle size. If hydrogen sorption is determined on a specimen of known surface area/volume ratio, the amounts adsorbed and dissolved can be determined by a simple calculation. The volume of palladium can be determined from the amount of hydrogen contained in β phase Pd—H, as the possible change of adsorption in the narrow potential range of phase transformation will be entirely negligible besides the large amount of dissolved hydrogen. The surface area of palladium can be determined from measurements of oxygen adsorption.

Measurements were carried out in a usual three-compartment cell in N $HClO_4$ solution, the electrodes being platinum wires on which palladium black was deposited at varying current densities and lengths of time. The amounts of palladium were so chosen that the hydrogen and oxygen adsorption capacities of the supporting platinum were negligible. Each measurement was started by setting the electrode potentiostatically to 1450 mV as referred to the rhe, until the passage of current practically ceased. Subsequently a constant negative current was applied to the electrode and the change of potential with time recorded. The three characteristic portions of the charging

curve, oxygen desorption, charging of the α phase of the Pd—H system and the assumed parallel hydrogen adsorption capacity and finally charging of the β phase were taken at different current intensities according to convenience.

In Fig. 1 the three characteristic sections of the charging curve of a typical palladium electrode are plotted together, the time coordinate restarted from 0 at the outset of each section. The charge of adsorbed oxygen (O_a) and of hydrogen absorbed in the β phase transformation (H_β) were determined from the product of the intervals between the intersections of the tangents of the respective parts of the charging curve and the corresponding currents. The sum of the charges of hydrogen absorbed in the α phase (H_α) and of hydrogen adsorbed simultaneously (H_a) was determined in 20 mV intervals in an analogous way, subtracting the charge of the double layer represented by the extension of the tangent of the corresponding section of the charging curve between about 400 and 700 mV.

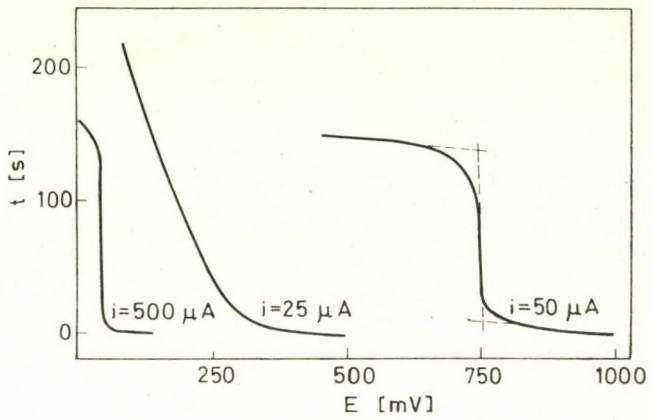

Fig. 1

The result of measurements of 10 specimens are tabulated. The separation of hydrogen adsorption and absorption is carried out according to the following equation. $H(E) = H_a(E) + H_\alpha(E) = a(E)O_a + \alpha(E)H_\beta = [a(E)_\gamma + a(E)]H_\beta$ where the symbols in capitals denote charges while (E) means that the given quantity is a function of potential. The factors

$$a\,(E) = \frac{H_a\,(E)}{O_a} \text{ and } \alpha\,(E) = \frac{H_\alpha\,(E)}{H_\beta}$$

are assumed to be independent of the nature of the specimen and depend on potential only, while

$$\gamma = \frac{O_a}{H_\beta},$$

Table I

Specimen	$H\beta$	O_a	H(E) E [mV] 80	100	120	140	160	180	200	220
1	90	1.77	6.3	4.5	3.45	2.7	2.15	1.75	1.35	1.05
2	90	1.64	6.0	4.35	3.3	2.6	2.1	1.7	1.3	1.05
3	74.5	5.85	7.8	5.8	4.65	2.85	3.15	2.55	2.05	1.6
4	74.5	5.55	7.45	5.6	4.5	3.75	3.1	2.5	2.0	1.6
5	72.5	6.10	9.35	6.7	5.1	4.1	3.25	2.55	1.9	1.3
6	78.5	5.95	9.2	6.9	5.45	4.55	3.65	2.85	2.1	1.4
7	78.0	8.85	10.2	7.75	6.3	5.25	4.2	3.3	2.35	1.6
8	78.0	8.25	8.6	6.45	5.1	4.15	3.3	2.5	1.7	1.1
9	68.5	8.35	9.3	7.15	5.95	4.95	4.1	3.3	2.55	1.95
10	68.5	8.35	8.8	6.75	5.6	4.7	3.75	3.15	2.35	1.75

the ratio of surface area/volume is different for each specimen. a(E) and α(E) can be determined if two specimens with different γ are available, while further specimens may serve as a check. This check showed the best agreement for specimens 1, 3 and 10 with values of γ of 0.0197, 0.079 and 0.122, respectively.

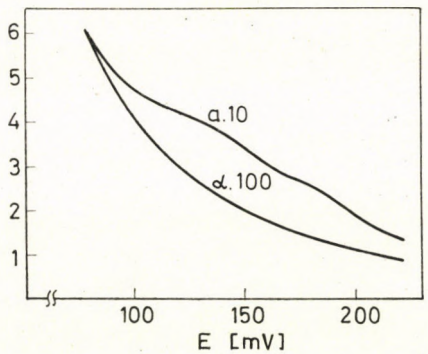

Fig. 2

In Fig. 2 a and α determined in the above way are plotted. As may be seen, the course of a, the charging curve of hydrogen adsorption resembles that of platinum both in quality and amount. The wavyness of the curve, though also resembling that of platinum, cannot be taken as significant because of the small number of points measured and the general uncertainty of the determination. The finer details of the hydrogen charging curve of platinum

are known from measurements of differential capacity. The method outlined here is, in principle, also applicable to measurements of differential capacity on palladium. Such measurements, however, have not been carried out so far because of technical difficulties.

REFERENCE

1. VERT, ZH. L., MOSEVICH, I. A., TVERDOVSKY, I. P.: Dokl. A.N. S.S.S.R. **140,** 149 (1961)

Iván TELCS; Budapest II., Pusztaszeri út 59—67.

Acta Chimica Academiae Scientiarum Hungaricae, Tomus 72 (2), pp. 213—220 (1972)

PREPARATION OF 2,3-DIHYDRO-4*H*-1,3-BENZOTHIAZINE DERIVATIVES*

J. SZABÓ, I. VARGA, E. VINKLER and É. BARTHOS

(Department for Pharmaceutical Chemistry, Medical University, Szeged)

Received June 12, 1970

The condensation of 2-mercaptobenzylamine and its derivatives with oxo compounds in alkaline medium gives 2,3-dihydro-4*H*-1,3-benzothiazine derivatives. The procedure described is a new method for the preparation of 2,3-dihydro-4*H*-1,3-benzothiazine derivatives.

The syntheses of various oxo-, thione- and imino derivatives of 2,3-dihydro-4*H*-1,3-benzothiazine have been described in several papers [2—27]. However, the preparation of 2,3-dihydro-4*H*-1,3-benzothiazine derivatives containing no oxo-, thione- or imino groups has only recently been achieved.

BOURGOIN-LEGNAY and BOUDET [28] obtained 2,3-dihydro-2-phenyl-4*H*-1,3-benzothiazine by means of the lithium aluminium hydride reduction of 4-oxo-2,3-dihydro-2-phenyl-4*H*-1,3-benzothiazine. SZABÓ, VARGA and VINKLER [29] prepared different 2-aryl- and 2-aryl-3-alkyl-2,3-dihydro-4*H*-1,3-benzothiazine derivatives by the reduction of 2-aryl-4*H*-1,3-benzothiazine derivatives and 2-aryl-3-alkyl-4*H*-1,3-benzothiazinium bromides with zinc in acid medium. 4,5-Dimethoxy-2-mercaptobenzyl ammonium chloride [30] (**I**), N-ethyl-4,5-dimethoxymercaptobenzyl ammonium bromide [31] (**IV**) and 2-mercaptobenzyl ammonium chloride [32], being bidentate compounds, seemed to be suitable starting materials for the preparation of 2,3-dihydro-4*H*-1,3-benzothiazine derivatives in condensation reactions with oxo compounds.

At first, 4,5-dimethoxy-2-mercaptobenzyl ammonium chloride (**I**) was condensed with formaldehyde. In this case, even if the stoichiometrically required amount of formaldehyde was applied, 3,3'-methylene-bis(2,3-dihydro-6,7-dimethoxy-4*H*-1,3-benzothiazine) (**III**) was obtained instead of the expected 2,3-dihydro-6,7-dimethoxy-4*H*-1,3-benzothiazine (**II**). Most probably, compound **II** is immediately condensed with formaldehyde to give the methylene-bis-derivative (**III**).

* Partly presented on the meeting of the Organic Chemical Committee of the Hungarian Academy of Sciences, February 22, 1966. [1]

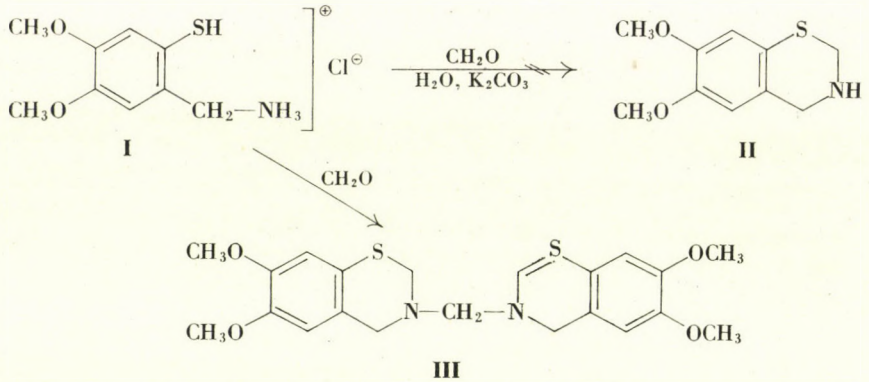

I II III

This assumption is supported by the reaction of N-(ethyl)-4,5-dimethoxy-2-mercaptobenzyl ammonium bromide (**IV**) with formaldehyde, resulting in the expected compound, 3-ethyl-6,7-dimethoxy-2,3-dihydro-4*H*-1,3-benzothiazine (**V**).

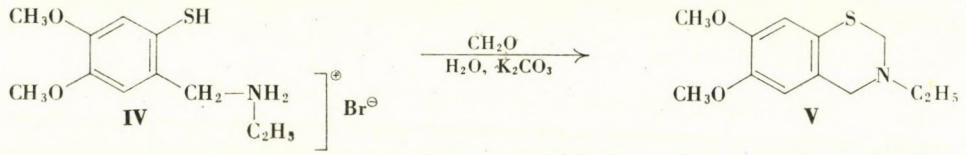

IV V

Here, the tertiary nitrogen atom of compound **V** is unable to undergo further condensation reactions. The formation of **III** is in accordance with the 1,3-benzoxazine cyclization reaction of 2-hydroxybenzylamine with formaldehyde, studied by HOLLY and COPE [33].

The structures of compounds **III** and **V** have been verified by their NMR spectra, in addition to the elemental analyses and molecular weight determinations (Figs 1 and 2).

δ 3.45 (NCH_2N, bridge, 1H); δ 4.60 ($ArCH_2N$, 2*H*—4); δ 3.97 (SCH_2N, 2H—2); δ 6.55 (ArH, 1H—5); δ 6.67 (ArH, 1H—8); δ 3.70 (OCH_3, 6H—6, 7);

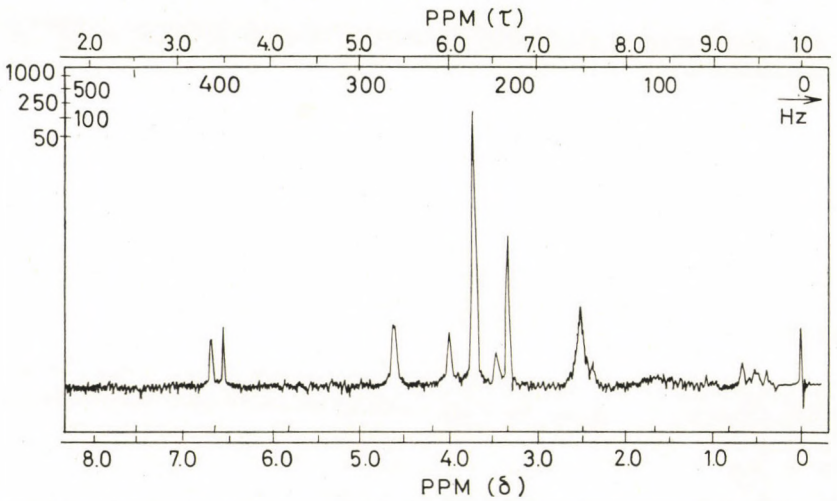

Fig. 1. NMR spectrum of 3,3'-methylene-bis(2,3-dihydro-6,7-dimethoxy-4*H*-1,3-benzothiazine) in DMSO-d_6

δ 1.09 (CH_3, triplet, ethyl, 3H); δ 4.55 ($ArCH_2N$, 2H-4); δ 3.90 (SCH_2N, 2H-2); δ 6.55 (ArH, 1H-5); δ 6.68 (ArH, 1H-8); δ 3.72 (OCH_3, 6H-6, 7); the δ CH_2 signal is fused with the absorption of the solvent (DMSO-d_6)

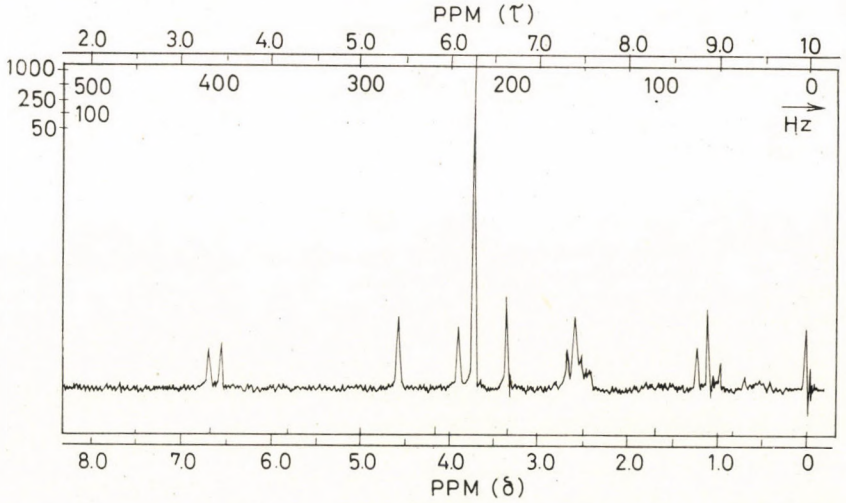

Fig. 2. The NMR spectrum of 3-ethyl-6,7-dimethoxy-2,3-dihydro-4*H*-1,3-benzothiazine in DMSO-d_6

4,5-Dimethoxy-2-mercaptobenzyl ammonium chloride (**I**) and 2-mercaptobenzyl ammonium chloride were successfully condensed with both aliphatic and aromatic aldehydes and ketones, resulting in 2,3-dihydro-4*H*-1,3-benzothiazine derivatives (**VIa**—**h**).

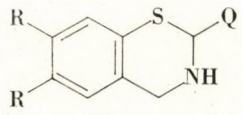

VI

a. R = OCH_3 Q = CH_3; **b.** R = OCH_3 Q = C_6H_5; **c.** R = H Q = C_6H_5; **d.** R = OCH_3 Q = 3,4—$(CH_3O)_2C_6H_3$; **e.** R = OCH_3 Q = 4—NC—C_6H_4; **f.** R = OCH_3 Q = 2-furyl; **g.** R = OCH_3 Q = $(CH_3)_2$; **h.** R = OCH_3 Q = $-CH_2(CH_2)_3-CH_2-$;

Of these derivatives compounds **VIb**, **VIc** and **VId** — also prepared by independent syntheses [29] — were in all respects indentical with the products obtained by reduction.

N-(Ethyl)-4,5-dimethoxy-2-mercaptobenzyl ammonium bromide (**IV**) was successfully converted with aromatic aldehydes in pyridine solutions to the

corresponding 3-ethyl-2,3-dihydro-4*H*-1,3-benzothiazine derivatives (**VIIa—f**). In this case the cyclization experiments failed with aliphatic aldehydes and ketones.

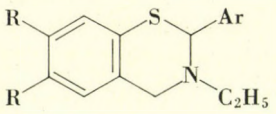

VII

a. R = OCH_3 Ar = C_6H_5; **b.** R = OCH_3 Ar = 3,4—$(CH_3O)_2C_6H_3$; **c.** R = OCH_3 Ar = 4—$(CH_3)_2N$—C_6H_4; **d.** R = OCH_3 Ar = 4—NC—C_6H_4; **e.** R = OCH_3 Ar = 4—$CH_3OC_6H_4$; **f.** R = OCH_3 Ar = 2-furyl

The NMR spectrum of compound **VIIa** is in agreement with the assumed structure (Fig. 3).

δ 1.09 (CH_3, triplet, ethyl, 3H, J=7 Hz); δ 3.81—3.83 ($ArCH_2N$, 2H—4); δ 5.88 (CH, 1H—2); δ 6.70 (ArH, 1H—5); δ 6.75 (ArH, 1H—8); δ 3.70, 3.75 (OCH_3, 6H—6, 7); δ Ph (5H) 430—460 Hz. The δ CH_2 signal is fused with the absorption of the solvent (DMSO—d_6).

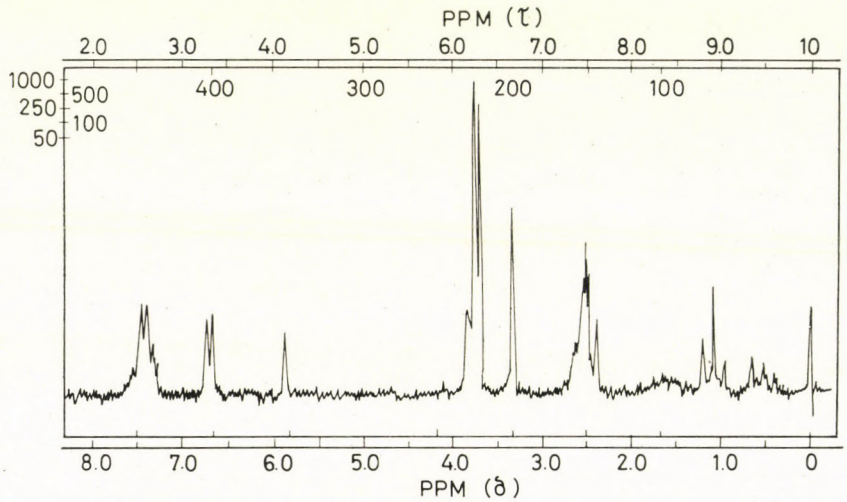

Fig. 3. The NMR spectrum of 2-phenyl-3-ethyl-6,7-dimethoxy-2,3-dihydro-4*H*-1,3-benzothiazine (m.p. 95—96°C) in DMSO-d_6

In the case of 2-phenyl-3-ethyl-6,7-dimethoxy-2,3-dihydro-4*H*-1,3-benzothiazine (**VIIa**), the existence of polymorphism was observed. Crystallization from ethanol resulted in two kinds of colourless radial needles melting at 81—82°C and 95—96°C, respectively. The structures of the two modifications were verified by the analytic data and their identical infrared spectra (Fig. 4).

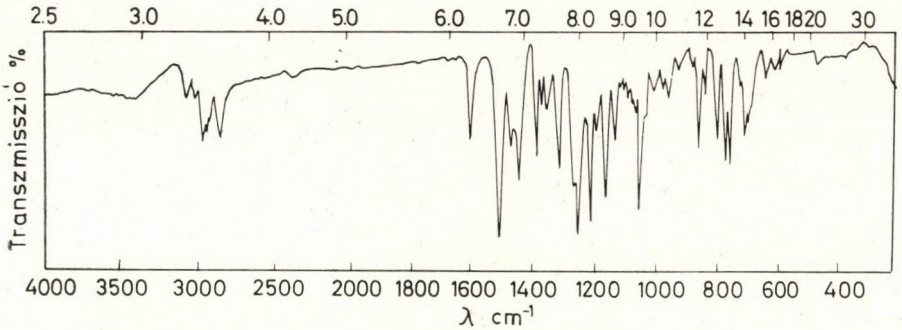

Fig. 4. The infrared spectrum of 2-phenyl-3-ethyl-6,7-dimethoxy-2,3-dihydro-4*H*-1,3-benzothiazine (m.p. 81—82°C or 95—96°C) in KBr

Experimental

(Melting points are uncorrected)

1) 3,3'-Methylene-bis(2,3-dihydro-6,7-dimethoxy-4*H*-1,3-benzothiazine) (III)

0.47 g (0.002 mole) of 4,5-dimethoxy-2-mercaptobenzyl ammonium chloride **(I)** was dissolved in 10 ml of water, and 0.5 ml of 30% formaldehyde solution and 0.1 g of potassium carbonate were added. The crystalline reaction product was filtered off, washed with water and recrystallized from ethanol; colourless powder-like crystals, m.p. 172—173°C; 0.21 g (48.4%).

$C_{21}H_{26}N_2O_4S_2$ (434,57). Calcd. C 58.04; H 6.03; N 6.45. Found C 58.31; H 5.80; N 6.44%.

Molecular weight found: 425—450.

2) 3-Ethyl-6,7-dimethoxy-2,3-dihydro-4*H*-1,3-benzothiazine (V)

0.62 g (0.002 mole) of N-(ethyl)-4,5-dimethoxy-2-mercaptobenzyl ammonium bromide **(IV)** was dissolved in 10 ml of water, and 0.5 ml of 30% formaldehyde solution and 0.1 g of potassium carbonate were added to the solution. The oily reaction product which separated was extracted with ether. After evaporation of the solvent, the oily residue was dissolved in ethanol and the solution was mixed with ethanol containing hydrogen chloride. The product, 3-ethyl-6,7-dimethoxy-2,3-dihydro-4*H*-1,3-benzothiazinium chloride, was precipitated with ether; pale yellow needles, m.p. 201—202°C (d.).

$C_{12}H_{18}ClNO_2S$ (275.79). Calcd. C 52.26; H 6.58. Found C 51.94; H 6.46%.

The base, liberated from the aqueous solution of the hydrochloride with sodium carbonate, was extracted with ether, dried over anhydrous sodium sulfate and the solvent was evaporated. The residue was crystallized from 50% ethanol to give colourless prisms, m.p. 72.5—74°C.

$C_{12}H_{17}NO_2S$ (239.33). Calcd. C 60.22; H 7.16. Found C 60.59; H 6.99%.

Molecular weight of the base found: 222 (ebullioscopic method).

3) 2-Methyl-6,7-dimethoxy-2,3-dihydro-4*H*-1,3-benzothiazine (VIa)

0.24 g (0.001 mole) of 4,5-dimethoxy-2-mercaptobenzyl ammonium chloride **(I)** was dissolved in 5 ml of water and the solution was saturated with acetaldehyde under cooling in ice. After this, 0.1 g of potassium carbonate was added to the reaction mixture, it was allowed to stand for 30 min., and the crystalline precipitate was filtered off to obtain 0.21 g of the product; colourless prisms (from anhydrous ether), m.p. 107—109°C.

$C_{11}H_{15}NO_2S$ (225.30). Calcd. C 58.64; H 6.26. Found C 58.79; H 6.58%.

4) 2-Phenyl-6,7-dimethoxy-2,3-dihydro-4*H*-1,3-benzothiazine (VIb)

0.47 g (0.002 mole) of 4,5-dimethoxy-2-mercaptobenzyl ammonium chloride (**I**) was dissolved in 10 ml of water, and mixed with a solution of 0.2 ml of benzaldehyde in 6 ml of ethanol and 0.2 g of potassium carbonate. The crystalline precipitate was filtered off, washed with 50% ethanol, dried and crystallized to obtain 0.49 g (87.5%) of colourless needles (from ethanol), m.p. 156—157°C; this product gave no m.p. depression with the compound prepared by reduction [29].

$C_{16}H_{17}NO_2S$ (287.37). Calcd. C 66.87; H 5.96; N 4.87. Found C 67.20; H 5.85; N 4.80%.

5) 2-Phenyl-2,3-dihydro-4*H*-1,3-benzothiazine (VIc)

0.35 g (0.002 mole) of 2-mercaptobenzyl ammonium chloride [32] and 0.20 ml of benzaldehyde were allowed to react in the same way as given in Experiment 4) to obtain 0.35 g (78%) of nacreous plates (from ethanol), m.p. 123.5—124°C; this product gave no melting point depression with the substance obtained by reduction [29].

$C_{14}H_{13}NS$ (227.31). Calcd. C 73.96; H 5.76; N 6.15. Found C 73.80; H 5.70; N 6.12%.

6) 2-(3',4'-Dimethoxyphenyl)-6,7-dimethoxy-2,3-dihydro-4*H*-1,3-benzothiazine (VId)

0.47 g (0.002 mole) of 4,5-dimethoxy-2-mercaptobenzyl ammonium chloride (**I**) and 0.34 g (0.002 mole) of veratraldehyde were allowed to react as described in Experiment 4) to obtain 0.57 g (81.4%) of **VId**: colourless radial needles (from ethanol), m.p. 169—170°C; it gave no melting point depression with the product prepared by reduction [29].

$C_{18}H_{21}NO_4S$ (347.42). Calcd. C 62.23; H 6.09; N 4.03. Found C 62.50; H 6.20; N 4.00%.

7) 2-(4'-Nitrilophenyl)-6,7-dimethoxy-2,3-didihydro-4*H*-1,3-benzothiazine (VIe)

0.47 g (0.002 mole) of 4,5-dimethoxy-2-mercaptobenzyl ammonium chloride (**I**) and 4-nitriloaldehyde were allowed to react as described in Experiment 4) to yield 0.57 g (92%) of **VIe**: colourless needles (from benzene–petroleum ether), m.p. 166—168°C.

$C_{17}H_{16}N_2O_2S$ (312.38). Calcd. C 65.36; H 5.16. Found C 65.59; H 4.97%.

8) 2-(2'-Furyl)-6,7-dimethoxy-2,3-dihydro-4*H*-1,3-benzothiazine (VIf)

0.24 g (0.001 mole) of 4,5-dimethoxy-2-mercaptobenzyl ammonium chloride (**I**) and 0.1 ml of 2-furfurylaldehyde were allowed to react as described in Experiment 4) to obtain 0.22 g (81.5%) of **VIf**: colourless needles (from ether), m.p. 136—137°C.

$C_{14}H_{15}NO_3S$ (277.33). Calcd. C 60.63; H 6.49; Found C 60.18; H 6.30%.

9) 2,2-Dimethyl-6,7-dimethoxy-2,3-dihydro-4*H*-1,3-benzothiazine (VIg)

0.24 g (0.001 mole) of 4,5-dimethoxy-2-mercaptobenzyl ammonium chloride (**I**) and 1 ml of acetone were allowed to react as described in Experiment 4) to give 0.18 g (75.3%) of **VIg**: colourless prisms (from ether), m.p. 117—118°C.

$C_{12}H_{17}NO_2S$ (239.33). Calcd. C 60.22; H 7.16; N 5.83. Found C 60.30; H 7.00; N 5.92%.

10) 2,2-Pentamethylene-6,7-dimethoxy-2,3-dihydro-4*H*-1,3-benzothiazine (VIh)

0.24 g (0.001 mole) of 4,5-dimethoxy-2-mercaptobenzyl ammonium chloride (**I**) and 0.1 ml of cyclohexanone were allowed to react as described in Experiment 4) to obtain 0.24 g (85.5%) of compound **VIh**: colourless prisms (from 50% ethanol), m.p. 97—98°C.

$C_{15}H_{21}NO_2S$ (279.39). Calcd. C 64.48; H 7.58; Found C 64.17; H 7.31%.

11) 2-Phenyl-3-ethyl-6,7-dimethoxy-2,3-dihydro-4*H*-1,3-benzothiazine (VIIa)

0.62 g (0.002 mole) of N-(ethyl)-4,5-dimethoxy-2-mercaptobenzyl ammonium bromide (**IV**) was dissolved in 3 ml of pyridine and after the addition of 0.21 g (0.002 mole) of benzaldehyde, the solution was boiled for 30 min. The pyridine was distilled off in vacuum, the residue diluted with 20 ml of water and extracted with ether. The solvent was distilled off and the residue crystallized from ethanol to give 0.35 g (55.5%) of **VIIa**; colourless radial needles, m.p. 81—82°C. This substance gave no melting point depression with the product prepared by reduction [29].

$C_{18}H_{21}NO_2S$ (315.42). Calcd. C 68.54; H 6.71; N 4.44; S 9.84. Found C 68.33; H 6.72; N 4.40; S 9.55%.

Colourless radial needles (from ethanol); m.p. 95—96°C.

$C_{18}H_{21}NO_2S$ (315.42). Calcd. C 68.54; H 6.71; N 4.44. Found C 68.70; H 7.15; N 4.65%.

12) 2-(3',4'-Dimethoxyphenyl)-3-ethyl-6,7-dimethoxy-2,3-dihydro-4*H*-1,3-benzothiazine (VIIb)

0.31 g (0.001 mole) of N-(ethyl)-4,5-dimethoxy-2-mercaptobenzyl ammonium bromide (**IV**) and 0.17 g (0.001 mole) of veratraldehyde were allowed to react as described in Experiment 11) to obtain 0.28 g (75%) of **VIIb**: colourless prisms from ethanol, m.p. 138—139°C. The substance gave no melting point depression with the product obtained by reduction [29].

$C_{20}H_{25}NO_4S$ (375.47). Calcd. C 63.97; H 6.71; N 3.73. Found C 64.11; H 6.49; N 3.70%.

13) 2-(4'-Dimethylaminophenyl)-3-ethyl-6,7-dimethoxy-2,3-dihydro-4*H*-1,3-benzothiazine (VIIc)

0.15 g (0.0005 mole) of N-(ethyl)-4,5-dimethoxy-2-mercaptobenzyl ammonium bromide (**IV**) and 0.075 g (0.0005 mole) of 4-dimethylaminobenzaldehyde were allowed to react as described in Experiment 11) to obtain 0.1 g (55%) of **VIIc**: pale yellow plates (from 50% ethanol), m.p. 96—97°C.

$C_{20}H_{26}N_2O_2S$ (358.49). Calcd. C 67.00; H 7.81; N 7.81. Found C 67.25; H 7.70; N 7.61%.

14) 2-(4'-Nitrilophenyl)-3-ethyl-6,7-dimethoxy-2,3-dihydro-4*H*-1,3-benzothiazine (VIId)

1.5 g (0.005 mole) of N-(ethyl)-4,5-dimethoxy-2-mercaptobenzyl ammonium bromide (**IV**) and 0.65 g (0.005 mole) of 4-cyanobenzaldehyde were allowed to react as described in Experiment 11) to yield 0.5 g (29.4%) of **VIId**: colourless needles (from 60% ethanol), m.p. 115—116°C.

$C_{19}H_{20}N_2O_2S$ (340.43). Calcd. C 67.03; H 5.92. Found C 66.96; H 6.03%.

15) 2-(4'-Methoxyphenyl)-3-ethyl-6,7-dimethoxy-2,3-dihydro-4*H*-1,3-benzothiazine (VIIe)

0.75 g (0.0025 mole) of N-(ethyl)-4,5-dimethoxy-2-mercaptobenzyl ammonium bromide (**IV**) and 0.35 g of 4-methoxybenzaldehyde were allowed to react as described in Experiment 11) to obtain 0.38 g (45.2%) of **VIIe**: colourless prisms (from ethanol), m.p. 79—80.5°C.

$C_{19}H_{23}NO_3S$ (345.44). Calcd. C 66.06; H 6.86. Found C 66.09; H 6.92%.

16) 2-(2'-Furyl)-3-ethyl-6,7-dimethoxy-2,3-dihydro-4*H*-1,3-benzothiazine (VIIf)

0.31 g (0.001 mole) of N-(ethyl)-4,5-dimethoxy-2-mercaptobenzyl ammonium bromide (**IV**) and 0.3 ml of 2-furfurylaldehyde were allowed to react as described in Experiment 4) to obtain 0.09 g (29.4%) of **VIIf**: colourless needles (from 60% ethanol), m.p. 80—81°C.

$C_{16}H_{19}NO_3S$ (305.38). Calcd. C 62.92; H 6.27. Found C 62.91; H 6.68%.

*

The authors' thanks are due to Dr. P. SOHÁR for the recording and evalution of the IR and NMR spectra.

REFERENCES

1. SZABÓ, J., VINKLER, E., VARGA, I., BARTHOS, É.: Kémiai Közlemények **26,** 21 (1966)
2. INGRAM, I. S., MC CLELLAND, E. W.: J. Chem. Soc. **63,** 763 (1947)
3. BÖHME, H., SCHMIDT, W.: Arch. Pharm. **286,** 330 (1953)
4. BÖHME, H., SCHMIDT, W.: Arch. Pharm. **286,** 437 (1953)
5. BOUDET, R.: Bull. soc. chim. France (1955). 1618
6. WRIGHT, W. B.: U. S. Pat. 2.776.281 (1957)
7. HASSPACHER, K.: U.S. Pat. 2.978.448 (1961)
8. HASSPACHER, K.: German Pat. 1.096.361 (1961)
9. BÖHME, H., BÖING, H.: Arch. Pharm. **294,** 556 (1961)
10. HASSPACHER, K.: German Pat. 1.079.050 (1960)
11. HASSPACHER, K.: German Pat. 1.105.874 (1958)
12. MOREAU, R. C., DELACOUX, E.: Bull. soc. chim. France (1962) 502
13. LOEV, B., KÖRMENDY, M.: J. Org. Chem. **27,** 3365 (1962)
14. KRETOV, A. E., BESPALY, A. S.: Zh. Obshch. Khim. **33,** 213 (1963)
15. PALAZZO, S., LOMBARDO, G.: Gaz. Chim. Ital. **93,** 207 (1963)
16. LOEV, B.: J. Org. Chem. **28,** 2160 (1963)
17. PONCI, R., BARUFFINI, A., GIALDI, F.: Farmaco (Pavia) Ed. Sci. **18,** 653 (1963)
18. KRETOV, A. E., BESPALYI, A. S.: Zh. Obshch. Khim. **34,** 1307 (1964)
19. ZINNES, H., COMES, R. A.: Org. Chem. **29,** 2068 (1964)
20. LOEV, B.: U.S. Pat. 3.149.106 (1964)
21. FENECH, G., BASILE, M., VIGORITA, G.: Ann. Chim. (Rome) **54** (6) 607 (1964)
22. BOUDET, R., BOURGOIN-LEGAY, D.: Compt. rend. Ser. C. **262,** 596 (1966)
23. LANGE, W. E., ANDERSON, I. C.: French Pat. 1.481.713 (1967)
24. WAGNER, G., RICHTER, P.: Pharmazie **22,** 611 (1967)
25. WAGNER, G., RICHTER, P.: Pharmazie **24,** 100 (1969)
26. KRAPCHO, J.: U. S. Pat. 3.459.748 (1969)
27. KRAPCHO, J.: U.S. Pat. 3.455.915 (1969)
28. BOURGOIN-LEGAY, D., BOUDET, R.: Compt. rend. Ser. C. **263,** 77 (1966)
29. SZABÓ, J., VARGA, I., VINKLER, E.: In press
30. SZABÓ, J., VINKLER, E., VARGA, I.: Acta Chim. Acad. Sci. Hung. **58,** 179 (1968)
31. SZABÓ, J., VARGA, I., VINKLER, E., BARTHOS, É.: In press
32. BOUDET, R., BOURGOIN-LEGAY, D.: Compt. rend. Ser. C. **262,** 596 (1966)
33. HOLLY, F. W., COPE, A. C.: J. Am. Chem. Soc. **66,** 1875 (1944)

János SZABÓ
István VARGA
Elemér VINKLER
Éva BARTHOS

Szeged, Eötvös u. 2. Hungary.

Acta Chimica Academiae Scientiarum Hungaricae, Tomus 72 (2), pp. 221—230 (1972)

ALKALOIDS CONTAINING THE INDOLO [2,3-c] QUINAZOLINO [3,2-a] PYRIDINE SKELETON, I

NEW SYNTHESES AND REDUCTION OF RUTECARPINE

O. CLAUDER and K. HORVÁTH-DÓRA

(Institute of Organic Chemistry, Faculty of Pharmaceutical Sciences, Semmelweis Medical University, Budapest)

Received November 5, 1970

New syntheses of rutecarpine **2** were developed. In the first procedure the well-known methods have been simplified, the second is a new synthesis, using *N*-carbobenzyloxytryptamine **19** as starting material. The so-called 'adduct' intermediate prepared from 1,2,3,4-tetrahydro-1-oxo-β-carboline **9** with $POCl_3$ was found to be suitable for the preparation of rutecarpine **2** and its substituted derivatives.

3,14-dihydrorutecarpine **20** was obtained from the product **21** of the reaction between tryptamine **18** and *ortho*-formic acid ethyl ester.

The reduction of rutecarpine **2** with $LiAlH_4$ was also investigated and rutecarpene **23** or rutecarpane **22** was obtained, depending on the nature of the solvent used.

Two alkaloids, evodiamine **1** and rutecarpine **2** were isolated from *Evodia rutaecarpa* fruits by ASAHINA *et al.* [1]. They stated that these two alkaloids have similar structures [2]. The treatment of evodiamine **1** with alcoholic potassium hydroxide resulted 3,4-dihydro-β-carboline **3** and *N*-methylanthranilic acid **4**, while in the hydrolysis of rutecarpine **2** with potassium hydroxide in amyl alcohol, tryptamine-2-carboxylic acid **5** and anthranilic acid **6** were obtained (Fig. 1).

According to the above authors [3, 4], evodiamine **1** can be converted to rutecarpine **2** by treatment with alcoholic hydrochloric acid and subsequent heating. The intermediates of the reaction involving demethylation are isoevodiamine **7** and anhydroisoevodiamine **8** (Fig. 2).

The first synthesis of rutecarpine **2** was accomplished by ASAHINA, MANSKE and ROBINSON [5], by the condensation of 1,2,3,4-tetrahydro-1-oxo-β-carboline **9** with anthranilic acid methyl ester **10** in the presence of PCl_3.

In another procedure they used tryptamine-2-carboxylic acid as starting material [6]. First its *o*-nitrobenzoyl derivative **11** was prepared, which was reduced **12** and cyclized with $POCl_3$, resulting in rutecarpine **2**.

OHTA [7] modified the first ASAHINA synthesis, using 1,2,3,4-tetrahydro-1-oxo-β-carboline **9** and anthranilic-*N*-carboxylic anhydride **13** in the condensation reaction.

SCHÖPF and STEUER [8] synthesized it from 3,4-dihydro-β-carboline **3** with *o*-aminobenzaldehyde **14** under conditions similar to the physiological ones. An aminocarbinol **15** was obtained in the first step, its oxidation resulted in rutecarpine **2**.

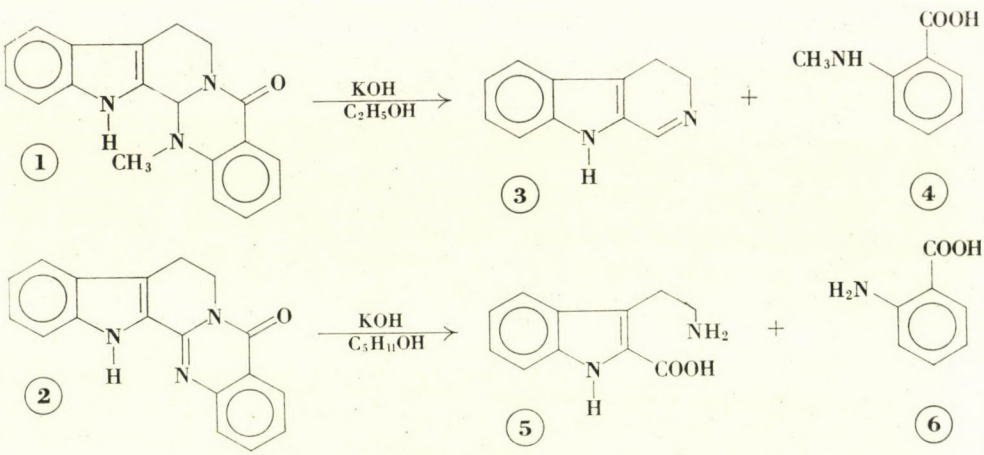

Fig. 1

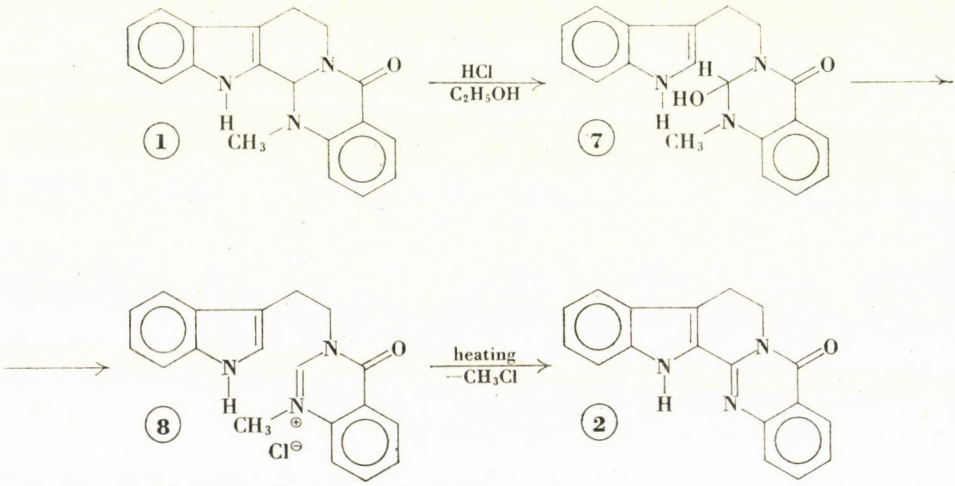

Fig. 2

PETERSEN and TIETZE [9] also prepared rutecarpine **2** from 3,4-dihydro-1-methoxy-β-carboline **16** and anthranilic acid **6** by refluxing them in methanol (Fig. 3).

We carried out the synthesis of rutecarpine **2** by simplifying the ASAHINA synthesis [5]. 1,2,3,4-Tetrahydro-1-oxo-β-carboline **9** was directly condensed with anthranilic acid **6** in benzene in the presence of $POCl_3$. In 5 hours, rutecarpine **2** was obtained in nearly quantitative yield. After recrystallization from ethanol or benzene, the substance was identified on the basis of its melting point, as well as its ultraviolet and infrared spectra, by making comparisons with the data of the spectrum catalogues compiled by HESSE [11] and NEUSS [12].

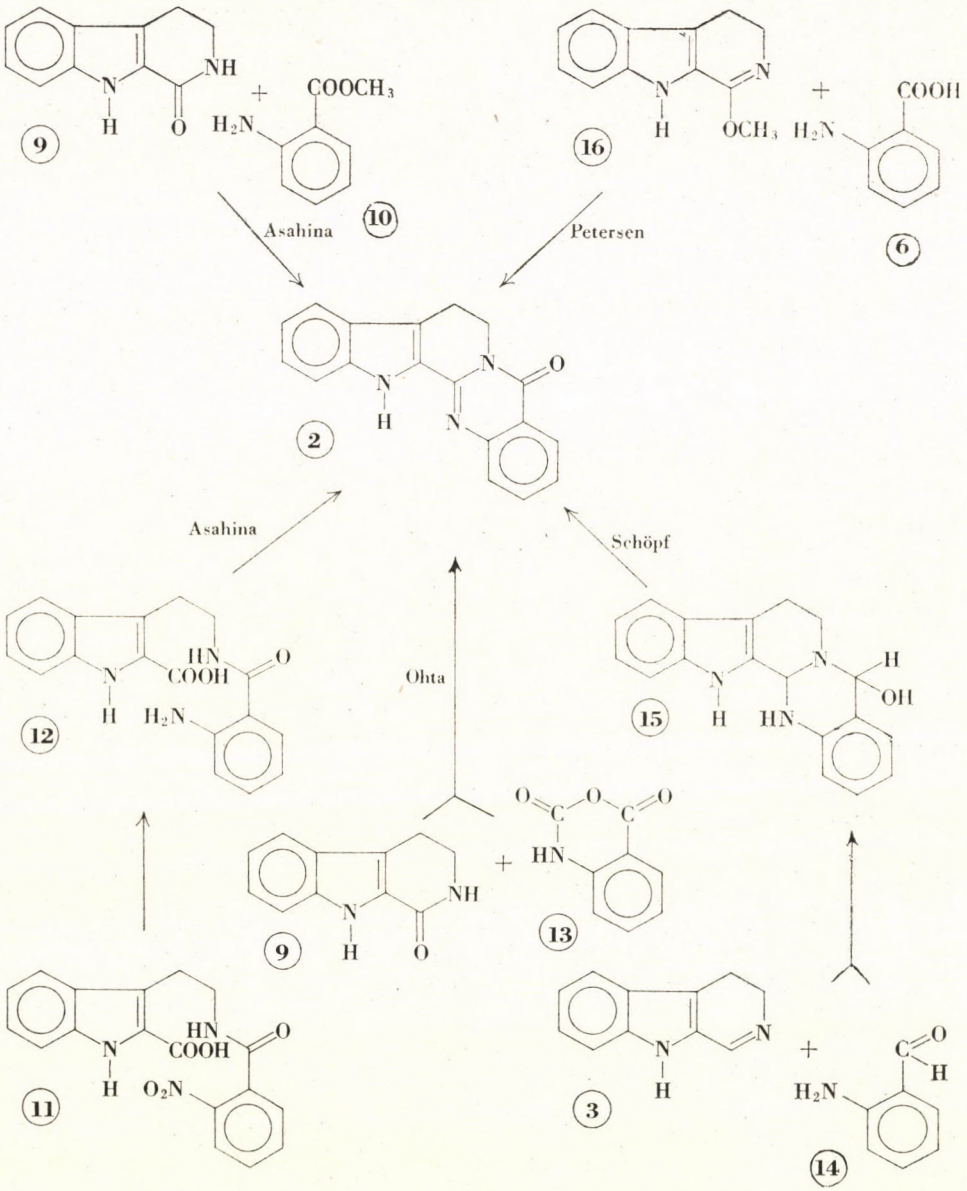

Fig. 3

In order to modify our previous method of synthesis, the following reaction was carried out. 1,2,3,4-tetrahydro-1-oxo-β-carboline **9** and $POCl_3$ were heated without solvent. After cooling and precipitating with ether, a very reactive substance was obtained, its hypothetic structure, according to LORENZ [13] corresponded to 3,4-dihydro-1-chloro-β-carbolium, PO_2Cl_2 **17**. The author refers to this compound simply as an 'adduct'. Heating of this 'adduct'

in absolute benzene with anthranilic acid **6** also resulted in rutecarpine **2**. The advantage of the procedure is that it eliminates discolouration of the solution and the formation of tarry materials, as no excess of phosphoryl chloride is present. This may be of great importance in the preparation of rutecarpine derivatives containing sensitive substituents (Fig. 4).

Another synthesis of rutecarpine was also developed. According to the BERGMAN—ZERVAS method, *N*-carbobenzyloxytryptamine **19** was prepared from tryptamine **18** and chlorocarbonic acid benzyl ester in a benzene-sodium hydroxyde medium. As in the previous procedure, it was reacted with anthranilic acid **6** in benzene in the presence of $POCl_3$, resulting in rutecarpine **2**.

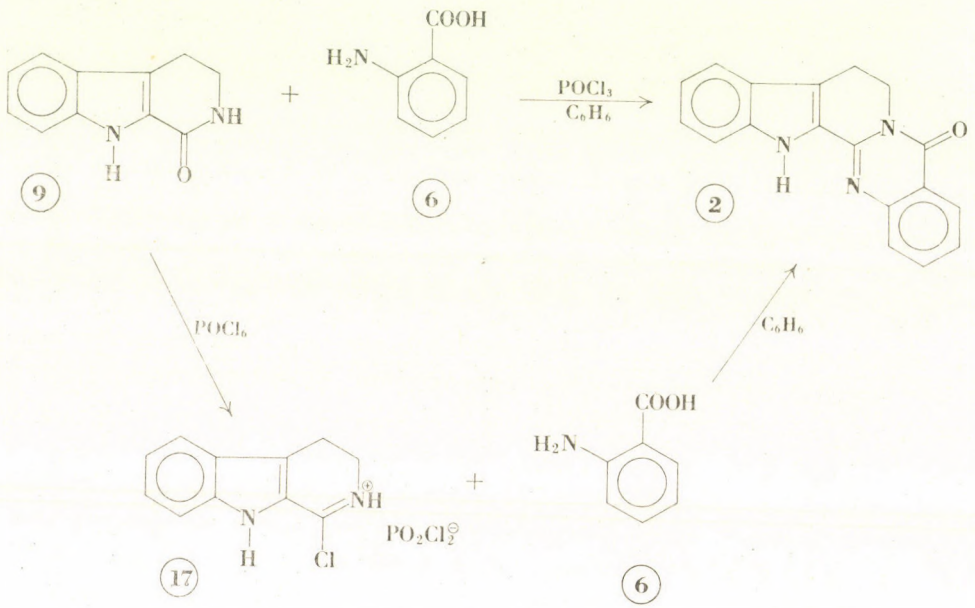

Fig. 4

With certain modification, the procedure is also suitable for the preparation of the hydrated derivative of rutecarpine, *i.e.*, 3,14-dihydrorutecarpine **20**. In the reaction of tryptamine **18** with methyl formate or orthoformic acid ethyl ester, with subsequent addition of anthranilic acid **6** in absolute benzene in the presence of $POCl_3$, 3,14-dihydrorutecarpine **20** is formed. It should be noted that this compound has not been prepared by hydration of rutecarpine **2** up to now (Fig. 5).

In the reaction of tryptamine **18** with ortho-formic ester a crystalline material was obtained which, however, was not homogeneous. On the basis of its infrared spectra it is assumed to be a mixture of formyltryptamine

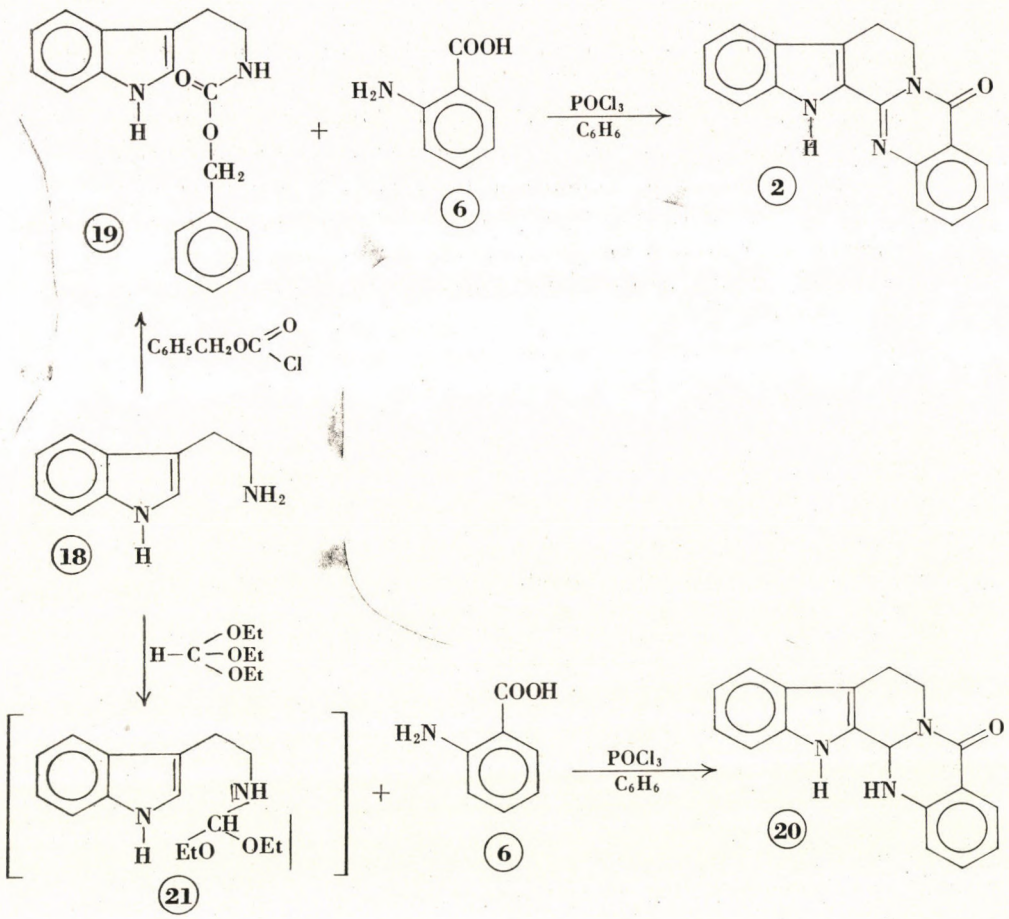

Fig. 5

iminoether and acetal. The exact determination of its structure requires further investigations.

In the following, the reduction of rutecarpine **2** will be discussed. TERZIAN *et al.* [10] described the reduction of rutecarpine **2** with $LiAlH_4$ in absolute ether; the C_3 and N_{14} double bonds and the C=O group were reduced and dl-rutecarpane **22** was obtained. The reduction procedure was repeated by us. After 20 hrs of reaction, the mixture was decomposed with water and the ethereal solution extracted with 2 *M* hydrochloric acid. The acid solution was made alkaline with ammonia. Rutecarpane separated in crystalline form **22**. It was recrystallized from ethanol and its ultraviolet and infrared spectra were recorded. Its ultraviolet spectrum is of the indole type (Fig. 8), and its infrared spectrum did not contain the band assigned to the C=O group in the acid amide (1660 cm^{-1}). The appearance of the Bohlmann bands at

2850—2750 cm^{-1} indicates the *trans* anellation of the C—D rings and the presence of a 3 α H.

The reduction was carried out also in absolute tetrahydrofurane. After 20 hrs the reaction mixture was processed and 21-desoxorutecarpine, *i.e.*, rutecarpene **23** was obtained. Similarly, rutecarpene **23** was formed upon using a 3 or 6-fold amount of $LiAlH_4$, as well as on accomplishment of the reaction at 35°C (the b.p. of ether). These experiments prove the dependence of the reduction on the nature of the solvent applied (Fig. 6).

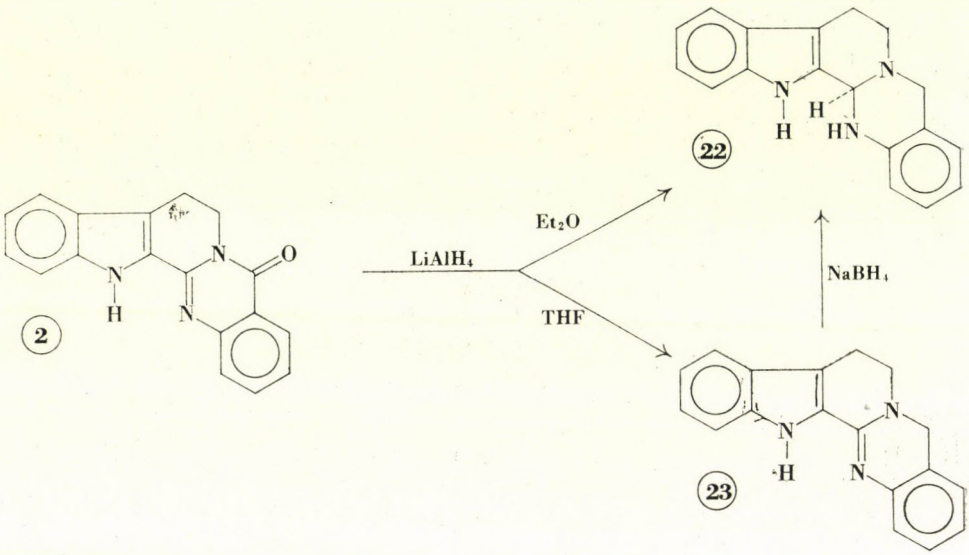

Fig. 6

Rutecarpene **23** has a characteristic ultraviolet spectrum (Fig. 8). In its infrared spectrum the C=O band of the acid amide (1660 cm^{-1}) is not present. The maximum assigned to the NH stretching vibration of indole also disappeared. Presumably, in the absence of the C=O group the electron pair of the N(b) nitrogen atom gives rise to strong electron displacement towards C_3, resulting in the development of a negative charge at N_{14} **24**. Its protonation with the hydrogen of the N(a) nitrogen, through the formation of the intermediate anhydronium base **25** may cause further electron displacement thus giving rise to a quinoidal structure **26** (Fig 7).

On treatment with hydrochloric acid, **23** gave a hydrochloride at the N(b) nitrogen atom only.

The C=N double bond of rutecarpene **23** could be reduced in the usual way, *e.g.* with $NaBH_4$, and 3-α-rutecarpane **22** was obtained, in accordance with the well-known and thoroughly studied reaction of the indole alkaloids (Fig. 6).

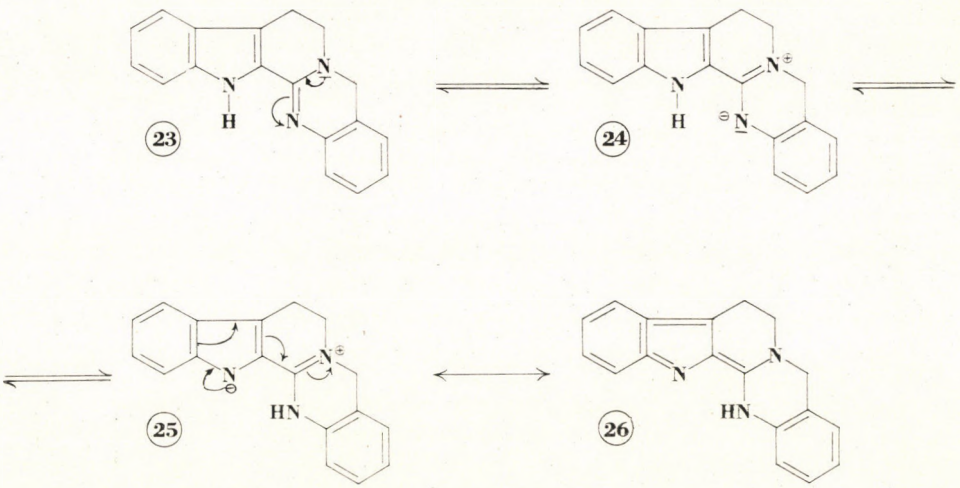

Fig. 7

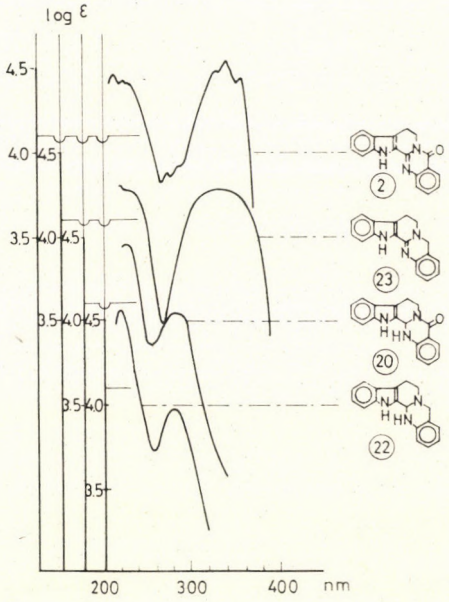

Fig. 8

Our reduction experiments indicate that in rutecarpine **2**, an extended conjugation should be supposed which hinders the hydrogenation of the C_3 and N_{14} double bonds. The weakening of conjugation by reduction of the C=O group, the first step of the reduction procedure, facilitates the attack on the C=N bond, *e.g.* for $NaBH_4$.

Comparison of the ultraviolet spectra of the substances prepared shows the following. Rutecarpine **2**, owing to extended conjugation, gives a characteristic, rich spectrum (maxima at 278, 290, 332, 345, 364 nm). Reduction of the oxogroup of the carboxylic amide makes the spectrum of rutecarpene **23** simpler: strongly shifted indole spectrum appears, owing to conjugation of the CN double bond with the electron system of indole (maximum at 336 nm, minimum at 270 nm). Further reduction results in rutecarpane **22**, which has an indole spectrum as a consequence of the strong suppression of conjugation (maximum at 283 nm, minimum at 258 nm). Also synthetically prepared 3,14-dihydrorutecarpine **20** shows an indole spectrum (maximum at 284 nm, minimum at 255 nm) (Fig. 8).

Experimental

Rutecarpine 2

(a) 1.86 g (0.01 mol) of 1,2,3,4-tetrahydro-1-oxo-β-carboline **9** and 1.37 g (0.01 mol) of anthranilic acid **6** were mixed with 25 ml of absolute benzene. 10 ml of $POCl_3$ was added dropwise to the mixture while cooling with water. The crystals became slightly oily and the solution became red. The mixture was refluxed under continuous stirring on a hot water bath for 5 hrs. After boiling for about 15 min the crystals dissolved and a few minutes later the solution became cloudy and precipitation of yellow crystals started. After the refluxing period it was cooled and filtered off. 20 ml of 20% Na_2CO_3 solution was poured onto the crystals under cooling with water. After thorough stirring the crystals were filtered off and washed with water. I. Yield 1.70 g. The benzene filtrate of the crystals was evaporated in vacuum on a water bath. 20 ml of water was poured onto the residue under cooling. Yellowish-beige crystals separated. The mixture was made alkaline with 20% Na_2CO_3 and the crystals were filtered off. II. Yield 1.15 g (99%). After recrystallization from 96% ethanol or glacial acetic acid the melting point of the substance was 256—58°C.

$C_{18}H_{13}N_3O$ (287).	Calcd.	C 75.27; H 4.52; N 14.63
	Found	C 75.20; H 4.80; N 14.60%.
UV spectrum: λ ethanol max.		278 nm (log ε = 3.88)
		290 nm (log ε = 3.92)
		332 nm (log ε = 4.48)
		345 nm (log ε = 4.54)
		364 nm (log ε = 4.44)
IR spectrum (KBr):		3350 cm^{-1} (ν NH indole)
		1660 cm^{-1} (ν CO acid amide)
		765 and 725 cm^{-1} (γ CH o-disubsts.)

(b) 0.25 g (0.00125 mol) of 1,2,3,4-tetrahydro-1-oxo-β-carboline **9** was converted to the 'adduct' **17** according to LORENZ [13]: 2.5 ml of $POCl_3$ was added to it and the mixture was kept on a water bath at 60°C until dissolution (about 2 min). A clear, orange solution was obtained. It was cooled quickly, and 10 ml ether was added to it. An orange-yellow oil separated which gave lemon-coloured crystals on rubbing. These were filtered off quickly and 0.17 g of anthranilic acid **6** was added to the crystals. After thorough mixing, 5 ml of absolute benzene was poured onto the mixture and it was refluxed on a water bath for 2 hrs. The crystals did not dissolve. At the beginning they became somewhat oily, but later on solidified again. On cooling this solid gave crystals. The yellow crystals were filtered off and rubbed with 20% Na_2CO_3 solution, according to Procedure *(a)*. Yield 0.30 g (86%).

(c) 0.47 g (0.0015 mol) of *N*-Cbo-tryptamine **19** was dissolved in 5 ml of absolute benzene. 2 ml of $POCl_3$ was added to it dropwise while cooling with water, then the solution was boiled on a water bath for 1 hr. A clear, red-brown solution was obtained. It was cooled and 0.20 g (0.0015 mol) of anthranilic acid **6** was added to it, then it was boiled on a water bath for 5 more hours. A reddish oil separated on the wall of the flask. The solution was concentrated in vacuum on a water bath. The oily residue was rubbed with 15 ml of water. The mixture

was made alkaline with conc. NH_4OH under cooling and was extracted with 3×20 ml of chloroform. The chloroform solution was dried over Na_2SO_4 and evaporated in vacuum on a water bath at 50°C. The residue was an orange-yellow oil, which completely solidified. Yield: 0.25 g (60 %).

N-Carbobenzyloxytryptamine 19

0.32 g (0.002 mol) of tryptamine **18** was mixed with 30 ml of absolute benzene and the mixture was cooled to +5°C. At this temperature a solution of 0.68 g (0.004 mol) of chlorocarbonic acid benzyl ester in 6 ml of absolute benzene and 6 ml of 1 *M* sodium hydroxide were simultaneously added in a dropwise manner. Stirring was continued for 10 min at +5°C then for 1 1/2 hrs at room temperature. The solution was transferred to a separatory funnel and the benzene phase was separated. The aqueous phase was extracted with 10 ml of benzene. The combined benzene phases were washed with 2×10 ml of 0.5 *M* HCl and 1×10 ml of water in order to remove the unreacted tryptamine. The solution was dried over Na_2SO_4 and evaporated to dryness in vacuum on a water bath. A light red-brown, oily residue was obtained, which crystallized on standing. Yield 0.55 g (93%). After recrystallization from absolute ethanol, white needle-shaped crystals were obtained. M.p. 45—50°C.

$C_{18}H_{18}N_2O_2$ (294). Calcd. C 73.48; H 6.12; N 9.52.
Found C 73.68; H 6.24; N 9.54%.

Reaction of tryptamine with ortho-formic acid ethyl ester 21

0.40 g (0.0025 mol) of tryptamine base **18** was boiled with 3.7 g of freshly distilled *ortho*-formic acid ethyl ester (0.0025 mol) in a N_2 atmosphere, on a paraffin bath at 150°C for 5 hrs, then it was evaporated to dryness in vacuum. A clear, oily residue was obtained, which solidified completely. Yield: 0.40 g. According to the infrared spectrum, this product is a mixture of *N*-formyltryptamine acetal and iminoether. It can be easily hydrolyzed to *N*-formyltryptamine. Its reaction with $POCl_3$ in absolute toluene gives 3,4-dihydro-β-carboline.

3,14-Dihydrorutecarpine 20

0.25 g (0.001 mol) of the mixture of *N*-formyltryptamine acetal and iminoether **21** or 0.19 g of *N*-formyltryptamine was dissolved in 5 m of absolute benzene. 0.14 g (0.001 mol) of anthranilic acid **6** was added. After cooling, 1.5 ml of $POCl_3$ was added dropwise. The solution became slightly red, then it was refluxed on a water bath under continuous stirring for 5 hrs. A violet-coloured mixture of solution and precipitate was obtained, which was evaporated to dryness in vacuum on a water bath. After adding some ice it was made alkaline with conc. NH_4OH. The heterogeneous mixture was transferred into a separatory funnel and extracted with 1×20 and 3×15 ml of chloroform. The chloroform solution was extracted with 1×20 and 3×15 ml of 2 *M* HCl. The hydrochloric acid solution was made alkaline with 20% sodium hydroxide. Beige crystals precipitated. Yield: 0.10 g (35%). After recrystallization from ethanol, the m.p. was 250—55°C (d).

$C_{18}H_{15}N_3O$ (289). Calcd. C 74.74; H 5.19; N 14.53.
Found C 74.33; H 5.42; N 14.60%.
UV spectrum: λ ethanol max. 284 nm (log $\varepsilon = 4.04$)
292 nm (log $\varepsilon = 4.02$)
λ ethanol min. 255 nm (log $\varepsilon = 3.84$)
IR spectrum (KBr): 3250 cm^{-1} (ν NH secondary amine)
1660 cm^{-1} (ν CO acid amide)
745 cm^{-1} (γ CH *o*-disubst.)

Rutecarpane 22

(a) 0.23 g (0.006 mol) of $LiAlH_4$ was added to 40 ml of absolute ether. After thorough stirring, 0.28 g (0.001 mol) of rutecarpine **2** was added to it in two portions. After refluxing for 20 hrs under continuous stirring, the mixture was decomposed with 2 ml of water. The precipitate was filtered off and washed with 2×5 ml of ether. The combined ethereal solutions were extracted with 1×20 and 1×15 ml of 2 *M* HCl. On making the hydrochloric solution alkaline with conc. NH_4OH, lustrous crystals precipitated. The mixture was cooled and filtered. Yield: 0.20 g (74%). After recrystallization from ethanol, the m.p. was 161—63°C.

$C_{18}H_{17}N_3$ (275). Calcd. C 78.55; H 6.18; N 15.27.
Found C 78.60; H 6.30; N 15.20%.
UV spectrum: λ ethanol max. 283 nm (log $\varepsilon = 3.96$)
λ ethanol min. 258 nm (log $\varepsilon = 3.72$)
IR spectrum (KBr): 3400 cm^{-1} (ν NH indole)
3250 cm^{-1} (ν NH secondary amine)
2850—2750 cm^{-1} (ν CH Bohlmann)
745 cm^{-1} (γ CH o-disubst.)

(b) 0.05 g (0.0002 mol) of rutecarpene **23** was dissolved in 10 ml of methanol by boiling. The solution was cooled and 0.07 g (0.002 mol) of $NaBH_4$ was added while cooling. The solution was refluxed for 3 hrs and evaporated in vacuum on a water bath. 10 ml of water was poured onto the solid residue and it was extracted with 3×10 ml of ether. The ethereal solution was extracted with 20 ml of 2 *M* HCl. The hydrochloric acid solution was made alkaline with 2 *M* NaOH, resulting in the precipitation of beige-white lustrous crystals which, after cooling in a refrigerator, were filtered off. Yield: 0.03 g (60%).

Rutecarpene 23

(a) 0.28 g (0.001 mol) of rutecarpine **2** was thoroughly mixed with 20 ml of absolute tetrahydrofurane. The greatest part of the substance dissolved. 0.12 g (0.003 mol) of $LiAlH_4$ was added to the solution, then it was refluxed on a water bath for 20 hrs. 2 ml of water was used for decomposition. The precipitate was filtered off and washed with 2×5 ml of chloroform. The solvent mixture was dried over Na_2SO_4 and evaporated in vacuum on a water bath. A yellow, solid residue was obtained. Yield: 0.25 g (93%). After recrystallization from absolute ethanol, m.p. 205—7°C.

$C_{18}H_{15}N_3$ (273). Calcd. C 79.19; H 5.49; N 15.38.
Found C 79.30; H 5.54; N 15.42%.
UV spectrum: λ ethanol max. 336 nm (log $\varepsilon = 4.28$)
λ ethanol min. 270 nm (log $\varepsilon = 3.45$)
IR spectrum (KBr): 760 and 740 cm^{-1} (γ CH *o*-disubst.)

(b) According to Procedure *(a)*, 0.28 g (0.001 mol) of rutecarpine **2** was reduced with 0.23 g (0.006 mol) of $LiAlH_4$. After processing the reaction mixture, 0.25 g of rutecarpene **23** was obtained (yield 92%).

Hydrochloride (recrystallized from ethanol) m.p. 271—73°C (d).
$C_{18}H_{16}N_3Cl$ (309.5) Calcd. Cl 11.4. Found Cl 11.6%.

REFERENCES

1. Asahina, Y., Kashiwiaki, K.: J. Pharm. Soc. Japan No. 405, 1293 (1915); C.A. **10**, 607 (1916)
2. Asahina, Y., Mayeda, S.: J. Pharm. Soc. Japan No. 416, 871 (1916); C. A. **11**, 332 (1917)
3. Asahina, Y., Ohta, T.: J. Pharm. Soc. Japan No. 530, 293 (1926); C. A. **21**, 2134 (1927)
4. Asahina, Y., Ohta, T.: J. Pharm. Soc. Japan **49**, 1025 (1929); C. A. **24**, 1386 (1930)
5. Asahina, Y., Manske, R. H. F., Robinson, R.: J. Chem. Soc. **1927**, 1708
6. Asahina, Y., Irie, T., Ohta, T.: J. Pharm. Soc. Japan No. 543, 51 (1927); C. A. **21**, 3054 (1927)
7. Ohta, T.: J. Pharm. Soc. Japan **60**, 311 (1940); C. A. **34**, 7291 (1940)
8. Schöpf, C., Steuer, H.: Ann. **558**, 124 (1947)
9. Petersen, S., Tietze, E.: Ann. **623**, 166 (1959)
10. Terzian, A. G., Safrazbekyan, R. S., Khaznakyan, L. V., Tatevosyan, G. T.: Izv. Akad. Nauk. Arm. SSR, Khim. Nauki **14**, 393 (1961)
11. Hesse, M.: Indolalkaloide in Tabellen 90. Springer Verlag 1964
12. Neuss, N.: Physical data of indole and dihydroindole alkaloids 103. Eli Lilly & Comp. Indianapolis, Indiana, USA, 1960
13. Lorenz, R.: Ger. 1.039.065. Sept. 18, 1958 (Cl. 12 p).

Ottó Clauder
Klára Horváth-Dóra } Budapest IX., Hőgyes E. u. 7.

INDEX

INORGANIC AND ANALYTICAL CHEMISTRY — ANORGANISCHE UND ANALYTISCHE CHEMIE — НЕОРГАНИЧЕСКАЯ И АНАЛИТИЧЕСКАЯ ХИМИЯ

BODOR, E., JÓNÁS, K. and WELTHER, M.: Thermal Decomposition of Pyridine-Borane 111

PHYSIKAL CHEMISTRY — PHYSIKALISCHE CHEMIE — ФИЗИЧЕСКАЯ ХИМИЯ

ILLÉS, V.: The Pyrolysis of Gaseous Hydrocarbons, V. The Kinetics of the Thermal Decomposition of an Isobutane–*n*-Butane Mixture 117

ILLÉS, V.: The Pyrolysis of Gaseous Hydrocarbons, VI. Product Distribution as the Function of the Degree of Decomposition in the Pyrolysis of an Isobutane–*n*-Butane Mixture 133

KISS, A. B., HOLLY, S. and HILD, E.: Characteristic Vibrational Frequencies of Crystalline Ammonium Polymolybdates Consisting of Octahedral MoO_6 Units, in the 400—4000 cm^{-1} Range 147

HORÁNYI, G., KŐNIG, P. and TELCS, I.: Oxidation of Secondary Alcohols on a Platinum Electrode, I. The Oxidation Products 165

HORÁNYI, G., VÉRTES, G. and KŐNIG, P.: Oxidation of Secondary Alcohols on a Platinum Electrode, II. Study of the Connection between Oxygen Adsorption and the Reaction 179

KALLÓ, D., DETREKŐY, E. and SCHAY, G.: Mechanistic Study of the Isomerization of *n*-Butene on Acid Catalysts, I. Kinetics of Monomolecular Catalytic Interconversion of Three Components 189

TELCS, I.: A Method for the Determination of Hydrogen Adsorption on Palladium Electrodes (Short Communication) 209

ORGANIC CHEMISTRY — ORGANISCHE CHEMIE — ОРГАНИЧЕСКАЯ ХИМИЯ

SZABÓ, J., VARGA, I. VINKLER, E. and BARTHOS, É.: Preparation of 2,3-Dihydro-4*H*-1,3-Benzothiazine Derivatives 213

CLAUDER, O. and HORVÁTH-DÓRA, K.: Alkaloids Containing the Indolo [2,3-c] Quinazolino [3,2-a] Pyridine Skeleton, I. New Syntheses and Reduction of Rutecarpine 221

ACTA CHIMICA

ТОМ 72 — ВЫП 2

РЕЗЮМЕ

Термическое разложение пиридин-борана

Э. БОДОР, К. ЙОНАШ и М. ВЕЛТХЕР

С помощью методов дериватографии, ИК спектрофотометрии и химического анализа было доказано, что при нагреве пиридин-борана протекает экзотермическая реакция перегруппировки, а именно, миграция атомов водорода, присоединенных к бору, на пиридиновое кольцо с частичным насыщением последнего. Вероятно, что параллельно с перегруппировкой, в некотором определенном интервале температуры, происходит также термическая диссоциация пиридин-борана. Главным конечным продуктом является цепной полимер, основанный на связи бор-бор. Согласно исследованиям с подобными системами, при нагреве барановых аддуктов, содержащих донорный азот в ароматической системе, всегда протекает, в большей или меньшей степени, экзотермическая реакция перегруппировки, т. е. частичное насыщение ароматического кольца.

Пиролиз газообразных углеводородов, V

Кинетика терморазложения смеси изобутан—*н*-бутан

В. ИЛЛЕШ

Было изучено терморазложение эквимолярной смеси изобутан — *н*-бутан в проточном реакторе, при общем давлении 1 атм и в области температур 640—790°С.

Было показано, что величина расширения смесей при пиролизе может быть рассчитана аддитивно из пиролитических данных чистых углеводородов.

Были определены константы кинетических уравнений, описывающих скорость реакций разложения компонентов исходной смеси *н*-бутана и изобутана.

Для характеристики степени разложения углеводородных смесей, вводилась сумма конверсий компонентов исходной смеси, взвешенная по молярным долям, а в случае многокомпонентной смеси — относительное расширение. Заменяя в кинетических уравнениях, выведенных для проточного реактора, конверсию на степень разложения, были получены зависимости, описывающие бруттоскорость разложения углеводородов. Из полученных зависимостей может быть рассчитана величина степени разложения для данного времени реакции, при данной температуре.

Пиролиз газообразных углеводородов, VI

Распределение продуктов пиролиза смеси изобутан—*н*-бутан в зависимости от степени разложения

В. ИЛЛЕШ

Было исследовано распределение продуктов реакции при различных температурах зависимости от степени разложения. Качественное и количественное распределения продуктов реакции и изменения в нем интерпретировались на основе теории цепных свободнорадикальных реакций.

Было установлено, что изменение выхода основных продуктов реакции и молекулярного веса смеси на выходе из реактора в зависимости от степени разложения—в области температур и времен реакции, используемых при пиролизе в промышленных масштабах — не зависит от температуры и описывается «единственными кривыми».

Было получено выражение, на основе которого из пиролитических данных чистых компонентов, составляющих смесь, рассчитываются выходы продуктов пиролиза смеси.

Характерные колебательные частоты кристаллических полимолибдатов аммония, построенных из октаэдрических блоков MoO_6 в области 400—4000 $см^{-1}$

Б. А. КИШ, Ш. ХОЛЛИ и Е. ХИЛЬД

Изучались колебательные частоты микрокристаллических аммоний-полимолибдатов в области 400—4000 $см^{-1}$. ИК спектры очень чувствительны к структурным изменениям полианионов, построенных из блоков MoO_6. Производились приближенные отнесения частот валентных колебаний Mo—O и мостов Mo—O—Mo, содержащих атомы кислорода в различных координациях. Характер валентных колебаний в случае гепта- и октамолибдата определялся с помощью корреляции $O_h \rightarrow C_{2v} \rightarrow C_{2h}$ и $O_h \rightarrow C_{2h} \rightarrow C_i$.

Смещение частот связей Mo—O(I) в ИК и Раман спектрах приводились в зависимости от изменения степени поликонденсации, от среднего координационного числа центральных ядер Mo, а также от изменения отношения $[NH_4^+] : [Mo—O(I)]$, характеризовавшегося через K. Подобным образом объяснялось смещение частоты колебания $\nu_3(F_2)$ иона NH_4^+. Полученные зависимости позволяют оценить числа связей Mo—O(I) в полианионах неизвестного строения, а в некоторых простых случаях и положения ионов NH_4^+. Вероятно, что ионы NH_4^+ октамолибдата располагаются симметрично по *i*-центру триклиновой ячейки C_i^1.

Окисление вторичных спиртов на платиновом электроде, I

Продукты окисления

ДЬ. ХОРАНИ, П. КЁНИГ и И. ТЕЛЬЧ

Электроокисление вторичных спиртов (изопропанол, *втор.* -бутанол и циклогексанол) было исследовано в кислых средах. Результаты, полученные из исследований стационарным и потенциодинамическим методами, были классифицированы в группы.

Было найдено, что химические явления при окислении спиртов следует разделять на две группы.

1. Взаимодействие металла со спиртом является необратимой адсорбцией, сопровождаемой переносом заряда; это не является ступенью стационарного окисления.

2. Существует хорошо выраженный путь реакции, исходящий из растворенного исходного вещества и приводящего к растворенному продукту.

Было найдено, что продуктами окисления являются соотвествующие кетоны.

Изучение окисления вторичных спиртов на платиновом электроде, II

Исследование взаимосвязи между адсорбцией кислорода и реакцией

ДЬ. ХОРАНИ, ДЬ. ВЕРТЕШ и П. КЁНИГ

1. Изучалось окисление вторичных спиртов на поверхности платины, частично или полностью покрытой кислородом.

2. Было установлено, что окисление протекает с заметной скоростью лишь на свободной поверхности платины.

3. При исследовании реакции окисления открывается возможность изучения адсорбционных и десорбционных свойств адсорбированного кислорода.

Изучение механизма изомеризации н-бутена, протекающей на кислом катализаторе, I

Кинетика каталитических мономолекулярных взаимных превращений трех компонентов

Д. КАЛЛО, Э. ДЕТРЕКЁИ и Г. ШАЙ

Были выведены уравнения скоростей превращений какого-либо компонента i для следующих возможных механизмов: 1. при превращении как в j, так и в k происходит адсорбция, реакция на поверхности и десорбция, 2. без реакции на поверхности одна из адсорбированных форм i десорбируется в виде j, а другая в виде k, 3. i адсорбируясь, превращается в адсорбированные j и k, которые затем десорбируются, 4. общая адсорбированная форма двух компонентов превращается в адсорбированную форму третьего компонента, 5. компоненты превращаются друг в друга через общие поверхностные промежуточные продукты. Для отдельных механизмов при выводе уравнений скорости ступенями, лимитирующими скорость, считали либо реакцию на поверхности, либо сорбцию. Легче оценивать такие уравнения начальной скорости превращения $i \rightarrow j$ для r^0_{ij}, которые в зависимости от начального давления p^0_i всегда могут быть выражены в виде уравнения $1/r^0_{ij} = m_{ij}/p^0_i + b_{ij}$ (при небольших покрытиях поверхности $m_{ij}/p_i \gg b_{ij}$, а при больших — $m_{ij}/p^0_i \ll b_{ij}$). Если $b_{ij} \neq b_{ik}$, то принципиально элементарные ступени мономолекулярных взаимных превращений трех компонентов протекают согласно Δ-схеме [(1) и (2) механизмы и (3), если реакция на поверхности является лимитирующей скорость процесса]; если $b_{ij} = b_{ik}$, то может наблюдаться лишь то, что превращение протекает согласно Y-схеме через общие промежуточные продукты или в равновесной смеси продуктов [механизмы (3), (4) и (5), когда лимитирующими процесс являются ступени сорбции]; если между двумя какими-либо компонентами быстро устанавливается равновесие, то реакция протекает согласно механизму (4) через медленную реакцию на поверхности. Кинетический метод, помимо выяснения механизма процесса, в некоторых случаях позволяет определить константы скоростей элементарных ступеней.

Получение производных 2,3-дигидро-4H-1,3-бензтиазина

Й. САБО, И. ВАРГА, Э. ВИНКЛЕР и Е. БАРТОШ

При конденсации 2-меркаптобензиламина и его производных с оксосоединениями в щелочной среде образуются производные 2,3-дигидро-4*H*-1,3-бензтиазина. Данный способ является новым методом получения производных 2,3-дигидро-4*H*-1,3-бензтиазина.

Алкалиоды со скелетом индоло [2,3-c] хиназолино [3,2-a] пиридина, I

Новые синтезы рутекарпина и его восстановление

О. КЛАУДЕР, К. ХОРВАТХ-ДОРА

Были разработаны новые синтезы рутекарпина. В одном случае цель была достигнута за счет упрощения известных синтезов, а в другом случае, исходя из N-карбобензилокситриптамина, был разработан новый метод. Полученный из 1,2,3,4-тетрагидро-1-оксо-β-карболина с помощью $POCl_3$ в качестве промежуточного продукта, так называемый «аддукт», *17*, может быть использован для получения рутекарпина и замещенных производных.

Из продукта, полученного при реакции триптамина с этиловым эфиром ортомуравьиной кислоты, был синтезирован 3,14-дигидрорутекарпин.

Исследовалось восстановление рутекарпина с помощью $LiAlH_4$ и в зависимости от используемого растворителя был получен либо рутекарпен, либо рутекарпан.

Printed in Hungary

A kiadásért felel az Akadémiai Kiadó igazgatója — Műszaki szerkesztő: Várhelyi Tamás

A kézirat nyomdába érkezett: 1971. XI. 5. — Terjedelem: 11,25 (A/5) ív, 75 ábra

72.72639 Akadémiai Nyomda, Budapest — Felelős vezető: Bernát György

The Acta Chimica publish papers on chemistry in English, German, French and Russian.

The Acta Chimica appear in volumes consisting of four parts of varying size, 4 volumes being published a year.

Manuscripts should be addressed to

Acta Chimica
Budapest 112/91 Műegyetem

Correspondence with the editors should be sent to the same address.

The rate of subscription is $ 16.00 a volume.

Orders may be placed with "*Kultúra*" Foreign Trade Company for Books and Newspapers (Budapest I., Fő utca 32. Account No. 43-790-057-181) or with representatives abroad.

Les Acta Chimica paraissent en français, allemand, anglais et russe et publient des mémoires du domaine des sciences chimiques.

Les Acta Chimica sont publiés sous forme de fascicules. Quatre fascicules seront réunis en un volume (4 volumes par an).

On est prié d'envoyer les manuscrits destinés à la rédaction à l'adresse suivante:

Acta Chimica
Budapest 112/91 Műegyetem

Toute correspondance doit être envoyée à cette même adresse.

Le prix de l'abonnement est de $ 16.00 par volume.

On peut s'abonner à l'Entreprise pour le Commerce Extérieur de Livres et Journaux «*Kultúra*» (Budapest I., Fő utca 32. Compte-courant No. 43-790-057-181) ou à l'étranger chez tous les représentants ou dépositaires.

«*Acta Chimica*» издают трактаты из области химической науки на русском, французском, английском и немецком языках.

«*Acta Chimica*» выходят отдельными выпусками разного объема. 4 выпуска составляют один том. 4 тома публикуются в год.

Предназначенные для публикации рукописи следует направлять по адресу:

Acta Chimica
Budapest 112/91 Műegyetem

По этому же адресу направлять всякую корреспонденцию для редакции.

Подписная цена – $ 16.00 за том.

Заказы принимает предприятие по внешней торговле книг и газет «*Kultúra*» (Budapest I., Fő utca 32. Текущий счет № 43-790-057-181) или его заграничные представительства и уполномоченные.

Reviews of the Hungarian Academy of Sciences are obtainable at the following addresses:

ALBANIA

Drejtorija Qändrone e Pärhapjes
dhe Propagandimit tä Librit
Kruga Konferenca e Päzes
Tirana

AUSTRALIA

A. Keesing
Box 4886, GPO
Sydney

AUSTRIA

GLOBUS
Höchstädtplatz 3
A-1200 Wien XX

BELGIUM

Office International de Librairie
30, Avenue Marnix
Bruxelles 5
Du Monde Entier
5, Place St. Jean
Bruxelles

BULGARIA

HEMUS
11 pl Slaveikov
Sofia

CANADA

Pannonia Books
2, Spadina Road
Toronto 4, Ont.

CHINA

Waiwen Shudian
Peking
P. O. B. 88

CZECHOSLOVAKIA

Artia
Ve Smečkách 30
Praha 2
Poštovní Novinová Služba
Dovoz tisku
Vinohradská 46
Praha 2
Mad'arská Kultura
Václavské nám. 2
Praha 1
SLOVART A. G.
Gorkého
Bratislava

DENMARK

Ejnar Munksgaard
Nörregade 6
Copenhagen

FINLAND

Akateeminen Kirjakauppa
Keskuskatu 2
Helsinki

FRANCE

Office Internationa' de Documentation
et Librairie
48, rue Gay-Lussac
Paris 5

GERMAN DEMOCRATIC REPUBLIC

Deutscher Buch-Export und Import
Leninstraße 16
Leipzig 701
Zeitungsvertriebsamt
Fruchtstraße 3—4
1004 Berlin

GERMAN FEDERAL REPUBLIC

Kunst und Wissen
Erich Bieber
Postfach 46
7 Stuttgart S.

GREAT BRITAIN

Blackwell's Periodicals
Oxenford House
Magdalen Street
Oxford
Collet's Subscription Import
Department
Dennington Estate
Wellingsborough. Northants.
Robert Maxwell and Co. Ltd.
4—5 Fitzroy Square
London W. 1

HOLLAND

Swetz and Zeitlinger
Keizersgracht 471—487
Amsterdam C.
Martinus Nijhof
Lange Voorhout 9
The Hague

INDIA

Hind Book House
66 Babar Road
New Delhi 1

ITALY

Santo Vanasia
Via M. Macchi 71
Milano
Libreria Commissionaria Sansoni
Via La Marmora 45
Firenze
Techna
Via Cesi 16
40135 Bologna

JAPAN

Kinokuniya Book-Store Co. Ltd.
826 Tsunohazu 1-chome
Shinjuku-ku
Tokyo
Maruzen and Co. Ltd.
P. O. Box 605
Tokyo-Central

KOREA

Chulpanmul
Phenjan

NORWAY

Tanum-Cammermeyer
Karl Johansgt 41—43
Oslo 1

POLAND

RUCH
ul. Wronia 23
Warszawa

ROUMANIA

Cartimex
Str. Aristide Briand 14—18
Bucureşti

SOVIET UNION

Mezhdunarodnaya Kniga
Moscow G—200

SWEDEN

Almquist and Wiksell
Gamla Brogatan 26
S—101 20 Stockholm

USA

F. W. Faxon Co. Inc.
15 Southwest Park
Westwood Mass. 02090
Stechert Hafner Inc.
31. East 10th Street
New York, N. Y. 10003

VIETNAM

Xunhasaba
19, Tran Quoc Toan
Hanoi

YUGOSLAVIA

Forum
Vojvode Mišića broj 1
Novi Sad
Jugoslovenska Knjiga
Terazije 27
Beograd

ACTA CHIMICA

ACADEMIAE SCIENTIARUM HUNGARICAE

ADIUVANTIBUS

V. BRUCKNER, GY. DEÁK, K. POLINSZKY,
E. PUNGOR, G. SCHAY, Z. G. SZABÓ

REDIGIT

B. LENGYEL

TOMUS 72 FASCICULUS 3

AKADÉMIAI KIADÓ, BUDAPEST

1972

ACTA CHIM. (BUDAPEST) ACASA 2 72 (3) 231—358 (1972)

ACTA CHIMICA

A MAGYAR TUDOMÁNYOS AKADÉMIA KÉMIAI TUDOMÁNYOK OSZTÁLYÁNAK IDEGEN NYELVŰ KÖZLEMÉNYEI

SZERKESZTI

LENGYEL BÉLA

TECHNIKAI SZERKESZTŐK

DEÁK GYULA és HARASZTHY-PAPP MELINDA

Az Acta Chimica német, angol, francia és orosz nyelven közöl értekezéseket a kémiai tudományok köréből.

Az Acta Chimica változó terjedelmű füzetekben jelenik meg, egy-egy kötet négy füzetből áll. Évente átlag négy kötet jelenik meg.

A közlésre szánt kéziratok a szerkesztőség címére (Budapest 112/91 Műegyetem) küldendők.

Ugyanerre a címre küldendő minden szerkesztőségi levelezés. A szerkesztőség kéziratokat nem ad vissza.

Megrendelhető a belföld számára az „Akadémiai Kiadó"-nál (Budapest V., Alkotmány utca 21. Bankszámla 05-915-111-46), a külföld számára pedig a „Kultúra" Könyv- és Hírlap Külkereskedelmi Vállalatnál (Budapest I., Fő utca 32. Bankszámla: 43-790-057-181) vagy annak külföldi képviseleteinél és bizományosainál.

Die Acta Chimica veröffentlichen Abhandlungen aus dem Bereiche der chemischen Wissenschaften in deutscher, englischer, französischer und russischer Sprache.

Die Acta Chimica erscheinen in Heften wechselnden Umfanges. Vier Hefte bilden einen Band. Jährlich erscheinen 4 Bände.

Die zur Veröffentlichung bestimmten Manuskripte sind an folgende Adresse zu senden:

Acta Chimica
Budapest 112/91 Műegyetem

An die gleiche Anschrift ist auch jede für die Redaktion bestimmte Korrespondenz zu richten. Abonnementspreis pro Band: $ 16.00.

Bestellbar bei dem Buch- und Zeitungs-Außenhandels-Unternehmen »*Kultúra*« (Budapest I., Fő utca 32. Bankkonto No. 43-790-057-181) oder bei seinen Auslandsvertretungen und Kommissionären.

Acta Chimica Academiae Scientiarum Hungaricae, Tomus 72 (3), pp. 231—240 (1972)

ÜBER DIE ANWENDUNG ZWEIATOMIGER MOLEKÜLE ALS VERGLEICHSELEMENTE BEI DER SPEKTROCHEMISCHEN ANALYSE NICHTLEITENDER STOFFE

J. LITOMISKÝ

(Institut für mineralische Rohstoffe, Kutná Hora, ČSSR)

Eingegangen am 10. Dezember 1970

Die in der Arbeit angeführten Beispiele bestätigen die Möglichkeit der analytischen Verwendung der molekularen Emissionsspektren. Bisher wurden diese Spektren für einen unerwünschten Ballast gehalten, welcher die Auswertung des Spektrogramms erschwert.

Die vorgelegten Resultate zeigen aber, daß sie als Vergleichselement (Bezugselement) zum Bilden analytischer Linienpaare mit Erfolg verwendet werden können.

Die Entstehung der molekularen Bandenspektren ist an solche Elemente gebunden, welche die Matrix des analysierten Systems bilden, gleich wenn sie der Bestandteil der Probe oder der Elektroden sind. Dadurch fällt die Notwendigkeit weg, »fremdes« Vergleichselement der Probe zuzusetzen, so daß die Vorbereitung der Probe zur Analyse in einfacherer Weise geschieht.

Einführung

Die quantitative spektrochemische Analyse leitender und nichtleitender Stoffe verdankt ihre außerordentliche Verbreitung der Einführung des Vergleichselementes, früher »Innerstandard« genannt. Das Vergleichselement beseitigt oder unterdrückt die Fehler, die durch die Anwendung der absoluten Intensität der Spektrallinie des analysierten Elementes als Maß seines Gehaltes in der Probe entstanden sind.

Die Ansichten darüber, welche Eigenschaften ein Vergleichselement besitzen sollte, entwickelten und änderten sich im Laufe der letzten 20 bis 30 Jahre, gestützt auf viele experimentell festgestellte Daten. Etwa in den sechziger Jahren waren schon die allgemein geltenden Richtlinien für die Wahl des Vergleichselementes bekannt [1, 2].

Wahl eines Vergleichselementes

Die erwähnten allgemeingültigen Richtlinien führen an erster Stelle die Flüchtigkeit des Vergleichselementes an, die der Flüchtigkeit des analysierten Elementes tunlichst ähnlich sein soll. Weiters sollen die beiden Elemente ähnliche Anregungspotentiale besitzen. Die ausgewählte Bezugslinie soll selbstabsorptionsfrei sein.

Beim Ausarbeiten konkreter analytischer Vorgänge ist es notwendig, zu überprüfen und dann zu entscheiden, ob als ein Vergleichselement dasselbe Element angewandt werden kann, das den Bestandteil der Probe darstellt

(meistens als Hauptkomponente), oder ob man gezwungen ist, ein Element zu verwenden, das keinen Bestandteil der Probe darstellt. Das erste Verfahren wird meistens bei der Spektralanalyse der Metalle und Legierungen benützt. Man kann es auch verwenden — wie weiter noch gezeigt wird — bei der Analyse pulverförmiger Stoffe. Als Vergleichselement, das kein Bestandteil der Probe ist, kann uns einen guten Dienst leisten

a) ein Element, das zur Probe in kleiner, konstanter Menge zugegeben wird,

b) ein Element, das den Hauptbestandteil der Trägerelektrode oder Gegenelektrode bildet,

c) ein Element, das der Bestandteil des Zusatzes (Puffers) ist; dieses wird in großer, aber konstanter Menge zur Probe zugegeben (siehe Tabelle I).

Übereinstimmung des energetischen Zustandes des Analysenlinienpaares

Bei der Wahl des Vergleichselementes herrschte früher die Ansicht vor, daß die Übereinstimmung des energetischen Zustandes beider Partner des analytischen Paares der maßgebliche Faktor sei. Das heißt, daß nur die Paare Atom/Atom oder Ion/Ion als analytische dienen sollten.

AHRENS und TAYLOR [3] haben an einer Reihe von Beispielen gezeigt, daß es möglich ist, auch die Paare Atom/Ion oder Ion/Atom zu benutzen und dabei eine befriedigende Reproduzierbarkeit der Resultate zu erreichen. Die einzige Bedingung ist, daß die Entladung zwischen den Elektroden glatt und ruhig brennen soll.

Tabelle I

Beispiele für die Auswahl eines Vergleichselementes (Innerstandard)

Vergleichselement (Innerstandard)			
1	2		
	Kein Bestandteil der Probe		
Bestandteil der Probe	*a)* wird der Probe zugegeben (kleine konstante Menge)	*b)* Hauptbestandteil der Elektrode (Träger- oder Gegenelektrode)	*c)* Bestandteil des Zusatzes (Puffer)
Metallurgie: Fe in Stählen, Al in Al-Legierungen — Pulverige Proben (SiO in Quarzit — diese Arbeit)	Silikatanalyse nach AHRENS [6]: In für leichtflüchtige, Pd für schwerflüchtige Elemente	Metallurgie (die Methode »point to plane«) — Pulverige Proben: Cu für Mo in Gesteinen [7] CN (aus Graphit) für Nb in Gesteinen [8]	Zn aus ZnS für leichtflüchtige Elemente in Gesteinen [9] — OH aus C_2H_5OH für Mo in Gesteinen [10] — NO aus KCN für Te in Gold [11]

Als Beispiel kann ich meine eigene Erfahrung mit einem solchen heterogenen Paar anführen. Bei der Bestimmung von Strontium in Apatit [4] habe ich gute Resultate mit dem Linienpaar Sr II 346,4 nm/Ca I 346,8 nm gewonnen. Zur Anregung der Spektren wurde der Wechselstromdauerbogen benutzt. AHRENS und TAYLOR arbeiteten mit dem Gleichstrombogen.

Esergibt sich daraus, daß der glatte Verlauf der Entladung nicht nur durch die Parameter der Anregungsquelle, sondern auch durch das Material und die Form der Elektroden und durch andere, wenn auch scheinbar untergeordnete Faktoren beeinflußt werden kann.

Molekülspektren

Bei der thermischen Zersetzung der Probe entstehen auch zweiatomige Moleküle. Diese können Restpartikeln von ursprünglichen, komplizierten Molekülen sein, aber auch neuentstandene Partikeln aus den Reaktionen der freigesetzten Atome und Ionen der Probe, aus der Trägerelektrode oder sogar aus der Luft.

Diese zweiatomigen Moleküle, ähnlich den Atomen und Ionen, können durch Einwirkung von energiereichen Partikeln angeregt werden und dann Spektrallinien aussenden. Zum Unterschied von Atomen und Ionen ist das molekulare Spektrum sehr kompliziert [5].

Es ist verursacht durch die Fähigkeit der Moleküle, zu rotieren (es rotiert das ganze Molekül), zu schwingen (es schwingen die Atome in dem Molekül) und sich anregen zu lassen (es handelt sich um äußere Elektronen). Solange sich das Molekül im Gaszustand befindet, wird die Energie von ihm in Quanten aufgenommen und ausgesendet. Die kleinste Energiemenge ist zur Rotation nötig, viel größer ist die zur Vibration verbrauchte Energie (meistens etwa hundertmal größer) und am größten die zur Anregung von Elektronen verbrauchte. Die Energie der Elektronenniveaus ist mit der von Bogenanregungsquellen gelieferten Energie vergleichbar. Deswegen findet man molekulare Emissionsspektren meistens bei der Spektralanalyse von Proben, die durch einen elektrischen Bogen angeregt wurden.

Bei der Anregung von molekularen Elektronenspektren entstehen gleichzeitig Vibrations- und Rotationsspektren. Die letzteren bilden die sogenannte Rotationsfeinstruktur der molekularen Spektren.

Die molekularen Bandenspektren verursachen bei der Spektralanalyse eine Reihe von Schwierigkeiten beim Auswerten der Spektren durch häufige Interferenzen mit den analytischen Spektrallinien.

Analytisch wurden bisher nur die Moleküle des Typs CaF zur Fluorbestimmung benutzt.

Im Vergleich zu den Atom- und Ionenspektren erscheinen die Molekülspektren erst bei höheren Konzentrationen der Elemente, die das emittierende

Molekül bilden. So z. B. erscheint die Atomlinie von Beryllium 234,861 nm bei der Bestimmung von Be im Flußspat schon beim Gehalt von 0,8 ppm Be, dagegen sind die stärksten Bandenköpfe von BeF (300,99 nm, 301,30 nm und 301,8 nm) im Spektrogramm erst beim Gehalt von über 0,2% Be nachweisbar [12]. Zur völligen Besetzung aller Energieniveaus und zur völligen Entwicklung des gesamten Molekularbandenspektrums kommt es erst dann, wenn die Konzentration der Elemente, die das Molekül bilden, genügend hoch ist (z. B. beim SiO Molekül muß die Probe mindestens 10% SiO_2 enthalten).

Das molekulare Spektrum als Vergleichselement

Interessanterweise wurden die molekularen Bandenspektren bisher nur in sehr beschränktem Maße analytisch ausgenutzt. Ich habe mir das Ziel gesetzt, sie als ein Vergleichselement bei der Emissionsspektralanalyse zu verwenden. In der mir zugänglichen Literatur habe ich nur einen einzigen diesbezüglichen Hinweis gefunden. Im Buch von AHRENS und TAYLOR [13] wird die Dissertationsarbeit von R. H. SERAPHIM zitiert. SERAPHIM hat — offensichtlich zum erstenmal — die Molekülbande CaO 548,8 nm als Vergleichselement zum Bandenkopf CaF 529,1 nm benutzt. Es handelte sich um die Fluorbestimmung in Silikatgesteinen. In diesem Falle wurde das Paar Molekül/Molekül benutzt. Beide Partikel sind bezüglich Zusammensetzung, Masse und Energiegehalt sehr ähnlich. Es ist aber möglich, exakte Resultate der Analyse auch mit den Paaren Atom/Molekül oder Ion/Molekül zu erreichen. Nur muß die AHRENS—TAYLORsche Bedingung eines glatten, regelmäßigen Entladungsverlaufes erfüllt sein.

So z.B. wurde das Paar Atom/Molekül bei der Molybdänbestimmung in Gesteinsproben gewählt [7]. Auf einer kupfernen Schalenelektrode wurde die Probe mit 50%igem Äthanol befeuchtet und mittels einer kondensierten Funkenentladung zur Strahlung angeregt. Als analytisches Paar wurden die Molybdänlinie Mo I 317,035 nm und eine Linie aus der Molekülbande OH (Bandenkopf 306,4 nm) mit der Wellenlänge 309,0 nm verwendet.

Das Paar Ion/Molekül hat sich bei der Zirkoniumbestimmung in Abfallsprodukten bei der Kaolinaufbereitung als besonders erfolgreich erwiesen. Deshalb soll diese Methode hier ausführlicher beschrieben werden.

Quantitative Bestimmung von Zirkonium in Abfallprodukten der Kaolinaufbereitung

Das Abfallprodukt enthielt mehr als 90% SiO_2. Die Standardproben wurden aus brasilianischem Bergkristall (95%), Aluminiumoxid (2,5%) und Limonit (2,5%) vorbereitet. Zu diesem Gemisch wurde Zirkonium in Form von $ZrOCl_2$ zugesetzt und eine Reihe von 6 Standardproben mit Zirkoniumgehalten von 1,00% bis 0,0032% hergestellt.

Analytische Bedingungen:

Spektrograph: Zeiss Q 24. Spaltbreite 0,006 mm, Hartmannblende T-10-5, Zwischenabbildungsblende 3,2 mm; Kammerblende 1 : 15.

Anregungsquelle: Wechselstrombogen, I = 8A. Sowjetischer Generator DG-1.

Elektroden: Kohleelektroden (quasiamorphes Material). Stäbchen von quadratischem Querschnitt (ČKD Prag). Trägerelektrode mit zylindrischer Aushöhlung, Querschnitt 2,5 mm, Tiefe 4,5 mm, Kanten gebrochen. Gegenelektrode mit pyramidalem Ende. Elektrodenabstand 3 mm.

Vorbereitung der Probe: Die Probe wird mit dem zweifachen Gewicht an Kohlepulver vermischt und in die Trägerelektrode gestampft.

Photographische Behandlung: Photoplatte Foma super ortho 6×24 cm (18 DIN). Expositionszeit 20 s ohne Vorbrennen. Entwickler AGFA 40, Entwicklungszeit 2,5 min/20 °C.

Vier Standardproben (0,100—0,003% Zr) wurden unter den genannten Bedingungen analysiert. Die Analyse wurde nach einem längeren Zeitabstand wiederholt. Die Spektren wurden auf eine Platte anderer Emulsionsnummer aufgenommen. Die analytischen Linien Zr II 339,198 nm und Zr II 343,823 nm kamen deutlich auch in der letzten Standardprobe (0,0032% Zr) zum Vorschein. Zum Messen ihrer optischen Dichte wurde die s.p.d.-Skala nach ADDINK [14] mit 21 Stufen, eigener Herstellung, verwendet.

Es zeigte sich, daß die Absolutwerte der optischen Dichte der Zr-Linien stark von der Güte der photographischen Emulsion abhängig sind (siehe Abb. 1).

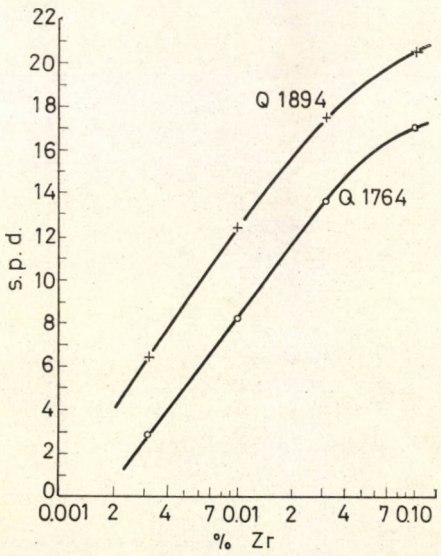

Abb. 1. Abhängigkeit der optischen Dichte der Spektrallinie Zr II 339,2 nm von der Güte der photographischen Emulsion. Analyse der Standardproben Nr. 3—6. Gemessen mit der s. p. d.-Skala

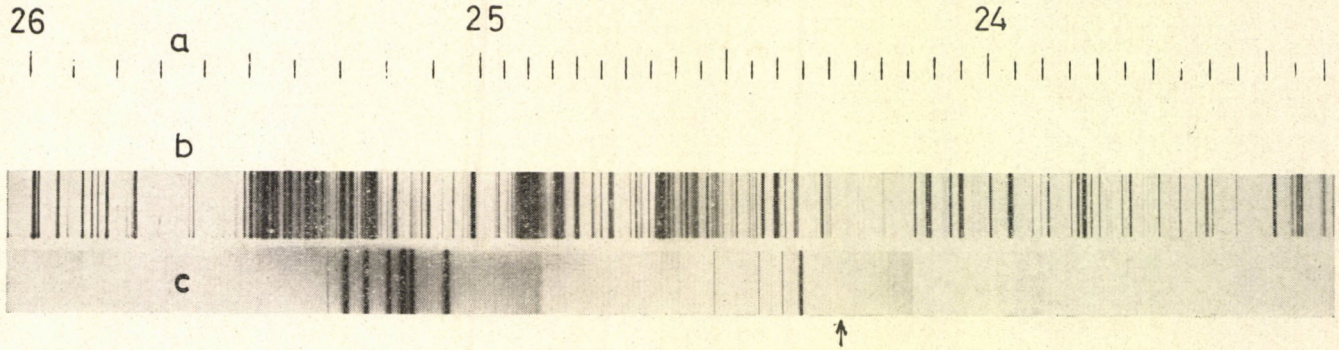

Abb. 2. Emissionsbandenspektrum des Moleküls SiO. Der intensivste Teil zwischen 236 und 260 nm. a — Wellenlängenskala; b = Eisenspektrum; c = Bandenspektrum des Moleküls SiO (gemeinsam mit den Atomlinien des Siliziums). Die mit dem Pfeil bezeichnete Linie wurde als die Vergleichslinie verwendet

Es wurde klar gezeigt, daß zur Ausschaltung dieses ungünstigen Einflusses (und selbstverständlich auch der Unregelmäßigkeiten des Anregungsprozesses) ein geeignetes Vergleichselement gefunden werden muß. Zuerst wurde eine Linie von Silizium gesucht, das — als Hauptkomponente anwesend — sich direkt als Vergleichselement anbot. Alle Siliziumlinien waren aber von so großer Intensität, daß sie für Vergleichszwecke nicht verwendbar waren. Um die Analyse durch den Zusatz eines fremden Vergleichselementes nicht komplizieren zu müssen, habe ich einen Versuch mit dem Molekülspektrum von SiO vorgenommen.

Dieses Bandenspektrum liegt im ultravioletten Bereich zwischen 293 und 210 nm [15]. Einzelne Banden mit zahlreichen scharfen Linien der Rotationsfeinstruktur nehmen den Anlauf von Vibrationskanten zu längeren Wellenlängen.

Der benutzte Spektrograph Q 24 hat im Bereich zwischen 260 und 200 nm ein gutes Auflösungsvermögen, so daß die einzelnen Linien der Rotationsfeinstruktur der SiO-Bande gut getrennt sind.

Aus dem ganzen Spektrum des Moleküls SiO sind die Banden mit Köpfen der Wellenlängen 248,680 nm (v', $v'' = 0, 2$) und 241,377 nm (v', $v'' = 0, 1$) die intensivsten. Aus dem Bande v', $v'' = 0, 1$ habe ich eine Linie mit der Wellenlänge 242,75 nm als Vergleichslinie ausgewählt. Die Lücke zwischen dieser und der benachbarten Linie genügte eben zum Dazwischenlegen einer Meßlinie der s.p.d.-Skala. Eine Übersicht über die Meßergebnisse gibt Tabelle II.

Tabelle II

Analyse der Standardproben für die Zr-Bestimmung in Quarz

Photoplatte Nr.	Standard-probe (Nr.)	Gehalt an Zr (in %)	s.p.d.-Werte*		Δ s.p.d. Zr—SiO
			Zr 339,2	SiO 242,7	
Q 1764	3	0,100	17,0	8,2	+8,8
	4	0,032	13,7	8,3	+5,4
	5	0,010	8,2	7,8	+0,4
	6	0,0032	2,8	7,8	−5,0
Q 1894	3	0,100	20,5	12,5	+8,0
	4	0,032	17,7	12,2	+5,5
	5	0,010	12,5	12,5	0,0
	6	0,0032	6,5	12,5	−6,0

* Mittelwert von drei Messungen.

Die Arbeitskurve, aus den Werten Δs.p.d. Zr—SiO und Logarithmen des Zr-Gehaltes konstruiert, ist in Abb. 3 veranschaulicht. Sie hat einen geradlinigen Verlauf im Konzentrationsbereich von 0,0032% bis 0,032% Zr.

Durch dieses Verfahren sind einige Proben von Quarzsanden analysiert worden. Eine von diesen wurde auch auf chemischem Wege (kolorimetrisch) analysiert. Die gewonnenen Resultate an Zirkonium:

Probe Nr. 60351

Spektralanalytisch ..... 0,022% Zr
Kolorimetrisch ..... 0,020% Zr

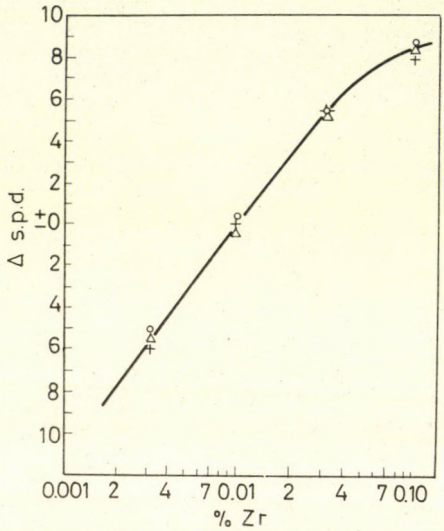

Abb. 3. Arbeitskurve zur Bestimmung von Zirkonium in Proben mit einer Siliziumoxidmatrix. ○—○ Zr II 339,198 nm — SiO 242,75 nm. Diese Werte wurden aus Photoplatten mit +—+ verschiedenen Emulsionsnummern entnommen. △—△ Zr II 343,823 nm — SiO 242,75 nm

Mit der Zr-Linie 339,198 nm fällt die Atomlinie des Thoriums Th I 339,204 nm zusammen. Enthält die Probe auch Thorium, so ist es notwendig, die Zr-Linie Zr II 343,823 nm zu verwenden. Dies war der Fall bei der Bestimmung von Zr im Monazitsand. Nach vorläufigen Versuchen wurde die Probe mit Siliziumdioxyd (Quarzsand) zehnmal verdünnt und unter den obenerwähnten Bedingungen analysiert. Die Meßergebnisse zeigt die Tabelle III.

In der ursprünglichen Probe wurde durch Umrechnen 0,13% Zr gefunden. Die kolorimetrische Bestimmung [16] ergab 0,150% Zr. Die Übereinstimmung beider Resultate ist befriedigend. Die Reproduzierbarkeit der Resultate, durch die Standardabweichung ausgedrückt, beträgt $\pm 5\%$ (für Hundertstel % Zr) und $\pm$ 12% (für Tausendstel % Zr).

Es ist beachtenswert, daß die Δs.p.d.-Werte der beiden verwendeten Linienpaare innerhalb der Fehlergrenzen die gleichen sind (siehe Tab. II und III). Sie bilden also eine einheitliche Arbeitskurve (s. Abb. 3).

Dieses Beispiel zeigt mit genügender Signifikanz, daß die molekularen Spektren der zweiatomigen Moleküle als Vergleichselement genauso geeignet

sind wie die Atom- oder Ionenlinien. Sie haben den bedeutenden Vorteil, daß sie von Selbstabsorption frei sind; dies gilt besonders für die Linien der Rotationsfeinstruktur.

Tabelle III

Die Bestimmung des Zr-Gehaltes in Monazitsand

Probe	Durchschnittswerte s.p.d.		Δs.p.d. Zr—SiO	Gehalt an Zr (in %)
	Zr 343,8	SiO 242,7		
Stand. Nr. 3	17,0	8,5	+8,5	0,100
Nr. 4	13,83	8,5	+5,33	0,032
Nr. 5	7,83	8,16	−0,33	0,010
Nr. 6	2,83	8,33	−5,50	0,0032
Monazitsand mit SiO_2 verdünnt	10,0	9,0	+1,0	0,013

Weitere Beispiele der Anwendung von Bandenspektren als Vergleichselement

Auf Grund dieser anregenden Resultate wurden die Bandenspektren als Vergleichselement auch in anderen Verfahren erprobt. So bei der Lösungsspektralanalyse des gediegenen Goldes [11], in welchem die Elemente Ag, Bi, Cu, Hg, Pb und Te bestimmt wurden, entstand ein intensives, ultraviolettes Band des Moleküls NO während der Bogenbrennung. Es zeigte sich, daß es für die Tellurbestimmung als ein Vergleichselement mehr geeignet ist als Gold, das sonst mit den übrigen Elementen befriedigende Linienpaare geschaffen hat.

Bei anderer Gelegenheit ist festgestellt worden, daß die Möglichkeit besteht, auch molekulare Spektren, die durch Reaktionen des Elektrodenmaterials entstehen, zu verwenden. So bei der Bestimmung von Niob in Gesteinsproben hat sich als Vergleichselement der Kopf des Schwanzbandes (tailband) des Moleküls CN (Wellenlänge 314,26 nm) am besten bewährt [8]. Dieser Bandenkopf wurde mit der Spektrallinie Nb II 316,34 nm kombiniert. Die Konstruktion von Streudiagrammen nach HOLDT [17] hat die Vorteile dieser Kombination im Vergleich mit anderen Linienpaaren erwiesen.

In manchen Fällen hat sich gezeigt, daß nur ein Vergleichselement nicht fähig ist, alle Intensitätsschwankungen der Analysenlinie auszugleichen. Hier ist es zu einer Besserung gekommen, wenn zwei Linien von zwei verschiedenen Partikeln verwendet wurden:

$$\Delta Y = \text{Be I } 265{,}06\,\text{nm} - \frac{\text{SiO } 243{,}17\,\text{nm} + \text{CN } 343{,}25\,\text{nm}}{2} \quad [15],$$

$$\Delta\text{s.p.d.} = \text{Sr II } 346{,}45\,\text{nm} - \frac{\text{CN } 351{,}5\ \text{nm} + \text{Ca } I\ 346{,}85\,\text{nm}}{2} \quad [13].$$

Das Resultat dieser Kombinationen war in den meisten Fällen eine Verminderung des Streubereiches der ΔY- (Δs.p.d.-)Werte und darauffolgende erhöhte Genauigkeit der Analyse. In einigen Fällen ist es gelungen, die Arbeitskurve geradlinig zu gestalten, ihren Anstieg zu steigern, was eine weitere Präzisionserhöhung der Analyse zur Folge hatte.

Abschluß

Die in der Arbeit angeführten Beispiele bestätigen die Möglichkeit der analytischen Verwendung der molekularen Emissionsspektren. Bisher wurden diese Spektren für einen unerwünschten Ballast gehalten, der die Auswertung des Spektrogramms erschwert.

Die vorgelegten Resultate zeigen aber, daß sie als Vergleichselement (Bezugselement) zum Bilden analytischer Linienpaare mit Erfolg verwendet werden können.

Die Entstehung der molekularen Bandenspektren ist an solche Elemente gebunden, die die Matrix des analysierten Systems bilden, gleich ob sie Bestandteile der Probe oder der Elektroden darstellen. Hiermit fällt die Notwendigkeit weg, »fremdes« Vergleichselement der Probe zuzusetzen, so daß die Vorbereitung der Probe zur Analyse auf einfachere Weise geschieht.

LITERATUR

1. Scheller, H.: Einführung in die angewandte spektrochemische Analyse. VEB Verlag Technik, Berlin, 1953, S. 64
2. Ahrens, L. H., Taylor, R. S.: Spectrochemical Analysis, 2nd Ed. Addison-Wesley Publishing Co., Reading, London, 1961, S. 90
3. Ahrens, L. H., Taylor, R. S.: *ibid.* S. 96
4. Litomiský, J.: Čas. miner. geol. **9**, Nr. 1, 9, 1964
5. Harrison, G. R., Lord, R. C., Loofbourow, J. R.: Practical Spectroscopy. Prentice-Hall, New York, 1948
6. Ahrens, L. H., Taylor, R. S.: *ibid.* S. 183
7. Litomiský, J.: Diplomarbeit, Karls Universität Prag, 1953, S. 10. (Résumé: Chem. Listy **48**, 1437, 1954)
8. Litomisky, J.: Abschlußbericht des Institutes für mineralische Rohstoffe, Kutná Hora, 1966, S. 100 (nicht veröffentlicht)
9. Litomiský, J.: Chemia Analit. (Warszawa), **7**, No. 2, 409, 1962
10. Litomiský, J.: Diplomarbeit, S. 25
11. Litomiský, J., Kupková, D.: Acta geologica et geografica Universitatis Comenianae, Geologica Nr. 6, S. 464, 1961
12. Litomiský, J.: Abschlußbericht des Institutes für mineralische Rohstoffe, Kutná Hora, 1958 (nicht veröffentlicht)
13. Ahrens, L. H., Taylor, R. S.: *ibid.* S. 280
14. Addink, N. W. H.: Spectrochim. Acta **4**, 36, (1949)
15. Rosen, B. *et al.*: Tables de constantes et données numériques 4. Constantes sélectionnées. Données spectroscopiques concernant les molécules diatomiques. Hermann et Cie, Paris, 1951, S. 278
16. Valcha, Z.: Geologický průzkum **5**, Nr. 5, 145, 1963
17. Holdt, G.: In »Emissionsspektroskopie«, Akademie-Verlag, Berlin, 1964, S. 63

Jaromír Litomiský; Kutná Hora, Šmeralova ul. 532, ČSSR.

Acta Chimica Academiae Scientiarum Hungaricae, Tomus 72 (3), pp. 241—253 (1972)

ELECTRONIC STRUCTURE OF ISOELECTRONIC MOLECULES

S. SZŐKE G. JALSOVSZKY and E. DUDAR*

*(Central Research Institute for Chemistry of the Hungarian Academy of Sciences, Budapest and *Chinoin Pharmaceutical and Chemical Works, Budapest)*

Received February 25, 1970

The electronic structure and orbital configuration of pyridine-*N*-oxide have been investigated by the PPP and EH methods. It has been found that in polar solvents the orbital configuration of the N–O bond in pyridine-*N*-oxide is similar to that of monofluorobenzene, while in nonpolar solvents the well known acceptor–donor structure exists. The differences in electronic spectra in nonpolar solvents have been interpreted by assuming that the nitrogen is doubly charged in the N–O bond. Compared to the more compact configuration of the C–F bond in monofluorobenzene, this structure gives rise to lower transition energies in the near ultraviolet region.

Several parameters of isoelectronic molecules are nearly equal, or, at least, have similar values. There are different degrees of isoelectronicity, ranging from equality of the total number of electrons to the identity of orbital configurations. Consequently, in the first case less, in the second case more parameters of isoelectronic molecules have nearly the same values. If the orbital configurations of isoelectronic molecules are exactly the same, interatomic distances will be nearly equal to each other, and in addition to the molecular parameters, certain terms of the Hamiltonian, and the kinetic and potential energy matrices will also agree [1—4].

Due to the isoelectronicity, a number of quantum-chemical terms have similar values. Several authors have pointed out that in the simplest semiempirical methods the diagonal terms of the Hamiltonian matrix are proportional to the electronegativity. PRITCHARD and SUMNER [5, 6] have even elaborated a quantum-chemical method for determining electronegativities.

By twos, the diagonal terms of the original PPP Hamiltonian represent a chemical bond, so the diagonal elements constructed from atomic parameters belonging to isoelectronic bonds add up to nearly the same value.

The trace of a matrix determines the sum of its eigenvalues, which, in turn, influences orbital energies, *i.e.*:

$$\sum_{u=1}^{s} F_{uu} = \sum_{u} \left[-I_u + \frac{1}{2} P_{uu}\gamma_{uu} + \sum_{v} (P_{uv} - Z_v)\gamma_{uv} \right] = \sum_{u} \lambda_u \qquad (1)$$

where F_{uu} is the diagonal term of the PPP Hamiltonian,

I_u is the ionization potential of atoms contributing π-electrons,

γ_{uu} denotes one-center Coulomb integrals,
γ_{uv} denotes two-center Coulomb integrals,
P_{uu} denotes charges on atoms,
P_{uv} denotes bond orders,
Z_v denotes core charges;
eigenvalues are denoted by λ_u, and s is the number of centers.

One-center repulsion integrals, γ_{uu}, are related to Mulliken atomic electronegativities; more precisely, they differ only in a multiplication factor of two, which is balanced by a 1/2 factor in Eq. (1). The principle of equalized electronegativities is, of course, also valid for Mulliken electronegativities, and so one can refer to bond electronegativities also in this case. Summing the γ_{uu} integrals over bonds, the equalized or mean electronegativities of the bonds are obtained, and these quantities are nearly the same in isoelectronic molecules. Similarly, due to the fact that in isoelectronic diatomic molecules (and, in several cases, also in bonds) the mean ionization potentials are nearly the same, these ionization potentials contribute the same partial sums to the trace of the F matrix.

As an example for this statement, let us consider the mean ionization potentials of C—F and N—O bonds, calculated from parameters used later in the paper:

$$I_C + I_F = 11.16 + 33.58 = 44.74 \text{ eV},$$

$$I_N + I_O = 14.12 + 30.15 = 44.27 \text{ eV}.$$

The sum of P_{uu}'s (charges on atoms) and that of P_{uv}'s agree, by definition, with the corresponding quantities of isoelectronic molecules. The second equality is one of the determining features of isoelectronicity. The same holds for Z_v's, the effective core charges.

Two-center repulsion integrals are evaluated by the expression e^2/r (POPLE [7]), or by the expression $e^2/(r + a)$ (MATAGA–NISHIMOTO approximation), where e denotes the charge of the electron. Regarding that in isoelectronic molecules of the same orbital configuration the value of the interatomic distance (r) is approximately the same, and that the constant a in the MATAGA–NISHIMOTO approximation is, in fact, the mean Mulliken electronegativity of the bond, the value of γ_{uv} should be the same, or at least nearly the same for isoelectronic bonds.

In addition to the facts given above, there are several other analogous features in connection with potential energy functions, electronic and vibrational spectra.

In this work the π-electron distribution and the electronic transition energies of two isoelectronic molecules, pyridine-*N*-oxide and monofluorobenzene, are studied in order to understand the relations between electronic structure and isoelectronicity.

Isoelectronicity of pyridine-N-oxide and monofluorobenzene

Some authors noticed long ago that the vibrational spectra of the above molecules and of their derivatives have numerous similar features. This means not only the similar position of certain bands but closer similarities in the whole structure of the spectra and even the agreement of the majority of force field elements [2, 3, 9, 10].

On the basis of these analogies in the vibrational spectra it has been assumed that these molecules are isoelectronic in the sense that their orbital configurations are the same, including those of the C–F and N–O bonds.

This assumption seems to be surprising because the diatomic CF and NO molecules are not isoelectronic in this sense, their orbital configurations and vibrational frequencies being rather dissimilar. Moreover, the nitrogen atom contributes three electrons and the oxygen two electrons to the N–O bond, giving rise to an odd total number of electrons and a half integer bond order. On the other hand, in aromatic *N*-oxides N–O bonds are of dative character, and the π-electrons are contributed by the nitrogen.

In order to elucidate the electronic structure of pyridine-*N*-oxide and monofluorobenzene, first of all the π-electron system was studied, assuming that the influence of other bonds as well as that of σ–π interactions are the same in the two molecules.

Numerous studies have been carried out on the character of the C–F bond in fluorobenzenes, and the bond has been found definitely covalent. No such definite statement can be made for the *N*-oxides, where not even the final assignment of electronic spectra has been accepted so far.

Apart from gross isoelectronicity, the isoelectronicity of characteristic groups often causes surprising similarities in the spectra, so it had to be studied whether it is the identical structure of certain characteristic groups, or the agreement of the total number of electrons that gives rise to the analogous features. In order to extend this line of analysis, pyridine-N^+-OH was also studied, since the structure of this molecule is intermediate between those of the above mentioned two molecules.

Models for the calculations

The electronic structure of pyridine-*N*-oxide is studied on the basis of two different models:

(1) Model I is based on the isoelectronicity with fluorobenzene. The N–O bond is assumed to have a nitrogen atom of $trtrtr^2\pi$ configuration. Two of its four hybrid electrons occupy the empty $2p_y$ and $2p_z$ orbitals of oxygen. This rearrangement is, in fact, a charge transfer, *i.e.* the nitrogen atom becomes more positive and the oxygen more negative. The bond becomes thereby more similar to the C–F bond. The remaining two hybrid electrons of the nitrogen

are bonded to carbon atoms, and the p-electron is delocalized. So a closed shell is formed around the oxygen, just like around the fluorine in the fluorobenzenes (Fig. 1).

According to the above, in model I it is assumed that the orbital configurations of the two molecules are the same (including the electrons of the substituents and of the bonds directed to the substituents). The correctness of this

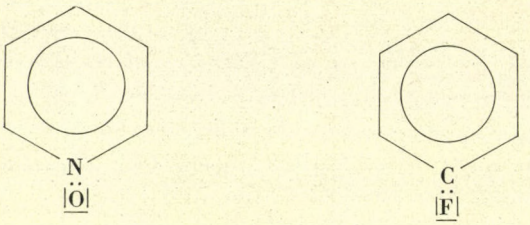

Fig. 1. Orbital configuration of pyridine-N-oxide and monofluorobenzene

assumption is apparent from the good agreement of bond order and total electronic energy values. The aim of the PPP calculations was, first of all, to check the validity of this assumption. In the calculations, dipole moment and molecular ionization potentials were used as adjusting parameters.

(2) The calculation on pyridine-N-oxide can also be carried out by assuming that the nitrogen directly contributes two $2p$ electrons, and the oxygen atom only one electron, to the delocalized system (model II).

In model I the contribution of oxygen is 2 electrons to the delocalized system, just like that of fluorine in the C–F bond, and therefore the core charge of oxygen is taken to be 2. The nitrogen atom contributes only one electron to the π-sextet, giving rise to a singly charged core.

The two models lead to different matrix elements in the PPP Hamiltonian, due to the different ionization potentials and different one- and two-center integrals.

The method applied

Regarding that it is first of all the mobile π-electron system that determines the structural characteristics of the above molecules, the PPP approximation was chosen for the investigation. The use of this method is particularly justified here, because it suits our assumptions concerning isoelectronic molecules, namely that the influence of π-electrons and that of the σ–π interaction are nearly the same due to the similar structure and, therefore, differences can be expected only in the behaviour of π-electrons.

Our first aim was to determine bond orders, on the basis of which the transferability of force constants could be interpreted [4, 10]. The charges on atoms, on the other hand, are related to the ionicity and mean electronegativities.

The reliability of the calculated π-electron distribution is based on the reproduction of electronic transition energies, calculated from the orbital energies by taking configuration interaction into account.

The total π-electron energy (E_π) was evaluated from the following expression:

$$E_\pi = \sum_{i=1}^{n/2} \left\{ \varepsilon_i^{SCF} + \sum_{u=1}^{s} c_{iu}^{SCF} \left[(-I_u - \sum_{v=1}^{s} Z_v \gamma_{uv}) c_{iu}^{SCF} + \sum_{u \neq v} \beta_{uv} c_{iu}^{SCF} \right] \right\} \qquad (2)$$

where ε_i denotes the energy of the i-th molecular orbital, I_u stands for the ionization potential of atom u, Z_v is the virtual core charge of atom v, γ_{uv} denotes repulsion integrals ($u \neq v$), β_{uv} denotes two-center core integrals, n is the number of π-electrons, and s the number of $2p$ basis orbitals.

Molecular orbitals, ψ_i, are obtained by the following transformation:

$$\psi_i = \sum_{u=1}^{s} c_{iu} \varphi_u$$

where φ_u denotes $2p$ atomic orbitals centered on atom u, and s is the number of centers contributing electrons to the π-electron system and, at the same time, is the dimension of the PPP matrix.

The diagonal terms of this matrix are given by Eq. (1), whereas the off-diagonals are given by the following expression:

$$F_{uv} = \beta_{uv} - 1/2 P_{uv} \gamma_{uv}. \qquad (3)$$

The elements of the configuration interaction matrix are as follows:

$$\langle \chi_{i \to k} | H | \chi_{j \to l} \rangle = \delta_{ij} \delta_{kl} (\varepsilon_k - \varepsilon_i) + \sum_{u,v} (2 c_{uj} c_{ul} c_{iv} c_{ik} - c_{ui} c_{uk} c_{vj} c_{vl}) \gamma_{uv} \qquad (4)$$

where $\chi_{i \to k}$ and $\chi_{j \to l}$ are the wave functions belonging to the corresponding electronic transitions, H denotes the Hamiltonian operator, ε_i and ε_k denote orbital energies, c_{uj} etc. are LCAO coefficients and δ is the Kronecker symbol.

In the calculation of one-center repulsion integral terms, problems arise very often due to the uncertainty of electron affinity values, particularly in cases when one of the atoms contributes two electrons to the delocalized π-system. In such cases the usual ionization potential values cannot be used.

Several methods have been recently recommended for overcoming the difficulties due to the uncertain value of the electron affinity, a rather widely used one being that of PAOLONI [11], according to which the one-center repulsion integral of carbon is used for evaluating the terms corresponding to other atoms, by the means of Slater exponents of $2p$ orbitals. Similarly, CHALVET

and LEIBOVICI [12], whose parameters were used in this work for the fluorobenzene calculations, have given a simple expression for the repulsion integral of fluorine:

$$\gamma_{FF} = \gamma_{CC} \frac{\xi_F}{\xi_C} \tag{5}$$

where ξ_F and ξ_C denote the corresponding Slater exponents. The terms used for the approximation of repulsion integrals are, in fact, the Mulliken electronegativities of the atoms in question.

The Slater exponents used in Eq. (5) are in linear correlation with the Pauling electronegativities [13]:

$$\xi_A = 0.65\ P_A \tag{6}$$

where P_A denotes the Pauling electronegativity of atom A. Consequently, Eq. (5) can be rewritten as

$$\gamma_{FF} = \gamma_{CC} \frac{P_F}{P_C} . \tag{7}$$

The near identity of the ratio of orbital exponents is not restricted to the first row of the periodic table. In the second period the constancy of this ratio becomes more pronounced if the orbital exponents are calculated by taking into account d-orbitals as well (SANTRY and SEGAL [14]).

Based on the above considerations, the calculation of one-center repulsion integrals, γ_{AA}, can be traced back to the proportionality between electronegativities.

Parameters used in the calculations

In the PPP method, one-center core integrals are approximated by ionization potentials, two-center ones by empirical parameters characteristic of a given bond type.

As has been mentioned earlier in the paper, in the calculation of monofluorobenzene, the parameters of CHALVET and LEIBOVICI [12] were used without any alteration. The authors of Ref. [12] determined the electronic transitions and π-electron distributions of 12 fluorinated molecules.

The properties of pyridine-*N*-oxide and of pyridine-N^+-OH were calculated using the parameters given by BAILEY [15]. She has studied a great number of azacyclic molecules. These calculations were based on the ionization potential and electron affinity values reported by HINZE and JAFFÉ and by NISHIMOTO and FORSTER. One-center repulsion integrals were evaluated by

the method of KWIATKOWSKI. In cases when an atom contributes two π-electrons to the conjugated system, the integral is given by the following expression:

$$W_x = \langle\varphi_x|T(i) + U_x^{++}(i)|\varphi_x\rangle = -I(X{-}H){-}\gamma_{xx} \qquad (8)$$

where I_A denotes the first ionization potential of atom A; the other symbols are those used in Refs. [15] and [16].

The parameters of the carbon atom as well as the two-center core integrals of C–C bond are, as almost generally accepted, the same in all of the mentioned papers for both molecule series. The parameters used in this work are listed in Tables I and II.

Table I

b) *one-center repulsion integrals (in eV)*
a) *one-center core integrals*

	C	F	N	Ñ	O	Ö
Monofluorobenzene	a) 11.16	33.58				
	b) 11.13	17.81				
Pyridine-*N*-oxide	a) 11.16		14.12	25.73	17.70	30.15
	b) 11.13		12.34	16.76	15.23	19.32

Table II

Two-center core integrals (in eV)

	CF	CC	CN	NO
Fluorobenzene	−2.31	−2.39		
Pyridine-*N*-oxide				
Ia		−2.39	−1.6	−1.6
Pyridine-*N*-oxide				
Ib		−2.39	−2.6	−2.6
Pyridine-*N*-oxide				
II (1,2)		−2.39	−2.0	−2.0

Two-center repulsion integrals were calculated by the MATAGA—NISHIMOTO approximation [8].

Electronic spectra

The spectra of pyridine-*N*-oxide have been reported by a number of authors [17—23]. According to these studies, the first transition can be observed at 215 nm with a relatively high intensity ($\varepsilon = 10\,000$, $f = 0.012$),

and the second, most intense band ($\varepsilon = 18\,000$, $f = 0.0173$ [23]) is at 280 nm, in hexane. The third, low intensity band ($\varepsilon = 3000$) has been observed at 325 nm, in nonpolar solvents.

The recent opinion of a part of the authors is that the first three bands are due to $\pi \rightarrow \pi^*$ transitions; MURREL [24], however, on the basis of SIDMAN's measurements [25], assigns the band at 320 nm to an $n \rightarrow \pi^*$ transition. The most up-to-date calculations on pyridine-*N*-oxide and a number of related molecules were carried out by EVLETH [23]. In his opinion this band also corresponds to a $\pi \rightarrow \pi^*$ transition.

The gas phase spectra of fluorobenzenes were reported by KIMURA and NAGAKURA [26]. For the sake of better comparability, we have recorded the spectrum of monofluorobenzene in the same solvents in which the spectra of pyridine-*N*-oxide were taken. No characteristic differences were found between the spectra in solution and gas phase, and the $\pi \rightarrow \pi^*$ character of the 4.8 and 6.0 eV transitions appears to be doubtless. On comparing the electronic spectrum and the transition energy values of monofluorobenzene with those of pyridine-*N*-oxide, and pyridine-N^+-OH it can be observed that the characteristic values of the first two are more similar than those of the first and third. At any rate, the greater similarity can be attributed to the covalency of bonds directed to the substituent.

Results of the calculations

The measured dipole moment and electronic transition energy values can be best reproduced by model II. The agreement of the calculated and experimental transition energies is very good, as can be seen from Table IV. Input data used for the calculations are given in Tables I and II. The agreement of experimental and calculated dipole moments, 4.19 and 4.56 D, respectively, is also acceptable.

Using model I, the agreement obtained for both the $\pi \rightarrow \pi^*$ and the $n \rightarrow \pi^*$ assignments was still acceptable. Two different sets of parameters were used in this model, differing in the values of β. In the first case (model Ia) the following two-center core integrals were used:

$$\beta(\mathrm{CC}) = -2.39 \text{ eV},$$
$$\beta(\mathrm{CN}) = -1.6 \text{ eV},$$
$$\beta(\mathrm{NO}) = -1.6 \text{ eV},$$

while the parameters used in model Ib were:

$$\beta(\mathrm{CC}) = -2.39 \text{ eV},$$
$$\beta(\mathrm{CN}) = -2.6 \text{ eV},$$
$$\beta(\mathrm{NO}) = -2.6 \text{ eV}.$$

The differences in the parametrization influence the values of the off-diagonal terms in the PPP Hamiltonian, and cause considerable shifts in the eigenvalues.

In model II the following β parameters were used:

$$\beta(\mathrm{CC}) = -2.39 \text{ eV},$$
$$\beta(\mathrm{CN}) = -2.0 \text{ eV},$$
$$\beta(\mathrm{NO}) = -2.0 \text{ eV}.$$

Table III

Orbital energies (in eV)

Fluorobenzene	−16.99	−13.06	−10.30	−9.99	−0.76	−0.63	2.29
Pyridine-*N*-oxide Ia	−13.46	−12.02	−10.34	−9.42	−1.83	−0.74	1.68
Pyridine-*N*-oxide Ib	−15.86	−12.06	−10.20	−9.10	−0.65	−0.53	2.53
Pyridine-*N*-oxide II	−15.88	−12.74	−11.46	−0.41	−2.15	−1.86	1.01

The orbital energies obtained by these three models are listed in Table III. The energy of the highest occupied molecular orbital is the ionization potential of the molecule. The same value, 9.4 eV, was obtained for this quantity by models Ia and II, and the value obtained by model Ib (9.1 eV) is but slightly different.

Using SCF orbital energies and eigenvectors, the matrix elements given by Eq. (4) were calculated, and the transition energies were determined by taking configuration interaction into account. The observed and calculated transition energy values are compared in Table IV. The results are so different that from the results of model Ib one might even doubt that the first band of the electronic spectrum (at 3.9 eV) is due to a $\pi \rightarrow \pi^*$ transition.

Table IV

Electronic transition energies (in eV)

Fluorobenzene	calcd.	4.84	6.09	6.92	6.95
	exptl.	4.8	6.1	6.9	
Pyridine-*N*-oxide Ia	calcd.	4.11	4.4	5.78	
Pyridine-*N*-oxide Ib	calcd.	4.48	5.73	6.33	
Pyridine-*N*-oxide II	calcd.	3.81	4.35	5.67	
Pyridine-*N*-oxide	exptl.	3.95	4.4	5.7	

Among the different parametrizations a definite choice can be made only on the basis of the calculated dipole moment. Due to symmetry reasons, the π-component of the dipole moment should lie in the σ_v plane. According to KUBOTA, the experimental value is —4.19 D. Using the calculated density matrix, P, the dipole moment is determined from the following equation:

$$\vec{\mu} = e \sum_v (Z_v - P_{vv}) \vec{r}_v, \tag{9}$$

where $\vec{\mu}$ denotes the dipole moment due to the π-electrons and the core, Z_v is the core charge and $\vec{r}_v$ is the position vector of atom v.

Model I, even with different parametrizations, was unable to reproduce the dipole moment value, so model II has been accepted. At the same time, it has been concluded that the bands in the electronic spectrum are all due to $\pi \rightarrow \pi^*$ transitions. From model II —4.56 D was obtained for the z-component of the π-dipole (Fig. 2).

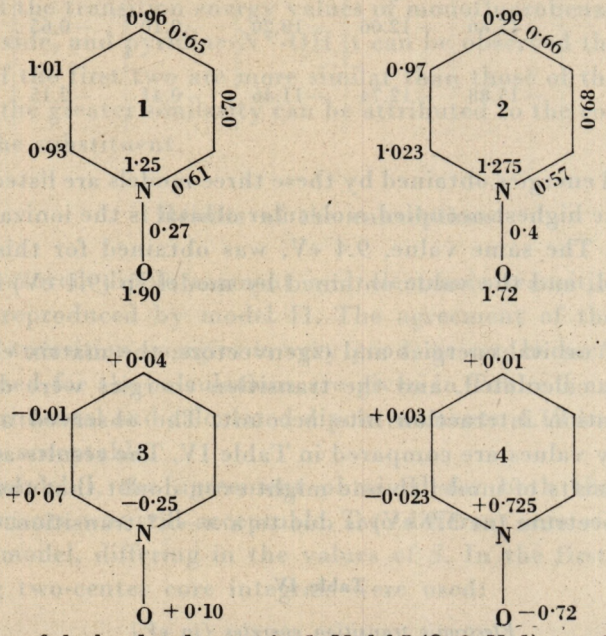

Fig. 2. Elements of the bond order matrix. 1. Model I (O: 2; N: 1) $\mu = 4.56$ D. 2. Model II (O: 1; N: 2) $\mu = 0.20$ D. 3. Model I, net charge. 4. Model II, net charge

Spectra in polar solvents

In polar solvents the third band of pyridine-*N*-oxide disappears and the second band is strongly shifted towards shorter wavelengths. If the parametrization is retained, obviously, a different model should be used for the reproduction of the spectrum.

In strongly acidic media, pyridine-*N*-oxide is protonated and its electronic transitions appear at 4.7 and 5.8 eV. These energy values could be reproduced only by model I. EVLETH applied model II to this problem, and obtained 5.1 eV for the second transition; this is by all means a poor approximation. In pyridine-N^+-OH the covalent character of the bond directed to the substituent increases and the oxygen contributes two electrons to the delocalized system. If the optimal β-parameters of model II are combined with the ionization potential values and γ_{uu} terms of model I, the transition energies observed in polar solvents can be reproduced within 2—4%. The transition energies of pyridine-*N*-oxide measured in polar solvents (*e.g.* water, ethanol) are very close to those of monofluorobenzene (4.7, 5.85, and 4.8, 6.1 eV, respectively).

Bond orders and vibrational spectrum

The vibrational frequencies assigned to the C–F and N–O stretching modes are very close to each other (1220 and 1255 cm^{-1}, respectively). As discussed in a previous paper [4], the kinetic energy matrix elements belonging to the stretching coordinates of isoelectronic molecules have nearly the same values (which fact follows first of all from the agreement of reduced masses). Consequently, the corresponding potential energy terms should also agree within a few per cents.

The potential energy terms are, of course, to a certain extent also influenced by the neighbouring bonds. These effects, however, are the same, to a very good approximation, in the isoelectronic molecules under study. The π-bond order of the C–F bond in monofluorobenzene is 0.21, that of the N–O bond is 0.27 according to model I, and 0.39 according to model II. Taking into account that in vibrational problems the total bond order is the relevant factor, and adding σ-bond orders to the above quantities, the difference between the two molecules becomes small, even in the less favourable case of model II.

Vibrational spectra can be well interpreted by the total bond order values of 1.21 and 1.4. As a comparison, it should be mentioned that the bond orders of CF and NO diatomics are 1.5 and 2.5, respectively, and their vibrational normal frequencies are 1280 and 1904 cm^{-1}.

Discussion

The results, first of all the agreement of electronic transition energies and dipole moment values, support the $\pi \rightarrow \pi^*$ assignment of the 320 nm band. The fact, however, that by altering the two-center core integrals alone the electronic transitions observed in water or in polar solvents can be reproduced with model I, indicates that in polar solvents the N–O bond becomes covalent. This accounts for the analogous features with fluorobenzene. The

above argument is also supported by the fact that the transition energies of fluorobenzene are very close to those of pyridine-*N*-oxide measured in polar solvents.

On the basis of the isoelectronic principle the eigenvalues and, consequently, the orbital energies and the total energy could be expected to be approximately the same in the above molecules. Indeed, if the ionization potentials and the repulsion integrals are calculated by using electronegativities, the sum of the orbital energies and the total electronic energy of the two molecules differ only by 1—2 per cents.

Our study was completed with Extended Hückel calculations. As known, σ–π interaction is neglected in the PPP approximation, but is overemphasized in the EH method. It has turned out from the analysis of orbital populations that the relative electronegativities of neighbouring atoms have a great influence on the atomic charges, bond orders and bond moments.

The results of EH calculations can be summarized as follows. Much higher values were obtained for the dipole moment of both molecules than the measured values; the calculated dipole moment of fluorobenzene is 3.0 D, almost twice as large as the experimental value (1.6 D). Approximately the same ratio was found in the case of pyridine-*N*-oxide, when assuming that the nitrogen and oxygen atoms contribute 5 and 6 electrons, respectively. A better result can be obtained if the semipolar character of the N–O bond is taken into account, and it is assumed that the nitrogen atom, contributing two electrons to the bond, holds only 4 electrons in the valence state, and the oxygen atom holds 7 electrons. A similar assumption was used in the PPP calculations, when nitrogen was taken as a doubly, and oxygen as a singly charged core. Using this approximation, 6.0 D was obtained for the dipole moment of pyridine-*N*-oxide, while the original model led to a value of 12.0 D.

*

The calculations were carried out on an ICT 1905 computer. The original version of the PPP program was kindly supplied by J. C. PACKER, Nottingham University.

REFERENCES

1. MULLIKEN, R. S.: Intern. J. Quant. Chem. **1,** 1 (1967)
2. MIRONE, P.: Atti Acad. Nazl. Lincei, Rend., Classe Sci. Fis. Mat. Nat. **35,** 530 (1963)
3. COSTA, G., GALASSO, V., SARTORI, G.: Atti Acad. Nazl. Lincei, Rend., Classe Sci. Fis. Mat. Nat. **37,** 289 (1964)
4. SZŐKE, S., VARSÁNYI, GY., BAITZ, E.: Acta Chim. Acad. Sci. Hung. **54,** 145 (1967)
5. PRITCHARD, H. O., SUMNER, F. H.: Proc. Roy. Soc. (London) **A 235,** 136 (1956)
6. BAIRD, N. C., SICHEL, J. M., WHITEHEAD, M. A.: Theoret. Chim. Acta (Berlin) **11,** 38 (1968)
7. POPLE, J. A.: Trans. Faraday Soc. **49,** 1375 (1953)
8. MATAGA, N., NISHIMOTO, K.: Z. Phys. Chemie (Frankfurt) **13,** 140 (1957)
9. SZŐKE, S., VARSÁNYI, GY., BAITZ, E.: Acta Chim. Acad. Sci. Hung. **53,** 347 (1967)
10. SZŐKE, S., JALSOVSZKY, GY.: J. Mol. Structure **2,** 93 (1968)
11. PAOLONI, L.: Nuovo Cimento **4,** 410 (1956)

12. CHALVET, O., LEIBOVICI, C.: Theoret. Chim. Acta (Berlin) **13**, 297 (1969)
13. SZŐKE, S.: Acta Chim. Acad. Sci. Hung. **58**, 390 (1968)
14. SANTRY, D. P., SEGAL, G. A.: J. Chem. Phys. **47**, 158 (1967)
15. BAILEY, L. M.: Theoret. Chim. Acta (Berlin) **13**, 56 (1969)
16. KVIATKOWSKY, S.: Acta Phys. Polon. 29, 477 (1966)
17. KUBOTA, T.: J. Chem. Soc. Japan **79**, 930 (1958)
18. KUBOTA, T.: J. Chem. Soc. Japan **80**, 578 (1959)
19. KUBOTA, T.: Bull. Chem. Soc. Japan **35**, 946 (1962)
20. ITO, M., HATA, N.: Bull. Chem. Soc. Japan **28**, 260 (1955)
21. ITO, M., HATA, N.: J. Chem. Phys. **24**, 495 (1956)
22. KUBOTA, T., WATANABE, H.: Bull. Chem. Soc. Japan **36**, 1093 (1963)
23. EVLETH, E. M.: Theoret. Chim. Acta (Berlin) **11**, 145 (1968)
24. MURREL, J. N.: Theory of the Electronic Spectra of Organic Molecules, Methuen and Co. Ltd., London, 1963
25. SIDMAN, J.: Chem. Rev. **58**, 689 (1958)
26. KIMURA, K., NAGAKURA, S.: Mol. Phys. **9**, 117 (1965)
27. KOBINATA, L., NAGAKURA, S.: Theoret. Chim. Acta (Berlin) **15**, 415 (1969)

Sándor SZŐKE
György JALSOVSZKY } Budapest II., Pusztaszeri út 57—69.

Erzsébet DUDAR; Budapest IV., Tó u. 1—5.

Acta Chimica Academiae Scientiarum Hungaricae, Tomus 72 (3), pp. 255—259 (1972)

INFLUENCE OF HYDROGEN ION CONCENTRATION ON THE ANODIC POLARIZATION OF *p*-GERMANIUM ELECTRODES

D. SINGH and A. N. DWIVEDI

(Electrochemical Research Laboratory, Banaras Hindu University, India)

Received October 8, 1970

Anodic polarization of *p*-Ge electrodes has been studied in solutions of the composition 0.02 *N* TEA Br + *x N* HBr, where *x* denotes the normality of the acid. The anode characteristics of *p*-Ge of different resistance are identical, differing only at higher current densities. The Tafel relation, $\eta = a + b \log i$, is valid for *p*-Ge anodes over limited current densities. Anodic polarization diminishes with increasing pH, and an anode reaction occurs vigorously with water in acidic solutions. The slopes of Tafel plots vary from 0.094 to 0.123 V, indicating that the overvoltage is restricted mainly to the Helmholtz double layer region.

Introduction

The low concentration of free charges (electrons and holes) in semiconductors has an interesting effect on the electrochemical behaviour of germanium electrodes. All anode reactions are oxidations which may involve either dissolution of the electrode material or oxidation of ions in the solution. Germanium can be electrolytically dissolved in most electrolytes.

The investigations of BRATTAIN and GARRETT [1], demonstrating that the rate of the anodic dissolution process is controlled by the supply of holes at the germanium electrode surface, which is changed by the influence of light, developed a new field of electrochemistry. JIRSA [2] has studied the anodic dissolution of germanium in acidic and alkaline solutions and reported that germanates are formed in alkaline and the corresponding germanium salts in acidic medium. UHLIR studied the electrolytic dissolution of germanium in both aqueous and non-aqueous solutions [3].

The anodic reactions of germanium in aqueous solutions have been studied by several authors [4—6]. TURNER [7] confirmed the Tafel relation, $\eta = a + b \log i$, in both acidic and alkaline media below 0.3 mA · cm^{-2} (η is the overpotential at C. D. i; a and b are constants). This author has concluded that germanium goes into sulution and the overall process involves two holes and two electrons for the dissolution of each germanium atom. BECK and GEIISCHER [8] have offered a more elaborate mechanism for such reactions. YAKOVLEVA *et al.* [9] suggest that the concentration of holes on the surface increases, and that of electrons decreases, with increasing anodic polarization.

The purpose of this study is to elucidate the nature of the electrode reaction at the germanium–electrolyte interface.

Experimental

Materials

The Ge-crystals used as electrode were supplied by Mullard House, Torrington Place, London, and were rectangular in shape, affording a large face-to-edge ratio. Their resistance was determined by D. C. current–potential measurement; the type of germanium was confirmed by Hall-effect experiments. The electric connections were made with silver electrodes deposited by evaporation on the samples in an Edward High Vacuum coating unit at 10^{-5} Torr. The orientation of two large faces is (110), as determined by a back reflection X-ray technique. The ohmic contact with the germanium electrodes was made by soldering copper wire with a lead–tin alloy, using zinc chloride as flux to avoid rectifying contacts; the copper wire was threaded through a glass tube to avoid its contact with the electrolyte solution and cemented with Araldite. The large face of the germanium electrode was ground with 800 mesh carborundum powder, and the surface was etched for 1.5 min. in a CP-4 solution (15 ml HF, 25 ml HNO_3 and 15 ml glacial acetic acid with 0.3 ml bromine) and immediately rinsed thoroughly with conductivity water; this treatment provides a smooth and reproducible surface. A 1 cm^2 area of the germanium surface was coated with paraffin wax (E. Merck) and this was used n the polarization measurements. All solutions were prepared from AnalaR (BDH) grade recrystallized chemicals dissolved in doubly distilled water.

Apparatus and procedures

The experiments were carried out in a modified H-shape Jena glass cell [10]. The cell was placed into an air thermostat box containing a stirrer, a toluene–mercury thermoregulator, an electronic relay and a Beckmann and a standard thermometer; this arrangement permitted to maintain the temperature within ± 0.01 °C. To eliminate the effect of light on the germanium electrode, a 100 W electric bulb coated with aluminium foil was used as heater. Current–potential data were recorded galvanostatically in an unstirred solution, using the direct method. The auxiliary platinum and the germanium electrode were connected to a constant current device (KT_2 valve); the potential of the polarized germanium electrode against the S. C. E. was measured with a portable potentiometer (Pye-Catalog No. 7569P), an external galvanometer (multiflex galvanometer MG-4) being used as detector. The S.C.E. was connected through a calomel compartment containing a buggin capillary which was positioned at 0.05 mm from the Ge-electrode to avoid an ohmic drop. The calomel compartment was filled with the experimental electrolyte solution purified by pre-electrolysis for 3—4 hrs. Polarization results were obtained by passing the current for 1 min. intervals, whereas steady state polarization results were obtained by passing the current for a considerable time. The results reported in this work are the average from several experiments.

Results and discussion

The results in Fig. 1 illustrate the steady state anodic polarization of *p*-Ge (4—8 ohm·cm) in 0.02 *N* tetraethylammonium bromide (TEABr) solutions of different pH at 25 °C. The plots are linear over the limited current range from 0.020 to 0.580 mA · cm^{-2}. At higher current densities (above 1.780 mA · cm^{-2}) these curves coincide. The slopes vary from 0.094 to 0.121 V. Thus the Tafel equation, $\eta = a + b \log i$, is obeyed. The anodic polarization changes with the pH of the electrolyte and if the acid concentration is decreased, the anode polarization diminishes. Fig. 2 illustrates the steady state current–potential results for *p*-Ge (0.2—0.3 ohm · cm) in the above solutions. The slope, $dV/d \log i$, varies from 0.102 to 0.123 V. The curves obey the Tafel equation over the whole range of current densities. From these curves it is

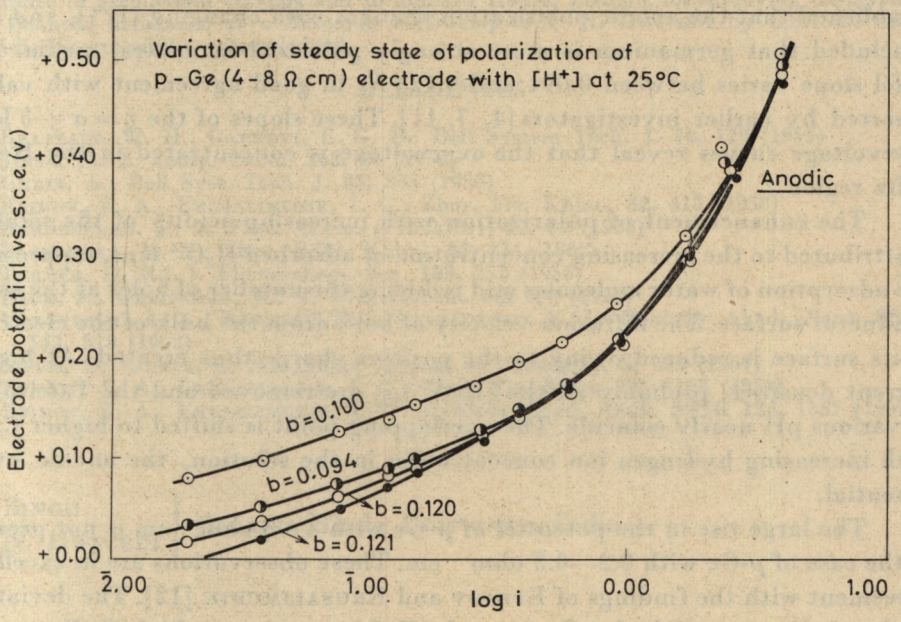
Variation of steady state of polarization of
p-Ge (4-8 Ω cm) electrode with [H+] at 25°C
Anodic
b=0.100
b=0.094
b=0.120
b=0.121
Electrode potential vs. s.c.e.(v)
+0.50
+0.40
+0.30
+0.20
+0.10
+0.00
2̄.00
1̄.00
0.00
1.00
log i

Fig. 1

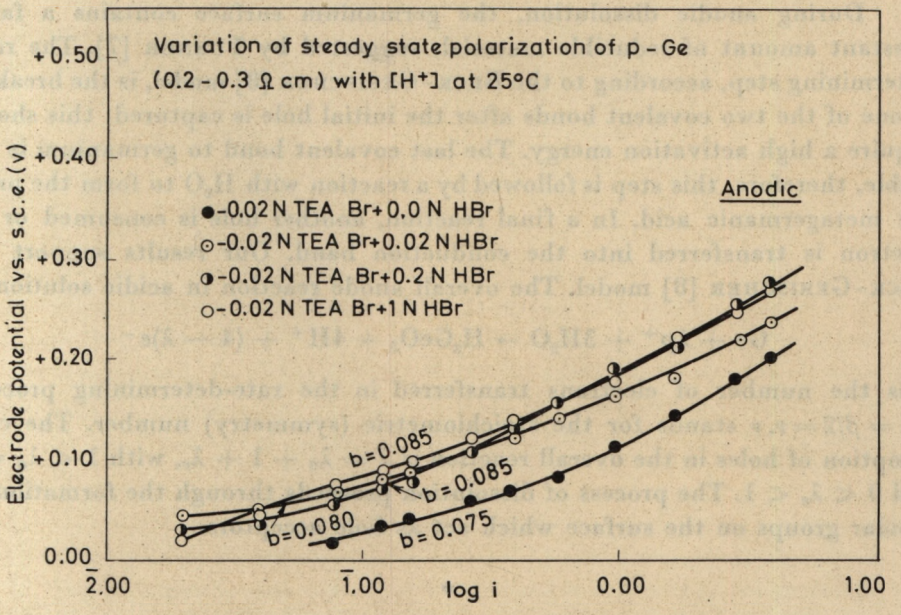
Variation of steady state polarization of p-Ge
(0.2-0.3 Ω cm) with [H+] at 25°C
Anodic
●-0.02N TEA Br+0,0 N HBr
⊙-0.02N TEA Br+0.02 N HBr
◑-0.02 N TEA Br+0.2 N HBr
○-0.02 N TEA Br+1 N HBr
b=0.085
b=0.085
b=0.080
b=0.075
Electrode potential vs. s.c.e.(v)
+0.50
+0.40
+0.30
+0.20
+0.10
0.00
2̄.00
1̄.00
0.00
1.00
log i

Fig. 2

established that the anodic polarization changes with changing $[H^+]$, and it is concluded that germanium is more strongly polarized in neutral media. The Tafel slope varies between 0.094 and 0.123 V, in good agreement with values reported by earlier investigators [4, 7, 11]. These slopes of the $\eta = a + b \log i$ overvoltage curves reveal that the overvoltage is concentrated in the Helmholtz region.

The enhancement of polarization with increasing acidity of the solution is attributed to the increasing concentration of adsorbed H_3O^+ ions, suppressing the adsorption of water molecules and reducing the number of holes at the semiconductor surface. The diffusion velocity of holes from the bulk of the electrode to its surface is reduced owing to the positive charge thus created. At higher current densities, probably all the $(H_3O^+)_{ads}$ are removed and the Tafel plots at various pH nearly coincide. The overlapping point is shifted to higher C. D. with increasing hydrogen ion concentration in the solution, the anodic overpotential.

The large rise in the potential of *p*-Ge with 4—8 ohm · cm is not present in the case of *p*-Ge with 0.2—0.3 ohm · cm. These observations are in excellent agreement with the findings of EFIMOV and ERUSALIMCHIK [12]. The deviation in the anode potential of *p*-Ge from the Tafel equation at high C. D. can be attributed to two IR drops; one in the germanium and the other in an anodic layer of germanium dioxide which is formed more rapidly than it can be dissolved by the electrolyte.

During anodic dissolution, the germanium surface contains a fairly constant amount of reducible material, suggested by TURNER [7]. The rate-determining step, according to the BECK–GERISCHER [8] model, is the breaking of one of the two covalent bonds after the initial hole is captured; this should require a high activation energy. The last covalent bond to germanium is unstable, therefore, this step is followed by a reaction with H_2O to form the product metagermanic acid. In a final reaction, another hole is consumed or an electron is transferred into the conduction band. Our results support the BECK–GERISCHER [8] model. The overall anode reaction in acidic solution is:

$$Ge + \lambda p^+ + 3H_2O \rightarrow H_2GeO_3 + 4H^+ + (4 - \lambda)e^-$$

λ is the number of electrons transferred in the rate-determining process; $1/\lambda = \beta/2 = \nu$, ν stands for the stoichiometric (symmetry) number. The consumption of holes in the overall reaction is $\lambda = \lambda_a + 1 + \lambda_e$, with $1 \leqslant \lambda_a \leqslant 2$ and $0 \leqslant \lambda_e \leqslant 1$. The process of dissolution proceeds through the formation of dipolar groups on the surface which act as hole acceptors.

*

The authors express their thanks to Mr. K. N. RAI, Solid State Physics Research Laboratory, B.H.U., for the help rendered in the determination of plane orientation, type aud

resistance of germanium crystals and to Mullard House, London, for supplying Ge-crystals. The financial assistance as a Research Fellowship to A. N. DWIVEDI by C.S.I.R., Govt. of India, is gratefully acknowledged.

REFERENCES

1. BRATTAIN, W. H., GARRETT, C. G. B.: Bell System Tech. J. **34**, 129 (1955)
2. JIRSA, F.: Z. anorg. Chem. **268**, 84 (1952)
3. UHLIR, A.: Bell Syst. Tech. J. **35**, 333 (1956)
4. EFIMOV, E. A., ERUSALIMCHIK, I. G.: Zhur. Fiz. Khim., **32**, 413 (1958)
5. BARDELEBEN. J.: Z. Phys. Chem. (Frankfurt) **17**, 39 (1958)
6. PLATONOVA, M. N.: Zhur. Prikl. Khim., **35**, 334 (1962)
7. TURNER, D. R.: J. Electrochem. Soc. **103**, 252 (1956)
8. BECK, F., GERISCHER, H.: Z. Elektrochem. **63**, 500 (1959)
9. YAKOVLEVA, A. A., BORISOVA, T. I., VASELOVSKII, V. I.: Doklady Akad. Nauk SSSR **145**, 373 (1962)
10. SINGH, D., GUPTA, A. N.: Indian Journal of Chemistry, **5**, 383 (1967)
11. EFIMOV, E. A., ERUSALIMCHIK, I. G.: Zhur. Fiz. Khim. **32**, 1103 (1958)
12. EFIMOV, E. A., ERUSALIMCHIK, I. G.: Doklady Akad. Nauk. SSSR **134**, 1387 (1960)

D. SINGH
A. N. DWIVEDI
Banaras Hindu University, India.

Acta Chimica Academiae Scientiarum Hungaricae, Tomus 72 (3), pp. 261–268 (1972)

INVESTIGATION OF ADSORPTION PHENOMENA ON PLATINIZED PT ELECTRODES BY TRACER METHODS, X

STUDIES WITH ^{14}C-LABELLED ACETONE

GY. HORÁNYI and F. NAGY

(Central Research Institute for Chemistry, Hungarian Academy of Sciences, Budapest)

Received November 30, 1970

1. The behaviour of ^{14}C-labelled acetone was studied on a platinum electrode in the potential interval of 0—1000 mV.

2. A study was made of how the gaseous products formed during the electrohydrogenation and electrooxidation of acetone affect the tracer measurements.

3. From the observations, general conclusions were drawn with regard to the phenomena observed in the adsorption of individual organic substances.

Earlier studies on the electrohydrogenation and oxidation of acetone [1, 2] required that we use the possibilities provided by the tracer technique to obtain further information on the processes undergone by the acetone on the platinum—electrolyte boundary surface, and on the phenomena connected with these. These studies recently became of interest from another point of view too. A paper was published not long ago on the adsorption, mobility, and exchange of water adsorbed on platinum [3]. On the basis of the experimental observations a proposal is made as to the mechanisms of adsorption and electrosorption of organic substances on a platinum electrode. In one of the essential stages of these studies [3] the platinum electrode is washed with acetone. According to our earlier observations regarding the adsorption of acetone [1], there is such a strong interaction between acetone and the platinum surface that the acetone cannot be considered an inert washing solution. Taking this into account, in our opinion, those theoretical conclusions which support the proposal as to the mechanism of the adsorption (reported not only in Ref. [3] but by other authors too [4]) cannot be drawn from the observations presented in the work cited. In the following, with the application of a tracer technique, we attempt to answer the question of what happens to acetone dissolved in an aqueous medium on a platinized platinum electrode and in its immediate vicinity.

Experimental

The investigations were carried out with the aid of the method and apparatus already described [5]. The acetone used had a specific activity of a few mCi/mmol and was labelled with ^{14}C in positions 1 and 3. The required amount of labelled acetone was dissolved in a 1*N* $HClO_4$ background solution.

Potential dependence of the adsorption

In one of our earlier publications [6] it was shown that the potential dependence of the adsorption of some substance can be given unambiguously only if the reactions (oxidation or reduction) occurring with the substance in question demonstrably do not disturb the adsorption equilibrium. This requirement at all events forces us to carry out polarization studies prior to the study of the adsorption.

In Fig. 1 is shown the potentiostatic polarization curve determined at an acetone concentration of 0.1 *M*. It can be seen clearly from the Figure that the

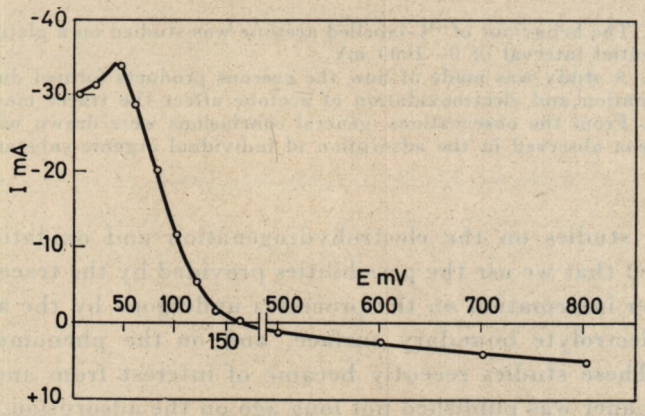

Fig. 1. Polarization curve determined with the potentiostatic method for an acetone concentration of 0.1 *M*. (*E* is the potential against a 1 atm H_2 electrode immersed in 1 *N* $HClO_4$.)

potential interval in which it is not necessary to consider either oxidation or reduction is relatively narrow (200—500 mV). According to our earlier work and to other evidence in the literature, on the cathodic branch of the polarization curve [1, 7] the main reaction is

$$CH_3-\underset{\underset{O}{\|}}{C}-CH_3+4H^++4e \longrightarrow CH_3-CH_2-CH_3+H_2O \qquad (1)$$

with a smaller contribution from the process

$$CH_3-\underset{\underset{O}{\|}}{C}-CH_3+2H^++2e \longrightarrow CH_3-\underset{\underset{OH}{|}}{CH}-CH_3 \qquad (2)$$

During the oxidation (anodic branch), however, presumably [8] the reaction

$$CH_3-\underset{\underset{O}{\|}}{C}-CH_3+6\,OH^- \longrightarrow CO_2+CH_3COOH+3H_2O+6e \qquad (3)$$

occurs. It is evident from the above equations that on both the cathodic and anodic branches of the polarization curve gas evolution must be reckoned with. As will be seen below, this condition determines to a decisive extent how far the adsorption during the reaction can be studied with the tracer technique.

At low acetone concentrations the potential dependence of the adsorption can be characterized by the curve shown in Fig. 2. Thus, in a narrow potential interval the adsorption does not depend on the potential. The decrease in

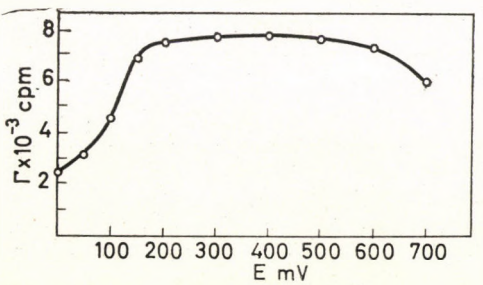

Fig. 2. Potential dependence of the count rate (proportional to the adsorption) at an acetone concentration of 5×10^{-4} *M*

adsorption on both sides of this interval is presumably related to reactions (1) and (2) or to (3). Evidence for this is also provided by the fact that with increasing acetone concentration the length of the above interval also increases, and further, by the earlier observation [1] that the adsorbed, labelled acetone can be exchanged with inactive acetone only extremely slowly. At potentials more negative than 100—150 mV the rate of the hydrogenation reaction increases with increasing acetone concentration and hence so does the rate of gas evolution. The possibility of the study of adsorption is greatly affected by the appearance of the labelled gaseous product formed from the dissolved labelled component.

Simultaneous study of the electrohydrogenation and adsorption of labelled acetone

Our method of study, as was shown [9] in the case of the electrohydrogenation of phenylacetic acid, is suitable for the elucidation of the connection between the adsorption, the coverage and the reaction rate. Essentially, it is a matter of measuring continuously the amount of the labelled, reacting component adsorbed on the surface of the electrode and present in its immediate vicinity, while recording the polarization curve by a potentiostatic or a galvanostatic method. The principle of the measurement (with reference to our earlier publication [5]) is illustrated in Fig. 3. The results of the galvanostatic

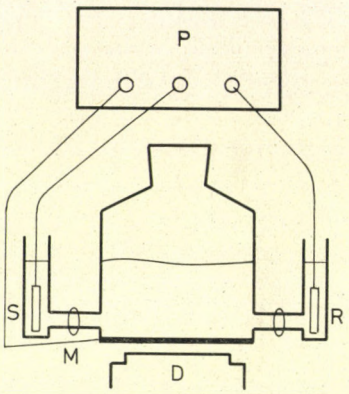

Fig. 3. Scheme of the experimental set-up: *M:* the main electrode forming the bottom of the cell; *S:* auxiliary electrode; *R:* reference electrode; *D:* the radiation detector (scintillation pick-up); *P:* potentiostat

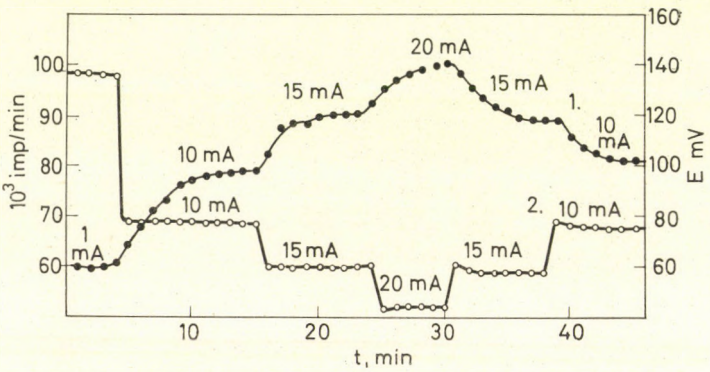

Fig. 4. Change of the potential (2) and the count rate (1) with time in the case of a galvanostatic measurement (5×10^{-2} *M*)

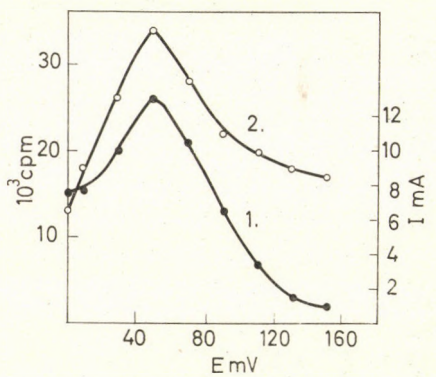

Fig. 5. Potential dependence of the current (1) and the count rate (2) in the case of a potentiostatic measurement (2×10^{-2} *M*)

measurements can be seen in Fig. 4. It is clear from this Figure that an increasing count rate is related to increasing currents, that is the departure of the labelled product from the surface is impeded.

From the potentiostatic current vs. count rate curves too (Fig. 5) it can be seen that the count rate changes in parallel with the current, and what is more, according to a maximum curve.

It is shown in the following that the observed phenomena are related to the fact that the propane formed accumulates in the pores and on the surface of the platinum black in the form of bubbles. These phenomena appear only at relatively high acetone concentrations when the hydrogenation rates become so high that bubble formation must be considered as a result of the slow diffusion of dissolved propane.

Accumulation of the gaseous, labelled component in the form of bubbles on the solid–liquid boundary surface

Let us assume that in the case of the experimental set-up shown in Fig. 3, a weakly adsorbed gaseous product is formed by some reaction from the dissolved component labelled with a soft β-emitting isotope, *e.g.* ^{14}C and this product, or a part of it, adheres to the surface in the form of bubbles. If the size of the bubbles is not too large (their radius $r \ll 1$ cm), then the self-adsorption of β-radiation in the bubbles need not be considered. For the purposes of radiation measurements, the bubbles adhering to the surface can be substituted by a gas layer in direct contact with the solid phase, with thickness l, for which the relation $V_b = l$ is valid, where V_b is the total volume of bubbles on 1 cm^2 of the geometrical surface. (The system is thus comprised of liquid phase–gas layer-adsorption phase–solid phase.) It must be stressed that electrically this model is not correct, because in such a system the conduction of current would cease.

In our earlier publications a study was made of what the distribution of the given labelled component between the liquid and adsorption phases must be, in order that the adsorption can be measured. We now seek an answer to the question of how the appearance of the labelled component as a gas affects the possibilities of studying the adsorption. Let us consider this first of all in the case of a smooth adsorbent surface. The radiation originating from the gas phase, from the bubbles, and reaching the detector will then be proportional to $\frac{P}{RT}\, l$, and that originating from the adsorption phase will be proportional to Γ. If the radiation originating from the liquid phase is disregarded, the two radiations will become comparable in the case of an average layer thickness

$l = \frac{RT}{P}\Gamma$, and obviously at layer thicknesses greater than this, in comparison to the radiation originating from the bubbles, that from the adsorption will begin to become negligible.

Assuming a pressure of 1 atm for the gas at 20 °C, and taking the specific adsorbed amount as $\Gamma = 10^{-10}$ mol/cm^2, a value of 2.4×10^{-6} cm is obtained for l. It can be seen that the amount of labelled substance in a single bubble with a radius somewhat less than 10^{-2} cm is equivalent to the amount of substance adsorbed on 1 cm^2.

Applying the above considerations in the case of a platinized surface, the expression

$$l = \gamma \frac{RT}{P}\Gamma$$

will be valid, where γ is the roughness factor of the adsorbent surface studied, *i.e.* the quotient of the true and geometrical surfaces. Considering that on the platinized platinum electrodes used by us this value is usually about 100, we obtain a value of $l = 2.4 \times 10^{-4}$ cm. This means that the radiation originating from the substance contained in a single gas bubble with a radius of 5×10^{-2} cm is equivalent to the radiation from the amount of material adsorbed on 1 cm^2 geometrical or 100 cm^2 true surface.

In the case of the platinized electrodes, the high roughness factor can only come about if the platinum black possesses some structure. The roles of the structure and porosity of the platinum black in measurements with the tracer technique were treated in an earlier publication [10]. In the platinum-black layer there are cavities, and from these the gas-phase products can displace the solution. The result of this will be that the average concentration (defined in the paper cited) of the labelled component in the disperse adsorption phase will change, generally increase, because under the usual conditions of study the concentration of the labelled component is smaller than that in the gas phase or in a bubble containing gas at a pressure of about 1 atm.

The removal of the bubbles formed in the cavities may be difficult, depending on the conditions, and so a significant increase in the count rate (a 'background increase') can occur.

Interpretation of the phenomena observed in the electrohydrogenation of acetone

On the basis of what has been said in the previous section, the phenomenon observed in the galvanostatic measurements, *viz.* that the count rate increases with increasing current, can be explained in terms of higher gas production at higher currents, resulting in formation of more or larger bubbles.

In the studies with the potentiostatic method too the current and the count rate change in parallel. The probable cause of the maximum on the polarization curves determined by the potentiostatic method has been dealt with in an earlier publication [1]. It has been established that at negative or small positive potentials process (2) begins to come into the foreground compared with process (1), and if the rate of replacement of acetone is limited (diffusion or adsorption control) then, upon changing the potential in the negative direction, the current and the amount of the gaseous product are decreased. The maximum observed in the count rate *vs.* potential curves is in complete agreement with this.

Phenomena in the electrooxidation of acetone

In the electrooxidation of acetone (although we are concerned with a process which takes place at a much lower rate than the electrohydrogenation) the observed phenomena are similar to those described above.

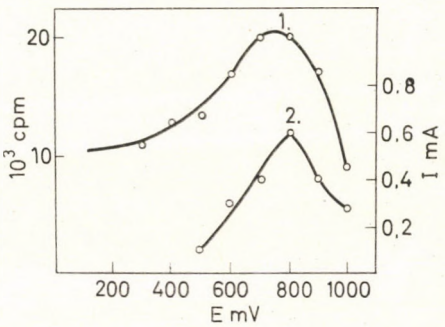

Fig. 6. Potential dependence of the count rate and the current in the case of the oxidation of acetone ($c = 5 \times 10^{-2}$ *M*)

In Fig. 6 can be seen the phenomena observed during electrooxidation in the case of a labelled acetone concentration of 5×10^{-2} *M* with a potentiostatic method. The parallel change of the count rate and the current can presumably be attributed to the gas bubbles accumulating on the surface.

Conclusions

In the study of the adsorption of water on a platinum electrode in the paper cited above, the procedure was to maintain the electrode at a constant potential in an HTO solution. The electrode was then lifted out of the solution, washed with acetone, and the tritium activity measured [3]. As a result of the

experimental observations presented above, the conclusion must be reached that after the acetone washing the bulk of the adsorbed water scarcely remains on the electrode surface, because

(1) the adsorption of acetone is fast;

(2) the rate of desorption of the adsorbed acetone is low.

It is conceivable that the tritium appears on the surface as a result of hydrogen exchange between HTO and the organic molecule adsorbed on the surface.

In this connection we must refer again to the work of DE HEMPTINNE and SCHUNCK [7]. In the course of the electrohydrogenation of deuterated acetone in ordinary water and of light acetone in heavy water they found that the hydrogen atoms of acetone adsorbed on platinum exchange with the hydrogen atoms of the solvent.

If it is also considered that acetone can undergo chemical reactions depending on the electrode potential, then the validity of the mentioned method of studying the adsorption of water must be considered as even more doubtful.

In addition to this, from the experiments with acetone the important conclusion can be drawn that at potentials where a gaseous product is formed from the labelled component during adsorption measurements with the tracer technique (disregarding the quite small adsorptive concentrations), the experimental results can no longer (or only after careful consideration) be considered characteristic of the adsorption.

Such phenomena must be considered in the case of alcohols, and this question will be dealt with in our next publication.

REFERENCES

1. HORÁNYI, GY., SOLT, J., SZABÓ, S., NAGY, F.: Magy. Kém. Foly. **76**, 333 (1970); Acta Chim. Acad. Sci. Hung. **68**, 205 (1971)
2. HORÁNYI, GY., KŐNIG, P., TELCS, I.: Acta Chim. Acad. Sci. Hung. **72**, 165 (1972)
3. SCHULTZE, J. W.: Ber. Bunsenges. physik. Chem. **73**, 483 (1969)
4. Electrosorption. Ed. by E. Gileadi. Plenum Press, New York, 1967
5. SOLT, J., HORÁNYI, GY., NAGY, F.: Acta Chim. Acad. Sci. Hung. **63**, 385 (1970)
6. HORÁNYI, GY., SOLT, J., NAGY, F.: Acta Chim. Acad. Sci. Hung. **68**, 39 (1971)
7. DE HEMPTINNE, X., SCHUNCK, K.: Trans. Faraday Soc. **65**, 591 (1969)
8. KHOMYAKOV, V. G., BAKHCHISARYAN, N. G., TOMILOV, A. P.: Trudi chetvortovo soviesh-chaniya po elektrokhimii, p. 287. Izd. Akademii Nauk, Moscow 1959
9. HORÁNYI, GY., NAGY, F.: Acta Chim. Acad. Sci. Hung. **68**, 229 (1971)
10. HORÁNYI, GY., RIZMAYER, E. M., NAGY, F.: Acta Chim. Acad. Sci. Hung. **69**, 35 (1971)

György HORÁNYI
Ferenc NAGY
Budapest II., Pusztaszeri út 59—67.

Acta Chimica Academiae Scientiarum Hungaricae, Tomus 72 (3), pp. 269—275 (1972)

INVESTIGATION OF ADSORPTION PHENOMENA ON PLATINIZED PT ELECTRODES BY TRACER METHODS, XI

STUDY OF THE ADSORPTION OF ISOPROPANOL

GY. HORÁNYI, P. KŐNIG* and F. NAGY

*(Central Research Institute for Chemistry, Hungarian Academy of Sciences, Budapest, and *Isotope Institute of the Hungarian Academy of Sciences, Budapest)*

Received November 30, 1970

1. A study was made of the adsorption of isopropanol on a platinized platinum electrode in acidic medium.

2. It was found that the adsorption is irreversible, and the adsorbed molecules do not take part in the oxidation reaction of the isopropanol leading to the formation of acetone.

3. In the reduction the adsorbed isopropanol is converted to a gaseous product. In connection with this the conditions of measurement of the labelled gas-phase product accumulating in the platinum black were examined. The supposition was arrived at that the surface complexes formed during the adsorption of isopropanol and acetone are probably the same.

From our earlier work in connection with the oxidation of secondary alcohols [1] we have come to the conclusion that there is no direct relation between the alcohol adsorption phenomena and the oxidation reaction resulting in the formation of the ketone from the alcohol.

This finding was based primarily on the observation that the rate of oxidation of ^{14}C-labelled isopropanol adsorbed on the electrode surface is very low. From the point of view of studies aimed at elucidating the oxidation mechanism of secondary alcohols, it seemed important to examine thoroughly, with the aid of a tracer technique, the phenomena taking place during the adsorption of isopropanol and the properties of adsorbed isopropanol.

Independently of this object, there is the hope that the tracer study of isopropanol adsorption may perhaps contribute to a decision between the contradictory views in the literature concerning the adsorption of alcohols. Of the alcohols, so far the adsorption of methanol has been studied the most thoroughly, both with tracer techniques and by electrochemical methods [2, 3]. The findings and conclusions drawn on the basis of the measurements with the various methods primarily differ from each other with regard to the potential-dependence of the adsorption and the adsorption isotherm.

Experimental

The apparatus and method used in the investigation have already been described [4]. The specific activity of the ^{14}C-labelled isopropanol used varied in the range 0.1—10 mCi/mM. Similarly as in our previous work, 1 N $HClO_4$ was used as background solution.

As can be seen in Fig. 1, the curve describing the potential-dependence of the adsorption is very similar in nature to the curves obtained during the study of the adsorption of other alcohols [2]. It must be stressed that this curve can still not be regarded as characteristic of the adsorption, since at potentials greater than 400 mV the oxidation of the alcohol takes place at an appreciable rate, while at 800 mV it is already necessary to consider the appearance of adsorbed oxygen, too. At potentials more negative than 300 mV, on the other hand, a part may be played by hydrogen adsorption. All this shows that the curve to be seen in Fig. 1 comes about as the result of several factors. In our view, a possibility is provided for the study of the adsorption of isopropanol, independently of other factors, by a study of the mobility of the adsorbed isopropanol.

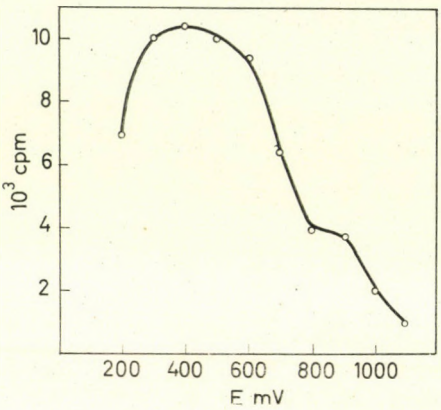

Fig. 1. Variation of the count rate (proportional to the amount adsorbed) as a function of the potential in the case of an isopropanol concentration of 10^{-3} *M*. (*E* is the potential against a 1 atm H_2 electrode immersed in 1 *N* $HClO_4$)

Study of the mobility and reaction of adsorbed isopropanol by a tracer technique

A study of the desorption and the rate of desorption of the adsorbed substance must be considered important because on the basis of these studies there is a possibility to take a stand in questions connected with the adsorption isotherm of the substance, and with the potential-dependence of its adsorption. In the course of our earlier informatory investigations [1], it was already found that the rate of desorption of the adsorbed isopropanol is very small. The method used for the study of the exchange between adsorbed isopropanol and that in the solution phase was as follows: after the adsorption processes of the labelled substance had gone to completion, the solution phase was removed and, after washing, the apparatus was refilled with pure background solution. A potentiostat ensured that the potential of the electrode should not change. The electrode potential was adjusted in advance to a value at which the oxidation of isopropanol need still not be considered.

In agreement with what has already been said, under such conditions the radioactivity originating from the labelled substance adsorbed on the electrode does not vary, or to only a small extent. (Naturally, the total count

rate observed, which also included the radiation arising from the labelled component in the solution, decreased. The intensity of the radiation from the solution was also determined separately. In our experiments its magnitude never attained 10% of the intensity of radiation arising from the adsorption.)

A relatively large amount of unlabelled isopropanol was next added to the system, and the potential of the electrode was then gradually changed in the positive direction in order that the behaviour of the labelled, adsorbed molecules could be studied during the oxidation of the added unlabelled isopropanol. The results of our observations are reflected by the curves to be seen in Fig. 2.

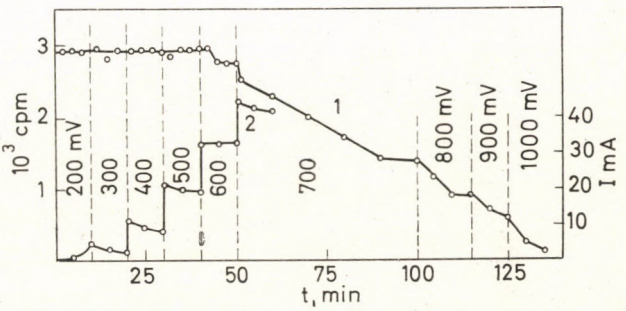

Fig. 2. Study of the mobility of labelled isopropanol adsorbed on the electrode in the presence of 5×10^{-2} *M* of inactive isopropanol. Curve 1 refers to the count rate, and curve 2 to the rate of oxidation

The above experiment was carried out in such a way that at first unlabelled isopropanol was brought into contact with the electrode. After a suitable waiting period this solution was removed from the apparatus and replaced by a solution containing labelled isopropanol. The phenomena observed when

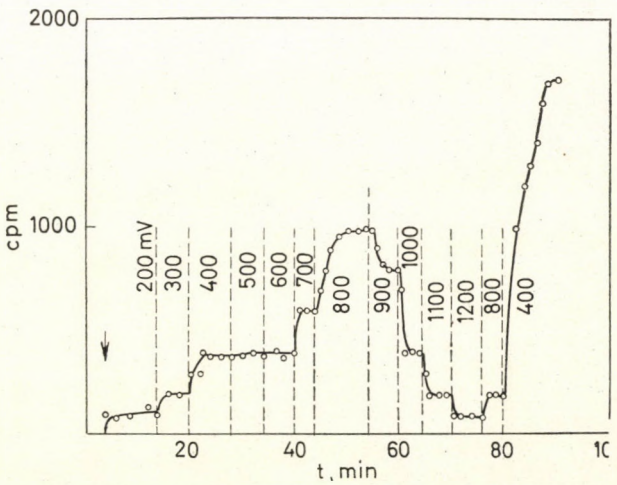

Fig. 3. Potential dependence of the adsorption of labelled isopropanol when inactive isopropanol has previously been adsorbed on the surface

changing the potential as a function of time are shown in Fig. 3. In the curves to be seen in Fig. 3, a considerable increase of the count rate occurs only at potentials more positive than 600 mV, in agreement with the observations in Fig. 2; thus, it was seen that the removal of the previously adsorbed molecules from the surface begins to take place with an appreciable rate only at such potentials. On returning from high (1200 mV) potentials to lower (400 mV) potentials, the adsorption of isopropanol again occurs.

Based on the experimental results presented, the following can be stated.

1. The adsorbed substance formed from the isopropanol cannot be exchanged.

2. The adsorbed molecules are still not oxidized even when an oxidation reaction (resulting primarily in acetone) is already taking place at an appreciable rate with the component in the solution phase.

3. The departure of the adsorbed component from the surface occurs at potentials more positive than 600 mV, and it probably involves a reaction independent of the oxidation leading to the formation of the oxo compound from the alcohol. Naturally, it cannot be excluded either that the adsorption of oxygen also plays a part in the decrease of the alcohol adsorption.

From Figs 2 and 3 it also appears that for reasons of principle we cannot speak of the adsorption isotherm of isopropanol and of the potential-dependence of the adsorption, for the molecules in the solution phase and in the adsorption phase are not identical. The phenomena arising on the change of the electrode potential in the negative direction bear witness to the fact that isopropanol undergoes significant changes during adsorption.

In the case when, similarly to the experiments previously described, after the adsorption of the labelled component at 200 mV the apparatus is washed out and refilled with background solution, and the potential is then changed in the negative direction, an increase of the count rate is observed, as can be seen in Fig. 4.

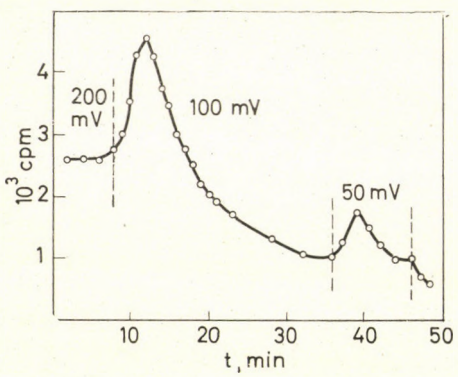

Fig. 4. Phenomena arising with labelled isopropanol adsorbed at 200 mV, when the potential is changed in the negative direction

Considering that the amount of labelled substance on the washed electrode cannot increase, the increase in the count rate can come about only as a result of changes in the self-absorption and geometrical conditions in the adsorbent–adsorptive system. According to the literature [5], if solutions of alcohols come into contact with a platinum electrode, and in the case of the change of the electrode potential in the negative direction, hydrocarbons are formed. If it is accepted that such phenomena occur in this case too, then the observed phenomena can be explained.

In one of our earlier publications [6] it was shown that the platinized platinum can be regarded as an agglomeration of particles, the average density of which is given by the relation

$$(1 - \varepsilon)\varrho_m + \varepsilon\varrho_0 = \bar{\varrho} \tag{1}$$

where ε is the porosity, and ϱ_m and ϱ_0 are the densities of the metallic platinum and the medium filling the space between the particles, respectively.

In the case when there is no labelled substance in the space between the particles, the intensity (I) of the radiation originating from the labelled substance adsorbed on the particles is given by the relation

$$I = \frac{\alpha q I_0}{\mu\bar{\varrho}} [(1-\varepsilon)\,\varrho_m\, a_s\, \Gamma](1 - e^{-\mu\varrho k}) \tag{2}$$

where α is the efficiency of the measurement, I_0 is the specific activity of the labelled substance, μ is the mass absorption coefficient, q is the area of the surface, a_s is the specific surface of the adsorbent, Γ is the amount of substance adsorbed on 1 cm^2 of the surface, and k is the thickness of the platinum black. If the aqueous solution ($\varrho_{0w} \approx 1$ g/cm^3) is displaced from the space between the particles by a gas ($\varrho_{0g} \approx 10^{-3}$ g/cm^3), the average density of the entire system, and hence its self-absorption too, change.

From Eqs (1) and (2), the ratio of the intensities of the radiation observed in the two cases is given by the expression

$$\frac{I_2}{I_1} = \frac{1 - e^{-\mu\bar{\varrho}_2 k}}{1 - e^{-\mu\bar{\varrho}_1 k}} \frac{\bar{\varrho}_1}{\bar{\varrho}_2} \tag{3}$$

It can be seen from Eq. (3) that in the limiting case when $\mu\bar{\varrho}_2 k$ and $\mu\bar{\varrho}_1 k \gg 1$, one obtains

$$\frac{I_2}{I_1} = \frac{\bar{\varrho}_1}{\bar{\varrho}_2}\,. \tag{4}$$

From relation (1), on the other hand, it can be seen that at high porosities ($1 > \varepsilon > 0.9$) a significant change is caused in the average density if the liquid medium is exchanged for a gas.

On the basis of the above, when the potential is changed in the negative direction the increase in the count rate and the maximum observed in its time dependence are explained by the fact that the gas-phase products formed by hydrogenation of the labelled, adsorbed substance partially or completely displace the liquid from the pores and the interstices of the platinum black.

In agreement with the views of other authors, the experimental results presented and the conclusions drawn from them bring us to the assumption that the adsorption of isopropanol be considered as a dehydrogenation reaction. The simplest product of the dehydrogenation and oxidation of isopropanol is acetone, which was found in an earlier paper [7] to be irreversibly adsorbed in a fairly wide potential interval. It appears very probable that the adsorbed complexes formed on the adsorption of acetone and isopropanol are essentially the same; in agreement with observations on the electrohydrogenation of acetone in acidic media, the adsorbed complex must be reduced to the same products, primarily propane, in both cases. (Naturally, because of the possible splitting of the C–C bonds the formation of other hydrocarbons cannot be excluded.)

Thus, the following proposed scheme can be given for the adsorption and reduction of isopropanol and acetone:

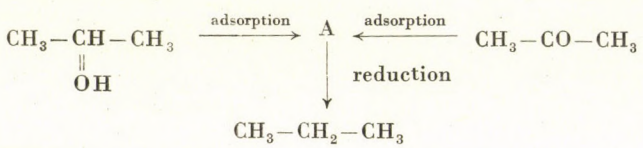

where A is the adsorbed molecule.

Our investigations to support the above conceptions, primarily with regard to the analysis of the gaseous products, are in progress.

REFERENCES

1. HORÁNYI, GY.. KŐNIG, P., TELCS, I.: Acta Chim. Acad. Sci. Hung. **72,** 165 (1972)
2. SMITH, R. E., URBACH, H. B., HARRISON, J. H., HATFIELD, N. L.: J. Phys. Chem. **71,** 1250 (1967);
   STENIN, V. F., KAZARINOV, V. E., PODLOVCHENKO, B. I.: Elektrokhimiya, **5,** 442 (1969)
3. BREITER, M. W.: Electrochim. Acta **7,** 533 (1962);
   BREITER, M. W.: Trans. Faraday Soc. **64,** 79 (1968);
   BREITER, M. W.: J. Electroanal. Chem. **15,** 221 (1967);
   BREITER, M. W.: J. Electroanal. Chem. **14,** 407 (1967);
   PODLOVCHENKO, B. I., FRUMKIN, A. N., STENIN, V. F.: Elektrokhimiya **4,** 339 (1968);
   BAGOTSKI, V. S., VASILIEV, YU. B.: Electrochim. Acta **12,** 1323 (1967)
   BIEGLER, T., KOCH, D. F. A.: J. Electrochem. Soc. **114,** 904 (1967);
   PODLOVCHENKO, B. I., KAZARINOV, V. E., STENIN, V. F.: Elektrokhimiya **6,** 252 (1970)
4. SOLT, J., HORÁNYI, GY., NAGY, F.: Acta Chim. Acad. Sci. Hung. **63,** 385 (1970)

5. PODLOVCHENKO, B. I., GORGONOVA, E. P.: D. A. N. SSSR. **156,** 673 (1964); PODLOVCHENKO, B. I.: Elektrokhimiya **1,** 101 (1965)
6. HORÁNYI, GY., RIZMAYER, E. M., NAGY, F.: Acta Chim. Acad. Sci. Hung. **69,** 35 (1971)
7. HORÁNYI, GY., SOLT, J., SZABÓ, S., NAGY, F.: Magyar Kém. Foly. **76,** 333 (1970)

György HORÁNYI, Ferenc NAGY } Budapest II., Pusztaszeri út 59—67.

Péter KŐNIG Budapest XII., Konkoly Thege M. út

Acta Chimica Academiae Scientiarum Hungaricae, Tomus 72 (3), pp. 277—280 (1972)

C_5-CYCLIZATION OF UNSATURATED HYDROCARBONS ON PLATINUM BLACK

(SHORT COMMUNICATION)

Z. PAÁL and P. TÉTÉNYI

(Institute of Isotopes of the Hungarian Academy of Sciences, Budapest)

In 1954 it was discovered by KAZANSKY, LIBERMAN *et al.* that in the presence of a Pt/C catalyst saturated hydrocarbons, among them *n*-hexane, are transformed to cyclopentane derivatives in a reaction termed C_5-dehydrocyclization [1, 2]. This process may also be catalyzed by oxide-carrier [3—5] or carrier-free [5, 6] platinum or palladium [7].

It was assumed by LIBERMAN that the C_5-dehydrocyclization and the hydrogenolysis of the five-membered ring take place *via* a common surface intermediate formed with the participation of hydrogen [8]:

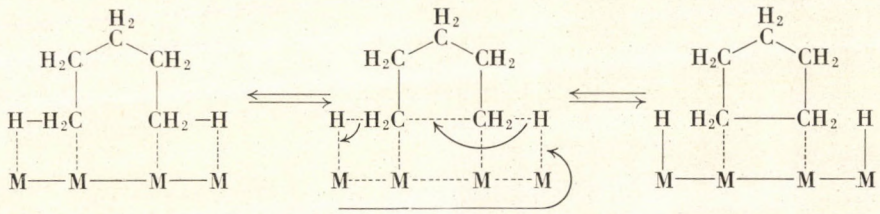

(1)

At the same time GAULT *et al.* conceived the formation of the cyclopentane ring *via* unsaturated intermediates [5]:

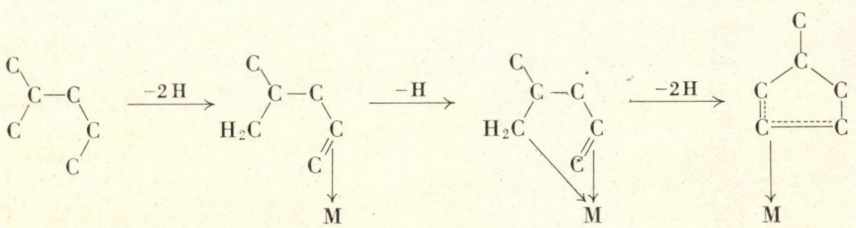

(2)

In fact, it has recently been observed that five-membered cyclic compounds can also be formed from hexene-1, hexadiene-1,5 [7] and hexatriene-1,3,5 [9]: these are methyl-cyclopentane, or alternatively methyl-cyclopentene and methylcyclopentadienes. This observation indicates again that it is necessary to study the role of unsaturated compounds in C_5-dehydrocyclization more thoroughly.

A systematic study was recently made of the transformations of various saturated and unsaturated hydrocarbons in the presence of hydrogen. It was found that in the presence of a hydrogen excess (but only then) methylcyclopentane is formed from *n*-hexane and from methylpentanes [6, 10]. In the presence of hydrogen, the formation of *methylcyclopentene-1* was almost always observed from unsaturated hydrocarbons (*n*-hexene, hexadiene isomers and hexatriene). Its amount was relatively low, and it disappeared very rapidly during the deactivation of the catalyst.

These studies showed that the peak found in the aromatization of *n*-hexene-1 in our earlier experiments [11] (believed to be epoxide impurity) was in fact methylcyclopentene-1.

In Table I are given the product-compositions obtained in the transformations of various hexadiene isomers and *trans*-hexatriene-1,3,5 in hydrogen. It can be seen that the amount of methylcyclopentene-1 formed depends considerably on the structure of the starting hydrocarbon: for hexadiene-1,5 it was a few per cent, whereas for all the other hexadienes and for hexatriene it was only a few tenths of one per cent. In some cases methylcyclopentadienes could be detected, too.

Table I

C_5-cyclization of hexadienes and hexatriene

Catalyst: 0.4 g Pt; t = 360 °C; carrier-gas 20% H_2 + 80% He, 60 ml/min; 5 μl hydrocarbon

Starting hydrocarbon	No. of impulse	Composition, mass %							
		Cracked products	Hexane	Hexenes + MCP	Hexadienes	Hexatriene-1,3,5	Methylcyclopentene-1	Methylcyclopentadienes	Benzene
hexadiene-1,5	I	9.5	61.9	18.3	—	—	1.5	0.3	8.7
	V	5.9	45.4	38.7	—	—	2.5	0.4	7.2
hexadiene-1,4	I	19.9	63.6	5.8	—	—	0.2	0.1	10.5
	V	13.0	69.5	8.9	—	—	0.6	—	7.9
hexadiene-1,3	I	19.0	65.7	4.3	—	—	0.4	0.1	8.4
	V	13.9	68.8	9.1	—	—	0.8	—	7.5
c,t-hexadiene-2,4	I	25.4	58.8	4.0	—	—	0.2	—	11.6
	V	15.5	69.9	7.4	—	—	0.6	—	6.8
t,t-hexadiene-2,4	I	21.3	61.5	4.3	—	—	0.2	—	12.8
	V	12.2	73.8	6.6	—	—	0.6	—	6.8
t-hexatriene-1,3,5	I	16.6	55.4	9.4	—	—	0.7	0.1	17.7
	V	7.3	45.7	28.6	0.3	—	1.6	—	16.5

From the fact that the C_5-cyclization of hexadiene-1,5 is outstandingly large compared with those of the other hydrocarbons listed, it was concluded that of all the hexadiene isomers hexadiene-1,5 had the most favourable structure for C_5-cyclization.

The fact that the amount of methylcyclopentene-1 *increases* with the decrease of the *dehydrogenating* activity of the catalyst, points to the direct hexadiene-1,5→methylcyclopentene-1 reaction; that is, the observed cycloolefin is the primary product of the ring-closure, and is not formed from methylcyclopentane (*cf.* the product-compositions for impulses I and V in Table I).

It is assumed that the ring-closure takes place similarly to the route described by GAULT *et al.*, with the difference that here the adsorption of the two terminal π-bonds of the molecule and hydrogen-shift must be presumed:

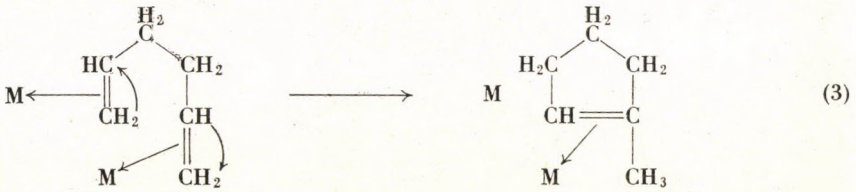

(3)

The C_5-cyclizations of the other mono- and polyolefins proceed either much more slowly or they are absent; in this latter case the formation of the five-membered ring would be preceded by the formation of hexadiene-1,5 from hexene by dehydrogenation, from hexadienes by isomerization, and from hexatriene by hydrogenation.

Attention must be drawn to the fact that the formation of five-membered rings from both saturated and unsaturated hydrocarbons was observed only in a hydrogen excess. This points to the relationship of these two reactions: the C_5-dehydrocyclization of *n*-hexane and the cyclization of hexadiene. In agreement with LIBERMAN's conception in the course of the reaction therefore, the presence of hydrogen is necessary, but the surface intermediate is not necessarily of a saturated nature. In the case of C_6-dehydrocyclization leading to aromatization it was shown that this is a simple cyclization following dehydrogenation. Such a mechanism may also be assumed for the formation of the five-membered ring. The final elucidation of the mechanism, however, requires still further experimental work.

REFERENCES

1. KAZANSKY, B. A., LIBERMAN, A. L., ALEKSANIAN, V. T., STERIN, H. F.: Dokl. Akad. Nauk SSSR, **95**, 77 (1954)
2. KAZANSKY, B. A., LIBERMAN, A. D., LOZA, G. V., CHANG MING-NAN: Dokl. Akad. Nauk SSSR, **120**, 789 (1958)
3. FOMICHOV, YU. V., GOSTUNSKAYA, I. V., KAZANSKY, B. A.: Izv. Akad. Nauk SSSR Ser. Khim., 1112 (1968)
4. DAUTZENBERG, F. M., PLATTEEUW, J. C.: J. Catalysis, **19**, 41 (1970)
5. BARRON, Y., MAIRE, G., MULLER, J. M., GAULT, F. G.: J. Catalysis, **5**, 428 (1966)
6. PAÁL, Z., TÉTÉNYI, P.: Dokl. Akad Nauk SSSR, **201**, 1119 (1971)
7. KAZANSKY, B. A., FADEEV, V. S., GOSTUNSKAYA, I. V.: Izv. Akad. Nauk SSSR, 677 (1971)
8. LIBERMAN, A. L.: Kinetika i kataliz, **5**, 128 (1964)

9. FADEEV, V. S., GOSTUNSKAYA, I. V., KAZANSKY, B. A.: Dokl. Akad. Nauk SSSR, **199,** 622 (1971)
10. PAÁL, Z., TÉTÉNYI, P.: Dokl. Akad. Nauk SSSR, **201,** 868 (1971)
11. PAÁL, Z., TÉTÉNYI, P.: Acta Chim. Acad. Sci. Hung. **53,** 193 (1967)

Zoltán PAÁL
Pál TÉTÉNYI
} Budapest XII., Konkoly Thege M. u.

Acta Chimica Academiae Scientiarum Hungaricae, Tomus 72 (3), pp. 281—296 (1972)

ХИМИЯ 1,3-БИФУНКЦИОНАЛЬНЫХ СОЕДИНЕНИЙ, XIII*

ИЗУЧЕНИЕ ПРЕВРАЩЕНИЙ ЦИКЛИЧЕСКИХ АЦЕТАЛЕЙ НА КАТАЛИЗАТОРЕ Pt/T С ПОМОЩЬЮ МИКРОРЕАКТОРНОЙ ТЕХНИКИ. 1,3-ДИОКСОЛАНЫ И 1,3-ДИОКСЕПАНЫ

Й. АПЬОК и М. БАРТОК

(Институт Органической Химии Университета им. А. Йожефа, Сегед, Венгрия)

(Поступило в редакцию: 22 октября 1969 г.; в переработанной форме: 20 сентября 1970 г.)

Описываются контактно-каталитические превращения некоторых пяти- и семичленных циклических ацеталей (1,3-диоксоланы и 1,3-диоксепаны). Исследования проводились на катализаторе Pt/T, содержащем 10% платины, в атмосфере водорода и с помощью микрореакторной техники. Были определены основные направления превращений, и результаты сравнивались с наблюдениями для 1,3-диоксанов. Были сделаны заключения относительно зависимостей относительных реакционных способностей от числа членов цикла в гомологическом ряду циклических ацеталей.

На основе исследований было установлено, что в случае 1,3-диоксепанов, в противоположность пяти- и шестичленным циклическим ацеталям, отсутствует реакция изомеризации, приводящая к образованию сложного эфира, а другие направления реакций, такие как изомеризация в алкоксиальдегид, гидрогенолиз кольца с образованием моноэфира диола, а также фрагментация кольца, являются общими направлениями превращений для всех трех циклических ацеталей. Уменьшение числа членов цикла приводит, как правило, к уменьшению реакционной способности. Изменение направлений превращений циклических ацеталей и их реакционных способностей в зависимости от числа членов цикла, вероятно, вызвано различиями в конформациях этих соединений.

1,3-Диоксоланы и 1,3-диоксепаны** можно рассматривать как 5- и 7-членные гомологи 1,3-диоксана. Эти соединения могут быть получены аналогичным путем из диолов и оксосоединений, и в некоторых реакциях, как например гидролиз или полимеризация, ведут себя подобным путем. В литературе [1] приводятся сравнительные данные относительно скорости гидролиза всех трех групп соединений, на основе которых можно заключить, что, несмотря на аналогию в строении этих соединений, существуют различия в их реакционной способности.

В то же время в литературе практически отсутствуют данные относительно превращений циклических ацеталей, протекающих на контактах. Рондестведт с сотр. [2] сравнивали превращения циклических ацеталей при изомеризации 1,3-диоксанов на пемзе и силикагеле, однако, выбор условий реакции, как например катализатора и температуры, в некоторой степени был произвольным. Интересным казалось бы изучение превращений 1,3-диок-

* Предыдущее сообщение: Acta Chim. Acad. Sci. Hung. **70,** 133 (1971)

** Получение 1,3-диоксоланов и 1,3-диоксепанов проводилось из диолов и оксосоединений согласно [16].

соланов и 1,3-диоксепанов, при таких условиях, при которых уже изучались контактно-каталитические превращения 1,3-диоксанов [3—10], что позволило бы делать сравнения относительно направлений превращений и их относительных скоростей.

В настоящем сообщении приводятся результаты исследований превращений 1,3-диоксоланов и 1,3-диоксепанов на катализаторе Pt/T* в присутствии водорода и эти результаты сравниваются с результатами, полученными для 1,3-диоксанов. Исследования проводились с помощью микрореакторной техники [11].

На основе наших исследований, превращения пяти-, шести- и семичленных циклических ацеталей, протекающие на катализаторе Pt/T в присутствии водорода, могут быть представлены в виде следующей схемы:

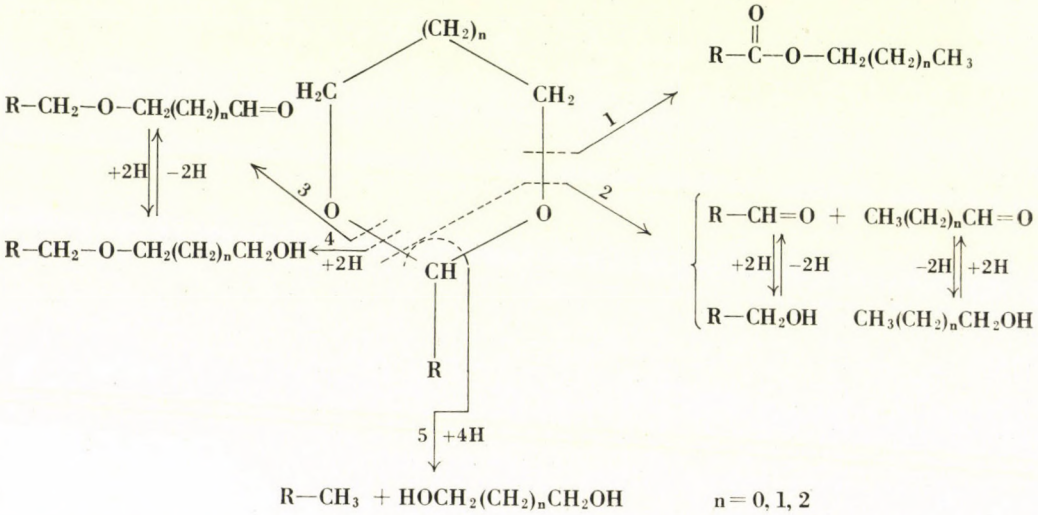

Количественные данные относительно этих превращений представлены в таблице 1.

Таблица 1

Максимальные выходы продуктов превращений циклических ацеталей, выраженные в %-ах по отношению к исходному соединению

n	Изомеризация, %, в сложные эфиры (направление 1)	Фрагментация, %, в окси-, оксо-соединения и углеводороды (направление 2)	Изомеризация, %, в алкокси-альдегиды (направление 3)	Гидрогенолиз, %, в моноэфиры диола (направление 4)	Гидрогенолиз, %, в диол + углеводород (направление 5)
0	89	10,5	0,5	2,9	~1%
1	81	60	15	14	—
2	—	57,6	35,8	37	—

* Приготовление и свойства катализатора Pt/T могут быть найдены в литературных ссылках [11, 12].

Очевидно, что среди процессов, изображенных на общей схеме превращений, изомеризация (направление 1) отсутствует для семичленного циклического ацеталя ($n = 2$), в то время как для пяти- и шестичленных циклических ацеталей (R = алкил) она представляет собой направление, дающее наибольший процент превращения.

Эти главные процессы сопровождаются вторичными процессами, как например гидрирование, дегидрирование, декарбонилирование и др. Степень превращения, а также %-ный состав образующихся продуктов зависят от температуры и от природы заместителя R, если другие параметры совпадают или не изменяются в одной серии измерений.

Проведение исследований с 1,3-диоксоланами и 1,3-диоксепанами в аналогичных условиях позволяет делать сравнения с результатами, полученными для 1,3-диоксанов [3—10].

Экспериментальные результаты и их обсуждение

I. Каталитические превращения 1,3-диоксоланов*

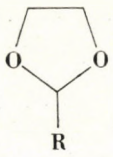

где R = CH_3 (I);
изо—C_3H_8 (II);
C_6H_5 (III).

2-Метил-1,3-диоксолан (I)

Соединение I подвергалось каталитическим превращениям на Pt/T в присутствии водорода. На основе результатов газохроматографического анализа были определены состав катализата и степени превращения I, в зависимости от температуры (см. табл. 2 и рис. 1.).

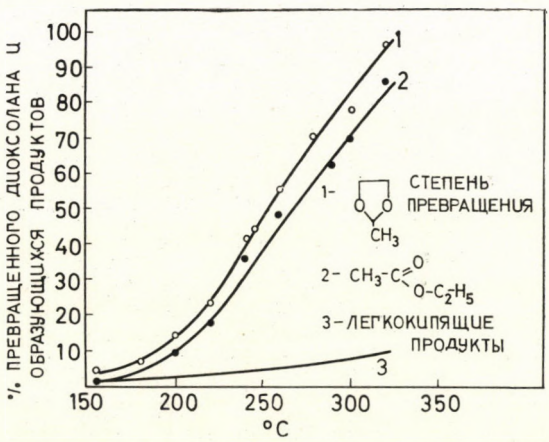

Рис. 1. Изменение степени превращения 2-метил-1,3-диоксолана (I) и %-ного состава образующихся продуктов в зависимости от температуры

* Физические константы [12]: I Т. кип.: 81—82°C, $n_D^{27} = 1{,}3926$; II Т. кип.: 123°C, $n_D^{27} = 1{,}4072$; III Т. Кип.: 106—107°C (11 мм рт. ст.), $n_D^{27} = 1{,}5220$

Таблица 2

Степени превращения 2-метил-1,3-диоксолана (I) и %-ный состав образующихся продуктов в зависимости от температуры а) — относительно исходного и б) — относительно превращенного диоксолана

Температура, °C	Степень превращения диоксолана, %	Образование сложного эфира, % (направл. 1)		Фрагментация, % (направл. 2)		Образование алкоксиальдегида (направл. 3) и моноэфира диола (направл. 4), %	
		а	б	а	б	а	б
180	3,5	1	28,6	1,5	42,8	1	28,6
200	7	3	42,8	3	42,8	1	14,3
220	14,5	10	69	3,5	24,1	1	6,9
240	42	36,7	87,4	4,3	10,2	1	2,4
260	55,4	49	88,5	5,4	9,7	1	1,8
280	71,2	63,3	88,9	6,9	9,7	1	1,4
300	78,3	70,3	89,8	7,5	9,6	0,5	0,6
320	97	87	89,7	10	10,3	—	—

Как видно из данных таблицы 2 и рисунка 1, в ходе превращений образуется этилацетат с хорошей селективностью. Количество продуктов с низкой температурой кипения достигает 10%-ов лишь при 320°C. Основным направлением превращений является изомеризация в сложные эфиры, обозначенная на общей схеме ($R = CH_3$; $n = 0$) как 1-ое направление. Фрагментация соединения I (2-ое направление), изомеризация в альдегид (3-ье направление) и гидрогенолиз (4-ое направление) не играют важной роли в превращениях диоксоланового кольца. В катализате были найдены лишь следы этиленгликоля, что свидетельствует о незначительной роли 5-ого направления.

Хроматограмма, характеризующая превращения соединения I представлена на рис. 2.

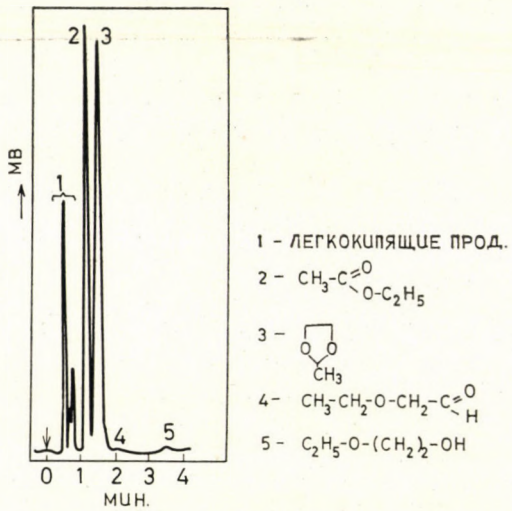

Рис. 2. Хроматограмма, характеризующая превращения 2-метил-1,3-диоксолана (I) Экспериментальные условия: а) 1 мл Pt/T, H_2,260 °C; б) 2 м 20% полипропиленгликольадипата, 142°C, 60 мл H_2/мин, 140 ма, предельное отклонение компензографа 8 мв.

2-Изопропил-1,3-диоксолан (II)

При превращениях соединения II на катализаторе Pt/T образуются также в основном жидкие продукты (см. табл. 3 и рис. 3).

Как видно из данных таблицы 3 и рисунка 3, основным продуктом превращений является этилизобутират. Другие продукты, включая и низкокипящие продукты, были найдены в катализате лишь в небольших количествах.

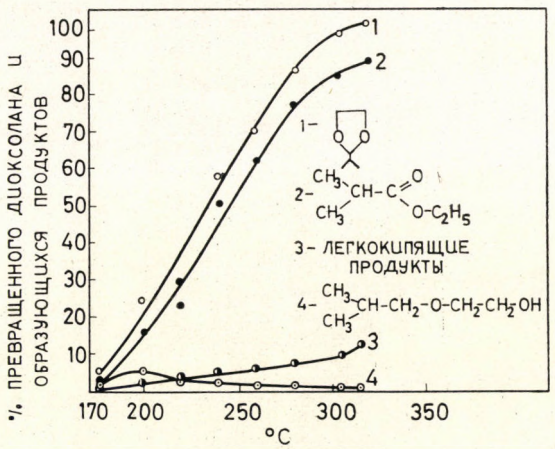

Рис. 3. Изменение степени превращения 2-изопропил-1,3-диоксолана (II) и %-ного состава образующихся продуктов в зависимости от температуры

Таблица 3

Степени превращения 2-изопропил-1,3-диоксолана (II) *и %-ный состав образующихся продуктов в зависимости от температуры а) — от исходного и б) — от превращенного диоксолана*

Температура, °C	Степень превращения диоксолана, %	Образование сложного эфира, % (направл. 1)		Фрагментация % (направл. 2)		Образование алкоксиальд. % (направл. 3)		Образование моноэфира диола, % (направл. 4)	
		а	б	а	б	а	б	а	б
175	4,6	2,5	54,4	0,5	10,8	0,1	2,2	1,5	32,6
200	24,4	16	66,7	2,5	10,2	0,2	0,8	5,7	23,3
220	29,6	23,2	78,4	3,2	10,8	0,3	1	2,9	9,8
240	58,8	50,5	85,8	5	8,5	0,5	0,9	2,8	4,8
260	71	62,1	87,5	6,7	9,4	0,2	0,3	2,0	2,8
280	86,7	77,4	89,3	7,5	8,6	сл.	сл.	1,8	2,1
305	96,7	85,9	88,6	9,8	10,1	—	—	1	1,1
315	100	89	89	10,5	10,5	—	—	0,5	0,5

При превращениях II доминирующим процессом является изомеризация в сложный эфир (1-ое направление). Фрагментация диоксоланового кольца (2-ое направление) и вторичные превращения продуктов обеспечивают легкокипящую часть катализата. Общее

количество их при 240°С не достигает 5%-ов и достигает 10%-ов лишь при 315°С. При 200°С количество 2-изобутоксиэтанола (4-ое направление) превышает 5%-ов и сповышением температуры уменьшается равномерно. На рис. 4 представлена хроматограмма, характеризующая превращения II.

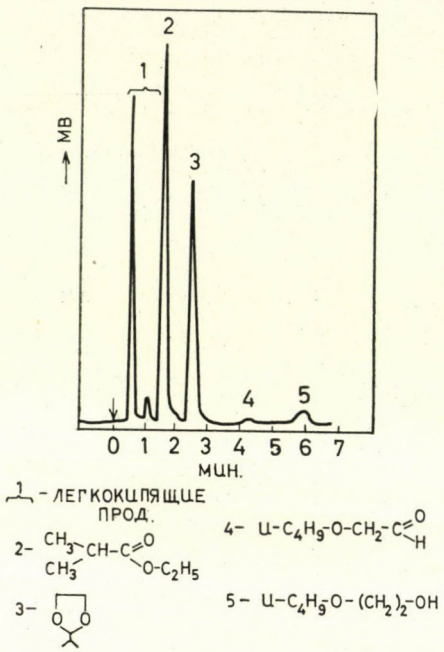

Рис. 4. Хроматограмма, характеризующая превращения 2-изопропил-1,3-диоксолана (II) Экспериментальные условия: а) 1 мл Pt/T, H_2, 240°С; б) 2 м 20% полипропиленгликольадипата, 142°С, 60 мл H_2/мин, 160 ма, предельное отклонение компензографа 8 мв

2-Фенил-1,3-диоксолан (III)

В таблице 4 и на рисунке 5 представлены данные превращений III на Pt/T в присутствии водорода.

Таблица 4

Степени превращения 2-фенил-1,3-диоксолана (III) *и %-ный состав образующихся продуктов в зависимости от температуры а) — исходного и б) — превращенного диоксолана*

Температура, °С	Степень превращения диоксолана, %	Образование сложного эфира, % (направл. 1)		Фрагментация, % (направл. 2)		Образование алкоксиальдегида, (направл. 3) и моноэфира диола (направл. 4), %	
		а	б	а	б	а	б
220	33,3	6,2	18,6	12,5	37,6	14,6	43,8
235	41	10	24,4	13,5	32,9	17,5	42,7
250	61	21	34,4	15	24,6	25	41
265	67	26	38,8	17	25,4	24	35,8
285	83,2	39	46,9	19	22,9	25,2	30,2
300	91	49	53,8	23	25,3	19	20,9

Среди продуктов превращений, особенно при более высоких температурах, значительное место занимает этилбензоат.

С повышением температуры степень образования сложного эфира монотонно возрастает и при 300°C количество образующегося этилбензоата достигает 54%-ов от всего превращенного диоксолана III, т. е. 1-ое направление становится доминирующим.

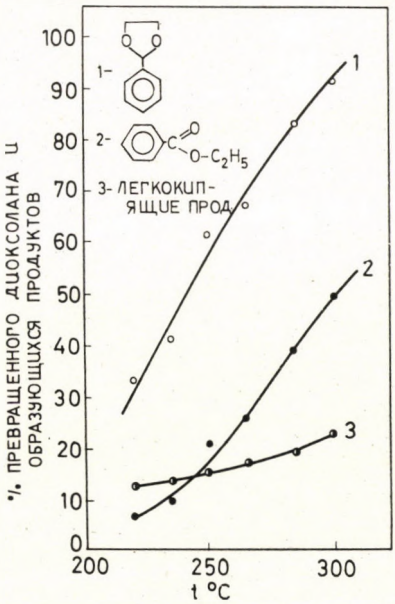

Рис. 5. Изменение степени превращения 2-фенил-1,3-диоксолана (III) и %-ного состава образующихся продуктов в зависимости от температуры

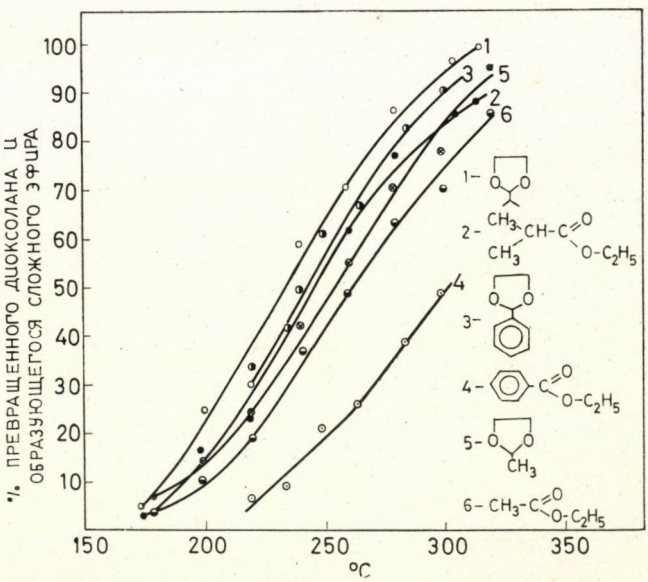

Рис. 6. Изменение степеней превращений 1,3-диоксоланов и выхода образующихся продуктов в зависимости от температуры

II. Сравнение реакционных способностей 1,3-диоксоланов и 1,3-диоксанов

Изученные на Pt/T в присутствии водорода 1,3-диоксоланы с хорошим выходом превращаются в соответствующие сложные эфиры (рис. 6).

Диоксоланы, на основе температурных величин, соответствующих 50%-ному превращению, могут быть помещены в следующий ряд: 2-изопропил- > 2-фенил- > 2-метил-1,3-диоксолан. Приводимый ряд отражает склонность 1,3-диоксоланов к превращениям (реакционную способность) в данных условиях контактного катализа на Pt/T в присутствии водорода. На основе выхода сложного эфира склонность к изомеризации уменьшается в следующем ряду: 2-изопропил- > 2-метил- > 2-фенил-1,3-диоксолан. Рисунки 7 и 8 служат для сравнения реакционной способности некоторых 2-алкил-1,3-диоксоланов и 1,3-диоксана. Согласно рис. 7, 2-метил-1,3-диоксолан (I) является более реакционноспособным и обладает большей склонностью к изомеризации в сложный эфир, чем 2-метил-1,3-

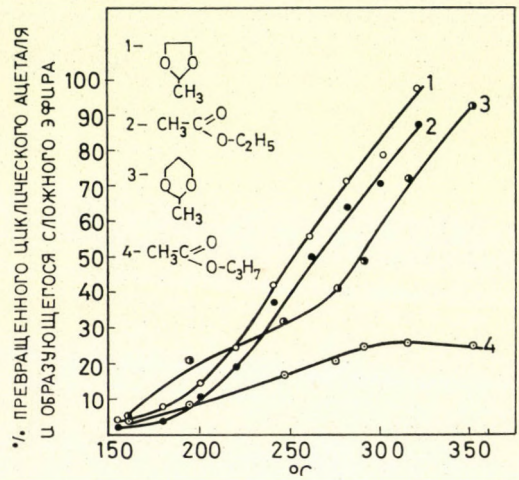

Рис. 7. Изменение степеней превращений 2-метил-1,3-диоксолана и 2-метил-1,3-диоксана, а также выхода образующихся продуктов в зависимости от температуры

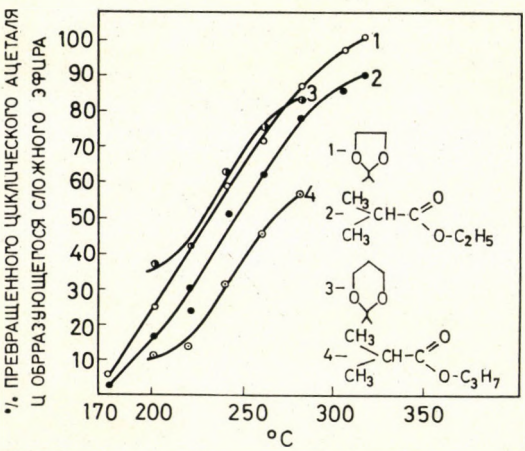

Рис. 8. Изменение степеней превращений 2-изопропил-1,3-диоксолана и 2-изопропил-1,3-диоксана, а также выхода образующихся продуктов в зависимости от температуры

диоксан. Изменения степеней превращения 2-изопропил-замещенных циклических ацеталей относительно близки, однако, на основе выхода сложного эфира 2-изопропил-1,3-диоксолан (II) превышает 2-изопропил-1,3-диоксан (рис. 8.). При превращениях 2-изопропил-1,3-диоксана можно наблюдать образование значительных количеств алкоксиальдегида (14,5%) и алкоксипропанола (14%) [9], в то время как в случае 2-изопропил-1,3-диоксолана (III) выход соответствующих продуктов значительно меньше (всего макс. 6%).

На основе сравнения результатов, полученных для превращений 2-алкил-замещенных 1,3-диоксоланов и диоксанов было установлено, что склонность к изомеризации в сложные эфиры (разрыв связи C(4)—O(3))является более выраженной у диоксоланов, чем у диоксанов. В то же самое время диоксаны более склонны по сравнению с диоксоланами к гидрогенолизу с разрывом связи C(2)—O(3), и изомеризации, с образованием алкоксиальдегида.

III. Каталитические превращения 1,3-диоксепанов*

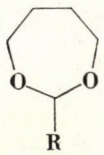

где R = C_3H_7 (IV);
изо-C_3H_7 (V).

2-Пропил-1,3-диоксепан (IV)

Процентный состав основных продуктов превращения соединения IV на Pt/T в присутствии водорода определялся газохроматографическим методом (см. табл. 5).

Таблица 5

Степени превращения 2-пропил-1,3-диоксепана (IV) *и %-ный состав образующихся продуктов в зависимости от температуры а)— исходного и б)— превращенного диоксепана*

Температура, °C	Степень превращения диоксепана, %	Фрагментация, % (направл. 2)		Образование алкоксиальдегида, % (направл. 3)		Образование моноэфира диола, % (направл. 4)	
		а	б	а	б	а	б
180	71	6,5	9,1	27,2	38,2	37,3	52,6
200	73,5	11,7	16	29,5	40,5	32	43,5
220	74,2	24,4	32,9	24,9	33,5	24,9	33,5
230	84	40,2	47,9	23,4	27,8	20,4	24,3
255	85	52,5	61,7	16,7	19,7	15,8	18,6
270	88,5	57,6	65,1	15,1	17,1	15,8	17,8

Данные таблицы изображены в виде графика на рис. 9. Как видно из рис. 9, в процессе превращений IV с увеличением температуры уменьшается общий выход алкоксиальдегида и моноэфира диола, благоприятствуя образованию легкокипящих продуктов. Это явление указывает на возрастающее значение фрагментации диоксепана, а также на ускорение вторичных процессов, в результате которых образующиеся алкоксиальдегид и моноэфир диола разлагаются далее. Так как изомеризация в сложный эфир (1-ое на-

* Физические константы [12]: IV Т. кип.: 75—77°C (45—50 мм рт. ст.) n_D^{25} 1,4293; V Т. кип.: 69—71°C (45—50 мм р$_D^{25}$т. ст.) n 1,4289.

правление) отсутствует, то главными направлениями превращений становятся изомеризация в алкоксиальдегид (3-ье направление) и гидрогенолиз (4-ое направление). С повышением температуры, наряду с фрагментацией, протекают гидрогенолиз, дегидрирование, дегидратация, декарбонилирование и др. образовавшихся продуков. Хроматограмма, характеризующая продукты превращеиий соединения IV, представлена на рис. 10.

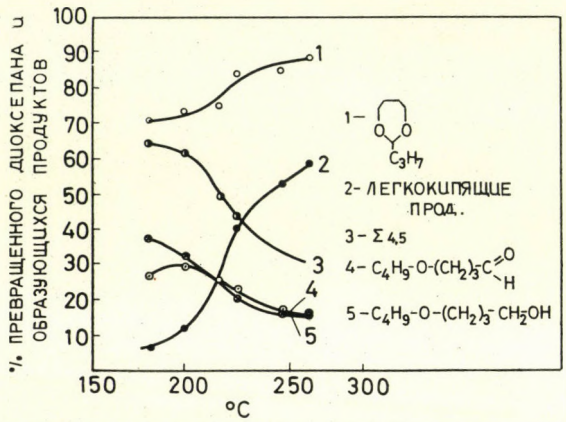

Рис. 9. Изменение степени превращения 2-пропил-1,3-диоксепана (IV) и %-ного состава образующихся продуктов в зависимости от температуры

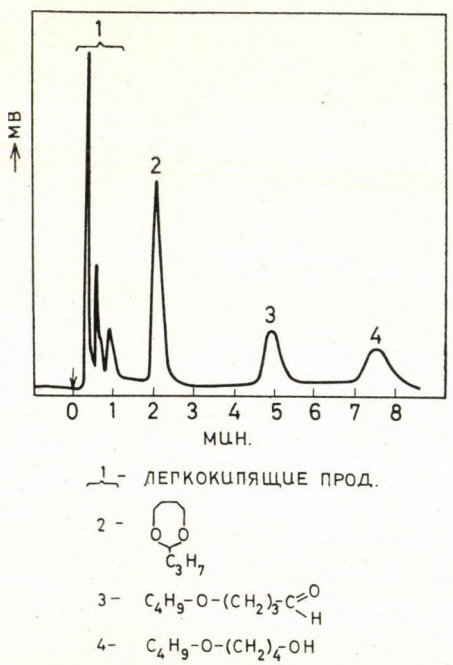

Рис. 10. Хроматограмма, характеризующая превращения 2-пропил-1,3-диоксепана. Экспериментальные условия: а) 1 мл Pt/T, H_2, 220°C; б) 1 м 20% полипропиленгликольадипата, 162°C, 60 мл H_2/мин, 140 ма, предельное отклонение компензографа 8 мв

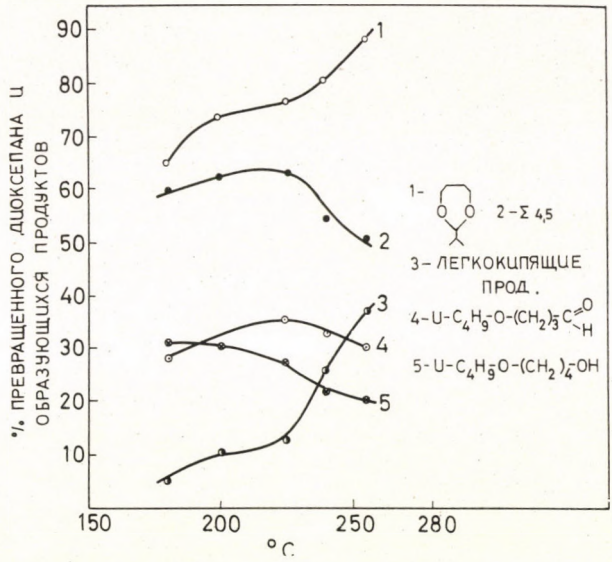

Рис. 11. Изменение степени превращения 2-изопропил-1,3-диоксепана (V) и %-ного состава образующихся продуктов в зависимости от температуры

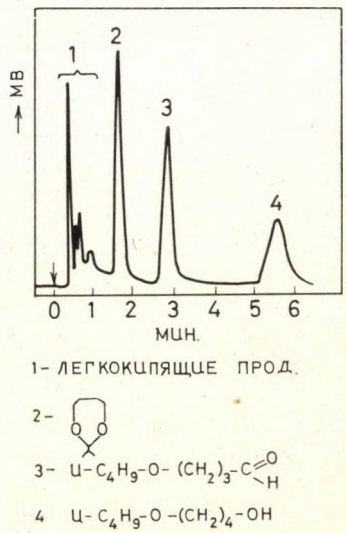

Рис. 12. Хроматограмма, характеризующая превращения 2-изопропил-1,3-диоксепана (V) Экспериментальные условия: а) 1 мл Pt/T, H_2, 200°C; б) 1 м 20% полипропиленгликольадипата, 162°C, 60 мл H_2/мин, 140 ма, предельное отклонение компензографа 8 мв

2-Изопропил-1,3-диоксепан (V)

Соединение V ведет себя на Pt/T и в токе водорода подобно соединению IV, однако, наблюдаются некоторые расхождения в поведении двух изомеров IV и V относительно количественных отношений образующихся продуктов.

В случае соединения V в изученном интервале температур общий выход алкоксиальдегида и моноэфира диола превышает количество легкокипящих продуктов (см. табл. 6 и рис. 11).

Таблица 6

Степени превращения 2-изопропил-1,3-диоксепана (V) и %-ный состав образующихся продуктов в зависимости от температуры а) — исходного и б) — превращенного диоксепана

Температура, °C	Степень превращения диоксепана, %	Фрагментация, % (направл. 2)		Образование алкоксиальдегида, % (направл. 3)		Образование моноэфира, % (направл. 4)	
		а	б	а	б	а	б
180	65	5,5	8,5	28,5	43,8	31	47,7
200	73,8	10,8	14,6	32,5	44	30,5	41,4
225	76,3	13	17	35,8	47	27,5	36
240	80,5	25,7	32	32,4	40,2	22,4	27,8
255	88,5	37,3	42,2	30,5	34,4	20,7	23,4

В процессе превращений соединения V при температуре 255°C выход алкоксиальдегида в полтора раза превышает количество моноэфира диола, в то время как в случае соединения IV выходы этих двух продуктов гораздо меньше различаются в тех же самых условиях. На рис. 12 представлена хроматограмма, характеризующая превращения соединения V.

IV. Сравнение реакционных способностей 1,3-диоксепанов, 1,3-диоксанов и 1,3-диоксоланов

В превращениях 1,3-диоксепанов не наблюдалось образование сложных эфиров. В то же время, два изомерных диоксепена (IV и V), на основе сравнения их степеней превращения, обладают почти одинаковой реакционной способностью, независимо от структуры алкильного заместителя. Иначе говоря, решающим фактором, определяющим направление и скорость превращений, является семичленная циклическая структура, а алкильный заместитель с разветвленной цепочкой в положении 2 препятствует процессу фрагментации.

В случае 1,3-диоксанов алкильный заместитель с разветвленной цепочкой в положении 2 оказывает также значительное влияние и на степень изомеризации в сложный эфир (степень превращения 2-изопропил-1,3-диоксана превышает степень превращения его изомера 2-пропил-1,3-диоксана; см. рис. 13).

2-Изопропил-производные циклических ацеталей, на основе температур, при которых достигается 50%-ное превращение, могут быть представлены в следующем ряду реакционных способностей:

1,3-диоксепан $\gg$ 1,3-диоксан $>$ 1,3-диоксолан.

Для склонности к гидрогенолизу циклических ацеталей получаем обратный порядок. В таблице 7 приводятся ряды реакционных способностей циклических ацеталей, измеренных при различных условиях, в зависимости от числа членов цикла.

Таблица 7

Реакционная способность циклических ацеталей

Основа сравнения	Зависимость реакционной способности от размеров кольца	Литература
Энтальпия образования	$5 > 7 > 6$	13
Скорость гидролиза	$5 > 6 > 7$	14
Полимеризационная способность	$7 \geq 5 \gg 6$	15
Контактно-каталитические превращения, Pt/T; H_2:		
Степень превращения	$7 \gg 6 \geq 5$	
Изомеризация в алкоксиальдегид	$7 \gg 6 > 5$	a
Гидрогенолиз в моноэфир диола	$7 \gg 6 > 5$	
Изомеризация в сложный эфир	$5 > 6$	

a — на основе экспериментальных данных для 2-изопропил-производных, приводимых в настоящем сообщении.

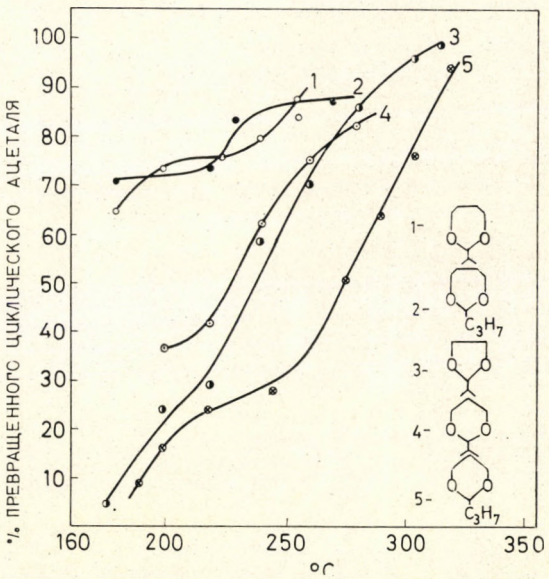

Рис. 13. Изменение степеней превращений 2-пропил- и 2-изопропил-замещенных циклических ацеталей в зависимости от температуры.

V. О механизме химических превращений пяти-, шести- и семичленных циклических ацеталей на Pt/T в присутствии водорода

Пяти- и шестичленные циклические ацетали на катализаторе Pt/T в присутствии водорода с хорошим выходом превращаются в сложные эфиры в процессе изомеризации, являющимся главным направлением превращений. Насколько удивительным является селективность превращений в случаях 1,3-диоксоланов и 1,3-диоксанов, не менее особенным кажется тот факт, что в гомологическом ряду циклических ацеталей для случая семичленных 1,3-диоксепанов изомеризация с образованием сложного эфира отсутствует в

полной мере, а вместо этого, через раскрытие связи между углеродом в положении 2 и соседним кислородом, происходит образование алкоксиальдегида и моноэфира диола. Образование сложного эфира не наблюдалось и в случае линейных ацеталей, превращения которых проводились также на катализаторе Pt/T в присутствии водорода.

В литературе приводятся данные относительно того, что в жидкой фазе при условиях протекания радикальных реакций (УФ-облучение, присутствие перекисей) пяти- и шестичленные циклические ацетали, а также ацетали с открытой цепочкой превращаются с образованием сложного эфира [17—22]. Можно полагать, что при подобных условиях 1,3-диоксепаны будут претерпевать аналогичные превращения. Помимо этого, в двух работах по термической изомеризации в паровой фазе 5-метилен-1,3-диоксанов сообщается об образовании металлиловых сложных эфиров [23, 24]. В некоторых вышеперечисленных случаях ацетальная связь находится в сопряжении с двойной связью (сопряжение аллильного типа), так что всеми авторами, обсуждающими механизм реакции, в качестве начальной ступени реакции полагается без исключения радикальная реакция с потерей водорода, протекающая на углероде второй степени окисления (для циклических ацеталей на атоме C(2)).

Изучая превращения ацеталей, протекающие на Pt/T в присутствии водорода, было установлено, что характерное образование сложного эфира в случае пяти- и шестичленных циклических ацеталей, можно представить как формальную 1,3-перегруппировку, связанную с разрывом связи O(3)—C(4).

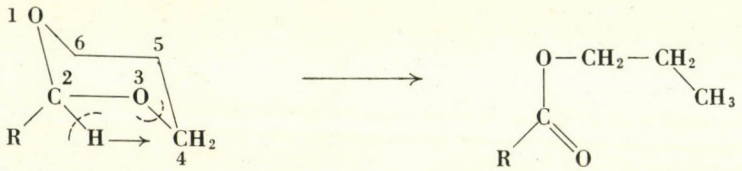

Относительно термодинамических сил, движущих процессом (стабильности циклического ацеталя и сложного эфира), имеются лишь сравнительные данные, согласно которым сложные эфиры являются более стабильными, чем циклические ацетали по отношению к терморазложению и контактно-каталитическим превращениям [12, 25]. Отсюда следует полагать, что при контактно-каталитических превращениях, образованию и дальнейшим превращениям переходного комплекса, необходимого для изомеризации обычно реакционноспособного 1,3-диоксепана в сложный эфир, препятствуют не энергетические, а адсорбционные геометрические факторы, исходящие из конформации цикла. Для пяти-, шести- и семичленных алициклических углеродных соединений имеются в распоряжении надежные конформационные данные [26, 27]. На основе подобия в конформациях пяти- и шестичленных ацеталей с соответствующими им алициклическими соединениями [26, 28—30] можно полагать, что 1,3-диоксепаны следует рассматривать в корреляции с циклогептаном.

Полагая конформацию с минимальной энергией и переходы между экваториальными аксиальными положениями алкильных заместителей при атоме C(2), можно обнаружить, что в случае 1,3-диоксолана и 1,3-диоксана кислороды, примыкающиеся к атому C(2), находятся в одной плоскости и, помимо этого, у 1,3-диоксолана второй центр превращения, приводящего к образованию сложного эфира, а именно атом C(4) в основном своем состоянии находится в той же самой плоскости. В случае 1,3-диоксепанов такая копланарность центров, принимающих участие в реакции, в конформации, означающей минимальное энергетическое состояние, еще более затруднена по сравнению с 1,3-диоксанами, не говоря уже об ацеталях с открытой цепочкой. На этой основе могут быть объяснены результаты, относящиеся к изомеризации ацеталей. Количественные различия в изомеризации пяти- и шестичленных циклических ацеталей (см. табл. 1) переходят в качественное отличие — отсутствие данного направления реакции для случая 1,3-диоксепанов. На этой же основе следует рассматривать и отсутствие образования сложного эфира у ацеталей с открытой цепочкой. С другой стороны, что касается точного механизма, а именно выяснения вопроса о том, что переход водорода происходит меж- или внутримолекулярно, необходимы дополнительные исследования. Хемосорбированный на поверхности платины водород может вступать в сложные реакции на поверхности, и тем самым, образование сложного эфира возможно и не за счет внутримолекулярного переноса водорода. В атмосфере гелия изомеризация в сложный эфир не протекает, а протекают другие не каталитические, а в основном пиролитические процессы.

Среди прочих превращений циклических ацеталей на катализаторе Pt/T в атмосфере водорода, важное место занимают изомеризация с образованием алкоксиальдегида за счет разрыва связи C(2)-O, и гидрогенолиз до моноэфира диола. В случае 1,3-диоксепанов наблюдаются почти только эти два процесса, в то время как в гомологическом ряду ацеталей с уменьшением числа членов цикла и молекулярного веса алкильного заместителя в положении 2, они становятся все менее важными. Образование алкоксиальдегида является также процессом изомеризации, только направление переноса водорода явялется обратным по сравнению с изомеризацией, приводящей к образованию сложного эфира. Отношение образующихся алкоксиальдегида и моноэфира диола особенно трудно определяется при повышенных температурах, вследствие возможных гидрирования — дегидрирования и прочих вторичных процессов. Однако, и в данном случае было определено, что с увеличением числа членов цикла увеличивается образование алкоксиальдегида и моноэфира диола, что, вероятно, связано с вытекающими из конформаций циклических ацеталей адсорбционно-геометрическими условиями, благоприятствующими процессам такого направления.

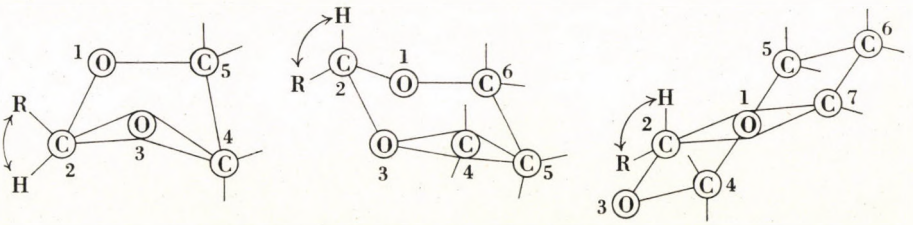

Summary

The heterogeneous catalytic transformations of some 5 and 7-membered cyclic acetals, 1,3-dioxolans and 1,3-dioxepans, have been studied in a microreactor, using a Pt/T catalyst with a Pt content of 10%, in the presence of hydrogen. The general direction of the reactions involved has been established and compared with the findings for 1,3-dioxans. Conclusions were drawn concerning the relative reactivity of homologous cyclic acetals, depending on the number of atoms in the ring.

It has been established that, in contrast to 5 and 6-membered cyclic acetals, isomerization to the ester does not occur in the case of 1,3-dioxepans. However, the other typical reactions such as isomerization to alkoxyaldehyde, ring hydrogenolysis to diol monoether and ring fragmentation are common characteristic features of all the 3 cyclic acetals. The decrease in the number of ring atoms, in general, leads to a decreased reactivity. The dependence of the reactions and reactivities of cyclic acetals on the number of ring atoms can probably be attributed to differences in their conformation.

ЛИТЕРАТУРА

1. Апьок, Й., Барток, М., Караханов, Р. А., Шуйкин, Н. И.: Успехи Химии, **38,** 72 (1969).
2. Rondestvedt, C. S., Mantell, G. J.: J. Am. Chem. Soc., **84,** 3307 (1962)
3. Апьок, Й., Барток, М., Караханов, Р. А., Шуйкин, Н. И.: Изв. АН СССР, сер. хим., *1968,* 2357.
4. Apjok, J., Bartók, M., Karakhanov, R. A., Kovács, K.: Acta Phys. et Chem. Szeged, **14,** 99 (1968)
5. Караханов, Р. А., Блинов, Б. Б., Апьок, Й., Барток, М., Шуйкин, Н. И.: Всесоюзный Симпозиум, Рига, 1969.
6. Apjok, J., Bartók, M., Kovács, K.: MKE Vegyészkonferencia, Szeged, 1969.
7. Bartók, M., Apjok, J., Karakhanov, R. A., Kovács, K.: Acta Chim. Acad. Sci. Hung., **61,** 315 (1969).
8. Apjok, J., Bartók, M.: Acta Phys. et Chem. Szeged, **17,** 55 (1971).
9. Apjok, J., Bartók, M., Karakhanov, R. A., Kovács, K.: Acta Phys. et Chem., Szeged **15,** 141 (1969).
10. Apjok, J., Bartók, M., Kovács, K.: Acta Chim. Acad. Sci. Hung. **69,** 445 (1971).
11. Bartók, M., Fényi, Sz.: Acta Phys. et Chem., Szeged, **12,** 157 (1966).
12. Апьок, Й.: Кандидатская диссертация, Москва, 1969.

13. Скуратов, С. М., Стрепихеев, А. А., Штехер, С. М., Волохина А. В.: ДАН СССР, *117*, 263 (1957).
14. Leutner, R.: Monatshefte, **60,** 317 (1932).
15. Стрепихеев, А. А., Волохина, А. В.: ДАН СССР, *94*, 407 (1959).
16. Апьок, Й., Барток, М., Караханов, Р. А., Шуйкин, Н. И.: Изв. АН СССР, сер. хим., 2352 (1968).
17. Ikeda, C. K., Braun, R. A., Sorenson, B. E.: J. Org. Chem., **29,** 286 (1964).
18. Seyfarth, M. E., Reiche, A., Hesse, A.: Chem. Ber., **100,** 624 (1967).
19. Huyser, E. S., Garcia, Z.: J. Org. Chem., **27,** 2716 (1962).
20. Huyser, E. S., Wang, D. T.: J. Org. Chem., **29,** 2720 (1964).
21. Kuhn, L. P., Wellman, C.: J. Org. Chem., **22,** 774 (1957).
22. Elad, D., Youssefyeh, R. D.: Tetrahedron Letters, 2189 (1963).
23. Weiss, F., Isard, A., Bensa, R.: Bull. Soc. Chim. France, 1358 (1965).
24. Weiss, F., Isard, A., Bonnard, G.: Bull. Soc. Chim. France, 2332 (1965).
25. Bilger, E. M., Hibbert, H.: J. Am. Chem. Soc., **58,** 823 (1936).
26. Eliel, E. L., Allinger, N. L., Angyal, S. J., Morrison, G. A.: «Conformational Analysis», John Wiley and Sons, Inc., N. Y., 1965.
27. Hendrickson, J. B.: J. Am. Chem. Soc., **89,** 7036, 7043, 7047 (1967).
28. Kankaanperä, A.: Ann. Univ. Turku, Ser. A I. N 95 (1966).
29. Pihlaja, K.: Ann. Univ. Turku, Ser. A. I. N 114 (1967).
30. Pihlaja, K.: Acta Scand., **21,** 2390, 2430 (1967); **22,** 716 (1968).

József Apjok
Mihály Bartók } Szeged, Dóm-tér 8. Hungary.

Acta Chimica Academiae Scientiarum Hungaricae, Tomus 72 (3), pp. 297—307 (1972)

THE CHEMISTRY OF 1,3-BIFUNCTIONAL SYSTEMS, XIV

KINETIC STUDY OF THE ALKALINE HYDROLYSIS OF THE 2,2-DISUBSTITUTED HOMOLOGUES OF TRIMETHYLENE CHLOROHYDRIN

M. Bartók, G. Bozóki-Bartók and K. Kovács

(Department of Organic Chemistry, A. József University, Szeged)

Received October 27, 1969,
in revised form July 15, 1970

The kinetics of alkaline hydrolysis of the 2,2-disubstituted homologues [2,2-dimethyl (**I**), 2,2-diethyl (**II**), 2-methyl-2-propyl (**III**), 2-ethyl-2-butyl (**IV**), 2,2-diisopropyl-3-chloropropanol (**V**)] of trimethylene chlorohydrin were studied. From the experimental data, the rate constants, activation energies and entropies, and preexponential factors have been determined for the formation of oxacyclobutane homologues.

We have reported in two communications on a kinetic investigation of the alkaline hydrolysis of 1,3-chlorohydrins [1, 2].

In this paper we wish to report the results obtained with the following model compounds belonging to the group of 2,2-disubstituted 1,3-chlorohydrins:

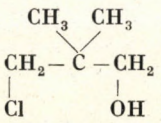

I

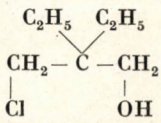

II

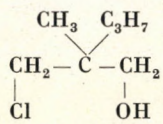

III

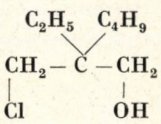

IV

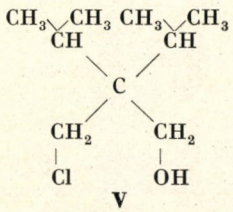

V

Beyond a simple description of the experimental results we shall examine the validity of the reaction mechanism suggested earlier [1] and the effect of substituents introduced into the trimethylene chlorohydrin molecule on the kinetic parameters.

In our preparative work we were able to confirm that when boiled in an alkaline medium, compounds (**I**) to (**V**) and their acetals are converted mainly into the corresponding oxetanes [1, 3].

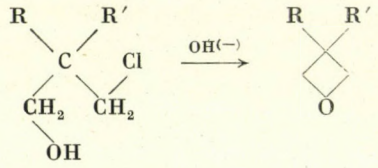

where R and R′ represent methyl—methyl, ethyl—ethyl, methyl—propyl, ethyl—butyl and isopropyl—isopropyl radicals.

The formation of oxetanes is accompanied by some minor fragmentation [1]. According to our recent investigations, in a 0.2 *M* aqueous barium hydroxide solution too the main reaction is oxetane formation.

On the basis of the mechanism suggested in our earlier work [1] the formation of 2,2-disubstituted oxetanes may be explained as follows:

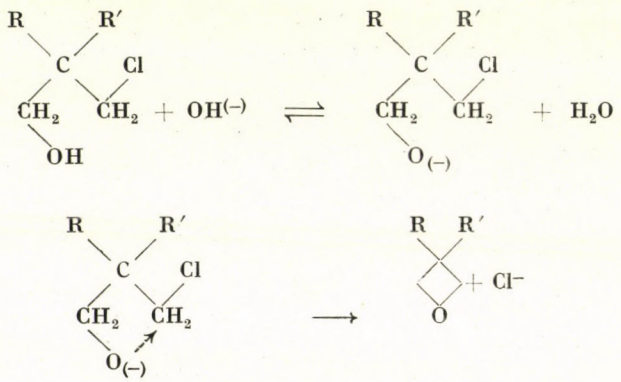

The kinetic results are summarized in Table I. The rate constants have been calculated in accordance with [1] from a second order rate equation. The Table contains beside the experimental conditions the rate constants *(k)*, the activation energies ($\Delta H^{\ddagger}$), the preexponential factors (A) and the activation entropies ($\Delta S^{\ddagger}$).

The experimental data listed in the Table are in satisfactory agreement with a second order rate equation, which confirms the validity of the suggested reaction mechanism (1) also for this type of chlorohydrins. The rate constants measured at various temperatures can be satisfactorily described by means of the Arrhenius equation (Fig. 1). The validity of the proposed reaction mechanism is supported by the values of $\Delta H^{\ddagger}$ and $\Delta S^{\ddagger}$ calculated from the experimental data.

Table I

Kinetic data of the alkaline hydrolysis of 1,3-chlorohydrins of the type

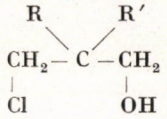

	°C	Chlorohydrin conc. mol/l.	[OH⁻] geq/l	k l · mol^{-1} · min^{-1}	$\Delta H^{\ddagger}$ kcal · mol^{-1}	A l · mol^{-1} · min^{-1}	$\Delta S^{\ddagger}$ e.u.
	80	0.01005	0.01806	0.023			
	85	0.01011	0.01610	0.043			
	90	0.01005	0.01623	0.065			
I	90	0.01005	0.01480	0.076	23.6	1.2×10^{13}	— 7.2
	195	0.01003	0.01610	0.105			
	95	0.01006	0.01480	0.115			
	100	0.01011	0.01480	0.195			
	100	0.01003	0.01834	0.200			
	80	0.01001	0.09510	0.076			
	80	0.01003	0.01571	0.071			
II*	85	0.01004	0.01623	0.115	21.9		
	90	0.01005	0.01630	0.175			
	95	0.01001	0.01687	0.254		2.4×10^{12}	—10.4
	95	0.01003	0.01571	0.235			
	80	0.01012	0.01687	0.044			
III	85	0.01001	0.01610	0.069	23.1		
	90	0.01005	0.01623	0.109			
	95	0.01014	0.01610	0.167		8.6×10^{12}	— 7.9
	80	0.01005	0.01687	0.060			
IV	85	0 01005	0.01610	0.098	22.0		
	90	0.01001	0.01623	0.145			
	95	0.01010	0.01610	0.213		2.3×10^{12}	—10.5
	75	0.01007	0.01687	0.162			
	80	0.01007	0.01687	0.234			
	80	0.01004	0.01554	0.216			
	80	0.00993	0.01554	0.224	22.0		
V	80	0.01005	0.01939	0.245			
	85	0.01007	0.01918	0.382			
	90	0.01007	0.01918	0.571			
	95	0.01001	0.01554	0.747			
	95	0.01003	0.02087	0.716		9.1×10^{12}	— 7.8
	95	0.01007	0.01918	0.802			

* Experimental data taken from Ref. [1]

Comparison of the rate constants in the Table with the rate constant of the parent substance — trimethylene chlorohydrin — under identical experimental conditions [2], e.g. at 80 °C where the latter is 0.024 1 · mol^{-1} · min^{-1}, shows that the presence of the two alkyl groups has considerably raised the rate of alkaline hydrolysis despite the fact that the substituents are not attached to carbon atoms participating directly in the reaction. The most probable cause for the higher rate constants should be sought in the development of a favourable conformation necessary for the S_Ni process to take place. The simultaneous presence of two substituents on carbon atom 2 forces the molecule to take up this favourable conformation.

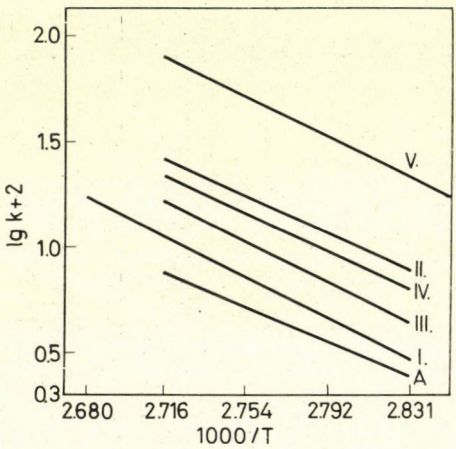

Fig. 1. Variation of the alkaline hydrolysis rate of the 2,2-disubstituted homologues of trimethylene chlorohydrin with the temperature. **A**: trimethylene chlorohydrin. **I**: 2,2-dimethyltrimethylene chlorohydrin. **II**: 2,2-diethyltrimethylene chlorohydrin. **III**: 2-methyl-2-propyltrimethylene chlorohydrin. **IV**: 2-ethyl-2-butyltrimethylene chlorohydrin. **V**: 2,2-diisopropyltrimethylene chlorohydrin

Experimental

The 1,3-chlorohydrins were prepared by the deacetylation of the corresponding chloroacetates in the presence of methanol [1]. The yields were about 80%. The purity of the starting materials was checked by gas-liquid chromatography. The physical parameters of the starting substances are listed in Table II.

Table II

Symbol of compound	Boiling point		n_D^{25}	Cl %	
	°C	mmHg		calcd.	found
I	93	40	1.4440	28.92	28.51
II	117	40	1.4596	23.54	23.50
III	117	40	1.4532	23.54	22.87
IV	143	40	1.4600	19.77	19.36
V	115	20	1.4642	19.77	19.22

I

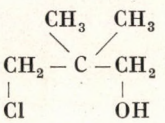

80 °C
$a = 0.01806$
$b = 0.01005$

No.	t	x	k
1	150	0.00066	0.025
2	215	0.00097	0.027
3	275	0.00133	0.029
4	335	0.00156	0.029
5	395	0.00181	0.029
6	455	0.00204	0.029
7	510	0.00227	0.030

$k_{1-7} = 0.029$

85 °C
$a = 0.01610$
$b = 0.01011$

No.	t	x	k
1	60	0.00044	0.046
2	120	0.00081	0.044
3	180	0.00110	0.041
4	230	0.00142	0.042
5	280	0.00162	0.041
6	300	0.00181	0.043
7	320	0.00189	0.042
8	340	0.00199	0.042

$k_{1-8} = 0.043$

90 °C
$a = 0.01623$
$b = 0.01005$

No.	t	x	k
1	55	0.00055	0.065
2	78	0.00076	0.063
3	130	0.00126	0.066
4	170	0.00158	0.066
5	220	0.00195	0.065
6	280	0.00241	0.066
7	340	0.00278	0.064
8	400	0.00310	0.063

$k_{1-8} = 0.065$

90 °C
$a = 0.01480$
$b = 0.01005$

No.	t	x	k
1	50	0.00062	0.086
2	102	0.00104	0.075
3	150	0.00157	0.081
4	200	0.00192	0.076
5	250	0.00226	0.075
6	300	0.00270	0.077
7	350	0 00293	0.076
8	400	0.00323	0.075

$k_{2;\,4-8} = 0.076$

II

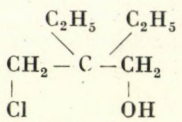

95 °C
$a = 0.01610$
$b = 0.01003$

No.	t	x	k
1	45	0.00075	0.108
2	85	0.00138	0.113
3	125	0.00186	0.109
4	165	0.00226	0.104
5	205	0.00271	0.105
6	245	0.00309	0.104
7	285	0.00341	0.102
8	325	0.00372	0.097

$k_{1-8} = 0.105$

95 °C
$a = 0.01480$
$b = 0.01006$

No.	t	x	k
1	44	0.00067	0.109
2	83	0.00125	0.112
3	120	0.00176	0.115
4	155	0.00222	0.118
5	195	0.00263	0.116
6	235	0.00307	0.118
7	280	0.00349	0.118
8	320	0.00372	0.113

$k_{1-8} = 0.115$

100 °C
$a = 0.01480$
$b = 0.01011$

No.	t	x	k
1	20	0.00052	0.179
2	40	0.00105	0.191
3	60	0.00152	0.193
4	80	0.00195	0.195
5	100	0.00243	0.203
6	120	0.00291	0.213

$k_{1-6} = 0.195$

100 °C
$a = 0.01834$
$b = 0.01003$

No.	t	x	k
1	21	0.00067	0.188
2	42	0.00135	0.196
3	61	0.00198	0.208
4	82	0.00252	0.207
5	100	0.00288	0.201
6	121	0.00333	0.201
7	140	0.00369	0.200

$k_{1-7} = 0.200$

III

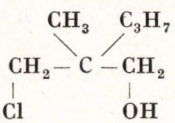

80 °C
a = 0.01687
b = 0.01012

No.	t	x	k
1	68	0.00057	0.050
2	120	0.00092	0.048
3	180	0.00127	0.047
4	240	0.00160	0.044
5	300	0.00189	0.041
6	360	0.00226	0.045
7	420	0.00248	0.043
8	480	0.00278	0.043

k_{2-8} = 0.044

85 °C
a = 0.01610
b = 0.01001

No.	t	x	k
1	60	0.00066	0.072
2	120	0.00120	0.068
3	180	0.00172	0.068
4	230	0.00208	0.068
5	280	0.00250	0.069
6	300	0.00260	0.068
7	320	0.00277	0.069
8	340	0.00292	0.070

k_{1-8} = 0.069

90 °C
a = 0.01623
b = 0.01005

No.	t	x	k
1	30	0.00053	0.113
2	65	0.00111	0.115
3	102	0.00184	0.130
4	135	0.00290	0.107
5	168	0.00235	0.106
6	200	0.00271	0.107
7	230	0.00308	0.109
8	260	0.00334	0.108

$k_{1-2;\,4-8}$ = 0.109

95 °C
a = 0.01610
b = 0.01014

No,	t	x	k
1	20	0.00053	0.169
2	40	0.00104	0.173
3	60	0.00154	0.179
4	80	0.00186	0.167
5	100	0.00218	0.162
6	120	0.00261	0.168
7	140	0.00287	0.164
8	160	0.00319	0.180

k_{1-8} = 0.170

IV

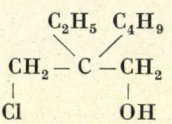

80 °C
a = 0.01687
b = 0.01005

85 °C
a = 0.01610
b = 0.01005

No.	t	x	k	No.	t	x	k
1	68	0.00072	0.066	1	60	0.00083	0.091
2	120	0.00112	0.060	2	120	0.00211	0.130
3	180	0.00175	0.066	3	180	0.00226	0.095
4	240	0.00203	0.059	4	230	0.00294	0.104
5	300	0.00249	0.060	5	280	0.00328	0.099
6	360	0.00278	0.058	6	300	0.00341	0.099
7	420	0.00316	0.059	7	320	0.00363	0.099
8	480	0.00349	0.059	8	340	0.00377	0.099

k_{1-8} = 0.060 k_{3-8} = 0.098

90 °C
a = 0.01623
b = 0.01001

95 °C
a = 0.01610
b = 0.01010

No.	t	x	k	No.	t	x	k
1	23	0.00053	0.144	1	20	0.00058	0.186
2	58	0.00124	0.144	2	40	0.00130	0 219
3	95	0.00194	0.148	3	60	0.00178	0.211
4	128	0.00242	0.145	4	80	0.00229	0.214
5	161	0.00286	0.142	5	100	0.00274	0.215
6	193	0.00334	0.146	6	120	0.00306	0.207
7	223	0.00368	0.144	7	140	0.00325	0.192
8	253	0.00397	0.143	8	160	0.00346	0.184

k_{1-8} = 0.145 k_{2-6} = 0.213

V

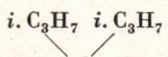

75 °C
a = 0.01687
b = 0.01007

No.	t	x	k
1	15	0.00043	0.173
2	30	0.00077	0.157
3	45	0.00112	0.159
4	60	0.00122	0.132
5	78	0.00179	0.157
6	90	0.00213	0.167
7	105	0.00239	0.164
8	120	0.00258	0.160

$k_{1-3;5-8}$ = 0.162

80 °C
a = 0.01687
b = 0.01007

No.	t	x	k
1	10	0.0003828	0.226
2	20	0.0006559	0.198
3	30	0.001039	0.219
4	40	0.001460	0.243
5	52	0.001650	0.215
6	60	0.002068	0.241
7	70	0.002355	0.242
8	80	0.002680	0.251

$k_{1;3-8}$ = 0.234

80 °C
a = 0.01554
b = 0.009927

No.	t	x	k
1	30	0.00103	0.244
2	60	0.00185	0.236
3	90	0.00246	0.222
4	120	0.00320	0.236
5	180	0.00414	0.227
6	210	0.00443	0.216
7	240	0.00473	0.211

k_{2-7} = 0.224

80 °C
a = 0.01939
b = 0.01005

No.	t	x	k
1	15	0.00076	0.277
2	45	0.00196	0.262
3	75	0.00291	0.255
4	105	0.00364	0.246
5	130	0.00418	0.243
6	140	0.00429	0.235

k_{3-6} = 0.245

80 °C
a = 0.01554
b = 0.01004

No.	t	x	k
1	10	0.00039	0.256
2	60	0.00182	0.228
3	125	0.00325	0.228
4	180	0.00411	0.221
5	240	0.00468	0.204
6	300	0.00485	0.173
7	360	0.00581	0.200

$k_{2-5;7}$ = 0.216

85 °C
a = 0.01918
b = 0.01007

No.	t	x	k
1	10	0.00059	0.319
2	20	0.00136	0.397
3	30	0.00187	0.376
4	40	0.00235	0.370
5	50	0.00296	0.397
6	60	0.00335	0.390
7	70	0.00368	0.380
8	80	0.00399	0.369

k_{2-8} = 0.383

V

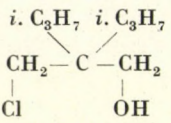

90 °C
$a = 0.01918$
$b = 0.01007$

95 °C
$a = 0.01554$
$b = 0.010005$

No.	t	x	k	No.	t	x	k
1	8	0.00073	0.499	1	20	0.00205	0.795
2	17	0.00165	0.575	2	40	0.00346	0.781
3	25	0.00224	0.558	3	65	0.00452	0.715
4	32	0.00279	0.574	4	80	0.00512	0.699
5	39	0.00327	0.579	5	120	0.00595	0.633
6	47	0.00377	0.585	6	160	0.00654	0.567
7	57	0.00425	0.572	7			
8	67	0.00461	0.552				

$k_{2-8} = 0.571$

$k_{1-4} = 0.747$

95 °C
$a = 0.02087$
$b = 0.01003$

95 °C
$a = 0.01918$
$b = 0.010073$

No.	t	x	k	No.	t	x	k
1	10	0.00129	0.721	1	5	0.00059	0.640
2	20	0.00234	0.695	2	15	0.00191	0.770
3	30	0.00349	0.764	3	20	0.00255	0.816
4	40	0.00410	0.716	4	25	0.00296	0.788
5	50	0.00461	0.682	5	30	0.00341	0.795
6	60	0.00502	0.651	6	35	0.00381	0.797
7	70	0.00563	0.677	7	40	0.00421	0.802
8	80	0.00598	0.660	8	45	0.00459	0.816

$k_{1-5} = 0.716$

$k_{2-8} = 0.802$

The chlorohydrins crystallize on standing.

The methods of kinetic measurements and calculations have been described in full detail in our earlier communication [1]. In the kinetic calculations the rate constants of chlorohydrins measured up to a 30—40% conversion have been used.

Experimental data

The following notations are used:
t: time (min)
a: initial concentration of hydroxide ions [$Ba(OH)_2$, geq/l]
b: initial concentration of chlorohydrin (mol/l)
k: second order rate constant ($l \cdot mol^{-1} \cdot min^{-1}$).

REFERENCES

1. Bartók, M., Bozóki-Bartók, G., Kovács, K.: Acta Chim. Acad. Sci. Hung. **66,** 115 (1970)
2. Bartók, M., Láng-Lakos, K., Bozóki-Bartók, G.: Acta Chim. Acad. Sci. Hung. **70,** 133 (1971)
3. Shuikin, N. I., Bartók, M., Kozma, B.: Izv. A. N. SSSR, Ser. Khim. 1967, 153
4. Bartók, M., Kozma, B., Gilde, A. S.: Acta Phys. et Chem. Szeged **11,** 35 (1965)

Mihály Bartók
Gizella Bozóki-Bartók
Kálmán Kovács
Szeged, Dóm-tér 8. Hungary.

Acta Chimica Academiae Scientiarum Hungaricae, Tomus 72 (3), pp. 309—316 (1972)

N-GLYCOSIDES, XV*

THE VALIDITY OF HUDSON'S ISOROTATIONAL RULE FOR AROMATIC O- AND N-GLUCOSIDE DERIVATIVES OF ANALOGOUS STRUCTURES

A. LIPTÁK and R. BOGNÁR

(Organic Chemical Institute, L. Kossuth University, Debrecen)

Received May 6, 1970,
in revised form March 15, 1971

In secondary glucosylamine derivatives, the designation of the configuration based on the direction and magnitude of the optical rotation also gives the correct absolute configuration. The Hudson $2B$ values of these compounds are comparable with the corresponding values of O-glucosides of analogous structures in the free N-aryl-D-glucopyranosylamine group only. In glucosides, tetraacetates and tetramethyl ethers the differences in the $2B$ values increase with increasing polarizability of the aglycones.

In the free O-glucosides and their O-acetyl derivatives examined by us, ARNDT's quantitative relationship was stated between the polarizability of the aglycones (α) and the molar rotation. It has been shown that in the two anomers the contributions of the aglycones to the molar rotation are not equal. The participation in molar rotation increases with increasing polarizability of the aglycone.

On the basis of the van't Hoff theory on optical superposition [1], HUDSON [2] found a relationship between the optical rotation of the glycoside carbon atom and the other active centres in sugars with cyclosemiacetal structures.

The validity of the rule has been studied on several groups of carbohydrate derivatives and it was found to be applicable for acetylated glycosides [3], methylpentoses [4], sugar phosphates [5], deoxyamino sugars [6] and acetohalogen sugars [7]. The limit of the applicability of this rule was pointed out primarily by BONNER [8], who emphasized that in the presence of polar aglycones a very strong variation in the $2B$ values should be expected.

Special attention is to be paid to glycosylamine derivatives, since in tertiary glycosylamine derivatives a rotational irregularity was observed which put an end to the unequivocal designation of the anomeric configuration on the basis of the direction and magnitude of the optical rotation. Thus, *e.g.*, the β-anomers of all pyrimidine nucleosides show higher positive rotation than the corresponding α-anomers [9, 10].

According to the investigations of BERTHO [11] and FRUSH and ISBELL [12], primary glycosylamine derivatives follow the Hudson rule. In secondary glycosylamines, the $2B$ values calculated for the anomeric tetraacetates can be compared in some cases with those of the aromatic O-glycoside tetraacetates of analogous structures, as indicated by the investigations of PIGMAN [13] and BOGNÁR and NÁNÁSI [14].

* Part XIV: R. BOGNÁR, H. FRENZEL, I. FARKAS: Acta Chim. Acad. Sci. Hung. **60**, 163 (1969)

Both anomers of several N-aryl-D-glucopyranosylamine derivatives have been prepared lately; thus the $2B$ and $2A$ values of N- and O-glucosides of similar structures can be calculated from the specific rotations measured under identical conditions in absolute methanol, and they may be compared. In Tables I—III the $2B$ values of the compounds examined are given.

Table I

2B values of some aromatic N- and O-glucosides

Aglycone	2B		Δ2B	Ref.
	NH-glucosyl	O-glucosyl		
C_6H_5-	29.600	33.900	4.300	[15]
p-$CH_3-C_6H_4-$	33.600	33.800	200	[16]
p-$Br-C_6H_4-$	42.400	41.100	−1.300	[16]
$NO_2-C_6H_4-$	51.600	45.500	−6.100	[16]
$C_6H_5-CH_2-$	—	26.800	—	

Table II

2B values of some aromatic N- and O-glucoside tetraacetates

Aglycone	2B		Δ2B	Ref.
	NH-glucosyl $(OAc)_4$	O-glycosyl $(OAc)_4$		
C_6H_5-	69.500	58.100	−11.400	[15]
p-$CH_3-C_6H_4-$	76.300	57.300	−19.000	[16]
p-$Br-C_6H_4-$	47.200	65.200	18.000	[16]
p-$NO_2-C_6H_4-$	60.800	69.400	8.600	[16]
$C_6H_5-CH_2$	—	43.100	—	

Table III

2B values of some aromatic N- and O-glucoside tetramethyl ethers

Aglycone	2B		Δ2B	Ref.
	NH-glucosyl $(OCH_3)_4$	O-glucosyl $(OCH_3)_4$		
C_6H_5-	—	33.000	—	
p-$CH_3-C_6H_4-$	50.000	38.000	−12.000	[17]
p-$Br-C_6H_4-$	65.000	42.500	−23.500	[17]
p-$NO_2-C_6H_4-$	48.000	20.600	−27.400	[17]
$C_6H_5-CH_2-$	—	39.900	—	

The $2B$ values of the aromatic O- and N-glucoside derivatives of analogous structures show, in general, a good agreement with a maximum deviation of about $\pm 10\%$. In both series an increase of the $2B$ values can be observed in the direction phenyl→*p*-NO_2-phenyl.

In the case of glucoside tetraacetates the deviation between the compared values is far greater. In O-glucoside tetraacetates the $2B$ values increase again in the same order as above; in N-glucoside tetraacetates no similar regularity can be detected.

There is a significant difference between the analogous N- and O-glucoside derivatives in the group of glucoside tetramethyl ethers; however, the changes of the $2B$ values with respect to direction and magnitude are nearly identical in both series. Similarly to the tetraacetates, the $2B$ values of the O-glucoside tetramethyl ethers are lower than those of N-glucoside tetramethyl ethers. In all three groups, the $2B$ values of the O-benzyl glucosides are also given; these are very near to the corresponding data of the aromatic glucoside derivatives.

Investigating the dependence of the $2B$ values on the aglycone of the two glucoside groups, the differences between the optical data appear in a different light.

YAMANA [18, 19] and ARNDT [20] studied acetohalogen sugars and some glucoside tetraacetates, respectively, and stated that in tetraacetyl-D-glucopyranose derivatives substituted at C-1 by X (halogen, OH, O—C_6H_5, SCH_3, OAc, $OC(CH_3)_3$), the molar rotation of the anomers and the polarizability of the free X^- ions (α) were in a linear relationship with each other. In the case of the two anomers this dependence is different, thus the Hudson B value also depends on the polarizability of the aglycone (the anion derived from the aglycone), according to the following formula:

$$M_{\alpha \text{ or } \beta} = A_{\alpha \text{ or } \beta} + B'$$

where

$$A_\alpha = m_\alpha \cdot \alpha; \quad A_\beta = m_\beta \cdot \alpha$$

and

$$B_{\text{Hudson}} = (m_\alpha + m_\beta)\, \alpha/2 + B'$$

It also follows from the equations that in contradiction to HUDSON's original formulation $(A_\alpha) \neq (A_\beta)$, *i.e.*, the degrees of participation of the two aglycones in the molar rotation are not equal to each other.

In the knowledge of the polarizability (α) and the B' values published by ARNDT for tetraacetyl-D-glucopyranosyl derivatives, we have calculated the polarizability values (α) of the anions derived from the aglycones of the glucosides examined by us. The following values were obtained: C_6H_5O—: 39; *p*-CH_3—C_6H_4—O—: 41; *p*-Br—C_6H_4—O—: 55—56; *p*-NO_2—C_6H_4—O—: 59—

$60 \cdot 10^{-25}$ cm^3. This made possible the calculation of the dependence of the molar rotation of the anomers on the polarizability of the aglycone ($\Delta M_\alpha/\Delta\alpha$ and $\Delta M_\beta/\Delta\alpha$), as well as the change in the B values per unit polarizability ($\Delta B/\Delta\alpha$), and further on, the molar rotation (B') of 1,5-anhydrosorbite derivatives, for all the three O-glucoside groups (Figs 1—3 and Table IV). In the case of O-glucoside tetramethyl ethers the scattering of the measured data is high, the slopes of the lines are uncertain, thus the values per unit polarizability are not given numerically.

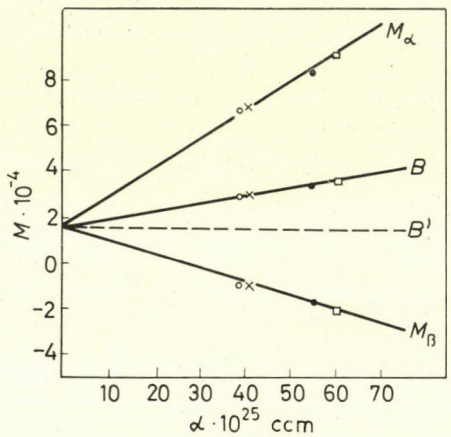

Fig. 1. Molar rotation (M_α and M_β) and the Hudson B values of anomeric aromatic O-glucosides as a function of the polarizability of the phenolate anion (α). ○ phenyl-; ● *p*-Br-phenyl-; × *p*-cresyl-; □ *p*-NO_2-phenyl-

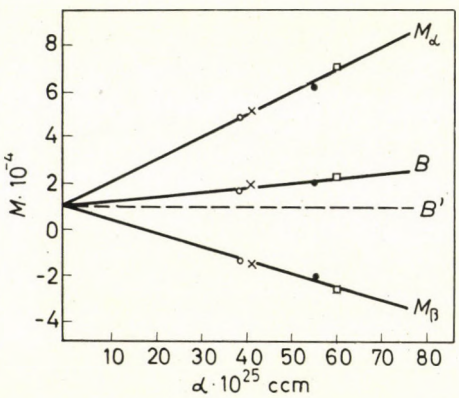

Fig. 2. Molar rotation (M_α and M_β) and the Hudson B values of anomeric aromatic O-glucoside tetraacetates as a function of the polarizability of the phenolate anion (α). ○ phenyl-; ● *p*-Br-phenyl-; × *p*-cresyl-; □ *p*-NO_2-phenyl-

Table IV

Molar rotations of the anomers, B values per unit polarizability and molar rotations of 1,5-anhydrosorbite derivatives

	$\frac{M_\alpha/10^4}{\alpha \cdot 10^{24}}$	$\frac{M\beta/10^4}{\alpha \cdot 10^{24}}$	$\frac{B}{\alpha \cdot 10^{24}}$	B'*
Aromatic O-glucosides	+0.98°	−0.58°	+0.20°	$+1.0° \cdot 10^4$
Aromatic O-glucoside tetraacetates	+1.22°	−0.60°	+0.31°	$+1.5° \cdot 10^4$

On the basis of the B' values the specific rotations of 1,5-anhydrosorbite and tetraacetyl-1,5-anhydrosorbite were found to be +54° (+43°) and +46° (+40°), respectively. (The literature data are given in parentheses.)

The differences in the optical behaviour of the two groups of glucosides are not satisfactorily explained.

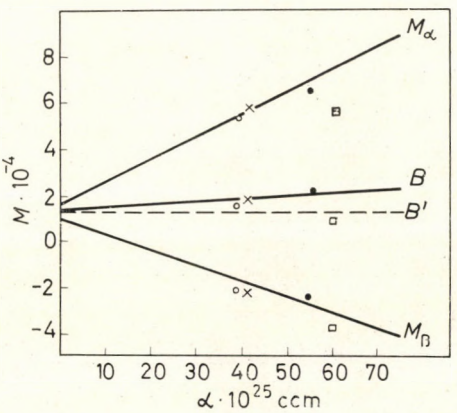

Fig. 3. Molar rotation (M_α and M_β) and the Hudson B values of anomeric aromatic O-glucoside tetramethyl ethers as a function of the polarizability of the phenolate anion (α). ○ phenyl-; ● *p*-Br-phenyl-; × *p*-cresyl-; □ *p*-NO_2-phenyl-

The anomers of the N-glucosides may not have been quite pure in spite of their careful preparation under mild reaction conditions and purification. Another possible cause of the deviations may be the difference between the conformations of the two glucoside groups, which can be attributed to the different valence angles of oxygen and nitrogen. Though this difference is not very great, it may be enough to give rise to a different degree of conformational deformation of the glucopyranosyl group. The polarizing effect of solvent may increase this difference so much that the optical behaviours of the two groups of compounds cannot longer be compared. This assumption is confirmed by our

*B' is the molar rotation of the hypothetic glucopyranosyl cation or the tetraacetylglucopyranosyl cation, its numerical value being equal to the molar rotation of 1,5-anhydrosorbite and tetraacetyl-1,5-anhydrosorbite, respectively.

observation that the lowest difference is found between the optical behaviour of the free N- and O-glucosides. Namely, in these compounds the polar hydroxyl groups in the glucopyranosyl part stabilize an actual conformer much more than the apolar substituents of a tetraacetyl- or, particularly, a tetramethylglucopyranosyl group.

According to ARNDT's investigations, the compounds which follow the rule have identical conformations, as shown by NMR spectroscopy.

On the basis of recent conformational studies, the B values should always be compared using the same solvent, because the dominant conformations of the anomers may be different or even opposite in an actual solvent; thus the direction of the variation may differ in different solvents [21].

Table V

2A values of aromatic O- and N-glucopyranosides

Aglycone	O-glucoside				N-glucoside
	A_α	A_β	$(\|A_\alpha\| + \|A_\beta\|)$	$2A$	$2A$
C_6H_5-	28.220	−22.620	60.840	64.300	83.200
p-$CH_3-C_6H_4-$	40.180	−23.780	63.960	70.200	87.900
p-$Br-C_6H_4-$	53.900	−31.900	85.800	79.500	115.900
p-$NO_2-C_6H_4-$	58.800	−34.800	93.600	99.500	150.700

Table VI

2A values of aromatic O- and N-glucopyranoside tetraacetates

Aglycone	O-glucoside $(OAc)_4$				N-glucoside $(OAc)_4$
	A_α	A_β	$(\|A_\alpha\| + \|A_\beta\|)$	$2A$	$2A$
C_6H_5-	47.580	−23.400	70.980	83.100	112.300
p-$CH_3-C_6H_4-$	50.020	−24.600	74.620	84.700	123.200
p-$Br-C_6H_4-$	67.100	−33.000	100.100	90.400	100.500
p-$NO_2-C_6H_4-$	73.200	−36.000	109.200	109.600	153.700

Table VII

2A values of aromatic O- and N- glucopyranoside tetramethyl ethers

Aglycone	O-glucoside $(OCH_3)_4$				N-glucoside $(OCH_3)_4$
	A_α	A_β	$(\|A_\alpha + \|A_\beta\|)$	$2A$	$2A$
C_6H_5-	37.440	−23.400	60.840	74.200	—
p-$CH_3-C_6H_4-$	39.360	−24.600	63.960	78.400	96.300
p-$Br-C_6H_4-$	52.800	−33.000	85.800	88.700	122.200
p-$NO_2-C_6H_4-$	57.600	−36.000	93.600	94.400	173.600

Table VIII

Physical constants and elemental analyses of phenyl-D-glucopyranoside tetramethyl ethers substituted in the aromatic ring

-D-glucoside $(OCH_3)_4$	M.p., or b.p./0.09 torr	$[\alpha]_D$ (in methanol)	Yield, %	Crystallization g/ml solvent	Analysis
α-phenyl	136—7°	+171.6	84.4	—	$C_{16}H_{24}O_6$ (312.35). Calcd. C 61.52; H 7.77; OCH_3 39.74. Found C 61.41; H 7.73; OCH_3 38.91%.
β-phenyl	78°	— 66.0	84.5	3 (P)	$C_{16}H_{24}O_6$ (312.35). Calcd. C 61.52; H 7.77; OCH_3 39.74. Found C 62.05; H 7.77; OCH_3 38.16%.
α-*p*-cresyl-	24—28°	+180.1	97.2	1 (P)	$C_{17}H_{26}O_6$ (326.38). Calcd. C 62.55; H 8.03; OCH_3 38.03. Found C 62.31; H 8.00; OCH_3 37.73%
β-*p*-cresyl-	52°	— 61.9	70.4	3 (P)	$C_{17}H_{26}O_6$ (326.38). Calcd. C 62.55; H 8.03; OCH_3 38.03. Found C 62.51; H 8.17; OCH_3 37.50%
α-*p*-Br-phenyl-	58.5°	+167.7	77.8	1.5 (P)	$C_{16}H_{23}O_6Br$ (391.26). Calcd. C 49.11; H 5.92; Br 20.42; OCH_3 31.72. Found C 49.09; H 6.08; Br 20.66; OCH_3 31.08%
β-*p*-Br-phenyl-	89—90°	— 59.2	60.9	2.5 (P)	$C_{16}H_{23}O_6Br$ (391.26). Calcd. C 49.11; H 5.92; Br 20.42; OCH_3 31.72. Found C 49.80; H 5.90; Br 20.49; OCH_3 31.71%
α-*p*-NO_2-phenyl-	syrup	+160.8	99.6	—	$C_{16}H_{23}O_8N$ (357.32). Calcd. C 53.77; H 6.48; N 3.92; OCH_3 34.73. Found C 53.57; H 6.42; N 3.99; OCH_3 34.18%
β-*p*-NO_2-phenyl-	109°	—103.4	54.5	35 (P)	$C_{16}H_{23}O_8N$ (357.32). Calcd. C 53.77; H 6.48; N 3.92; OCH_3 34.73. Found C 53.76; H 6.94; N 4.23; OCH_3 34.46%
β-*o*-NO_2-phenyl-	90.5°	—105.2	65.5	4 (A)	$C_{16}H_{23}O_8N$ (357.32). Calcd. C 53.77; H 6.48; N 3.92; OCH_3 34.73. Found C 53.97; H 6.66; N 4.13; OCH_3 34.56%
α-benzyl-	161—2°	+162.7	87.1	—	$C_{17}H_{26}O_6$ (326.38). Calcd. C 62.55; H 8.03; OCH_3 38.03. Found C 62.60; H 8.22; OCH_3 37.84%
β-benzyl-	161—4°	— 40.4	94.4	—	$C_{17}H_{26}O_6$ (326.38). Calcd. C 62.55; H 8.03; OCH_3 38.03. Found C 62.54; H 8.00; OCH_3 38.00%

Abbreviations: A = ethyl alcohol
P = petroleum ether

Experimental

The $2A$ and $2B$ values in the paper were calculated from specific rotation values measured in absolute methanol.

The α- and β-anomers of phenylglucosides and tetraacetates substituted in the aromatic ring were prepared as described in the literature.

The anomeric glucoside tetramethyl ethers were obtained by methylation of the corresponding glucoside anomers according to KUHN [22], under the reaction conditions discussed in detail below.

The syntheses and rotational values of the anomeric N-glucosides, N-glucoside tetraacetates and N-glucoside tetramethyl ethers are given in the literature [15—17].

The specific rotations of all compounds examined were measured in absolute methanol with a Schmidt-Haensch polarimeter in 10 cm tubes, at room temperature (20—22 °C); the rotation values were read 2 minutes after dissolving the sample. During this time no significant mutarotation took place.

The melting and boiling points given are uncorrected.

Methylation of the substituted phenyl-D-glucopyranosides was carried out according the following general procedure:

3—6 g (1 mole) of the phenylglucoside anomer substituted in the aromatic ring was dissolved in 20—40 ml of dimethylformamide, with stirring. A calculated amount (20 mole) of methyl iodide was added to the solution in one portion, then active silver oxide was added in small portions, under continuous stirring, during 15 min. The amount of silver oxide in grams was equal to the number of milliliters of methyl iodide added to the reaction mixture. The temperature of the reaction mixture was kept below 30 °C. When no more heat evolved, the mixture was stirred further for 10—12 hrs. at room temperature.

Diluting the reaction mixture with 50—100 ml of chloroform, the silver iodide precipitated from the solution; the precipitate was filtered off on a G4 sintered glass filter and washed with chloroform. The dimethylformamide-chloroform filtrate was washed with water, 1% KCN solution, then again with water. The solution was dried over Na_2SO_4 and the solvent was evaporated in vacuum. The residue was crystallized or distilled under reduced pressure.

The physical constants of the products obtained, yields, the conditions of crystallization, and elemental analyses are summarized in Table VIII.

REFERENCES

1. MICHEEL, F.: Chemie der Zucker und Polysaccharide. Akademische Verlagsgesellschaft Leipzig, 1956
   PIGMAN, W. W.: The Carbohydrates, Academic Press, New York, 1957
   STANEK, J., CERNY, M., KOCOUREK, J., PACÁK, J.: The Monosaccharides. Prague, 1963
2. HUDSON, C. S.: J. Am. Chem. Soc. **41,** 66 (1909)
3. SYKORA, V.: Chemie (Prague) **9,** 400 (1957); C. A. **52,** 8033 (1958)
4. YAMANA, S.: Bull. Chem. Soc. Japan **31,** 564 (1958); C. A. **57,** 9070 (1959)
5. PUTMAN, E. W., HASSID, W. Z.: J. Am. Chem. Soc. **79,** 5057 (1957)
6. NEUBERGER, A., RIVERS, R. R.: J. Chem. Soc. **1939,** 122
7. KORYTNYK, W.: J. Chem. Soc. **1959,** 650
8. BONNER, W. A., KUBITSCHEK, M. M. J., DRISKO, R. W.: J. Am. Chem. Soc. **74,** 5082 (1952)
9. FOX, J. J., WEMPEN, I.: Adv. Carbohydrate Chem. **13,** 430 (1959)
10. EMERSON, T. R., ULBRICHT, T. L. V.: Chem. Ind. (London) **1964,** 2129
11. BERTHO, A.: Ann. **562,** 229 (1949)
12. FRUSH, H. L., ISBELL, H. S.: J. Research Natl. Bur. Standards **47,** 239 (1951)
13. PIGMAN, W., JOHNSON, K. C.: J. Am. Chem. Soc. **75,** 3464 (1953)
14. BOGNÁR, R., NÁNÁSI, P.: Vegyipari Kut. Int. Közl. **IV,** 183 (1954)
15. HONEYMAN, J., TATCHELL, A. R.: J. Chem. Soc. **1950,** 867
16. NÁNÁSI, P., BOGNÁR, R.: J. Chem. Soc. **1961,** 323
17. BOGNÁR, R., NÁNÁSI, P., LIPTÁK, A.: Acta Chim. Acad. Sci. Hung. **45,** 47 (1965)
18. YAMANA, S.: J. Org. Chem. **31,** 3698 (1966)
19. YAMANA, S.: Tetrahedron **24,** 1559 (1968)
20. ARNDT, O.: Ann. **695,** 184 (1966)
21. LEMIEUX, R. U., PAVIA, A. A.: Can. J. Chem. **46,** 1453 (1968)
22. KUHN, R., TRISCHMAN, A., LÖW, I.: Angew. Chem. **67,** 32 (1955).

András LIPTÁK
Rezső BOGNÁR
} Debrecen 10. Hungary.

Acta Chimica Academiae Scientiarum Hungaricae, Tomus 72 (3), pp. 317—322 (1972)

PHYTOCHEMICAL INVESTIGATION OF CERTAIN *CESTRUM* SPECIES GROWING IN EGYPT

ALKALOIDS AND SAPONINS

M. S. KARAWYA,* A. M. RIZK, F. M. HAMMOUDA, A. M. DIAB and Z. F. AHMED**

(Pharmaceutical Sciences Laboratory, National Research Centre, Dokki, Cairo, U.A.R.)

Received November 30, 1970

Solanidine and solasodine were isolated from *Cestrum purpureum*, while *C. aurantiacum* and *C. diurnum* were devoid of any steroidal alkaloid. Quantitative determination of the alkamines was carried out by titrimetric and colorimetric methods. Investigation of the saponin content showed that both *C. aurantiacum* and *C. purpureum* contain the same saponin, *viz.* digitonin while *C. diurnum* contains tigonin; their identity was proved by acid hydrolysis and identification of the steroid sapogenins (digitogenin and tigogenin) and the sugar components.

Introduction

The review of literature reveals that some *Cestrum* species *(Solanaceae)* contain steroid alkaloids and/or steroid sapogenins. MERCIER *et al.* [1] reported in 1913 that *C. parqui L'Her* contains a bitter alkaloid parquine ($C_{21}H_{39}O_8N$) which has a mixed effect of strychnine and atropine; later several authors [2—4] failed to isolate from this plant either parquine or any other alkaloid. SILVA *et al.* [5] in 1962 were able to isolate solasonine from *C. parqui*. The sapogenins gitogenin and digitogenin were obtained after hydrolysis of the neutral glycosides of both *C. laevigatum* and *C. parqui* [5—7], while the saponin of *C. diurnum* [8, 9] was found identical with tigonin which on mild hydrolysis yields tigogenin and the sugars xylose, glucose and galactose. Tigogenin and yuccagenin were also isolated from the hydrolysate of the saponins prepared from *C. nocturnum* [10].

The present work deals with the study of the alkaloids and saponins of certain *Cestrum* species growing in Egypt *viz. C. aurantiacum* Lindl., *C. diurnum* L. and *C. purpureum* Stand.

Results and discussion

The phytochemical screening of the three *Cestrum* species studies revealed the presence of alkaloids only in *C. purpureum*. Two procedures were applied for the preparation of the alkaloids of *C. purpureum*. In the first method the dry, powdered leaves were extracted with methanol, containing acetic

* Faculty of Pharmacy, Cairo University.
** Deceased on 30.1.1971.

acid to take up the alkamines and saponins, and the extract, after defatting with benzene–ether, was made alkaline with ammonia to give a fraction of alkaloid matter. In the second method the defatted, powdered leaves were extracted with 5% acetic acid and the concentrated extract was treated with ammonia to precipitate the alkamines. The alkaloids, prepared by the two methods, were found by thin-layer chromatography, using different solvent systems, to consist of solasodine and solanidine. The mixture was resolved by fractional crystallization as well as by solvent fractionation procedures.

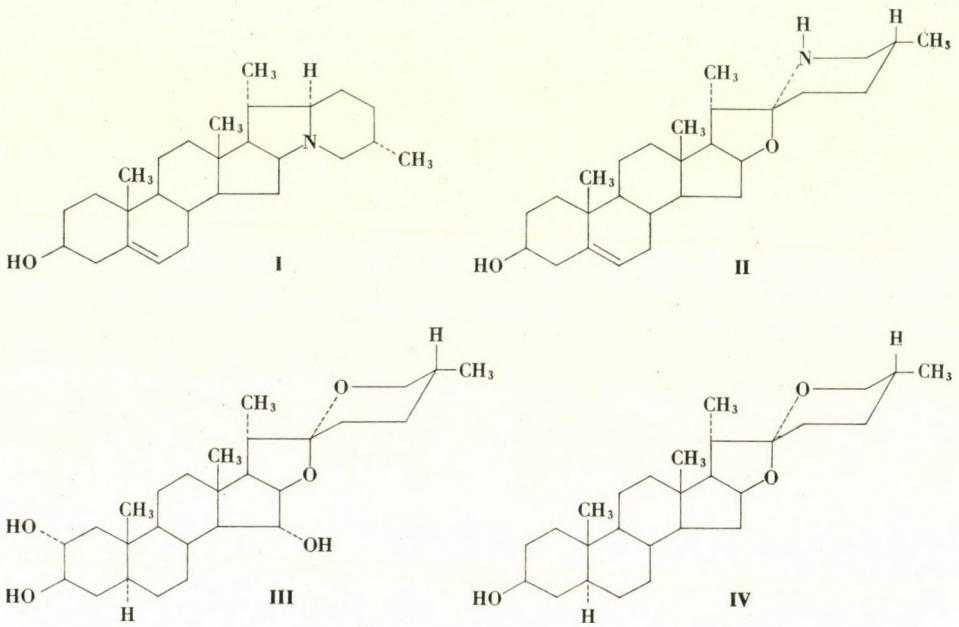

Fig. 1

Fractional crystallization from methanol–water afforded at first solanidine; the mother liquor, after being treated with a few more drops of water, gave solasodine. On the other hand, extraction of the whole alkaloid mixture with acetone and then with methanol resulted in the isolation of solanidine and solasodine, respectively.

TLC investigation of the methanolic extract of *C. purpureum* revealed the presence of only solasodine and solanidine and the absence of any traces of glycoalkaloids.

The identities of the isolated solanidine(**I**) and solasodine(**II**) were established by TLC, preparation of crystalline derivatives, *viz.* hydrochloride, picrate, acetate and O-benzoate, as well as by comparative IR spectra and mixed m.p. with the corresponding authentic alkamines.

The quantitative determination of the alkamines was carried out using both titrimetric and spectrophotometric methods [11]. Non-aqueous potentiometric titration of the isolated alkamines was assumed to provide the amount of solasodine, while the colorimetric method was used to assay the individual alkamine. No marked differences were observed between the results obtained by the two methods. Aluminium oxide for TLC was used as adsorbent in the quantitative assay instead of silica gel which entailed difficulties in the elution of the strongly adsorbed alkamines, even with acetic acid as eluting agent. The results obtained are shown in Table I.

Table I

Alkamine content of C. purpureum

Method	Solanidine	Solasodine	Total
Gravimetry	0.012	0.032	0.044
Titrimetry	—	—	0.054
Colorimetry	0.016	0.039	0.055

The saponins of the species studied were prepared by butanol extraction of the ammoniacal filtrate after isolation of the alkamines, followed by precipitation with cholesterol. The free saponins were obtained by treatment with pyridine, in the manner recommended by WALL *et al.* [12]. Investigation of the saponin content by TLC revealed that both *C. aurantiacum* and *C. purpureum* contain the same saponin, *viz.* digitonin, while *C. diurnum* contains a different saponin, *viz.* tigonin. Study of the acid hydrolysate of the saponins revealed the presence of the expected sugars (*viz.* galactose, glucose and xylose in *C. diurnum*; galactose and glucose in *C. aurantiacum* and *C. purpureum*) as well as the expected sapogenins, *viz.* digitogenin (**III**) and tigogenin (**IV**) (Table II).

Table II

Saponin content, sapogenins and the component sugars of the Cestrum species studied

Species	Saponin %	Steroid sapogenin	Sugars
C. aurantiacum	0.09	Digitogenin	Galactose, glucose
C. diurnum	0.05	Tigogenin	Galactose, glucose, xylose
C. purpureum	0.10	Digitogenin	Galactose, glucose

The identities of the isolated sapogenins were confirmed by TLC m.p., m.m.p., IR and the preparation of the acetate derivatives.

Experimental

Plant material

C. aurantiacum Lindl., *C. diurnum* L. and *C. purpureum* Stand. were collected in April from the Ornamental Plants Farm, Horticulture Dept., Cairo University. The plants were kindly authenticated by Prof. V. TÄCKHOLM, Faculty of Science, Cairo University.

Thin-layer chromatography

Adsorbents:

Silica gel G and alumina.

Solvent systems [13—16]:

For alkaloids: Benzene–methanol (5 : 1)
Ethanol–chloroform–ammonia 1% (2 : 2 : 1)
Acetic acid–ethanol (1 : 3)

For saponins and sapogenins: Benzene–methanol (15 : 2, 5 : 1).

Spraying reagents:

The following reagents were used for alkamines, neutral glycosides and sapogenins: Dragendorff's antimony trichloride [17] (33% solution in chloroform), 10% aqueous sulfuric acid, *p*-anisaldehyde in acetic acid containing sulfuric acid [15, 18] (followed by UV examination), CLARK's [19] 1% paraformaldehyde in 80% phosphoric acid and iodine vapours.

(A) Alkamines

Preparation of the alkamines

Method 1: The dried, powdered leaves of *C. purpureum* (850 g) were macerated with 2 l of 80% methanol containing 5% acetic acid at room temperature for 48 hrs., filtered and the marc re-extracted twice the same solvent (1 l each time). The combined extract, after concentration to about 150 ml, was treated with an equal volume of 10% acetic acid, then allowed to stand overnight and freed from the deposited resinous matter. The solution was defatted by repeated extraction with benzene–ether (1 : 1), heated to about 70 °C, adjusted with an ammonia solution to pH 10, and allowed to stand overnight. The precipitated steroidal alkaloidal bases were separated by centrifugation, refined by repeated dissolution in 5% acetic acid and precipitation with ammonia. This process gave about 0.5 g of crude material.

Method 2: 1 kg of the defatted, powdered *C. purpureum* was macerated with 3 l of 5% acetic acid for 48 hrs. and the marc was re-extracted twice with acetic acid. The concentrated acidic solution was treated with an ammonia solution (pH 10) and left to stand at room temperature for 48 hrs. The precipitated alkaloidal mixture, after separation and purification as mentioned above, gave about 0.63 g of crude material.

Isolation of solanidine and solasodine

1. Fractional crystallization. The purified alkaloidal mixture (0.5 g) was refluxed with successive portions of methanol. The combined methanolic solution was concentrated to about 30 ml, when a crystalline substance began to separate. A few drops of water were added and the solution was left at room temperature for 48 hrs.; the crystalline deposit was removed by filtration (solanidine). The filtrate was treated with another few drops of water till turbidity occurred, left to crystallize at room temperature for 72 hrs. and the crystalline deposit was filtered (solasodine).

2. Solvent fractionation. The crude alkaloidal mixture (0.6 g) was extracted in a Soxhlet apparatus with acetone and the acetone-insoluble residue was exhausted with methanol. The solvent-free acetone extract, after boiling in methanol with activated charcoal and crystallization from methanol–water, gave solanidine while the methanol extract treated in the same manner gave solasodine.

Solanidine

Solanidine, crystallized from methanol–water melted at 219 °C (undepressed by authentic solanidine); $[\alpha]_D$ —27° (in chloroform), λ_{max}, 205 mμ, its IR spectrum was identical with an authentic sample. The prepared hydrochloride melted at 345 °C (undepressed) and the acetate at 204 °C (undepressed).

Solasodine

Solasodine, crystallized from methanol–water melted at 197 °C (undepressed by an authentic sample of solasodine); $[\alpha]_D$ —92° (in benzene), λ_{max} 210 mμ; its IR spectrum was identical with the authentic sample. The following derivatives were prepared: hydrochloride, m.p. 280 °C (Ref. [15]: 277—280 °C), picrate, m.p. 142 °C (undepressed) (Ref. [20]: 144 °C), O-benzoate, m.p. 219 °C (Ref. [21]: 216—217 °C), and acetate, m.p. 195 °C (undepressed).

Quantitative determination of the alkamines

1. Titrimetric determination. 50 mg of the alkaloidal residue, prepared as mentioned above, was dissolved in 20 ml of glacial acetic acid and a few drops of acetic anhydride were added. Titration was carried out with 0.1 *N* perchloric acid in glacial acetic acid and the end-point was detected potentiometrically.

2. Colorimetric determination. A 0.1% methanolic solution of the alkamines was quantitatively applied on the plates coated with alumina. After developing with the solvent, the plates were dried and dipped vertically in a jar containing solid iodine. After the alkamines were stained brown, the corresponding areas were marked and kept overnight at room temperature to remove iodine. The zones with the adsorbed alkamine and areas of the same size from a blank plate were scraped off and transferred to separate, glass-stoppered tubes. To each sample was added 5 ml of 1% H_2SO_4 in ethanol, then 5 ml of conc. H_2SO_4 (added gradually then vigorously shaken), followed after one minute by the addition of 2.5% of 1% formaldehyde solution. After cooling the tubes were centrifuged, the optical density of the supernatant was measured at 570 mμ and the concentration determined from the standard curve of each alkamine.

(B) Saponins

Preparation. The ammoniacal filtrate, remaining after removal of the steroidal alkaloids *(C. purpureum)* was concentrated, sodium chloride was added, followed by conc. HCl to bring the pH between 4.0 and 5.0. The solution was then shaken with an equal volume of *n*-butanol (previously saturated with water). The combined butanol extract was distilled *in vacuum*, the residue was dissolved in methanol, boiled with charcoal, filtered and the filtrate evaporated *in vacuum*. The residue was dissolved in chloroform–90% ethanol. Cholesterol in ethanol was added, and the mixture boiled on a water bath for 15 min and left in a refrigerator for 2 days. The precipitated cholesterol complex was filtered, washed with ethanol, decomposed with pyridine and the saponins were precipitated with ether.

The saponins of the other two species, *viz. C. aurantiacum* and *C. diurnum*, were prepared as follows:

1 kg of the defatted, powdered plant was extracted with 80% ethanol. The ethanol extract was concentrated until alcohol free, and the aqueous solution was then treated as mentioned above.

Hydrolysis. 0.5 g of the saponin, obtained from *C. purpureum*, was dissolved in 2 *N* H_2SO_4 in 50% ethanol (100 ml) and refluxed on a water bath for 2 hrs. The solution was cooled and the precipitate thus obtained was extracted with chloroform. The crude tarry sapogenin was refluxed for 1/2 hr. with a mixture of 400 ml benzene and 200 ml of 5% methanolic KOH. The solution was then cooled and filtered and the residue was washed with hot benzene containing 10% ethanol. The filtrate and washings were combined. Water (10 ml) was added and the aqueous solution was drawn off and re-extracted twice with benzene (100 ml each). The benzene solutions were combined, washed with distilled water, dried over anhydrous sodium sulfate and evaporated to dryness.

Digitogenin

Digitogenin, crystallized from chloroform–methanol, melted at 295—296 °C both alone and when admixed with authentic digitogenin. The digitogenin acetate prepared melted at 188—190 °C (undepressed).

The remaining aqueous layer containing the sugar substances, after extraction of the sapogenin matter, was neutralized with $BaCO_3$ and the solution was investigated for the sugar components by paper chromatography. The chromatogram was obtained with ethyl acetate–pyridine–water (2 : 1 : 2) and the spots were developed by spraying with aniline–oxalic acid reagent [22].

Investigation of the saponins of the other two *Cestrum* species was restricted to comparative chromatographic analysis (Table II).

*

The authors are grateful to Prof. K. R. FELL, Leeds College of Technology, England and Dr. G. WILLUHN, Institut für Pharmakognosie der Phillips Universität, Marburg, Germany, for kindly supplying the authentic samples.

REFERENCES

1. MERCIER *et al.*; cited in Watt, M. J. and Breyer-Brandwijk, G. M.: "The Medicinal and Poisonous Plants of Southern and Eastern Africa", 2nd ed., E. S. Levingstone Ltd., Edinburgh and London (1962)
2. MESSNER, E.: Rev. Med. Vet. Uruguay, **15** (1918)
3. HUG, E.: Ann. Soc. Rur. Argentina **54,** 445 (1919)
4. PEREZ, M., ANDERSEN, H.: Rev. Soc. Med. Vet. Chili **4,** 1 (1953)
5. SILVA, M., MANCINELLI, P., CHEUL, M.: J. Pharm. Sci. **51,** 289 (1962)
6. CANHAM, P. A. S., WARREN, F. L.: J. S. Afr. Chem. Inst. **3, 9** (1950)
7. CANHAM, P. A. S., WARREN, F. L.: J. S. Afr. Chem. Inst. **3,** 63 (1950)
8. CHAKRAVARTI, R. V., DATTA, S., MITRA, M. V.: Bull. Calcutta School Trop. Med. **10,** 123 (1962)
9. CHAKRAVARTI, R. V., DATTA, S., MITRA, M. V.: Bull. Calcutta School Trop. Med. **11,** 20 (1963)
10. CHAKRAVARTI, R. V., DATTA, S., MITRA, M. V.: Bull. Calcutta School Trop. Med. **11,** 56 (1963)
11. CROMWELL, B. T.: in PEACH, K. and TRACEY, M. V.: "Modern Methods of Plant Analysis", Vol. **IV,** Springer-Verlag, Berlin—Göttingen—Heidelberg (1955)
12. WALL, M. E., KRIDER, M. M., ROTHMAN, E. S., EDDY, C. R.: J. Biol. Chem. **198,** 533 (1952)
13. PAUQIN, R.: J. Chromatog. **12,** 57 (1962)
14. BOLL, P. M.: Acta Chem. Scand. **17,** 1852 (1963)
15. FAYEZ, M. B. E., SALEH, A. A.: Phytochemistry **6,** 433 (1967)
16. FAYEZ, M. B. E., SALEH, A. A.: Planta Medica **15,** 430 (1967)
17. NEHER, R.: Steroid Chromatography, 2nd ed., Elsevier Publishing Co., New York (1964)
18. STAHL, E.: Dünnschicht-Chromatographie, Springer-Verlag, Berlin—Heidelberg—New York (1967)
19. CLARK, E. G. C.: Nature **181,** 1152 (1958)
20. BELL, R. C., BRIGGS, L. H., CARROLL, J. J.: J. Chem. Soc. **12,** (1942)
21. BRIGGS, L. H., OSHA, T.: J. Chem. Soc. **1654,** (1952)
22. HARROCKS, R. H., MANNING, G. B.: Lancet **18,** 1042 (1949)

Abdel-Fattah M. RIZK; Pharmaceutical Sciences Laboratory,
National Research Centre, Dokki, Cairo, U.A.R.

M. S. KARAWYA
F. M. HAMMOUDA
Z. F. AHMED
Faculty of Pharmacy, Cairo University

Acta Chimica Academiae Scientiarum Hungaricae, Tomus 72 (3), pp. 323—327 (1972)

CALCULATION OF THE INFRARED CARBONYL STRETCHING FREQUENCIES AND IONIZATION POTENTIALS OF 4-SUBSTITUTED ACETOPHENONES

Z. DINYA

(Institute of Organic Chemistry, L. Kossuth University, Debrecen, Hungary)

Received December 4, 1970

The first ionization potentials of 4-substituted acetophenones were calculated directly, with good accuracy, by means of the simple HMO method.

A linear correlation was found between the measured carbonyl stretching frequencies and the χ HOMO energy-level coefficients, by which a linear equation can be directly given for the approximate calculation of stretching frequencies.

Introduction

In an earlier communication [1] we reported the results of our calculations made for 4-substituted acetophenones by infrared spectroscopy and the Hückel Molecular Orbital (HMO) method. The present paper described the calculation of the expected carbonyl stretching frequencies and ionization potentials of the compounds investigated.

Many communications deal with the theoretical determination of the expected stretching frequencies of carbonyl groups [1, 2a, b, c, d, e, f, g, h, i, j]. In each case, the π bond order of the carbonyl group is determined by some quantum chemical approximation method, and this value is used for the calculation of the force constant and the group frequency, by means of various formulas. However, calculations of this type are rather complicated.

A simpler approach to the problem is possible with the use of the ionization potentials (Ip) of the molecules. A linear correlation was found [3] between the first ionization potentials and C=O stretching frequencies of carbonyl compounds. According to KOOPMANS [4], the first ionization potential of a molecule is the negative values of the energy of the highest occupied molecular orbital (HOMO). This view has been generally accepted in the literature [5a, b, c]. However, it must be noted that this holds precisely for SCF LCAO calculations only [6a, b].

Calculation

The calculations were carried out, after an appropriate choice of the parameters [1] by a computer of ODRA-1013 type, applying the simple HMO method. Ionization potentials were calculated by the method of CHIN *et al.* [8].

Experimental

The infrared spectra of the investigated compounds were recorded in carbon tetrachloride solution ($c = 0.1—0.3$ mole/liter; $d = 0.1—0.5$ mm), using a Zeiss UR-10W spectrophotometer. The accuracy of measurement was ± 2 cm^{-1}.

Results

The experimental and calculated data are presented in Table I.

Table I

4-R substituent	ν (C=O) experimental, cm^{-1} A	Ip* experimental, eV B	χ_{HOMO} C	Ip* calcd., eV D	Ip* calcd., eV E	ν (C=O)** calcd., cm^{-1} F
—NH_2	1675	8.33	0.6191	8.65	9.11	1671
—OH	1680	—	0.7693	9.02	9.24	1675
—CH_3	1688	9.31	0.9938	9.58	9.55	1687
—H	1692	9.53	1.0000	9.60	9.72	1690
—Cl	1692	9.58	1.0000	9.60	9.69	1690
—Br	1693	9.47	0.9958	9.59	9.72	1690
—I	1693	—	1.0031	9.61	9.72	1691
—NO_2	1700	10.16	1.1370	9.94	9.96	1698

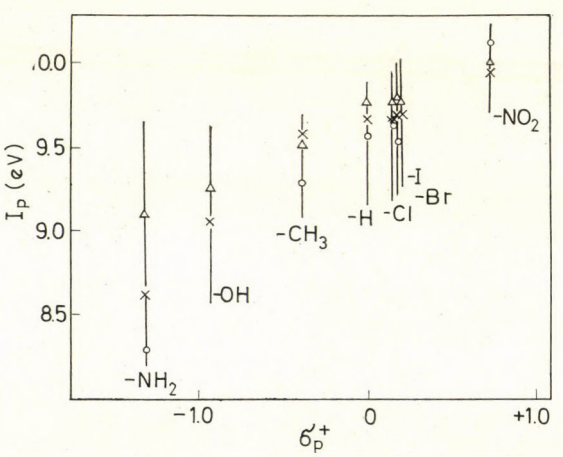

Fig. 1. The first ionization potential as a function of σ_p^+. ○ experimental values [8] (column B); × values calculated from χ_{HOMO}; ▲ values calculated by the Cook equation [3]

* $\pm$ 0.1 eV
** rounded values
*** χ_{HOMO}: coefficient for the energy level of HOMO $E_{HOMO} = \alpha_0 + \chi_{HOMO}\,\beta_0$

Discussion

The data listed in Table I show that the values of the first ionization potential established experimentally (column B) and those calculated by us (column D) are in good agreement (taking into account the nature of the calculation method applied). The scattering is greater in the values of the first ionization potentials (column E) calculated by Cook's [3] equation from the measured carbonyl frequencies. This can be seen in Fig. 1 where the Ip values are plotted against the σ_p^+ values of the substituents [9]. On plotting the measured carbonyl stretching frequencies against the χ_{HOMO} values (column C), the graph shown in Fig. 2 is obtained.

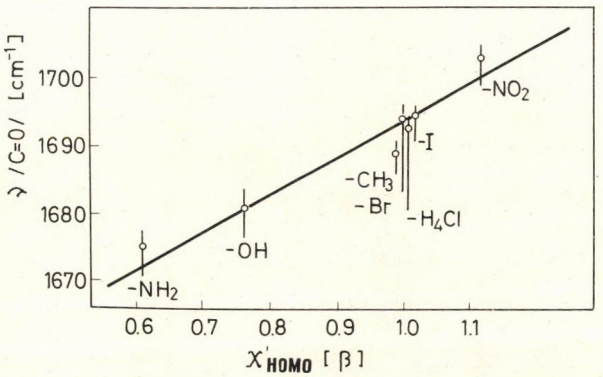

Fig. 2. Dependence of the value $\nu_{(C=O)}$ on χ_{HOMO}

It can be seen that in agreement with the general results reported in the literature [3, 4, 5], a linearly rising straight is obtained. Thus, on the basis of this correlation, a direct formula can be given for the relation between the carbonyl stretching frequency and the χ_{HOMO} energy-level coefficients

$$\nu_{C=O}\ (cm^{-1}) = 1618.0 + 73\ \chi_{HOMO} \pm 3.2.$$

The carbonyl frequencies calculated from this formula (column F) agree well with the experimentally established values (column A).

This is also proved by Fig. 3 where the experimentally established (column A) and calculated (column F) carbonyl frequencies are plotted against the σ_p^+ values of the substituents applied.

It appears from Fig. 3 that the straights plotted on the basis of the measured and calculated values run practically parallel, and their character is identical with the data published in the literature [10].

In general, the equation

$$\nu_{(C=O)}\ (cm^{-1}) = 1615.32 + 73\ \chi_{HOMO} \pm 6$$

can be successfully applied for the simple approximate calculation of the expected carbonyl stretching frequencies of aromatic carbonyl compounds.

For example, in the case of the chalcone (benzalacetophenone):

$\nu_{(C=O)}$ experimental: 1672 cm^{-1}

$\nu_{(C=O)}$ calculated: 1673 cm^{-1}

(Parameters: ho: 2.0 $k_{CO} : \sqrt{2}$)

$k_{C-C} : 0.9$

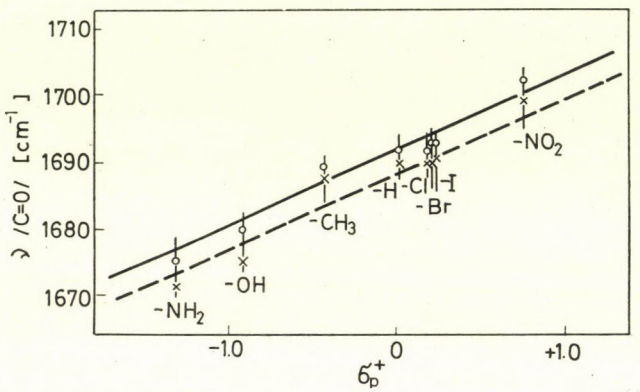

Fig. 3. Dependence of the values of $\nu_{(C=O)}$ on σ_p^+. ○ experimental values; × calculated values

*

The author's thanks are due to the First Department of Natural Sciences of the Hungarian Academy of Sciences for sponsoring the present work, and to the research workers of the Computer Centre of the L. Kossuth University for their assistance in the calculations.

REFERENCES

1. Dinya, Z., Szabó, S.: Acta Chim. Acad. Sci. Hung. (In press)
2. a. Bonino, G. B., Scrocco, E.: Rend. Accad. Naz. Linc. **6,** 421; **8,** 183 (1950)
   b. Scrocco, E., Chiorboli, P.: Rend. Accad. Naz. Linc. **8,** 248 (1950)
   c. Berthier, G., Pullman, B., Pontis, J.: J. Chim. Phys. **41,** 367 (1952)
   d. Josien, M. L., Deschamps, J.: J. Chim. Phys. **52,** 213 (1955)
   e. Baudet, J., Berthier, G., Pullman, B.: J. Chim. Phys. **54,** 282 (1957)
   f. Deschamps, J.: Compt. Rend. **246,** 3661 (1958)
   g. Bratož, S., Besnainou, S.: J. Chim. Phys. **56,** 555 (1959)
   h. Forsen, S.: Spectr. Acta **18,** 595 (1962)
   i. Bratož, S., Besnainou, S.: J. Chem. Phys. **34,** 1142 (1961)
   j. Jensen, H. H.: Acta Chem. Scand. **23,** 3163 (1969)
3. Cook, D.: J. Am. Chem. Soc. **80,** 49 (1958)
4. Koopmans, T.: Physicas Grav. **1,** 104 (1933)
5. a. Streitwieser, A.: Molecular Orbital Theory for Organic Chemists, p. 188. John Wiley and Sons, N. Y., 1961
   b. Peacock, T. E.: Electronic Properties of Aromatic andHeterocyclic Molecules, pp. 26. Acad. Press, N. Y., 1865
   c. Tajima, S., Wasado, N., Tsuchija, T.: Tetrahedron Letters **1970,** 139

6. a. FLURRY, R. L.: Molecular Orbital Theories of Bonding in Organic Molecules, pp. 197. Dekker Inc., N. Y., 1968
b. STREITWIESER, A.: Molecular Orbital Theory for Organic Chemists, pp. 193. John Wiley and Sons, N. Y., 1961
7. HEILBRONNER, E., BOCK, H.: Das HMO-Modell und seine Anwendung, Vol. I. pp. 317. Verlag Chemie, GmbH., Weinheim, 1968
8. CHIN, M. S., HARRISON, A. G.: Org. Mass Spectr. **2**, 1073 (1969)
9. BROWN, H. C., OKAMOTO, Y.: J. Am. Chem. Soc. **80**, 4974 (1958)
10. a. GROSS, R. F., FUGASI, P.: J. Am. Chem. Soc. **71**, 223 (1949)
b. FRIESS, S. L., SOLOWSKY, A. H.: J. Am. Chem. Soc. **73**, 3968, 5000 (1951)
c. FUSON, N., JOSIEN, M. L., SHELTON, E. M.: J. Am. Chem. Soc. **76**, 2526 (1954)
d. BELLAMY, L. J.: J. Chem. Soc. **1955**, 4221
e. TANAKA, J., NAGAKURA, S., KOBAYASHI, M.: J. Chem. Phys. **24**, 311 (1956)
f. JONES, R. N., FORBES, W. F., MUELLER, W. A.: Can. J. Chem. **35**, 505 (1957)
g. JONES, R. N., SPINNER, E.: Can. J. Chem. **36**, 1020 (1958)
h. ROSCETTI, G. P., SUSZ, B. P.: Helv. Chim. Acta **47**, 299 (1964)

Zoltán DINYA; Debrecen 10. Hungary.

Acta Chimica Academiae Scientiarum Hungaricae, Tomus 72 (3), pp. 329—339 (1972)

СИНТЕЗ МОНО- И ДИСУЛЬФОПРОИЗВОДНЫХ ДИФЕНИЛПИКРИЛГИДРАЗИЛА (ДФПГ)

Г. В. ПУТЫРСКАЯ и Ю. СИЛАДИ
(Центральный Исследовательский Институт Химии ВАН, Будапешт)

Поступила 25. I. 1971 г.

Описывается синтез моно- и дисульфопроизводных 1,1-дифенил-2-пикрилгидразила. Синтез осуществлялся ступеньчато: сульфированием асс. дифенилгидразина хлорсульфоновой кислотой, конденсацией полученного сульфопроизводного асс. гидразина с пикрилхлоридом и окислением продукта конденсации перекисью свинца. Варьированием молярного отношения асс. дифенилгидразина и хлорсульфоновой кислоты реакцию можно направлять в сторону получения моно- или ди-производного сульфогидразина. Приводятся ИК спектры соединений и дается их оценка.

Со времени синтеза первого стабильного радикала 1,1-дифенил-2-пикрилгидразила [1] синтезировано большое количество его аналогов с различными заместителями и функциональными группами в фенильных и пикрильном кольцах ([2—5] и др.), исследованы их стабильность и химические свойства в зависимости от типа и количества заместителей, а также их положения в молекулах. Эти свободные радикалы в силу своей природы оказались весьма полезными соединениями для изучения кинетики полимеризационных, биологических и радиационно-химических процессов. Особый интерес представляют водорастворимые стабильные радикалы для изучения радиолиза воды и водных растворов.

Впервые упоминание о существовании водорастворимого аналога ДФПГ с сульфо-группой в орто-положении пикрильного кольца содержится в работе [6], в которой сообщалось о результатах исследования парамагнитных свойств этого соединения, но не содержалось никаких сведений о его синтезе. В одной из наших работ [7] нами описывается синтез другого аналога ДФПГ, а именно п,п'-дисульфо-1,1-дифенил-2-пикрилгидразила, который однако оказался недостаточно устойчивым в водном растворе. Поэтому представлял интерес синтез моно-сульфо-производного ДФПГ и исследование его свойств в надежде на его большую устойчивость в водных растворах.

В основу синтеза моно-сульфо-производного ДФПГ нами взят тот же ход реакций, что и при получении дисульфо-производного [7], т. е. сульфирование асс. дифенилгидразина в сухом нитробензоле хлорсульфоновой кислотой с последующей конденсацией полученного продукта в спирто-водной среде с пикрилхлоридом по нижеследующей схеме:

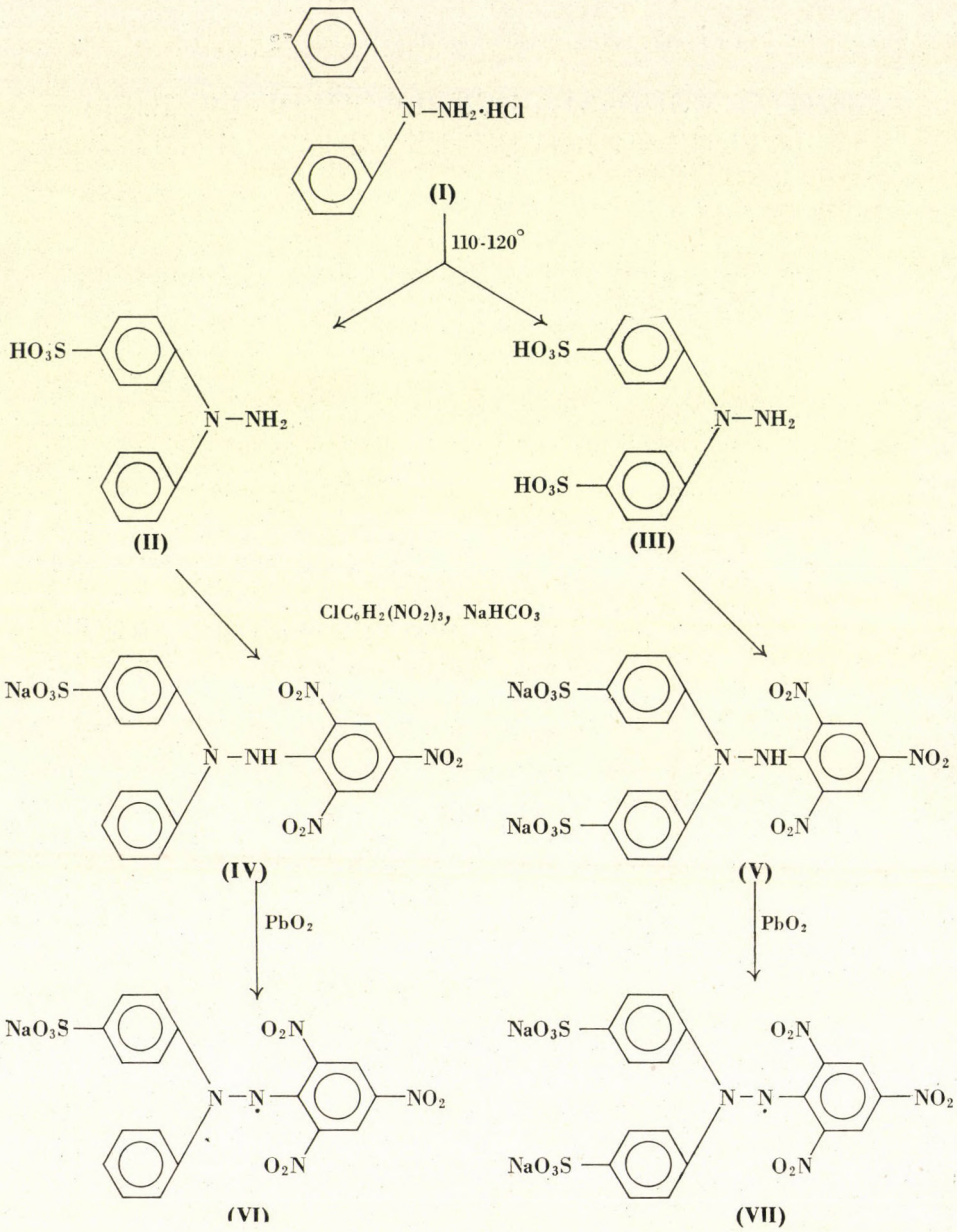

Изменением соотношения дифенилгидразина и хлорсульфоновой кислоты, как показали предварительные опыты, реакцию можно направить в сторону получения или моносульфо-производного (**II**) или дисульфо-производного дифенилгидразина (**III**). Так как в ходе синтезов по сравнению с прописью [7] введены некоторые изменения, в данной статье будут описаны синтезы обоих производных ДФПГ.

Экспериментальная часть

I. Получение п-сульфо-1,1-дифенил-2-пикрилгидразила (VI)

1. Исходные продукты

Необходимый для реакции асс. дифенилгидразин (I) получался восстановлением N-нитрозодифениламина [8] в среде абс. эфира $LiAlH_4$ [9]. Очищенные двух- или трехкратной перекристаллизацией из этилового спирта игольчатые кристаллы серо-зеленого цвета имели температуру разложения 139—142°C. Следует заметить, что успех синтеза всегда зависел от чистоты асс. дифенилгидразина.

Другие исходные вещества, такие, как хлорсульфоновая кислота (Fluka AG. Buchs SG. pract), нитробензол (Fabrika Odczynnikow Chemicznych, puriss) и пикрилхлорид (Laboratory Reagent, the British drug Houses LTD, p.a.) использовались без дополнительной очистки.

2. Сульфирование асс. дифенилгидразина

20 г асс. дифенилгидразина (I) при энергичном перемешивании небольшими порциями добавлялось к раствору 6,5 мл хлорсульфоновой кислоты (мол. соотношение 1 : 1) в 200 мл сухого нитробензола. Реакция начиналась сразу же с выделением пузырьков хлористого водорода и с небольшим разогревом (30—35°). Полученная зеленоватая липкая масса медленно нагревалась до 110—120° при непрерывном перемешивании. По истечении 10—15 минут вся масса превращалась в черный рассыпчатый продукт, который после охлаждения отделялся от реакционной смеси простым фильтрованием, многократно промывался небольшими порциями нитробензола и бензола, а затем высушивался над хлористым кальцием.

Если молекулярное соотношение дифенилгидразина и хлорсульфоновой кислоты бралось в пределах 1 : 1, то продукт (III) образовывался в небольших количествах.

3. Получение п-сульфо-1,1-дифенил-2-пикрилгидразина (IV) (конденсация)

Хорошо высушенный и измельченный сульфогидразин (II) вносился в смесь 400 мл этилового спирта с 70 мл воды и нейтрализовался бикарбонатом натрия, затем очищался от примесей непродолжительным кипячением с активированным углем, фильтровался. К еще теплому раствору добавлялось 8 г бикарбоната натрия и 22 г пикрилхлорида, предварительно растворенного при нагревании в 100 мл этанола. Реакционная смесь выдерживалась при температуре 60—70° в течение примерно 2-х часов до полного прекращения выделения пузырьков двуокиси углерода. При этом смесь окрашивалась в красновато-коричневый цвет. Под пониженным давлением из нее отгонялся избыток растворителя, остаток же высаживался нагретым до 60° изо-амиловым спиртом (около 600 мл). После охлаждения изоамиловый спирт декантировался, смолообразный остаток же экстрагировался 4 раза бензолом и высушивался над хлористым кальцием. Полученный гидразин (IV) очищался от примесей методом распределительной хроматографии на колонках с последующей перекристаллизацией из спирта.

4. Хроматографическая очистка (IV)

Предварительные опыты хроматографии на бумаге показали, что наиболее подходящим для хроматографирования составом является смесь н-бутанола, уксусной кислоты и воды, взятых в объемном отношении 3 : 1 : 1. Значение коэффициента $R_f = 0{,}67$ для моносульфогидразина (IV).

Для распределительной хроматографии пользовались колонкой размером 4,5×50 см, заполненной целлюлозной пудрой марки Schuchardt. Хроматографируемая смесь наносилась из метанолового раствора на небольшое количество целлюлозной пудры, целлюлоза высушивалась и вносилась в колонку. Скорость подачи растворителя поддерживалась 1 мл/мин. Собранные фракции высушивались под вакуумом в тонком слое. Хроматографирование повторялось два-три раза. Отбирались те фракции, которые давали положительную реакцию на свободный радикал при окислении их перекисью свинца (метаноловый раствор окрашивался в лиловый цвет). Для элементарного анализа полученный гидразин (IV) перекристаллизовался из этанола. Результаты анализа указаны в таблице 1.

5. Получение п-сульфо-1,1-дифенил-2-пикрилгидразила (VI) (окисление)

Высушенный после конденсации продукт может быть окислен без дополнительной очистки. Навеску 4 г растворяли в 200 мл метилового спирта, к смеси добавляли 30 г перекиси свинца и встряхивали в течение двух часов до получения лилового окрашивания реакционной смеси. Раствор фильтровался от шламма и испарялся в струе воздуха от растворителя до наступления кристаллизации. Выпавшие мелкие кристаллы отфильтровывались и на фильтре промывались попеременно водой и спиртом до получения промывных вод чистого лилового цвета. Кристаллы, напоминающие по внешнему виду сажу, высушивались над пятиокисью фосфора. Выход их составлял 0,7—1 г. Свободный радикал может быть перекристаллизован из этанола, но может быть использован и без дополнительной очистки. Из сделанной для проверки чистоты продукта бумажной хроматограммы видно, что весь продукт переместился в виде одной полосы без расслоения. Спектроскопические испытания же показали, что даже в перекристаллизованном стабильном радикале содержатся следы исходного гидразина (**IV**). Результаты анализа приведены в таблице 1. Дериватографические исследования по определению кристаллизационной воды были проведены на кафедре Общей и Аналитической Химии Будапештского Политехнического Института Ш. Галом и Т. Мейзелем, за что авторы приносят им свою благодарность.

Опыт показал, что наибольший выход стабильного радикала получался при окислении небольших порций гидразина (**IV**), не превышающих 4—6 г. Окисление можно проводить и из ацетонового раствора. Так как полученный свободный радикал представляет собой гигроскопический продукт, целесообразно хранить его над пятиокисью фосфора. В этих условиях он может сохраняться без изменений годами.

II. Получение п,п'-дисульфо-1,1-дифенил-2-пикрилгидразила (VII)

1. Сульфирование дифенилгидразина

Дисульфогидразин (**III**) получался по тому же рецепту, что и (**II**), но с тем отличием, что отношение хлорсульфоновой кислоты к дифенилгидразину бралось в пределах от 2-х до 4-х. Выход продукта (**III**) получался заниженным по сравнению с получением (**II**) в предыдущем синтезе за счет частичного осмоления продуктов избытком хлорсульфоновой кислоты. Параллельно с дисульфо-производным (**III**) всегда образовывался в небольших количествах и (**II**). Их разделение целесообразно проводить после конденсации.

2. Получение п,п'-дисульфо-1,1-дифенил-2-пикрилгидразина (V) (конденсация)

Полученный после сульфирования продукт (**III**) после сушки и измельчения вносился в раствор 400 мл этанола и 70 мл воды, нейтрализовался примерно 22 г бикарбоната натрия и очищался небольшим количеством активированного угля от примесей. После фильтрования получалась жидкость лилово-розового цвета. К ней при перемешивании добавлялся раствор 24 г пикрилхлорида в 100 мл этанола и 8 г бикарбоната натрия. В дальнейшем ход реакции и обработка продуктов совпадает с получением (**IV**).

Как уже упоминалось выше, при сульфировании одновременно с продуктом (**III**) образуется в небольших количествах и продукт (**II**), который может быть легко отделен от дисульфопроизводного после конденсации. Разделение производится высаждением дисульфопикрилгидразина из метанолового раствора ацетоном, т. к. последнее нерастворимо в ацетоне, а моно-сульфогидразин (**IV**) хорошо в нем растворим.

3. Разделение (IV) и (V)

10 г сухого неочищенного после конденсации продукта при небольшом нагревании растворялось в 50 мл метанола и высаждалось при энергичном перемешивании в 500 мл ацетона. При этом дисульфопикрилгидразиновая фракция (**V**) высаживалась в виде светло-коричневых хлопьев, а гидразин (**IV**) оставался в ацетоновом растворе. Для предотвращения осмоления продукта (**V**) к концу фильтрации к осадку добавлялось небольшое количество н-бутанола, вещество высушивалось над хлористым кальцием, а затем очищалось методом распределительной хроматографии на колонках, который полностью совпадает с методом очистки продукта (**IV**). Значение $R_f = 0{,}20$ для продукта (**V**) было определено в предварительных опытах на бумажной хроматограмме.

Дисульфодифенилпикрилгидразин (**V**) может быть перекристаллизован после хроматографирования из этилового спирта. Результаты элементарного анализа приведены в таблице 1.

4. Получение п,п'-дисульфо-1,1-дифенил-2-пикрилгидразила (VII) (окисление)

4 г очищенного гидразина (**V**) растворялось в 80 мл метанола и окислялось 30-ю граммами перекиси свинца в течение 2-х часов при энергичном перемешивании. Смесь отфильтровывалась через обычный бумажный фильтр, фильтрат обрабатывался двумя путями:

1) быстрым испарением метанола в струе воздуха или азота,

2) частичной отгонкой большей части растворителя и высаждением стабильного радикала сухим бензолом.

Следует заметить, что моно-сульфо-ДФПК оказался более устойчивым в водных растворах, чем дисульфопроизводное. Элементарный анализ соединения (**VII**) указан в таблице 1.

Для подтверждения строения полученных соединений были проведены спектроскопические исследования.

III. Спектроскопические исследования

Изменения в инфракрасных спектрах, которые возникают при переходах от (**IV**) к (**VI**) и от (**V**) к (**VII**), т. е. при окислении сульфированных пикрилгидразинов в свободные радикалы лучше всего могут быть определены при сравнении их с более простыми, но хорошо изученными моделями такими, как пара 1,1-дифенил-2-пикрилгидразин — 1,1-дифенил-2-пикрилгидразил (ДФПГ).

У 1,1-дифенил-2-пикрилгидразина, как это видно из спектра 1, полоса

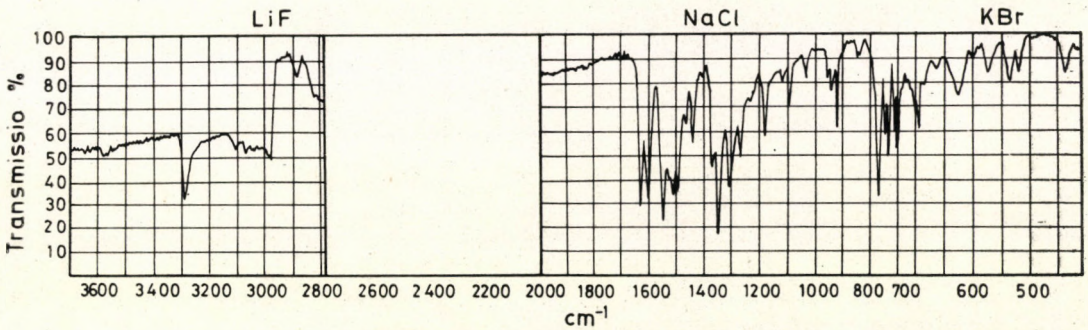

Рис. 1. ИК-спектр 1,1-дифенил-2-пикрилгидразина

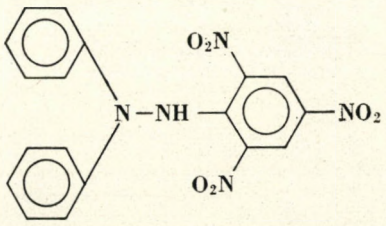

Таблица 1

Результаты элементарного анализа

	Соединение	Вид продукта	Результаты анализа рассчитанные			
			C	H	N	S
1.	п-сульфо-1,1-дифенил-2-пикрилгидразин (**IV**) $C_{18}H_{12}N_5O_9SNa \cdot C_2H_5OH$	коричн. мелкие крист.	44,10	3,32	12,90	5,90
2.	п-сульфо-1,1-дифенил-2-пикрилгидразил (**VI**) $C_{18}H_{11}N_5O_9SNa \cdot 2H_2O$	черные мелкие крист.	40,61	2,84	13,15	6,02
3.	п,п'-дисульфо-1,1-дифенил-2-пикрилгидразин (**V**) $C_{18}H_{11}N_5O_{12}S_2Na_2 \cdot CH_3OH$	желтокоричн. крист.	36,21	2,22	11,07	10,01
4.	п,п'-дисульфо-1,1-дифенил-2-пикрилгидразил (**VII**) $C_{18}H_{10}N_5O_{12}S_2Na_2 \cdot C_2H_5OH$	черные мелкие крист.	38,12	3,22	10,01	9,28

	Соединение	Вид продукта	Результаты анализа полученные			
			C	H	N	S
1.	п-сульфо-1,1-дифенил-2-пикрилгидразин (**IV**) $C_{18}H_{12}N_5SNa \cdot C_2H_5OH$	коричн. мелкие крист.	43,82	3,46	13,19	6,34
2.	п-сульфо-1,1-дифенил-2-пикрилгидразил (**VI**) $C_{18}H_{11}N_5O_9SNa \cdot 2H_2O$	черные мелкие крист.	40,31	3,07	13,05	6,20
3.	п,п'-дисульфо-1,1-дифенил-2-пикрилгидразин (**V**) $C_{18}H_{11}N_5O_{12}S_2Na_2 \cdot CH_3OH$	желтокоричн. крист.	36,48	2,21	11,38	10,28
4.	п,п'-дисульфо-1,1-дифенил-2-пикрилгидразил (**VII**) $C_{18}H_{10}N_5O_{12}S_2Na_2 \cdot C_2H_5OH$	черные мелкие крист.	38,30	2,98	10,22	9,76

валентных колебаний группы NH имеет частоту 3290 $см^{-1}$. Валентные колебания ароматического скелета могут быть приписаны полосам с частотами 1625, 1600, 1495 и 1440 $см^{-1}$ (хотя спектр снят в парафиновом масле, очень тонкий слой — 0,02 мм — все же дает возможность описать также и область, лежащую в районе 1460 $см^{-1}$).

В спектре 2 1,1-дифенил-2-пикрилгидразила недостает полосы валентных колебаний группы NH, и картина области поглощения ароматического скелета по сравнению с соответствующим спектром 1 для 1,1-дифенил-2-пикрилгидразина также изменилась. Так, например, полоса с частотой 1625 $см^{-1}$ на спектре 1 переместилась к 1580 $см^{-1}$ из-за изменения условий сопряжения.

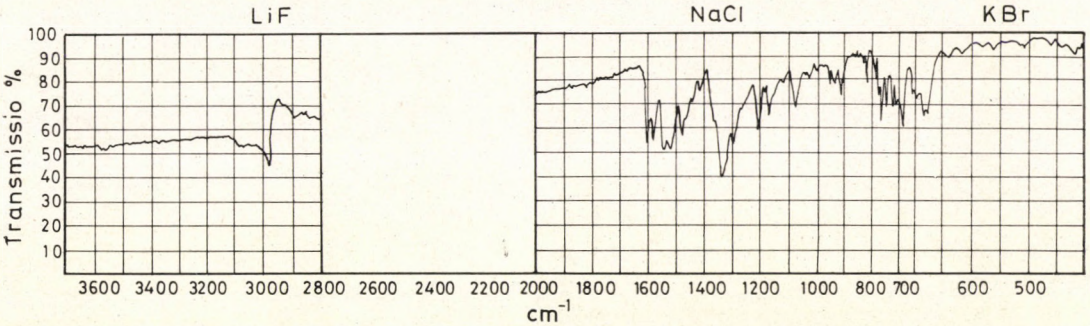

Рис. 2. ИК-спектр 1,1-дифенил-2-пикрилгидразила (ДФПГ)

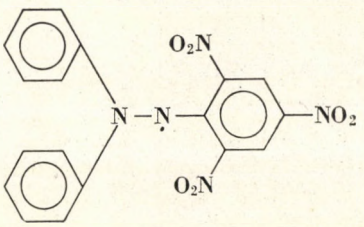

На спектре 3, принимая во внимание спектр 1, полоса валентных колебаний группы NH имеет частоту 3285 $см^{-1}$. Широкая полоса поглощения с минимумом 3440 $см^{-1}$, характерная для колебаний групп OH, а также колебания в области между 3000—2800 $см^{-1}$ (полосы алифатических частот CH) указывают на присутствие в веществе некоторого количества спирта, оставшегося после перекристаллизации. В спектре можно найти полосы валентных колебаний ароматического скелета с частотами 1620, 1600, 1570, 1495 и 1440 $см^{-1}$. Полоса $\nu_{acc.}$ SO_3^-, характерная для группы NaO_3S^-, из-за большого молекулярного веса проявляется слабее, чем обычно, и имеет частоту 1228 $см^{-1}$ (целесообразно интенсивность полосы $\nu_{acc.}$ SO_3^- отнести к интенсивности полосы $\nu_{сим.}$ NO_2, имеющей частоту 1340 $см^{-1}$, т. к. таким образом можно легче заметить возрастание количества сульфо-групп в парах (**IV**) и (**V**), (**VI**) и (**VII**).

В спектре 4 вещества (**VI**) практически отсутствует полоса группы NH. Небольшой изгиб на кривой с частотой 3290 $см^{-1}$ указывает на то, что процесс окисления произошел не на все 100%. Это подтверждается и тем фактом, что полоса с частотой 1620 $см^{-1}$ спектра 3, характерная для валентных колебаний ароматического скелета, хотя и с очень небольшой интенсивностью,

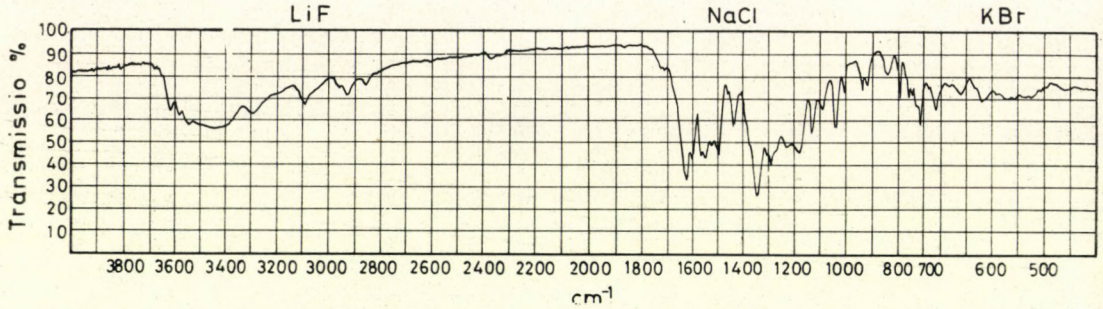

Рис. 3. ИК-спектр п-сульфо-1,1-дифенил-2-пикрилгидразина (**IV**)

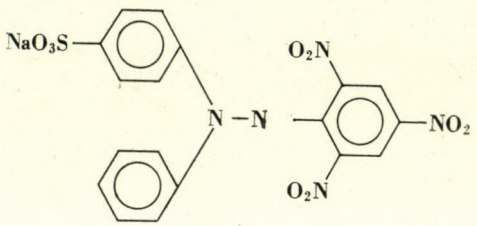

но появляется и здесь. Влияние изменения условий сопряжения при переходе к свободному радикалу появляется и в данном случае: полоса (**IV**) с частотой 1620 $см^{-1}$ перемещается в спектре соединения (**VI**) к 1580 $см^{-1}$. Точно также изменением условий сопряжения объяснимо то обстоятельство, что в спектре (VI) интенсивнее появляется полоса $\nu_{acc.}$ SO_3^- приблизительно у 1215 $см^{-1}$, чем в спектре 3. Следует заметить, что полоса на спектре 4 с минимумом 3450 $см^{-1}$ обязана своим появлением кристаллизационной воде (ν OH).

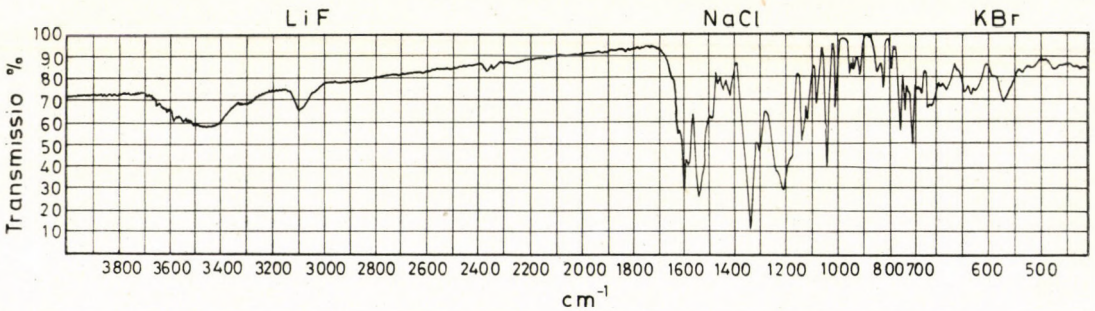

Рис. 4. ИК-спектр п-сульфо-1,1-дифенил-2-пикрилгидразила (**VI**)

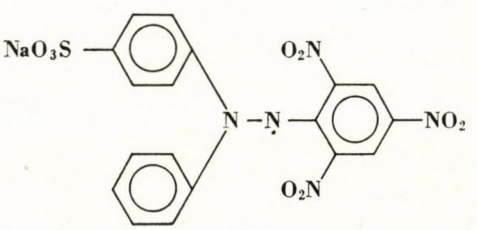

На спектре 5 соединения (**V**) полоса валентных колебаний группы NH имеет частоту 3295 $см^{-1}$, а полосы валентных колебаний ароматического скелета — 1623, 1600, прибл. 1560 (эта полоса появляется в виде небольшого изгиба и сливается с полосой $\nu_{сим.}$ NO_2 с частотой 1545 $см^{-1}$), 1500 и 1440 $см^{-1}$. Полоса с минимумом 3440 $см^{-1}$ относится к валентным колебаниям групп OH, и полосы поглощения в области 3000—2800 $см^{-1}$, характерные для алифатических CH-групп, обязаны своим происхождением спирту, из которого производилась перекристаллизация. Полоса поглощения, характерная для $\nu_{acc.}$ SO_3, с частотой 1200 $см^{-1}$, в этом спектре более интенсивна, чем в спектре вещества (**IV**).

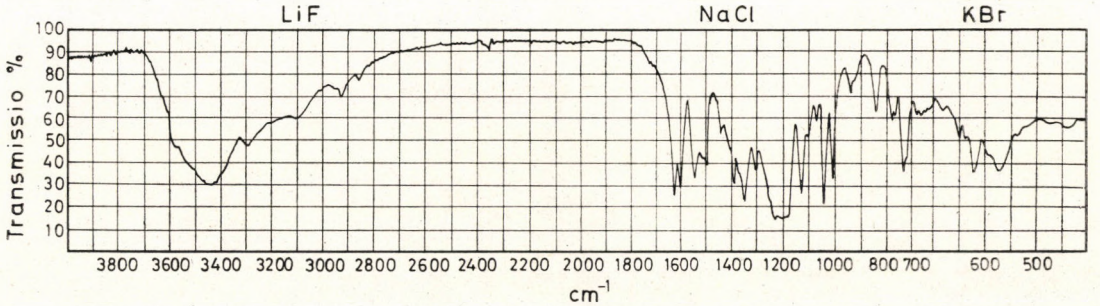

Рис. 5. ИК-спектр п,п'-дисульфо-1,1-дифенил-2-пикрилгидразина (**V**)

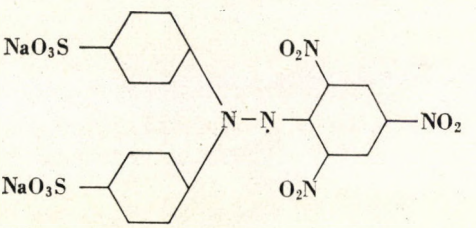

В спектре 6 небольшой изгиб у частоты у 3290 $см^{-1}$ указывает на присутствие следов группы NH. Изменение области полос ароматического скелета по сравнению с предыдущими двумя спектрами, здесь не настолько значительное. Большее количество оставшегося гидразина по сравнению со спектром 4 соответственно проявляется в некотором увеличении интенсивности полосы с частотой 1623 $см^{-1}$. Новая полоса, которая появляется при переходе от гидразина к свободному радикалу, здесь перемещается от 1623 $см^{-1}$ и сливается с полосой ароматического скелета у 1600 $см^{-1}$, вызывая ее уширение. Широкая полоса с минимумом у 3450 $см^{-1}$ — следствие присутствия в молекуле кристаллизационной воды или спирта.

Спектры снимались на инфра-красном спектрометре Цейса типа UR-10 с использованием программы щели 4. В случае 1,1-дифенил-2-пикрилгидразина и соответствующего ему свободного радикала использовалась техника NUJOL (спектры 1 и 2), остальные четыре спектра снимались по KBr технике.

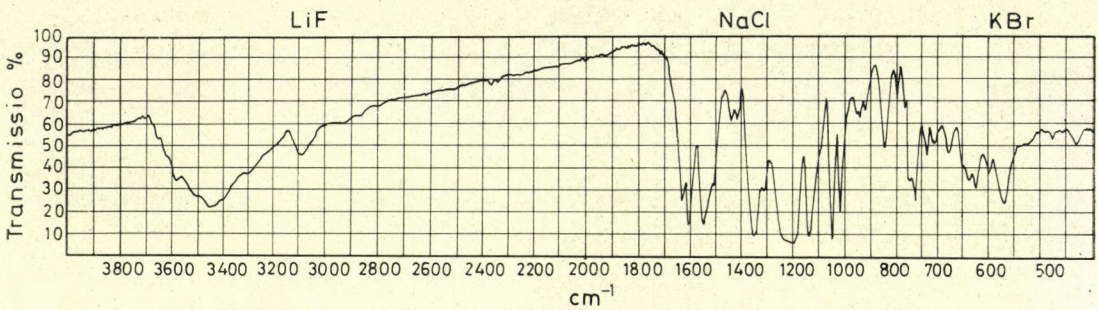

Рис. 6. ИК-спектр п,п'-дисульфо-1,1-дифенил-2-пикрилгидразила (VII)

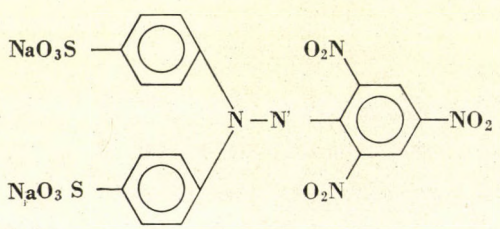

*

В заключение считаем своим приятным долгом выразить благодарность канд. хим. наук Ш. Холли за снятие и оценку ИК спектров.

Summary

The synthesis of mono- and disulfonated derivatives of 1,1-diphenyl-2-picrylhydrazyl (DPPH) is described. The synthesis was carried out step by step: by sulfonation of the asymmetric diphenylhydrazine with chlorosulfonic acid, by condensation of sulfonated derivative formed with picrylchloride and by subsequent oxidation of the condensation product with lead peroxide. Variation of the mole ratio of the asymmetric diphenylhydrazine and chlorosulfonic acid leads to the formation of either the mono- or the disulfonated hydrazine derivative. The IR spectra and their characteristics are described.

ЛИТЕРАТУРА

1. Goldschmidt, S.: Ber., **53**, 44 (1920)
2. Valter, R. J., Cordington, R. S., Amado, F. D., Torrey, J. R.: J. Chem. Phys., **25**, 319 (1956)

3. Tüdős, F., Azori, M.: Magy. Kém. Foly. **64,** 305 (1958)
4. Р. О. Матевосян, И. Я. Постовский и А. К. Чирков: Ж. О. Х., **29,** 858 (1959)
5. М. А. Икрина и Р. О. Матевосян: Ж. О. Х., **32,** 3952 (1962)
6. Jarett, H. S.: J. Chem. Phys., **21,** 761 (1953)
7. Putirszkaja, G. V.: MTA KKKI Közleményei, **8,** 39 (1963)
8. В. В. Некрасов: «Малый практикум по органической химии», Москва, 229 (1950)
9. Poirier, R. H., Benington, F.: J. Am. Chem. Soc., **74,** 3192 (1952)

Г. В. Путырская
Ю. Силади

Центральный Исследовательский Институт Химии Венгерской Академии Наук, Будапешт II, Пуста-сери ут 57—63.

Acta Chimica Academiae Scientiarum Hungaricae, Tomus 72 (3), pp. 341—348 (1972)

INFRARED ABSORPTION BANDS ASSOCIATED WITH THE SULTAM RING

S. H. Doss

(Organisch-Chemisches Institut der Universität Bonn, German Federal Republic)

Received January 25, 1971,
in revised form May 20, 1971

The infrared spectra of various aromatic and aliphatic six-membered cyclic sultams have been studied. The characteristic frequencies and shifts are discussed.

Sultams are cyclic sulfonamides, analogous to the γ-, δ- and ε-lactams, and may contain five- or six-membered rings. They are well crystallized substances; their solubilities in alkalies are due to the formation of metal salts. The "imino group" has an acid nature due to the influence of the negative SO_2 group [1].

Few observations have been reported on the infrared spectra benzene- and toluene-sulfonamides [2, 3].

ADAMS and TJEPKEMA [4] found a strong band at 1180—1160 cm^{-1} as the characteristic frequency for several N,N-disubstituted sulfonamides.

BAXTER *et al.* [5] studied the infrared spectra of 25 sulfonamides and found that all sulfonamides had two strong bands at frequencies near 1160 and 1350 cm^{-1} which are due to the symmetric ν_s and antisymmetric ν_{as} vibrations of the two S—O bonds.

In the present work the spectra of 17 compounds listed in Table I were measured between 4000 and 650 cm^{-1} in KBr pellets and in acetonitrile. The principal results are summarized in Table II (acetonitrile) and Table III (KBr).

Experimental

The IR spectra were obtained with a Perkin-Elmer model 221 spectrophotometer containing a prism grating interchange unit. The spectra were measured in both the solid form using KBr and in solution using acetonitrile, which dissolved most compounds under investigation and was suitable for the region studied.

Results and discussion

When the sulfonamide group cyclizes forming the sultam ring, its two characteristic bands at 1180—1160 cm^{-1} and 1360—1330 cm^{-1}, respectively, are shifted to lower frequencies. These shifts appear clearly when the spectra are run in KBr. The frequency due to the symmetric vibration ν_s is always near 1130 cm^{-1} (± 10 cm^{-1}), while the other frequency which is assigned to the antisymmetric vibrations ν_{as} is variable and depends on the nature of the neighbouring carbon atom, whether aliphatic or aromatic, as will be shown later.

Table I

No.	Compound	Ref.
I	Bis-1,2-(4-chloro-*n*-butane-1-sulfonamide)-ethane (**I**, $n = 2$)	[6]
II	Bis-1,3-(chloro-*n*-butane-1-sulfonamide)-propane (**I**, $n = 3$)	[6]
III	Bis-1,6-(4-chloro-*n*-butane-1-sulfonamide)-hexane (**I**, $n = 6$)	[6]
IV	Bis-1,2-((N)-1,4-*n*-butanesultamyl)-ethane (**II**, $n = 2$)	[6]
V	Bis-1,3-((N)-1,4-*n*-butanesultamyl)-propane (**II**, $n = 3$)	[6]
VI	Bis-1,6-((N)-1,4-*n*-butanesultamyl)-hexane (**II**, $n = 6$)	[6]
VII	*p*-(N-(4-Chloro-*n*-butane-1-sulfonyl)-amino)-N-methyl-N-acetylbenzylamine (**III**)	[7]
VIII	*p*-(1,4-*n*-Butanesultamyl-(N))-N′methyl-N′-acetylbenzylamine (**IV**, R = CO−CH_3)	[7]
IX	*p*-(1,4-*n*-Butanesultamyl-(N))-N′methylbenzylamine (**IV**, R = H)	[7]
X	Bis-(N-sultamyl-(1,4)-benzyl)-methylamine (**V**)	[7]
XI	N-(4-Acetaminophenyl)-butanesultam-(1,4) (**VI**, R = CO−CH_3)	[8]
XII	N-((4-Aminophenyl)-butanesultam-(1,4) (**VI**, R = H)	[8]
XIII	Butanesultam-(1,4) (**VII**)	[9]
XIV	N-Benzylbutanesultam-(1,4) (**VIII**)	[10]
XV	N-(*p*-Tolyl)-butanesultam-(1,4) (**IX**, R = CH_3)	[10]
XVI	N-(*p*-Nitrophenyl)-butanesultam-(1,4) (**IX**, R = NO_2)	[10]
XVII	N,N-*p*-Phenylamine-bis-butanesultam-(1,4), (**X**)	[10]

The results obtained here are in agreement with those published by BAXTER *et al.* [5], if we consider the data given by DIRSCHLER *et al.* [9] for the six-membered unsubstituted sultam ring **XIII** as the ideal case. When the spectra are run in KBr, in addition to the band at the high frequency of ca. 1300 cm^{-1}, we find another band, with nearly the same or somewhat smaller intensity, between 1291 and 1270 cm^{-1} in all sultams (Table III). We suggest that this band is due to the sultam ring.

This assignment should be, however, substantiated, because the two CH_2-deformation frequencies occur at 1433 cm^{-1} and 1440 cm^{-1}; other shifts also occur when the grouping is attached to other atoms such as nitrogen or sulfur [11].

The following considerations and facts enable us to reach our conclusion safely:

(1) The above restriction is not well defined and depends to some extent on the nature of the other attachments to these atoms [11].

(2) These bands are rather far from our band region, *i.e.* 1291—1270 cm^{-1}.

(3) According to the observations of BROWN *et al.* [12], the wagging vibration γ_s CH_2 appears as weak bands near 1240 cm^{-1} and 1300 cm^{-1}.

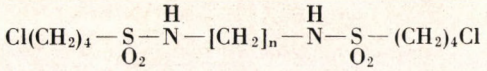

I

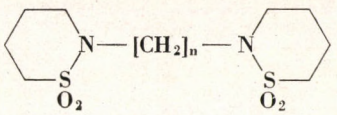

II

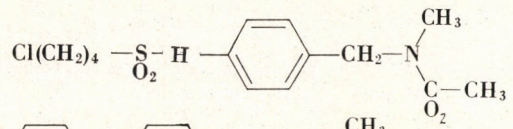

III

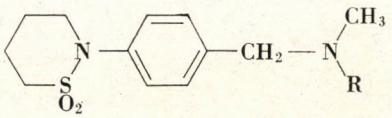

IV

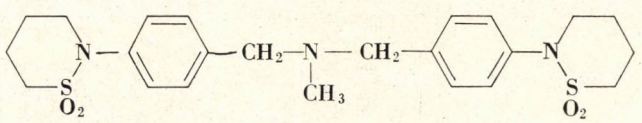

V

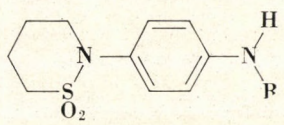

VI

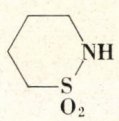

VII

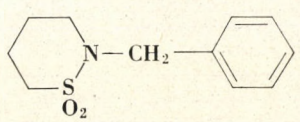

VIII

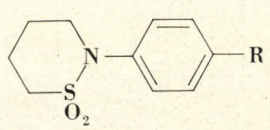

IX

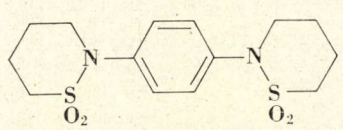

X

Table II

Spectra obtained in acetonitrile

No.	S—O stretching vibration		S—N stretching vibration	Suggested peak for sultam
	Symm.	*Asymm.*		
I	1128 (s)	1295 (s)	870 (w)	—
II	1129 (s)	1298 (s)	910 (m)	—
III	1128 (s)	1295 (s)	910 (m)	—
IV	1128 (s)	1305 (s)	890 (m)	1285 (s)
V	1125 (s)	1294 (s)	890 (w)	1280 (w)
VI	1128 (s)	1305 (w)	875 (s)	1280 (s)
VII	1138 (s)	1325 (m)	897 (w)	—
VIII	1128 (s)	1305 (s)	890 (s)	1288 (s)
IX	1130 (s)	1308 (s)	880 (s)	1288 (s)
X	1125 (s)	1312 (s)	872 (s)	1282 (s)
XI	1129 (s)	1315 (s)	878 (s)	1280 (s)
XII	1129 (s)	1320 (s)	910 (s)	1280 (m)
XIII	1120 (s)	1300 (s)	900 (w)	1278 (s)
XIV	1130 (s)	1308 (s)	905 (s)	1290 (m)
XV	1130 (s)	1320 (s)	875 (s)	1290 (s)
XVI	1140 (s)	1340 (s)	872 (s)	1285 (w)
XVII	1130 (s)	1320 (s)	870 (s)	1180 (s)

m = moderate intensity
s = strong
w = weak

Table III

Spectra obtained in KBr pellets

No.	S—C stretching vibration		S—N stretching vibration	Suggested peak for sultam
	ν_s	ν_{as}		
I	1128 (s)	1292 (s)	870	—
IV	1130	1298 (s)	890	1285
X	1125	1312 (s)	872 (s)	1282 (s)
XI	1130 (s)	1305 (s)	878 (s)	1280 (s)
XII	1130 (s)	1310 (s)	878 (m)	1280 (m)
XIII	1120 (s)	1300 (s)	900 (w)	1275 (s)
XV	1130 (s)	1320 (s)	875 (s)	1290 (s)
XVI	1140 (s)	1340 (s)	870 (s)	1285 (w)
XVII	1131 (s)	1320 (s)	870 (s)	1282 (m)

(4) MARISSON [13] reported that cyclohexane derivatives have bands in the ranges 1005—952 cm^{-1} and 1005—1000 cm^{-1}.

(5) Comparing the spectra of sulfonamides and the corresponding cyclized sulfonamides (sultams) in acetonitrile, we have observed the presence of only two bands in sulfonamides, in the region between 1328 and 1300 cm^{-1}. In the case of sultams, in addition to these bands, 1 to 3 bands more appear in this region (1350—1100 cm^{-1}) (Figs 1 and 2); in all sultam samples a regu-

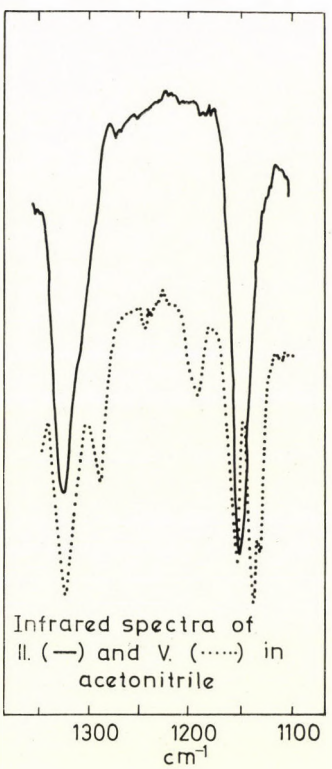

Fig. 1

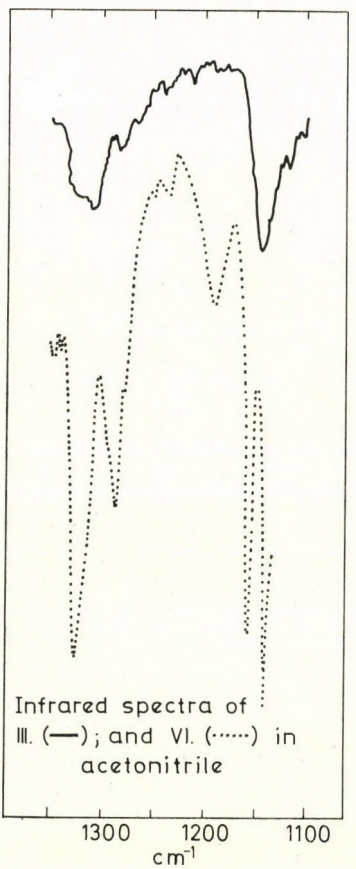

Fig. 2

lar band with medium intensity always appears between 1291 and 1270 cm^{-1}. The other two weak bands occupy the regions 1226—1291 cm^{-1} and 1191—1185 cm^{-1}.

(6) Comparing aromatic and aliphatic sultams, *e.g.*, compounds **XII** and **IV** (Fig. 3), we find that both of them exhibit the same bands in solution (acetonitrile); this proves that the benzene ring plays no part in these spectra.

(7) Comparing the sulfonamide **VII** and the acetylsultam **VIII** with the free aminosultam **IX** (Fig. 4), we find the same bands in the spectra of the sultam and acetylsultam, in addition to the two characteristic bands of sulfonamide. This proves that these bands are not due to the acetyl group.

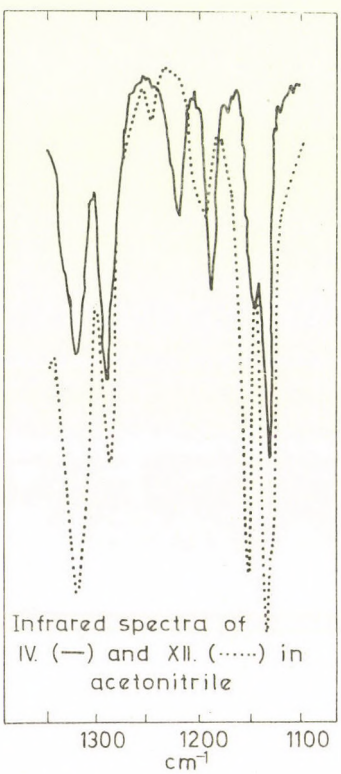

Fig. 3

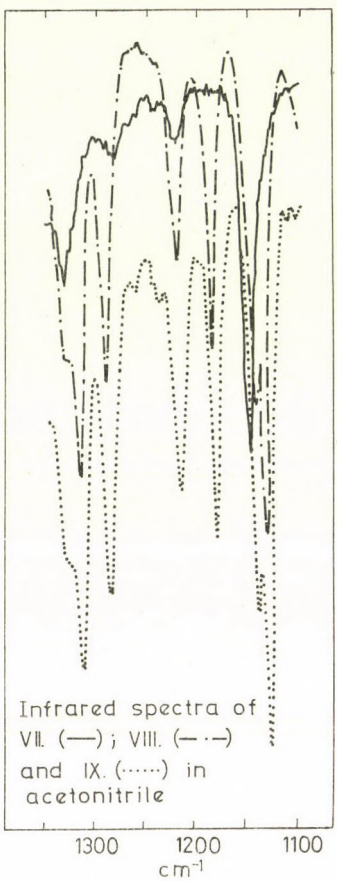

Fig. 4

(8) Comparing the bis-sultam like compound **X** with the monosultam **XV**, we observe the same bands (Fig. 5); this adds further evidence to our observation that the band at 1291—1270 cm^{-1} is unique and characteristic of the sultam ring. The band of higher frequency (ca. 1300 cm^{-1}) shows a slight increase on aromatic substitution (Fig. 6) rather than when aliphatic groups are introduced (Fig. 7), as far as can be judged from the compounds studied (Table III) and from the results of BAXTER *et al.* [5].

Regarding the S—N bond, ANGUS *et al.* [3] reported that the characteristic band lies between 1100—1070 cm^{-1} as shown by his Raman spectral study of five compounds containing S—N linkage. We believe that this band

is not characteristic for the S—N bond because (a) monosubstituted benzene rings absorb weakly in this region [14], (b) the observations of HOFFMAN *et al.* [15] are in contradiction with this data, finally, (c) this band does not appear regularly in our samples.

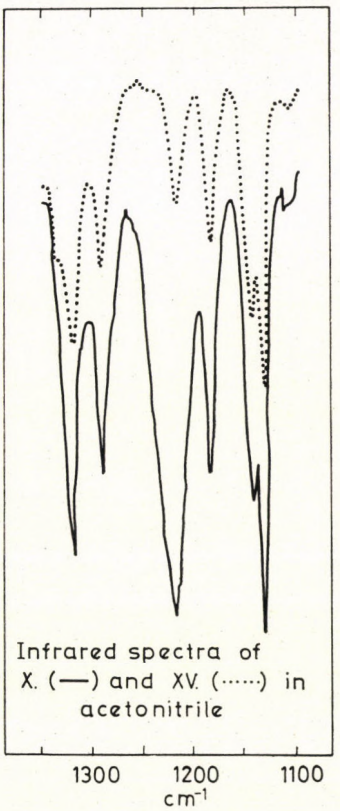

Fig. 5

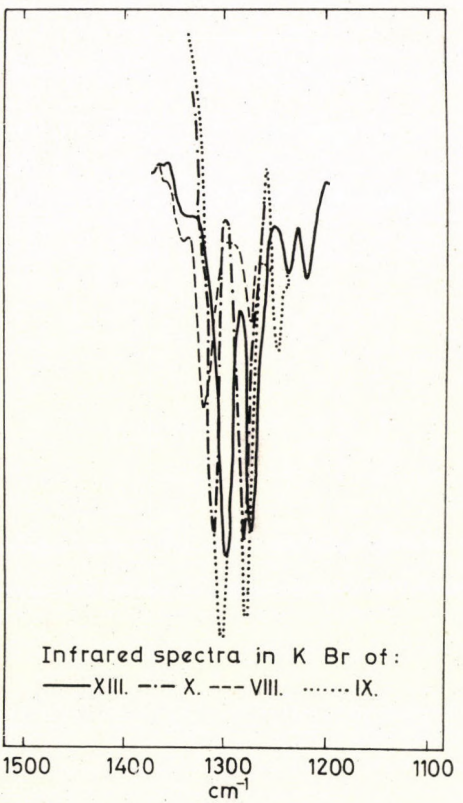

Fig. 6

MASCHKA *et al.* [16] found νS—N lines in the region between 900 and 800 cm^{-1}.

KATRITZKY *et al.* [17] assign the νS—N stretching vibration in several sulfonamide derivatives to a band with medium intensity in the region 912—866 cm^{-1}.

HADZI [18] reported that in N-methyl-*p*-tolylsulfonamides the νS—N stretching frequency band appears at 839 cm^{-1}.

The results of the present study agree with those reported by KATRITZKY *et al.* [17] as the νS—N band is found between 910 and 870 cm^{-1}.

It can be concluded that the band between 1291—1270 cm^{-1} is probably the characteristic band of the six-membered sultame ring, and the νS—N band lies between 910 and 870 cm^{-1}.

*

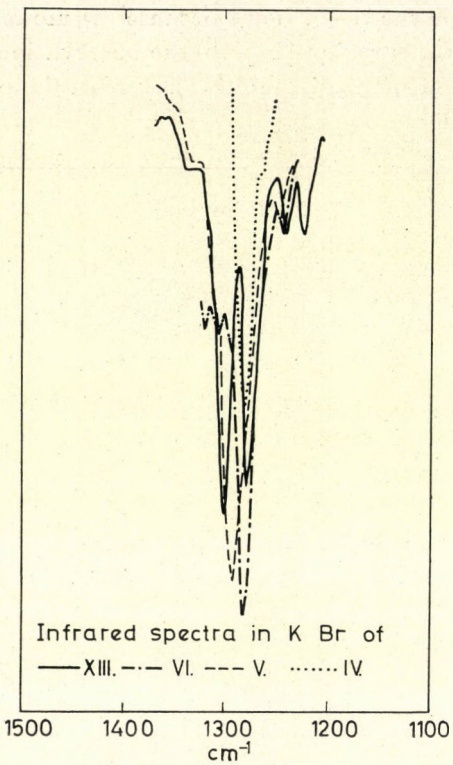

Fig. 7

The author's thanks are due to the directors of the Alexander von Humboldt Stiftung for a scholarship award, to Prof. Dr. B. HELFERICH for his kind encouragement and for a gift of samples **XIV**—**XVII**, and to Prof. Dr. G. SNATZKE for reading the manuscript and very helpful discussion.

REFERENCES

1. MUSTAFA, A.: Chem. Rev. **54,** 195 (1954)
2. SCHREIBER, K. C.: Anal. Chem. **21,** 1168 (1949)
3. ANGUS, W. R., LECKIE, A. H., WILLIAMS, T. I.: Trans. Faraday Soc. **34,** 793 (1938)
4. ADAMS, R., TJEPKEMA, J. J.: J. Am. Chem. Soc. **70,** 4202 (1948)
5. BAXTER, J. N., CYMERMAN-CRAIG, J., WILLIS, J. B.: J. Chem. Soc. 669 (1955)
6. HELFERICH, B., BETTIN, L., DOSS, S. H.: Ann. **741,** 139 (1970)
7. HELFERICH, B., DOSS, S. H.: Ann. **747,** 107 (1971)
8. HELFERICH, B., KLEB, K. G.: Ann. **635,** 91 (1960)
9. DIRSCHERL, W., WEINGARTEN, F. W.: Ann. **588,** 200 (1954)
10. HELFERICH, B., DHEIN, R., GEIST, K., JUNGER, H., WIEHLE, D.: Ann. **646,** 32 (1961)
11. BELLAMY, L. J.: Infrared Spectra of Complex Molecules, 2nd ed. p. 22. Methuen et Co. Ltd., London (1966)
12. BROWN, J. K., SHEPPARD, N., SIMPSON, D. M.: Discuss. Faraday Soc. **9,** 261 (1950)
13. MARISSON, L. W.: J. Chem. Soc. **1951,** 1614.
14. COLTHRUP, N. B.: J. Opt. Soc. Amer. **40,** 397 (1950)
15. HOFFMAN, H. J., ANDRESS, K. R.: Naturwiss. **4,** 94 (1954)
16. MASCHKA, A., AUST, H.: Monatsh. **85,** 891 (1954)
17. KATRITZKY, A. R., JONES, R. A.: J. Chem. Soc. **1960,** 4497
18. HADZI, D.: J. Chem. Soc. **1957,** 847.

S. H. Doss; 53 Bonn, Meckenheimer Allee 168, DBR.

Acta Chimica Academiae Scientiarum Hungaricae, Tomus 72 (3), pp. 349—353 (1972)

ALKALINE CLEAVAGE OF SOME (1-PHENYLSULFONYL-2-PYRAZOLIN-5-YLMETHYL) KETONES

(SHORT COMMUNICATION)

M. LEMPERT-SRÉTER and K. LEMPERT

(Department of Organic Chemistry, L. Eötvös University, and Department of Organic Chemistry, Technical University, Budapest)

Received July 27, 1971

In connection with the synthesis of heteroaromatic ammonioamidates of type **2**, starting with pyrylium salts of type **1** and substituted hydrazines, there arose recently some interest in the chemistry of (2-pyrazolin-5-ylmethyl) ketones (**3**, X = HN, RN, $PhSO_2N$), the alternative products of the above reactions, as well as of the related 2-isoxazolines (e.g., **4**) [1—4].

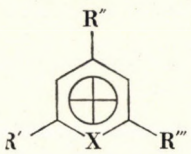

1: X = O

2: X = N—$\ddot{N}^{\ominus}$—R

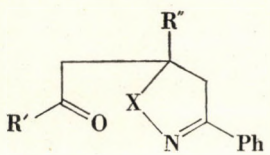

3a: R′ = R″ = Ph; X = $PhSO_2N$

b: R′ = Ph; R″ = H; X = $PhSO_2N$

c: R′ = Me; R″ = Ph; X = $PhSO_2N$

4: R′ = R″ = Ph; X = O

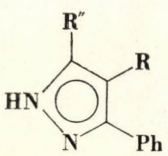

5a: R = H; R″ = Ph

b: R = H; R″ = $BzCH_2$

c: R = H; R″ = COOH

d: R = Ph; R″ = $BzCH_2$

e: R = Ph; R″ = H

f: R = $BzCH_2$; R″ = Ph

Having recently studied the cleavage of the (1-phenylsulfonyl-2-pyrazolin-5-ylmethyl) ketones **3a**—**c** under acidic conditions [4], we have now investigated the products of their alkaline cleavage, emphasis being laid prima-

Table I

Melting points, elemental compositions and spectra of some pyrazoles and pyridazines

Compound	M.p. (Recryst.)	Formula	IR (KBr)	NMR	UV (EtOH)*
A = 5b	153—4 °C (EtOH)	$C_{17}H_{14}N_2O$	νNH 3330, νC=O 1665 cm^{-1}	DMSO-d_6: **NH** 12.75 δ (b), Ph 500—420 Hz (10 H), 4—**H** 6.58δ, $\geqslant$C—CH_2—CO 4.43 δ (s)	~200 (~4.7), 249 (4.47), ~314 (2.46) sh.
D = 5f	177—8 °C (MeOH)	$C_{23}H_{18}N_2O$	νNH 3400—2800, local maximum at 3190, νC=O 1688 cm^{-1}	$CDCl_3$: **NH** 8.6 δ (b), Ph 490—430 Hz. (m, 15 H), $\geqslant$C—CH_2—CO 4.3 δ (s)	202 (4.76), 243 (4.56), ~310 (2.15) sh.
3,5-Diphenyl-pyrazole **(5a)** [10]					205 (4.56), 254 (4.50), ~310 (1.9) sh.
3(5),4-Diphenyl-pyrazole **(5e)** [12]					204 (4.57), 228 (4.28), 254 (4.06)
5d	188—9 °C (EtOH)	$C_{23}H_{18}N_2O$	νNH 3250 (b), νC=O 1695 cm^{-1}	DMSO—d_6: Ph 490—415 Hz (15 H), $\geqslant$C—CH_2—CO 4.37 δ (s)	201 (4.78), 242 (4.41), 320 (2.62) sh.
E = 7d	141—3 °C (EtOH)	$C_{23}H_{16}N_2O$	νC=O 1665 cm^{-1}; *no* NH band	$CDCl_3$: Ar**H** 500—425 Hz; *no* other signals	~200 (~4.75), 263 (4.53), ~330 (~3.0) sh.
F = 7e	140—2 °C (MeOH)	$C_{23}H_{18}N_2O$	νOH 3400—3100 cm^{-1}; *no* C=O band	$CDCl_3$: Ar**H** 500—405 Hz (m, 16 H), ArAr'C**H**OH 6.05 δ (s), OH ~ 5.1 δ (b)	~200 (~4.7), 255 (4.43), ~326 (~2.75) sh.
7a [15]					~200 (~4.75), 259 (4.48), ~320 (~2.9) sh.
7b [14]					202 (4.70), 266 (4.40), 330 (2.7) sh.
7c	203—4 °C lit.[16] 200 °C				~200 (~4.65), 271 (4.43)

* The UV spectra have been published in full in Ref. [17].

rily on the structure elucidation of the cleavage products of **3a**. While only a single compound (**A** and **B**, respectively) could be isolated upon alkaline cleavage of both **3b** and **3c**, at least four products (**C**—**F**), separable by chromatography, were formed upon similar treatment of **3a**.* **

A, which was obtained in 53% yield, could be identified with 2-[5(3)--phenyl-3(5)-pyrazolyl]-acetophenone (**5b**) (1) by its elemental composition and spectra, (2) by oxidation ($KMnO_4$ in aqueous t-butanol) to the known [5] 5(3)-phenyl-3(5)-pyrazolecarboxylic acid (**5c**), and (3) by synthesis from 1,5--diphenyl-1,3,5-pentanetrione [6] and hydrazine hydrate. Formation of **5b** may possibly be explained by assuming base-induced concerted or stepwise elimination of benzenesulfinic acid from **3b** to yield the 3*H*-pyrazole **6b** which subsequently isomerizes into **5b**, the course of the elimination step being determined by the better leaving group properties of the benzenesulfinate as compared with the acetophenone enolate anion.***

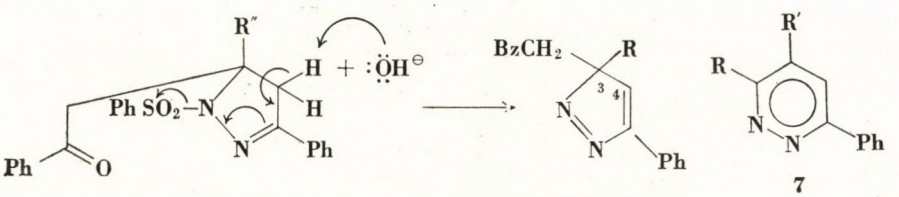

7

3a: R″ = Ph
3b: R″ = H

6a: R″ = Ph
6b: R″ = H

a: R = H; R′ = Ph
b: R = Ph; R′ = $PhCH_2$
c: R = Ph; R′ = Bz
d: R = Bz; R′ = Ph
e: R = PhCHOH; R′ = Ph

B — m.p. 72—3 °C (ligroin), $C_{18}H_{15}N$, 40—50% yield — was found to be identical (mixed m.p., IR spectra) with an authentic sample of 2-methyl-4,6--diphenylpyridine [8], and **C** — m.p. 138—140 °C (MeOH), $C_{23}H_{17}N$, 32% yield — could similarly be identified with 2,4,6-triphenylpyridine [9].

The close resemblance of the UV spectra of **D** (obtained in 11% yield), of **A** and of 3,5-diphenylpyrazole (**5a**) [10], as well as other properties of **D** suggested the structure of a 2-(diphenylpyrazolyl)-acetophenone for **D**, a possible mode of its formation involving the intermediacy of **6a** which could yield **D** by a subsequent van Alphen type rearrangement [11]. Since, so far, only aryl groups were found to migrate in the course of van Alphen rearrange-

* For the elemental compositions and the physical properties of compounds **A**—**F** as well as of some reference substances, see Table I.

** All new compounds described in the present communication gave correct microanalyses.

*** Similar reactions, yielding 5-arenesulfonamido-1-phenylpyrazolines and alkali arenesulfinates, were observed by H. Dorn *et al.* [7] when treating 3-arenesulfonamido-1-arylsulfonyl-2-phenyl-3-pyrazolines with alkalies.

ments (suffering thereby intramolecular electrophilic substitution (*cf.* [11c]), **D** was originally thought to be identical with 2-[4,5(3)-diphenyl-3(5)-pyrazolyl]-acetophenone (**5d**). The dissimilarity of the UV spectra of **D** and of 3(5),4-diphenylpyrazole (**5e**) [12] casted, however, doubts on the correctness of the above structure assignment, and an authentic sample of **5d**, prepared from 1,2,5-triphenyl-1,3,5-pentanetrione [13] with hydrazine hydrate, proved to be different from **D**. Thus, **D** had and, indeed, was shown to be identical with 2-(3,5-diphenyl-4-pyrazolyl)-acetophenone (**5f**), an authentic sample of which was prepared by reacting 2-benzoyl-1,4-diphenyl-1,4-butanedione [14] with hydrazine hydrate. If, then, **D** = **5f** is in fact formed through **6a**, the rearrangement step constitutes the first example of a novel type of the van Alphen rearrangement in which a non-aromatic group migrates in preference to an aryl group. Since van Alphen rearrangements of 3*H*-pyrazoles *un*substituted in position 4 (the so-called A type rearrangements [11c]) were hitherto induced thermally or by acid catalysis while in our case the medium was alkaline, the reversal of the usual order of the migratory aptitudes may easily be understood: the acidic methylene group of **6a** is apparently ionized, and, as a consequence, its ability of being attacked electrophilically becomes enhanced to such an extent that attack of the neighbouring carbon atom (C—4) occurs at this site rather than at the phenyl group.

The close resemblance of the UV spectra of **E** and **F**, which were formed in 5 and 24% yield, respectively, suggested closely related structures for these two compounds; this was confirmed by $LiAlH_4$ reduction (anhydrous THF) of **E** to **F**, as well as by $KMnO_4$ oxidation (aqueous t-butanol) of **F** to **E**. Moreover, the similarity of the UV spectra of **E** and **F**, on the one hand, and of 3,5-diphenylpyridazine (**7a**) [15] and 4-benzyl-3,6-diphenylpyridazine [14] (**7b**), on the other, as well as the IR and NMR spectra of **E** and **F** suggested the structure of a diphenylpyridazinyl phenyl ketone, *viz.* either **7c** or **7d** (their carbon skeletons being identical with those of **D** = **5f** and **3a**, respectively) for **E**, and that of the corresponding alcohol for **F**. Since **7c**, obtained by chromic acid oxidation of **7b*** was clearly different from **E**, the correct structures of **E** and therefore of **F** are **7d** and **7e**, respectively.**

REFERENCES

1. BALABAN, A. T.: Tetrahedron **26,** 739 (1970)
2. BALABAN, A. T.: Tetrahedron **24,** 5095 (1968)
3. KUMLER, P. L., PEDERSON, C. L., BUCHARDT, O.: Acta Chem. Scand. **22,** 2719 (1968)
4. LEMPERT-SRÉTER, M., LEMPERT, K.: Acta Chim. Acad. Sci. Hung. **65,** 443 (1970)
5. SJOLLEMA, B.: Liebigs Ann. Chem. **279,** 251 (1894)
6. MILES, M. L., HARRIS, TH. M., HAUSER, CH. R.: J. Org. Chem. **30,** 1007 (1965)
7. DORN, H., HILGETAG, G., ZUBEK, A.: Chem. Ber. **98,** 3357 (1965)

* For another synthesis of **7c**, see [16].

** *Added in proof:* Corroboration of structure **7d** assigned to **E** was obtained by cleavage of **E** by the potassium t-butoxide—H_2O—1,2-dimethoxyethane reagent (*cf.* [18]) to **7a**.

8. GASTALDI, C.: Gazz. chim. ital. **52, I,**, 169 (1922)
9. WISLICENUS, J., NEWMANN, F. H.: Liebigs Ann. Chem. **302,** 236 (1898)
10. KNORR, L., DUDEN, P.: Ber. **26,** 111 (1893)
11. (a) VAN ALPHEN, J.: Rec. trav. chim. Pays-Bas **62,** 485, 491 (1943)
(b) HÜTTEL, R., RIEDL, J., MARTIN, H., FRANKE, K.: Chem. Ber. **93,** 1425 (1960)
(c) HÜTTEL, R., FRANKE, K., MARTIN, H., RIEDL, J.: Chem. Ber. **93,** 1433 (1960)
12. WISLICENUS, W., RUTHING, A.: Liebigs Ann. Chem. **379,** 229 (1911)
13. STAVAUX, M., LOZAC'H, N.: Bull. soc. chim. France **1967,** 2082
14. BAILEY, PH. S. *et al.*: J. Org. Chem. **21,** 297 (1956)
15. WASSERMANN, H. H., BROUS, J. B.: J. Org. Chem. **19,** 515 (1954)
16. SPRIO, V., MADONIA, P.: Ann. Chim. [Rome] **50,** 1827 (1960)
17. LÁNG, L., (Ed.): Absorption Spectra in the Ultraviolet and Visible Regions, Vol. XVI, Publishing House of the Hungarian Academy of Sciences, Budapest, 1971.
18. DAVIES, D. G., DERENBERG, M., HODGE, P.: J. Chem. Soc. (C) **1971,** 455

Magda LEMPERT-SRÉTER, Budapest VIII., Múzeum krt. 4/B
Károly LEMPERT, Budapest XI., Gellért tér 4.

Acta Chimica Academiae Scientiarum Hungaricae, Tomus 72 (3), pp. 355–356 (1972)

ALKALOIDS FROM VINCA MAJOR L. (APOCYNACEAE)

(±)-VINCADIFFORMINE

(PRELIMINARY COMMUNICATION)

B. ZSADON, GY. ÁRVAY and P. TÉTÉNYI*

*(Department of Chemical Technology, L. Eötvös University, Budapest and *Research Institute for Medicinal Plants, Budapest)*

Received September 3, 1971

In the course of studies concerning the *Aspidosperma* alkaloids, recently we isolated racemic vincadifformine (I) [1, 2] from the alkaloid mixture obtained by extraction of *Vinca major* sprouts. So far 24 alkaloids have been isolated from or detected in this plant [3]. All these are indole alkaloids, but do not include either vincadifformine or other compounds belonging to the group of *Aspidosperma* alkaloids.

Racemic vincadifformine has been isolated hitherto from *Vinca difformis* [1], *Rhazya stricta* [4], *Vinca minor* [5] and *Vallesia dichotoma* [6]. From the first two plants (+)-vincadifformine [4], while from the third one (−)-vincadifformine [7], too, could be isolated.

Extraction with methanol of air-dry sprouts (2 kg) of *Vinca major* gave 18 g of a crude alkaloid mixture. It was fractionated by partitioning between dilute aqueous citric acid and benzene, and the benzene phase containing the weak bases (1.8 g) was chromatographed on a column of aluminium oxide with a 1 : 1 (vol) mixture of benzene and heptane. The eluate contained one alkaloid only and, according to thin-layer chromatography, it was identical with vincadifformine.

Evaporation of this eluate gave 130 mg of colourless substance, which on crystallization from ethanol yielded 45 mg crystalline, optically inactive product, identical in all respects with (±)-vincadifformine (I). M. p. 124°, UV spectrum λ_{max} 226, 300 and 328 nm. No m. p. depression was observed with an authentic sample.

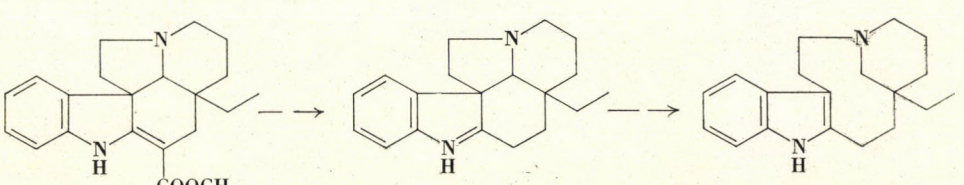

(I) (II) (III)

In order to obtain further evidence concerning the identity of the crystalline product, it was saponified and decarboxylated in a known manner

[2, 8, 9], and the resulting (±)-1,2-dehydroaspidospermidine (**II**) was reduced with sodium borohydride in hot ethanol to give (±)-quebrachamine (**III**).

The experiments were carried out with botanically identified *Vinca major* plants of New Zealand origin grown in the Research Institute for Medicinal Plants, Budapest, and collected in September 1970.

REFERENCES

1. Gosset, J., Le Men, J., Janot, M. M.: Ann. Pharm. Fr. **20,** 448 (1962)
2. Djerassi, C., Budzikiewicz, H., Wilson, J. M., Gosset, J., Le Men, J., Janot, M. M.: Tetrahedron Letters 235 (1962)
3. Hesse, M.: Indolalkaloide in Tabellen. Springer 1964, Ergänzungswerk 1968
4. Smith, G. F., Wahid, M. A.: J. Chem. Soc. 4002 (1963)
5. Mokry, J., Kompis, I., Dubravková, L., Sefcovic, P.: Experientia **20,** 311 (1963)
6. Walser, A., Djerassi, C.: Helv. Chim. Acta **48,** 391 (1965)
7. Plat, M., Le Men, J., Janot, M. M., Budzikiewicz, H., Wilson, J. M., Durham, L. J., Djerassi, C.: Bull. Soc. Chim. France 2237 (1962)
8. Smith, G. F., Wrobel, J. T.: J. Chem. Soc. 793 (1960)
9. Zsadon, B., Otta, K.: Acta Chim. Acad. Sci. Hung. **69,** 87 (1971)

Béla Zsadon
György Árvay } Budapest VIII., Múzeum krt. 6—8.
Péter Tétényi; Budapest XII., Dániel út 40.

RECENSIONES

Topics in Current Chemistry; Volume 18

R. C. BINGHAM and P. v. R. SCHLEYER: Chemistry of Adamantanes, 102 pages

Springer-Verlag, Berlin—Heidelberg—New York, 1971

The new volume of this journal deals with a well defined topic of organic chemistry, namely the chemistry of adamantane and related polycyclic hydrocarbons. This special field of chemistry has rapidly developed since 1956, when the rearrangement of tetrahydrocyclopentadiene to adamantane was discovered by P. v. R. SCHLEYER. The popularity of the chemistry of "cage-like" hydrocarbons has not been due to any unique properties associated with the cage structures of the molecules, as these systems are typically hydrocarbon in nature. The usefulness of these compounds lies in their conformational rigidity, eliminating the structural variables found in normal hydrocarbons.

The monograph is divided into five chapters; the first (20 pages) deals with the preparation of diamonoid structures by the rearrangement of polycyclic hydrocarbons; the second (17 pages) with the synthesis and chemistry of polycyclic hydrocarbons related to adamantanes, including protoadamantanes, twistanes, tricyclodecanes, homoadamantanes, noradamantanes, bisnoradamantanes, dehydroadamantanes, dehydrohomoadamantanes and ethanoadamantanes. The third chapter (10 pages) deals with the physical properties, the fourth (19 pages) with the chemical properties, and the last (5 pages) with the biological properties of adamantane derivatives.

The authoritativeness of this monograph is guaranteed by the personality of the writers, as one of them (P. v. R. SCHLEYER) was the initiator of the whole adamantane chemistry and co-author of the first summary (Chem. Rev. **64**, 277 (1964)) dealing with the chemistry of "cage-like" compounds. Thus the chapters dealing with the physical and chemical properties of adamantane derivatives are of outstanding value, as they comprise, among others, the newest results achieved at the Princeton University under the leadership of Prof. SCHLEYER.

The last chapter, "Adamantane Derivatives in Pharmacology and Biochemistry", deserves special interest. Here we can find not only a summary of the antiviral activity of 1-adamantanamine hydrochloride discovered in 1964, but also some very interesting structure-activity relationships. This chapter contains even speculations concerning the biological pathways of pharmacologically active adamantane derivatives.

The up-to-dateness of the monograph can also be seen from the references (372), the latest of which quotes the literature of 1970. A special "Addendum" (2 pages) can be found at the end of the book, dealing with the most recent literature published up to January 1971.

The monograph can be recommended to all chemists who want to get a complete and up-to-date survey of this special field of organic chemistry, as it is both highly theoretical and practical.

J. KUSZMANN

Methoden der Analyse in der Chemie, Band 8

W. BENZ: Massenspektrometrie Organischer Verbindungen, 424 S.

Akademische Verlagsgesellschaft, Frankfurt am Main, 1969

Die Massenspektrometrie hat sich in den letzten zehn Jahren als eine sehr erfolgreiche Methode erwiesen, und findet auf einem sich dauernd erweiternden Einsatzgebiet sowohl in der Molekülstrukturforschung als auch zur Lösung analytischer Aufgaben Anwendung. Besonders schnell wächst die Zahl jener organischen Chemiker, die diese Methode zur Lösung ihrer organisch-chemischen strukturellen oder analytischen Probleme anwenden möchten.

Das Buch kann eben diesen Chemikern wertvolle Hilfe leisten, denn es ist vor allem für Leser gedacht, die auf dem Gebiete der Massenspektrometrie Anfänger sind, jedoch über gewisse organisch-chemische Kenntnisse verfügen. In Einklang damit, wird das Gewicht in erster Linie auf technische und methodische Fragen in Verbindung mit der Aufnahme, Auswertung und Interpretation der Massenspektren gelegt.

Die Massenspektrometer werden — richtigerweise — nicht eingehend beschrieben, statt dessen werden im ersten kurzen Abschnitt, etwa als Einleitung, die Arbeitsprinzipien und Aufbauschemen der Meßinstrumente kurz angegeben.

Die vom Gesichtspunkte der Aufnahme von Massenspektren besonders wichtigen technischen Geräte, die sogenannten Einlaßsysteme, verschiedene Probeneinführungsmethoden, werden im zweiten Abschnitt beschrieben. Besonders wertvoll in diesem Abschnitt sind jene Teile, die die verschiedenen Varianten der sog. direkten Einführung schwerflüchtiger organischer Verbindungen sowie die mit angeschlossenem Gaschromatographen verwendeten technischen Lösungen und Probleme beschreiben.

Im dritten Abschnitt diskutiert der Verfasser, auf verschiedene massenspektrometrische Aufgaben spezialisiert, die mit der Aufnahme und Auswertung der Massenspektren verbundenen methodologischen Probleme und Griffe (Probleme des Untergrundes, der Auflösung, der Bestimmung der Massenzahl, die Auswertungstechnik metastabiler Peaks usw.), mit Ausnahme der Probleme bezüglich Massenspektren hoher Auflösung, die in einem besonderen Abschnitt behandelt werden.

Besonders wertvoll und gleichzeitig von größtem Umfang (mehr als 100 Seiten) ist der vierte Abschnitt. Dieser Abschnitt wird vom Autor der Diskussion des Zusammenhanges zwischen Massenspektrum und Molekülstruktur gewidmet, um damit der Interpretation der Massenspektren eine Basis zu schaffen. Der Aufbau dieses Teiles folgt vor allem den Gesichtspunkten der Strukturidentifikation. Die wichtigsten Elektronenstoß-induzierte Fragmentationsvorgänge werden im wesentlichen in die von K. BIEMANNS Buch (»Mass Spectrometry, Organic Chemical Applications«, McGraw-Hill, 1962) bekannten Typen getrennt diskutiert und die einzelnen Typen an Hand von Beispielen illustriert. Die Beispiele für die Umlagerungsreaktionen sind besonders gut gelungen. Am Ende des Abschnittes werden die Massenspektren einiger wichtiger Verbindungsgruppen kurz charakterisiert. Jede Verbindungsgruppe wird durch ein separates Literaturverzeichnis ergänzt, was den Wert dieses Abschnittes noch erhöht. Der Abschnitt ist gedrängt abgefaßt und enthält eine sehr große Menge von Informationen. Doch scheinen auf Grund des Abschnittes die Zusammenhänge zwischen Massenspektrum und Molekülstruktur stellenweise zu einfach und problemfrei zu sein.

Der fünfte Abschnitt, welcher sich mit der Interpretation von Massenspektren befaßt, ist eine nützliche Sammlung zahlreicher methodologischer Griffe. Beispiele und Probleme der Interpretation der Spektren heben noch den Wert des Abschnittes.

Der Diskussion der auf dem Gebiet der quantitativen chemischen Analyse verwendeten massenspektrometrischen Methoden (Gemischanalyse organischer Substanzen, Isotopenanalyse) wird ein separater Abschnitt gewidmet.

Der siebente Abschnitt befaßt sich mit den speziellen meß- und auswertungstechnischen Problemen der modernen hochauflösenden Massenspektrometrie (Spektrumaufnahme-Technik, »peak matching«, Bestimmungsmethoden der Bruttoformel, Beschreibung und Diskussion der Sinnvoll und nützlich im Anhang beigefügten Tabelle von HENNEBERG und CASPER). Der Abschnitt behandelt auch zahlreiche spezielle Fragen der Aufarbeitungstechnik von Spektren hoher Auflösung (z. B. »element map«). Die Möglichkeit der Datenverarbeitung von Spektren mit Computern werden auch erwähnt.

Im achten, relativ kurzen Abschnitt illustriert der Verfasser an Hand einiger Beispiele, wie die Interpretation von Massenspektren durch die chemische Umwandlung der zu untersuchenden Probe erleichtert werden kann.

Jeder Abschnitt des Buches wird durch ein entsprechendes Literaturverzeichnis ergänzt, welches auch zahlreiche Referate aus dem Jahr 1968 enthält. Die praktische Verwendbarkeit des Buches wird durch die Tabellen im Anhang noch verbessert. Unter diesen befinden sich auch die vollen Massenspektren zahlreicher (etwa 350) organischer Verbindungen, die die wichtigsten Gruppen der organischen Verbindungen vertreten.

Wie bereits einleitend erwähnt wurde, wird das Buch »Massenspektrometrie organischer Verbindungen« von W. BENZ vor allem solchen Chemikern eine große Hilfe sein, die auf diesem Gebiet noch Anfänger sind, doch kann das Buch auch den in der Massenspektrometrie aktiv Tätigen sowie jenen von Nutzen sein, die sich über die Anwendungsmöglichkeiten der Massenspektrometrie in der organischen Chemie orientieren wollen.

J. TAMÁS

INDEX

INORGANIC AND ANALYTICAL CHEMISTRY — ANORGANISCHE UND ANALYTISCHE CHEMIE — НЕОРГАНИЧЕСКАЯ И АНАЛИТИЧЕСКАЯ ХИМИЯ

LITOMISKÝ, J.: Über die Anwendung zweiatomiger Moleküle als Vergleichselemente bei der spektrochemischen Analyse nichtleitender Stoffe. (On the Use of Diatomic Molecules as Comparing Elements in the Spectrometric Analysis of Non-Conducting Substances) 231

PHYSICAL CHEMISTRY — PHYSIKALISCHE CHEMIE — ФИЗИЧЕСКАЯ ХИМИЯ

SZŐKE, S., JALSOVSZKY, G. and DUDAR, E.: Electronic Structure of Isoelectronic Molecules 241

SINGH, D. and DWIVEDI, A. N.: Influence of Hydrogen Ion Concentration on the Anodic Polarization of *p*-Germanium Electrodes 255

HORÁNYI, GY. and NAGY, F.: Investigation of Adsorption Phenomena on Platinized Pt Electrodes by Tracer Methods, X. Studies with ^{14}C-labelled Acetone 261

HORÁNYI, GY., KŐNIG, P. and NAGY, F.: Investigation of Adsorption Phenomena on Platinized Pt Electrodes by Tracer Methods, XI. Study of the Adsorption of Isopropanol 269

PAÁL, Z., and TÉTÉNYI, P.: C_5-Cyclization of Unsaturated Hydrocarbons on Platinum Black (Short Communication) 277

ORGANIC CHEMISTRY — ORGANISCHE CHEMIE — ОРГАНИЧЕСКАЯ ХИМИЯ

АПЬОК, Й и БАРТОК, М.: Химия 1,3-бифункциональных соединений, XIII. Изучение превращений циклических ацеталей на катализаторе Pt/T с помощью микрореакторной техники. 1,3-диоксоланы и 1,3-диоксепаны (Apjok, J. and Bartók, M.: The Chemistry of 1,3-Bifunctional Systems, XIII. Conversions of Cyclic Acetals on Pt/T Catalysts, Studied by Micro-reactor Technique. 1,3-Dioxelans and 1,3-Dioxepans) 281

BARTÓK, M., BOZÓKI-BARTÓK, G. and KOVÁCS, K.: The Chemistry of 1,3-Bifunctional Systems, XIV. Kinetic Study of the Alkaline Hydrolysis of the 2,2-Disubstituted Homologues of Trimethylene Chlorohydrin 297

LIPTÁK, A. and BOGNÁR, R.: N-Glycosides, XV. The Validity of Hudson's Isorotational Rule for Aromatic O- and N-Glucoside Derivatives of Analogous Structures 309

KARAWYA, M. S., RIZK, A. M., HAMMOUDA, F. M., DIAB, A. M. and AHMED, Z. F.: Phytochemical Investigation of Certain *Cestrum* Species Growing in Egypt. Alkaloids and Saponins 317

DINYA, Z.: Calculation of the Infrared Carbonyl Stretching Frequencies and Ionization Potentials of 4-Substituted Acetophenones 323

Г. В. Путырская и Ю. Силади- Синтез моно: и дисульфопроизводных дифенилпикрилгидразила (ДФПГ) (PUTIRSKAJA, G. V. and SZILÁGYI, J.: Synthesis of Mono- and Disulfonated Derivatives of 1,1-Diphenyl-2-picrylhydrazyl (DPPH)) 329

DOSS, S. H.: Infrared Absorption Bands Associated with the Sultam Ring 341

LEMPERT-SRÉTER, M. and LEMPERT, K.: Alkaline Cleavage of Some (1-Phenylsulfonyl-2-Pyrazolin-5-Ylmethyl) Ketones (Short Communication) 349

ZSADON, B., ÁRVAY, Gy. and TÉTÉNYI, P.: Alkaloids from *Vinca Major* L. (Apocynaceae) (±)-Vincadifformine (Preliminary Communication) 355

RECENSIONES 357

ACTA CHIMICA
ТОМ 72 — ВЫП. 3

РЕЗЮМЕ

Использование диатомных молекул в качестве сравнительных элементов в спектроскопии

Й. ЛИТОМИСКИ

Обсуждаемые примеры подтверждают возможность аналитического использования спектров молекулярной эмиссии. До сих пор эти спектры рассматривались как нежелательный балласт, затрудняющий оценку спектрограмм.

Приводимые же примеры указывают на возможности успешного применения их в качестве сравнительного элемента при аналитическом построении пар линий.

Построение молекулярных полосатых спектров связано с такими элементами, которые составляют матрицу изучаемой системы даже в том случае, когда они являются составляющими образца или электрода. В результате этого отпадает необходимость в добавлении «инородного» сравнительного элемента и, тем самым, открывается возможность простого приготовления образца для анализа.

Электронное строение изоэлектронных молекул

Ш. СЁКЕ, ДЬ. ЯЛШОВСКИ и Э. ДУДАР

Влияние электронного строения и орбитальной конфигурации изучалось с помощью методов П. П. П. и Э. Х. На основе результатов измерений было установлено, что в полярных растворителях спектр молекулы N-окси-пиридина приближается к спектру монофторбензола, в то время как в неполярных растворителях сохраняется акцепторно-донорный характер. Что же касается различий в электронных спектрах, то это объясняется удвоенной заряженностью основного характера азота в связи N—O, приводящей к пониженным энергиям перехода в близкой УФ-области, по сравнению со связью C—F монофторбензола.

Алгольная программа KDF-9 была любезно предоставлена в наше распоряжение Дж. К. Пакером и модифицирована нами для проведения некоторых, интересующих нас проблем.

Расчеты были произведены на машине ICT-1905 ЦИИФ АН Венгрии.

Влияние концентрации водородного иона на поляризацию p-германиевых электродов

Д. СИНГ и А. Н. ДВИВЕДИ

Анодная поляризация *p*-германиевых электродов была изучена в растворах (0,02N ТЭА Br + x N HBr), где x — нормальность кислоты. Анодные характеристики p—Ge с различным сопротивлением идентичны и лишь различаются при более высоких плотностях тока. Уравнение Тафеля $\eta = a + b \log i$ справедливо для p—Ge анодов лишь при ограниченных плотностях тока. Анодная поляризация уменьшается с уменьшением pH, и анодные реакции с молекулами воды протекают бурно в кислых средах. Тангенс угла наклона прямых Тафеля изменяется от 0,094 до 0,123 в. Это указывает на тот факт, что перенапряжение повышается в области двойного слоя Гельмгольца.

Изучение адсорбционных явлений на платиновом электроде с помощью техники радиоактивного мечения, X

Исследования с ацетоном, меченым C^{14}

ДЬ. ХОРАНИ и Ф. НАДЬ

1. Изучалось поведение ацетона, меченого C^{14}, на платиновом электроде в интервале потенциалов 0—1000 мв.

2. Было исследовано влияние газообразных продуктов, образующихся при электрогидрировании или электроокислении ацетона, на измерения с помощью радиоактивной техники.

3. Согласно наблюдениям были сделаны общие заключения относительно явлений, происходящих при адсорбции отдельных органических веществ.

Изучение адсорбционных явлений на платиновом электроде с помощью техники радиоактивного мечения, XI

Исследование адсорбции изопропанола

ДЬ. ХОРАНИ, П. КЁНИГ и Ф. НАДЬ

1. Адсорбция изопропанола изучалась в кислых средах на электроде платинированной платины.

2. Было установлено, что адсорбция является необратимой и адсорбированные молекулы не принимают участия в окислении изопропанола до ацетона.

3. При восстановлении адсорбированного изопропанола образуется газообразный продукт. В связи с этим изучались возможности измерения меченого газообразного продукта, накапливающегося на платиновой черни. Было сделано заключение, что поверхностный комплекс, образующийся при адсорбции изопропанола и ацетона, вероятно, один и тот же.

Химия 1,3-бифункциональных систем, XIV

Кинетика реакции щелочного гидролиза 2,2-дизамещенных гомологов триметиленхлоргидрина

М. БАРТОК, Г. БОЗОКИ-БАРТОК и К. КОВАЧ

Исследовалась кинетика щелочного гидролиза 2,2-дизамещенных гомологов триметиленхлоргидрина: 2,2-диметил-(I), 2,2-диэтил-(II), 2-метил-2-пропил-(III), 2-этил-2-бутил-(IV) и 2,2-диизопропил-3-хлорпропанолов(V). На основе экспериментальных данных рассчитывались константы скоростей, энергии активации, энтропии активации и предэкспоненциальные множители в уравнении констант скоростей процессов, приводящих к образованию гомологов оксациклобутана.

N-Гликозиды, XV

Справедливость изоротационного привила Хадсона среди производных ароматических O- и N-глюкозидов аналогичного строения

А. ЛИПТАК и Р. БОГНАР

Для производных вторичных глюкозил-аминов конфигурационное обозначение, основанное на направлении и величине оптического вращения, дает также правильную абсолютную конфигурацию. Величина 2B по Хадсону этих соединений может быть сравнима лишь для свободных N-арил-O-глюкопиранозиламинов с соответствующей величиной O-глюкозидов аналогичного строения. У тетраацетатов и тетраметильных эфиров глюкозидов расхождения в значениях 2B увеличиваются с увеличением поляризуемости аглюконов.

Для изученных свободных O-глюкозидов и их O-ацетил-производных была установлена количественная зависимость по Арндту между поляризуемостью аглюконов (α) и молярным вращением. Далее было показано, что в случае двух аномеров доля участия аглюконов в молярном вращении различается. Это участие увеличивается с повышением поляризуемости аглюконов.

Фотохимическое исследование некоторых представителей Cestrum, произрастающих в Египте

(Алкалоиды и Сапонины)

М. С. КАРАВЯ, А. М. РИЗК, Ф. М. ХАММОУДА, А. М. ДИАБ и З. Ф. АХМЕД

Соланидин и соласидин были изолированы из *Cestrum purpureum* в то время как *C. Aurantiacum* и *C. diurnum* были лишены каких-либо стероидальных алкалоидов. Количественное определение алкаминов производилось титрометрическим и колориметрическим методами. На основе исследования состава сапонина было обнаружено, что *C. aurantiacum* и *C. purpureum* содержат один и тот же сапонин, а именно дигитонин, в то время как *C. diurnum* содержит тигонин; их идентичность была доказана кислым гидролизом, а также идентификацией стероидных сапогенинов (дигитогенин и тигогенин) и сахарных компонентов.

Расчет ИК частоты валентного колебания карбонила и ионизационного потенциала 4-замещенных ацетофенонов

З. ДЫНЯ

С помощью простого метода НМО непосредственно и с хорошей точностью были рассчитаны первые ионизационные потенциалы 4-замещенных ацетофенонов.

Была найдена линейная зависимость между измеряемой частотой валентного колебания карбонила и энергетическим коэффициентом ($\varkappa_i$) наивысшей заполненной молекулярной орбиты. На этом основании может быть дано линейное уравнение для приближенного расчета частоты валентного колебания.

Полосы ИК поглащений, характерные для кольца сультама

С. Х. ДОСС

Были сняты ИК спектры различных ароматических и алифатических шестичленных циклических сультамов. Обсуждаются характерные частоты и сдвиги.

Printed in Hungary

A kiadásért felel az Akadémiai Kiadó igazgatója — Műszaki szerkesztő: Várhelyi Tamás

A kézirat nyomdába érkezett: 1971. XII. 6. — Terjedelem: 11,5 (A/5) ív, 71 ábra

72.72785 Akadémiai Nyomda, Budapest — Felelős vezető: Bernát György

The Acta Chimica publish papers on chemistry, in English, German, French and Russian.

The Acta Chimica appear in volumes consisting of four parts of varying size, 4 volumes being published a year.

Manuscripts should be addressed to

Acta Chimica
Budapest 112/91 Műegyetem

Correspondence with the editors should be sent to the same address.

The rate of subscription is $ 16.00 a volume.

Orders may be placed with "*Kultúra*" Foreign Trade Company for Books and Newspapers (Budapest I., Fő utca 32. Account No. 43-790-057-181) or with representatives abroad.

Les Acta Chimica paraissent en français, allemand, anglais et russe et publient des mémoires du domaine des sciences chimiques.

Les Acta Chimica sont publiés sous forme de fascicules. Quatre fascicules seront réunis en un volume (4 volumes par an).

On est prié d'envoyer les manuscrits destinés à la rédaction à l'adresse suivante:

Acta Chimica
Budapest 112/91 Műegyetem

Toute correspondance doit être envoyée à cette même adresse.

Le prix de l'abonnement est de $ 16.00 par volume.

On peut s'abonner à l'Entreprise pour le Commerce Extérieur de Livres et Journaux «*Kultúra*» (Budapest I., Fő utca 32. Compte-courant No. 43-790-057-181) ou à l'étranger chez tous les représentants ou dépositaires.

«*Acta Chimica*» издают трактаты из области химической науки на русском, французском, английском и немецком языках.

«*Acta Chimica*» выходят отдельными выпусками разного объема. 4 выпуска составляют один том. 4 тома публикуются в год.

Предназначенные для публикации рукописи следует направлять по адресу:

Acta Chimica
Budapest 112/91 Műegyetem

По этому же адресу направлять всякую корреспонденцию для редакции.

Подписная цена — $ 16.00 за том.

Заказы принимает предприятие по внешней торговле книг и газет «*Kultúra*» (Budapest I., Fő utca 32. Текущий счет № 43-790-057-181) или его заграничные представительства и уполномоченные.

Reviews of the Hungarian Academy of Sciences are obtainable at the following addresses:

ALBANIA

Drejtorija Qëndrone e Përhapjes
dhe Propagandimit të Librit
Kruga Konferenca e Pazes
Tirana

AUSTRALIA

A. Keesing
Box 4886, GPO
Sydney

AUSTRIA

Globus
Höchstädtplatz 3
A-1200 Wien XX

BELGIUM

Office International de Librairie
30, Avenue Marnix
1050 Bruxelles
Du Monde Entier
162, rue du Midi
1000 Bruxelles

BULGARIA

Hemus
11 pl Slaveikov
Sofia

CANADA

Pannonia Books
2, Spadina Road
Toronto 4, Ont.

CHINA

Waiwen Shudian
Peking
P. O. B. 88

CZECHOSLOVAKIA

Artia
Ve Smečkách 30
Praha 2
Poštovní Novinová Služba
Dovoz tisku
Vinohradská 46
Praha 2
Mad'arská Kultura
Václavské nám. 2
Praha 1
Slovart A. G.
Gorkého
Bratislava

DENMARK

Ejnar Munksgaard
Nörregade 6
Kopenhagen-K

FINLAND

Akateeminen Kirjakauppa
Keskuskatu 2
Helsinki 10

FRANCE

Office International de Documentation
et Librairie
48, rue Gay-Lussac
Paris 5

GERMAN DEMOCRATIC REPUBLIC

Deutscher Buch-Export und Import
Leninstraße 16
Leipzig 701
Zeitungsvertriebsamt
Fruchtstraße 3—4
1004 Berlin

GERMAN FEDERAL REPUBLIC

Kunst und Wissen
Erich Bieber
Postfach 46
7 Stuttgart 1

GREAT BRITAIN

Blackwell's Periodicals
Oxenford House
Magdalen Street
Oxford
Collet's Subscription Import
Department
Dennington Estate
Wellingsborough. Northants.
Robert Maxwell and Co. Ltd.
4—5 Fitzroy Square
London W. 1

HOLLAND

Swetz and Zeitlinger
Keizersgracht 471—478
Amsterdam C.
Martinus Nijhof
Lange Voorhout 9
The Hague

INDIA

Hind Book House
66 Babar Road
New Delhi 1

ITALY

Santo Vanasia
Via M. Macchi 71
Milano
Libreria Commissionaria Sansoni
Via La Marmora 45
Firenze
Techna
Via Cesi 16.
40135 Bologna

JAPAN

Kinokuniya Book-Store Co. Ltd.
826 Tsunohazu 1-chome
Shinjuku-ku
Tokyo
Maruzen and Co. Ltd.
P. O. Box 605
Tokyo-Central 100-31

KOREA

Chulpanmul
Phenjan

NORWAY

Tanum-Cammermeyer
Karl Johansgtan 41—43
Oslo 1

POLAND

Ruch
ul. Wronia 23
Warszawa

ROUMANIA

Cartimex
Str. Aristide Briand 14—18
Bucureşti

SOVIET UNION

Mezhdunarodnaya Kniga
Moscow G—200

SWEDEN

Almquist and Wiksell
Gamla Brogatan 26
S—101 20 Stockholm

USA

F. W. Faxon Co. Inc.
15 Southwest Park
Westwood Mass. 02090
Stechert Hafner Inc.
31. East 10th Street
New York, N. Y. 10003

VIETNAM

Xunhasaba
19, Tran Quoc Toan
Hanoi

YUGOSLAVIA

Forum
Vojvode Mišića broj 1
Novi Sad
Jugoslovenska Knjiga
Terazije 27
Beograd

16. VI. 1972

Index: 26.007

ACTA CHIMICA

ACADEMIAE SCIENTIARUM HUNGARICAE

ADIUVANTIBUS

V. BRUCKNER, GY. DEÁK, K. POLINSZKY,
E. PUNGOR, G. SCHAY, Z. G. SZABÓ

REDIGIT

B. LENGYEL

TOMUS 72 FASCICULUS 4

AKADÉMIAI KIADÓ, BUDAPEST

1972

ACTA CHIM. (BUDAPEST) ACASA 2 72 (4) 359–468 (1972)

ACTA CHIMICA

A MAGYAR TUDOMÁNYOS AKADÉMIA KÉMIAI TUDOMÁNYOK OSZTÁLYÁNAK IDEGEN NYELVŰ KÖZLEMÉNYEI

SZERKESZTI

LENGYEL BÉLA

TECHNIKAI SZERKESZTŐK

DEÁK GYULA és HARASZTHY-PAPP MELINDA

Az Acta Chimica német, angol, francia és orosz nyelven közöl értekezéseket a kémiai tudományok köréből.

Az Acta Chimica változó terjedelmű füzetekben jelenik meg, egy-egy kötet négy füzetből áll. Évente átlag négy kötet jelenik meg.

A közlésre szánt kéziratok a szerkesztőség címére (Budapest 112/91 Műegyetem) küldendők.

Ugyanerre a címre küldendő minden szerkesztőségi levelezés. A szerkesztőség kéziratokat nem ad vissza.

Megrendelhető a belföld számára az „Akadémiai Kiadó"-nál (Budapest V., Alkotmány utca 21. Bankszámla 05-915-111-46), a külföld számára pedig a „Kultúra" Könyv- és Hírlap Külkereskedelmi Vállalatnál (Budapest I., Fő utca 32. Bankszámla: 43-790-057-181) vagy annak külföldi képviseleteinél és bizományosainál.

Die Acta Chimica veröffentlichen Abhandlungen aus dem Bereiche der chemischen Wissenschaften in deutscher, englischer, französischer und russischer Sprache.

Die Acta Chimica erscheinen in Heften wechselnden Umfanges. Vier Hefte bilden einen Band. Jährlich erscheinen 4 Bände.

Die zur Veröffentlichung bestimmten Manuskripte sind an folgende Adresse zu senden:

Acta Chimica
Budapest 112/91 Műegyetem

An die gleiche Anschrift ist auch jede für die Redaktion bestimmte Korrespondenz zu richten. Abonnementspreis pro Band: $ 16.00.

Bestellbar bei dem Buch- und Zeitungs-Außenhandels-Unternehmen »*Kultúra*« (Budapest I., Fő utca 32. Bankkonto No. 43-790-057-181) oder bei seinen Auslandsvertretungen und Kommissionären.

Acta Chimica Academiae Scientiarum Hungaricae, Tomus 72 (4), pp. 359–362 (1972)

HYDRAZO-9-ACRIDINE, A NEW ACID–BASE INDICATOR FOR TITRATIONS IN GLACIAL ACETIC ACID, I

L. LADÁNYI, PHAM HAI TUNG*, G. FAUVELOT** and G. SZÓKÁN***

*(Institute of Inorganic and Analytical Chemistry, L. Eötvös University, Budapest, * Permanent address: Institute of Analytical Chemistry, Faculty of Pharmacy, Hanoi, Vietnam, ** Department of Organic Chemistry, E. S. C. P. I., Paris, France, *** Institute of Organic Chemistry, L. Eötvös University, Budapest)*

Hydrazo-9-acridine is recommended as an acid–base indicator in acetic acid medium for the titration of bases with pK_{H_2O} values higher than 5. The precision obtainable is greater than that using Crystal Violet.

Introduction

Potentiometric titration is a convenient method of end-point detection in acid–base titrations in glacial acid, if the titration curve has an easily determined inflexion point coinciding with the equivalence point. Nevertheless, this does not eliminate the need for indicators which function effectively in such a medium, and this prompted the present study of the dye hydrazo-9-acridine(I).

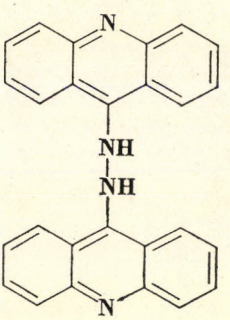

I

Compounds of this type were first synthesized by LUCIUS and BRÜNIG [1] from 9-halogenoacridines with hydrazine. According to CAUQUIS and FAUVELOT [2] hydrazo-9-acridine is a bivalent base in CH_3CN which can be protonated in two consecutive steps. On reaction with one equivalent of perchloric acid the orange solution of the dye becomes red; reaction with a second equivalent of the acid changes the colour to yellow. On the basis of these reactions we supposed that the substance has acid–base indicator properties and

is suitable for end-point detection in non-aqueous media. In fact, in glacial acetic acid hydrazo-9-acridine can be successfully used in the titration of bases of various strengths. The colour of the 'basic' form of the indicator is rose, that of its 'acid' form is yellow. Even at $2.5 \cdot 10^{-5}M$ concentration of the dye, using $0.05N$ perchloric acid as the titrant, the colour change is very sharp.

Experimental

Titrations in glacial acetic acid using hydrazo-9-acridine indicator

Instruments. A Radelkis Precision pH-meter, type OP-205, equipped with a magnetic stirrer was employed for all potentiometric titrations. Glass-Ag/AgCl electrode-pairs filled with acetic acid and saturated solutions of potassium chloride in acetic acid, respectively (Tacussel AcOH B.10 and AgCl 10 model) were used; the systems attained equilibrium rapidly.

Chemicals. All chemicals, if not stated otherwise, were of analytical grade of purity.

Acetic acid used in the preparation of all solutions was purified according to GYENES [3] (water content less than 0.06%). Hydrazo-9-acridine ($2.5 \cdot 10^{-3}M$ in acetic acid) and Crystal Violet (0.1 g in 100 ml of acetic acid) were applied as indicator stock solutions.

Titration of bases. For the standardization of perchloric acid the routine procedure was followed [3] using 1,1'-diphenylguanidine as standard. The effectiveness of hydrazo-9-acridine was compared with that of Crystal Violet in the potentiometric and visual titrations of some bases and hydrochlorides of bases (*e.g.*, pyridine, papaverine HCl, methylamine HCl, urea and α-naphtylamine). In titrations of the hydrochlorides of bases, $Hg(CH_3COO)_2$ was added and the acetates which formed were then determined. The results were evaluated statistically. The effect of moisture in the solvent on the colour change of the indicator was also investigated.

Results

The results of the potentiometric titrations are shown in Fig. 1.

It can be seen that the colour change of Crystal Violet is gradual, while that of hydrazo-9-acridine from rose to yellow is very sharp.

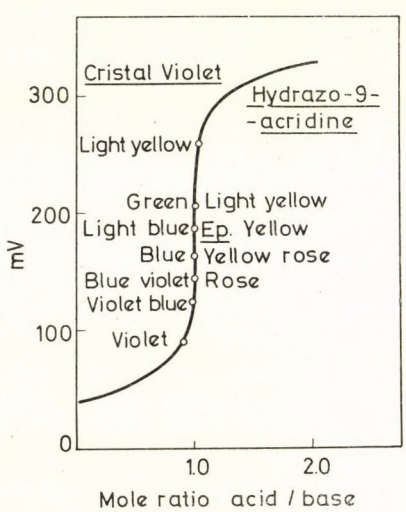

a

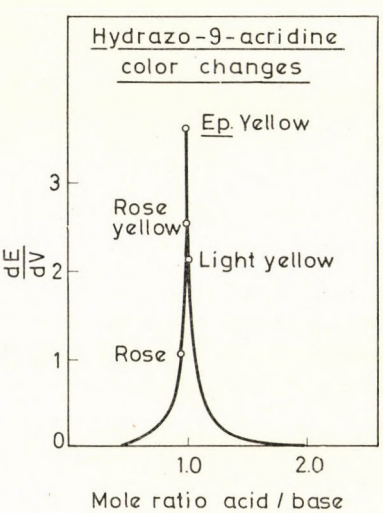

b

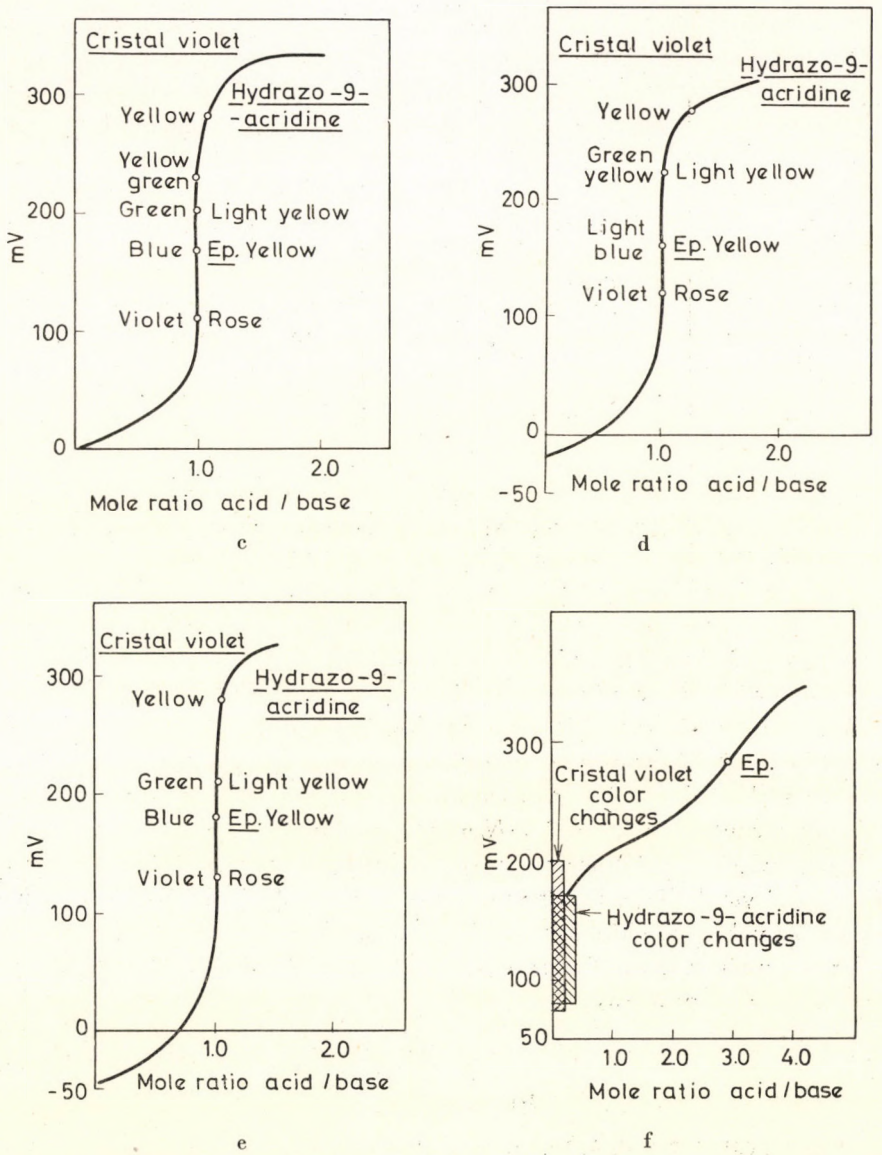

Fig. 1. Potentiometric titration curves showing a comparison between Crystal Violet and hydrazo-9-acridine indicators. a) Diphenylguanidine 0.05 *N*, b) Diphenylguanidine 0.05 *N*, Derivative curve, c) Pyridine 0.05 *N*, d) Methylammonium chloride 0.05 *N*, e) Papaverine hydrochloride 0.05 *N*, f) Urea 0.05 *N*

Fig. 1b illustrates the first derivative of the titration curve and the colour change of hydrazo-9-acridine in the case of 1,1'-diphenylguanidine.

Table I shows that both indicators give very good results, but the precision and accuracy of hydrazo-9-acridine is higher.

Table I

Titrations of bases in glacial acetic acid with 0.05 N $HClO_4$

Base	Indicator	Number of determinations	Mean normality	Standard deviation of a single dtn., %
1,1-diphenyl-quanidine	Crystal Violet	10	0.0490	0.29
	Hydrazo-9-acridine	10	0.0489	0.25
Pyridine	Crystal Violet	6	0.0501	0.45
	Hydrazo-9-acridine	6	0.0501	0.42
Papaverine hydrochloride	Crystal Violet	10	0.0430	0.27
	Hydrazo-9-acridine	10	0.0429	0.21
Methylammonium chloride	Crystal Violet	10	0.0493	0.27
	Hydrazo-9-acridine	10	0.0493	0.17

In the case of pyridine ($pK_{H_2O} = 5.2$), papaverine and methylamine hydrochloride the colour change of Crystal Violet is relatively difficult to perceive and requires much practice; when hydrazo-9-acridine indicator is used it is more easy to evaluate. This is reflected in the standard deviations. For urea ($pK_{H_2O} = 0.4$) and α-naphtylamine ($pK_{H_2O} = 4.0$) the colour change does not coincide with the equivalence point.

According to GYENES [3] if the perchloric acid solution is not weaker than 0.1*N*, up to about 1% water does not interfere with the colour change of Crystal Violet; with hydrazo-9-acridine indicator the response is still sharp up to 1.25% water content using a 0.05*N* solution of perchloric acid.

Therefore, in glacial acetic acid medium hydrazo-9-acridine seems to be better than Crystal Violet for the titration of dilute (0.05*N*) solutions of bases whose pK_{H_2O} values are higher than 5.

Experiments for the determination of some physico-chemical properties of the dye are in progress.

REFERENCES

1. Ger. Pat. 364 031 (1922); C. A. **18**, 1131 (1924)
2. CAUQUIS, G., FAUVELOT, G.: Polarography 1964, p. 848. MacMillan, London, 1964
3. GYENES, I.: Titration in Non-aqueous Media, Akadémiai Kiadó, Budapest, 1967
4. CHARLOT, G., TRÉMILLON, B.: Les réactions chimiques dans les solvants et sels fondus. p. 221. Gautier Villars Ed., Paris, 1963

László LADÁNYI
Pham Hai TUNG
Gérard FAUVELOT
Gyula SZÓKÁN

Budapest VIII., Múzeum krt. 4/b.

Acta Chimica Academiae Scientiarum Hungaricae, Tomus 72 (4), pp. 363–369 (1972)

HYDRAZO-9-ACRIDINE, A NEW ACID–BASE INDICATOR FOR TITRATIONS IN GLACIAL ACETIC ACID, II*

DETERMINATION OF THE INDICATOR DISSOCIATION CONSTANT

PHAM HAI TUNG** and L. LADÁNYI

*(Institute of Inorganic and Analytical Chemistry, L. Eötvös University, Budapest, ** Permanent address: Institute of Analytical Chemistry, Faculty of Pharmacy, Hanoi, Vietnam)*

Received January 5, 1971

The acid–base equilibrium of hydrazo-9-acridine has been studied and the indicator dissociation constant ($pK_I = pHClO_4$) determined in glacial acetic acid.

Introduction

In a previous paper* a new acid–base indicator (hydrazo-9-acridine, further: *I*) has been described that proved to be useful for the titrations of bases of various strengths ($pK_{H_2O} > 5$) in glacial acetic acid. The present communication deals with the investigation of some physico-chemical properties and the mechanism of colour change of this dye.

According to HIGUCHI [1] the colour change of an acid–base indicator in acetic acid depends upon the relative concentration of the base to that of its conjugate acid.

If another base (*B*) is present in the solution besides the solvent and the indicator, the resultant process can be written as:

$$BH^+A^- + IH^+Ac^- \rightleftharpoons BH^+Ac^- + IH^+A^-$$

where

BH^+A^- — the salt of base *B* formed with the strong acid used for the titration

BH^+Ac^- — the acetate of base *B*

IH^+A^- — the acid form of the indicator

IH^+Ac^- — the base form of the indicator.

For the equilibrium constant of this process we have:

$$K = \frac{|BH^+Ac^-|\ |IH^+A^-|}{|BH^+A^-|\ |IH^+Ac^-|} = \frac{K_{ind}}{K_{base}} . \qquad (1)$$

* Part I: Acta Chim. Acad. Sci. Hung. **72**, 359 (1972)

This expression can be used for the determination of the dissociation constant of the indicator. The value of $| BH^+Ac^- | / | BH^+A^- |$ in this expression can be adjusted arbitrarily with the aid of buffer solutions.

The ratio $| IH^+A^- | / | IH^+Ac^- |$ can be determined spectrophotometrically from Eq. (2):

$$\frac{|IH^+A^-|}{|IH^+Ac^-|} = \frac{E_B - E_1}{E_1 - E_A} \tag{2}$$

where:

E_B — the absorbance of the solution, when the total quantity of the indicator is present in its base form (at a given wavelength)

E_A — the absorbance of the solution, when the total quantity of the indicator is present in its acid form (at the same wavelength)

E_1 — the absorbance measured at the given wavelength when both forms are present.

LAPIDUS, LUCAS and TRÉMILLON [2] proposed a graphical method for the determination of pK_{ind} by plotting $\lg | IH^+Ac^- | / | IH^+A^- |$ as a function of $\lg | BH^+Ac^- | / | BH^+A^- |$. This gives a straight line of unit slope and when $| BH^+Ac^- | = | BH^+A^- |$, one has:

$$\lg \frac{|IH^+Ac^-|}{|IH^+A^-|} = pK_{ind} - pK_{base}. \tag{3}$$

Instead of pK_{base} and pK_{ind} it is possible to use the constant K_{BHA} and K_I for the equilibria including BHA and IH^+A^-, respectively.

$$K_{BHA} = \frac{|B|\,|HA|}{|BH^+A^-|}. \tag{4}$$

In this case Eq. 3 can be written as follows:

$$\lg \frac{|IH^+Ac^-|}{|IH^+A^-|} = pK_{BHA} - pK_I \tag{5}$$

When perchloric acid is used as a strong acid, pK_{BHA} is observed as the $pHClO_4$ value (5) of base B in glacial acetic acid. Thus, the calculated pK_1 can be placed directly on the $pHClO_4$ basicity scale of the same solvent.

Experimental

The following buffer systems were used: lithium acetate–lithium perchlorate; sodium acetate–sodium perchlorate; and antipyrine acetate – antipyrine perchlorate. The buffers were prepared by partial neutralization of their basic components with perchloric acid. The final

concentration of I was in all cases $2.5 \cdot 10^{-5} M$. In order to obtain the spectra of I in the 'pure acid' and 'pure base' forms, they were recorded in the presence of excess perchloric acid and a sufficiently strong base, respectively, so that no spectral change occurred even if a stronger base was employed.

The spectra of I were recorded in CH_3CN, both in non-buffered and acidic media. A stock solution of $0.1N$ perchloric acid in CH_3COOH was prepared and suitable quantity of this was added to the solution of I in CH_3CN by a Hamilton microsyringe.

The absorption spectra were obtained at room temperature with a Unicam SP 700 spectrophotometer using quartz cells of 1 cm length.

The chemicals used were commercial products of analytical grade of purity.

Hydrazo-9-acridine was prepared according to CAUQUIS and FAUVELOT [3].

The solvents were purified by conventional methods. The water content of the solvents was less than 0.06%.

Results and discussion

The absorption spectra of hydrazo-9-acridine recorded in various antipyrine acetate–antipyrine perchlorate buffer solutions are shown in Fig. 1. The absorption maxima of the 'pure base' and 'pure acid' forms of I are at

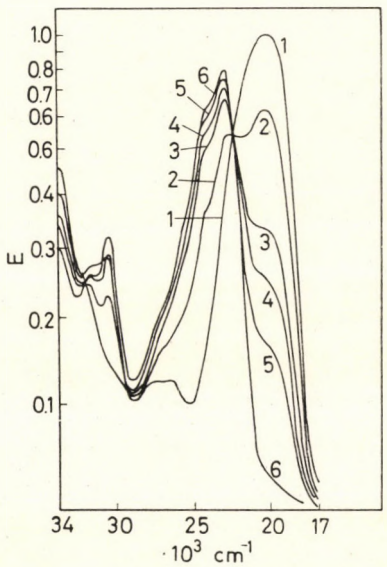

Fig. 1. Absorption of hydrazo-9-acridine in antipyrine acetate—antipyrine perchlorate buffer solutions in acetic acid

19.500 and 23.500 cm^{-1}, respectively. Only one isobestic point is found indicating one true acid–base equilibrium. At 19.500 cm^{-1} the absorbance of the 'pure acid' form is negligible.

The calculation of pK_I of hydrazo-9-acridine is shown in Table I.

By using the graphical method mentioned above, the pK_I is determined as shown in Fig. 2. For other buffer systems, the pK_I ($pHClO_4$) values are summarized in Table II.

Table I

Solution	Molar concentration of buffer components		Absorbance at 19.500 cm^{-1}	$\frac{\lvert IH^+Ac^-\rvert}{\lvert IH^+A^-\rvert}$	pK_I ($p\mathrm{HClO_4}$)
	Antipyrine acetate	Antipyrine perchlorate			
1	0.0500	0 .00	1.00	—	—
2	0.0179	0.0321	0.62	1.63	6.48
3	0.0072	0.0428	0.33	0.50	6.48
4	0.0051	0.0449	0.26	0.35	6.45
5	0.0035	0.0465	0.17	0.20	6.51
6	0.000	0.0500	0.00	—	—

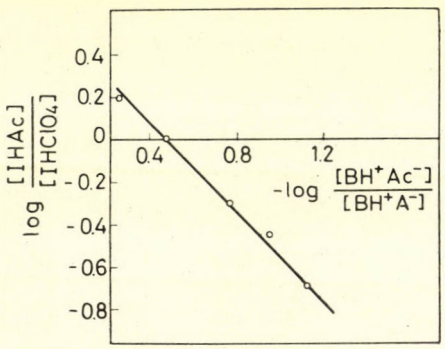

Fig. 2. Determination of pK_I in antipyrine perchlorate – antipyrine acetate buffer solutions

Table II

Buffer solution	pK_I
Lithium acetate–lithium perchlorate	6.47±0.02
Sodium acetate–sodium perchlorate	6.30±0.30

In the case of the buffer system sodium acetate–sodium perchlorate the error in pK_I is considerably greater. This can be due to the fact that the colour change of I is not gradual enough even if the perchloric acid is added in very small quantities. Moreover, small amounts of perchloric acid cannot be introduced with sufficient precision.

On the $p\mathrm{HClO_4}$ basicity scale, the pK_I value of hydrazo-9-acridine lies very near to that of Crystal Violet as shown in Fig. 3.

In Fig. 4 the absorption spectra of *I* in CH_3CN are shown.

When one equivalent amount of $HClO_4$ is added to the non-buffered solution of *I* in CH_3CN, the absorption spectrum is practically identical with that of the 'pure base' form in CH_3COOH (Curve 1). After the second equivalent of $HClO_4$ has been added, the absorption spectrum becomes similar to that of the 'pure acid' form in CH_3COOH, but the equilibrium is not completely shifted

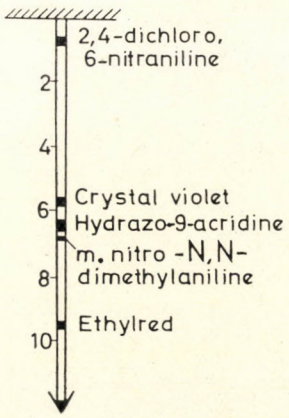

Fig. 3. $pHClO_4$ Basicity scale in acetic acid

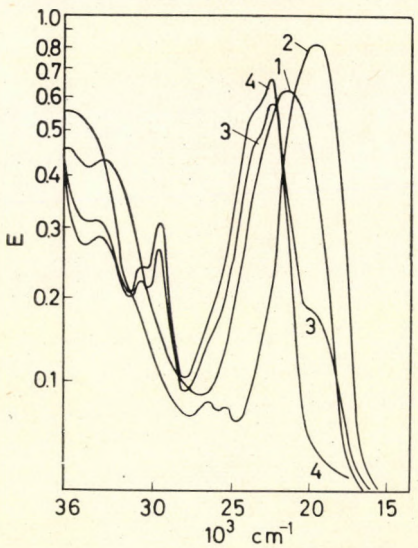

Fig. 4. Absorption spectra of hydrazo-9-acridine in acetonitrile. 1 — Indicator in acetonitrile. 2 — Indicator + 1 equivalent of $HClO_4$ in acetonitrile. 3 — Indicator + 2 equivalents of $HClO_4$ in acetonitrile. 4 — Indicator + 3,4,5-equivalents of $HClO_4$ in acetonitrile

to the right-hand side (Curve 2). In the presence of 3 or 4 equivalents of $HClO_4$, the spectra are very similar to that of the 'pure acid' form in CH_3COOH.

The fact that hydrazo-9-acridine reacts with only one molecule of $HClO_4$ during its colour change at the equivalent point in CH_3COOH was also proved in another way. The results obtained at 23.500 and 19.500 cm^{-1} in antipyrine acetate-antipyrine perchlorate buffers were evaluated by a computer program. The program does not involve any approximations and calculates the constant parameters of the following equation:

$$\frac{A}{C_I} = \frac{\varepsilon_0 + \sum_1^N \varepsilon_n \beta_n a^n}{1 + \sum_1^N \varepsilon \cdot \beta_n \cdot a^n}$$

where

A — absorbance measured
C_I — total concentration of I
ε_n — molar extinction coefficient of the nth form at the given wavelength
β_n — formation constant of the nth form

and by the definition:

$$a = \frac{K_{BHA}\,|BH^+A^-|}{|B|}\,.$$

The results of the calculation proved that N is equal to 1 in the system under discussion, *i.e.* the indicator behaves as a one-equivalent base. The final value for pK_I is:

$$pK_I = 6.43 \pm 0.03_5.$$

The calculated molar extinction coefficients for the 'pure base' and 'pure acid' forms are $1.73 \cdot 10^4$ and $2.90 \cdot 10^4$ at 23.500 cm^{-1} and $3.89 \cdot 10^4$ and $1 \cdot 10^{-1}$ at 19.500 cm^{-1}, respectively. The corresponding measured values were: $1.80 \cdot 10^4$, $2.80 \cdot 10^4$ and $4.00 \cdot 10^4$ and 0. There is a very good agreement between the data given in Table I and those obtained by the computer method.

According to the above results, the following equilibria and colour change mechanism can be written for I in acetic acid:

$$\underset{\substack{\text{orange in}\\ CH_3CN}}{I + HAc} \quad \rightleftharpoons \quad \underset{\substack{I' \text{ rose in } CH_3COOH\\ \text{('pure basic' form).}}}{IH^+Ac^-} \qquad (6)$$

This process takes place immediately when I is dissolved in acetic acid; the equilibrium is markedly shifted to the right-hand side.

At the equivalent point the second protonation takes place and the colour is changed to yellow.

$$\underset{\text{rose}}{I'} + \underset{(HClO_4 \text{ in } CH_3COOH)}{H_2Ac^+ClO_4^-} \rightleftharpoons \underset{\text{yellow ('pure acidic' form in } CH_3COOH)}{I'H^+ClO_4^-} + HAc \qquad (7)$$

*

We are very indebted to Miss M. KÁLDY and Dr. L. BARCZA for valuable discussions during the course of this work and for the computer calculations.

REFERENCES

1. HIGUCHI, T., FELDMANN, A., REHM, R.: Anal. Chem. **28,** 1120 (1956)
2. LAPIDUS, M., LUCAS, M., TRÉMILLON, B.: Bull. soc. chim. **1960,** 1949
3. CAUQUIS, G., FAUVELOT, G.: Polarography, 1964, p. 847. MacMillan, London, 1964
4. GYENES, I.: Titration in Non-aqueous Media, Akadémiai Kiadó, Budapest, 1967
5. CHARLOT, G., TRÉMILLON, B.: Les réactions chimiques dans les solvants et sels fondus. Gauthier Villars Ed., Paris, 1963

Pham Hai TUNG
László LADÁNYI
Budapest VIII., Múzeum krt. 4/b.

Acta Chimica Academiae Scientiarum Hungaricae, Tomus 72 (4), pp. 371—391 (1972)

INVESTIGATIONS ON THE THERMOCONDENSATION OF AMMONIUM PARATUNGSTATE PENTAHYDRATE BY A COMBINED THERMOANALYTICAL AND IR SPECTROPHOTOMETRIC METHOD, AND ADDITIONAL METHODS

A. B. KISS, P. GADÓ and A. J. HEGEDŰS

(Tungsram Research Institute, Budapest, Újpest)

Received February 1, 1971

The thermocondensation of ammonium paratungstate.5-hydrate was investigated by combined thermoanalytical and IR spectrophotometric gas analytical methods. By separating graphically the IR absorption maxima of gas products moles of released NH_3 and H_2O were determined, and the composition of intermediate phases, formed in overlapping net processes, was given. During the processes changes in crystal structures were followed too. It has been discovered that, between 195 and 230 °C there is a change in the structure of the paracrystal. In this phase the following composition was established: $3.75(NH_4)_2O \cdot 12WO_3 \cdot 3.25H_2O$, the same as calculated previously from spectrophotometric data. X-ray analytical and IR spectrophotometric characteristics of this phase were given. By analysing the gas products we have found that NH_3 is released from the crystal lattice partly alone, partly together with H_2O. Moreover, it was found that after the release of dry NH_3 gas covalently bonded OH groups remained attached to the WO_6 octahedrons of the polyanion.

Experiments have unambiguously shown that in 5-hydrates there is one mole of loosely bonded water and two moles of water of crystallization; consequently, in the case of 5-hydrates the structure of the paratungstate anion cannot be $[W_{12}O_{36}(OH)_{10}]^{10-}$, as accepted previously.

Ammonium paratungstate hydrates including also the pentahydrate, are starting materials for the industrial production of tungsten metal. The properties of tungsten filament depend very much on the composition and structure of the starting paratungstate, on the thermodynamical and kinetical conditions of its decomposition to WO_3 and on the reduction of the latter metallic tungsten.

Although the thermal decomposition of ammonium paratungstates in air has been widely studied [1—5], sure knowledge on this is far from being unambiguous. This manifests itself *e.g.* at the interpretation of TG curves [3], because on the basis of thermogravimetric measurements alone, if more than one gas is released, the quality and quantity of the gas products cannot be directly assigned to the consecutive steps of the TG curve. Although AHN [2] obtained satisfactory results by titrating the released ammonia, he, however, did not interpret the initial stage of the reaction. Others studied only the transformation of ammonium tungsten bronze to WO_3 [1, 4, 5].

Earlier [1] we attempted to elucidate the details of the thermal decomposition of ammonium paratungstate. GTA measurements were carried out in different gas atmospheres by a Chevenard-type thermobalance. The results of these studies are given in Figs 1 and 2 as well as in Table I. Temperature inter-

Acta Chim. (Budapest) 72, 1972

Table I

Molecular weight values related to 1 WO_3 at the inflexions of the TG curve

TG	in air			in N_2			$N_2 : H_2O$ 97 : 3 volume ratio		$N_2 : H_2O$ 90 : 10 volume ratio		
	Mw	C°	phase	Mw	C°	phase	Mw	C°	Mw	C°	phase
orig.	262.2	20	ASTM 1—0040	262.3	20	ASTM 1—0040	262.3	20	—		
1. infl.	258.5	49— 72	ASTM 1—0040	258.3	49— 62	ASTM 1—0040	259.0	68— 84	260.4	20	ASTM 1—0040
2. infl.	255.6	89—130	ASTM 1—0040	255.2	98—104	ASTM 1—0040	254,0	134—147	257.7	100	ASTM 1—0040
3. infl.	250.8	181—203	ASTM 1—0040	250.4	181—187	ASTM 1—0040 greyish	251.0	178—200	250.9	191	ASTM 1—0040
4. infl.	238.8	258—272	amorphous greyish w.	239.6	249—262	amorphous blueish-greyish	240.0	226—271	240.9	274	amorphous greyish
5. infl.	235.4	299—329	amorphous yellowish w.	235.6	300—312	amorphous blueish grey	235.6	300—349	236.4	306	amorphous blueish grey
6. infl. (step)	231.9	above 427	WO_3 + bronze light orange	231.3	above 467	WO_3 + bronze dark blue	231.9	above 400	231.9	above 400	WO_3 yellowish green

TG	in NH_3		$NH_3 : H_2O$ 97 : 3 volume ratio			in H_2			$H_2 : H_2O$ 97 : 3 volume ratio		90 : 10 volume ratio	
	Mw	C°	Mw	C°	phase	Mw	C°	phase	Mw	C°	Mw	C°
orig.	262.3	20	262.3	20	ASTM 1—0040	262.3	20	ASTM 1—0040	262.3	20	—	
1. infl.	260.9	29— 36	260.7	47	ASTM 1—0040	259.0	43— 77	ASTM 1—0040	260.9	67— 78	260.3	20
2. infl.	258.7	63— 68	258.8	64— 77	ASTM 1—0040	256.2	82—153	ASTM 1—0040	254.7	131—145	258.8	70
3. infl.	256.1	98—112	256.1	111—119	ASTM 1—0040	252.3	160—222	ASTM 1—0040	251.8	151—167	251.9	180
4. infl.	244.7 greyish	257—281	245.5 greyish	257—275	ASTM 1—0040	243.5	231—273	amorphous blueish black	240.6	257—262	241.2	270
			241.5 greyish green	302	—			amorphous				
5. infl.	236.1 blueish black	356	236.2 greyish green	357—365	bronze	238.1 236.0 235.3	262—343 297—301 305—403	amorphous bronze dark blue	236.8	294—301	236.8	314
6. infl. (step)	— blueish black	400	— dark blueish-green	400	bronze	232.7 230.8	351—475 383—534	bronze bronze blueish black	232.5 227.6	360—380 492	232.8 230.4 217.6	377—447 541—564 640

vals are indicated in the Table because the temperature data corresponding to the inflection points are influenced both by the rate of heating and by that of the gas flow. These parameters were deliberately varied in the experiments. As it can be seen from Table I and Fig. 1, the thermolysis of ammonium paratungstate proceeds in 6 steps in air, nitrogen, moist nitrogen, and dry ammonia,

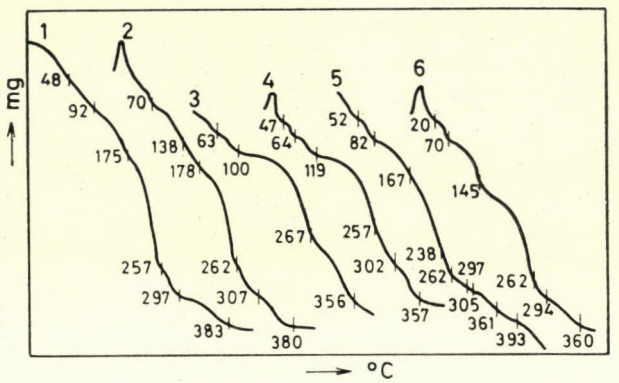

Fig. 1. TG curves measured in different gas atmospheres

1. Air (1686.3 mg)
2. N_2+H_2O (1477.2 mg)
3. NH_3 (1175.6 mg)
4. NH_3+H_2O (1189.0 mg)
5. H_2 (1321.5 mg)
6. H_2+H_2O (1132.0 mg)

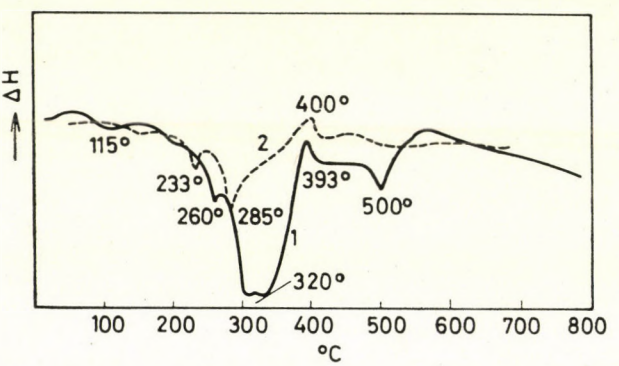

Fig. 2. DTA curves. 1. in air; 2. in hydrogen

respectively. In moist ammonia step 5 splits into two steps, *i.e.* a total of 7 steps was observed. The same number of steps was observed at the thermolysis in moist hydrogen, but in this case step 6 was split. In dry hydrogen both step 5 and step 6 were split so the entire thermolysis consisted of 9 steps. It can be seen from Table I, moreover, that the 1st and 2nd inflections are sensitive to water vapour and ammonia, the 4th and 6th ones are sensitive to ammonia and hydrogen, the 3rd one only to ammonia, while the 5th one presumably only to

hydrogen. These facts may indicate that before the 2nd step mainly H_2O and NH_3, before the 3rd one NH_3, and before the 4th and 6th steps NH_3, or possibly N_2 and H_2 are the products of the thermolysis. These latters combine catalytically to form NH_3. Process 5 is probably split into more processes by reactions leading to bronze formation due to H_2. The data of X-ray analysis in Table I are included only for preliminary information; more precise phase analyses will be given later in the paper. According to the DTA results, shown in Fig. 2, up to 400 °C essentially the same processes take place both in air and in hydrogen, except that the endothermic peaks appear at lower temperature, *i.e.* at higher molecular weight values, and that the endothermic process with a maximum at 500 °C measured in air cannot be observed in hydrogen.

Due to the qualitative nature of the above information the thermal decomposition of ammonium paratungstate was reinvestigated by the combined thermogravimetric and IR spectrophotometric method developed in this laboratory [6—8]. The same method was used in the studies on ammonium paramolybdate [9].

Experimental

1. TG—IR, and DTA measurements

Ammonium paratungstate samples of Tungsram and Fluka AG p.a. products were used throughout the experiments. According to X-ray diffraction data and IR spectra the two products had similar structural characteristics, only their water content differed slightly (Table II).

Table II

Analysis data

	Tungsram	Fluka
WO_3%	88.73	89.17
NH_3%	5.43	5.45
H_2O%	5.84	5.38
WO_3 moles	12.00	12.00
NH_3 moles	9.99	9.98
H_2O moles	10.17	9.32
Composition	$\approx 5(NH_4)_2O \cdot 12WO_3 \cdot 5H_2O$	$\sim 5(NH_4)_2O \cdot 12WO_3 \cdot 4.5H_2O$
Molecular weight	3133.52	3124.51

Combined TG and continuous IR spectrophotometric gas analytical measurements have confirmed that the samples yield WO_3 in six steps (Figs 3 and 4), and from the derivatograms (Figs 5 and 6) the same qualitative conclusions can be drawn.

Contrary to the decomposition of ammonium heptamolybdate.4-hydrate (paramolybdate) [7—9] the thermal decomposition steps of paratungstates are overlapping, which fact renders the qualitative and quantitative analysis of the process more difficult. Despite these

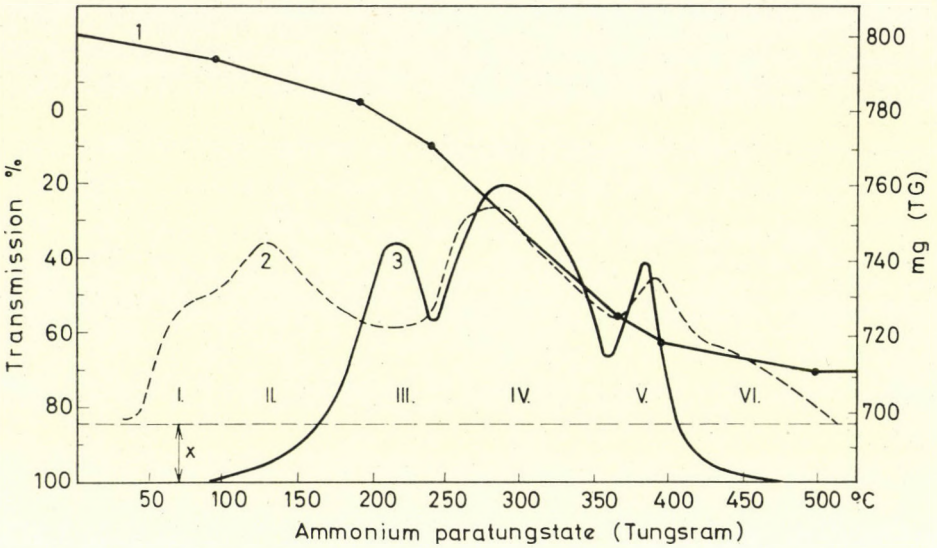

Fig. 3. Tungsram sample. 1. TG curve, 2. IR H_2O (C_2H_2) curve, 3. IR NH_3 curve, *x*. the equilibrium moisture content of the carrier gas

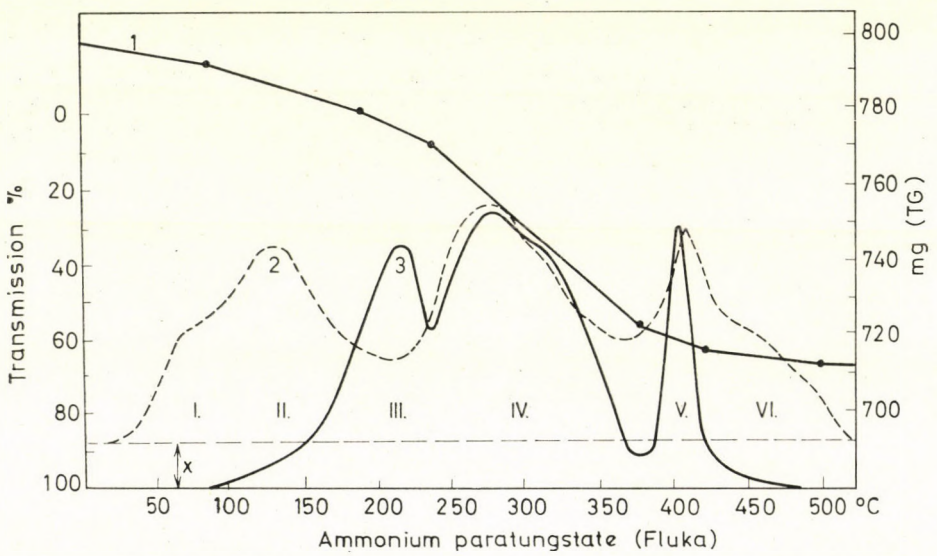

Fig. 4. Fluka sample. 1. TG curve, 2. IR H_2O (C_2H_2) curve, 3. IR NH_3 curve, x. the equilibrium moisture content of the carrier gas

difficulties the results of IR spectrophotometric gas analysis (Figs. 3 and 4) clearly indicate the order of appearance of NH_3 and H_2O with the temperature rise as well as the composition of the gas phase above the solid phase during the thermolysis* (Table III).

* On the basis of TG studies on 7-hydrates WANEK [3] concluded that between 240 and 380 °C NH_3 is released in one step and is not accompanied by H_2O. We have observed, however, several NH_3 maxima in the thermolysis curves of paratungstate 11- and 7-hydrates.

The amount of the gases formed can be estimated after redrawing Figs 3 and 4 [7, 8]. Figs 7 and 8 obtained this way express even better the facts given in Table II, and at the same time the slight differences between the decomposition of the tungstate products can also be observed. It is apparent that e.g. in the decomposition of the Fluka sample steps IV and V are almost separated in comparison with the Tungsram sample, and the variation of NH_3 concentration in the gas phase at step V shows a very sharp maximum. It is also apparent that the weight loss corresponding to step III is mainly due to the release of dry NH_3.

Knowing the total area below the maximum curves in Figs 7 and 8, and the total weight change data, obtained from the TG curves (see Table IV, Nos. 1. 2, 5 and 6), the spectrophoto-

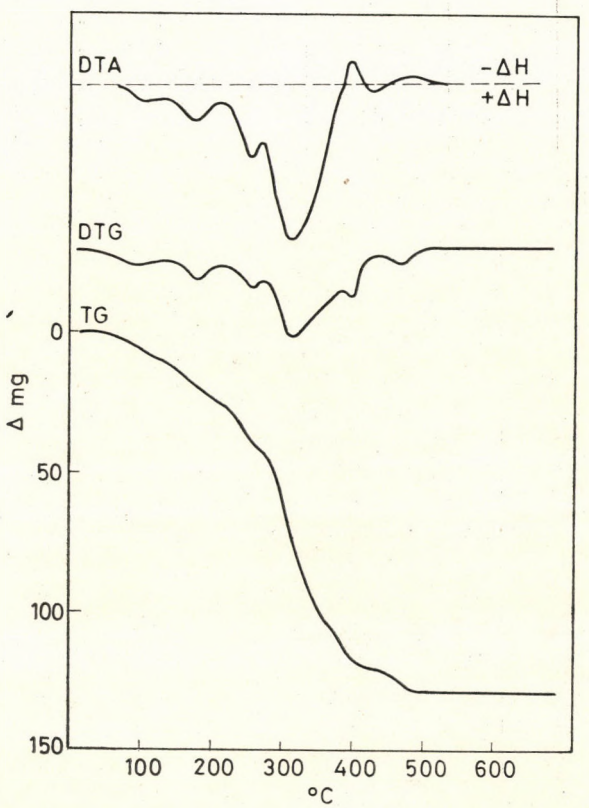

Fig. 5. Tungsram sample. Weight: 1.1790 g, DTA: 1/10, DTG: 1/5, TG: 200

Table III

Released gases

TG steps	I	II	III	IV	V	VI
Temperature range	20—130	70—170	100—280	190—390	340—480	460—450
Gas products	H_2O	H_2O	NH_3	NH_3+H_2O	NH_3+H_2O	H_2O

Table IV

Experimental conditions of the measurements and the planimetrically determined

No.	Sample mg	Δm mg	Flow rate lit/h	Heating rate °C/h	Gas measured	T'_1	T'_2
1	800	89.5	15.35	300	NH_3	—	—
2	800	89.5	15.01	300	C_2H_2	46.0	97.0
3	400		15.66	300	NH_3	—	—
4	800		15.52	150	NH_3	—	—
5	800	87,3	15.47	300	NH_3	—	—
6	800	87.3	15.55	300	C_2H_2	27.1	98.0

1—4: "Tungsram" paratungstate
5, 6: "Fluka" paratungstate

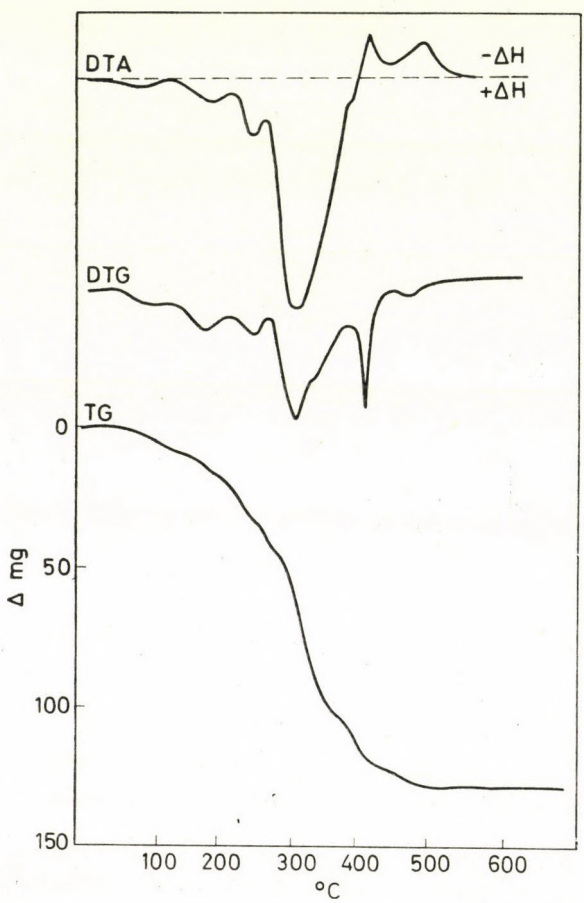

Fig. 6. Fluka sample, Weight: 1.1791 g, DTA: 1/10, DTG: 1/5, TG: 200

values proportiomal to the areas below the IR maxima absorption

T'_3	T'	T'_5	T'_6	$\Sigma T'_i$	Measured T(tot)	Difference
160.0	390.2	84.6	—	634.8	640.0 (T_1)	—5.2
—	252.5	50.5	22.2	468.2	472.5 (T_3)	—4.3
78.3	202.0	46.2	—	326.5	330.2	—3.7
156.0	398.0	84.0	—	638.0	635.3	+2.7
149.0	396.5	69.0	—	614.5	618.0 (T_1)	—3.5
—	241.7	55.0	26.8	448.6	455.0 (T_3)	—6.4

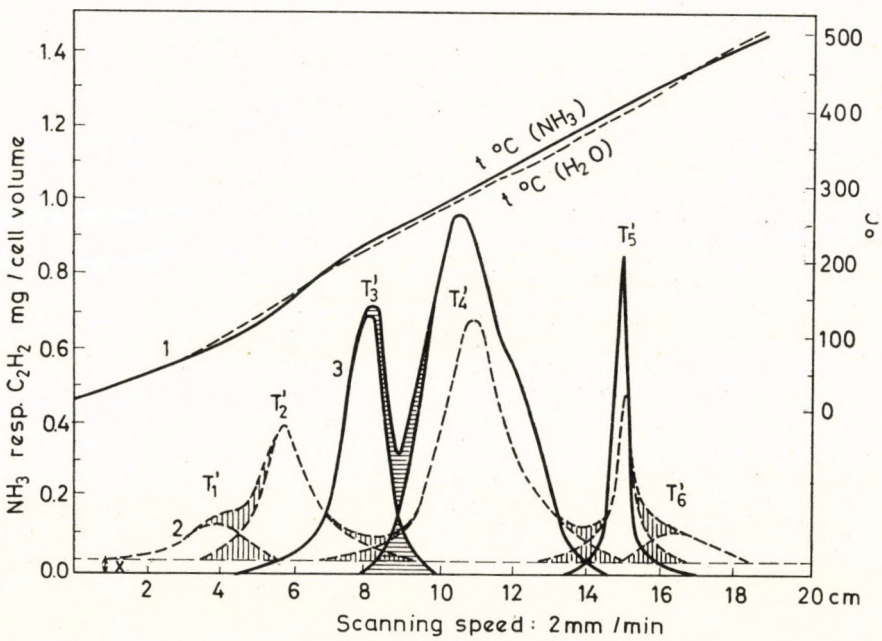

Fig. 7. Tungsram sample. 1. Heating rate, 2. H_2O (C_2H_2), 3. NH_3

metrically determined NH_3 and H_2O contents of the starting material were compared with those determined by chemical analysis. The following equations are valid [8]:

$$\frac{m_1}{m_2} = \frac{T_1 \cdot M_3 \cdot \eta_1 \cdot V_1}{n_L \cdot T_3 \cdot M_2 \cdot \eta_3 \cdot V_3} = K$$

$$m_1 = \Delta m \left(\frac{K}{K+1}\right) \qquad m_2 = \Delta m \left(1 - \frac{K}{K+1}\right)$$

or, in moles

$$N_1 = \frac{M_{pw} \cdot m_1}{G \cdot M_1 \cdot 1000} \qquad N_2 = \frac{M_{pw} \cdot m_2}{G \cdot M_2 \cdot 1000}$$

where

m_1 and m_2 denote the total amounts of NH_3 and H_2O (in mg) released;
Δm denotes the total weight change obtained from the TG curve;
T_1 and T_3 denote the total areas below the maximum curves of NH_3 and C_2H_2 (Table IV, meas. T_{tot});
η_1 and η_3 denote flow factors concerning the given experimental system and characteristic of NH_3 and C_2H_2 ($\eta_1 : \eta_3 = 1.155$) [8];
n_L denotes the apparent mole number ratio of the reaction between CaC_2 and H_2O ($n_L = 2.34$) [8];
V_1 and V_3 denote the flow rates of carrier gas at the measurement of NH_3 and H_2O (1 air/h);
M_1, M_2 and M_3 are the molecular weights of NH_3, H_2O and C_2H_2, respectively;
M_{pw} is the molecular weight of paratungstate;
N_1 and N_2 denote the number of NH_3 and H_2O moles in the starting substances;
G denotes the weight of the sample (g).

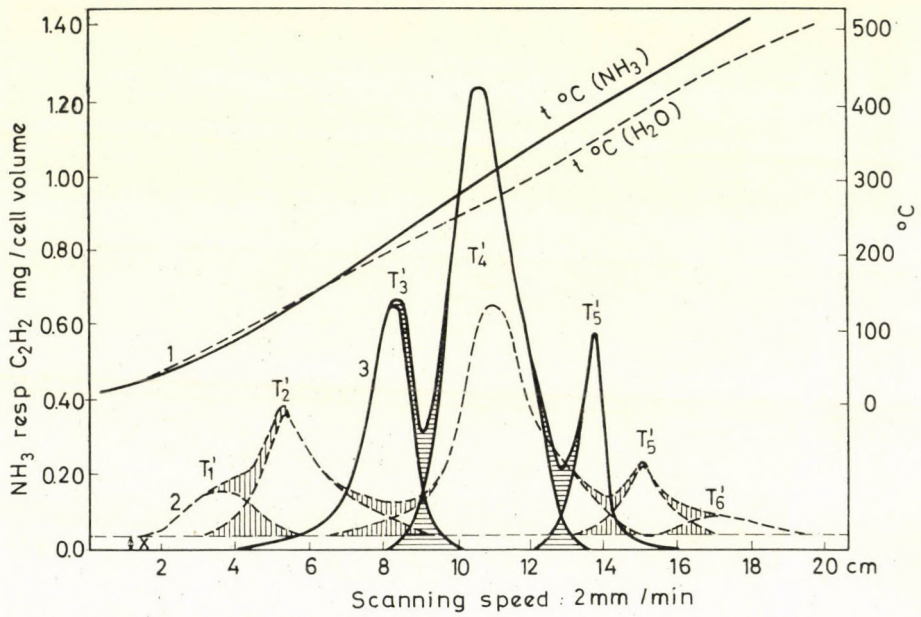

Fig. 8. Fluka sample. 1. Heating rate, 2. H_2O (C_2H_2), 3. NH_3

The good agreement between the data obtained by these expressions and by chemical analysis (Table V) indicates that the area below the IR maximum curves and the total amount of gas products formed are in a satisfactory correlation.

In the measurements of gas products formed in the consecutive steps it is a good approximation to assume that the maxima curves of NH_3 and H_2O are Gaussian. (After the minima of the curves of NH_3 and H_2O the preceding reaction causes nearly the same weight change as the next reaction has caused before the minimum.) The area below the overlapping maximum curves in Figs 7 and 8 was determined by planimetry (Table IV), and the mole numbers of

Table V

Comparison of the data obtained spectrophotometrically and by chemical analysis

Sample	NH_3 moles		Difference mole%	H_2O moles		Difference mole%
	Chemical anal.	IR spect. anal.		Chemical anal.	IR spect. anal.	
Tungsram	10	10.25	+2.50	10	9.83	—1.70
Fluka	10	9.79	—2.10	9.5	9.65	+1.58

NH_3 and H_2O released in independent processes were determined by the following equation [8]:

$$n_i = \frac{N \cdot T_i'}{\sum_{i=1}^{n} T_i'}$$

where n_i denotes the number of NH_3 and H_2O moles formed in the ith step, N denotes the number of NH_3 and H_2O moles in the starting substance, while T_i' is a number proportional to the area below the maximum curves corresponding to the ith step. The results are shown in Table VI.

Table VI

The amount of gaseous product (in moles) released in the reaction steps

No.	Gas product	n_1	n_2	n_3	n_4	n_5	n_6	$N = \Sigma n_i$
1	NH_3	—	—	2.52	6.15	1.33	—	10
2	H_2O	0.98	2.07	—	5.40	1.08	0.46	10
3	NH_3	—	—	2.41	6.19	1.40	—	10
4	NH_3	—	—	2.43	6.25	1.32	—	10
5	NH_3	—	—	2.42	6.45	1.12	—	10
6	H_2O	0.57	2.07	—	5.12	1.16	0.56	9.5

1—4: "Tungsram" paratungstate 5, 6: "Fluka" paratungstate

Since even in the case of different sample weights and heating rates, *i.e.* independently of the kinetic conditions of the reaction, the results, shown in Table VI, are nearly the same (and the same is true for the molecular weight values given in Table I), it is very probable that the data obtained are indeed characteristic of the decomposition process itself. From data in Table VI those in Table VII can readily be obtained. Table VII contains the composition related to 12 WO_3 and the molecular weight related to 1 WO_3 of the intermediate phases formed in the subsequent temperature ranges. The molecular weights given in this Table and corresponding data of Table I are in a good agreement.

Table VII

The composition of the phases

TG steps IR maxima	°C	$(NH_4)_2O$	WO_3	H_2O	Molecular weight related to 1 WO_3
Tungsram sample	20	5.0	12	5.0	261.1
I.	20—130	5.0	12	4.0	259.6
II.	70—170	5.0	12	2.0	256.6
III.	100—280	3.75	12	3.25	253.1
IV.	190—390	0.67	12	0.83	236.0
V.	240—480	—	12	0.5	232.6
VI.	460—550	—	WO_3	—	231.9

2. IR spectrophotometric and X-ray analytical study of the phase

Under the experimental conditions applied in the measurements yielding Figs 3 and 4, *i.e.* in crucible containing several hundred mg of sample, there are mixed phases present at the minima of the IR curves, due to the overlapping reaction steps. To avoid this, 30—40 mg of paratungstate samples were used, placed on a silica plate of 15 mm in diameter, forming a thin and evenly distributed layer. Samples were heated to a given temperature at a heating rate of 150 °C/h. After cooling the samples in a desiccator ower P_2O_5 the analyses were immediately started. In each successive procedure the final temperature was increased with 15—20 °C, and the structural changes of the phases were detected. Under these conditions the phases were formed within well defined temperature ranges. Both for spectrophotometry and for X-ray analysis sufficiently pure samples were obtained. The results obtained are summarized as follows:

20—180 °C range: apart from minor changes 4- and 2-hydrates retain their original crystal structure.
195—230 °C range: the structure is modified in step III (all W—O bands frequencies change in the IR spectra).
240—320 °C range: amorphous tungsten bronze is formed
320—350 °C range: some minor signs of the crystallization of ammonium bronze can be observed.
350—440 °C range: structural characteristics of WO_3 appear; according to IR spectra and gas analytical data hydrated WO_3 is formed.

Comparing the above structural transitions with the data taken from the literature, attention should be called to the phase transition observed around 200 °C. The change of diffraction pattern in the vicinity of 200 °C was also observed by AHN [2], but neither the composition nor the crystallographical characteristics of the phase formed in this temperature range were given. On the other hand, our observations — except the appearance of hydrated WO_3 — on the phases which occur during the ammonium tungsten bronze and WO_3 formations essentially agree with those published in the literature [1, 4, 5].

As far as structural changes are concerned, paratungstate samples of Fluka and Tungsram products behave identically. The only difference is that the bronze formed from Fluka tungstate is more crystalline in character in the temperature range between 320 and 350 °C. This latter might be the reason that the overlap of steps IV and V is smaller and that a separate NH_3 maximum is formed in step V (see Fig. 8).

The chemical composition of the sample prepared at 220 °C and stored in a desiccator over P_2O_5 was determined and the following result was obtained: $3.71\ (NH_4)_2O \cdot 12WO_3 \cdot 3.42\ H_2O$, which is in a good agreement with the composition corresponding to step III, given in

Table VII.* Taking also into account that the composition corresponding to step IV is also in a reasonable agreement with the composition of ammonium bronzes determined by other authors [1], the stoichiometric data given in Table VI can be accepted.

Since a more detailed study of the structural problems of ammonium paratungstate hydrates and of the intermediates formed from them is going to be published in a separate paper dealing with infrared spectroscopic investigations, this paper reports only the crystallographic and IR spectrophotometric features of the so far not isolated phase formed in step III, in comparison with the corresponding features of the starting material (Tables VIII and IX).

Table VIII

X-ray diffraction data

$5(NH_4)_2O \cdot 12WO_3 \cdot 5H_2O$			$3.75(NH_4)_2O \cdot 12WO_3 \cdot 3.25H_2O$		
$\sin^2\Theta \cdot 10^5$ obs.	$\sin^2\Theta \cdot 10^5$ calc.	hkl	$\sin^2\Theta \cdot 10^5$ obs.	$\sin^2\Theta \cdot 10^5$ calc.	hkl
560	556	001	563	563	001
818	821	111	832	840	111
1083	1090	$10\bar{1}$	1103	1107	$10\bar{1}$
1365	1379	$11\bar{1}$	1393	1398	$11\bar{1}$
1430	1412	120	1446	1429	120
1661	1688	121	1707	1713	121
2221	2220	002	2256	2252	002
2287	2304	300	2298	2271	$12\bar{1}$
2508	2505	012	2542	2541	012
3080	3070	122	3124	3123	122
3303	3319	122	3362	3366	$11\bar{2}$
3641	3625	230	3720	3726	$13\bar{1}$
3723	3696	$30\bar{1}$	3780	3785	$30\bar{1}$
4227	4190	$12\bar{2}$	4478	4495	103
4431	4414	103	4646	4656	040

X-ray diffraction data listed in Table VIII were obtained by the evaluation of Guiner-type measurements (Cu K_α radiation, KCl internal standard); the wave number values given in Table IX were obtained from the spectra of KBr disc samples.

On the basis of Table X one can see that the lattice parameters of Tungsram paratungstate are very close to those given in the literature [10], and the density ($\varrho = 4.41_5$) and the cell parameter values measured satisfy the requirements for $Z = 2$. In step III the partly dry release of NH_3 causes a change in the dimension and form of the cell. The measured density value of the sample prepared at 200 °C according to the above described process was found to be $\varrho = 4.66$. Taking the composition corresponding to this density and assuming an $(NH_4)_2O$ and WO_3 content that is the possibly nearest to this composition, or contains different integer numbers of said groups, the $(NH_4)_2O$:WO_3 ratio, however, kept nearly constant, the most likely Z-value was determined.

* Allowing to stand on air, the compound transforms into 5-hydrate; the $(NH_4)_2O$: WO_3 ratio and structural features remain unchanged.

On the basis of Table XI ratio $5(NH_4)_2O : 16WO_3$ can be disregarded. Although in all other cases the calculated Z-values are nearly integer numbers, ratios 4 : 13 and 8 : 26 should be distinguished. Assuming that molecules containing an odd number of WO_3-group are less probable, the most probable composition of the new phase is $8(NH_4)_2O \cdot 26WO_3 \cdot 7H_2O$, and the unit cell contains only one molecule.

Table IX

Characteristics of the infrared spectra

$5(NH_4)_2O \cdot 12WO_3 \cdot 5H_2O$ cm^{-1}	$3.75(NH_4)_2O \cdot 12WO_3 \cdot 3.25H_2O$ cm^{-1}	Assignment
702 vs, vb	721 vs, vb	ν W—O—W
745 sho		
765		
	800 w	W—OH, W—OH_2
818 s, b	828 s, b	
834 sho		
870 s, b	880 s, b	
918 s sh, p	928 s sh, p	terminal
934 b sh, p	942 b sh, p	ν W—O
951 sh, p	963 sh, p	
	1100 w, sh	W—OH, W—OH_2
1403 vs, sh	1408 s, sh	$\nu_4(F_2)$ NH_4^+
1468 sho		
1630 m	1645 w	δ OH (H_2O)
1678 w		NH_4^+ ?
2810 w	2825 w	$2\nu_4$ NH_4^+
2900 w	2885 w	?
3020 m, b	3035 m, b	$\nu_2 + \nu_4$ NH_4^+
3135 s, b	3150 s, b	$\nu_3(F_2)$ NH_4^+
3380 m, b		ν OH (H_2O)
3450 sho	3420 m, b w	ν OH (H_2O)
	3510 w	ν OH (W—OH)
	3615 w	ν OH (W—OH)

s: strong, sh: sharp, w: weak, b: broad, p: peak, sho: shoulder, v: very, m: medium

Table X

Crystallographic parameters

Sample	Unit cell parameters Å				Density	Number of molecules in the unit cell Z
	a	b	c	$\beta°$		
Hähnert Ref [10]	15.54	14.53	11.02	108.75	4.40	1.99 ≈ 2
Tungsram	16.419	14.356	11.151	111.67	4.415	2.06 ≈ 2
New phase	16.094	14.302	11.028	111.25	4.660	2.012 ≈ 2
						1.006 ≈ 1

Table XI

The most probable composition of the new phase

Possible compositions	Molecular weight	Z
$3.75(NH_4)_2O \cdot 12WO_3 \cdot 3.25H_2O$	3036.54	2.17
$4(NH_4)_2O \cdot 13WO_3 \cdot 3.5H_2O$	3285.96	$2.012 \approx 2$
$8(NH_4)_2O \cdot 26WO_3 \cdot 7H_2O$	6571.92	$1.006 \approx 1$
$5(NH_4)_2O \cdot 16WO_3 \cdot 5H_2O$	4061.20	1.628
$5(NH_4)_2O \cdot 16WO_3 \cdot 4H_2O$	4043.19	1.636
$4(NH_4)_2O \cdot 12WO_3 \cdot 3H_2O$	3045.04	2.171

Discussion

Summarizing the results obtained, the transformation of ammonium paratungstate · 5–hydrate to WO_3 in air is the following:

$$5(NH_4)_2O \cdot 12WO_3 \cdot 5H_2O \xrightarrow[20-130\,^\circ C]{-H_2O} 5(NH_4)_2O \cdot 12WO_3 \cdot 4H_2O$$

$$\xrightarrow[70-170\,^\circ C]{-2H_2O} 5(NH_4)_2O \cdot 12WO_3 \cdot 2H_2O \xrightarrow[100-280\,^\circ C]{-2 \cdot 5NH_3}$$

$$3.75(NH_4)_2O \cdot 12WO_3 \cdot 3.25H_2O \xrightarrow[190-390\,^\circ C]{-(3.08(NH_4)_2O+2.42H_2O)}$$

$$0.67(NH_4)_2O \cdot 12WO_3 \cdot 0.83H_2O \xrightarrow[340-480\,^\circ C]{-(0.67(NH_4)_2O+0.33H_2O)}$$

$$12WO_3 \cdot 0.5H_2O \xrightarrow[460-550\,^\circ C]{-0.5\ H_2O} \text{orthorhombic } WO_3 .$$

On the basis of Figs 7 and 8 as well as Tables VI and VII it can be established that in steps I, II and III phases of the same structure and composition are formed from both substances. Consequently, these processes are generally characteristic of paratungstate 5-hydrates.

On the other hand, differences can be found in the formation and decomposition of ammonium tungsten bronzes of slightly different composition ($0.67—0.56\,(NH_4)_2O \cdot 12WO_3 \cdot 0.6—0.5H_2O$). It is well known, however, that bronzes are non stoichiometric compounds, and a given type of crystal structure may exist over a reasonably wide range of composition [1]. The kinetic differences to be seen on Figs. 5 and 6 are most likely due to differences in crystalline character and in the morphological features of predominantly amorphous phases.

The difference between the composition of the bronzes obtained by IR gas-analytical method probably has a connection with the exothermic process indicated by the DTA curves. This process may be due to the combustion of a small amount of ammonia. With the Fluka tungstate the exothermic peak and the temperature corresponding to the maximum is higher. With the Tungsram tungstate the amount of oxidized ammonia may not be significant because, according to Table V, there is no loss in ammonia at the composition calculated from the total area of the IR peaks. With the Fluka tungstate, although the data of Table V are still within the experimental error, the sign of the percentage error is reversed, which fact may be related to the slightly higher exothermic peak in the DTA curve of Fig. 6. This effect may slightly modify the composition determined for the Fluka bronze by spectrophotometric method, and may bring it closer to the composition of Tungsram sample.

The derivatograms are in accordance with our previous TG studies and with the present IR data. In Figs 3 and 4, and in the DTG curves of Figs 5 and 6 the shoulder which appears at step IV is not connected to the incidental formation of a new substance, more precisely, there could not be found a convincing proof for it, due to the predominantly amorphous structure. Since in this step, to some extent, crystallization of bronzes takes place [4, 5], which may affect the reaction rate, it seems to be evident that the shoulder is due to this effect. This conclusion is also supported by the fact that the bronze formed from the Fluka sample is more crystalline, and, at the same time, the shoulder found in the IR curve is more pronounced. (See Fig. 6.)

Processes in which H_2O and/or NH_3 are released are endothermic, regardless of the rearrangement of the crystal lattice. The same was found in the solid phase polycondensation reaction of ammonium heptamolybdate.4-hydrate [9]. The exothermic peak in the range of 460—480 °C is due to $WO_{3(\text{disordered})} \rightarrow WO_{3(\text{ordered})}$ transition.

The evolution of NH_3 on its own or together with water vapour suggests the assumption that there may be two different decomposition processes for the WO_6 groups of paratungstate anion compensated by NH_4^+ ion. Although, relying on the principle of uniform charge distribution of ionic crystals, there is no reason so far to assign NH_4^+ ions to certain oxygen atoms of the WO_6 octahedrons, as a working hypothesis, however, the conditions can be simplified according to the following scheme: —

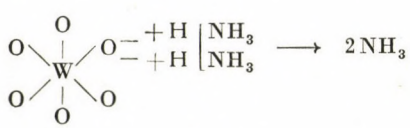

1. a

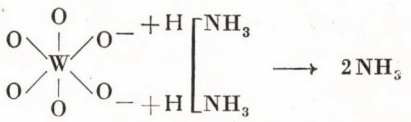

1.b

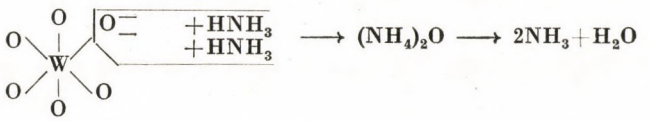

2

The changes in the spectra, given in Table IX, show a couple of features supporting the assumption that the phase of modified structure formed in step III contains —OH or OH_2 groups, coordinated to the metal. So, *e.g.* the shift of the bands toward higher wave numbers in the ν OH region, and the appearance of small individual maxima at 3510 and 3615 cm^{-1}, can generally be explained by the decreased strength of hydrogen bonds or, possibly, by the formation of free OH [11, 12] or W—OH [13—15] groups. The appearance of maxima at 1100 and 800 cm^{-1} is also consistent with the above assumption; these frequencies can generally be assigned to δ M—OH [11, 12, 16] and ϱ M—OH_2 [12, 16] vibration modes. Moreover, the shift of δ OH from 1630 to 1645 cm^{-1} may be characteristic *e.g.* of the deformation vibration of OH_2 groups coordinated to the metal [12].

Among the structural problems of hetero- and isopolyacids and their salts, *e.g.* paratungstates, the nature, bonding relations and crystallographic position of H_2O, OH, H_3O^+ and the basicity of the polyacids are among the most widely discussed issues. The structure of paratungstate anion was determined by LINDQVIST [17], in $5Na_2O \cdot 12WO_3 \cdot 28H_2O$. It has been established that the previously assumed [18] $[W_{12}O_{41}]^{10-}$ structure is incorrect, and, in fact, the structure of the anion is $[W_{12}O_{46}]^{20-}$. This structure, however, requires the protons to be bound to the anion (*e.g.* $[H_{10}W_{12}O_{46}]^{10-}$). The problems arising here have not been solved by LINDQVIST.

On the basis of IR and proton magnetic resonance measurements GLEMSER [19, 20] and SCHWARZMANN [21] concluded that the ten H-atoms are not acidic, and are present as OH groups. Based on this finding, the recently accepted structure is $Na_{10}[W_{12}O_{36}(OH)_{10}]23H_2O$. On the other hand, LIPSCOMB [22] has pointed out that on the basis of LINDQVIST's data besides $[W_{12}O_{46}]^{20-}$ other structures, *e.g.* $[W_{12}O_{42}]^{12-}$ can also be assumed. This latter assumption is also supported by recent X-ray studies of WEISS [23] on ammonium paratungstate.11-hydrate. In the case of 7- and 5-hydrates neither the position of tungsten atoms, nor their mode of bonding to the light atoms have been determined. Only the size and the symmetry of the unit cell are known [10, 24].

Insofar as the GLEMSER—SCHWARZMANN formula was regarded as general, 11-, 7- and 5-hydrates should have the following general composition:

$$5(NH_4)_2O \cdot 12WO_3 \cdot nH_2O = (NH_4)_{10}[W_{12}O_{36}(OH)_{10}]mH_2O$$

where n = 11, 7 or 5 and m = 6, 2, or 0.

HÄHNERT [10] reasoned on the basis of this formula that paratungstates containing less than five molecules of water, in analytical sense, cannot be precipitated aqueous solutions.

Consequently, 5-hydrate and its dehydrated products would not contain water molecules at all. This, however, contradicts our experimental findings, that water is released already at 25—30 °C. This could not be explained if the substance contained water only structurally. In such a case the oxygen atom of H_2O should be released from the lattice of the anion, and the considerable oxygen loss due to this process would result in the collapsing of the crystal lattice. We have found, however, that H_2O is released without structural changes in steps I and II. The distinct appearance of δOH frequencies in the spectrum at 1630 and 1645 cm^{-1} (Table IX), which frequencies characterize exclusively the deformation modes of H_2O molecules, is also a decisive proof. Consequently, it is obvious that the formula assumed by GLEMSER and SCHWARZMANN as well as, to certain extent, by HÄHNERT [25] can by no means hold in the case of 5-hydrates; and the experimental results should rather be interpreted on the basis of the LIPSCOMB—WEISS structure. It is, however, still an open question whether the protonated structure $[H_2W_{12}O_{42}]^{10-}$ or the structure — corresponding to GLEMSER's principle — $[W_{12}O_{40}(OH)_2]^{10-}$ is present.

The low temperature corresponding to step I as well as the stoichiometric differences found between tungstates of different products indicate that in 5-hydrates 1 mole or less amount of mobile water, bonded with absorption or capillary forces, is present. Step II indicates the presence of 2 moles of water of crystallization. The process of step III can less easily be accounted for. It should be assumed that in the outer coordination sphere of the ion the W—O^- . . . NH_4^+ groups, which are bonded with different energies, which in one case result in the thermal dissociation of NH_4^+ ions, in other cases to the splitting of $(NH_4)_2O$ groups containing an oxygen atom from the lattice.

The question necessarily emerges whether the hydrogen atoms remaining after the thermal dissociation of NH_4^+ ions are acidic hydrogens or they form W—OH groups bonded with covalent forces. One might decide on the basis of the following consideration. In hetero- and isopolyacids, so, in principle in the paratungstic acid not isolated so far, the analytically determinable water content consists of two parts: — 1. Salt 'forming water', the amount of which is exactly defined by the basicity of polyacids, 2. Water content independent of salt formation, which can be either H_2O bonded with forces of different nature

or OH or OH_2 groups, bonded with covalent forces, taking part in the structure of the polyanion.

If it is assumed that the residue is acidic hydrogen, the structure of the anion ought not to change, because in this case the degree of polycondensation, compared to the basic substance, does not change either, and it is known that in this step structural water is not released. Let us measure the degree of condensation by the ratio $\alpha = (NH_4)_2O : WO_3$, which ratio in turn, implicitly implies the change of charge with respect to 1 mole of WO_3. In this case, should acidic hydrogen remain, the following expressions will be equivalent, as far as the charge with respect to 1 mole of WO_3 is concerned: —

$$\alpha_{(5\text{-hydrate})} = \frac{[10NH_4^+ + 50^{2-}]}{[12WO_3]}, \quad \text{and}$$

$$\alpha_{(\text{step III})} = \frac{[7.5NH_4^+ + 3.5H^+ + 50^{2-}]}{[12WO_3]},$$

i.e. the extent of condensation will not change. Consequently, there would be no reason for a structural rearrangement.

According to the data of Table IX, however, the stretching frequencies of the terminal W—O groups as well as the ν_3 (F_2) frequency of NH_4^+ ion are shifted towards higher values, which facts are typical of changes in crystal structure connected with increasing degree of condensation [26]. The shifts in the spectrum given in Table IX, consequently, confirm the existence of a phase, containing covalently bonded OH groups. The phase is characterized by the ratio $\alpha = 3.75(NH_4)_2O : 12WO_3$.

The change of the condensation degree with α or $1/\alpha$ is also supported by the continuous shift of the phase density values. In Fig. 9 the densities of phases of different structure and the corresponding α values appear to be in a functional relationship, because the density value at a given composition of the phase belonging to step III, as well as that of a tungsten bronze fit well the plot drawn in Fig. 9.

Finally, it should be noted that also in the case of paratungstate → WO_3 reaction in the solid state, the word "thermolysis" is not quite adequate to characterize the process, it should rather be termed as a thermal polycondensation reaction, or as a thermocondensation. This terminology was also followed in our previous publications [9, 27].

Our further concern is to clarify the structure of paratungstate·5-hydrate and intermediate substances formed from it, by means of deuterium exchange and IR spectrophotometry.

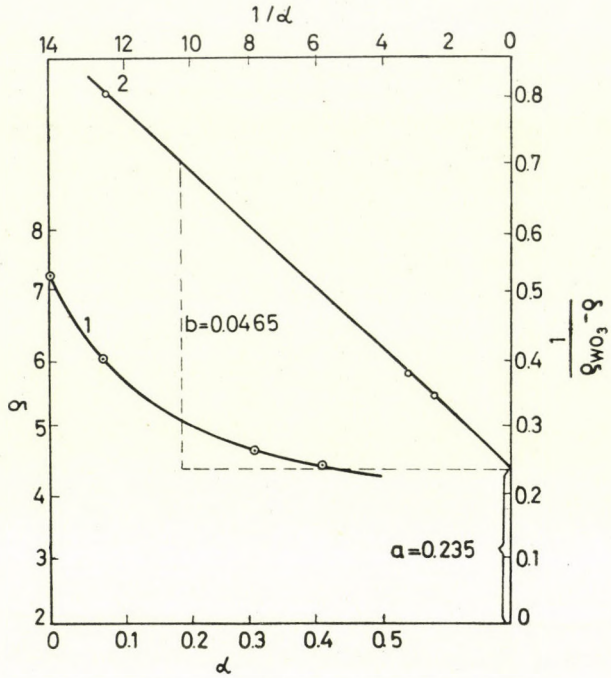

Fig. 9. The density variation of the phases

	α	ϱ
5-hydrate	0.416	4.415
substance of step III (220 °C)	0.312	4.66
ammonium bronze (350 °C)	0.081	6.04
WO_3	0.0	7.29 [28]

$$1.\ \varrho = \varrho_{WO_3} - \frac{1}{a + b/\alpha}$$

$$2.\ \frac{1}{\varrho WO_3 - \varrho} = a + b/\alpha$$

REFERENCES

1. NEUGEBAUER, J., HEGEDÜS, A. J., MILLNER, T.: Z. anorg. allg. Chem. **302,** 50 (1959); M. T. A. Kém. Tud. Oszt. Közl. **12,** 37 (1959)
2. AHN, J.: Bull. Chem. Soc. Japan **8,** 254 (1961)
3. WANEK, W.: Silikaty **6,** 70 (1962)
4. KOHLSTRUNG, G.: Phys. Stat. Sol. **2,** 85 (1962)
5. HENKES, H.: Phys. Stat. Sol. **9,** k 105 (1965)
6. HEGEDÜS, A. J., KISS, B. A.: Acta Chim. Acad. Sci. Hung. **51,** 251 (1967)
7. KISS, B. A.: Acta Chim. Acad. Sci. Hung. **61,** 207 (1969)
8. KISS, B. A.: Acta Chim. Acad. Sci. Hung. **63,** 243 (1970)
9. KISS, B. A., GADÓ, P., ASZTALOS, I., HEGEDÜS, A. J.: Acta Chim. Acad. Sci. Hung. **66,** 235 (1970); Magy. Kém. Foly. **76,** 358 (1970)
10. HÄHNERT, M.: Z. Krist. **120,** 216 (1964)
11. GLEMSER, O.: Angew. Chem. **73,** 785 (1961)
12. HENNING, O.: Wissenschaftliche Zeit. der Hochschule für Architektur und Bauwesen, Weimar **15,** 53 (1968)
13. YUKHNEVICH, G. V.: Russ. J. Inorg. Chem. **4,** 656 (1959)

14. BABUSKIN, A. A.: Izv. Akad. Nauk. SSSR. Ser. Fiz., **22,** 1131 (1959)
15. BABUSKIN, A. A., YUKHNEVICH, G. V., BEREZKINA, Y. F., SPITSYN, V. I.: Zhur. Neorg. Khim. **4,** 823 (1959)
16. NAKAMOTO, K.: Infrared Spectra of Inorganic and Coordination Compounds, John Wiley Publ. Co. London, 1963, pp 157 and 159
17. LINDQVIST, I.: Acta Cryst. **5,** 667 (1952)
18. SADDINGTON, K., CAHN, R. W.: J. Chem. Soc., 3526 (1950)
19. GLEMSER, O., SCHWARZMANN, E.: Naturwissenschaften **50,** 300 (1963)
20. GLEMSER, O., HOLZNAGEL, W., HÖLTJE, W., SCHWARZMANN, E.: Naturforschung, Band **20***b*, 725 (1965)
21. SCHWARZMANN, E.: Naturwissenschaften **50** 1 (1963)
22. LIPSCOMB, W. L.: Inorg. Chem. **4,** 132 (1965)
23. WEISS, G.: Z. anorg. allg. Chem. **368** 279 (1969)
24. HÄHNERT, M.: Berichte der Geologischen Gesellschaft, Heft 1, 64 (1961)
25. HÄHNERT, M.: Z. anorg. allg. Chem. **318,** 222 (1962)
26. KISS, B. A., HOLLY, S., HILD, E.: Acta Chim. Acad. Sci. Hung., **72,** 147 (1972)
27. HEGEDÜS, A. J., GADÓ, P., SCHLOSSER, G., NEUGEBAUER, J.: Acta Chim. Acad. Sci. Hung., **66,** 349 (1970) and M.T.A., MÜ.T.I.Közl. **0—2,** 143 (1969):
28. GEBERT, ACKERMANN, R. Inorg. Chem. **5,** 136 (1966).

András B. KISS
Pál GADÓ
András J. HEGEDÜS
Budapest IV., Váci út 77.

Acta Chimica Academiae Scientiarum Hungaricae, Tomus 72 (4), pp. 393—406 (1972)

ADSORPTION OF WATER VAPOUR ON THE CHEMICALLY TREATED SURFACE OF A GERMANIUM SINGLE CRYSTAL

J. GIBER,* M. WÉGNER* and O. DOBIS**

(Tungsram United Incandescent Lamp and Electrical Co., and ** Central Research Institute for Chemistry of the Hungarian Academy of Sciences)*

Received December 4, 1970

The interaction of water vapour with the surface of germanium single crystals, etched in alkaline H_2O_2 solution, was investigated. Using volumetric and tritium tracer techniques the amount of water adsorbed on the surface was measured as a function of temperature (between 16—80 °C), adsorption time and relative humidity (up to 0.8). The adsorption equilibrium is reached in 10 hrs. The adsorption isotherms in the 50—80 °C temperature range can be described by Freundlich's equation giving a value of 155×10^{-9} g/cm² for monolayer coverage of the surface. This adsorption has a "weak" chemisorption character, the isosteric heat of adsorption varies with the coverage between 13 and 23 kcal/mol. The kinetic results point to a diffusion controlled process in which the oxide layer becomes saturated with water vapour. The diffusion model leads to a diffusion coefficient of 5.8×10^{-18} cm²/sec at 80 °C. The activation energy of diffusion is about 4 kcal/mol, in good agreement with the apparent activation energy calculated from the kinetic curves of water vapour adsorption.

1. Introduction

The process of interaction between water vapour and the surface of germanium crystals or germanium dioxide powders has been studied by numerous authors [1—9]. Experiments have been carried out mostly on powdered samples of germanium [1, 3—6, 8, 9]. The surface was subjected to various physical treatments but only PRUDNIKOV and KISELEV [6] have employed chemical etching before adsorption. As regards to the mechanism of water adsorption on a real germanium surface covered by a thin oxide layer, SRINIVASAN *et al.* [4] have assumed a donor-acceptor interaction. KISELEV and PRUDNIKOV [7, 9] supposed the same mechanism on etched germanium surfaces. On the basis of ESR and NMR studies it was concluded that water adsorption at a coverage of $\Theta = 1$ takes place in the form of multilayers at located pits [9]. PRAVDIC, MCCAFFERTY and ZETTLEMOYER [8] have examined the conditions of water chemisorption on oxide coated germanium surfaces, as a function of the bulk carrier concentration.

The investigations reported in this paper are primarily concerned with the adsorption of water vapour on chemically etched surfaces of germanium single crystals over a wide range of temperature and relative humidity, in an atmosphere of purified N_2. The amount of adsorbed water was measured in the

'equilibrium' state and also as a function of time. The purpose of the kinetic study of water adsorption was to determine the mechanism of the overall process.

2. Experimental

The germanium samples were in the form of rectangular, $2\times2\times0.3$ mm slabs. They were cut from an N-type ingot parallel to the (111) face and polished on both sides with an aqueous suspension of silicon carbide powder. The ingot resistivity was 1.5 ± 1 Ohmcm and had a dislocation density in the range of 3000—5000 cm^{-2}.

The germanium plates were etched in alkaline hydrogen peroxide solution [250 ml hydrogen peroxide ($d_{15} = 1.104$) + 2 ml 25% (by weight) aqueous KOH solution]. The chemical

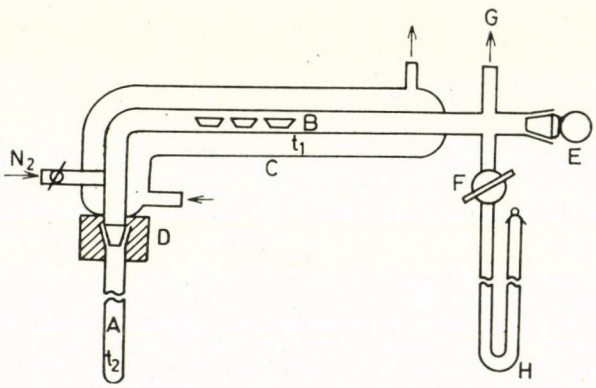

Fig 1. Apparatus for the measurement of water adsorption

etching was continued for 30 min at 110 °C under vigorous stirring. After washing and rinsing the samples in distilled water (conductivity 10^{-6} Ohm^{-1} cm^{-1}), they were baked for 100 hrs at 110 °C in purified air, then the temperature was raised to 300 °C for 10 hrs in vacuum (10^{-4} Torr).

The chemical treatment has removed from the surface all the abrasive layers created by polishing. It was controlled by measuring the homogeneity of X-ray diffraction. The thickness of the GeO_2 layer was found to be $(30 \pm 2)\times10^{-8}$ cm by ellipsometry.

The examination of the treated surface with an electron microscope has shown that the oxide layer on the surface of germanium is plane and compact. The specific surface area of the samples was determined by the BET method from low-temperature adsorption of krypton, and the roughness factor (r = specific surface/geometrical surface) was found to be 1.2—1.3.

Water adsorption was measured by the volumetric method [11, 12] in the relative humidity range $0.01 < p/p_0 < 0.3$ at 16 °C and by a method using tritium labelled water in the range $0.1 < p/p_0 < 0.8$.

With the radioactive tracer method the adsorption process was carried out in an atmosphere of purified nitrogen, at constant temperature (t_1) and relative humidity (p/p_0). A scheme of the apparatus is shown in Fig. 1. Containers with the germanium samples were placed into tube B maintained on temperature t_1. Tritiated water in reservoir A was thermostated at t_2 determining the vapour pressure (p) of the system ($t_1 > t_2$). Block D heated the nonthermostated parts of the system. Stopcock F and trap G were used for adjusting the atmospheric pressure and for quick setting of p/p_0. This static system maintains a controlled relative humidity up to 0.8.

The adsorption process was finished by removing the containers and pouring the germanium samples into arm 2 of the ampoule shown in Fig. 2, by fitting ground joint 3 to the open

end E of the adsorption apparatus. Then the ampoule was quickly connected to a vacuum system through ground joint 3 and immersed into liquid nitrogen. After a few minutes of cooling, it was evacuated to 10^{-4} Torr and sealed off at the side-pipe.

To determine the amount of water vapour adsorbed on germanium sample the tritiated water was converted into the form of tritiated hydrogen. Arm 1 of the ampoule was filled with a known amount of fresh aqua regia degassed twice in high vacuum under cooling with liquid nitrogen and the ampoule was sealed off at the side-pipe. Then the break-seal 6 was opened and aqua regia was distilled into arm 2 cooled with liquid nitrogen. The distilled aqua regia was a ring-shaped layer of frozen solid about 1 cm above the germanium samples. On rapid heating the ring dropped upon the samples which dissolved therein, with intense hydrogen evolution in 30 min.

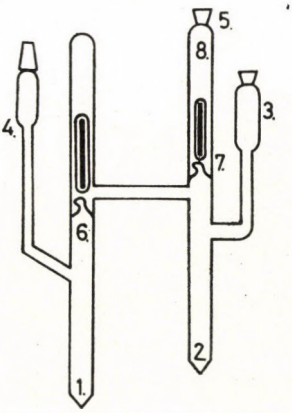

Fig. 2. Ampoule for the measurement of water adsorption

After the above operations, the ampoule was connected to the vacuum system through joint 5, break-seal 7 was opened and hydrogen was pumped into a GM counter of internal filling.

Hydrogen evolution may be interrupted by freezing at any stage of the dissolution. This method was applied for checking experimentally the stationarity of the specific radioactivity of the hydrogen formed. It seems that the tritium exchange is carried out before the evolution of hydrogen and the process of solution of germanium does not influence the specific radioactivity of tritiated hydrogen.

The adsorbed radioactive water vapour can also be converted into methane in a more convenient way. If arm 1 contains a known amount (about 1 g) of acetic acid with 0.1 weight per cent of acetic anhydride and the germanium samples are poured into this solution, after degassing, sealing-off and immersing it in a hot bath, the water will be completely desorbed within two hours. (The acetic anhydride content of acetic acid reacts to the desorbed water.) If arm 2 contains an adequate amount of degassed methylmagnesium iodide, then a few drops of acetic acid may distil into arm 1 on opening break-seal 6. The specific radioactivity of the methane formed will be the same as that of acetic acid.

The two methods of desorption give the same results with a deviation 3%.

The specific radioactivity of water in reservoir A was measured with a Packard liquid scintillation instrument which was correlated to the GM counters by the acetic acid method.

The amount of water adsorbed on the surface of germanium samples is proportional to the ratio of its specific radioactivity and the specific radioactivity of water in reservoir A:

$$a = \frac{G}{F \cdot r} = \frac{I \cdot S}{I_0 - I} \cdot \frac{1}{F \cdot r} \approx \frac{I \cdot S}{I_0 \cdot F \cdot r}$$

where

a: amount of water adsorbed on unit surface area, g/cm^2;
G: amount of water adsorbed by the surface of germanium samples, g;

F: geometric surface of the germanium sample, cm^2;
r: roughness factor;
S: the amount of hydrogen equivalent to the desorbing solvent, g;
I_0: specific radioactivity of water in reservoir A, cpm/Torr;
I: specific radioactivity of hydrogen or methane formed during the dissolution of the germanium sample, cpm/Torr.

The high sensitivity of the radioactive tracer method allowed carrying out the adsorption measurement on germanium samples with surface areas of 3—4 cm^2.

The vapour pressure and temperature can be accurately adjusted in the experimental system, whereas the measurement of the roughness factor and the radioactivity of adsorbed water give a $\pm 10\%$ standard deviation.

The results of the two different methods at 16 °C are in good agreement in the relative humidity range of 0.1—0.3 and point to a negligible isotope effect, as shown in Table I.

Table I

Amount of water (a_∞) adsorbed on unit area of the etched germanium surface, at "equilibrium" at 16 °C and different relative humidities (p/p_0)

p/p_0	$a_\infty \times 10^9$ (g/cm²) (volumetric method)	$a_\infty \times 10^9$ (g/cm²) (tracer method)
0.007	1.2	—
0.022	2.6	—
0.029	4.0	—
0.051	5.2	—
0.073	7.1	—
0.103	9.5	8.0
0.147	12.0	11.0
0.206	14.0	13.2
0.250	16.4	14.8
0.301	18.4	16.8

3. Isotherms of water vapour adsorption

For the purpose of determining the isotherms and isobars of adsorption, the amount of adsorbed water on the chemically etched surface of the germanium single crystal was measured by the radioactive tracer method, at various relative humidities and temperatures. The results are summarized in Table II. The values for the adsorbed amount of water in Table II are the average of 6—9 measurements during adsorption times ranging from 10 to 25 hrs, which is required for the process to reach the "equilibrium".

The data in Tables I and II yield five isobars with maximum adsorption at 50 °C, as shown in Fig. 3. The shape of isobars points to the existence of an activated adsorption process in which thermodynamic equilibrium is reached above 50 °C. Since the state of thermodynamic equilibrium can rarely be reach-

Table II

Amount of water adsorbed (a_∞) on unit area of the etched germanium surface at "equilibrium", at different temperatures and relative humidities (p/p_0)

p/p_0	$a_\infty \times 10^9$ (g · cm^{-2})				
	30 °C	50 °C	60 °C	70 °C	80 °C
0.10	40.8	70.0	65.4	49.7	30.9
0.30	50.4	90.5	81.5	68.9	52.0
0.50	52.9	104.5	97.7	88.0	79.6
0.65	64.0	113.0	106.5	97.5	88.8
0.80	70.5	122.5	116.5	109.0	99.0

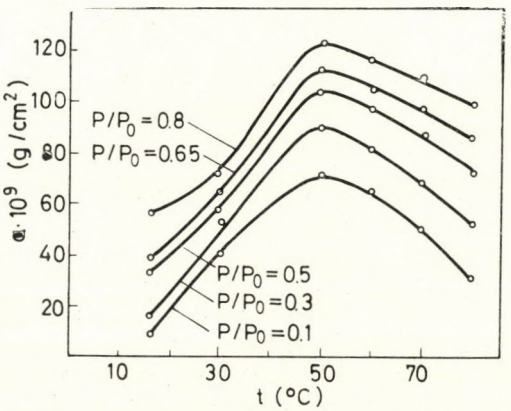

Fig. 3. Isobars of water vapour adsorption on etched germanium surfaces

ed in case of 'strong' chemisorption, we may suppose 'weak' chemisorption which prevails at low coverage followed by physical adsorption at higher coverages of the surface. The predominant process at 16 °C is physical adsorption: using the volumetric method, this has been proved by readsorption isotherms which are identical with the adsorption data within experimental error. The isotherms measured at 50, 60, 70 and 80 °C can be described by Freundlich's equation as shown in Fig. 4. The ordinate belonging to the intersection of the four straight lines gives the amount of adsorbed water at monomolecular coverage (a_0) of the surface. Using the least squares method one obtains: $a_0 = (155 \pm 14) \times 10^{-9}$ g · cm^{-2}. (Monomolecular coverage is an unrealistic state since the system is highly supersatureted with water vapour.)

Our results are in a good agreement with those in the literature. Comparison is made in Table III. Different germanium samples treated in a similar way give nearly identical isotherms at given parameters.

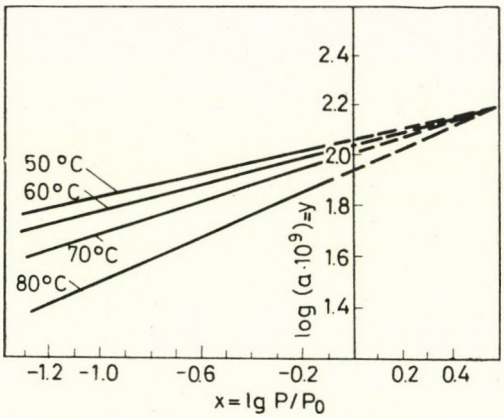

Fig. 4. Isotherms of water adsorption on the etched germanium surface plotted according to the parameters of Freundlich's equation

Table III

Comparison of water adsorption values on real germanium surfaces given by different authors

$a \times 10^9$ (g · cm^{-2})	P/P_0	t^* (°C)	R**	Vacuum treatment at (°C)	Germanium sample	Ref.
9.0 16.7	0.1 0.3	20		200	Ge powder etched in H_2O_2 and NaOH, N-type, $\varrho = 35$ Ohm · cm	[7]
		25	0.6	300	Ge powder, N-type, $\varrho = 0.14$ Ohm · cm	[4]
8.9 16.5	0.1 0.3	16 30	0.54 1.11	300	Ge plates etched in H_2O_2 and KOH, N-type, $\varrho = 1$ Ohm · cm	this work

* Temperature of adsorption measurements
** R = water area/argon area (The BET equation was applied to calculate the R values.)

The isosteric heat of adsorption, Q_i, is a logarithmic function of the amount of water adsorbed by unit area of the surface. This is characteristic of adsorption processes obeying Freundlich's equation. As is shown in Fig. 5, the isosteric heat of adsorption ranges from —23.3 kcal/mol (at a coverage of 0.36, corresponding to a rather high contribution of chemisorbed water vapour) to —13.3 kcal/mol (at a coverage of 0.71). The dependence of the heat of adsorption on the coverage points to chemisorption at $\Theta < 0.5$. The Q_i values calculated from calorimetric measurements [6] are much lower than ours. This may be caused by different contributions from chemisorption due to differences in the surface treatments and temperature.

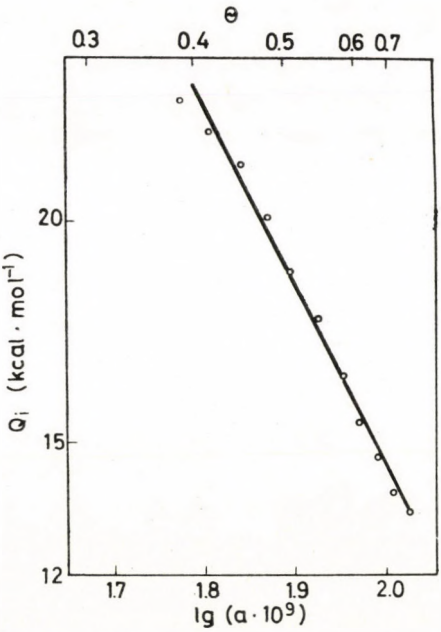

Fig. 5. Dependence of the heat (Q_i) of isosteric adsorption on the coverage (Θ) (upper scale) and on the amount of water adsorbed on unit area of the germanium surface (lower scale)

4. Kinetics of the interaction of water vapour with the etched germanium surface

Water adsorption is a time dependent process during the first 8-hour period. This period is sufficient for following the whole process as a function of time by the radioactive tracer method. The kinetic curves of water adsorption at four values of relative humidity and at 80 °C are shown in Fig. 6. The kinetics of the adsorption process were also measured at 50, 60 and 70 °C. This time dependent process cannot be described by a logarithmic rate equation valided for activated adsorption on heterogeneous surfaces. The relationship between Θ and $\ln(\tau + \tau_0)/\tau_0$, where τ denotes the time of the process, is not linear and the rate of adsorption does not increase unambiguously with the temperature. The calculated apparent energy of activation is about 4—7 kcal/mol and has no dependence on the coverage. The amount of adsorbed water vapour, a_τ, divided by that adsorbed at equilibrium, a_∞, is independent of the relative humidity, as checked in a wide range of p/p_0 at 80 °C. Therefore the kinetic measurements at other temperatures were carried out only at $p/p_0 = 0.50$ with a few control runs at other values of p/p_0. The results of kinetic measurements are summarized in Table IV (the range of adsorption times was 0.5—10 hrs).

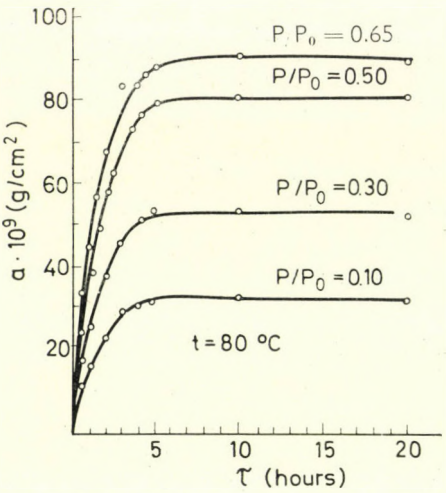

Fig. 6. Kinetics of water adsorption on the etched germanium surface at 80 °C

The features described above are not characteristic of pure adsorption processes. So we may suppose that the rate controlling step is not chemisorption but diffusion of water vapour through the oxide layer toward the boundary surface of germanium. The interpretation of the diffusion process in a germanium oxide layer involves the following assumptions.

(a) The adsorption of water vapour has a "weak" chemisorption character and is fast compared with diffusion.

(b) The adsorption of water vapour begins at the surface of germanium oxide but takes place inside the entire oxide layer.

(c) Water vapour diffuses into the oxide layer but cannot diffuse into the germanium singlecrystal at the temperatures of the experiments.

(d) The diffusion coefficient is a function of the temperature only.

Fick's equation for diffusion in one dimension is:

$$\frac{\partial c}{\partial \tau} = D \frac{\partial^2 c}{\partial x^2} \tag{1}$$

where c denotes the water vapour concentration, τ is the time of diffusion, x stands for the coordinate perpendicular to the germanium surface and D represents the diffusion coefficient of water vapour.

The scheme of water vapour diffusion is shown in Fig. 7. The oxide layer occupies the $0 < x < b$ interval. The decrease of water concentration along the oxide layer is stopped at the surface of germanium metal, *i.e.* the point $x = b$ represents an impermeable wall for water vapour. Since the amount of

Table IV

Amount of water (a_τ) adsorbed on unit area of the etched germanium surface, as a function of time (τ) at different temperatures (t) and relative humidities (p/p_0)

t (°C)	τ (hrs)	$a_\tau \times 10^9$ (g/cm²)			
		$p/p_0 = 0.1$	$p/p_0 = 0.3$	$p/p_0 = 0.5$	$p/p_0 = 0.65$
50	0.5	—	—	15.2	
	1.0	16.9	22.0	28.6	
	1.5	—	—	50.1	
	2.0	—	—	64.0	
	2.5	—	—	73.1	
	3.0	50.6	56.0	78.7	
	3.5	—	—	81.5	
	4.0	—	—	88.0	
	4.5	—	—	91.6	
	5.0	68.2	95.2	99.6	
	10.0	68.4	85.2	106.8	
60	0.5	—	—	19.0	
	1.0	14.6	22.8	34.7	
	1.5	—	—	49.1	
	2.0	—	—	61.0	
	2.5	—	—	69.8	
	3.0	50.9	62.8	75.7	
	3.5	—	—	80.0	
	4.0	—	—	83.6	
	4.5	—	—	88.5	
	5.0	—	78.9	97.3	
	10.0	66.1	82.7	99.6	
70	0.5	—	—	22.7	
	1.0	28.8	34.6	47.5	
	1.5	—	—	53.9	
	2.0	—	—	64.5	
	2.5	—	—	68.6	
	3.0	42.9	60.1	77.7	
	3.5	—	—	78.0	
	4.0	—	—	81.0	
	4.5	—	—	83.3	
	5.0	48.6	66.0	86.2	
	10.0	48.6	70.3	92.5	

Table IV (cont.)

t (°C)	τ (hrs)	$a_\tau \times 10^9$ (g/cm²)			
		$p/p_0 = 0.1$	$p/p_0 = 0.3$	$p/p_0 = 0.5$	$p/p_0 = 0.65$
	0.5	10.8	16.6	23.7	32.7
	1.0	15.6	24.3	38.4	45.0
	1.5	20.1	33.4	49.5	56.4
	2.0	23.1	38.2	57.6	68.2
	2.5	26.2	41.2	62.6	—
80	3.0	28.7	45.4	73.5	82.7
	3.5	26.9	47.0	71.7	—
	4.0	29.6	50.5	76.0	83.6
	4.5	30.2	51.6	76.9	86.0
	5.0	30.7	53.7	79.8	87.9
	10.0	32.5	53.5	81.2	90.8

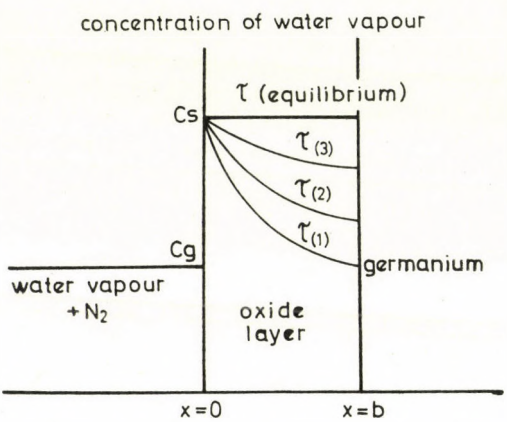

Fig. 7. Scheme of water vapour diffusion into the oxide layer with the boundary conditions

adsorbed water does not exceed 6×10^{-7} g, the concentration of water vapour (C_g) may be regarded as constant at the gas/solid boundary surface.

Owing to the prevailing vapour pressure, the equilibrium concentration of water (C_s) corresponding to the given temperature is rapidly achieved and remains constant during the process of diffusion. Therefore, the boundary conditions for diffusion are:

$$c(0, \tau) = C_s\,; \quad \left(\frac{\partial c}{\partial x}\right)_{x=b} = 0 \quad \text{for} \quad \tau > 0 \tag{2}$$

The initial condition for water vapour distribution in the oxide layer is described by the function $f(x)$:

$$c(x, 0) = f(x) \text{ at } 0 \leq x \leq b \tag{3}$$

With boundary conditions (2), function $f(x)$ satisfies the following equations:

$$f(x) - C_s = C_s - f(-x)$$

and

$$f(x + b) = f(b - x) \tag{4}$$

i.e. $f(x)$ is periodical with respect to 4 b.

Using conditions (2) and (3), the solution of Eq. (1), after substituting $c(x, 0) = C_1$, is [10]:

$$c(x, \tau) = C_s + (C_1 - C_s) \sum_{k=-\infty}^{+\infty} \left[\operatorname{erf}\left(\frac{x - 4Kb}{2\sqrt{D\tau}}\right) - \right.$$
$$\left. - \frac{1}{2} \operatorname{erf}\left(\frac{x - (4K-2)\,b}{2\sqrt{D\tau}}\right) - \frac{1}{2} \operatorname{erf}\left(\frac{x - (4K+2)\,b}{2\sqrt{D\tau}}\right) \right] \tag{5}$$

where K is an integer.

Since germanium samples were previously treated in vacuum at 300 °C, the initial distribution of water vapour in the oxide layer is: $c(x,0) = f(x) = 0$ and Eq. (5) takes the form:

$$c(x, \tau) = C_s \left\{ 1 - \sum_{k=-\infty}^{+\infty} \left[\operatorname{erf}\left(\frac{x - 4Kb}{2\sqrt{D\tau}}\right) - \frac{1}{2} \operatorname{erf}\left(\frac{x - (4K-2)\,b}{2\sqrt{D\tau}}\right) - \right.\right.$$
$$\left.\left. - \frac{1}{2} \operatorname{erf}\left(\frac{x - (4K+2)\,b}{2\sqrt{D\tau}}\right) \right] \right\}. \tag{6}$$

Our experimental results yield the amount of water adsorbed on unit surface area of the oxide layer as a function of the adsorption time (τ). Since $c(x, \tau)$ stands for the time dependent concentration, Eq. (6) has to be integrated with respect to x:

$$\frac{1}{C_s b} \int_0^b c(x, \tau)\, dx = 1 - \frac{1}{b} \int_0^b \sum_{k=-\infty}^{+\infty} \left[\operatorname{erf}\left(\frac{x - 4Kb}{2\sqrt{D\tau}}\right) - \right.$$
$$\left. - \frac{1}{2} \operatorname{erf}\left(\frac{x - (4K-2)\,b}{2\sqrt{D\tau}}\right) - \frac{1}{2} \operatorname{erf}\left(\frac{x - (4K+2)\,b}{2\sqrt{D\tau}}\right) \right] dx. \tag{7}$$

Eq. (7) can be integrated numerically but first we have to determine the thickness of the oxide layer and the order of magnitude of the diffusion coefficient.

The thickness of the oxide layer was found to be 30×10^{-8} cm by the ellipsometric method. The first term in the square brackets of Eq. (6) is suitable for estimating the diffusion coefficient at $K = 0$; it gives $D = 10^{-17} - 10^{-18}$ cm^2/sec in the temperature range studied. Under the experimental conditions, the value of the 'erf' function at $|K| > 1$ rapidly converges to unity. Considering the experimental error, it is not necessary to increase the number of terms in the approximation series. The calculations were performed with the values $K = 1, 0, -1$.

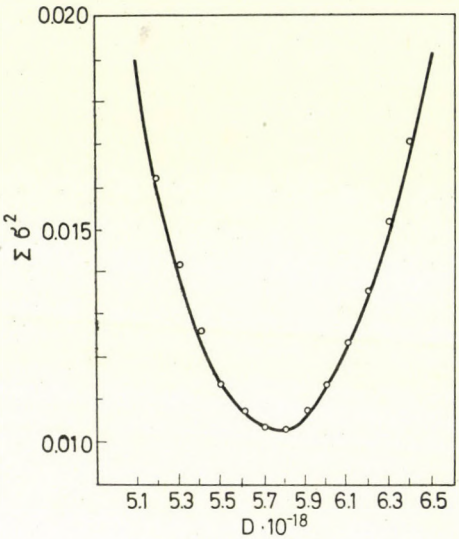

Fig. 8. The quadratic sum of deviation ($\Sigma\sigma^2$) between the experimental and theoretical data as a function of the diffusion coefficient (D) at 80 °C

By performing the numerical integration of Eq. (7) with various diffusion coefficients in the range of
$D = (1.5 - 7.0)\times10^{18}$ cm^2/sec with a deviation of $\Delta D = 0.1\times10^{-18}$, we have obtained the theoretical curves of the $a_\tau/a_\infty = f(\tau)$ function (where $a_\tau = \int_0^b c(x, \tau)dx$ and $a_\infty = C_S\, b$).

The experimental curves were fitted to the theoretical ones. Fig. 8 shows the sum of quadratic deviations of the experimental results measured at 80 °C from the calculated theoretical values, as a function of the diffusion coefficient. The minimum is at $D = 5.8\times10^{-18}$ cm^2/sec. In this point the ordinate has a small value indicating that the experimental data are in good agreement with those of the theoretical curve.

The diffusion coefficients at other temperatures were computed in the same way and the results are summarized in Table V.

Table V

Diffusion coefficients of water vapour in the oxide layer at different temperatures (t)

t (°C)	D (cm²/sec)
80	5.8×10^{-18}
70	4.8×10^{-18}
60	3.8×10^{-18}
50	3.3×10^{-18}

The estimated activation energy of the diffusion process is about 4 kcal/mol in the temperature range used in the experiments. That value is comparable to apparent activation energy calculated from the kinetic curves of water vapour adsorption.

5. Conclusions

The germanium singlecrystal etched in alkaline peroxide solution has a plane and compact surface, the thickness of the oxide layer being 30×10^{-8} cm. The water adsorption process on the surface of an etched germanium singlecrystal reaches thermodynamic equilibrium within a period of 10 hrs and the isotherms can be described by Freundlich's equation at 50, 60, 70 and 80 °C. The water adsorption has a 'weak' chemisorption character. The rate of the whole process is controlled by diffusion. The mechanism of water adsorption process involves rapid, 'weak' chemisorption on the boundary surface of the oxide layer, from where diffusion occurs toward the surface of germanium metal. The residence time of water vapour due to 'weak' chemisorption and the steric conditions of adsorption inside the oxide layer lead to a diffusion coefficient of the order of 10^{-18} cm$^2 \cdot$ sec^{-1}. This value is much lower than in case of pore diffusion. The estimated activation energy of diffusion is 4 kcal/mol, in good agreement with the apparent activation energy calculated from the kinetic curves of water vapour adsorption. Therefore, the process of water vapour diffusion through the germanium oxide layer is controlled by adsorption and steric conditions.

*

The authors are indebted to Mr. M. MEHN and Mr. J. ZSAK for programming and computing the diffusion equations, and to Dr. P. FEJES for his valuable comments.

REFERENCES

1. LAW, J. T.: J. Phys. Chem. **59,** 67 (1955)
2. KAWASAKI, K., KANOU, K., SEKITA, Y.: J. Phys. Soc. Japan, **14,** 233 (1959)
3. GREEN, M., MAXWELL, K. H.: J. Phys. Chem. Solids, **11,** 195 (1959)

4. SRINIVASAN, G., CHESSICK, J. J., ZETTLEMOYER, A. C.: J. Phys. Chem. **66,** 1819 (1962)
5. SPARNAAY, M. J.: Ann. New York Acad. Sci., **101,** 972 (1963)
6. PRUDNIKOV, R. V., KISELEV, V. F.: Zh. Fiz. Khim. **50,** 1396 (1966)
7. PRUDNIKOV, R. V., KISELEV, V. F., EGOROV, M. M.: Dokl. Akad. Nauk SSSR **166,** 395 (1966)
8. PRAVDIC, V., MCCAFFERTY, E., ZETTLEMOYER, A. C.: Surface Sci. **7,** 380 (1967)
9. KISELEV, V. F., KOZLOV, S. N., NOVOTOTSKY-VLASOV, Yu. F., PRUDNIKOV, R. V.: Surface Sci. **11,** 111 (1968)
10. HAUFFE, K.: Reaktionen in und an festen Stoffen, Springer Verlag, Berlin, 1966
11. GIBER, J.: Kém. Közl. **34,** 187 (1970)
12. KIRÁLY, J.: Magy. Kém. Foly. **68,** 77 (1962)

János GIBER
Mária WÉGNER } Budapest IV., Váci út 77.
Ottó DOBIS, Budapest II., Pusztaszeri út 57—59.

Acta Chimica Academiae Scientiarum Hungaricae, Tomus 72 (4), pp. 407—421 (1972)

UNTERSUCHUNGEN ZUM VERHALTEN DER URANYLSALZE IN WÄSSRIGEN BINÄREN UND TERNÄREN SYSTEMEN

E. KÁLMÁN

(Sektion Chemie der Technischen Universität Dresden, Bereich Elektrochemie und physikalische Chemie)

Eingegangen 28. Januar 1971

Es wird die Konzentrationsabhängigkeit verschiedener Eigenschaften von Uranylsalzlösungen in Wasser und in 0,1*m* $HClO_4$ untersucht. Die Meßergebnisse deuten auf die starke strukturbildende Wirkung des Uranylions hin. Auf Grund einer ausführlichen Betrachtung vorhandener Angaben, wurden die Anomalien dieser Lösungen auf die Bindungen (in der äquatorialen Ebene) zwischen den Liganden und dem Uran der Uranylgruppierung zurückgeführt. Es wird auf die Schwierigkeiten bei der Interpretation der Ergebnisse der Untersuchungen an konzentrierten Elektrolytlösungen hingewiesen.

In der Technik werden konzentrierte Elektrolytlösungen allein schon aus ökonomischen Gründen häufig angewendet. Die Eigenschaften dieser Lösungen lassen sich aber in sehr beschränktem Umfang erklären. Diese Schwierigkeiten sind zum Teil darauf zurückzuführen, daß die Struktur des flüssigen Wassers, also die des verwendeten Lösungsmittels selbst, noch ungeklärt ist, obwohl sie seit Jahrzehnten mit ständig neuen physikalischen und chemischen Methoden untersucht wird. Eine Zusammenstellung über die zur Zeit vorhandenen wichtigsten Modellvorstellungen zur Wasserstruktur zeigt Abb. 1.

Eine Strukturänderung des Wassers läßt sich unter anderem durch einen Elektrolytzusatz herbeiführen. Die Strukturmodelle der wäßrigen Elektrolytlösungen können ausgehend von der ersten Abbildung vielfältig ausgelegt werden. Bis zu einer Ionenstärke von 10^{-2}Mol/l lassen sich viele Eigenschaften der Elektrolytlösungen mit Hilfe der Debye-Hückel-Theorie voraussagen. Jedoch werden die notwendigen Vereinfachungen, die in verdünnten Lösungen zulässig sind, mit steigender Konzentration immer weniger erfüllt. Eine geeignete allgemeingültige Theorie für konzentrierte Elektrolytlösungen existiert trotz intensiver Bemühungen bis heute noch nicht. Deshalb sind auch die zahlreichen Bestrebungen, sie experimentell zu erforschen, verständlich. So konnte SCHWABE [2—5] an Hand seiner Untersuchungen des Neutralsalzeinflusses auf verdünnte Säure-, Basen-, oder Salzlösungen eine Deutung der pH-Verschiebung geben.

Da die konzentrierten Uranylperchloratlösungen in bezug auf ihre Aktivitätskoeffizienten ein interessantes Verhalten zeigen, wurden eingehende Unter-

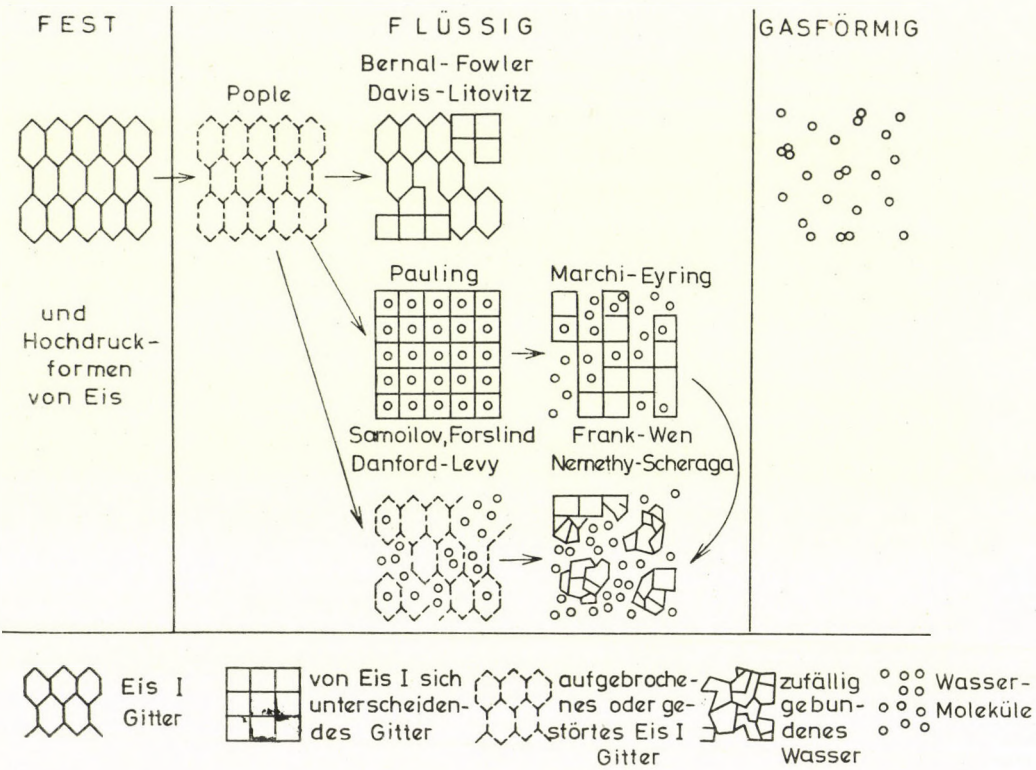

Abb. 1. Modellvorstellungen über die Struktur des Wassers [1]

suchungen an wäßrigen Uranylsalzlösungen durchgeführt [6]. Aus den folgenden Abbildungen geht das unterschiedliche Verhalten der verschiedenen Uranylsalzlösungen in Abhängigkeit von ihrer Konzentration hervor. Es werden zunächst die Aktivitätskoeffizienten betrachtet (s. Abb. 2).

Wie zu erwarten, erhält man wegen der äußerst geringen Komplexbildungsneigung des Perchlorations in Uranylperchlorat-Lösungen die höchsten Aktivitätskoeffizienten. Die niedrigsten Werte liegen dagegen auf Grund der starken Ionenpaarbildung in den Uranylsulfat-Lösungen vor. Die Aktivitätskoeffizienten für die Uranylnitrat- und Uranylchlorid-Lösungen liegen zwischen diesen beiden Extremwerten.

Welchen Einfluß die Anionen auf das Spektrum des Uranylions ausüben, geht aus Abb. 3 hervor.

Im Gebiet des steilsten Anstiegs der Absorptionsbande bei 418 nm kann man die Änderung des molaren Extinktionskoeffizienten, der ja ein Maß für die Beteiligung des absorbierenden Stoffes an einem konzentrationsabhängigen Gleichgewicht ist, in einer Uranylperchloratlösung durch Zusatz von $HClO_4$, HNO_3, HCl und H_2SO_4 sehen. Diese Reihenfolge (s. Abb. 3)

entspricht der Komplexbildungstendenz des Uranylions mit den entsprechenden Anionen.

Auch das Leitfähigkeitsverhalten der vier untersuchten Uranylsalzlösungen zeigt [6], daß bei diesen Salzen alle Arten der kovalenten Bindung

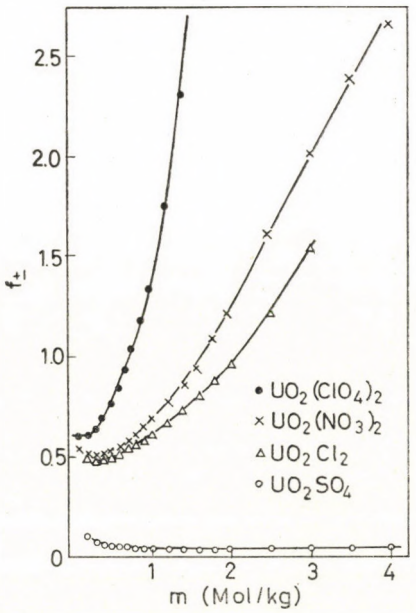

Abb. 2. Mittlere Aktivitätskoeffizienten der Uranylsalze in ihren wäßrigen Lösungen [7]

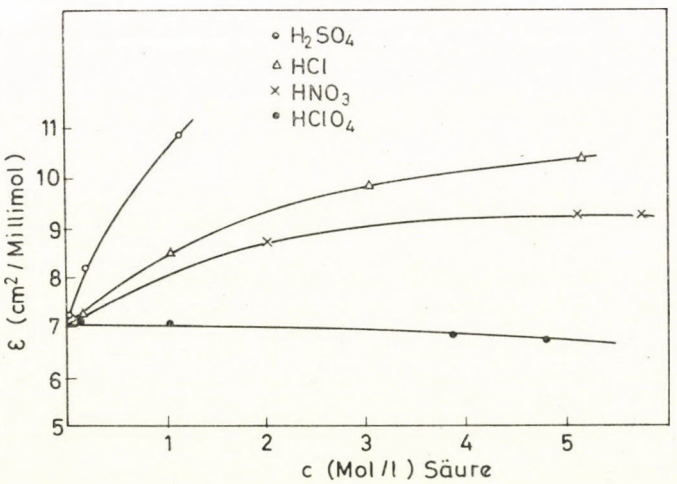

Abb. 3. Änderung der molaren Extinktionskoeffizienten des Uranylions in einer 1.25 Mol/l $UO_2(ClO_4)_2$-Lösung in Abhängigkeit von der Konzentration der zugesetzten Säure

— bei Uranylsulfat, wie schon erwähnt, Ionenpaarbildung, bei Uranylchlorid Komplexbildung und bei Uranylnitrat Assoziation — vorhanden sind. Auch in Uranylperchlorat-Lösungen tritt bei hohen Konzentrationen die sogenannte Bjerrumsche Ionenpaarbildung auf. Alle diese Effekte führen dazu, daß die Zahl der Ionen und auch deren Beweglichkeit herabgesetzt wird. Bei den sehr niedrigen Leitfähigkeitswerten der Uranylsulfat-Lösungen spielt außerdem

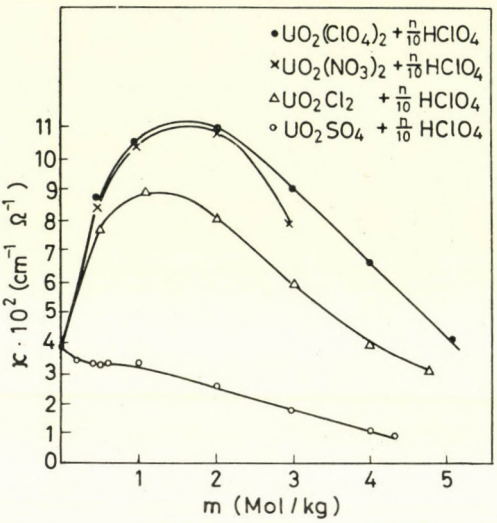

Abb. 4. Spezifische Leitfähigkeit von $UO_2(ClO_4)_2$, $UO_2(NO_3)_2$, UO_2Cl_2 und UO_2SO_4 in 0,1 m $HClO_4$ Lösungen in Abhängigkeit von der Salzkonzentration.

noch die hohe Viskosität eine Rolle. Die Leitfähigkeitsmaxima treten zwischen 1—2 Mol/kg auf. Etwa in diesem Konzentrationsbereich erfolgt der Übergang der Lösungsstruktur von der Wasserstruktur in die des Salzhydrats.

Wie in den binären, so zeigen die vier Uranylsalze auch in den ternären Systemen stark voneinander abweichende Werte der spezifischen Leitfähigkeit (s. Abb. 4).

Nach Abb. 5 erreicht die spezifische Leitfähigkeit in ternären Systemen ($\varkappa_{UO_2(ClO_4)_2 \text{ in } 0{,}1m\ HClO_4}$) nicht den Wert der Summe der Einzelleitfähigkeiten der beiden Komponenten (vgl. Additionskurve; $\varkappa_{add.} = \varkappa_{0{,}1m\ HClO_4} + \varkappa_{UO_2(ClO_4)_2}$)

Bei höheren Konzentrationen, oberhalb von etwa 2 Mol/kg nähern sich sogar die gemessenen Werte den Werten der reinen Salzlösungen. Dieses Phänomen läßt sich folgendermassen erklären: der Protonenaustausch wird durch die zunehmende Salzkonzentration immer mehr gehemmt, es entsteht letztlich eine geordnete Lösungsstruktur, die nur wenige »freie« Wassermoleküle enthält. Ein Protonentransport nach dem Sprungmechanismus kann kaum noch

erfolgen. Man muß sogar annehmen, daß die Protonen in die Hydrathülle des Uranylions einbezogen sind und daher nur mit diesem wandern. In konzentrierten Lösungen liefert die Säure also nur noch einen unwesentlichen Beitrag zur Leitfähigkeit. In Abb. 6 kann man diese Leitfähigkeitsverluste [$\varkappa$(W)]

$$\varkappa(\mathrm{W}) = (\varkappa_{0{,}1m\ \text{Säure}} + \varkappa_{\text{Salz}}) - \varkappa_{\text{gem.}}$$

verschiedener Salze in Abhängigkeit von der Konzentration sehen.

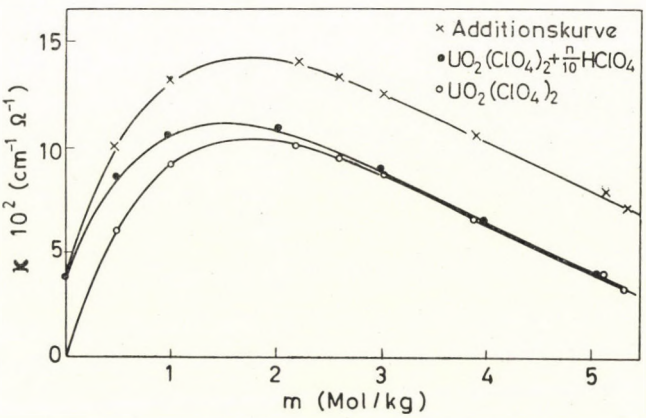

Abb. 5. Änderung der spezifischen Leitfähigkeit von $UO_2(ClO_4)_2$, 0.1 *m* $HClO_4$ + + $UO_2(ClO_4)_2$ in Abhängigkeit von der Konzentration (vgl. Additionskurve)

Die $\varkappa$(W)-Werte charakterisierten die Beseitigung des speziellen Transportmechanismus der Ionen des Wassers infolge der Zerstörung der Wasserstruktur und der Bindung des Wassers als Hydratwasser beim Salzzusatz. Die größten $\varkappa$(W)-Werte findet man in Aluminiumperchloratlösungen, nach diesen folgen die Uranylsalze: Perchlorat, Nitrat, Chlorid und Sulfat, abschließend $LiClO_4$, $NaClO_4$ und NH_4Cl. Es ist interessant festzustellen, daß die Uranylsalze, obwohl die Werte für ihre spezifischen Leitfähigkeiten sowohl im Wasser als auch in 0,1*m* Perchlorsäure stark voneinander abweichen, dicht beieinander liegende $\varkappa$(W)-Werte besitzen. Der große Leitfähigkeitsverlust kann demzufolge nur durch das Uranylion verursacht werden.

In diesem Zusammenhang wird kurz auf den Aufbau dieses Ions eingegangen. Die lineare Konfiguration der Uranylgruppe wurde sowohl in Salzen als auch in wäßrigen Lösungen bewiesen. Auf die hohe Stabilität der U—O-Bindung weist die große Kraftkonstante hin. Dagegen ist jedoch noch nicht einmal ein eindeutiger kristallographischer Radius des Uranylions bekannt. Für die Erklärung der Besonderheiten dieses Ions reicht das anschauliche Hantelmodell (s. Abb. 7. 1) nicht aus. Diese Tatsache kann man auch daraus

entnehmen, daß sich der U—O-Bindungsabstand »a« bei jedem untersuchten Uranylsalz ändert. Er kann ≈1,6—2,0 Å betragen, d. h. kleiner als die Summe der Radien von U^{6+} und O^{2-} sein. Auch andere Eigenschaften (Polarisierbarkeit, magnetische Suszeptibilität u. a.), die durch die Elektronendichte der Bindung bestimmt werden, hängen stark von den vorhandenen Liganden ab [8, 9].

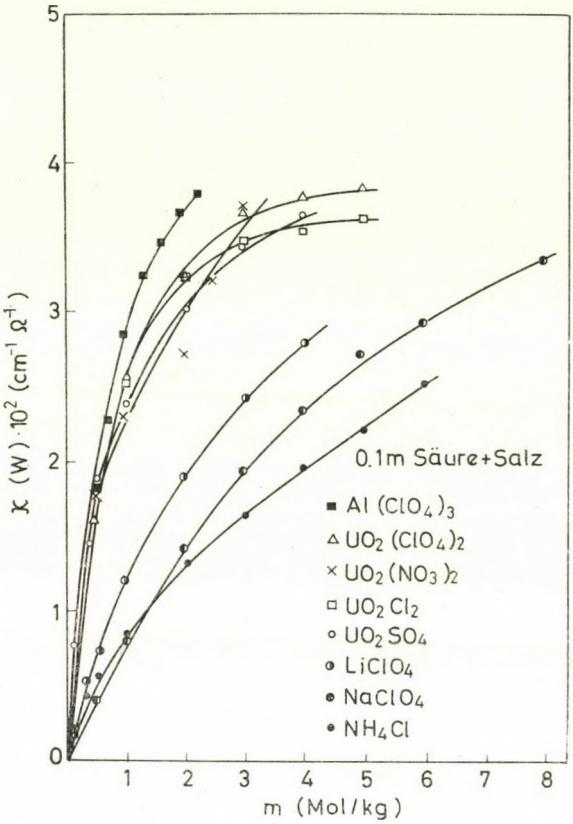

Abb. 6. Leitfähigkeitsverluste $\varkappa$(W) im ternären Systemen 0.1 *m* Säure + Salz

Die Betrachtung der Besetzung der Elektronenschale der Bausteine des Uranylions (s. Abb. 7.) ergibt das folgende Bild: im Uranatom gibt es neben den 6 Valenzelektronen noch eine ziemlich große Zahl freier Orbitale in den unteren Elektronen-Niveaus (6d, 5f). Es wird angenommen, daß im Uranylion außer der U=O—Doppelbindung eine zusätzliche Donator–Akzeptor-Gegenwirkung zwischen den einsamen Elektronpaaren der Sauerstoffatome und den freien Orbitalen des Uranatoms auftritt (s. Abb. 7. 2). (So kann man auch die hohe Kraftkonstante der U—O-Bindung, die einer Bindungsordnung größer

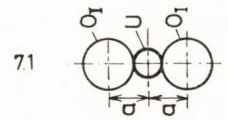

7.1

$r_{O^{2-}} = 1.32$ Å $\quad r_{O^{6+}} = 0.80$ Å

Uran	K^2	L^8	M^{18}	N^{32}	$5s^2$	$5p^6$	$5d^{10}$	$5f^3$	$6s^2$	$6p^6$	$6d^1$	$7s^2$
Elektronenkonfiguration der Valenzschale								$5f^3$			$6d^1$	$7s^2$
U^{6+}	K^2	L^8	M^{18}	N^{32}	$5s^2$	$5p^6$	$5d^{10}$		$6s^2$	$6p^6$		

Sauerstoff	K^2	$2s^2$	$2p^4$
O^{2-}	K^2	$2s^2$	$2p^6$

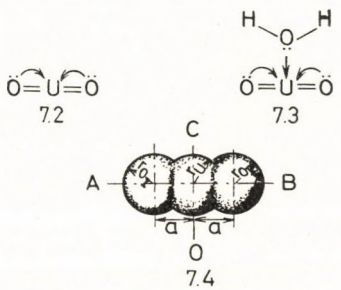

Abb. 7. Vorstellung zur Struktur und Konfiguration des Uranylions

als 2 entspricht, deuten.) Das schließlich dargestellte Modell (s. Abb. 7.4) beruht auf der gegenseitigen Überlappung der Elektronenwolken [10]. Mit anderen vorhandenen Molekülen, oder Ionen bildet sich eine Konkurrenz heraus. Die Ausbildung einer Koordinationssphäre von Wassermolekülen läßt sich auch so erklären (s. Abb. 7.3). Die Hydrathülle des Uranylions kann man sich als einen gefalteten Ring von kovalent gebundenen Wassermolekülen um das Uran des Uranylions vorstellen. Die Wassermoleküle können auch durch Anionen ersetzt werden. Der Einfluß aller Liganden bestimmt dann die Eigenschaften eines Uranylsalzes bzw. seiner wäßrigen Lösung. Hieraus läßt sich auch das gezeigte unterschiedliche Verhalten des Uranylions in Abhängigkeit von den Anionen qualitativ erklären. (Die Kationenhydratation in den verschiedenen Uranylsalzlösungen wurde auch mit Hilfe der PMR-Methode untersucht [11].)

Auf die starke strukturbildende Wirkung des Uranylions in wäßrigen Lösungen weist auch sein Entropie-Wert [12], der ja bekanntlich ein Maß für den Ordnungszustand ist, hin (s. Tab. I). Aus dem Entropie-Wert des

Uranylions von —17 cal/grd Mol kann man schließen, daß es die Wassermoleküle mit starken »spezifischen« Kräften anzieht.

Die Ausbildung einer sehr festen Hydrathülle mit kovalent gebundenen Wassermolekülen folgt auch aus dem Verlauf der scheinbaren Molvolumina der Uranylperchlorat-Lösungen in Abhängigkeit von der Konzentration (s. Abb. 8) Nach der MASSONschen Beziehung [15] nimmt das scheinbare Molvolumen eines starken Elektrolyten in wäßrigen Lösungen mit der Konzentration zu, so wie im Falle von Aluminium- und Magnesiumperchlorat-Lösungen (s. Abb. 8).

Tabelle I

Entropie-Werte einiger Kationen in ihren wäßrigen Lösungen [13] (als Vergleich werden die kristallographischen Radien angeführt [14])

Kation	Entropie [cal/grd Mol]	r [Å]
H^+	0,0	
Al^{+++}	—74,9	0,51
Mg^{++}	—28,2	0,66
UO_2^{++}	—17,0	
Cd^{++}	—14,6	0,97
Ca^{++}	—13,2	0,99
Sr^{++}	— 9,4	1,12
Ba^{++}	+ 3	1,34

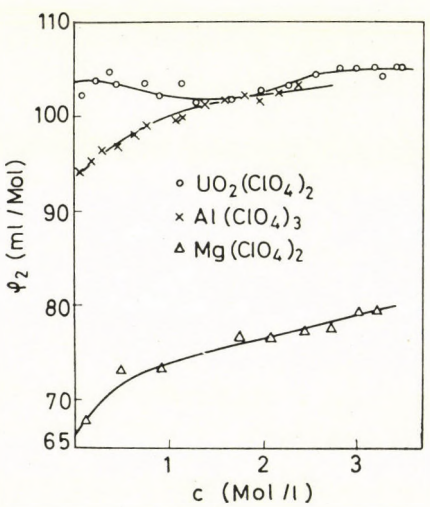

Abb. 8. Änderungen der scheinbaren Molvolumina φ_2 in wäßrigen $UO_2(ClO_4)_2$ -, $Al(ClO_4)_3$ -, $Mg(ClO_4)_2$-Lösungen in Abhängigkeit von der Konzentration

Diese Zunahme beweist, daß die Hydrathülle, in der das Wasser einer Kontraktion unterworfen ist, mit steigender Salzkonzentration abgebaut wird. Der fast geradlinige Verlauf des scheinbaren Molvolumens in wäßrigen Uranylperchlorat-Lösungen deutet an, daß das Uranylion neben den kovalent gebundenen Wassermolekülen kein elektrostatisch gebundenes Wasser enthält, es liegt, vielmehr in Übereinstimmung mit den spektroskopischen Untersuchungen [6], bis zu Sättigungskonzentration als Aquoion vor. Eine Diskon-

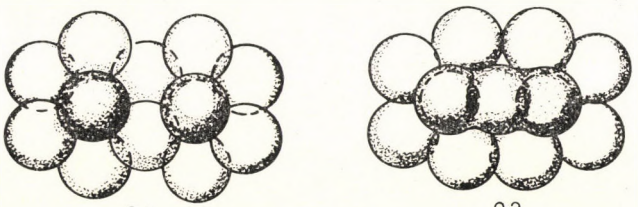

$$UO_2^{2+} + UO_2^{2+} + H_2O \rightleftharpoons 2H^+ + \left(\left[(UO_2)_2O\right]^{2+} \triangleq U_2O_5^{2+}\right)$$

$$\left[(UO_2)_2O\right]^{2+} + UO_2^{2+} + H_2O \rightleftharpoons 2H^+ + \left(\left[(UO_2)_3O_2\right]^{2+} \triangleq U_3O_8^{2+}\right)$$

$$\left[n\,UO_2^{2+}\,(n-1)\,O^{2-}\right]^{2+}$$

Abb. 9. Zur Hydrolyse des Uranylions [10]

tinuität kann man lediglich im Bereich von 1,3 bis 1,7 Mol/l beobachten. In diesem Konzentrationsinterval lag auch das Leitfähigkeitsmaximum, dementsprechend kann man auch dieses Phänomen mit strukturellen Effekten deuten.

An Hand der Struktur des Uranylions kann man auch seine Hydrolyse verstehen (vgl. Abb. 9). Zwischen Hydratation, partieller Hydrolyse, oder Hydrolyse gibt es keine großen Unterschiede. Durch Erhöhung des pH-Wertes über 2,5 oder durch Verdünnen wird Hydrolyse hervorgerufen. In Abb. 9.1 wurden zwei Uranylionen dargestellt, die nach LIPILINA [10] in zwei benachbarten Kanälen der Wasserstruktur untergebracht sind. (Erklärung zur Abb. 9.1: Die Bildebene steht senkrecht zur Kanalachse, mit der die Längsachse des Uranylions zusammenfällt. Die Projektion der Sauerstoffatome auf die Bildebene wurde durch gestrichelte Linien gekennzeichnet. Die dünnen geschlossenen Kreise stellen die Wassermoleküle dar.) Das $U_2O_5^{2+}$-Ion bildet sich nach der Abb. 9.2 aus zwei Uranylionen, die untereinander über O^{2-}-Ionen verbunden sind, d. h. es entstehen zwei senkrecht zueinander stehende U—O-Bindungen mit verschiedenem Abstand. Die Konturen dieses Komplexes in der äquatorialen Ebene sind mit einer dicken durchgehenden Linie gekennzeichnet. Analog bildet sich das nächste Hydrolyseprodukt $U_3O_8^{2+}$ und weitere mehrkernige Hydrolyseprodukte, die mit der allgemeinen Formel $(nUO_2^{2+}(n—1)O^{2-})^{2+}$ beschrieben werden können. Diese Vorstellung besitzt zweifellos qualitativen

Charakter. Man kann aber nur diese Art der Hydrolyseprodukte feststellen. Sie entstehen auch dann, wenn man UO_3 in Uranylsalzlösungen auflöst. Weiterhin wurde im Absoptionsspektrum des Uranylions infolge Hydrolyse weder eine neue Bande noch eine Bandenverschiebung zu größeren Wellenlängen beobachtet [16]. Das bedeutet in Übereinstimmung mit der Abb. 9, daß sich die Struktur und Konfiguration des Uranylions durch Hydrolyse nicht ändert. Durch eine Erhöhung der Konzentration wird jedoch die Hydrolyse zurückgedrängt. So beträgt zum Beispiel der Hydrolysegrad in einer 10^{-3} N Uranylnitrat-Lösung 10%. Wird nun die Konzentration auf 10^{-1} N erhöht, so sinkt er auf 2,7% ab [10].

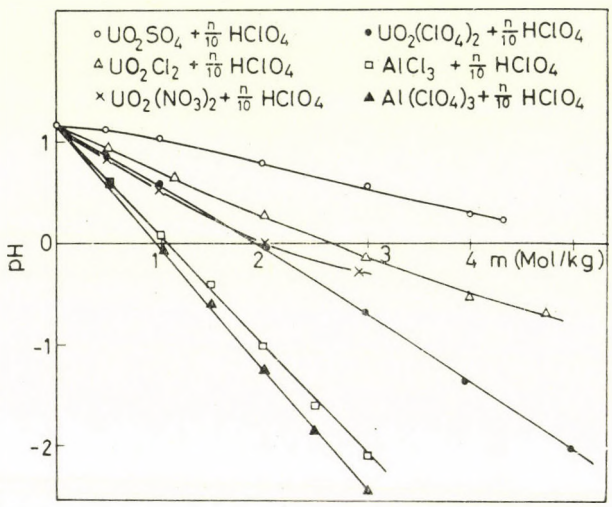

Abb. 10. Die pH-Verschiebung von 0.1 *m* $HClO_4$ durch Zusatz von UO_2SO_4, UO_2Cl_2, $UO_2(NO_3)_2$, $UO_2(ClO_4)_2$, $AlCl_3$ und $Al(ClO_4)_3$

Bei hohen Konzentrationen treten in den Uranylsalz-Lösungen sehr niedrige pH-Werte auf. Sie lassen sich durch den Salzeffekt auf die durch die Hydrolyse entstandene verdünnte Säure zurückführen [6]. In Abbildung 10 ist die pH-Verschiebung in einer 0,1 *m* $HClO_4$-Lösung durch Uranyl- und Aluminiumsalze zu sehen. Bei der Zugabe von Uranylsulfat tritt zunächst der allgemein bei Sulfaten beobachtete negative Salzeffekt gemäß $SO_4^{2-} + H^+ \rightleftharpoons HSO_4^-$ auf. Dagegen verursachen die anderen Uranylsalze (Chlorid, Nitrat und Perchlorat) und insbesondere auch die Aluminiumsalze, die zum Vergleich eingetragen wurden, eine große pH-Verschiebung, die mit der Zunahme der Aktivitätskoeffizienten des Protons gedeutet werden kann [2, 3].

In Abbildung 11 kann man die pH-Verschiebung einer 0,1 *m* $HClO_4$ durch Zusatz von Barium-, Calcium-, Magnesium-, Uranyl-, und Aluminium-

perchlorat sehen. Wie aus der Abbildung zu entnehmen ist, folgen die Geraden der Gleichung von SCHWABE [2, 3]:

$$pH_m = pH_0 - 0{,}0555\, m_s\, n_e \left[\frac{h_+}{r_+} - \frac{h_-}{r_-}\right]$$

$$pH_m = pH_0 - K\, m_s \quad K = f\left(\frac{1}{r}\right)$$

wobei:

pH_0 = pH-Wert der reinen Säurelösung
pH_m = pH-Wert der Säurelösung nach Neutralsalzzusatz
m_s = Fremdsalzkonzentration (Mol/kg)
n_e = elektrochemische Wertigkeit
h_+ bzw. h_- = Proportionalitätsfaktoren, die eine Funktion der Hydratationszahl der betreffenden Ionen sind.

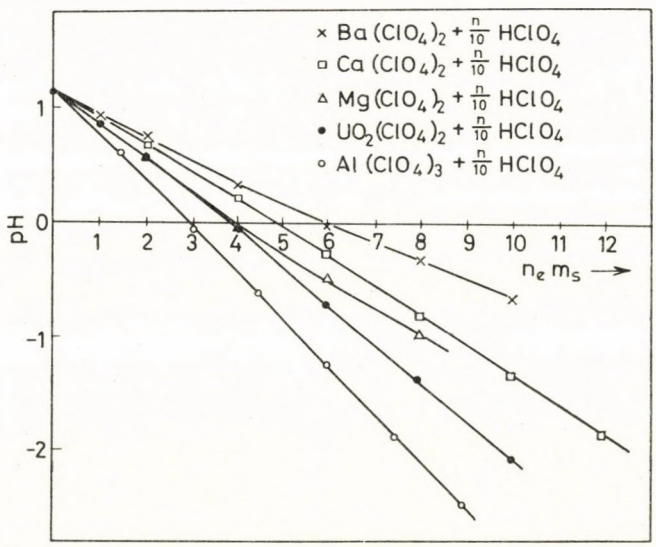

Abb. 11. Die Abnahme des konventionellen pH-Wertes beim Zusatz von Metallperchloraten zu 0.1 *m* Perchlorsäure

Diese Beziehung läßt sich theoretisch erklären, wenn man die elektrostatische Wechselwirkung zwischen den Protonen und den Ionen des Salzes für die pH-Verschiebung verantwortlich macht. Die Steigung K hängt vom Radius des Kations ab.

Einen Beitrag zur Problematik der starken Hydratation in wäßrigen Uranylperchlorat-Lösungen liefert auch die starke Erniedrigung der Aktivi-

tätskoeffizienten des Wassers bei Zusatz von $UO_2(ClO_4)_2$ (s. Abb. 12). SAMOILOV [17] wendet die Aktivitätskoeffizienten des Wassers für die Charakterisierung der Ionenhydratation folgendermaßen an:

Die Ionen wirken auf die Translationsbewegung der ihnen am nächsten gelegenen Wassermoleküle ein. Eine Abschwächung dieser Bewegung führt zu einer Verringerung der potentiellen Energie, d. h. zu einer Vergröße-

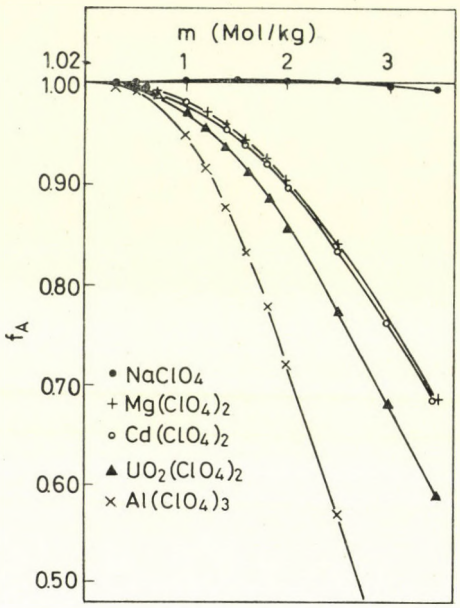

Abb. 12. Änderung der Aktivitätskoeffizienten des Wassers in Abhängigkeit von der Metallperchlorat-Konzentration

rung des negativen Potentials, also zu einer Verkleinerung der Aktivitätskoeffizienten des Wassers. Dagegen ist eine Vergrößerung von f_A auf den umgekehrten Effekt — die sogenannte negative Hydratation — zurückzuführen.

In Abb. 12 kann man die niedrigsten f_A-Werte in Aluminiumperchlorat-Lösungen sehen, danach folgen jedoch sogleich die des Uranylperchlorats. Es schließen dann die Werte für Cadmium-, Magnesium- und Natriumperchlorat an.

Es wurde auch eine Abschätzung der Hydratationszahlen vorgenommen [6]. Als Ausgangspunkt dienten die Wasseraktivitäten, die aus den Dampfdruckwerten der Lösungen berechnet wurden. Bei der Berechnung des Molenbruchs wurde die Inanspruchnahme des Wassers durch die Hydratation berücksichtigt. Nach einer graphischen Abschätzung könnte für das $UO_2(ClO_4)_2$

eine Hydratationszahl von etwa 7—8 erhalten werden. Der gleiche Wert wurde auch nach der Methode von PADOVA erhalten [siehe 18].

Aus dem Dargelegten kann man folgern, daß in Uranylperchlorat-Lösungen die Hydratation, insbesondere in den konzentrierten wäßrigen Lösungen, nicht ohne weiteres außer acht gelassen werden darf. Unter Verwendung des Hydratationsmodells von ROBINSON und STOKES [7, 19] bzw. GLUECKAUF

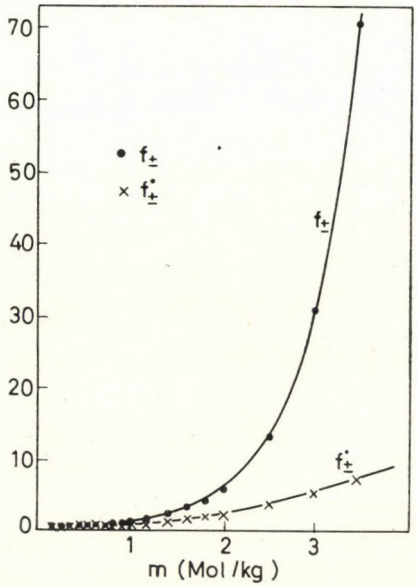

Abb. 13. Änderung des Aktivitätskoeffizienten $f_{\pm}$ des $UO_2(ClO_4)_2$ im Vergleich zur Änderung des Aktivitätskoeffizienten $f\dot{\pm}$, der unter Berücksichtigung der Hydratation berechnet wurde

[20] kann der Aktivitätskoeffizient des hydratisierten Gelösten berechnet werden. Eine Darstellung dieser Theorien sowie ihrer Mängel kann an dieser Stelle nicht gegeben werden. Es sei nur soviel erwähnt, daß diese Theorien oftmals mit den experimentellen Werten in Einklang gebracht werden können. Abb. 13 zeigt die unterschiedlichen Aktivitätskoeffizienten der Gelösten mit und ohne Berücksichtigung der Hydratation in wäßrigen Uranylperchlorat-Lösungen. Die mittleren Aktivitätskoeffizienten des Uranylperchlorats in ihrer wäßrigen Lösung weichen oberhalb einer Konzentration von etwa 1,4 Mol/kg* stark von denen ab, die unter Berücksichtigung der Hydratation berechnet

* Wie schon gezeigt wurde, tritt im gleichen Konzentrationsbereich eine Änderung anderer Eigenschaften, wie die der spezifischen Leitfähigkeit und des scheinbaren Molvolumens auf. Auch sie wurden auf Strukturänderungen in der wäßrigen Lösung zurückgeführt.

wurden. Die hydratationsbedingten Wechselwirkungsänderungen treten dann stark in den Vordergrund. In der konzentrierten Uranylperchlorat-Lösung liegt schon eine etwa hundertfache Abweichung vor.

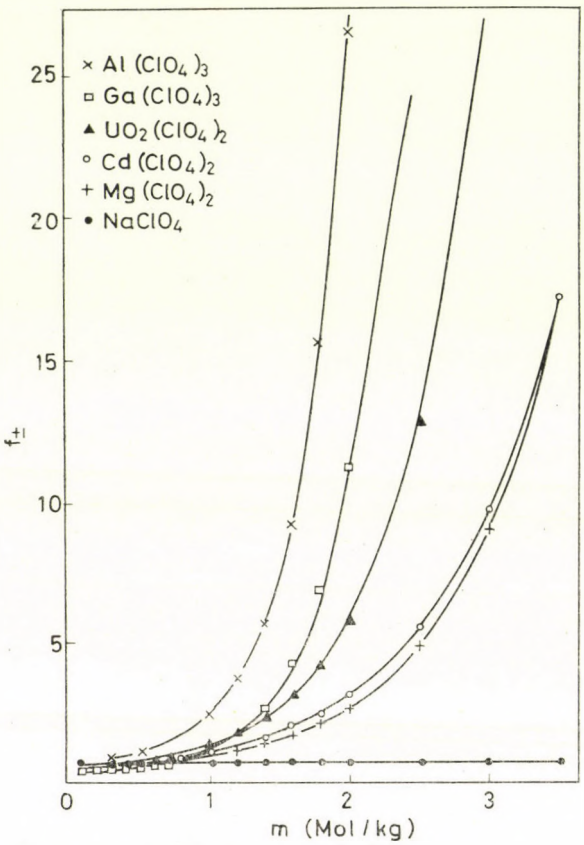

Abb. 14. Änderung der mittleren Aktivitätskoeffizienten einiger Metallperchlorate in Abhängigkeit von der Konzentration

Zu den Zahlenwerten des Aktivitätskoeffizienten in konzentrierten Elektrolytlösungen sei folgendes gesagt: unter dem Aspekt, daß der Aktivitätskoeffizient ein Maß der interionischen Wechselwirkung ist, ist seine Berechnung aus der Aktivität mit Hilfe der Konzentration aus der Einwaage nicht zulässig. Je nach der Art der vorliegenden Ionen sind nämlich alle Zwischenformen der Assoziation: von der rein elektrostatischen Bindung wie in den Ionenpaaren, über »undissoziierte Ionendipole« mit zunehmenden homöopolaren Bindungsanteil, bis zu Komplexionen mit überwiegend unpolarer Bindung möglich. Außerdem kann man noch Hydrolyse annehmen. Schließlich muß man noch

berücksichtigen, daß in konzentrierten Elektrolytlösungen neue Teilchenarten auftreten können, z. B. Ionen, die gegenüber dem Standardzustand teilweise desolvatisiert sind. Die ermittelten Aktivitätskoeffizienten (s. Abb. 14) sind lediglich als Faktoren zu betrachten, mit denen die analytische Konzentration der Elektrolyte multipliziert werden muß, um zu der wirksamen Konzentration zu gelangen. Es kann also allgemein festgestellt werden, daß die unmittelbar meßbaren Größen konzentrierter Elektrolytlösungen meistens eine Folgeerscheinung sehr verwickelter Wechselwirkungen sind, deren einzelne Faktoren sich nur schwierig voneinander trennen lassen. Für ihre Deutung ist demzufolge eine große Zahl von Meßergebnissen erforderlich.

*

Herrn Prof. Dr.-Ing. habil. Dr. rer. nat. h. c. Kurt SCHWABE sei für die Anregung zu dieser Arbeit und seine Unterstützung herzlich gedankt.

LITERATUR

1. GILLES, L.: Bibliographie, CEA—BIB-151, 24 (1969)
2. SCHWABE, K.: Österr. Chemiker Ztg. **65** 339 (1964)
3. SCHWABE, K.: Elektrochim. Acta, **12** 67 (1967)
4. SCHWABE, K.: Cronache di Chimica **24** 22 (1969)
5. SCHWABE, K.: J. Chim. physique 205 (1969)
6. KÁLMÁN, E.: Dissertation, TU Dresden, Sektion Chemie (1970)
7. ROBINSON, R. A., STOKES, R. H.: Electrolyte Solutions. Butterworths, London, 1959
8. DJATKINA, M. E., MICHAILOV, Ju. N.: J. Strukturchem. (Moskau) **3** 724 (1962)
9. RABINOWITSCH, E., BELFORD, R. L.: Spectroscopy and Photochemistry of Uranyl Compounds. Pergamon Press, 1964
10. LIPILINA, I. I.: Uranyl und seine Verbindungen, Verlag der Akademie der Wissenschaften der UdSSR, Moskau 1959
11. FRATIELLO, A., KUBO, V., LEE, R. E., SCHUSTER, R. E.: J. physic. Chem. **74** 3726 (1970)
12. COULTER, L. W., PITZER, K. S., LATIMER, W. M.: J. Amer. chem. Soc. **62** 2845 (1940)
13. LATIMER, W. M.: The Oxidations States of the Elements and Their Potentials in Aqueous Solutions. Prentice Hall Inc. New York 1952
14. WEAST, R. C., SELBY, S. M., HODGMAN, C. D.: Handbook of Chemistry and Physics, The Chemical Rubber Co. 1965, F-117
15. MASSON, D. O.: Philos. Mag. (7) **8** 218 (1929)
16. BELL, J. T., BIGGERS, R. E.: J. molecular Spectroscopy **22** 262 (1967)
17. SAMOILOV, O. Ja.: Die Struktur von wäßrigen Elektrolytlösungen. B. G. Teubner Verlagsgesellschaft, Leipzig 1961
18. FRITZSCH, M.: Diplomarbeit, TU Dresden, Sektion Chemie (1970)
19. STOKES, R. H., ROBINSON, R. A.: J. Amer. chem. Soc., **70** 1870 (1948)
STOKES, R. H., ROBINSON, R. A.: Trans. Faraday Soc., **53** 301 (1957)
20. GLUECKAUF, E.: Trans. Faraday Soc. **51** 1235 (1955); **53** 305 (1957)

Erika KÁLMÁN; Budapest VIII., Puskin u. 11—13.

Acta Chimica Academiae Scientiarum Hungaricae, Tomus 72 (4), pp. 423–432 (1972)

THE CHEMISTRY OF 1,3-BIFUNCTIONAL SYSTEMS, XV*

KINETIC STUDY OF THE ALKALINE HYDROLYSIS OF THE 1-MONOSUBSTITUTED HOMOLOGUES OF 3-CHLOROPROPANOL

M. BARTÓK and G. BOZÓKI-BARTÓK

(Department of Organic Chemistry, A. József University, Szeged)

Received December 11, 1969, in revised form July 15, 1970

The kinetics of alkaline hydrolysis of the 1-monosubstituted homologues (1-methyl **(I)**, 1-ethyl **(II)**, 1-butyl **(III)**, 1-cyclohexyl **(IV)**, 1-phenyl **(V)**) of 3-chloropropanol was studied. The reaction directions, rate constants, activation energies and entropies, as well as the preexponential factors were determined. The experimental results confirmed the validity of the reaction mechanism suggested earlier, for this type of compounds, too.

Studying the chemistry of certain 1,3-bifunctional systems, we investigated the transformation of various 1,3-chlorohydrins in alkaline media. In our earlier papers [1, 2, 3] a reaction mechanism was suggested and partly confirmed for the alkaline hydrolysis of 1,3-chlorohydrins containing a chlorine atom in the primary position. The model substances were the 2-mono- and 2,2-disubstituted homologues of 3-chloropropanol.

In the present work we wish to extend the reaction mechanism suggested earlier [1] to the explanation of the alkaline hydrolysis of the following 1,3-chlorohydrins:

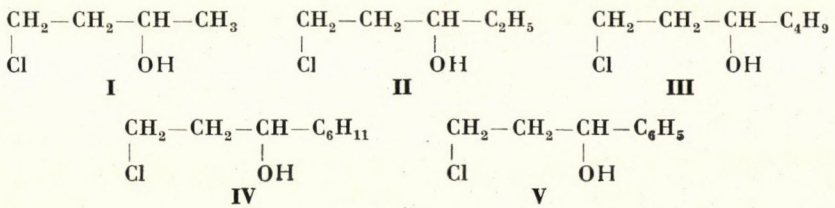

I **II** **III**

IV **V**

At the same time we intended to study the effect of the alkyl and aryl substituents in trimethylchlorohydrin on the kinetic parameters, report on the kinetic study of the alkaline hydrolysis of 1,3-chlorohydrin containing a secondary hydroxyl group.

It has been confirmed in our earlier preparative work [4], as well as by other authors (*e.g.* Ref. [5]), that in alkaline media the above compounds and their acetates are converted:

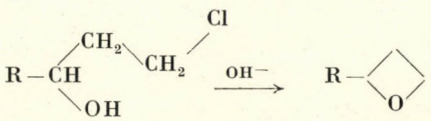

* Part XIV: Acta Chim. Acad. Sci. Hung. **72,** 297 (1972)

where R represents a methyl, ethyl, propyl, isopropyl, *n*-butyl or cyclohexyl group.

According to our more recent experiments, in the presence of 0.2 *M* barium hydroxide the formation of oxetanes is again the main direction of the reaction.

Because of the two directions of conversion observed in the alkaline hydrolysis of 3-chloro-2-phenylpropanol [2], in the case of 3-chloro-1-phenylpropanol preparative tests were carried out under the conditions of the kinetic measurements in order to prove the above direction of the process. GLC and infra-red spectroscopy have shown that the formation of 2-phenyltrimethylene oxide (20%) is accompanied by the formation of a considerable number of other by-products. Fragmentation leading to the formation of styrene may be considered the main direction of conversion, but 1,2-elimination and isomerization also take place. Since in our earlier work we were concerned merely with conversion mechanism of 1,3-chlorohydrins resulting in the formation of oxetanes, the various reaction directions observed in the case of 3-chloro-1-phenylpropanol are illustrated by the following reaction scheme without any attempt at a detailed description

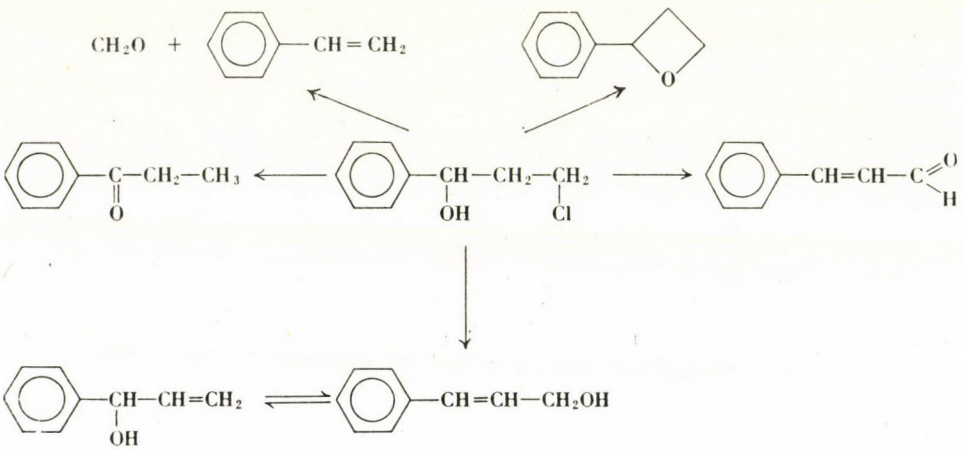

On the basis of the mechanism suggested in our earlier work [1] the formation of 2-monosubstituted oxetanes can be explained as follows:

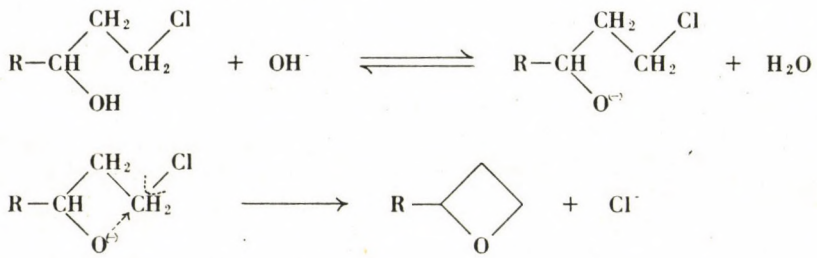

Table I

Kinetic data for the alkaline hydrolysis of 1,3-chlorohydrins of the type:

$$\begin{array}{l} CH_2-CH_2-CH-R \\ \quad | \qquad\quad | \\ \quad Cl \qquad OH \end{array}$$

Symbol of compound	t °C	Chlorohydrin conc. mole/l	[OH⁻] g-eq/l	k l · mole⁻¹ · min⁻¹	$\Delta H^{\ddagger}$ kcal · · mole⁻¹	A l · mole⁻¹ · · min⁻¹	$S^{\ddagger}$ e. u.
	80	0.0101	0.0147	0.051			
	85	0.0101	0.0147	0.082			
I	90	0.0101	0.0147	0.137			
	95	0.0101	0.0147	0.209	20.3	2.3×10^{11}	—15.0
	100	0.0101	0.0186	0.328			
	125	0.0101	0.0181	1.630			
	80	0.0101	0.0143	0.063			
	85	0.0101	0.0143	0.102			
II	90	0.0101	0.0143	0.149			
	95	0.0101	0.0143	0.221	20.3	2.4×10^{11}	—15.0
	100	0.0101	0.0186	0.369			
	125	0.0101	0.0186	1.811			
	80	0.0101	0.0181	0.067			
	85	0.0101	0.0148	0.121			
III	90	0.0101	0.0162	0.172			
	95	0.0139	0.0177	0.225	20.3	2.5×10^{11}	—15.0
	100	0.0101	0.0186	0.367			
	125	0.0101	0.0186	1.614			
	80	0.0101	0.0147	0.085			
IV	85	0.0101	0.0147	0.127			
	90	0.0101	0.0147	0.194			
	95	0.0101	0.0147	0.289	21.2	1.1×10^{12}	—12.2
	80	0.0100	0.0206	0.091			
	80	0.0100	0.0154	0.107			
	85	0.0100	0.0160	0.151			
	85	0.0100	0.0154	0.152			
V	90	0.0100	0.0180	0.242			
	90	0.0100	0.0154	0.243			
	95	0.0100	0.0154	0.362	23.4	2.9×10^{12}	— 5.5
	100	0.0100	0.0183	0.568			

The results obtained from the kinetic experiments for the five compounds under investigation are summarized in Table I. On the basis of our earlier work [1], the rate constants were calculated from second order rate equations. Beside the experimental results the Table includes the rate constants, apparent activation energies, the preexponential factors, and the activation entropies.

The experimental data in the Table can be satisfactorily evaluated by means of a second order rate equation. The logarithms of the rate constants obtained at four different temperatures, when plotted against 1/T, gave a straight line (Fig. 1). Using the Arrhenius equation, it was possible to calculate the activation energy of the process.

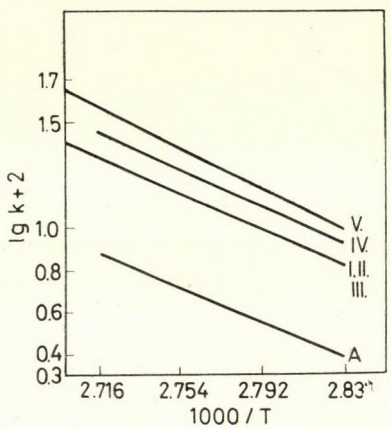

Fig. 1. Variation of the alkaline hydrolysis rate of the 1-R substituted homologues of 3-chloropropanol with the temperature. A: trimethylene chlorohydrin
I: R = methyl, **II**: R = ethyl, **III**: R = butyl, **IV**: R = cyclohexyl, **V**: R = phenyl

The kinetic parameters in Table I support the validity of the reaction mechanism suggested for the alkaline hydrolysis of 1,3-chlorohydrins in the case of this chlorohydrin type, too.

A detailed analysis of the kinetic data will be given later when further experimental results become available.

As it appears from Fig. 1, the introduction of an alkyl or aryl group into trimethylene chlorohydrin considerably raises the rate of alkaline hydrolysis. We are of the opinion that, beside the $+I$ effect of the substituents which understandably promotes the S_Ni process due to the increased electron density of the alkoxide ion, the steric effect is a decisive factor increasing the alkaline hydrolysis rate of derivatives containing electron donor substituents on the carbon atom linked to a hydroxyl group relative to trimethylene chlorohydrin. The alkyl groups tend namely to raise the rate of the second step

by promoting the formation of a favourable conformation for the S_Ni process of the intermediate, *i.e.* of the γ-chloroalkoxide ion. Hence the substituent effect is due to its decisive steric influence in the cyclization process.

The conversion of 1-phenyl-3-chloropropanol (V) proceeds at the highest rate which can be explained by reaction direction differing from those of the other four compounds. These different directions are the consequences of those structural characteristics of the molecule which result from the conjugation of the aromatic ring with the C—O bond. The $-I$ effect of the phenyl group and the mesomeric effect lead to a transition state whose conformation favours the elimination and fragmentation processes.

Experimental

The 1,3-chlorohydrins serving as starting materials were prepared as in Ref. [3]. Their purity was checked by GLC.

The methods of kinetic measurements and calculations have been described in an earlier communication [1]. In the kinetic measurements the highest conversion of chlorohydrin was 30—40%.

Experimental data

In the description of the experimental data the following symbols have been used:

t: time (min)
a: initial concentration of hydroxide ions ($Ba(OH)_2$ g-eq/l)
b: initial concentration of chlorohydrin (mole/l)
x: quantity of chlorohydrin converted in time t (mole/l)
k: second order rate constant ($l \cdot mole^{-1} \cdot min^{-1}$).

I.

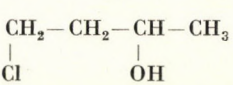

80 °C
$a = 0.01469$
$b = 0.01014$

85 °C
$a = 0.01469$
$b = 0.01014$

No	t	x	k	No	t	x	k
1	56	0.00043	0.052	1	35	0.00044	0.087
2	117	0.00083	0.051	2	111	0.00129	0.087
3	180	0.00123	0.051	3	155	0.00158	0.079
4	245	0.00158	0.050	4	200	0.00200	0.080
5	305	0.00193	0.050	5	245	0.00243	0.084
6	365	0.00229	0.052	6	290	0.00273	0.082
7	425	0.00260	0.052	7	335	0.00303	0.081

$k_{1-7} = 0.051$ $k_{1-8} = 0.082$

90 °C
$a = 0.01435$
$b = 0.010034$

No	t	x	k
1	30	0.00055	0.127
2	60	0.00111	0.536
3	90	0.00162	0.139
4	120	0.00205	0.139
5	150	0.00248	0.140
6	180	0.00284	0.139
7	210	0.00318	0.139

$k_{2-7} = 0.137$

95 °C
$a = 0.01435$
$b = 0.010034$

No	t	x	k
1	20	0.00053	0.186
2	40	0.00113	0.208
3	60	0.00159	0.206
4	80	0.00210	0.214
5	101	0.00248	0.208
6	120	0.00287	0.212
7	142	0.00323	0.210
8	161	0.00349	0.207

$k_{2-8} = 0.209$

100 °C
$a = 0.0186$
$b = 0.0101$

No	t	x	k
1	11	0.00058	0.289
2	20	0.00114	0.328
3	30	0.00168	0.335
4	40	0.00209	0.326
5	50	0.00252	0.328
6	60	0.00282	0.315
7	70.5	0.00328	0.336
8	80	0.00369	0.336

$k_{2-8} = 0.328$

125 °C
$a = 0.0181$
$b = 0.0101$

No	t	x	k
1	3	0.00062	1.161
2	6	0.00151	1.551
3	9	0.00223	1.632
4	12	0.00281	1.627
5	15	0.00329	1.605
6	18	0.00384	1.658
7	21	0.00434	1.707

$k_{2-7} = 1.63$

II.

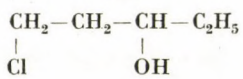

80 °C
$a = 0.01435$
$b = 0.010085$

No	t	x	k
1	35	0.00031	0.064
2	80	0.00070	0.064
3	121	0.00113	0.072
4	173	0.00137	0.062
5	230	0.00178	0.063
6	280	0.00202	0.060
7	335	0.00248	0.065
8	390	0.00272	0.063

$k_{1-2;\,4-8} = 0.063$

85 °C
$a = 0.01435$
$b = 0.010085$

No	t	x	k
1	39	0.00063	0.116
2	60	0.00078	0.107
3	115	0.00154	0.106
4	158	0.00200	0.105
5	235	0.00231	0.102
6	235	0.00257	0.097
7	275	0.00301	0.101
8	335	0.00337	0.097

$k_{2-8} = 0.102$

90 °C
$a = 0.01435$
$b = 0.010034$

No	t	x	k
1	31	0.00070	0.167
2	60	0.00087	0.109
3	90	0.00166	0.152
4	120	0.00217	0.154
5	165	0.00279	0.147
6	190	0.00306	0.151
7	215	0.00325	0.145
8	240	0.00347	0.143

$k_{3-8} = 0.149$

95 °C
$a = 0.01435$
$b = 0.010034$

No	t	x	k
1	20	0.00063	0.229
2	40	0.00123	0.239
3	60	0.00171	0.233
4	80	0.00202	0.213
5	136	0.00308	0.213
6	158	0.00342	0.213
7	180	0.00374	0.211

$k_{1-7} = 0.222$

100 °C
$a = 0.0186$
$b = 0.0101$

No	t	x	k
1	10	0.00065	0.362
2	20	0.00136	0.402
3	30	0.00175	0.357
4	45	0.00245	0.357
5	65	0.00335	0.369

$k_{1-5} = 0.369$

125 °C
$a = 0.0186$
$b = 0.0101$

No	t	x	k
1	2.5	0.00053	1.117
2	5.0	0.00121	1.410
3	7.5	0.00211	1.779
4	10.0	0.00245	1.608
5	12.5	0.00325	1.842
6	15.0	0.00354	1.727
7	17.5	0.00413	1.831
8	20.0	0.00456	1.876

$k_{3-8} = 1.811$

III.

$$CH_2-CH_2-\underset{\displaystyle OH}{\underset{|}{CH}}-C_4H_9$$
$$\quad\quad\quad

90 °C
a = 0.0162
b = 0.0101

No	t	x	k
1	34	0.00126	0.253
2	71	0.00199	0.204
3	104	0.00242	0.178
4	137	0.00291	0.170
5	169	0.00329	0.173
6	199	0.00348	0.150
7	229	0.00397	0.157

k_{2-7} = 0.172

95 °C
a = 0.0177
b = 0.0139

No	t	x	k
1	45	0.00235	0.245
2	78	0.00340	0.223
3	122	0.00445	0.205
4	160	0.00519	0.196
5	210	0.00601	0.188
6	270	0.00681	0.181
7	315	0.00735	0.179
8	360	0.00773	0.173

k_{1-3} = 0.225

100 °C
a = 0.0186
b = 0.0101

No	t	x	k
1	15	0.00085	0.395
2	30	0.00177	0.402
3	45	0.00235	0.364
4	60	0.00294	0.356
5	75	0.00337	0.338
6	90	0.00396	0.350

k_{1-6} = 0.367

125 °C
a = 0.0186
b = 0.0101

No	t	x	k
1	3	0.00068	1.631
2	6	0.00141	1.582
3	9	0.00202	1.531
4	12	0.00262	1.547
5	15	0.00318	1.573
6	18	0.00386	1.692
7	21	0.00427	1.677
8	24	0.00469	1.683

k_{1-8} = 1.614

IV.

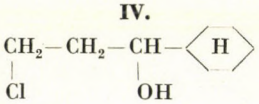

80 °C
a = 0.01469
b = 0.01007

No	t	x	k
1	72	0.00089	0.089
2	145	0.00158	0.085
3	185	0.00197	0.086
4	205	0.00211	0.085
5	237	0.00236	0.083
6	275	0.00262	0.082
7	315	0.00296	0.084
8	365	0.00328	0.084

k_{1-8} = 0.085

85 °C
a = 0.01469
b = 0.01007

No	t	x	k
1	68	0.00119	0.130
2	155	0.00243	0.133
3	179	0.00257	0.123
4	195	0.00280	0.127
5	210	0.00300	0.129
6	231	0.00319	0.128
7	251	0.00339	0.127
8	278	0.00353	0.121

k_{1-8} = 0.127

90 °C
a = 0.01469
b = 0.01004

No	t	x	k
1	30	0.00084	0.199
2	60	0.00157	0.201
3	90	0.00219	0.200
4	120	0.00263	0.189
5	150	0.00316	0.183
6	180	0.00359	0.193
7	210	0.00388	0.190
8	240	0.00439	0.195

k_{1-8} = 0.194

95 °C
a = 0.01469
b = 0.01004

No	t	x	k
1	20	0.00080	0.280
2	40	0.00149	0.285
3	60	0.00214	0.292
4	80	0.00263	0.284
5	101	0.00325	0.298
6	120	0.00360	0.291
7			

k_{1-6} = 0.289

V.

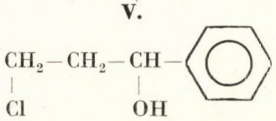

80 °C
a = 0.01806
b = 0.01010

No	t	x	k
1	30	0.00077	0.149
2	60	0.00122	0.123
3	90	0.00156	0.103
4	125.5	0.00199	0.103
5	175	0.00260	0.102
6	221	0.00301	0.098
7	255	0.00326	0.094
8	300	0.00372	0.096

k_{2-8} = 0.103

80 °C
a = 0.02063
b = 0.01035

No	t	x	k
1	25	0.00061	0.118
2	55	0.00103	0.094
3	85	0.00138	0.084
4	120	0.00184	0.083
5	180	0.00248	0.079
6	240	0.00292	0.072
7	300	0.00324	0.066
8	360	0.00349	0.061

k_{1-5} = 0.092

85 °C
a = 0.01598
b = 0.01002

No	t	x	k
1	40	0.00103	0.181
2	80	0.00173	0.156
3	120	0.00244	0.158
4	160	0.00297	0.153
5	200	0.00340	0.147
6	220	0.00360	0.146
7	250	0.00396	0.146

k_{2-7} = 0.151

90 °C
a = 0.01806
b = 0.01001

No	t	x	k
1	20	0.00097	0.289
2	45	0.00181	0.260
3	71	0.00253	0.244
4	95	0.00316	0.244
5	121	0.00367	0.235
6	150.5	0.00416	0.231
7	175	0.00464	0.231
8	200	0.00480	0.213

k_{1-8} = 0.243

100 °C $a = 0.01834$ $b = 0.01001$				95 °C $a = 0.0154$ $b = 0.0100$			
No	t	x	k	No	t	x	k
1	9	0.00101	0.659	1	10	0.00063	0.413
2	20	0.00189	0.560	2	20	0.00103	0.359
3	30	0.00261	0.593	3	33	0.00164	0.366
4	40	0.00315	0.567	4	40	0.00194	0.368
5	49	0.00373	0.584	5	50	0.00232	0.366
6	60	0.00420	0.567	6	60	0.00262	0.357
7	69	0.00458	0.564	7	70	0.00294	0.358
				8	80	0.00328	0.361
	k_2; $k_{4-7} = 0.569$				$k_{2-8} = 0.362$		

REFERENCES

1. BARTÓK, M., BOZÓKI-BARTÓK, G., KOVÁCS, K.: Acta Chim. Acad. Sci. Hung. **66,** 115 (1970)
2. BARTÓK, M., LÁNG-LAKOS, K., BOZÓKI-BARTÓK, G.: Acta Chim. Acad. Sci. Hung. **70,** 133 (1971)
3. BARTÓK, M., BOZÓKI-BARTÓK, G., KOVÁCS, K.: Acta Chim. Acad. Sci. Hung. **72,** 297 (1972)
4. BARTÓK, M., GILDE, A. S.: Acta Phys. et Chem. Szeged, **9,** 25 (1963)
5. FORSBERG, G.: Acta Chem. Scand. **8,** 135 (1954)

Mihály BARTÓK
Gizella BOZÓKI-BARTÓK
Szeged, Dóm-tér 8, Hungary.

Acta Chimica Academiae Scientiarum Hungaricae, Tomus 72 (4), pp. 433—440 (1972)

THE CHEMISTRY OF 1,3-BIFUNCTIONAL SYSTEMS, XVI*

REACTION KINETICAL STUDY OF THE ALKALINE HYDROLYSIS OF 1,1-DISUBSTITUTED DERIVATIVES OF 3-CHLORO-1-PROPANOL

M. BARTÓK and G. BOZÓKI BARTÓK

(Institute of Organic Chemistry, A. József University, Szeged)

Received July 16, 1970

The kinetics of the alkaline hydrolysis of some 1,1-dialkyl homologues (**I**: 1,1-dimethyl; **II**: 1-methyl-1-propyl; **III**: 1-methyl-1-isopropyl) of 3-chloropropanol have been studied. The rate constants of the alkaline hydrolysis of the three compounds, the activation energies, activation entropies and the action constants have been determined.

In our earlier papers [1—4] on the alkaline hydrolysis of 1,3-chlorohydrins we have reported the study by reaction kinetical methods of compounds containing primary chlorine atoms and primary or secondary hydroxyl groups.

In the present paper we shall describe the experimental results and reaction kinetical parameters of the alkaline hydrolysis of some 1,3-chlorohydrins containing primary chlorine atom and tertiary hydroxyl groups. The following 1,3-chlorohydrins were chosen as model compounds:

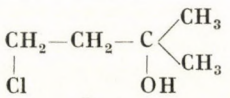

I

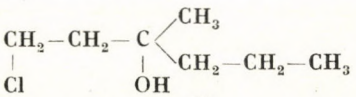

II

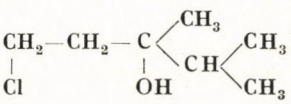

III

Several unsuccessful experiments were made to prepare 1,1-diisopropyl-3-chloro-1-propanol from ethyl-β-chloropropionate by means of Grignard reaction with isopropylmagnesium bromide.

In the course of our earlier preparative work [5] we found that in concentrated alkaline medium the above compounds were converted in very high yields into the corresponding oxacyclobutane homologues:

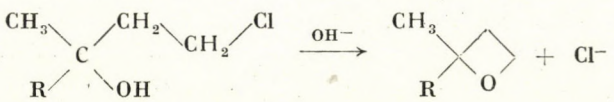

where R stands for methyl, propyl or isopropyl.

* Part XV: Acta Chim. Acad. Sci. Hung. **72**, 423 (1972).

According to the reaction mechanism suggested in an earlier communication [1], the formation of 2,2-disubstituted oxetanes can be explained as follows:

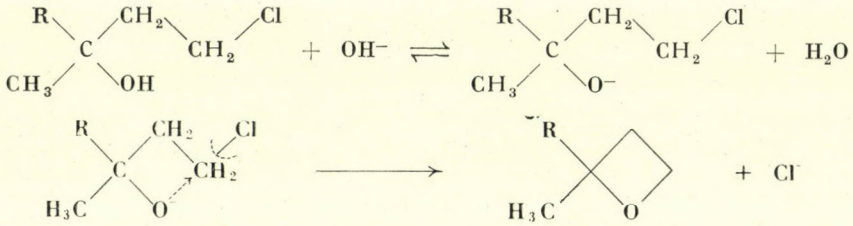

As it appears from Experimental, the kinetical measurements were made in dilute, and not in concentrated, alkali solution ($[OH^-] \simeq 0.02$ g-eq./l) in order to be able to follow accurately the rate of conversion. Even under these conditions relatively high rate constants were obtained. It may be expected from the reaction mechanism which has been suggested to explain the formation of four-membered cyclic ethers that the presence of water, and hence the hydroxyl ion concentration, will have a marked influence on the equilibrium, *i.e.* on the first step of the process. Similarly, it is to be expected that the presence of a tertiary hydroxyl group will multiply this effect, independently of the experimental fact which has been proved earlier that the yield of cyclic ethers is the highest in the case of compounds of this type. Therefore a kinetical investigation of the course of the conversion of chlorohydrins containing tertiary hydroxyl groups could not be omitted, though in had been proved for the other chlorohydrin types that the formation of cyclic ether is the main direction of alkaline hydrolysis.

The investigation of the conversions of 1,1-disubstituted derivatives of 3-chloro-1-propanol (*i.e.* 1,3-chlorohydrins containing tertiary hydroxyl groups) in alkaline medium and at low hydroxyl ion concentrations has shown that the transformations of these compounds are non-selective. The results of gas-liquid chromatographic analysis of the reaction products indicate the complex nature of the processes. Both simultaneous and consecutive conversions could be observed. Since in our earlier experimental work we dealt only with the mechanisms of the conversions leading to the formation of oxetanes, we illustrate here the various reaction directions in the case of compounds containing tertiary hydroxyl groups — without an attempt at completeness — by the reaction scheme on page 435.

Thus the conversion which takes place according to an S_Ni mechanism giving rise to the oxetanes, is accompanied by 1,2-elimination reactions resulting in the formation of unsaturated alcohols, further by 1,4-elimination producing olefines, and by substitution processes which give rise to the corresponding diols. According to our preliminary experiments, the extent to which

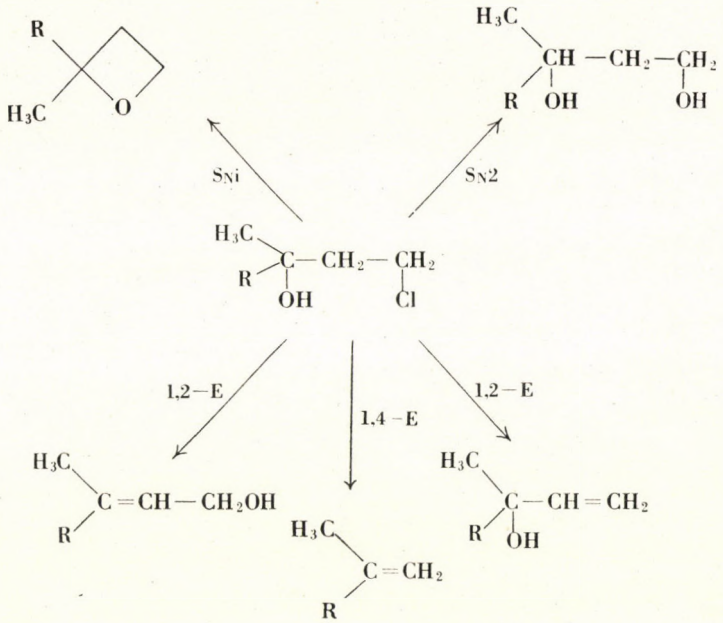

the reactions proceed in one or the other direction as sketched above can be significantly influenced by the hydroxyl ion concentration and by the nature of the base used.

When the hydroxyl ion concentration is 2 g-eq./l, there is a 70—90% conversion of the chlorohydrins into the corresponding oxetane derivatives. The main process is accompanied by a 1,4-elimination side-reaction. At lower hydroxyl ion concentrations mainly unsaturated alcohols and diols are formed, and the S_Ni process plays a subordinate part (maximum 10%).

The reaction directions observed in the case of 1,3-chlorohydrins containing tertiary hydroxyl groups have called attention not only to the investigation of the fine mechanism of the alkaline hydrolysis of this type of compounds, but the experimental data have also furnished new evidence for the two-step mechanism of oxetane formation.

The kinetic data obtained from the experiments for the three compounds are summarized in Table I. In Fig. 1 the temperature dependence of the reaction constants has been plotted. On the basis of our earlier work [1], the rate constants were calculated with the rate equation of second order reactions. The Table also contains the activation energy values, action constants and the values of activation entropy calculated from the experimental data.

Comparison of the reaction kinetical data of the alkaline hydrolysis of 1,1-dialkyl-3-chloro-1-propanols with those of other 1,3-chlorohydrins investigated earlier shows quite unambiguously that the reaction constants are the highest in the case of the compounds studied in the present work, while the

Table I

Reaction kinetical data of the alkaline hydrolysis of 1,3-chlorohydrins of the type:

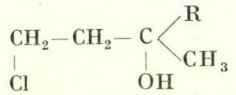

Compound	°C	Chlorohydrin concentration, mole/l	[OH⁻], g eq./l	k, $l \cdot mole^{-1} \cdot min^{-1}$	$\Delta H^{\ddagger}$ kcal · mole⁻¹	A, $l \cdot mole^{-1} \cdot min^{-1}$	$\Delta S^{\ddagger}$, cal · mole⁻¹ · °C⁻¹
	80	0.01006	0.01687	0.201			
	85	0.01008	0.01630	0.275			
I	85	0.01000	0.01432	0.293	19.0	1.2×10^{11}	—16.4
	90	0.01008	0.01630	0.407			
	95	0.01005	0.01432	0.602			
	80	0.01001	0.01687	0.248			
	85	0.01013	0.01598	0.366			
	85	0.01005	0.01630	0.369	19.7		
II	90	0.01005	0.01630	0.525			
	95	0.01010	0.01610	0.810			
	101.5	0.01092	0.02244	1.207			
	101.5	0.00960	0.02244	1.209		4.2×10^{11}	—13.9
	75	0.01011	0.01687	0.310			
III	80	0.01011	0.01687	0.454	18.4		
	85	0.01005	0.01630	0.659			
	90	0.01005	0.01630	0.903		1.1×10^{11}	—16.6

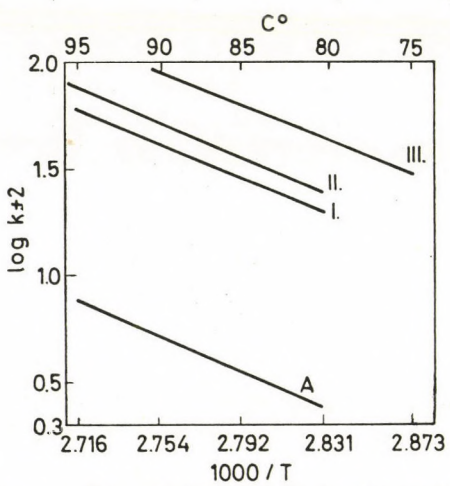

Fig. 1. Dependence of the rate of the alkaline hydrolysis of some 1,1-dialkyl homologues of 3-chloro-1-propanol as a function of the temperature. **A** 3-chloro-1-propanol, **I** 1,1-dimethyl-3-chloro-1-propanol, **II** 1-methyl-1-propyl-3-chloro-1-propanol, **III** 1-methyl-1-isopropyl-3-chloro-1-propanol

activation energy values are here the lowest. The relatively high rate increase compared with that found for the basic structure and for the other compound types can be explained by the elimination reactions occurring simultaneously.

The rate increase within the series cannot be satisfactorily explained by the very small differences in the reaction kinetical parameters calculated from the experimental data. The deviations found experimentally indicate some difference in the fine mechanism of the alkaline hydrolysis of 1,3-chlorohydrins; the study of this problem will be the subject of future work.

Experimental

The 1,3-chlorohydrins studied were prepared by the method described earlier [5]. Prior to the reaction kinetical measurements, the purity of the starting substances was checked by GLC.

The reaction kinetical measurements and calculation methods have been described in detail previously [1, 2].

In the description of the experimental results the following symbols are used:

: time in minutes
a: initial concentration of hydroxyl ions ($Ba(OH)_2$g-eq./l.)
b: initial chlorohydrin concentration
x: quantity of chlorohydrin converted in time t (mole/l.)
k: rate constant of second order ($l \cdot mole^{-1} \cdot min^{-1}$).

I.

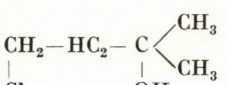

80 °C
$a = 0.01687$
$b = 0.01006$

No	t	x	k
1	15	0.00048	0.200
2	30	0.00095	0.206
3	45	0.00131	0.231
4	60	0.00172	0.198
5	75	0.00210	0.199
6	90	0.00244	0.199
7	105	0.00261	0.185
8	120	0.00292	0.187

$k_{1-8} = 0.201$

85 °C
$a = 0.01630$
$b = 0.01008$

No	t	x	k
1	10	0.00048	0.306
2	20	0.00081	0.269
3	30	0.00121	0.271
4	40	0.00157	0.273
5	50	0.00188	0.271
6	60	0.00217	0.265
7	70	0.00246	0.272
8	80	0.00277	0.272

$k_{1-8} = 0.275$

85 °C
$a = 0.01432$
$b = 0.010005$

No	t	x	k
1	10	0.00039	0.297
2	19	0.00073	0.290
3	30	0.00112	0.293
4	40	0.00144	0.291
5	50	0.00178	0.296
6	60	0.00207	0.294
7	70	0.00233	0.292
8	80	0.00257	0.288

$k_{1-8} = 0.293$

90 °C
$a = 0.01630$
$b = 0.01008$

No	t	x	k
1	7	0.00044	0.394
2	14	0.00094	0.441
3	21	0.00126	0.415
4	28	0.00169	0.427
5	35	0.00198	0.412
6	42	0.00220	0.388
7	49	0.00263	0.415
8	56	0.00283	0.399

$k_{1;3-8} = 0.407$

95 °C
$a = 0.01432$
$b = 0.010005$

No	t	x	k
1	5	0.00037	0.549
2	10	0.00086	0.658
3	15	0.00120	0.628
4	20	0.00149	0.597
5	30	0.00212	0.607
6	35	0.00236	0.590
7	40	0.00249	0.585

$k_{2-7} = 0.602$

II.

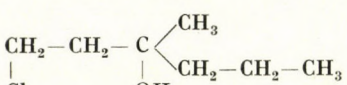

80 °C
$a = 0.01687$
$b = 0.01001$

No	t	x	k
1	15	0.00059	0.244
2	30	0.00104	0.223
3	45	0.00160	0.241
4	60	0.00208	0.252
5	75	0.02547	0.252
6	90	0.00292	0.251
7	105	0.00321	0.243
8	120	0.00368	0.258

$k_{1;3-8} = 0.248$

85 °C
$a = 0.01598$
$b = 0.01013$

No	t	x	k
1	10	0.00051	0.320
2	20	0.00102	0.337
3	30	0.00152	0.356
4	40	0.00203	0.374
5	50	0.00254	0.393
6	61	0.00289	0.381
7	70	0.00325	0.389
8	80	0.00350	0.381

$k_{1-8} = 0.366$

85 °C
a = 0.01630
b = 0.010045

90 °C
a = 0.01630
b = 0.010045

95 °C
a = 0.01610
b = 0.01010

No	t	x	k	No	t	x	k	No	t	x	k
1	10	0.00065	0.414	1	7	0.00051	0.458	1	6	0.00064	0.688
2	20	0.00108	0.363	2	14	0.00097	0.455	2	12	0.00150	0.877
3	30	0.00159	0.370	3	21	0.00159	0.495	3	17	0.00184	0.776
4	40	0.00198	0.360	4	28	0.00198	0.514	4	22	0.00239	0.827
5	50	0.00246	0.376	5	35	0.00246	0.535	4	27	0.00279	0.824
6	60	0.00285	0.377	6	42	0.00283	0.531	6	32	0.00319	0.827
7	70	0.00316	0.371	7	49	0.00324	0.546	7	37	0.00359	0.841
8	80	0.00345	0.366	8	56	0.00350	0.531	8	42	0.00385	0.817

k_{2-8} = 0.369 k_{3-8} = 0.525 k_{1-8} = 0.810

101.5 °C
a = 0.022447
b = 0.01092

101.5 °C
a = 0.022447
b = 0.00960

No	t	x	k	No	t	x	k
1	20	0.00457	1.363	1	20	0.00437	1.517
2	40	0.00655	1.237	2	40	0.00608	1.334
3	60	0.00777	1.180	3	60	0.00709	1.245
4	80	0.00851	1.172	4	80	0.00770	1.168
5	100	0.00906	1.086	5	100	0.00821	1.153
				6	120	0·00840	1.046
				7	140	0.00863	1.004

k_{1-5} = 1.207 k_{1-7} = 1.209

III.

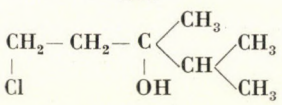

75 °C
a = 0.01687
b = 0.01011

80 °C
a = 0.01687
b = 0.01011

No	t	x	k	No	t	x	k
1	15	0.00081	0.336	1	10	0.00089	0.554
2	30	0.00144	0.315	2	20	0.00148	0.490
3	45	0.00206	0.320	3	30	0.00208	0.485
4	60	0.00256	0.314	4	40	0.00256	0.471
5	78	0.00311	0.310	5	52	0.00304	0.451
6	90	0.00340	0.303	6	60	0.00337	0.449
7	105	0.00368	0.291	7	70	0.00368	0.436
8	120	0.00401	0.289	8	80	0.00400	0.424

k_{1-8} = 0.310 k_{3-8} = 0.454

85 °C
$a = 0.01630$
$b = 0.010045$

90 °C
$a = 0.01630$
$b = 0.010045$

No	t	x	k	No	t	x	k
1	7	0.00072	0.664	1	5	0.00060	0.766
2	14	0.00132	0.649	2	10	0.00130	0.884
3	21	0.00196	0.675	3	15	0.00188	0.900
4	28	0.00254	0.694	4	20	0.00244	0.927
5	36	0.00307	0.711	5	25	0.00292	0.931
6	42	0.00329	0.649	6	30	0.00326	0.902
7	49	0.00372	0.664	7	35	0.00358	0.876
8	56	0.00403	0.652	8	40	0.00399	0.899

$k_{1-3;\,6-8} = 0.659$ $k_{2-8} = 0.903$

REFERENCES

1. Bartók, M., Bozóki-Bartók, G., Kovács, K.: Acta Chim. Acad. Sci. Hung. **66,** 115 (1970)
2. Bartók, M., Láng-Lakos, K., Bozóki-Bartók, G.: Acta Chim. Acad. Sci. Hung **70,** 133 (1971)
3. Bartók, M., Bozóki-Bartók, G., Kovács, K.: Acta Chim. Acad. Sci. Hung. **72,** 297 (1972)
4. Bartók, M., Bozóki-Bartók, G.: Acta Chim. Acad. Sci. Hung. **72,** 423 (1972)
5. Bartók, M.: Acta Chim. Acad. Sci. Hung. **55,** 365 (1968)

Mihály Bartók
Gizella Bozóki-Bartók
Szeged, Dóm tér 8, Hungary.

Acta Chimica Academiae Scientiarum Hungaricae, Tomus 72 (4), pp. 441—450 (1972)

CRYSTAL AND MOLECULAR STRUCTURE OF ACETONE 4-NITROPHENYLHYDRAZONE

GY. MENCZEL, G. SAMAY and K. SIMON

(Department for Experimental Physics, L. Eötvös University, Budapest)

Received October 2, 1970

The crystal and molecular structure determination of acetone 4-nitrophenylhydrazone has been performed by X-ray diffraction methods. The crystals are monoclinic, the space group is $P2_1/c$. The structure has been determined by Patterson's and molecular transform methods. The refinement has been carried out by differential syntheses and by least squares. The reliability index is $R = 10.9\%$. The bond relations in the benzene ring are asymmetrical. The bond lengths and angles are compared with data of acetone 3-nitrophenylhydrazone determined previously [1]. The equation of the best plane through the benzene ring, and those of the planes of the acetone and of two parts of the hydrazine, have been determined and the angles made by these planes have been computed.

The crystal and molecular structure of acetone 3-nitrophenylhydrazone (abbreviated: Ac-3-NPH) has been published recently [1]. As a further study of the bond relations of nitrophenylhydrazone derivatives, the X-ray diffraction investigation of acetone 4-nitrophenylhydrazone (abbreviated: Ac-4-NPH)

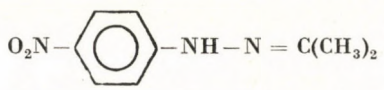

has been performed in the present work.

Experimental

The crystals were prepared by heating a mixture of acetone and *p*-nitrophenylhydrazine in aqueous alcohol [2]. The crystals are yellow monoclinic plates elongated in the direction of the *a* axis. Their length is 0.6—1.0 mm. The dimensions in the *b* and *c* directions are approximately 0.02 and 0.2 mm, respectively. The faces of the plates are the (010) planes. The crystals have little mechanical strength and cannot be cut without losing their single crystal character. The unit cell parameters were measured on oscillation and Weissenberg photographs.

Crystallographic data

(with standard deviations in parentheses)
Acetone 4-nitrophenylhydrazone, $C_9N_3O_2H_{11}$ (M. W. 193.23)
Monoclinic

$a = 4.053$ (15) Å
$b = 20.74$ (5) Å
$c = 11.80$ (3) Å
$\beta = 95.5°$ (4)
$Z = 4$
$V = 987$ (3) Å^3
$F(000) = 408$
$D_x = 1.30$ g · cm^{-3}, $D_m = 1.32$ (4) g · cm^{-3}
Systematic absences $h0l : l = 2n + 1$
$0k0 : k = 2n + 1$
Space group $P2_1/c$ (No. 14, C_{2h}^5)
μl (for Cu K α, $\lambda = 1.542$ Å) = 9.2 cm^{-1}.

The density was determined by flotation in aqueous $NaNO_3$ solution, in the presence of a few drops of isobutyl alcohol in order to remove air bubbles.

Weissenberg photographs were made by the equiinclination technique with unfiltered Cu radiation using the multiple film method. Intensity measurements were performed only from the layers $0kl$—$2kl$, owing to the fact that absorption had considerable effect on the photographs around the b and c axes. For this reason the common scale was obtained in the following way. A part of the $h = 0$ layer was recorded on one half of a film, while the $h = 1$ layer — with the same oscillation interval — was registered on the other half. Similarly, a common photograph of the layers $h = 0$ and $h = 2$ was prepared. The relative intensities were estimated visually using standard scale and were corrected for Lp-factors and spot shapes. The intensities of the unobserved reflexions were taken as the half of the minimum measured value. Thus 1087 independent reflexions were collected of which 566 had measurable intensities. The absolute scale and the mean temperature factor were determined by WILSON's method [3]. The scale factors were refined later in the course of the structure refinement.

Structure determination and refinement

The projection onto the (100) plane was determined first. The symmetry of this projection is *pgg*. The orientation of the molecule in the projection was found by a $P(v, w)$ Patterson synthesis: the two-dimensional Patterson map was compared with the projection of the theoretical vector set of the molecule. The a axis being short, the projection of the set of the intramolecular vectors was drawn by assuming that the molecule was plane, and the image of the molecule was not distorted significantly in the projection. After having found the orientation, the position of the molecule was fixed in relation to the b and c axes, applying the molecular transform method of TAYLOR and MORLEY [4]. A program in EFT autocode was written by SIMON for a URAL-2 computer to the computations [5].

The refinement for the projection, begun with a reliability index of $R = 46\%$, was carried out with successive differential syntheses and "diagonal matrix" least squares cycles. The R factor for the projection was then 27%. The Patterson syntheses were computed by a program written by CSORDÁS [6].

The rate of the shortening of the approximately known bond lengths in the projection and the assumption that the molecule was nearly plane, allowed us to determine roughly the orientation of the molecule in three dimensions. The position of the oriented molecule was still uncertain in the third (a) direction. The originally two-dimensional method of TAYLOR and MORLEY [4] was

then adopted for the one-dimensional problem and the previously applied computer program [5] was used for the computations of the x coordinates.

The three-dimensional model ($R = 52\%$) was refined by a 'block-diagonal matrix least squares' program. Three cycles were computed with isotropic and further nine cycles with anisotropic thermal parameters. In the three last cycles the parameter shifts showed only random fluctuations and were less than 10%

Table Ia

Positional parameters (with their standard deviations in parentheses)

	$x \cdot 10^4$	$y \cdot 10^4$	$z \cdot 10^4$
C(1)	9682 (26)	106 (2)	2768 (5)
C(2)	9801 (30)	—546 (3)	3416 (5)
C(3)	885 (25)	125 (3)	1574 (4)
C(4)	7157 (17)	1674 (1)	3294 (3)
C(5)	7491 (20)	2295 (2)	2780 (4)
C(6)	6281 (21)	2835 (2)	3332 (4)
C(7)	4840 (16)	2777 (1)	4342 (4)
C(8)	4376 (20)	2163 (2)	4850 (5)
C(9)	5643 (21)	1624 (2)	4312 (6)
N(1)	8325 (17)	565 (1)	3319 (3)
N(2)	8338 (16)	1167 (2)	2740 (4)
N(3)	3471 (19)	3330 (2)	4890 (4)
O(1)	4032 (19)	3862 (2)	4450 (4)
O(2)	2098 (14)	3270 (2)	5763 (4)

of the corresponding estimated standard deviation (e.s.d.) values. No hydrogen atoms were drawn into the computations. The final value of the reliability index for all reflexions was $R = 10.9\%$.

The atomic scattering factors for neutral atoms were taken from the *International Tables* [7]. Table Ia contains the final positional parameters with their e.s.d.'s, computed by the method of CRUICKSHANK [8]. Table Ib gives the final anisotropic temperature parameters.

The programs for the intensity corrections and for the differential synthesis were written in machine code for the Ural-2, while those for the least squares refinement and for the parameter error calculations were written in Algol-60 for RAZDAN-3 by one of us (Gy. M.).

The values of the observed and calculated structure factors are available from the authors.

Table Ib

Thermal parameters multiplied by 10^5.
The temperature factors are of the form:

$$T = \exp\left[-(b_{11}h^2+b_{22}k^2+b_{33}l^2+b_{12}hk+b_{13}hl+b_{23}kl)\right]$$

b_{23}	b_{11}	b_{22}	b_{33}	b_{12}	b_{13}	b_{23}
C(1)	2581	246	1024	731	—15	—232
C(2)	9449	297	1135	815	2531	—294
C(3)	2284	273	1431	962	1293	—172
C(4)	3280	254	806	—31	—682	23
C(5)	11300	314	739	—734	—32	—31
C(6)	5884	368	890	—577	483	—85
C(7)	6508	247	724	—61	924	—103
C(8)	3448	281	985	539	—675	61
C(9)	7313	297	754	—719	453	—95
N(1)	3262	263	855	147	—75	58
N(2)	10005	299	990	—1359	315	—84
N(3)	7641	323	897	—136	1085	—71
O(1)	11731	299	1586	620	5239	—313
O(2)	6199	328	936	437	1419	64

Description of the structure

Table II gives the interatomic distances with their e.s.d.'s. The bond angles are listed in Table III along with their e.s.d.'s calculated by the method of DARLOW [9]. The intramolecular distances and the bond angles are shown in Fig. 1a. For comparison purposes, Fig. 1b represents the bond relations in Ac-3-NPH.

The schematic drawing of the projection of the unit cell onto the (100) plane is shown in Fig. 2.

The main structural features of the two modifications do not show significant deviations. The bond relations of the benzene rings are asymmetrical in both compounds. The bond angle at the carbon atom where the nitro group is attached, is greater than 120° in both cases. The O(1)N(3)O(2) angles are also greater than 120°.

Considering the carbon–nitrogen bonds in the Ac-4-NPH and Ac-3-NPH molecules, the following comments can be made:

(*a*) The length of the bond between the aromatic carbon and the nitrogen of the nitro group is shorter in the *para* modification (1.453 Å), than in the ***meta*** nitro compound (1.489 Å). Comparing them by the method of CRUICKSHANK and ROBERTSON [10] it was shown that the difference (0.036 Å) is "significant".

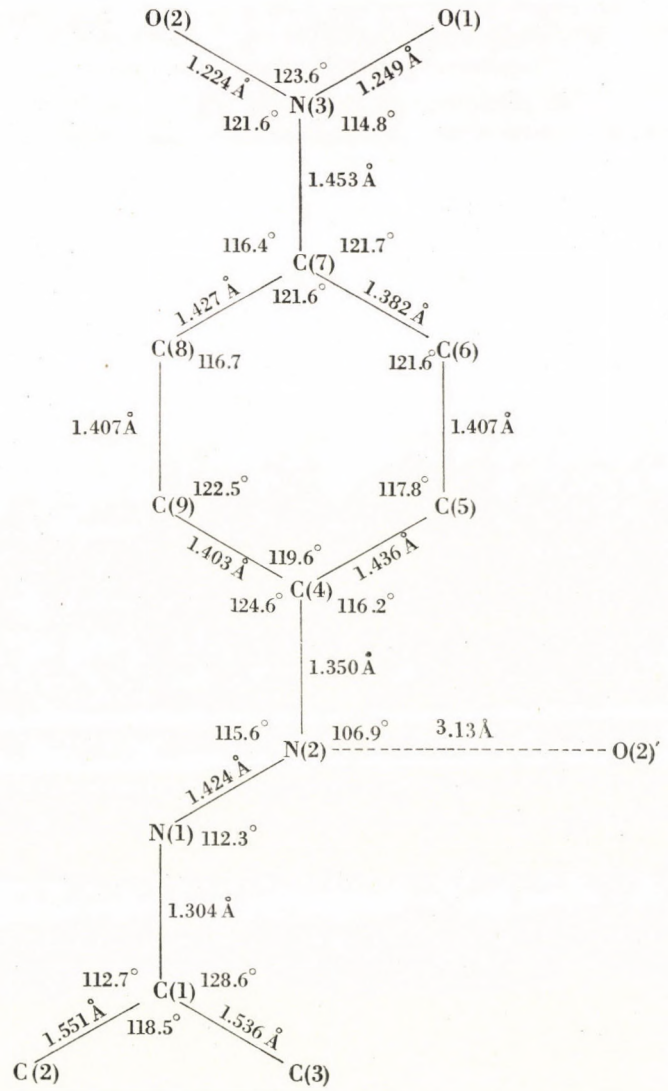

Fig. 1a. Bond lengths and angles in Ac-4-NPH

(*b*) The bond lengths between the aromatic carbon and the nitrogen of the hydrazine show no deviation (1.350 Å and 1.351 Å respectively) for the two compounds.

(*c*) The double bond between the N(1) nitrogen of the hydrazine and the C(1) carbon atom of the acetone is unusually short in the *meta* isomer: 1.273 Å. In the *para* modification this bond is a little longer and the deviation seems to be 'possibly significant' [10] too.

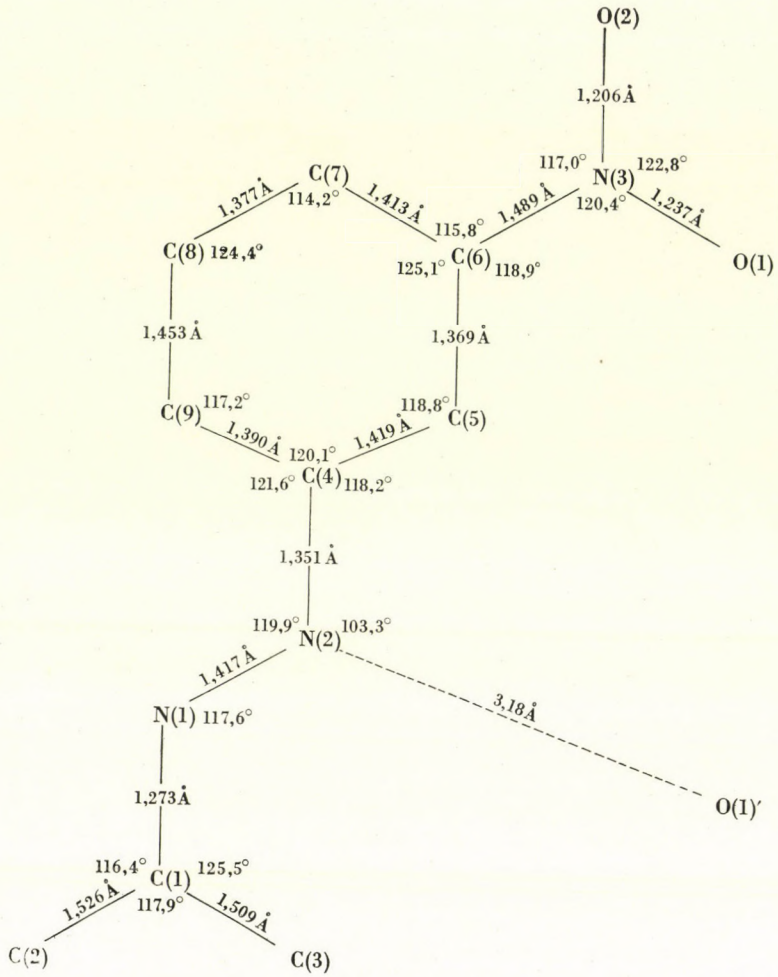

Fig. 1b. Bond lengths and angles in Ac-3-NPH

In Ac-4-NPH, the distance between 0(1)(x,y,z) and N(2)($x-1$, $1/2-y$, $1/2+z$) had the value of 3.13 Å. This is considerably shorter than the upper limit of the intermolecular distances between nitrogen and oxygen atoms connected by hydrogen bonding, which is reported by different sources to be between 3.17 and 3.22 Å [7, 11, 12]. The existence of such a hydrogen bond was shown by IR spectra, too [13]. The hydrogen bond connects here molecules which form infinite chains with axes parallel to the [201] direction (Fig. 2). The hydrogen bond in the *meta* isomer produces dimers by connecting molecules related by a centre of symmetry.

Table II

Interatomic distances (with their standard deviations in parentheses)

	Interatomic distances, Å
C(1)—C(2)	1.551 (11)
C(1)—C(3)	1.536 (10)
C(1)—N(1)	1.304 (13)
N(1)—N(2)	1.424 (6)
C(4)—N(2)	1.350 (6)
C(4)—C(5)	1.436 (7)
C(5)—C(6)	1.407 (8)
C(6)—C(7)	1.382 (7)
C(7)—C(8)	1.427 (8)
C(8)—C(9)	1.407 (9)
C(4)—C(9)	1.403 (8)
C(7)—N(3)	1.453 (7)
N(3)—O(1)	1.249 (8)
N(3)—O(2)	1.224 (7)

Table III

Bond angles

C(2)—C(1)—C(3)	118.5° (9)
C(2)—C(1)—N(1)	112.7 (6)
C(3)—C(1)—N(1)	128.6 (6)
C(1)—N(1)—N(2)	112.3 (5)
N(1)—N(2)—C(4)	115.6 (4)
N(2)—C(4)—C(5)	116.2 (6)
N(2)—C(4)—C(9)	124.6 (4)
C(5)—C(4)—C(9)	119.6 (5)
C(4)—C(5)—C(6)	117.8 (5)
C(5)—C(6)—C(7)	121.6 (5)
C(6)—C(7)—C(8)	121.6 (5)
C(7)—C(8)—C(9)	116.7 (5)
C(8)—C(9)—C(4)	122.5 (5)
C(6)—C(7)—N(3)	121.7 (5)
C(8)—C(7)—N(3)	116.4 (5)
O(1)—N(3)—O(2)	123.6 (5)
C(7)—N(3)—O(1)	114.8 (5)
C(7)—N(3)—O(2)	121.2 (5)

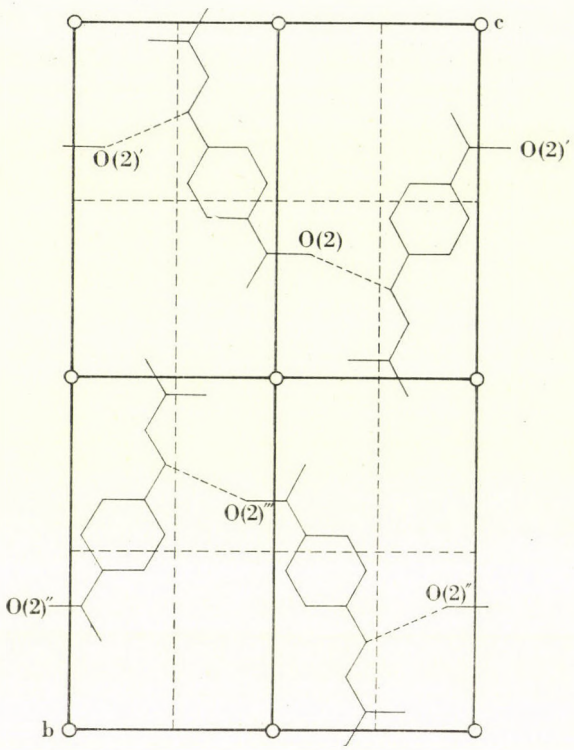

Fig. 2. Projection onto (010) of the unit cell of Ac-4-NPH

The equation of the 'best fitted plane', $P(1)$, through the atoms of the benzene ring was determined by the least squares procedure of SHOMAKER *et al.* [14]. This plane is almost perpendicular to the (010) plane (83.6°) and it is inclined to the (100) plane by 32.1°. The distances of the atoms from $P(1)$ are listed in Table IV.

The plane of the NO_2 group, $P(2)$, is slightly tilted to the plane $P(1)$ making an angle of 5.1° with it.

The equations of the following planes were also determined: $P(3)$ denotes the plane through the atoms C(2)C(1)C(3). $P(4)$ and $P(5)$ are the planes through the atoms C(1)N(1)N(2) and C(4)N(2)N(1), respectively. The equations of these planes refer to orthogonal axes X′, Y, Z′, where the transformation matrix is

$$\begin{bmatrix} 1 & 0 & \cos\beta \\ 0 & 1 & 0 \\ 0 & 0 & \sin\beta \end{bmatrix}.$$

The equations of the planes and the angles between the different planes are given in Table V. The e.s.d. of these angles is about $\pm 2°$.

Table IV

Deviations of the atoms from plane P(1)

	Deviation in 10^{-3} Å
C(1)	228
C(2)	455
C(3)	—286
C(4)	7
C(5)	—4
C(6)	—2
C(7)	21
C(8)	—14
C(9)	11
N(1)	160
N(2)	2
N(3)	—30
O(1)	54
O(2)	—55

Table V

(a) Equations of the planes

P1	$0.841\ X' + 0.112\ Y + 0.526\ Z' - 1.136 = 0$
P2	$0.840\ X' + 0.043\ Y + 0.541\ Z' - 0.719 = 0$
P3	$0.892\ X' + 0.209\ Y + 0.402\ Z' - 0.958 = 0$
P4	$0.849\ X' + 0.217\ Y + 0.484\ Z' - 1.244 = 0$
P5	$0.882\ X' + 0.186\ Y + 0.432\ Z' - 0.973 = 0$

(b) Angles between the different planes

	P2	P3	P4	P5	(100)	(010)
P1	5.1°	10.2°	7.3°	9.2°	32.1°	83.6°
P3	—	—	5.7°	2.5°	—	—
P4	—	—	—	4.4°	—	—

*

The authors are very grateful to Prof. A. GERECS and his co-workers (Department for Chemical Technology, L. Eötvös University, Budapest) for preparing the crystals, to Dr. L. CSORDÁS for his useful advice, to Prof. K. LEMPERT (Department for Organic Chemistry, Technical University, Budapest) for recording and evaluating the IR spectra, to Miss E. ZSOLDOS for help in making the calculations and drawings, and to the team of the University Computer Centre for their help in the computations.

REFERENCES

1. MENCZEL, GY.: Acta Chim. Acad. Sci. Hung. **62,** 41 (1969)
2. FÓTI, A.: Private communication
3. WILSON, A. J. C.: Nature **150,** 152 (1942)
4. TAYLOR, C. A., MORLEY, K. A.: Acta Cryst. **12,** 101 (1959)
5. SIMON, K.: Diploma Work, L. Eötvös Univ., Budapest, 1969
6. CSORDÁS, L.: Acta Chim. Acad. Sci. Hung. **57,** 147 (1968)
7. International Tables for X-Ray Crystallography, Vol. III, Kynoch Press, Birmingham
8. CRUICKSHANK, D. W. J.: Acta Cryst. **2,** 154 (1959)
9. DARLOW, S. F.: Acta Cryst. **13,** 683 (1963)
10. CRUICKSHANK, D. W. J., ROBERTSON, A. P.: Acta Cryst. **6,** 698 (1953)
11. FURBERG, S., PETERSON, C. S.: Acta Chim. Scand. **16,** 1539 (1962)
12. ROBERTSON, J. M.: Organic Crystals and Molecules, p. 243. Cornell University Press, Ithaca—New York, 1953
13. LEMPERT, K.: Private communication
14. SHOMAKER, V., WASER, J., MARSH, R. E., BERGMAN, G.: Acta Cryst. **12,** 600 (1959)
15. MENCZEL, GY.: Acta Chim. Acad. Sci. Hung. **60,** 135 (1969)

György MENCZEL; Budapest VIII., Múzeum krt. 6—8.
Géza SAMAY: Budapest XIV., Hungária krt. 114.
Kálmán SIMON; Budapest VII., Rottenbiller u. 26.

Acta Chimica Academiae Scientiarum Hungaricae, Tomus 72 (4), pp. 451–457 (1972)

THERMOLYTIC DISPROPORTIONATION OF CYANOACETATE SALTS

J. EGYED, P. VINKLER and S. GÁL*

*(Central Research Institute for Chemistry of the Hungarian Academy of Sciences, Budapest and *Department of General and Analytical Chemistry, Technical University, Budapest)*

Received October 18, 1970

Sodium cyanoacetate (**I**) decomposes over 180 °C to give carbon dioxide, acetonitrile and sodium-imidomethylenemalonic acid disodium salt (**II**). The mechanism of the reaction was examined. In the first step two molecules of **I** react to give cyanoacetic acid disodium salt (**III**) and cyanoacetic acid; the latter spontaneously decomposes at the temperature of the thermolysis to carbon dioxide and acetonitrile. The intermediary product **III** of carbanion structure can interact with the electrophilic carboxylate carbon atom of another **I** molecule and the resulting transition complex transforms to acetonitrile and **II**. In the presence of sodium methyl carbonate-^{14}C the thermolysis of **I** led to the incorporation of the radioactive carboxylate carbon atom into **II**, whose acid hydrolysis gave radioactive cyanoacetic acid, which was then isolated as the ethyl ester. Experiments with the Li, K and Ba salts of cyanoacetic acid revealed a dependence of the decomposition temperature upon the cation, but the decomposition products were identical with those of the sodium salt.

While the pyrolysis of aliphatic carboxylate salts yields, in general, ketones and carbonates [1], the thermolysis of cyanoacetates proceeds along a particular disproportionation pathway.

An examination of the properties of sodium cyanoacetate (**I**) has revealed that the compound melts at 182 °C and subsequently undergoes a gradual decomposition to carbon dioxide, acetonitrile and sodium-imidomethylenemalonic acid disodium salt (**II**). While carbon dioxide and acetonitrile are volatile at the temperature of the decomposition process, compound **II** is solid under these conditions. Hence the thermolytic decomposition can exactly be followed by the thermogravimetric technique (*cf.* Fig. 1) and this technique also makes possible the determination of the stoichiometry of the reaction:

$$\underset{\mathbf{I}}{3\ N\equiv C-CH_2-COONa} \rightarrow CO_2 + 2\ N\equiv C-CH_3 + Na-N=\underset{\mathbf{II}}{C=C\begin{matrix}COONa\\COONa\end{matrix}} \qquad (1)$$

The properties of compound **II** can be summarized as follows:

1. Compound **II** is a pale yellow, hygroscopic substance, insoluble in organic solvents and readily soluble in water. In aqueous solution compound **II** undergoes hydrolysis to give sodium cyanoacetate and sodium carbonate; the process can be followed by infrared spectrophotometry (Fig. 4).

2. In acidic milieu compound **II** undergoes a rapid decomposition to form cyanoacetic acid and carbon dioxide.

3. The infrared spectrum of compound **II** (Fig. 2) recorded with a UR-10 spectrophotometer in KBr pellet is different from that of the starting compound **I** (Fig. 3). The C—H frequencies are missing from the former, and the stretching vibration band of the nitrile appearing at 2263 cm^{-1} is replaced by an

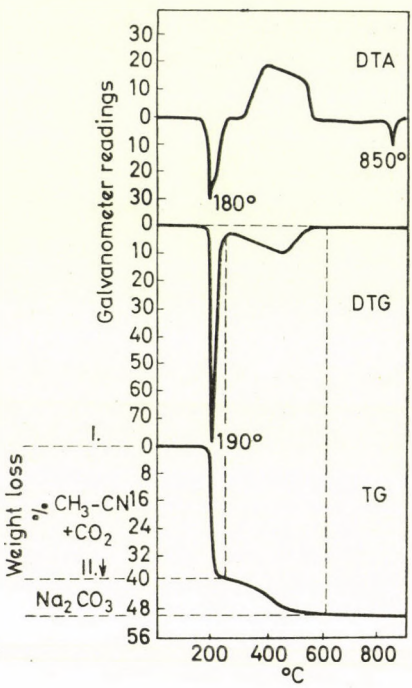

Fig. 1. TG, DTG and DTA diagrams of the thermolytic disproportionation of sodium cyanoacetate

intense absorption at 2170 cm^{-1}. According to the literature [3, 4], this latter absorption is associated with the antisymmetric stretching vibration of the ketenimine cumulated doublebond system. The absorption at 1158 cm^{-1} is presumably due to the symmetric stretching vibration of the C=C=N structural unit. The absorption bands appearing in the region 1600—1300 cm^{-1} refer to a dicarboxylate structure [2].

In the elucidation of the reaction mechanism, we started from the assumption that the mobility of the methylene hydrogen atoms, *i.e.* carbanion formation may play an important part in the process. (It is well known that cyanoacetic acid and related acids form dibasic salts with organometallic compounds: in addition to the carboxylic hydrogen atom, the methylene hydrogen is replaceable by metal [5].)

Therefore the thermolysis of compound **I** was accomplished in the presence of sodium methoxide. In this case no carbon dioxide was formed, and the products were acetonitrile, compound **II** and methanol. In the presence of sodium methoxide the thermolytic process followed the stoichiometry:

$$2\,\mathbf{I} + \mathrm{MeONa} \rightarrow \mathrm{MeOH} + \mathbf{II} + \mathrm{N} \equiv \mathrm{C}-\mathrm{CH_3}. \qquad (2)$$

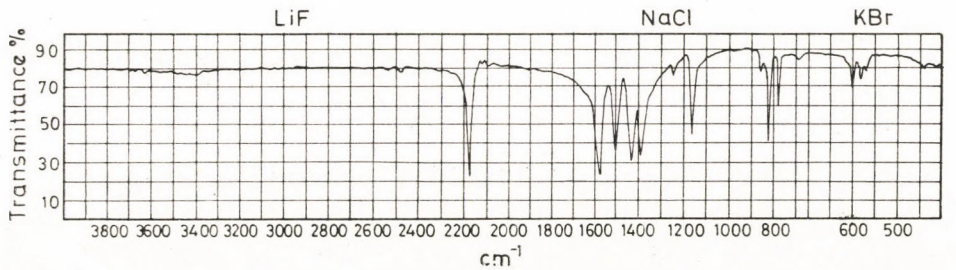

Fig. 2. Infrared spectrum of sodium-imidomethylene-malonic acid disodium salt (**II**)

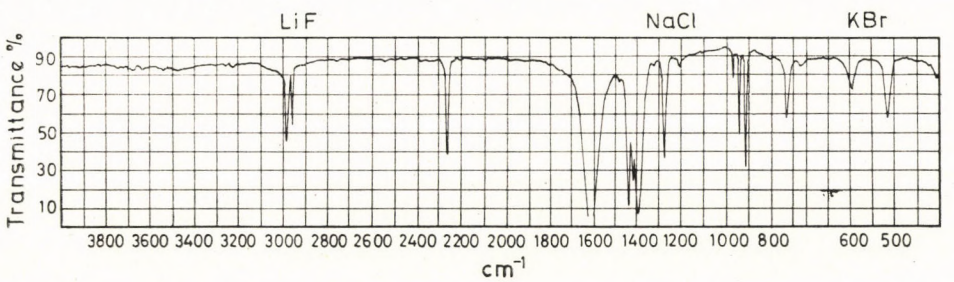

Fig. 3. Infrared spectrum of sodium cyanoacetate (**I**)

From this fact the conclusion may be drawn that the reaction proceeds through the intermediary product **III**, a carbanion-containing cyanoacetic acid disodium salt, which may be formed either from two molecules of **I** or from one molecule each of **I** and sodium methoxide. In the former case the formation of **III** is accompanied by that of cyanoacetic acid, which at the temperature of the thermolysis decomposes to acetonitrile and carbon dioxide. In the former case the formation of **III** is accompanied by that of cyanoacetic acid, which at the temperature of the thermolysis decomposes to acetonitrile and carbon dioxide. In the latter case, the other product is methanol.

$$\begin{aligned} 2\,\mathbf{I} &\rightarrow \mathrm{N} \equiv \mathrm{C}-\mathrm{CH_2}-\mathrm{COOH} + [\mathrm{N} \equiv \mathrm{C}-\mathrm{CH}-\mathrm{COONa}] \\ &\quad \downarrow \qquad\qquad\qquad\qquad\qquad\quad | \\ &\quad \mathrm{CO_2} + \mathrm{N} \equiv \mathrm{C}-\mathrm{CH_3} \qquad\qquad\quad \mathrm{Na} \\ &\qquad\qquad\qquad\qquad\qquad\qquad\qquad\quad \mathbf{III} \\ \mathbf{I} + \mathrm{MeONa} &\rightarrow \mathrm{MeOH} + \mathbf{III} \end{aligned} \qquad (3)$$

The mechanism of the formation of compound **II** can be elucidated on the basis of the stoichiometry shown in Eq. (2); the transition complex formed by the reaction of carbanion **III** and the electrophilic carboxylate carbon atom decomposes to acetonitrile and compound **II**:

$$\mathbf{III} + \underset{\mathbf{IV}}{Y-\overset{\overset{\displaystyle O}{\|}}{C}ONa} \rightarrow N\equiv C-\underset{\underset{\displaystyle ONa}{|}}{\underset{\underset{\displaystyle Y-C-ONa}{|}}{CH}}-COONa \rightarrow \mathbf{II} + HY \qquad (4)$$

a: $Y = -CH_2CN$
b: $Y = -OCH_3$

Eq. (4) represents a general description of the reaction between carbanion **III** and the electrophilic carboxylate carbon atom. Presumably, the practicability of the reaction is dependent upon the electrophilicity and detachability of the substituent connected to the carboxylic group.

A further piece of evidence for the validity of this generalization was provided by the fact that in the decomposition of sodium cyanoacetate in the presence of sodium methyl carbonate-^{14}C (**IVb**, $Y = OCH_3$) the radioactivity was incorporated into compound **II** formed. (In order to eliminate the interference from contaminations in the starting sodium methyl carbonate-^{14}C, compound **II** was transformed to cyanoacetic acid according to Eq. (5), esterified with ethanol and the radioactivity of this latter was measured.) The incorporation proceeded in alkaline medium, where no carbon dioxide could be formed and incorporated.

$$\mathbf{II} + H^+ \rightarrow CO_2 + N\equiv C-CH_2-COOH \rightarrow N\equiv C-CH_2-COOEt\,. \qquad (5)$$

Interestingly in Eq. (4) the carbon atom of the carboxylate anion is the electrophilic component of the S_E1 type substitution reaction. Similar reactions are known to proceed between carbanions and alkylmagnesium carbonates [6], however, in these processes the cyclic nature of the transition complex is considered to be the decisive factor, instead of the electrophilicity of the carboxylic carbon atom.

Finally, it is worth mentioning that the thermolysis of the Li, K and Ba salts of cyanoacetic acid was also studied and the temperature of decomposition of these salts was found to vary with the cation. The decomposition products were identical with those formed in the thermolysis of the sodium salt.

Experimental

Thermogravimetric examination of the thermolysis of cyanoacetate salts

The thermolysis processes of the lithium, sodium, potassium and barium salts of cyanoacetic acid were examined by means of an F. PAULIK—J. PAULIK—L. ERDEY type derivatograph [7, 8] (Hungarian Optical Works) with 200 mg samples, at 5 °C/min. rate of heating, in air and in some inert gas.

Fig. 1 shows the derivatogram of sodium cyanoacetate obtained in argon gas. The endothermic DTA peak at 180 °C indicates the melting of the sample and, together with the DTG and TG curves, it shows the proceeding of the decomposition process. Up to 240 °C the **I** → CO_2 + CH_3CN + **II** reaction proceeded quantitatively, as indicated by the good agreement between the calculated (39.3%) and measured (39.0%) weight loss values. The decomposition of the remaining solid product, compound **II**, only started above 300 °C and the rate of weight loss reached its maximum at about 450 °C (DTG curve). The residue of the decomposition which started at 300 °C was sodium carbonate formed in stoichiometric amount; this was proved besides the 50% weight loss by the appearance of an endothermic DTA peak at 850 °C indicating the melting of sodium carbonate. The gaseous decomposition products of compound **II** were not examined.

Similar results were obtained in the thermolysis of the other metal salts. The maximum rates of decomposition were observed at the following temperatures (DTG curves):

Li salt	245 °C
Na salt	190 °C
K salt	200 °C
Ba salt	245 °C.

The residues remaining after heating to above 600 °C consisted of the corresponding metal carbonates in each case.

The derivatographic measurements unequivocally proved the reaction: **I** → CO_2 + + CH_3CN + **II** and the subsequent decomposition of compound **II** to metal carbonate and gaseous products.

Thermolysis of sodium cyanoacetate (I) and identification of the decomposition products

The thermolysis was accomplished in a hermetically closed distillation apparatus connected to a vacuum manometer. 3.2 g (0.03 mole) of **I** was placed in the distillation flask, the receiver was cooled with liquid air and the sample heated to 200—220 °C. The substance melted above 180 °C and then a vigorous evolution of gas was observed. The residue gradually solidified in 15—20 min., which indicated the end of the reaction.

The reaction products were carbon dioxide, acetonitrile and sodium-imidomethylenemalonic acid disodium salt (**II**).

Carbon dioxide and acetonitrile condensed in the receiver. The carbon dioxide was identified as barium carbonate. The acetonitrile weighed 0.72 g (88% yield, based on Eq. (1)), b.p. 81 °C (only a negligible residue remained on distillation), and its infrared spectrum was identical with that of an authentic acetonitrile sample.

Compound **II** remained in the distillation flask; it weighed 1.85 g (95% yield, based on Eq. (1)).

$C_4NO_4Na_3$. Calcd. C 24.63; N 7.18; Na 35.37. Found C 24.80 and 25.23; N 7.23 and 7.35%.

Thermolysis of sodium cyanoacetate (I) in the presence of sodium methoxide

0.2298 g of sodium (0.01 g-atom) was dissolved in 4 ml methanol and 2.1438 g (0.02 mole) of **I** was added to the solution. The methanol was removed by distillation at room temperature in vacuum (2 Torr) and condensed in a receiver cooled with liquid air to recover 3 ml of methanol (no evolution of carbon dioxide was observed during the procedure). After changing the receiver, the pressure was adjusted again to 2 Torr and the thermolysis accomplished at 220 °C.

After the reaction was over, the pressure in the apparatus was 94 Torr at 22 °C, which practically corresponded to the tension of the methanol and acetonitrile produced. Accordingly, the thermolysis process followed Eq. (2) (the pressure of the carbon dioxide evolved according to Eq. (1) would have been 858 Torr at 22 °C).

Compound **II** obtained weighed 1.78 g, corresponding to 91.5% yield according to Eq. (2) and its infrared spectrum was identical with that of the product obtained in the preceding experiment.

The acetonitrile + methanol mixture weighed 1.10 g. According to gas-chromatographic analysis the mixture did not contain any other constituents.

Thermolysis of sodium cyanoacetate (I) in the presence of sodium methoxide and sodium methyl carbonate-^{14}C (IV-b)

The reactants were applied in stoichiometric amounts, according to Eq. (3).

0.5891 g of sodium (0.0256 g-atom) was dissolved in 10 ml methanol and the obtained sodium methoxide solution was treated with radioactive carbon dioxide evolved from 0.9956 g (0.00504 mole) of $Ba^{14}CO_3$ in the usual vacuum apparatus. In this way sodium methyl carbonate-^{14}C (**IV-b**) was synthesized in quantitative yield [9]. 3.7542 g (0.03508 mole) of **I** was added to the above suspension and subsequently the methanol was removed by distillation in vacuum using a water pump. Finally, the pressure was adjusted to 2 torr, the receiver cooled with liquid air, and the reaction mixture heated for 20 min. at 220 °C. By the end of the reaction the internal pressure rose to 82 Torr at 23 °C corresponding to the pressure of the methanol formed (practically no evolution of carbon dioxide was observed).

The solid residue remaining in the distillation flask (apparently compound **II** and perhaps unreacted starting materials including **IV-b**) was powdered, taken up in 40 ml of abs. ether and treated with 8.0 g (0.083) of methanesulfonic acid in the vacuum apparatus. The carbon dioxide formed during this decomposition step was introduced into an appropriate amount of phenylmagnesium bromide solution. The resulting benzoic acid was crystallized from water, dried (m.p. 124 °C) and its activity measured.

The ethereal cyanoacetic acid solution obtained on treatment of **II** with methanesulfonic acid was diluted with 70 ml of abs. ethanol, the ether removed by distillation and the ethanol solution refluxed for 6 hrs. to esterify the cyanoacetic acid. The solvent was removed by distillation, the residue dissolved in ether, the solution washed successively with sodium hydrogen carbonate solution and water, dried over anhydrous magnesium sulfate and distilled in vacuum to give 0.92 g of ethyl cyanoacetate, 103—104 °C/13 Torr. The radioactivity of the ethyl cyanoacetate-^{14}C was $6.459 \cdot 10^6$ dpm/mole, while that of the benzoic acid was $31.17 \cdot 10^6$ dpm/mole. The ethyl cyanoacetate-^{14}C contained 17.2% of the starting activity, which means that 34.4% of the starting activity had been incorporated into compound **II**.

Hydrolysis of sodium-imidomethylenemalonic acid disodium salt (II)

20 mg ($1.024 \cdot 10^{-4}$ mole) of **II** was dissolved in 0.1 ml distilled water and the hydrolysis was followed by infrared spectroscopy. The spectrum of the solution was recorded in every 2 minutes in the region 2100—2300 cm^{-1} with KRS-5 windows in 0.02 mm thickness at 35 °C. Inspection of the compensated spectra (Fig. 4), of which the first was recorded 2 min. after dissolution, reveals the gradual vanishing of the absorption band at 2160 cm^{-1}, characteristic of the ketenimine group and the parallel increase in intensity of the band at 2270 cm^{-1} associated with the stretching vibration of the nitrile group of the cyanoacetate ion. The eighth spectrum, recorded in the 16th min. of the hydrolysis reveals that the reaction was practically over by this time, since the band intensities were unchanged in the eighth and ninth spectra.

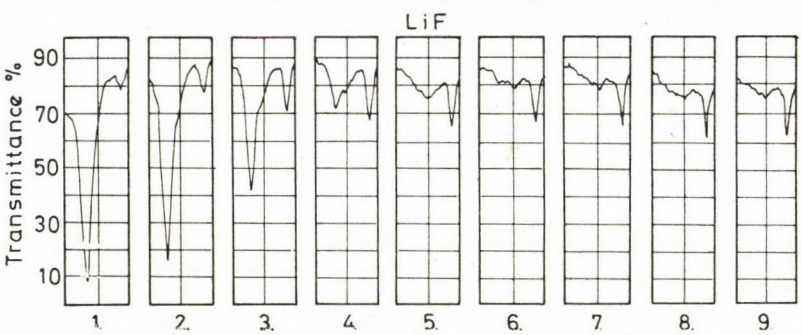

Fig. 4. Changes in the intensities of the $\nu\,C = C = N$ band (2160 cm^{-1}) of sodium-imidomethylenemalonic acid disodium salt (**II**) and the νCN band (2270 cm^{-1}) of sodium cyanoacetate (**I**) during the hydrolysis of compound **II**

REFERENCES

1. YAKERZON, V. I., RUBINSTEIN, A. M.: Reakcii i metodi issledovanija organicheskih soedinenii **13,** 128, Izdatelstvo Himija, Moscow, 1964
2. HARGREAVES, M. K., STEVINSON, E. A.: Spectrochim. Acta **21,** 1681 (1965)
3. STEVENS, C. L., FRENCH, I. C.: J. Am. Chem. Soc. **75,** 656 (1953)
4. DIJKSTRA, R., BACKER, H. I.: Rec. Trav. Chim. **73,** 575 (1954)
5. IVANOV, D., BLAGOV, B.: Bull. soc. chim. France **1963,** 1922
6. STILES, M., FINKBEINER, H. L.: J. Am. Chem. Soc. **81,** 505 (1959); **85,** 616 (1963); **86,** 961 (1964)
7. PAULIK, F., PAULIK, J., ERDEY, L.: Z. anal. Chem. **160,** 241 (1958)
8. PAULIK, F., PAULIK, J., ERDEY, L.: Z. anal. Chem. **160,** 321 (1958)
9. BOWEN, G.: U. S. Pat. 2,464,290 (1949); C. A. **43,** 6867f (1949).

János EGYED
Péter VINKLER
Budapest II., Pusztaszeri út 57—69, Hungary

Sándor GÁL; Budapest XI., Gellért tér 4, Hungary.

Acta Chimica Academiae Scientiarum Hungaricae, Tomus 72 (4), pp. 459—468 (1972)

METHANOLYSIS OF INULIN AND HYDROLYSIS OF METHYL-β-D-FRUCTOFURANOSIDE*

J. SZEJTLI, **R. D. HENRIQUES and **M. CASTIÑEIRA

*(Chinoin Pharmaceutical and Chemical Works Ltd., Budapest and **Escuela de Bioquimica-Farmaceutica, Universidad de La Habana, La Habana, Cuba)*

Received February 5, 1971

The preparation of methyl-β-D-fructofuranoside by methanolysis of inulin is described. The reaction rate constants for the methanolysis of inulin and saccharose as well as for the hydrolysis of the Me-β- and -α-D-fructofuranosides have been determined in the presence of HCl. The activation energy of methanolysis is considerably higher than that of hydrolysis, therefore, methanolysis is — at identical temperature and acid concentration — faster than hydrolysis. The activation entropy of methanolysis is +32 e.u., while that of hydrolysis is only +8 e.u., so it is concluded that the mechanism of alcoholysis differs from that of the hydrolysis. In glycosides, in which the aglycone moiety is bonded by a primary carbon atom to the bridging oxygen atom, the second atom of the aglycone exerts only a very small influence on the stability of the glycosidic bond. Therefore inulin may be considered a substituted methyl-β-D-fructofuranoside.

Introduction

The stability of the glycosidic bonds of β-D-fructofuranosides in acidic solutions has been investigated in our previous papers on the acid hydrolysis of saccharose, raffinose [1] and inulin[2]. These experiments furnished comparable data for cases in which a monosaccharide (in saccharose), a disaccharide (in raffinose) or a polysaccharide (in inulin) was joined to the fructofuranosyl moiety. For completing the investigation of this problem, it was deemed necessary to study the hydrolysis of methyl-β-D-fructofuranoside, the glycoside containing the smallest possible aglycone moiety. There are data in the literature [3] for the hydrolysis of methyl-α-D-fructofuranoside, but none are available for the β-anomer. Therefore, one of the aims of the present work was to determine the hydrolysis characteristics of methyl-β-D-fructofuranoside in a similar manner as it has been done in our previous papers [1, 2].

Methyl-β-D-fructofuranoside was prepared by the methanolysis of inulin. Another method of preparation, by the methanolysis of saccharose, has been described by HORVÁTH and METZENBERG [10]. Considering that relatively little is known about the methanolysis of glycosides, and the number of fractions formed upon the methanolysis of inulin was greater than expected, this

* The present paper is a part of a series; the previous part has been published in Acta Chim. Acad. Sci. Hung. **70,** 381 (1971).

reaction was subjected to more detailed studies for determining the optimal conditions of the process; simultaneously also some rate constants were determined for the methanolysis of saccharose.

Experimental

Determination of the rate of methanolysis

0.100 g of inulin (or saccharose), ground in a ballmill and dried over P_2O_5, and 1.0 ml of 0.14 *N* HCl in abs. methanol were put into 10 ml glass ampoules. After sealing, the ampoules were placed into an ultrathermostate of the appropriate temperature, and samples were taken out at definite time intervals. After opening the ampoules the refractivity of the supernatant was determined by an Abbé-type refractometer. Inulin and saccharose are insoluble in methanol, while the end products of methanolysis are soluble. It has been revealed by paper chromatography that the dissolved material contains only monosaccharides as well as their methylglycosides. The refractivity is directly proportional to the concentration of the dissolved material. The refractivity at zero reaction time ($\tau = 0$) is n_0 and the upper limit is n_{max} at $\tau = \infty$.

Table I

First order rate constants of methanolysis of inulin and saccharose

t (°C)	inulin $k_{met} \times 10^3$			saccharose $k_{met} \times 10^3$
	HCl = 0.0014 *N*	0.014 *N*	0.14 *N*	0.14 *N*
30.0	—	—	1.21	3.91
40.0	—	—	6.55	18.7
50.0	0.106	2.40	37.5	104.6

Determining the pairs of τ and n values, the first order rate constant of the methanolysis k_{met} can be calculated. Fig. 1 shows two methanolysis curves, one for inulin and one for saccharose; Fig. 2 shows the logarithmic plots for determining the rate constants of methanolysis. It is seen in Fig. 2 that, contrary to hydrolysis [2], these curves do not consist of two sections. The experimental k_{met} values are shown in Table I. The agreement between the obtained rate constants and those calculated from the data of HEIDT and PURVES [3] for similar reaction conditions is acceptable.

It is to be mentioned that the reaction may not be regarded as a pure methanolysis because considerable amount of reducing material is also formed. The reducing power of the reaction products in each methanolysis series of inulin has been determined in the last samples by the Somogyi—Nelson method [4]. Dissolution was practically complete in the last samples, and the reducing power reached 15.5% of the value obtained after complete acid hydrolysis of a parallel sample. Probably, this can be at least partly explained by the fact that the experiments have been performed under tropical conditions, in the rainy period at an extremely high air humidity.

Preparative methanolysis

A mixture of 12.87 g of dry, powdered inulin and 164 ml abs. methanolic HCl (0.11 *N*) was maintained at 40 °C for 4 hrs and then for 1 hr at 50 °C. The clear, slightly yellow solution formed was neutralized by shaking with dry $NaHCO_3$; after cooling, the inorganic residue was separated from the solution which contained 10.58 w% of organic material. This solution was used for preparative separations.

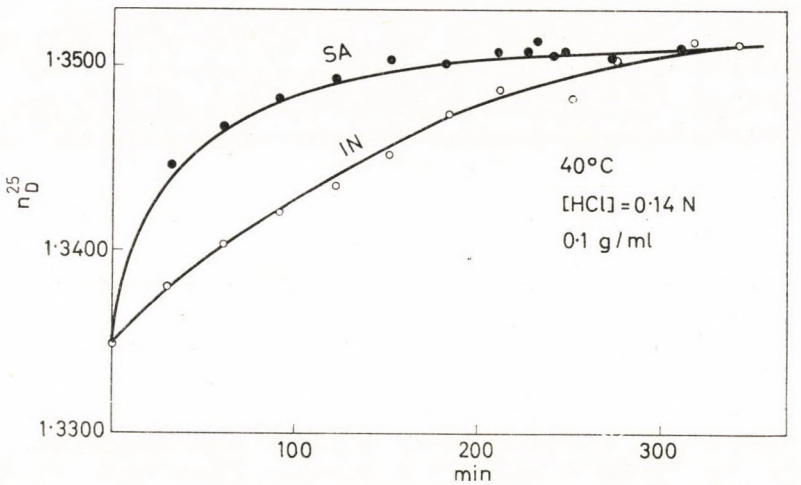

Fig. 1. Variation of the refractivity of inulin (IN) and of saccharose (SA) during their methanolysis

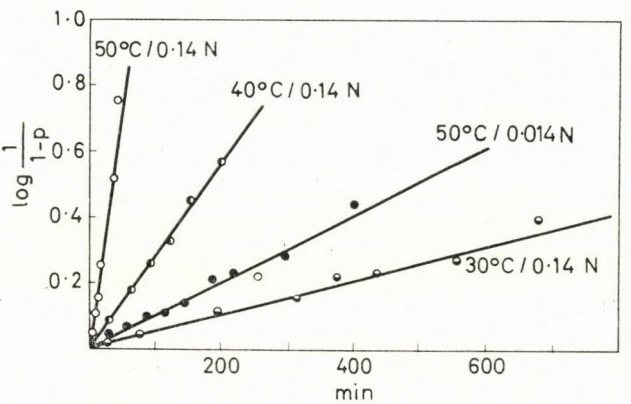

Fig. 2. Logarithmic inulin methanolysis curves

Paper electrophoresis

The conditions of paper electrophoresis used in studying the products of methanolysis were as follows. Buffer: 7.63 g sodiumborate + 0.62 g boric acid per liter, adjusted to pH = 9.2 with 2.0 *N* NaOH [5]. Paper: 4×30 cm strips (Filtrak F-1, "schnell laufend", 90 g/m²). Voltage: 300—350 V, 2 mA/strips; appropriate separation in 3—4 hrs. Sample weight in the case of glucose (as reference substance) 250 μg, and in the case of methanolysis products 700 μg, dissolved in 0.01 ml. After drying, the strips were sprayed with diphenylamine–aniline–phosphoric acid [6] and heated to 80 °C. In the case of mixtures containing also methylglycosides the separation of glucose and fructose did not occur. According to literature data [7], the M_G value (migration distance per migration distance of glucose) is 0.04 for methyl-β-D-fructofuranoside, and 0.60 for its α-anomer. The methanolysis of inulin yielded 4 components, their M_G values (corrected for electroosmosis) are shown in Table II. According to these data the first fraction is methyl-β-D-fructofuranoside, the third methyl-α-D-fructofuranoside, the fourth is a mixture of fructose and glucose; the second fraction has not been identified, it is presumably a methyl-pyranoside.

Table II

Characteristics of the fractions

Fraction	I	II	III	IV + V
R_F	0.764	0.694	0.976	0.642
M_G	0.040	0.40	0.63	1.00
Amount (% by electrophoresis)	21.6	33.3	30.2	15.5
Amount (% by paperchromatography)	24.2	27.2	33.2	14.8
Reducing power (expressed as fructose, %)	—	—	—	17.5
Stability in 0.01 *N* HCl at 60 °C	decomposes in 1.5 hr	stable	decomposes in 1.5 hr	increasing amount

Paper chromatography

Descending chromatography was applied with repeated development. The dry material content of the samples applied to the 4×56 cm strips was between 200 and 1000 μg. Solvents: pyridine: butanol: acetic acid = 6 : 4 : 3; detection of the spots as in paper electrophoresis. The glucose spot appeared with a blue tint, the fructose and its derivatives with a brown colour. The R_F values for the four spots after a single development are shown in Table II. One half of the most slowly moving spot had a bluish, the other half a brown colouration upon heating to 80 °C; this spot appeared also upon treatment with alkaline $AgNO_3$. Consequently this spot contained reducing sugars; the R_F values also revealed that this fraction was a mixture of glucose and fructose. The other three spots contained nonreducing glycosides.

Reducing power

The reducing power of the methanolysate made for preparative purposes, determined by the Somogyi-Nelson method [4], was equivalent to that of 12.8 mg/ml of fructose; the same value after a complete acid hydrolysis was 72.8 mg/ml, *i.e.* 17.5% of the total sugars were present as free sugars.

Quantitative determination of the various components

The fractions separated by paper electrophoresis were extracted from the strips and investigated by paper chromatography and vice versa. The fractions identified in this way were determined quantitatively by reducing power measurements following acid hydrolysis. The results are shown in Table II. Glucose and fructose can be separated by paper electrophoresis in the above buffer solution only in the absence of methylglycosides. Therefore, the methanolysate of inulin resulted in 4 fractions but after preliminary paperchromatographic separation, 5 fractions could be obtained. As seen in Table II, the stability to acid hydrolysis (60 °C, 0.01 *N* HCl) suggests that the Ist and the IIIrd fractions are furanosides, while the IInd fraction is probably a methylpyranoside.

Preparative separation of the fractions

The preparative separation was performed in borate buffer on a 25×2 cm Amberlite CG-400 resin column (chromatographic grade, 100—200 mesh) [9]. Inulin methanolysate equivalent to approximately 2.5 g fructose, dissolved in 5 ml 0.005 *M* potassiumtetraborate was charged on the column and, by increasing the borate concentration 15 ml fractions were collected (see Fig. 3). From the collector tubes 0.2 ml samples were taken and mixed with 1.8 ml

water and 4 ml anthrone reagent (0.2 g of anthrone dissolved in 100 ml of 95% sulfuric acid). After 30 min the optical density was measured at 630 mμ. As shown by Fig. 3, the separation of the first two fractions was complete; this was also proved by paper chromatography. The separation of the last two components was not complete, however, this is irrelevant for, interestingly the sequence of separation differs from that observed in paper electrophoresis. As first, fraction I (methyl-β-D-fructofuranoside) and as second, fraction III (methyl-α-D-fructo-

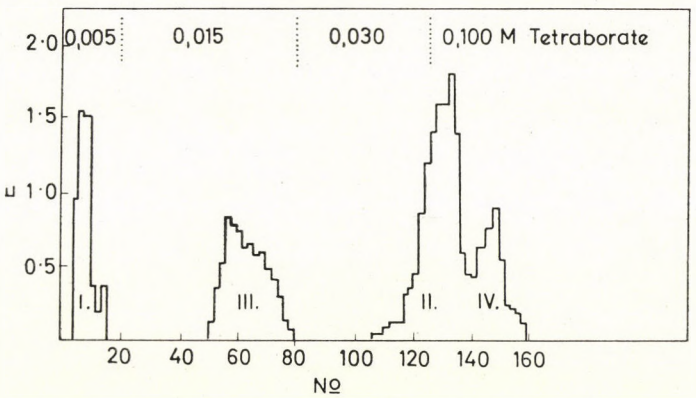

Fig. 3. Separation of the fractions by ion-exchange chromatography. Column: 2×25 cm Resin: Amberlite CG-400, 15 ml fractions were collected, flow-rate 1.5 ml/min, abscissa: tube N°

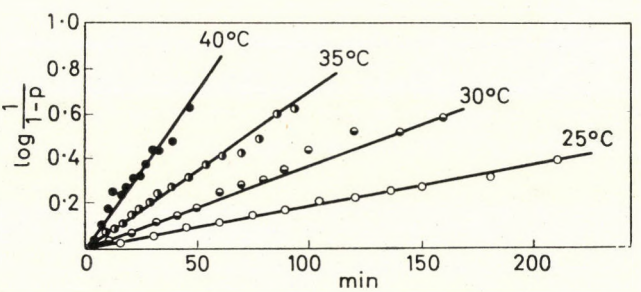

Fig. 4. Determination of first order rate constants for the hydrolysis of methyl-β-D-fructofuranoside in 0.0977 *N* HCl

furanoside) was eluted from the column. The contents of the corresponding tubes were combined and evaporated to dryness in vacuum. The residue was extracted first with cold methanol (insoluble residue discarded) and, after repeated evaporation, with pyridine. Potassiumtetraborate is insoluble in both solvents. The syrup obtained after the evaporation of pyridine proved to be homogeneous both by paper chromatography and paper electrophoresis. The quantity of the fractions agreed with the percent distribution shown in Table II.

Acid hydrolysis of methylfructofuranosides

80 mg syrupy methylfructofuranoside was dissolved in 40 ml 0.0977 *N* HCl of the appropriate temperature and kept in an ultrathermostate. At definite time intervals 2 ml samples were taken out and mixed immediately with 2 ml NaOH of the same normality. Reducing power was determined by the Somogyi-Nelson method [4]. The log $1/(1-p)$ values are shown in Fig. 4; the k values are shown in Table III. The E_a values for the methanolysis of inulin and saccharose as well as for the hydrolysis of methyl-β-D-fructofuranoside were determined graphically (Fig. 5).

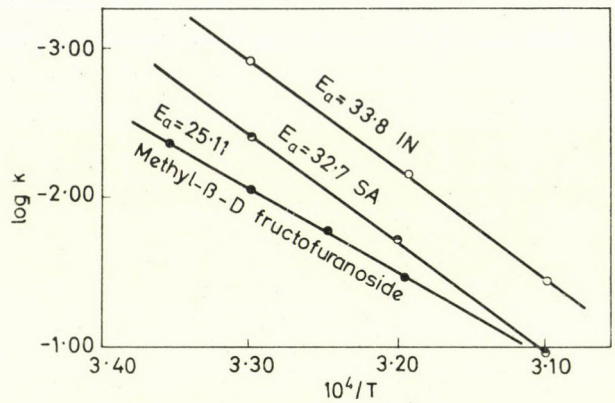

Fig. 5. Log k or log k_{met} values for the hydrolysis of methyl-β-D-fructofuranoside (in 0.0977 N HCl) and for the methanolysis of saccharose (SA) and inulin (IN) as a function of $1/T$; determination of the E_a values

Table III

First order hydrolysis rate constants of methyl-D-fructofuranosides in 0.0977 N HCl

t (°C)	$k \times 10^3$	k_r, 100 °C*
Me-β-D-fructofuranoside		
25.0	4.26	253
30.0	8.45	248
35.0	15.9	240
40.0	32.2	251
Me-α-D-fructofuranoside		
30.0	14.1	750+

+ = calculated on the basis of E_a reported by HEIDT and PURVES [3]

$$* = \log k_{r,100\,°C} = \log k_r + \frac{E_a}{4.575}\left(\frac{1}{T} - \frac{1}{373.2}\right)$$

Discussion

Methanolysis

Data concerning the mechanism of alcoholysis of glycosidic bonds are very scarce. It is known that an increase of the ethanol concentration up to about 70 vol% reduces, but above that limit increases the solvolysis rate of saccharose [11]. Presumably two opposing trends come into operation: with increasing ethanol concentration the hydrogen ion activity decreases up to about

80 vol% ethanol (the value of the H_0 function [12] increases), then the hydrolysis is replaced to an increasing extent by a more rapid reaction, alcoholysis. Above 80 vol% ethanol the value of the H_0 function begins to decrease, *i.e.*the activity of the acid to catalyze hydrolysis increases.

In all the investigated cases (*e.g.* saccharose [11], maltite [14], starch [14], cellulose [13]) the solvolysis of the glycosides in acidic absolute alcohols proved to be faster than the hydrolysis in an aqueous system at identical acid concentration and temperature. At higher temperatures the difference between the rates of alcoholysis and hydrolysis will be greater because the apparent activation energy of alcoholysis is considerably higher than that of hydrolysis.

Table IV

Characteristic data for hydrolysis and methanolysis of inulin and saccharose

	Inulin		Saccharose	
	hydrolysis	methanolysis	hydrolysis	methanolysis
E_a kcal/mole	25.5	33.8	25.5	32.7
ΔS^+ e.u.	+8.13	+32.30	+8.07	+32.63
g	1.062		1.038	
g^*		1.21		—
d	16.725	19.24	16.754	18.79
k_r, 100 °C	71.4		56.3	
$k_{r,met}$, 100 °C		437		1050

$$\Delta S^+ = 4.576\left[\log k_r - \log 1.025052 \cdot T \cdot \exp\left(-\frac{E_a - RT}{RT}\right)\right]$$

$$\log k_r = \log k + g \cdot \mathrm{pH} \qquad (k \text{ in } \mathrm{min}^{-1} \text{ and ln})$$

$$g = \Delta \log k / \Delta \mathrm{pH} \qquad g^* = \Delta \log k / \Delta (-\log [\mathrm{HCl}])$$

$$d = \frac{\Delta \log k}{\Delta \frac{10^3}{T}} \cdot \frac{1}{T_1} - \log k_{r1}$$

Thus for example, the E_a of cellulose hydrolysis in 1% aqueous sulfuric acid at 100—160 °C is 30.1 kcal/mole, while in 96% ethanol in the presence of 1% sulfuric acid, it is 33.3 kcal/mole [13]. As shown by Table IV, the activation energies of both inulin and saccharose are by 7—8 kcal/mole higher in methanol than in water. Consequently, the entropy of activation is also higher by about 24 e.u. than the one obtained for hydrolysis.

It is to be mentioned that for calculating comparable parameters a precondition is that the rate constants should refer to identical catalyst activities. In aqueous solutions this requirement is fulfilled by the so called reduced rate constant (k_r) which refers to pH = 0 or $H_0 = 0$ [15]; it is, however, not clear

which acidity function can guarantee in methanolic solutions the comparability of the calculated parameters with those corresponding to hydrolysis. The only feasible way was to refer k_{met} to unit acid concentration, *i.e.*:

$$\log k^*_{r,met} = \log k_{met} + g^*(-\log[HCl])$$

where $g^* = \Delta \log k_{met}/\Delta(-\log [HCl]) = 1.21$.

The errors associated with this simplification may make questionable the validity of the possible conclusions. In an aqueous solution the H_0 value for 0.1 *N* HCl is 0.97, while in 100% ethanol it is only 0.57 [12]. Presumably methanol does not differ strongly from ethanol in this sense, therefore, the log $k^*_{r,met}$ values calculated on the basis of —log [HCl] may deviate not more than by 0.4 units from the actual ones. The possible maximum deviation of the calculated values from the actual ones in the entropy of activation is 1.8 e.u. at most, and in the value of *d* at most 0.4 units, *i.e.* the maximum errors are about 6% and 2%, respectively. The maximum deviation of $k_{r,met}$ cannot exceed 2.5-times its actual value. However, the possible deviations do not influence the conclusions drawn, because the differences between the corresponding parameters of methanolysis and hydrolysis are much greater (see Table IV).

The above great differences in the ΔS^+ and E_a values suggest that the mechanism of methanolysis is not the same as that of hydrolysis. Probably also in this case the formation of a tertiary furanosyl cation is the rate-determining step; its higher stability and the high positive ΔS^+ value allow to conclude to this mechanism. However, the possibility of an open-chain mechanism does not seem to be excluded.

Swiderski and Temeriusz [16] have investigated the methanolysis of some methylglycosides in absolute methanol, in the presence of 1% HCl. They have concluded that in case of Me-β-D-gluco-, -β-D-galacto-, -α-D-galacto-, and -β-D-mannopyranosides the reaction proceeds through an acyclic intermediate, while the acid hydrolysis of the same glycosides occurs probably through a cyclic pyranosyl cation [8].

For an unambiguous clarification of this problem further studies are necessary.

Hydrolysis

Table V shows the hydrolysis characteristics of β-D-fructofuranosides as a function of the size of the aglycone moiety. These data suggest that already the second carbon atom of an aliphatic aglycone linked through a primary carbon atom to the glycosidic bridge-oxygen, exerts only a small influence on the stability of the glycosidic bond. This hypothesis is substantiated by the observation that the difference between the stability of the furanosyl-OCH_3

and furanosyl-OCH_2-(inulin) is less than that in the case of furanosyl-OCH_3 and furanosyl-O-(glucosyl). In the latter, the aglycone moiety (the glucosyl group) is bound through a secondary C-atom. Thus it is possible to predict that the stability of the 6-O-(β-D-fructofuranosyl)-D-glucopyranose, not yet studied, will fall between the stabilities of Me-β-D-fructofuranoside and of inulin, while the 6-O-(β-D-glucopyranosyl)-D-fructofuranose is about as stable as the isomaltose in acidic media.

The *n*-alkyl- and benzyl-glycosides, the 1,6-linked disaccharides and even the 1,6-linked dextran may be considered as substituted methylglycosides. It follows from the data of Table V that the same is true for inulin. The hydrolysis characteristics of such type of glycosides are closely related to those of the corresponding methylglycosides; the farther parts of the aglycone moiety,

Table V

Correlation between the size of the aglycone moiety and the stability of the glycosidic bond

Glycoside	Aglycone	E_a kcal/mole	ΔS^+ e. u.	k_r, 100 °C (min^{-1})
Raffinose	Melibiose	25.6	+8.34	48.3
Saccharose	Glucose	25.5	+8.07	55.3
Inulin	—CH_2—(Polysaccharide)	25.5	+8.13	71.4
Methyl-β-D-fructofuranoside	—CH_3	25.1	+9.55	253

joined to the —CH_2— group, exert much less influence on the stability of the glycosidic bond than the aglycone linked to the bridge-oxygen through a secondary carbon atom. Correspondingly the stability sequence is:

aglycone moiety is a disaccharide (*e.g.* in raffinose) >
monosaccharide (*e.g.* in saccharose) >
substituted methyl group (*e.g.* in inulin) >
methyl group (in methyl-β-D-fructofuranoside).

The correlation between the size of the aglycone and its hydrolysis rate is similar to the one observed in the case of pyranosides (*e.g.* maltose, homologues of maltose and amylose [17]). Other hydrolysis parameters (E_a and ΔS^+) are practically identical, which proves that the reaction mechanism is the same for all β-ketofuranosides. Thus the present work seems to support the hypothesis advanced in our previous papers [1, 2] for the mechanism of hydrolysis of furanosidic bonds.

According this hypothesis, in the case of saccharose the rate-determining step is not the formation of a glucosyl, but that of a tertiary furanosyl cation. A change of ring conformation can hardly have any significance in this case.

The entropy of activation of the alkylaldofuranosides is negative [18], which allows to conclude to an A-2 mechanism (the rate-determining step is a bimolecular attack of a solvent molecule on the protonated glycoside). In the case of β-fructofuranosides as well as other ketofuranosides investigated until now, and in the case of ketopyranosides, the ΔS^+ is positive [8], supporting the assumption of an A-1 mechanism (the rate-determining step is the monomolecular formation of a glycosyl cation, *i.e.* in this case of a cyclic tertiary cation).

REFERENCES

1. SZEJTLI, J., HENRIQUES, R. D., CASTIÑEIRA, M.: Acta Chim. Acad. Sci. Hung. **66,** 219 (1970)
2. SZEJTLI, J., HENRIQUES, R. D., CASTIÑEIRA, M.: Acta Chim. Acad. Sci. Hung. **70,** 381 (1971)
3. HEIDT, L. J., PURVES, C. B.: J. Amer. Chem. Soc. **60,** 1206 (1938); PURVES, C. B.: *ibid.*, **56,** 1969 (1934)
4. PAECH, K., TRACEY, M. V.: Moderne Methoden der Pflanzenanalyse, Vol. II. Springer Verlag, Berlin, 1955
5. DIAMOND, P. S., DENMAN, R. F.: Laboratory Techniques in Chemistry and Biochemistry. Butterworths, London, 1966
6. HAIS, I. M., MACEK, K.: Paper Chromatography. Czehoslovak Academy of Sciences, Prague, 1963.
7. FOSTER, A. B.: Adv. Carbohydrate Chem. **12,** 81 (1967)
8. SZEJTLI, J.: Säurehydrolyse glykosidischer Bindungen. Akadémiai Kiadó, Budapest; Fachbuchverlag, Leipzig, 1972
9. KHYM, J. X., ZILL, L. P.: J. Amer. Chem. Soc., **73,** 2399 (1961)
10. HORVÁTH, A. E., METZENBERG, R. L.: Biochim. Biophys. Acta, **74,** 165 (1963)
11. BURROWS, G. J.: J. Chem. Soc. **105,** 1260 (1914)
12. BRAUDE, E. A.: J. Chem. Soc. 1971 (1948); BRAUDE, E. A., STERN, E. S.: *ibid.* 1976 (1948)
13. SHARKOV, V. I., KOROLKOV, I. I., LEVANOVA, V. P.: Sbornik Trudov VNIIGS, Leningrad, **5,** 67 (1956)
14. KOROLKOV, I. I., SHARKOV, V. I., LEVANOVA, V. P.: Sbornik Trudov VNIIGS, Leningrad, **5,** 21 (1956)
15. SZEJTLI, J.: Acta Chim. Acad. Sci. Hung. **45,** 141 (1965)
16. SWIDERSKI, J., TEMERIUSZ, A.: Carbohydrate Res. **3,** 225 (1966—67)
17. SZEJTLI, J.: Stärke, **19,** 145 (1967)
18. BEMILLER, J. N.: Adv. Carbohydrate Chem. **22,** 25 (1967)

József SZEJTLI; Budapest IV., Tó u. 1—4.
Ruth Daisy HENRIQUES, Mirtha CASTIÑEIRA } Universidad de La Habana, Facultad de Ciencias, La Habana, Cuba.

INDEX

INORGANIC AND ANALYTICAL CHEMISTRY — ANORGANISCHE UND ANALYTISCHE CHEMIE — НЕОРГАНИЧЕСКАЯ И АНАЛИТИЧЕСКАЯ ХИМИЯ

LADÁNYI, L., PHAM HAI TUNG, FAUVELOT, G. and SZÓKÁN, G.: Hydrazo-9-Acridine, a New Acid–Base Indicator for Titrations in Glacial Acetic Acid, I 359

PHAM HAI TUNG and LADÁNYI, L.: Hydrazo-9-Acridine, a New Acid–Base Indicator for Titrations in Glacial Acetic Acid, II. Determination of the Indicator Dissociation Constant 363

KISS, A. B., GADÓ, P. and HEGEDÜS, A. J.: Investigations on the Thermocondensation of Ammonium Paratungstate Pentahydrate by a Combined Thermoanalytical and IR Spectrophotometric Method, and Additional Methods 371

PHYSICAL CHEMISTRY — PHYSIKALISCHE CHEMIE — ФИЗИЧЕСКАЯ ХИМИЯ

GIBER, J., WÉGNER, M. and DOBIS, O.: Adsorption of Water Vapour on the Chemically Treated Surface of a Germanium Single Crystal 393

KÁLMÁN, E.: Untersuchungen zum Verhalten der Uranylsalze in wäßrigen binären und ternären Systemen. (Investigation of the Behaviour of Uranyl Salts in Aqueous Binary and Ternary Systems) 407

ORGANIC CHEMISTRY — ORGANISCHE CHEMIE — ОРГАНИЧЕСКАЯ ХИМИЯ

BARTÓK, M. and BOZÓKI-BARTÓK, G.: The Chemistry of 1,3-Bifunctional Systems, XV. Kinetic Study of the Alkaline Hydrolysis of the 1-Monosubstituted Homologues of 3-Chloropropanol 423

BARTÓK, M. and BOZÓKI-BARTÓK, G.: The Chemistry of 1,3-Bifunctional Systems, XVI. Reaction Kinetical Study of the Alkaline Hydrolysis of 1,1-Disubstituted Derivatives of 3-Chloro-1-propanol 433

MENCZEL, GY., SAMAY, G. and SIMON, K.: Crystal and Molecular Structure of Acetone 4-Nitrophenylhydrazone 441

EGYED, J., VINKLER, P. and GÁL, S.: Thermolytic Disproportionation of Cyanoacetate Salts 451

SZEJTLI, J., HENRIQUES, R. D. and CASTIÑEIRA, M.: Methanolysis of Inulin and Hydrolysis of Methyl-β-D-Fructofuranoside 459

Printed in Hungary

A kiadásért felel az Akadémiai Kiadó igazgatója — Műszaki szerkesztő: Várhelyi Tamá

A kézirat nyomdába érkezett: 1971. XII. 23. — Terjedelem: 10 (A/5) ív, 76 ábra

72.72879 Akadémiai Nyomda, Budapest — Felelős vezető: Bernát György

ACTA CHIMICA

ТОМ 72 — ВЫП 4.

РЕЗЮМЕ

Гидразо-9-акридин — новый кислотно-основной индикатор, действующий в ледяной уксусной кислоте, I

Л. ЛАДАНИ, ФАМ ХАИ ТУНГ, Г. ФОВЕЛО и ДЬ. СОКАН

Описывается новый кислотно-основной индикатор (гидразо-9-акридин), действующий в ледяной уксусной кислоте, который может быть использован для индикации эквивалентной точки титрования оснований с $pK_{H_2O} > 5$. Точность титрования при использовании гидразо-9-акридина превышает точность при использовании индикатора кристаллфиолетового.

Гидразо-9-акридин — новый кислотно-основной индикатор, действующий в ледяной уксусной кислоте, II

Определение константы индикатора

ФАМ ХАИ ТУНГ и Л. ЛАДАНИ

Было исследовано кислотно-основное равновесие гидразо-9-акридина и была определена константа диссоциации индикатора ($pK_1 = pHClO_4$) в среде ледяной уксусной кислоты.

Исследование термоконденсации пятикратного гидрата аммониевого паравольфрамата с помощью термоаналитического, ИК спектрофотометрического и дополнительных методов

А. Б. КИШШ, П. ГАДО и А. Й. ХЕГЕДЮШ

Термоконденсация пятикратного гидрата аммониевого паравольфрамата была исследована при сочетании термоаналитического метода с ИК спектрофотометрическим методом измерения газов. Определяя число молей удаляющихся NH_3 и H_2O с помощью графического разделения инфракрасных пиков газовых продуктов, были рассчитаны составы промежуточных фаз, образующихся на ступенях процесса, перекрывающих друг друга. Следили также и за кристаллографическими превращениями. Следует отметить новое наблюдение, а именно, что на третьей стадии процесса в интервале температур 195 ÷ 230°C структура паракристалла модифицируется. Эта фаза разделялась соответствующим образом, и ее общий состав, рассчитанный спектрофотометрическим путем, оказался правильным и соответствует $3{,}75\ (NH_4)_2O \cdot 12WO_3 \cdot 3{,}25\ H_2O$. Приводятся рентгеноаналитические и ИК спектрофотометрические характеристики фазы. На основе измерения газообразных продуктов было установлено, что NH_3 удаляется из решетки либо с H_2O либо без нее. Было обнаружено, что при выделении сухого аммиака на октаэдре полианиона WO_6 остаются OH группы, связанные ковалентными силами. На основе исследований было однозначно доказано, что в пятикратных гидратах один моль воды присоединен слабо, а два моля являются кристаллической водой. Таким образом, принятая в настоящее время для паравольфраматного аниона структурная формула $[W_{12}O_{36}(OH)_{10}]^{-10}$ не применима для пятикратных гидратов.

Адсорбция водяного пара на химически обработанной поверхности монокристалла германия

Я. ГИБЕР, М. ВЕГНЕР и О. ДОБИШ

Было исследовано взаимодействие водяного пара с поверхностью монокристалла германия, вытравленной щелочным раствором перекиси водорода. Волюметрическим путем, а также радиоактивной индикацией измерялось количество воды, адсорбированной на поверхности, в зависимости от температуры (в интервале 16—80°С), времени взаимодействия и относительного содержания влаги ($p/p_0 < 0{,}8$). Приблизительно за 10 часов устанавливается адсорбционное равновесие. Изотермы, снятые в области температур 50—80°С, описываются уравнением Фрейндлиха; для мономолекулярного покрытия необходимо $155 \cdot 10^{-9}$ г/см² адсорбированной воды. Вода связана с поверхностью «слабыми» хемосорбционными силами, а теплота изостерической адсорбции колеблется в пределах 13—23 ккал/моль в зависимости от степени покрытия. Согласно кинетическим исследованиям, ступенью, лимитирующей скорость процесса, является диффузия. Коэффициент диффузии, рассчитанный на основе диффузионной модели, при 80°С равен $5{,}8 \cdot 10^{-18}$ см²/сек. Энергия активации диффузии равна прибл. 4 ккал/моль, что приблизительно совпадает с полученной величиной кажущейся энергии активации адсорбции.

Изучение свойств ураниловых солей в двойных и тройных системах

Э. КАЛЬМАН

Изучалось изменение свойств водных растворов ураниловых солей в зависимости от концентрации. Результаты указывают на сильное структуро-формирующее влияние уранилового иона. В согласии с литературными данными, аномальные свойства растворов ураниловых солей объяснялись связями, возникающими (в экваториальной плоскости) между ураном и другими лигандами, присутствующими в растворе. Были проанализированы проблемы, возникающие при интерпретировании термодинамических свойств более концентрированных растворов электролитов.

Химия 1,3-бифункциональных систем, XV

Изучение реакции щелочного гидролиза 1-монозамещенных гомологов 3-хлорпропанола

М. БАРТОК и Г. БОЗОКИ-БАРТОК

Исследовалась кинетика щелочного гидролиза 1-монозамещенных гомологов 3-хлорпропанола: 1-метил- (I), 1-этил- (II), 1-бутил- (III), 1-циклогексил-(IV) и 1-фенил-3-хлорпропанолов (V). Определялись направления реакции и рассчитывались константы скоростей, энергии активации, энтропии активации и предэкспоненциальные множители. Результаты измерений подтверждают механизм, предложенный авторами ранее, и для данного типа соединений.

Химия 1,3-бифункциональных систем, XVI

Кинетическое изучение щелочного гидролиза 1,1-дизамещенных производных 3-хлорпропанола

М. БАРТОК и Г. БОЗОКИ-БАРТОК

Рассматривался метод реакционной кинетики щелочного гидролиза некоторых 1,1-диалкильных гомологов 3-хлорпропанола [1,1-диметил- (I), 1-метил-1-пропил- (II), 1-метил-1-изопропил-3-хлорпропанол (III)].

На основе экспериментальных данных были определены константы скорости, энергии активации, энтропии активации, а также предэкспоненциальные множители щелочного гидролиза трех соединений.

Кристаллическое и молекулярное строение ацетон-4-нитрофенилгидразона

ДЬ. МЕНЦЕЛЬ, Г. ШАМАИ и К. ШИМОН

Кристаллическое и молекулярное строение ацетон-4-нитрофенилгидразона было определено рентгено-дифракционным методом. Кристалл — моноклинный, с пространственной группой $P2_1/C$. Строение определялось с помощью метода Паттерсона и молекулярно-трансформационного метода. Уточнения проводились с помощью дифференциального синтеза и метода наименьших квадратов. Индекс достоверности $R = 10{,}9\%$. Картина связей ароматического кольца асимметрическая. Длины и углы связей сравниваются со значениями для мета-соединений, определенными уже ранее [1]. Были определены уравнения плоскостей бензольного кольца и ацетоновой и гидразиновой частей, а также рассчитаны углы между этими плоскостями.

О диспропорционировании солей циануксусной кислоты под влиянием нагрева

Я. ЭДЬЕД, П. ВИНКЛЕР и Ш. ГАЛ

Было установлено, что натриевая соль циануксусной кислоты (I) при нагреве ее выше 180°С разлагается на двуокись углерода, ацетонитрил и двухнатриевую соль натрий-имидометиленмалоновой кислоты (II).

Изучался механизм этого процесса и было установлено, что первой ступенью его является образование 1 молекулы двухнатриевой соли циануксусной кислоты (III) и 1 молекулы циануксусной кислоты из 2 молекул I (последний продукт разлагается при данной температуре на двуокись углерода и ацетонитрил). Промежуточный продукт III карбанионного характера может образовывать связь с карбоксилатным углеродом I электрофильного характера. Образующийся таким образом промежуточный комплекс разлагается на ацетонитрил и II.

При проведении термического разложения I в присутствии метил-натрий-карбоната-C^{14}, радиоактивный карбоксилатный углерод встраивается в соединение II, при кислом разложении которого были выделены радиоактивная циануксусная кислота и этиловый эфир циануксусной кислоты.

Исследования с литиевыми, натриевыми, калиевыми и бариевыми солями циануксусной кислоты показали, что температура разложения их зависит от катиона, в то время как продукты разложения оказались идентичными.

Метанолиз инулина и гидролиз метил-β-D-фруктофуранозида

Й. СЕЙТЛИ, Р. Д. ХЕНРИКЕС и М. КАСТИНЕИРА

Получение метил-β-D-фруктофуранозида производилось с помощью метанолиза инулина. Были определены константы скорости метанолиза инулина и сахарозы, а также гидролиза метил-α- и -β-D-фруктофуранозидов в присутствии HCl. Энергия активации метанолиза значительно выше энергии активации гидролиза, поэтому метанолиз — при одинаковой температуре и концентрации кислоты — является более быстрой реакцией, чем гидролиз. Энтропия активации метанолиза равна +32 ед. энтр., в то время как для гидролиза была получена величина +8 ед. энтр. Таким образом, можно заключить, что механизм алкоголиза отличается от механизма гидролиза. В таких гликозидах, где агликоновое звено присоединяется к кислороду моста своим первичным атомом углерода, второй атом агликона оказывает лишь очень слабое влияние на стабильность гликозидной связи. Поэтому инулин можно рассматривать как замещенный метил-β-D-фруктофуранозид.

The Acta Chimica publish papers on chemistry in English, German, French and Russian.

The Acta Chimica appear in volumes consisting of four parts of varying size, 4 volumes being published a year.

Manuscripts should be addressed to

Acta Chimica
Budapest 112/91 Műegyetem

Correspondence with the editors should be sent to the same address.

The rate of subscription is $ 16.00 a volume.

Orders may be placed with "*Kultúra*" Foreign Trade Company for Books and Newspapers (Budapest I., Fő utca 32. Account No. 43-790-057-181) or with representatives abroad.

Les Acta Chimica paraissent en français, allemand, anglais et russe et publient des mémoires du domaine des sciences chimiques.

Les Acta Chimica sont publiés sous forme de fascicules. Quatre fascicules seront réunis en un volume (4 volumes par an).

On est prié d'envoyer les manuscrits destinés à la rédaction à l'adresse suivante:

Acta Chimica
Budapest 112/91 Műegyetem

Toute correspondance doit être envoyée à cette même adresse.

Le prix de l'abonnement est de $ 16.00 par volume.

On peut s'abonner à l'Entreprise pour le Commerce Extérieur de Livres et Journaux «*Kultúra*» (Budapest I., Fő utca 32. Compte-courant No. 43-790-057-181) ou à l'étranger chez tous les représentants ou dépositaires.

«*Acta Chimica*» издают трактаты из области химической науки на русском, французском, английском и немецком языках.

«*Acta Chimica*» выходят отдельными выпусками разного объема. 4 выпуска составляют один том. 4 тома публикуются в год.

Предназначенные для публикации рукописи следует направлять по адресу:

Acta Chimica
Budapest 112/91 Műegyetem

По этому же адресу направлять всякую корреспонденцию для редакции.

Подписная цена — $ 16.00 за том.

Заказы принимает предприятие по внешней торговле книг и газет «*Kultúra*» (Budapest I., Fő utca 32. Текущий счет № 43-790-057-181) или его заграничные представительства и уполномоченные.

Reviews of the Hungarian Academy of Sciences are obtainable at the following addresses:

ALBANIA

Drejtorija Qändrone e Pärhapjes dhe Propagandimit të Librit
Kruga Konferenca e Päzes
Tirana

AUSTRALIA

A. Keesing
Box 4886, GPO
Sydney

AUSTRIA

GLOBUS
Höchstädtplatz 3
A-1200 Wien XX

BELGIUM

Office International de Librairie
30, Avenue Marnix
Bruxelles 5
Du Monde Entier
162, rue du Midi
Bruxelles

BULGARIA

HEMUS
11 pl Slaveikov
Sofia

CANADA

Pannonia Books
2, Spadina Road
Toronto 4, Ont.

CHINA

Waiwen Shudian
Peking
P. O. B. 88

CZECHOSLOVAKIA

Artia
Ve Smečkách 30
Praha 2
Poštovní Novinová Služba
Dovoz tisku
Vinohradská 46
Praha 2
Mad'arská Kultura
Václavské nám. 2
Praha 1
SLOVART A. G.
Gorkého
Bratislava

DENMARK

Ejnar Munksgaard
Nörregade 6
Copenhagen

FINLAND

Akateeminen Kirjakauppa
Keskuskatu 2
Helsinki

FRANCE

Office International de Documentation et Librairie
48, rue Gay-Lussac
Paris 5

GERMAN DEMOCRATIC REPUBLIC

Deutscher Buch-Export und Import
Leninstraße 16
Leipzig 701
Zeitungsvertriebsamt
Fruchtstraße 3—4
1004 Berlin

GERMAN FEDERAL REPUBLIC

Kunst und Wissen
Erich Bieber
Postfach 46
7 Stuttgart S.

GREAT BRITAIN

Blackwell's Periodicals
Oxenford House
Magdalen Street
Oxford
Collet's Subscription Import Department
Dennington Estate
Wellingborough, Northants.
Robert Maxwell and Co. Ltd.
4—5 Fitzroy Square
London W. 1

HOLLAND

Swetz and Zeitlinger
Keizersgracht 471—487
Amsterdam C.
Martinus Nijhof
Lange Voorhout 9
The Hague

INDIA

Hind Book House
66 Babar Road
New Delhi 1

ITALY

Santo Vanasia
Via M Macchi 71
Milano
Libreria Commissionaria Sansoni
Via La Marmora 45
Firenze
Techna
Via Cesi 16.
40135 Bologna

JAPAN

Kinokuniya Book-Store Co. Ltd.
826 Tsunohazu 1-chome
Shinjuku-ku
Tokyo
Maruzen and Co. Ltd.
P. O. Box 605
Tokyo-Central

KOREA

Chulpanmul
Phenjan

NORWAY

Tanum-Cammermeyer
Karl Johansgt 41—43
Oslo 1

POLAND

RUCH
ul. Wronia 23
Warszawa

ROUMANIA

Cartimex
Str. Aristide Briand 14—18
Bucureşti

SOVIET UNION

Mezhdunarodnaya Kniga
Moscow G—200

SWEDEN

Almquist and Wiksell
Gamla Brogatan 26
S—101 20 Stockholm

USA

F. W. Faxon Co. Inc.
15 Southwest Park
Westwood Mass. 02090
Stechert Hafner Inc.
31. East 10th Street
New York, N. Y. 10003

VIETNAM

Xunhasaba
19, Tran Quoc Toan
Hanoi

YUGOSLAVIA

Forum
Vojvode Mišića broj 1
Novi Sad
Jugoslovenska Knjiga
Terazije 27
Beograd

30. VI. 1972 Index: 26.007